Environmental Studies No. 26

The ice environment of eastern Lancaster Sound and northern Baffin Bay

Northern Affairs Program

J.R. Marko
Arctic Sciences Limited

Published under authority of the Hon. John C. Munro,
P.C., M.P., Minister of Indian and Northern Affairs
Ottawa, 1982.
QS-8310-000-EF-A1

Catalogue No. R71-19/26-1982E
ISBN 0-662-12085-X

This report was prepared under contract for Petro-Canada as part of the Eastern Arctic Marine Environmental Studies (EAMES) program. The views, conclusions and recommendations expressed herein are those of the authors and not necessarily those of Petro-Canada or the Department.

A Canadian contribution to the Unesco Program on Man and the Biosphere (MAB).

Cette publication peut être aussi obtenue en français.

Table of Contents

Executive Summary iv

Acknowledgements xvi

List of Figures xvii

List of Tables xxiv

1. Introduction 1

2. Research Overview 1
   - 2.1 Historical 1
   - 2.2 The Petro-Canada - EAMES Program 13

3. The Ice Environment 14
   - 3.1 Ice Cover Characteristics 14
   - 3.2 Ice Characteristics 72
     - 3.2.1 Thickness and Old Ice Fractions 72
     - 3.2.2 Typical Ice Pack Configurations and Floe Sizes 78
   - 3.3 Ice Movements 100
   - 3.4 Icebergs 112
     - 3.4.1 Background 112
     - 3.4.2 Intrinsic Iceberg Parameters 123
       - 3.4.2.1 Numbers 123
       - 3,4.2.2 Shapes 130
       - 3.4.2.3 Dimensions 135
     - 3.4.3 Iceberg Motion 138

4. Summary and Recommendations 190

5. Bibliography 193

Appendix 1A: Best year in five (20 percentile) ice conditions 203

Appendix 1B: Average (50 percentile) ice conditions 205

Appendix 1C: Worst year in five (80 percentile) ice conditions 207

Appendix 2A: Greater Baffin Bay Ice Coverage, June 6-December 5, 1978 209

Appendix 2B:	Lancaster Sound and northwest Baffin Bay Ice Coverage, June 6-December 5, 1978	211
Appendix 3A:	Greater Baffin Bay Ice Coverage, June 12-November 13, 1979	213
Appendix 3B:	Lancaster Sound and northwest Baffin Bay Ice Coverage, June 12-November 13, 1979	215

EXECUTIVE SUMMARY

The sea-ice-and iceberg-related components of the 1978-1979 Petro-Canada-EAMES environmental programs have made major contributions to our knowledge of the Lancaster Sound-Baffin Bay ice cover. A particular, relatively unique, feature of some of the included studies was their repetition over a period of 2 or more years in order to obtain measure of year-to-year variability.

The present report integrates the new results with earlier data and interpretations to provide a current state of knowledge description of the Lancaster Sound-western Baffin Bay ice environment.

The 1978-1979 Petro-Canada-EAMES Ice Studies

After a review of previous work, several measurement-and data analysis-programs were included in the Petro-Canada-EAMES project to clarify relevant aspects of the regional sea-ice and iceberg properties. Specifically, information was sought on the numbers, physical dimensions, trajectories and general histories of icebergs and on the distributions and movements of sea-ice. The principal features of the individual projects are summarized in Table 1 with reference to the locations and areas of coverage indicated in Fig. 1.

Project results taken together with relevant portions of the accompanying oceanographic, meteorological and biological programs form a basis for:

a) assessing the sea-ice-iceberg threat to offshore drilling activities and;

b) evaluating the role of the ice cover in determining the physical and biological consequences of an accidental spillage of oil.

The results considered here include:

1) descriptions of seasonal changes in the ice cover in terms of fractional coverage of the surface, ice-thickness, -age and -floe sizes. Emphasis was placed upon representation of a year-to-year variability usually in terms of estimated mean and extremal conditions. Identifications were made of location and extents of landfast/consolidated ice and the ranges of dates associated with its formation, break up and clearing.

TABLE I
PETRO-CANADA-EAMES ICE-RELATED STUDIES
1978-1979

COMPONENT	PERIOD	ORGANIZATION	DESCRIPTION
1. Aerial Iceberg Surveys	July-October 1978, 1979	NORCOR Engineering & Research Ltd., Petro-Canada Ltd. (J. Miller)	Near-daily positioning, shape and dimension estimates of icebergs in Baffin Bay adjacent to Lancaster Sound entrance.
2. Satellite-Tracking of Icebergs	August, 1978-October, 1980	Arctic Sciences Ltd.	Intermediate accuracy (0.5-2.5 km) berg positioning several times daily in western Baffin Bay from 76°N to Hudson Strait.
3. Land-Based Radar-Tracking of Icebergs	July-October, 1978	Seakem Oceanography Ltd. and NORCOR Ltd.	High time-resolution (20 min. sampling) tracking of bergs in eastern Lancaster Sound and in Baffin Bay east of Devon Island.
4. Berg Profiling	August, 1978	Ice Engineering Ltd.	Measurements of berg draft and above-water dimensions using sonar and standard surveying techniques.
5. Statistical Sea-Ice Summaries	May-October, 1959-1974	Petro-Canada Ltd. (J. Miller)	Digitization and computation of statistical representations of weekly AES ice chart information on surface ice composition and floe sizes.
6. Satellite Imagery Studies of Floe Velocities	1974-1979	Arctic Sciences Ltd.	Extraction of velocity and seasonal patterns of motion data from NOAA and Landsat Satellite imagery.

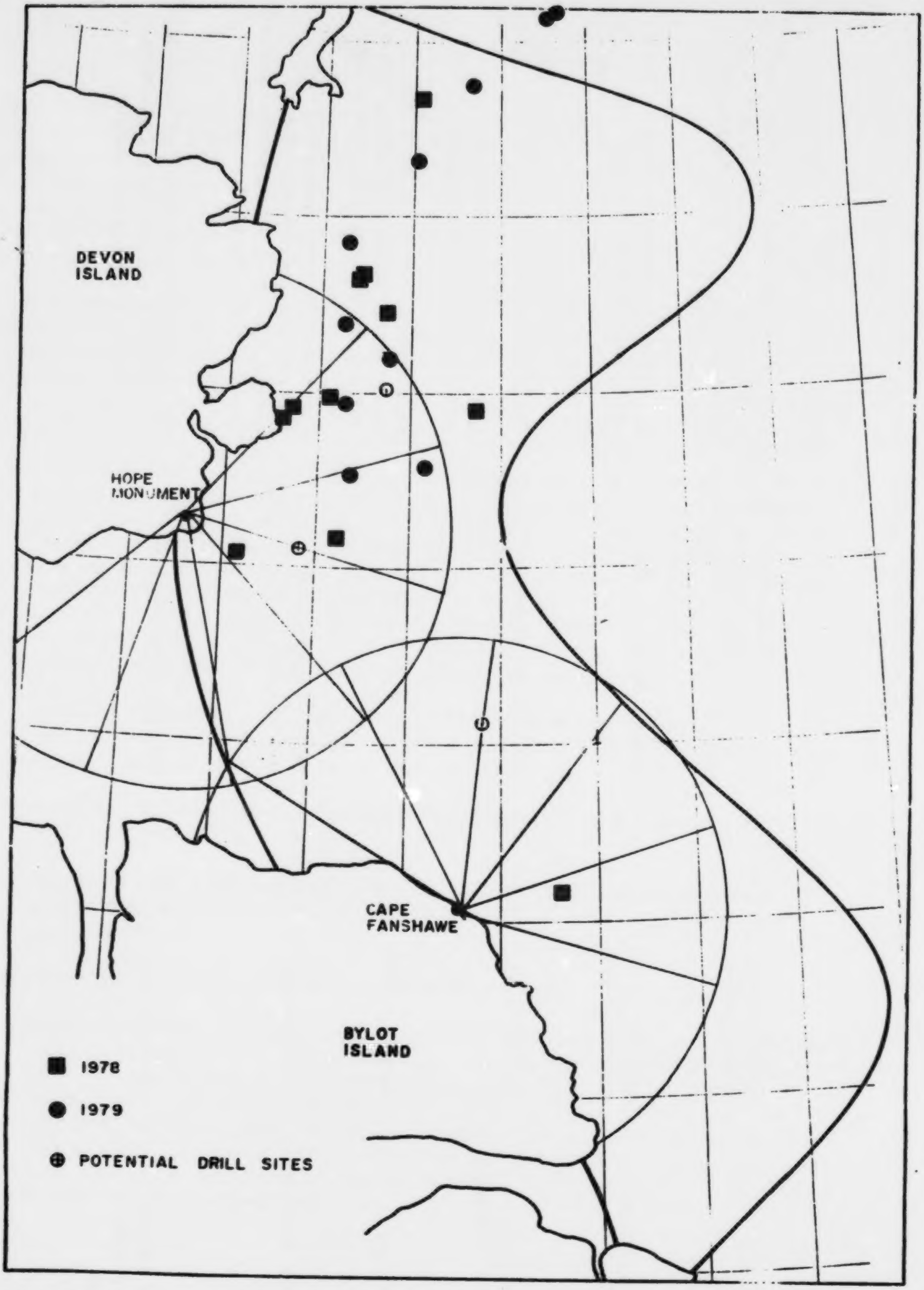
DEVON ISLAND
HOPE MONUMENT
CAPE FANSHAWE
BYLOT ISLAND
■ 1978
● 1979
⊕ POTENTIAL DRILL SITES

Figure 1: Locations of principal field operations, 1978-79 Petro-Canada-EAMES ice-related programs, including representation of the initial positions of 1978 and 1970 satellite-tracked bergs, the approximate range of the Hope Monument and Cape Fanshawe radar stations (semi-circles), and the boundaries of the aerial iceberg positions and dimension surveys (heavy lines).

2) descriptions of the seasonal sea-ice motions including their spatial- and time-dependences and their relationships to the atmospheric and oceanographic driving forces.

3) quantitative physical data on the regional iceberg population.

Sea-Ice Distributions

The large scale processes of change in the ice cover can be, to a first approximation, understood in terms of separate, relatively independent seasonal progressions taking place in Baffin Bay and Lancaster Sound, respectively. In the first instance, the Baffin Bay winter ice cover is made up of primarily first year ice due to the common near-completeness of the summer melt and the limited advection into the area. Winter coverage is usually total or 10/10 except in the "North Water" adjacent to Smith Sound and in the southeast where a large strip of open water extends northward along the west Greenland coast to very roughly 71°N.

Break-up of this winter ice cover is first noted in April as the north Water and West Greenland open water zones expand to the south and north respectively. Typically by July, large concentrations of pack ice in Baffin Bay are confined in a broad band bounded by the 67° and 76°N parallels of latitude and the 60° and 70°W lines of longitude. This ice typically dissipates by September with its last remnants usually lingering in the vicinity of Home Bay near 68°N off the east coast of Baffin Island. Baffin Island itself has an adjacent coastal landfast ice shelf which often extends outward for 70 km or more from the eastern Island shorelines. Break-up and clearance of this ice usually takes place in July and August. Smaller amounts of ice enter Baffin Bay in August and September from the break-up and clearing processes in Lancaster, Jones and Smith Sounds. New ice begins to form in September and October, beginning in the northern part of the region. Year-to-year variations in the spring-summer clearing process usually correspond to differences of roughly one month between the extremal "best" and "worst" conditions. Incomplete clearance of pack ice is a relatively common occurrence.

Although quantitative study of the phenomena is minimal, present understandings suggest that rates of clearing are governed by a combination of spring and summer winds and near-surface current patterns.

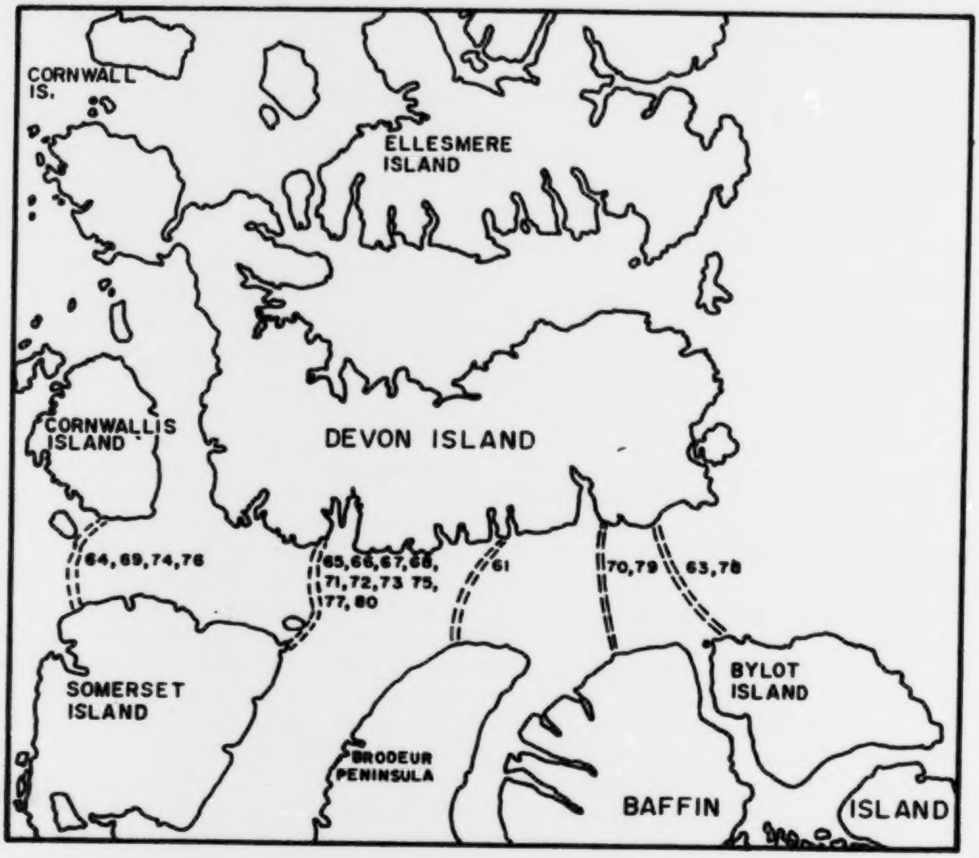
CORNWALL IS.
ELLESMERE ISLAND
CORNWALLIS ISLAND
DEVON ISLAND
64,69,74,76
65,66,67,68,
71,72,73 75,
77,80
61
70,79
63,78
SOMERSET ISLAND
BYLOT ISLAND
BRODEUR PENINSULA
BAFFIN
ISLAND

Figure 2 Approximate annual positions of the stable winter landfast ice edge, 1961-1980.

In Lancaster Sound and the adjacent Barrow Strait section of Parry Channel, additional complications arise from the presence of a landfast ice cover which extends fully across the Channel. This landfast ice is part of the great consolidated/landfast ice sheet which covers most of the Arctic Archipelago channels over the winter-spring period. In Parry Channel, coverage can be established as early as November or as late as April. The break-up of this ice cover usually begins in July. Important and large year-to-year variations occur in the eastern extent of the ice sheet as indicated by the approximate positions of the corresponding landfast ice edges as observed over the 1961-1980 period (Fig. 1-2). The most common ice edge position lies adjacent to Prince Leopold Island at the northeast corner of Somerset Island. Nevertheless, in approximately half of the years for which data are available the ice edge was located either in western Barrow Strait or in eastern Lancaster Sound. These shifts are significant because of the vastly different conditions obtained on the western and eastern sides, respectively, of the landfast ice edge. Over the winter period, areas to the east of the boundary are filled with a mixture of vast and smaller floes of dimensions often as large as 100 km, which move irregularly to the east with typical 10 km/day speeds. This process produces an open water/thin ice zone adjacent to the landfast ice edge and a mobile ice pack which gradually thickens to the east due to accretion during the easterly drift. At the junction with Baffin Bay, typical smooth ice thicknesses tend to be slightly less than the 2 m values typical of the Bay region.

By late April, large amounts of new ice are no longer generated and the continuing easterly drift of the remaining mobile floes generally gives rise by late May or early June to open-water or low ice-concentration conditions over most of Parry Channel east of the landfast ice edge. Under these circumstances, it is easily seen that the two extreme, westerly and easterly, edge positions correspond to alternative widely different spring and summer conditions over almost the entire length of Barrow Strait and Lancaster Sound. The westerly position usually leads to open conditions along the entire length of this sector from late May to sometime in July when the remaining consolidated ice packs begin to break apart. On the other hand, over this same period the easterly ice edge position generally leads to near total coverage of the same area by an originally 2 m thick mass of consolidated ice. In the last instance, even after break-up, the dissipation of the huge body of ice in this sector usually insures heavy ice conditions for much of the remaining summer period in Lancaster Sound and in the adjacent sector of Baffin Bay. In addition to these obvious effects on the region's ice conditions, differences in the thermal and radiative properties of open- and ice-covered-sea surfaces introduce a major source of variability in the regional energy budget.

Smaller year-to-year changes are also apparent in the extents and break-up dates of the regional coastal landfast ice shelves. In addition to the extensive landfast ice zone already noted off Baffin Island, important concentrations of such ice occur off the east coast of Devon Island, adjacent to Philpots Island, and in narrower most variable bands along the northern and eastern Bylot Island shorelines.

Sea-Ice Movements

Data on the movements of sea-ice were obtained from a seven year record of satellite imagery. At least two distinct seasonal patterns were identified associated with the November to May (winter-early spring) and May to October (spring and summer) periods respectively.

In the first instance, as noted above, the winter ice drift in Parry Channel tends to move the mobile ice away from the landfast ice edge. Box-averaging of observed daily floe drifts indicate typical easterly speeds are on the order of 10 km/day with somewhat higher values being obtained in the early winter and early spring periods. There is also an apparent tendency toward higher drift speeds in the southern Channel. The resulting easterly outflow of ice from eastern Lancaster Sound enters into the spatially uniform 10 to 15 km/day southerly drift of northwestern Baffin Bay with the easterly component of motion being observed as far east as 76°W.

During the spring and summer period, the simple rather uniform winter drift is replaced by a more complicated pattern that resembles greatly the surface current distributions identified in the oceanographic portions of the Petro-Canada-EAMES program. The movement of ice is, in this case, heavily concentrated in well-defined streams coinciding with the core of the Baffin Current which moves in a southerly direction along the continental slope of northwestern Baffin Bay before making a north to south intrusion into eastern Lancaster Sound, re-entering Baffin Bay where it flows south-southeasterly past Bylot and Baffin Islands. Ice drift speeds of 50 to 75 km/day are common in the rapid portions of the intrusive flow. On the other hand, adjacent regions have also been identified which correspond both to the weak flow/disordered zone where wind effects are important and to moderate speed, temporary eddy-like flow structures which have been identified in the oceanographic studies.

Icebergs

The great majority of icebergs in the western Baffin Bay - Lancaster Sound region originate from the coastal glaciers of western Greenland. Upon entry of calving into sea water, these bergs generally move northward along the West Greenland coastline before turning west somewhere in the northern reaches of Baffin Bay to enter the southward flowing Baffin Current. The latter flow moves along the eastern edge of the Arctic Archipelago and includes an important intrusion into eastern Lancaster Sound.

Aerial and radar surveys over a roughly 11 week period in 1978 identified approximately 1500 distinct bergs in the observation area with lengths in excess of 50 m. A small, approximately 20% reduction, was reported in the corresponding 1979 berg population.

On shorter time scales, 1978 radar data indicated a gradual increase in berg numbers through the summer corresponding to a 2.5 ratio of late to early season populations. Large random fluctuations in berg numbers were also present. Increasing in intensity in the late summer-early fall period. Anticipated "pulses" of large numbers of near-simultaneously arriving bergs were recorded in a few very narrow time intervals.

Median berg dimensions were on the order of 150 m in length, 8 m in mean height (relative to the water line) and 0.4×10^6 tonnes in mass. The largest berg observed was estimated to have a mass of 63×10^6 tonnes while the largest draft measured, in a 35 berg survey, was 220 m.

Non-uniformities in the spatial distributions of bergs were correlated with relatively well established patterns of movement as illustrated by the trajectories of 21 satellite-tracked bergs including in Fig. 3 a, b. The indicated berg trajectories follow closely the patterns of flow deduced from moored current meter measurements and from the drifts of sea-ice and drogued-buoys. Near-surface and deeper currents appear to be the dominant influence in berg motion. Approximately 90% of the bergs initially tracked in the east Devon-Coburg Island area entered Lancaster Sound, with most passing through an area near the southeastern corner of Devon Island where particularly high berg densities were recorded in the radar observation program. Only 2 of the tracked bergs penetrated Lancaster Sound west of 83°W. Most bergs tended to follow the main pathways of the intrusive flow with velocities (Fig. 4) comparable to those of the near-surface currents.

The trajectory data also indicate the presence of eddy-like berg movements chiefly to the north and east of Bylot Island. These motions tend to occur in fixed locations but do not appear to be permanent features of the berg circulation pattern. In this respect they resemble the temporary moderate flow features identified in the oceanographic studies of the region.

Upon leaving Lancaster Sound and passing through the eddy-zones to the east of Bylot Island, bergs tend to move to the southeast over the continental slope east of Baffin Island. Average drift velocities for moving bergs in this region tend to be on the order of 15 to 20 km/day. However, a tendency for the near-surface current to follow the bathymetric contour drives some bergs in shoreward directions along the underwater canyons which penetrate the continental shelf in several locations. Such bergs usually become grounded in adjacent shallow areas. Their escape from these areas and re-entry into the main flow along the continental slope is confined to the late July-early November period when the coastlines are partially or completely free of concentrations of inpenetrable landfast ice. Review of the 1978-1979 trajectory results suggest that under this complex interplay of current, bathymetry and ice processes, an average berg takes between two and three years to travel between Bylot Island and Cape Dyer in northern Davis Strait.

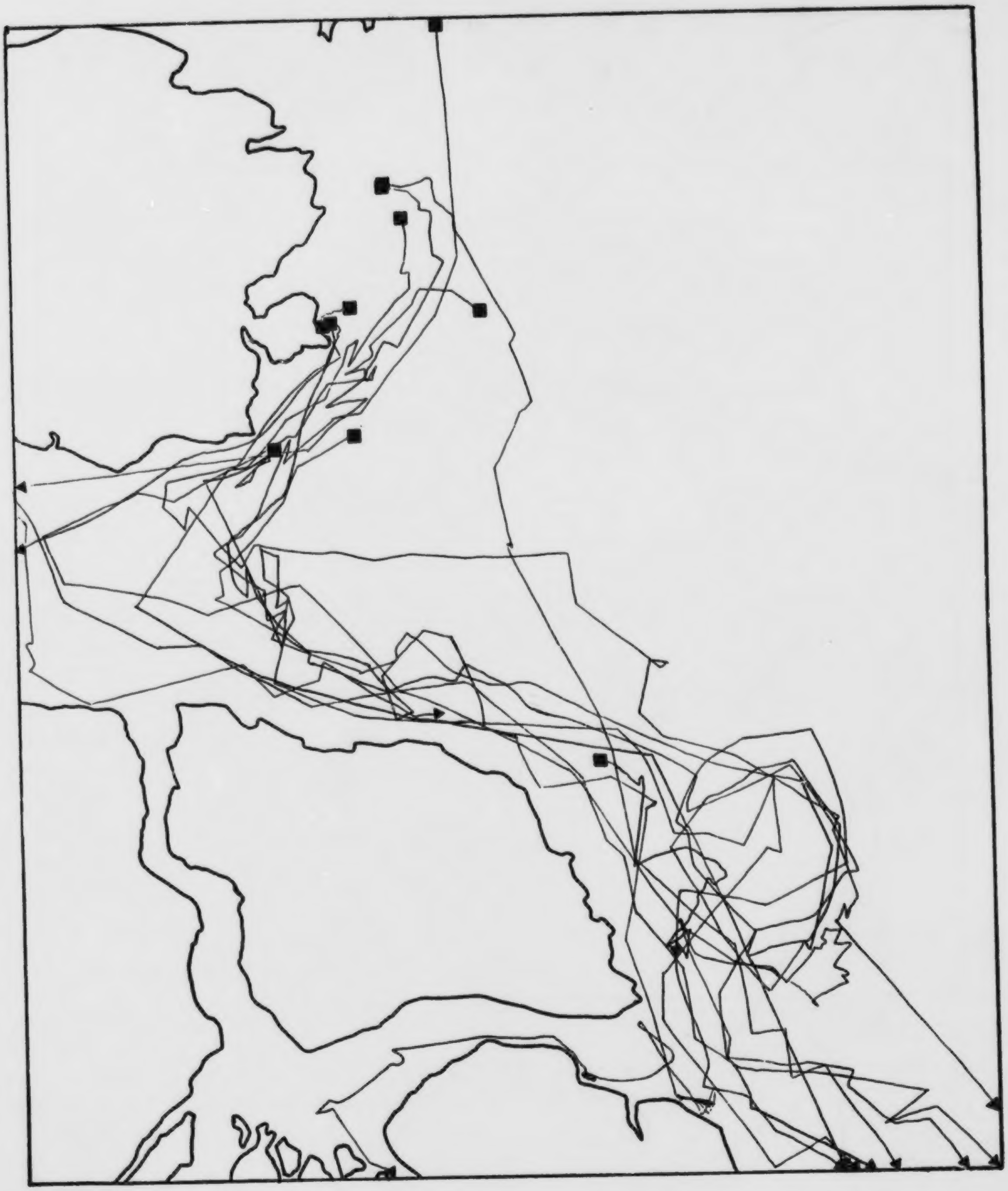

Figure 3a Trajectories of berg drifts from satellite-tracked data, 1978.

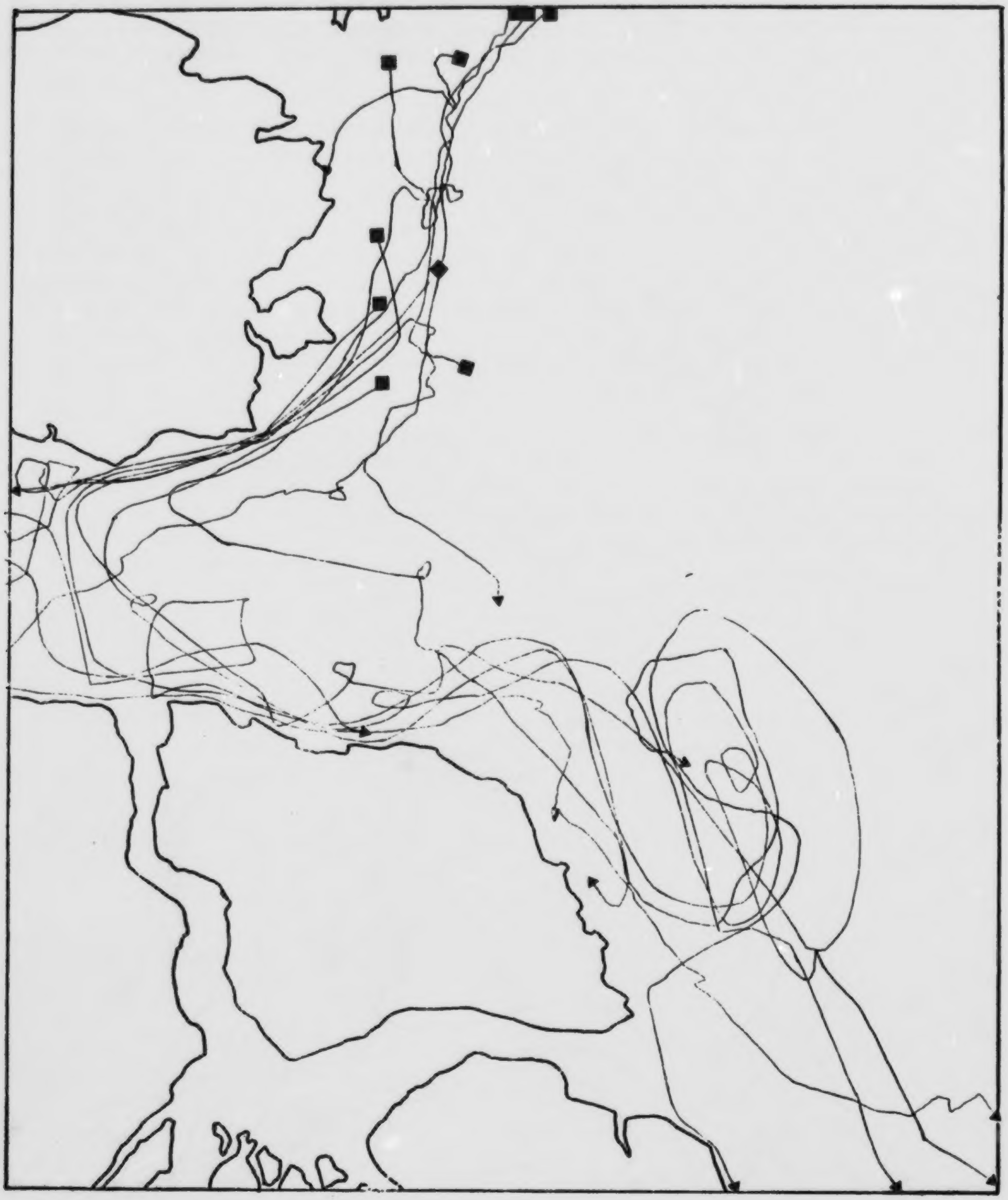

Figure 3b Trajectories of berg drifts from satellite-tracked data, 1979.

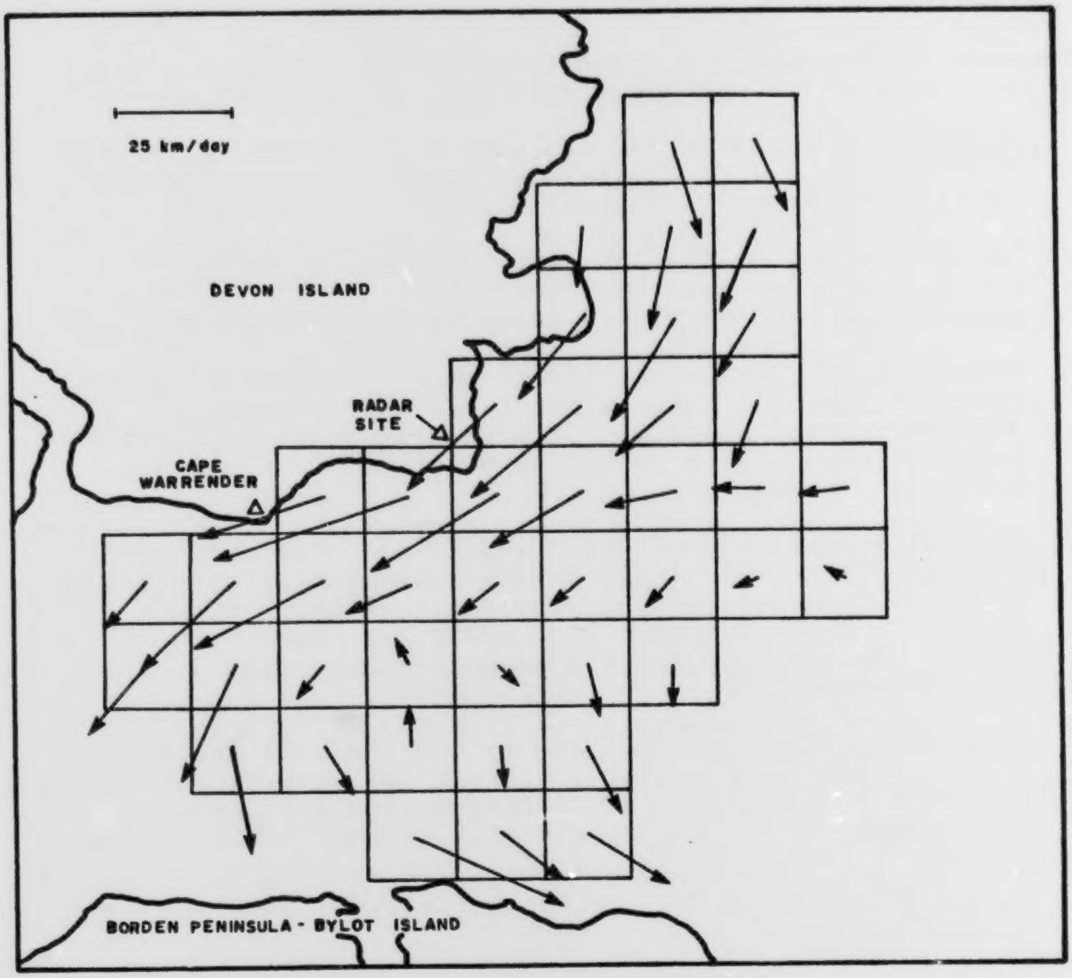
25 km/day
DEVON ISLAND
RADAR SITE
CAPE WARRENDER
BORDEN PENINSULA - BYLOT ISLAND

Figure 4 Average zonal velocity vectors, from 1978 Hope Monument radar-tracked berg data.

Acknowledgements

The present report and much of the original research upon which it was based was sponsored by Petro-Canada as part of the multi-disciplinary Eastern Arctic Marine Environmental Studies (EAMES) program, a joint industry-government undertaking.

Numerous individuals and organizations contributed to this review. Specific acknowledgements and appreciation are due:

Messrs. S.W. Speller, G. Glazier, B. Jonasson, J. Miller, J.M. Semples and Dr. J. Buckley and R. Wallace for their consistent support and assistance during the work.

Dr. H. Melling of the Institute of Ocean Sciences, Patricia Bay for numerous discussions and access to preliminary results of his Beaufort Sea studies.

Messrs. J.R. Birch, D.B. Fissel and D.D. Lemon of Arctic Sciences Ltd. for their general availability for discussions and sharing of insights on the relationship of sea-ice and icebergs to the oceanography of Lancaster Sound-Baffin Bay.

The scientific and technical staffs of other contractors to the Petro-Canada-EAMES program; particular note should be given to Messrs. R. Brown and R.J. Eley of NORCOR Engineering and Research Ltd. and B. de Lange Boom of Seakem Oceanography for providing documents and discussions.

Finally, to the technical and office staff of Arctic Sciences, with particular note to M. Wilson, D. Knight, S. Taylor, L. Miller, and J. Oberski for data and word-processing, drafting and editing contributions.

List of Figures

1.1	The principal area of interest in Lancaster Sound and northwest Baffin Bay	2
1.2	The greater Baffin Bay region	3
3.1.1 (a)	Ice conditions in Baffin Bay and the Arctic archipelago, April 19-24, 1955	16
3.1.1 (b)	Ice conditions in Baffin Bay and the Arctic archipelago, June 1-6, 1955	17
3.1.1 (c)	Ice conditions in Baffin Bay and the Arctic archipelago, June 13-18, 1955	18
3.1.1 (d)	Ice conditions in Baffin Bay and the Arctic archipelago, July 1-6, 1955	19
3.1.1 (e)	Ice conditions in Baffin Bay and the Arctic archipelago, August 1-6, 1955	20
3.1.1 (f)	Ice conditions in Baffin Bay and the Arctic archipelago, September 1-6, 1955	21
3.1.1 (g)	Ice conditions in Baffin Bay and the Arctic archipelago, October 7-12, 1955	22
3.1.1 (h)	Ice conditions in Baffin Bay and the Arctic archipelago, November 25-30, 1955	23
3.1.2	Mean monthly limits of 4/10 to 5/10 ice cover: (a) 1952-1960; (b) 1961-1970. Note differing rates of clearance.	24
3.1.3	NOAA satellite imagery, Eastern Parry Channel, April 16, 1975	26
3.1.4	NOAA satellite imagery Eastern Parry Channel, February 8, 1976	26
3.1.5	Approximate annual position of the stable landfast winter ice edge, 1961-1980	27
3.1.6	Ice freeze-up and breakup patterns, January-April, 1975 and 1976	30

3.1.7 Ice freeze-up and breakup patterns, June-November, 1975 and 1976 31

3.1.8 (a-m) Ice concentrations mapped at two-week intervals, June 18-December 3, 1975 32-45

3.1.9 (a-m) Ice concentrations mapped at two-week intervals, June 16-December 1, 1976 46-59

3.1.10 (a) NOAA satellite imagery, showing transient cross-channel lead formation, December 23, 1975 61

3.1.10 (b) NOAA satellite imagery, showing transient cross-channel lead formation, January 28, 1976 61

3.1.11 (a) NOAA satellite imagery, Eastern Parry Channel, January 20, 1978 64

3.1.11 (b) NOAA satellite imagery, Eastern Parry Channel, February 25, 1978 64

3.1.11 (c) NOAA satellite imagery, Eastern Parry Channel, March 10, 1978 64

3.1.11 (d) NOAA satellite imagery, Eastern Parry Channel, March 26, 1978 64

3.1.12 (a) NOAA satellite imagery, Eastern Parry Channel, November 28, 1978 66

3.1.12 (b) NOAA satellite imagery, Eastern Parry Channel, January 19, 1979 66

3.1.12 (c) NOAA satellite imagery, Eastern Parry Channel, February 1, 1979 66

3.2.1 Ice thickness vs. time-of-year at Resolute and Arctic Bay 75

3.2.2 Empirical growth curve of ice thickness in study area (Norcor, 1978) 75

3.2.3 Ice thicknesses measured May 2-10, 1970 from the S.S Manhattan 76

3.2.4 Location of AES ice-survey sites referred to in text 77

3.2.5	Landsat imagery, Sept. 17, 1977, showing an ice belt	92
3.2.6	Landsat imagery, June 9, 1974, showing an ice spiral	93
3.2.7 (a)	Landsat imagery, June 20, 1974, eastern Lancaster Sound	94
3.2.7 (b)	Landsat imagery, June 21, 1974, eastern Lancaster Sound	95
3.2.7 (c)	Landsat imagery, June 22, 1974, eastern Lancaster Sound	96
3.2.8	Percentage probabilities for exceeding the 3/10 and 8/10 levels of surface coverage by medium (> 100 m) floes - Site 520	97
3.2.9	Percentage probabilities for exceeding the 3/10 and 8/10 levels of surface coverage by medium floes - Site 502	98
3.2.10	Percentage probabilities for exceeding the 3/10 and 8/10 levels of surface coverage by medium floes - Site 598	99
3.3.1	Tracks of several ice beset vessels. Average net speeds are given for major segments of each track	101
3.3.2 (a)	Ice floe tracks from NOAA satellite imagery, March-May, 1976-1978	103
3.3.2 (b)	Ice floe drift tracks from NOAA satellite imagery, June-October, 1976-1978	104
3.3.2 (c)	Ice floe drift tracks from NOAA satellite imagery, November-February, 1976-1979	105
3.3.3 (a)	The division of Eastern Parry Channel into zones for the computation of average velocities	106
3.3.3 (b)	Average velocity distribution for ice floes in Eastern Parry Channel according to zone and time period	107

3.3.4 Vector averages of ice floe drift tracks from Landsat imagery, June-October, 1974-1979 110

3.3.5 Vector averages of ice floe drift tracks from Landsat imagery, March-May, 1974-1979 111

3.4.1. Major iceberg-producing glaciers of west Greenland 113

3.4.2 August, 1949 IIP iceberg counts in Baffin Bay and adjacent waterways 115

3.4.3 1969 IIP iceberg counts in Baffin Bay 116

3.4.4 (a) Iceberg densities, September and October, 1963-1969 118

3.4.4 (b) Iceberg densities, 1968-1970 119

3.4.4 (c) Iceberg densities, August-October, 1971 120

3.4.5 Initial positions of satellite-tracked bergs during the 1978 and 1979 seasons 121

3.4.6 (a) Distribution of icebergs, August 7, 1979 124

3.4.6 (b) Distribution of icebergs, August 24, 1979 125

3.4.7 Number of bergs observed over 6-hour periods from the Hope Monument radar station, 1978: (a) Week 1; (b) Weeks 2 and 3; (c) Weeks 4 and 5; (d) Weeks 6 and 7; (e) Weeks 8 and 9; (f) Weeks 10 and 11 126-128

3.4.8 Overall distribution of berg observations from Hope Monument radar station, 1978 129

3.4.9 Icebergs observed from Survey Vessel "Orion Arctic" August 7-September 24, 1973 131

3.4.10 Icebergs percentage recorded by area in ice patrols 132

3.4.11 Classification terminology of iceberg shapes, PC-EAMES studies: tabular, tilted tabular, pinnacled, blocky, domed, drydock 134

3.4.12 Percent exceedence iceberg waterline length 136

3.4.13 Percent exceedence iceberg height 136

3.4.14 Percent exceedence iceberg waterline area 137

3.4.15 Percent exceedence iceberg mass 137

3.4.16 Trajectories of berg drifts from satellite-tracked data, 1978 139

3.4.17 Trajectories of berg drifts from satellite-tracked data, 1979 (Fissel, 1980) 140

3.4.18 (a) Average velocity vectors, from 1978 satellite-tracked berg data 142

3.4.18 (b) Average velocity vectors, from 1979 satellite-tracked berg data 143

3.4.19 Average zonal velocity vectors, from 1978 Hope Monument radar-tracked berg data 144

3.4.20 Average velocity vectors, from 1978 and 1979 aerial observations 145

3.4.21 Regional pattern of near surface water flow, and zone scheme 147

3.4.22 Satellite-tracked berg trajectory: ID 1986, 8/9/79 to 24/11/79 149

3.4.23 Satellite-tracked berg trajectory: ID 1995, 9/9/79 to 4/10/79 150

3.4.24 Satellite-tracked berg trajectory: ID 1993, 8/9/79 to 16/9/79 151

3.4.25 Satellite-tracked berg trajectory: ID 1446, 3/9/78 to 27/9/78 152

3.4.26 Near-surface current data, summer 1979 (Dynamic height in cm., 300 db reference level) 154

3.4.27 (a) Radar-tracked berg trajectories - August 5-11, 1978 155

3.4.27 (b) Radar-tracked berg trajectories - September 2-8, 1978 156

3.4.28 Satellite-tracked berg trajectory: ID 1163, 28/8/78 to 22/12/78 157

3.4.29 Envelopes of the 1978 drifter tracks. Tracks were classified (Fissel, Lemon and Birch (1980)) according to two distinct modes. 158

3.4.30 Radar-tracked berg trajectories: September 12-18, 1978 159

3.4.31 Satellite-tracked berg trajectory: ID 1990, 12/8/79 to 7/9/79 160

3.4.32 Satellite-tracked berg trajectory: ID 1223, 1/9/78 to 13/10/78 161

3.4.33 (a) General iceberg drift pattern, July 13-27 163

3.4.33 (b) General iceberg drift pattern, July 28 - August 3 164

3.4.33 (c) General iceberg drift pattern, August 4-10 165

3.4.33 (d) General iceberg drift pattern, August 11-17 166

3.4.33 (e) General iceberg drift pattern, August 18-24 167

3.4.33 (f) General iceberg drift pattern, August 25-31 168

3.4.33 (g) General iceberg drift pattern, September 1-7 169

3.4.33 (h) General iceberg drift pattern, September 8-14 170

3.4.33 (i) General iceberg drift pattern, September 15-21 171

3.4.33 (j) General iceberg drift pattern, September 22-28 172

3.4.34 A general pattern of iceberg circulation deduced from radar-tracked iceberg data 173

3.4.35 Radar-tracked iceberg trajectory: ID 02A07, 1978 174

3.4.36 Average velocity vectors, from 1978 satellite-tracked berg data 176

3.4.37 Average velocity vectors, from 1979 satellite-tracked berg data 177

3.4.38 (a) Simplified trajectories of satellite-tracked bergs - 1978 drops 179

3.4.38 (b) Simplified trajectories of satellite-tracked bergs - 1978 drops 180

3.4.39 (a) Simplified trajectories of satellite-tracked bergs - 1979 drops 181

3.4.39 (b) Simplified trajectories of satellite-tracked bergs - 1979 drops 182

3.4.40 (a) Satellite-tracked berg trajectory: ID 1162, 6/7/79 to 11/10/79 183

3.4.40 (b) Satellite-tracked berg trajectory: ID 1162, 11/10/79 to 12/12/79 184

3.4.41 The 1978-1979 box-averaged daily iceberg drift vectors 185

3.4.42 Satellite-tracked berg trajectory: ID 1241, 18/9/78 to 9/10/78 186

3.4.43 Satellite-tracked berg trajectory: ID 1264, 21/9/78 to 2/10/78 187

3.4.44 Satellite-tracked berg trajectory: ID 1462, 6/7/79 to 7/12/79 188

List of Tables

3.1.1 Approximate timings for repeatable annual ice events over the period 1973-1979 68 - 71

3.2.1 Weekly cumulative probabilities for the occurrence of fractional old ice surface coverage - Site 520. Probabilities correspond to percentages of years in which the weekly old ice concentration equaled or fell below a given value (in tenths) 79

3.2.2 Weekly cumulative probabilities for the occurrence of fractional old ice surface coverage - Site 524 80

3.2.3 Weekly cumulative probabilities for the occurrence of fractional old ice surface overage - Site 540 81

3.2.4 Weekly cumulative probabilities for the occurrence of fractional old ice surface overage - Site 541 82

3.2.5 Weekly cumulative probabilities for the occurrence of fractional old ice surface overage - Site 557 83

3.2.6 Weekly cumulative probabilities for the occurrence of fractional old ice surface overage - Site 558 84

3.2.7 Weekly cumulative probabilities for the occurrence of fractional old ice surface overage - Site 569 85

3.2.8 Weekly cumulative probabilities for the occurrence of fractional old ice surface overage - Site 501 86

3.2.9 Weekly cumulative probabilities for the occurrence of fractional old ice surface overage - Site 502 87

3.2.10 Weekly cumulative probabilities for the occurrence of fractional old ice surface overage - Site 583 88

3.2.11 Weekly cumulative probabilities for the occurrence of fractional old ice surface overage - Site 598 89

3.3.1 A listing of the x (east) and y (north) components of the average summer (s) and non-summer (ns) velocities according to zone 108

1. Introduction

Ice has been the major physical obstacle in our efforts to inhabit, explore and exploit the Arctic regions. As a result, a combination of self interest and curiosity has motivated the accumulation of a centuries-old record of ice information. The present report begins with an overview of this process leading up to our present understanding of the Arctic sea-ice cover. This overview includes both a historical survey of relevant research and an outline of the 1978-1979 Petro-Canada-EAMES environmental programs in the Lancaster Sound-Baffin Bay Region. The later studies were most heavily concentrated in a roughly 45,000 km^2 region encompassing Lancaster Sound east of 83°W and areas of Baffin Bay off the eastern coasts of Devon and Bylot Islands. Considerable amounts of additional data were obtained in the adjoining central and western portions of Lancaster Sound and in Baffin Bay off the eastern coast of Baffin Island. The area of most intense study is outlined in Fig. 1-1 together with commonly used placenames in the Baffin Bay region. A similar reference map of greater Lancaster Sound is also included in Fig. 1-2.

Descriptions of the overall regional ice cover and the characteristics and movements of both sea-ice and bergs of terrestrial origin are given in subsequent sections of this report. In all cases, care is taken to provide measures of the year to year and shorter-term variabilities associated with all described results.

2. Research Overview

2.1 Historical

The earliest written accounts of man's contact with sea-ice arose out of the epic sea voyages which originated from the Norse settlements of Greenland and Iceland as well as from the British Isles (Mowat, 1960). The most significant explorations took place around 1000 A.D. led by Erik the Red, Bjarni Herjolfson and Thorfinn.Karlsefni. These parties covered much of Baffin Bay and its western shores as far south as Newfoundland. The success of their efforts was aided by their coincidence with the peak of the so-called "Little Climatic Optimum" which reportedly cleared the ice from Baffin Bay and, more arguably, from part of the Arctic Ocean.

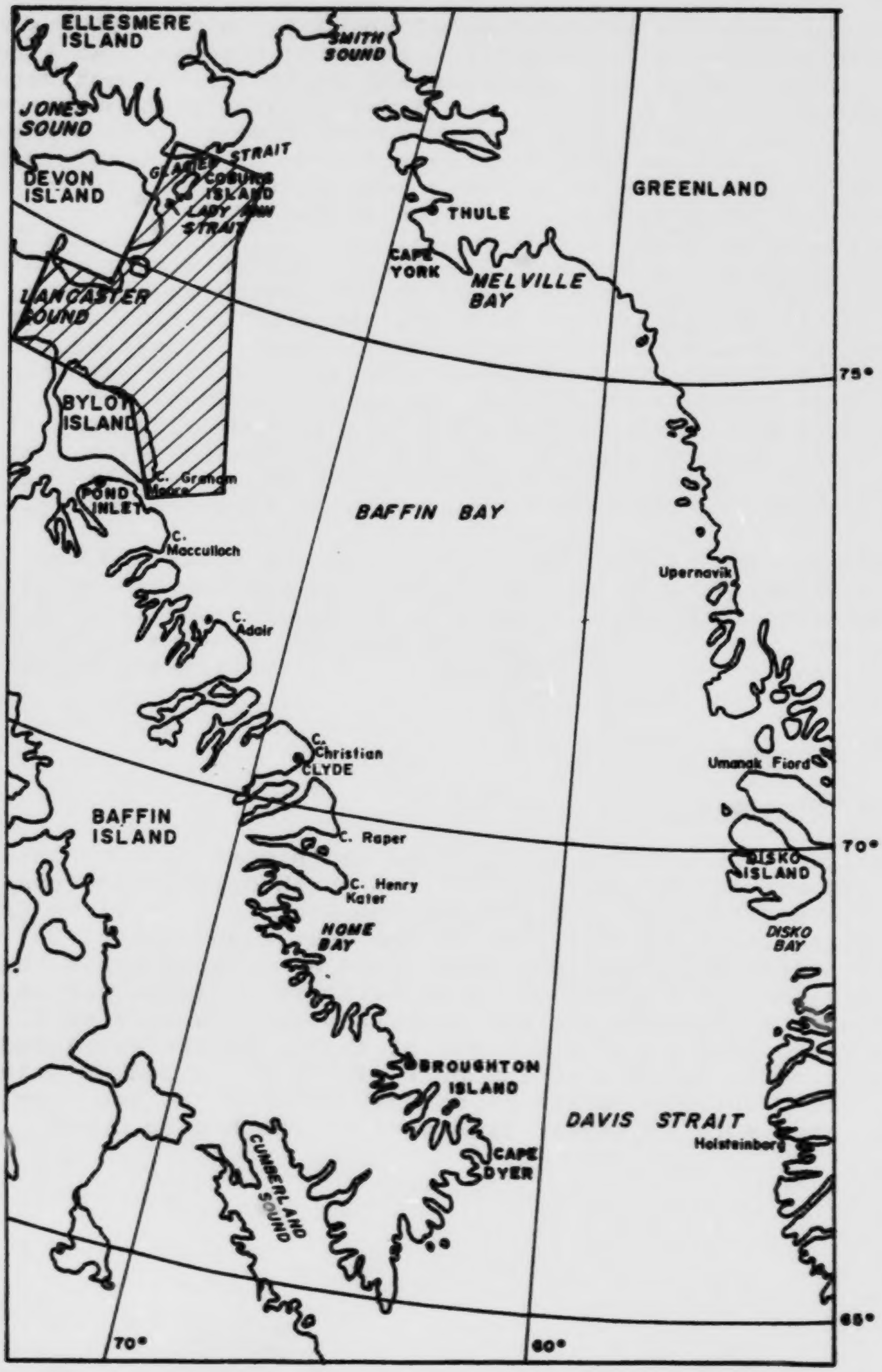
ELLESMERE ISLAND
SMITH SOUND
JONES SOUND
DEVON ISLAND
GLACIER STRAIT
COBURG ISLAND
LADY ANN STRAIT
GREENLAND
THULE
CAPE YORK
MELVILLE BAY
LANCASTER SOUND
75°
BYLOT ISLAND
C. Graham Moore
POND INLET
BAFFIN BAY
C. Macculloch
Upernavik
C. Adair
C. Christian
CLYDE
Umanak Fiord
BAFFIN ISLAND
C. Raper
70°
DISKO ISLAND
C. Henry Kater
HOME BAY
DISKO BAY
BROUGHTON ISLAND
DAVIS STRAIT
Holsteinborg
CAPE DYER
CUMBERLAND SOUND
65°
70°
60°

Figure 1.1: The principal area of interest in Lancaster Sound and northwest Baffin Bay

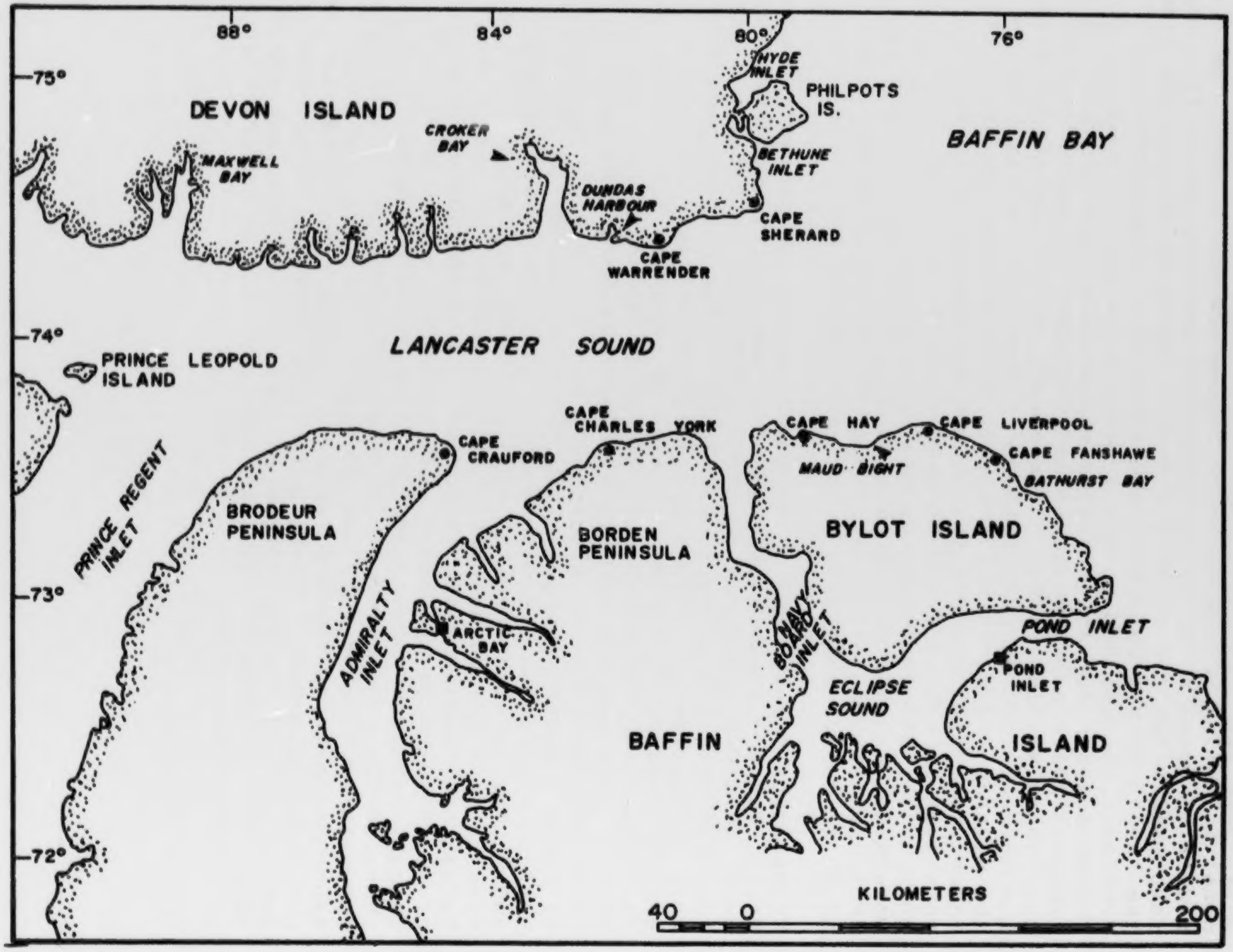
88°
84°
80°
76°
-75°
-74°
-73°
-72°
DEVON ISLAND
MAXWELL BAY
CROKER BAY
DUNDAS HARBOUR
CAPE WARRENDER
HYDE INLET
PHILPOTS IS.
BETHUNE INLET
CAPE SHERARD
BAFFIN BAY
LANCASTER SOUND
PRINCE LEOPOLD ISLAND
PRINCE REGENT INLET
BRODEUR PENINSULA
CAPE CRAUFORD
CAPE CHARLES YORK
BORDEN PENINSULA
ADMIRALTY INLET
ARCTIC BAY
CAPE HAY
MAUD BIGHT
CAPE LIVERPOOL
CAPE FANSHAWE
BATHURST BAY
BYLOT ISLAND
NAVY BOARD INLET
POND INLET
POND INLET
ECLIPSE SOUND
BAFFIN
ISLAND
KILOMETERS
40
0
200

Figure 1.2: The greater Baffin Bay region

Conditions more suitable for ice studies, if not for sea travel, attended upon the next major period of exploration running from approximately 1500 A.D. to 1800 A.D. This era overlapped the "Little Ice Age" (1650 - 1850) in which a general cooling of the northern hemisphere was noted. The resulting worsened ice conditions were perhaps partially responsible for the later decline in exploration activity from the levels of the late 16th and early 17th centuries when Frobisher, Davis, Hudson and Bylot all led major expeditions. The motivation for these latter explorations was provided by the need for a short route to Asia and the desire to expand the Hudson Bay fur trade. As a result, ice observations still tended to be of the practical sort, leading, for example, to the planning of routes and schedules which took advantage of the characteristic low early-summer ice densities of the southwest Greenland coast and avoided the congested regions to the east of Baffin Island. Occasional major contributions were made, such as Robert Bylot's discovery, in 1616, of the "North Water", a vast area of open-water and thin ice at the northern end of Baffin Bay.

Nevertheless, a systematic approach to the ice properties of Baffin Bay and areas to its west was not really forthcoming until 1818, when the end of the Napoleonic Wars initiated the "modern" era of exploration. Again, in the earlier part of this period, major efforts were devoted to geographical exploration, primarily of the maze of channels interior to the Canadian Arctic Archipelago. Lancaster Sound, after its re-discovery by Ross in 1818 and explorations by Parry in 1819-1820, soon was realized to be the likely eastern entrance of the Northwest Passage. From the tribulations of the various expeditions, the very broad outlines of ice properties and movements within the Archipelago began to emerge. Distinctions were drawn between those bodies such as McClintock Channel which tended to fill with massive jumbles of multi-year ice and those such as Lancaster Sound where lengthy ice-free summer conditions could be expected. Characteristic break-up and freeze-up dates were gradually accumulated in ship logs and expedition journals. Records kept on board ice-beset vessels were of particular use in providing measures of sustained ice drift rates. For many years, the positions reported in these drifts provided the only information available on the directions and magnitudes of the ice movements.

Nevertheless, it was difficult to derive a detailed or even descriptive understanding of the spatially and time-varying ice packs simply on the basis of the observations of men often functioning at the edge of survival. The necessary foundation for such understanding began to be established in the latter quarter of the 19th century when major scientific expeditions were sent forth by Denmark, Sweden and the United States. Of these, the Swedish "Sofia" expedition of 1883 (Hamburg, 1884) and the Danish "Fylla" voyages of 1884, 1886 and 1887 (Wandel, 1891) were most notable in that they established some major elements of the oceanography of Baffin Bay, Davis Strait and the southern approaches to Greenland. The description and identification of the source of the West Greenland current and the southward surface flow along the Baffin Island coast were essential first steps in deducing the pattern of ice movement in Baffin Bay. Inadvertently or, in some cases, deliberately ice-beset vessels continued to be important sources of data, particularly when the circumstances involved scientific field parties. Thus the works of Wayprecht (1879) and Petterson (1883) based upon measurements made during the drifts of the "Tegetthof" and the "Vega", respectively, provided early compilations of the physical properties of sea-ice. The most famous of the Arctic ice drift voyages was led by Nansen in the "Fram" during the 1893 - 1896 Norwegian North Polar Expedition. Among other valuable data, Nansen's careful recording of simultaneous drift and wind velocities established the tendency of ice to move to the right of the wind and, as such, led to major developments in boundary layer theory by Ekman (1902) and numerous other workers.

Data from the Danish "Ingolf" expeditions in 1895 and 1896 revealed the low temperature of the Labrador Sea relative to the waters to its east. This fact was essential in the understanding of iceberg survival rates at sub-Arctic latitudes. The iceberg drift problem was considered, on a quantitative basis, for the first time, by Mecking (1907) using data gathered by the increasing number of ships travelling in northern waters. The resulting record of iceberg counts for the period 1880 to 1899 was later shown (Smith, 1931) to have greatly overestimated the iceberg numbers due to Mecking's failure to account for multiple sightings of the same iceberg. Nevertheless, this work was significant in that it placed a reliable upper limit (several thousand) on the number of icebergs which appeared south of 48°N latitude.

The growing interest in icebergs also was evident in the first attempt by Steenstrup (1893) to relate the under-and-above-water berg dimensions. His results indicated (maximum) height to (maximum) draft ratios ranging from 1:7.4 to 1:8.2 or approximately equal to that expected of the freeboard and submerged ice masses. Other measurements by Rodman (1890), Krummel (1907) and Dawson (1907)indicated a slightly larger (1:5 to 1:6) median ratio and found unambiguous evidence for the occurrence of large, approximately 1:1 ratios.

The field work of the early twentieth century tended to build up the record of sea-ice observations and began to close major gaps in the oceanographic picture. Following the Danish "Tjalfe" expedition in West Greenland in 1908, Nielsen (1909, 1928) deduced major features of the eastern and southern Baffin Bay circulation including the fact that the underlying warm Atlantic water has no direct effect on the melting of the characteristic shallow-draft floe ice, since the surface layer temperatures of David Strait remain negative throughout the year. Other data of note were obtained by Kolchak (1928) and during Amundsen's (1918-1925) attempts to repeat the voyage of the Fram. The data obtained in the latter "Maud" expedition formed the basis for Malmgren's (1927) treatise on sea-ice properties and for Sverdrup's (1928, 1929) considerations of ice, wind and current relationships.

The sinking of the "Titanic" in a 1912 iceberg collision touched off major efforts in the study of sea-ice and icebergs. In particular, the sea-faring nations of the world were mobilized to establish the International Ice Patrol (IIP). This organization, under the administration of the U.S. Coast Guard, had as one of its tasks the gathering of sea-ice and iceberg observation data. By evaluating and correlating ship reports with the observations made by its own vessels, the IIP began to put iceberg studies on a quantitative basis. Initially, of course, efforts were directed toward locating and enumerating iceberg concentrations, drift rates, etc. in order to provide the IIP Grand Banks and North Atlantic shipping advisories. This responsibility eventually led to the development of the Coast Guard's present on-going program of oceanographic, meteorological and other environmental monitoring. Data-taking, initially, was carried out by cutters on surveillance duty. Later, specific expeditions were mounted on board the "Marion" and "General Greene" to obtain the data eventually used to derive much of our modern understanding of southern Baffin Bay, Davis Strait and more southern waters. A summation of the resulting sea-ice and iceberg data was provided by Smith (1931). This classic work put the monthly iceberg censuses on a more accurate footing, provided detailed experimental information on the properties of sea-ice and icebergs, and in general set up the groundwork for an iceberg condition forecast system based on an oceanographic and meteorological data-gathering program. A series of regular iceberg-census cruises in Baffin Bay and Davis Strait was begun in 1940 by the USCGC "Northland". However, the intervention of war prevented its continuation as a regular part of IIP activities until 1946 when PBY-5A Catalina and B-29 Super-Fortress aircraft were used in such studies. Data in the Canadian Zone at this time were obtained using American ice observers on-board R.C.A.F. aircraft. Particular attention to sea-ice, as opposed to iceberg monitoring, was forthcoming when such information was required by supply convoys enroute to the Thule, Greenland U.S. Air Force base. The resulting observing programme of the U.S. Naval Hydrographic Office began in 1952 with its surveys of ice concentration and character first appearing in published form in the following year (U.S.N. Hydrographic Office 1953-1959, 1962-1965).

Responsibility for ice reconnaissance in the Canadian Sector was assumed in 1957 by the Basic Weather Division of the Canadian Meteorological Branch with its reports gradually evolving into the current seasonal reviews, prognoses and weekly mappings of the distribution of ice concentrations, ages, floe sizes, etc. produced by the Ice Forecasting Centre of the Atmospheric Environment Service. Later statistical summaries of these data were compiled by Markham (1975, 1977) for areas of specific interest in the Beaufort Sea and Lancaster Sound-Baffin Bay. Additional Canadian efforts in areas more removed from the shipping lanes were begun in 1961 under the auspices of the Polar Continental Shelf Project of the Department of Energy, Mines and Resources. In addition to the annual summaries of such data (Black, 1961-1963), (Seifert, 1967-1968) this programme has also produced detailed mappings of conditions at approximately two-week intervals throughout most of the Arctic Archipelago in an atlas format for the 1961 - 1974 period (Lindsay 1976, 1977). This representation was, in many respects, more useful than those utilized in previous summary documents (Swithinbank, 1960, and Deutches Hydrographisches Institut, 1950).

The availability of detailed ice data stimulated several theoretical studies directed toward the development of methodologies of sea-ice forecasting (Brown, 1954) (Corton,

1954) (Callaway, 1954). With the aid of a large mass of data on ice growth and decay (Bilello, 1960, 1964), these early efforts evolved into later more detailed considerations of the thermodynamics of the sea-ice cover (Walmsley, 1966) (Vowinckel and Orvig, 1962) and (Maykut and Untersteiner, 1971). The latter studies formed much of the basis for later evaluations of disaster scenarios such as the possible removal of the polar ice cover by oil contamination (Walker, 1975) and long-term climatic changes (Kukla, 1978).

Aside from the initiation of regular sea-ice surveys and coastal ice thickness and air temperature monitoring, the 1950's and 1960's were still characterized by a relatively low level of actual "on the ice" study. The first attempts were made during this period to introduce the new techniques of: airborne radiation thermometry (IIP #52, 1964); radar and passive microwaves (IIP #52, 1967); and acoustical noise monitoring (Milne, 1963). With the exception of the latter work, most of these techniques have been heavily utilized in later satellite, air and land-based remote sensing studies. Acoustical techniques have as yet to be fully implemented in the non-military study of ice, although Milne (1970) has demonstrated the sensitivity of such measurements to the magnitudes of winter ice motion in the Arctic Archipelago.

Much of the work done in the later 1960's and in the very early part of the following decade was concerned with gleaning major features of the ice-cover behaviour from aerial overflights and primitive satellite imagery. Thus, Dunbar (1969) managed to deduce a value for the surface area of the North Water (1.66×10^5 km^2) and the timing of the maximum (March) and minimum (mid-September) extents of ice coverage in Baffin Bay. Aber and Vowinckel (1972), on the other hand, devised the Minimum Brightness Technique to follow the seasonal changes in the extent of this polynya on the basis of low resolution often cloud obscured, satellite imagery. Later, developments in satellite-tracked ice drifters were foreshadowed by a 1970 experiment in which radio beacons placed on the moving ice cover of Viscount Melville Sound were periodically located by tracking aircraft (Verral, Ganton and Milne, 1974).

Other more traditional measurements were also made in the ice surface during this period, most notably on the 1970 second voyage of the "Manhattan" (FENCO, 1974). Ice thicknesses were measured along the vessel's track through western Baffin Bay and eastern Lancaster Sound. Basic data on the pressure exerted by the ice on the ship's hull were also obtained and related in quantitative fashion to wind and coastline configurations (Bradford, 1971). More generalized experimental work was also being carried out to establish the microclimate immediately below a growing ice sheet (Lake and Lewis, 1970; Lewis and Walker, 1970; and Lake and Lewis, 1972). These studies tended to show that the structure of the isothermal water boundary layer, which controls critical energy exchange rates, depends upon a large number of factors including local run-off rate, advection and the conditions experienced during the previous summer. Results tended to call into question deductions of vertical energy flux based upon measurements at depths 1 metre or more below the lower ice surface.

Iceberg studies in the early seventies (Feazel and Kollmeyer, 1972, and Løken et al., 1972) were heavily concerned with establishing the origins of the bergs found in southern waters and in particular in determining the relative ratios of bergs arising from West Greenland, East Greenland and North American sources respectively. In the work of Løken et al (1972), magnitudes were given for the failure stresses in calving ice tongues or ramps and a well-known iceberg groundingyard staging area near Clyde on the east coast of Baffin Island was found to be associated with a submarine moraine which extends to the edge of the continental shelf. Analyses of southern iceberg counts (IIP, 1971)showed possible but inclusive correlations with factors such as the Belle Isle-Ivigtut air pressure difference and the Upernavik summer air temperature which were suspected to control the rate of southward berg movements and the supply of new bergs, respectively. Another approach to the iceberg density problem emerged in the 1971 Sea Ice Conference at Rejkjavik, Iceland where it was suggested (Dunbar, 1972) (see also Bradley, 1973) that the warming trend of the 1920 and 1930 decades had ended, and subsequent surveys indicated substantial and continued worsening of ice conditions in Baffin Bay and Davis Strait.Thus, for example, while "total" ice clearance was achieved in September in nine of the years 1950 - 1959, similar clearance occurred but once in the following decade. Dunbar identified 1963 as an approximate date for a shift to heavier conditions. At the same time, recognition was also given (Løken et al., 1971) to the interplay of sea-ice and iceberg effects, with Wittmann (1971) suggesting that the near simultaneous worsening of ice conditions and decreasing berg numbers may be evidence of an important sea-ice/berg interaction and control mechanism.

The basic physics of iceberg motion was explored in August, 1972 as part of an extended experimental program off Saglek Bay, Labrador (Allen, 1972). In this effort, which also included field work during the 1973 and 1974 seasons, berg-tracking was carried out by shore-based radar in conjunction with oceanographic and meteorological data = gathering including salinity and temperature profiling, surface temperature surveys (using a precision radiation thermometer) and current measurements from moored meters and tracked drogued drifters. Berg dimensions were recorded by stereo photography and sonar underwater profiling. The results of this study have just recently become available to the public. At nearly the same time, the U.S. Coast Guard and the International Ice Patrol began studies of the feasibility of berg trajectory prediction using air-deployed, expendable probes which, through the time-delayed release of two floats, offered measurement of the instantaneous surface current (Welsh and Phillips, 1973), (Broida and Richardson, 1972). Aside from the method's neglect of important sub-surface currents, deployment and interpretation difficulties were encountered which precluded any immediate improvement in predictive capabilities.

With the increasing recognition of the resource potential of Baffin Bay and Davis Strait, the Arctic Petroleum Operators Association (APOA) sponsored the 1972 summer cruise of the N.V. "Hans Egede" as part of a general regional environmental survey. Detailed shape and dimension data were obtained for some 350 icebergs as part of a rough mapping of the existing ice conditions (APOA, 1973). While the overall capability for ice mapping and berg tracking and counting was limited by the range of shipboard observations, the obtained data have since served as a useful basis of comparison for the results of more systematic studies.

This program was shortly followed, in 1973 and 1974, by the more localized studies of north Baffin Bay and Lancaster Sound, carried out from the M.V. "Orion Arctic" in connection with the hydrocarbon exploration plans of Norlands Petroleums Ltd. In the 1974 cruise, estimates were made of iceberg numbers and sizes, particularly in the eastern Lancaster Sound area of interest. In spite of visibility limitations, iceberg densities were inferred to be roughly four times larger than the average value of roughly one berg per 400 km^2 (26 bergs/ 10^3 mi^2) deduced from AES berg count data over the 1958 to 1976 period.

At nearly the same time (1973 - 1974), new developments in satellite and remote-sensing technology were beginning to yield detailed information on the large-scale behaviour of Arctic sea-ice. Imagery of nominal 80 m and 800 m resolution were available from the Landsat and NOAA = Tiros satellites respectively and the 8-11.6 micron band of the latter satellites gave, for the first time, a view of the ice during the winter dark period. Imagery reviews specific to the Beaufort Sea, the Central Arctic Archipelago and eastern Parry Channel were carried out by Marko (1975, 1977 and 1978) and an overall Arctic survey was provided by Arsenault et al. (1976). In the eastern Parry Channel data (Marko, 1978), quantitative estimates were available for the first time on both summer and winter ice drift velocities, ice-flow tendencies and the existence of prominent features such as a fall-early winter region of thin ice paralleling the northern edge of the Channel. Even more importantly, a cross-channel boundary was also noted separating the immobile, essentially landfast ice of the west from an eastern zone of moving ice. This boundary was observed to occur at a limited number of locations in Lancaster Sound and Barrow Strait, resembling to some extent the ice boundary at the northern edge of the North Water polynya. The latter feature was extensively studied, not only in the previously cited works of Dunbar (1969) and Aber & Vowinckel (1972), but also through the efforts of Muller and his co-workers in the North Water Project (1975).

Over the 1971 to 1977 period, a large international ice study, the Arctic Ice Dynamics Joint Experiment (AIDJEX), worked toward the development of models of sea-ice motions on scales down to tens of kilometres. In spite of its heavy theoretical and computational components, thus far it has been the program's advances in data-gathering instrumentation which have had the largest impact upon ice studies in the eastern Arctic. Of particular significance was the development of accurate positioning and data relay capabilities using drifting and floating "platforms", together with the Nimbus and other satellite communication systems. Such platforms, in the form of air-droppable (ADRAMS) buoys were utilized in a detailed 1978 study of the Beaufort Sea ice cover (Melling, to be published). Likewise, other new tools, such as real aperture side-looking radar (SLAR), synthetic aperture radar (SAR), and laser profilometers, received heavy application during the AIDJEX program. Together with the more conventional non-imaging radar utilized in land-based studies of Byam Martin Channel (de Lange Boom and Davidson, 1977) and Barrow Strait (MacNeill, and de Lange Boom, and Ramsden, 1978), these instruments now allow all-weather ice-monitoring and study programs and have been applied to a number of problems of continuing interest such as the North Water (Dunbar, 1979) and in the Petro-Canada-EAMES environmental studies of the Lancaster Sound-Baffin Bay region.

To date, no quantitative model has been developed for the dynamics of the ice cover of the Lancaster Sound-Baffin Bay region. This situation is, of course, to be expected in view of the extremely limited underlying data base. It also, however, reflects large differences in the area characteristics relative to the Arctic Ocean where major AIDJEX modelling efforts have thus far been concentrated. In the latter instance, attention was directed at establishing the dynamics of the deep-water, offshore portion of a pack composed primarily of multi-year ice. The effect of adjacent land masses were represented through the imposition of simplified boundary conditions. This procedure is clearly inappropriate in Lancaster Sound where the channel widths are barely comparable to the spacings of the AIDJEX modelling grids. Likewise, the predominantly first-year character of the eastern region ice and the normally higher surface current magnitudes limit the applicability of Arctic Ocean methodology. An alternative approach, specifically aimed at ice flow in narrow channels was suggested by Sodhi (1977) relevant to ice edge formation in Amundsen Gulf using analogies to soil mechanical and grain flow problems. To date, neither this approach nor a plastic collapsible model (Pritchard et al., 1974) have been applied to the Lancaster Sound-Barrow Strait ice edges. Such applications would, no doubt, be difficult at the present time, in view of the primitive data bases on ice thickness, year-old and multi-year ice concentrations, ridge densities, etc. Estimates of these parameters were given in a 1978 study (NORCOR, 1978) on the basis of overflight and satellite data and, as well, from a large number of ice thickness measurements taken in the Sverdrup Basin. Using simple assumptions on ice growth and ablation rates, rates and routes of ice export, etc., the major parameters were estimated in areas along potential transport routes. The ice thickness results reported for Lancaster Sound are particularly suspect in view of: 1)the area's great distance from the assumed Sverdrup Basin source of multi-year ice; 2) the neglect of multi-year ice from eastern Arctic sources; and 3) the neglect of the regional year-to-year variability associated with the different annual positions of the winter landfast ice boundary.

Considerable progress has recently been achieved in establishing relationships between observed ice conditions and the accompanying atmospheric pressure distributions. Of particular note have been the correlations found (Crane, 1979) between the ice advance/retreat timings in southwestern Davis Strait and the direction of airflow in terms of identified synoptic patterns in the 700 mb pressure data. Consideration of a larger geographical region by Jacobs et al. (1979) reported differences in the trends of east and west Baffin Bay respectively, and demonstrated that in both areas, the air temperatures of the summer and previous winter do not correlate with summer ice severity indices as observed in more enclosed areas such as Foxe Basin where in situ melting occurs. Instead, the over-riding importance of the Baffin Bay wind and current systems was established. Likewise, as part of an overall study of landfast ice Jacobs, et al., (1975) and Barry et al., (1978) demonstrated the dependence of the breakup of such ice upon wind and weather patterns of only a few days' duration, suggesting the limited utility of ice condition analysis in terms of monthly average winds. A more general and extensive approach considering the entire north polar region has also recently been put forth by Walsh and Johnson (1979) as part of a continuing study of long-term ice trends.

2.2 The Petro-Canada-EAMES Program

In 1978 and 1979, Petro-Canada initiated its Lancaster Sound - Baffin Bay research programs which attempted to: a) evaluate the likely impact of the ice environment upon proposed hydrocarbon explorations, and b) characterize the role of ice in determining the effects of a major oil spillage. In the absence of previous detailed area studies, bergs were assumed to be the principal threatening agent in the first respect, while sea-ice, on the other hand, was of significance primarily as a determinant of the extent and form of the resultant oil release.

As a result, initial assessment programs were heavily biased toward berg counting and tracking, utilizing land-based radar stations at: Hope Monument on Devon Island, and Cape Fanshawe on Bylot Island (see Figure 1-1); daily counting and tracking flights; and the placement of twenty satellite- tracked platforms on selected bergs. Underwater side-scan sonar profiling of 35 bergs was also carried out as a function of general berg type and above-water dimensions. Results from all programs were supplemented by relevant data available from the near-simultaneous oceanographic and meteorological programs.

Sea-ice, on the other hand, represented a much less tractable object for study in view of both its ubiquity and its enormous year-to-year variations in distribution and amount. Much of the data on its character and position had to be obtained from the historical AES compilations and from recent satellite imagery. The latter were of considerable use in illustrating the variety of ice configurations which could accompany offshore operations, acting both as an accident-inducing threat and as an obstacle to clean-up. The imagery also provided the only moderately extensive source of direct ice velocity information suitable for devising pollutant transport scenarios.

Shoreline contamination probabilities were addressed through video-taping overflights, field surveys and satellite imagery of the land-water boundary. Particular emphasis was laid upon estimating the concentration of shoreline ice. Such ice, in most cases, offers a measure of protection against shoreline contamination. On the other hand, similar ice concentrations could, in other instances, serve as intermediate sources of pollution by their ability to trap and hold oil in proximity to shorelines.

The results of these studies have been compiled in separate data and analysis reports. Their highlights and principal conclusions are incorporated in the environmental summaries of Section 3.

3. The Ice Environment

3.1 Ice Cover Characteristics

As indicated above, sixteen years of AES ice parameter data have now been digitized and processed as part of the Petro-Canada-EAMES programs (Miller, 1980). The portion of these results dealing with the fractional coverage of the sea surface can be usefully represented in terms of "best year in five", "average", and "worst year in five" configurations based respectively upon the 20, 50 and 80 percentile values of the ice concentrations recorded at weekly intervals at 135 individual sites in the AES observation area. These configurations have been plotted in Appendix 1 on a twice-monthly basis over the May to October period. Review of the figures indicates that in all three cases ("best", "average" and "worst") clearing proceeds with a south-southwestward extension of the North Water region of low ice concentration. There is roughly a one-month difference between the comparable stages of the "best" and "worst" case processes. Even larger spreads are evident in the corresponding clearing rates of Lancaster Sound.

These changes in local ice concentration may be related more clearly to events in the greater Eastern Arctic (by reference to larger-scale mappings such as those reproduced in Figure 3.1-1) corresponding to the rather typical evolution of the 1955 ice cover. The strong clearing in the northwest and southeast is evident as well as the tendency for ice to linger in a north-south strip, extending from Melville Bay to the Baffin Island coastline between Cape Adair and Cumberland Sound. The last major remnants of the summer ice pack are usually found in the vicinity of Cape Dyer and Home Bay, where in winter an extensive landfast ice zone reaches out some 70 km from shore to roughly the 180 depth contour (Jacobs et al., 1975). Accumulations of new ice appear first in these slow-clearing areas with, again, low ice concentrations remaining in effect longest in the extreme northwest of Baffin Bay and along the south-western Greenland coast.

The differing rates of clearance of the 1950 and 1960 decades were noted by Dunbar (1972) (Figure 3.1-3) who also found indications of a trend toward worsening ice conditions in the September data which indicated regular total clearances during the 1950's, but a similarly strong non-clearance record during the following decade. A review of the 1970 - 1979 data, however, indicated that measurable concentrations of ice were present throughout September in only three of the ten years studied, suggesting at least a strong fluctuation in the worsening trend postulated by Dunbar.

In the region of immediate interest to this review, note should again be made of the strong contrast between the "best" and "worst" configurations of the ice cover in Lancaster Sound and in the adjoining portion of Baffin Bay. In the first instance, Lancaster Sound is nearly ice-free to the 90° line of west longitude over most of the summer period, beginning in early June. In the "worst year in five" configuration, on the other hand, even by early July clearing has extended westward only to 82°W, reaching 90°W in the third week of August. The two extreme seasons thus respectively correspond to an ice-free or an ice-covered Lancaster Sound over the June-to-mid-August period. The two circumstances correspond

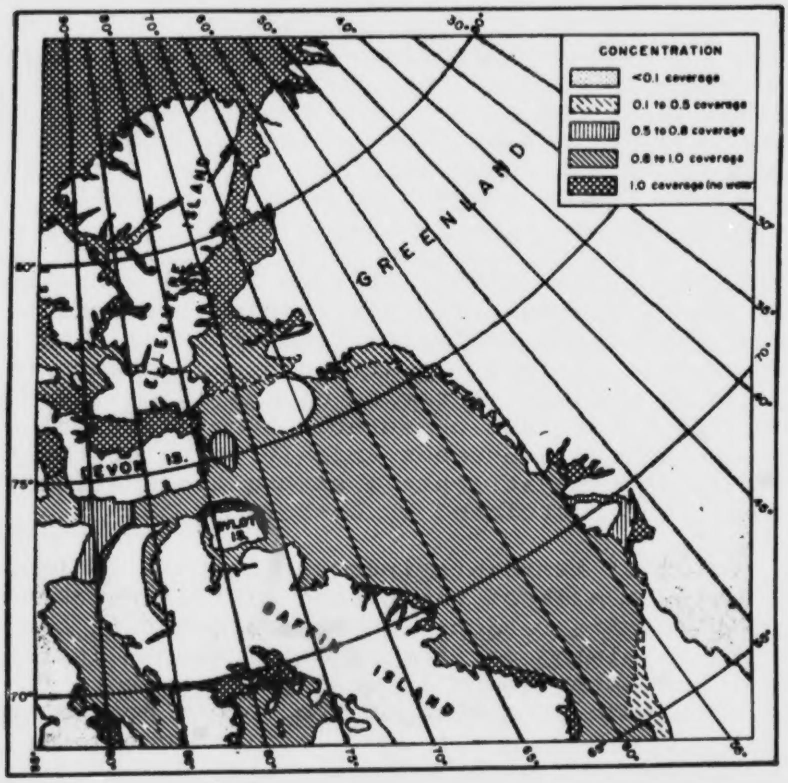
CONCENTRATION
<0.1 coverage
0.1 to 0.5 coverage
0.5 to 0.8 coverage
0.8 to 1.0 coverage
1.0 coverage (no water
GREENLAND
ELLESMERE ISLAND
DEVON IS.
BYLOT IS.
BAFFIN ISLAND
80°
75°
70°

Figure 3.1.1(a) Ice conditions in Baffin Bay and the Arctic archipelago, April 19-24, 1955

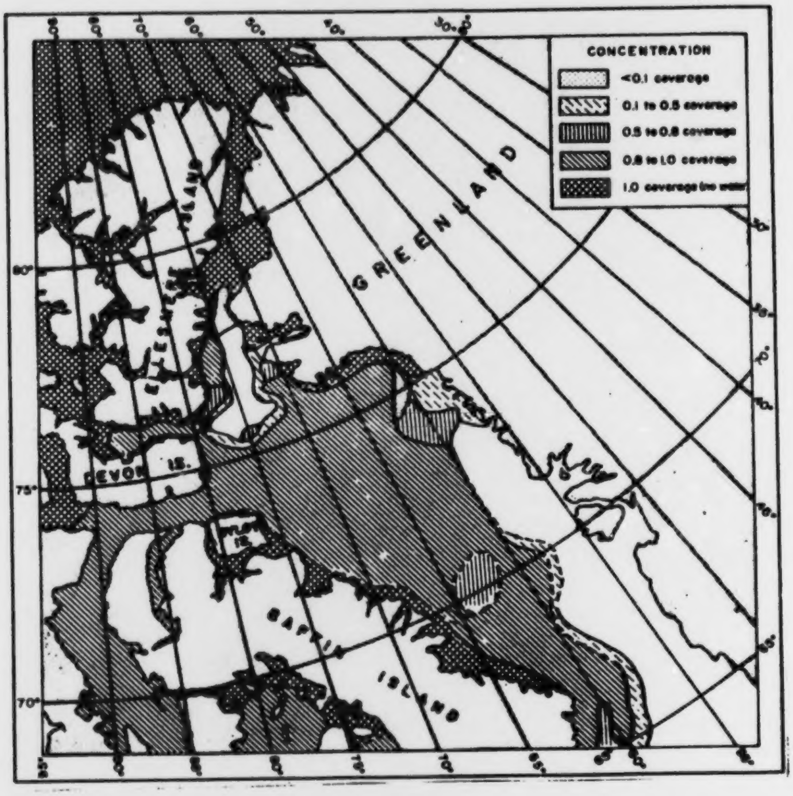
CONCENTRATION
<0.1 coverage
0.1 to 0.5 coverage
0.5 to 0.8 coverage
0.8 to 1.0 coverage
1.0 coverage (no water)
GREENLAND
ELLESMERE ISLAND
DEVON IS.
BAFFIN ISLAND
80°
75°
70°
30°
40°
50°
60°
70°
80°
90°

Figure 3.1.1(b) Ice conditions in Baffin Bay and the Arctic archipelago, June 1-6, 1955

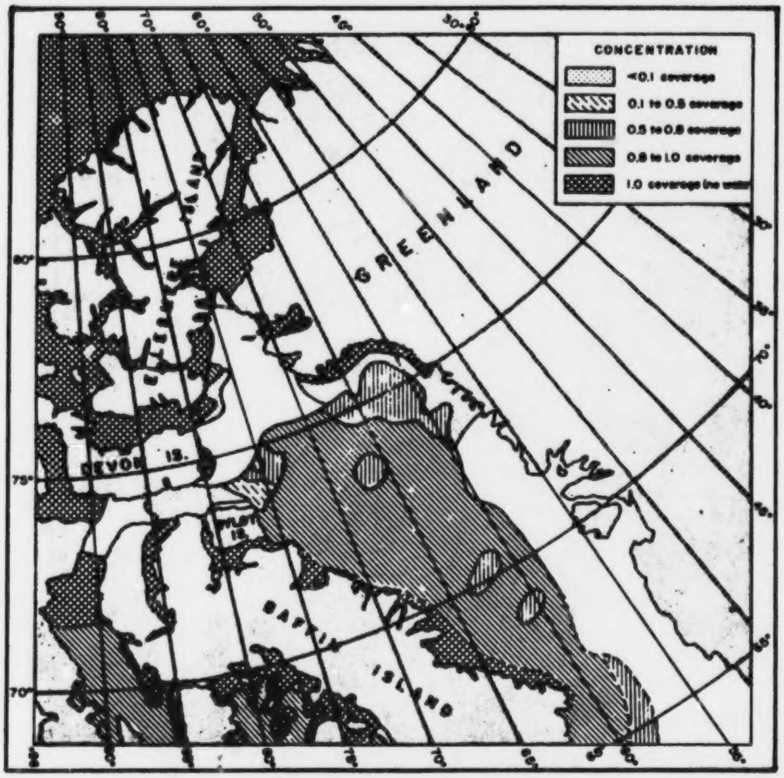
CONCENTRATION
<0.1 coverage
0.1 to 0.5 coverage
0.5 to 0.8 coverage
0.8 to 1.0 coverage
1.0 coverage (no
GREENLAND
DEVON IS.
BYLOT IS.
BAFFIN ISLAND
30°
40°
50°
60°
70°
80°
80°
75°
70°

Figure 3.1.1(c) Ice conditions in Baffin Bay and the Arctic archipelago, June 13-18, 1955

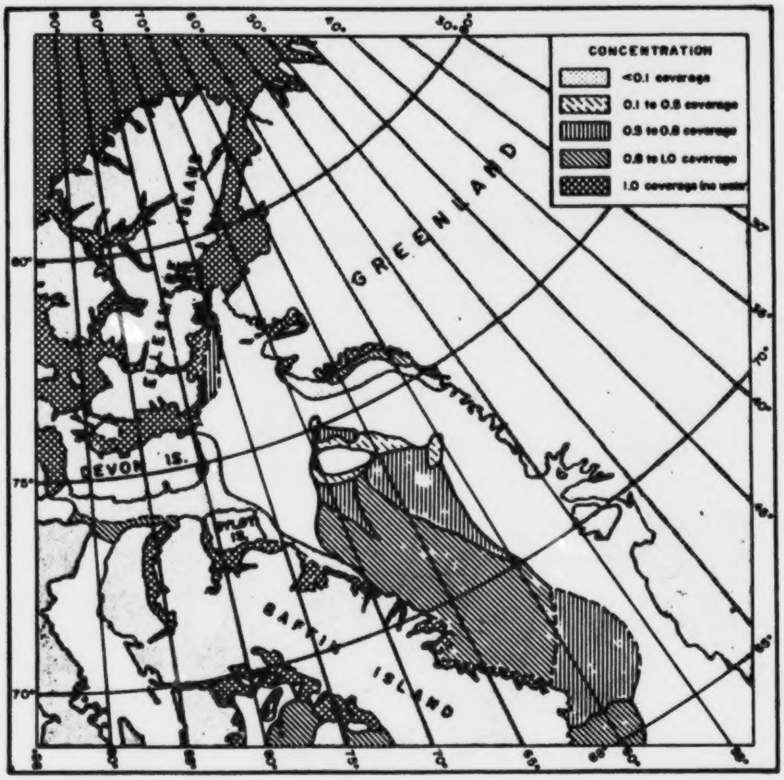
CONCENTRATION
<0.1 coverage
0.1 to 0.5 coverage
0.5 to 0.8 coverage
0.8 to 1.0 coverage
1.0 coverage (no wate
GREENLAND
DEVON IS.
BYLOT IS.
BAFFIN ISLAND
ELLESMERE ISLAND
80°
75°
70°

Figure 3.1.1(d) Ice conditions in Baffin Bay and the Arctic archipelago, July 1-6, 1955

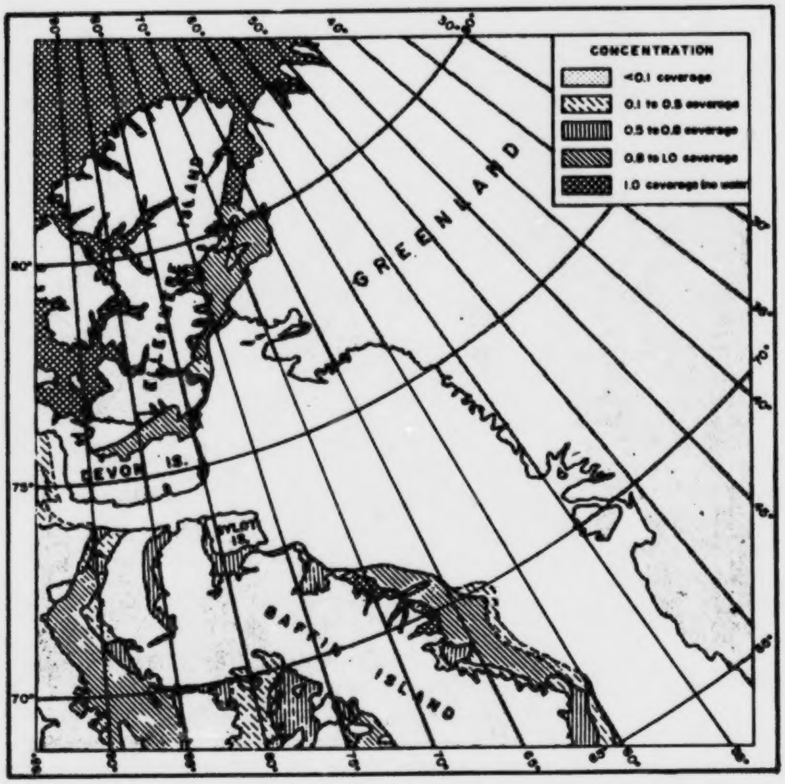
CONCENTRATION
<0.1 coverage
0.1 to 0.5 coverage
0.5 to 0.8 coverage
0.8 to 1.0 coverage
1.0 coverage (no
GREENLAND
DEVON IS.
BYLOT IS.
BAFFIN ISLAND
80°
75°
70°
90°
80°
70°
60°
50°
40°
30°

Figure 3.1.1(e) Ice conditions in Baffin Bay and the Arctic archipelago, August 1-6, 1955

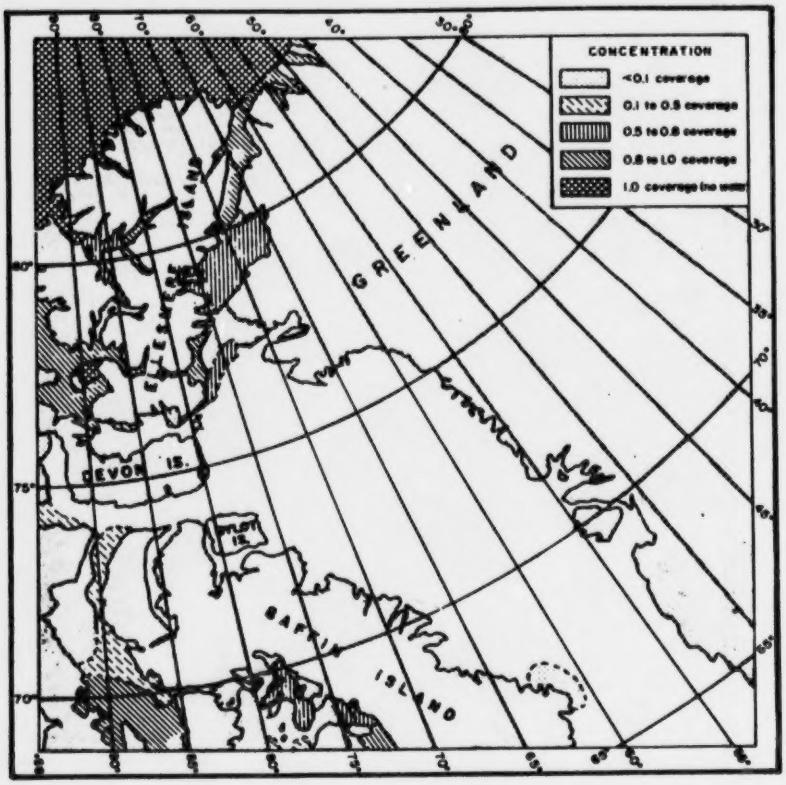
CONCENTRATION
<0.1 coverage
0.1 to 0.5 coverage
0.5 to 0.8 coverage
0.8 to 1.0 coverage
1.0 coverage (no water)
GREENLAND
ELLESMERE ISLAND
DEVON IS.
BYLOT IS.
BAFFIN ISLAND
80°
70°
60°
50°
40°
30°
80°
75°
70°
65°
60°

Figure 3.1.1(f) Ice conditions in Baffin Bay and the Arctic archipelago, September 1-6, 1955

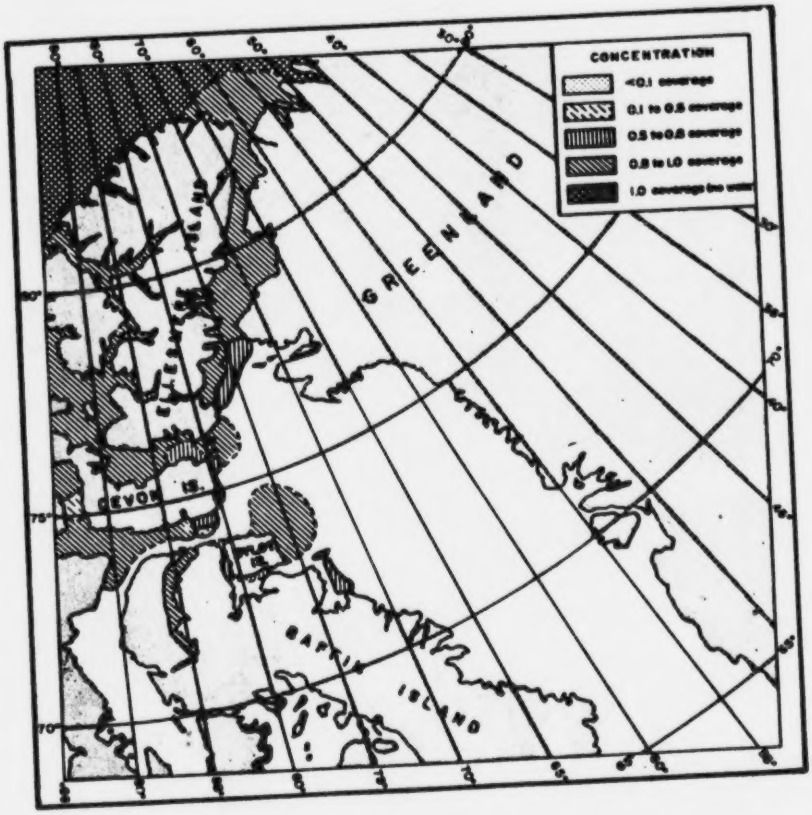
CONCENTRATION
<0.1 coverage
0.1 to 0.5 coverage
0.5 to 0.8 coverage
0.8 to 1.0 coverage
1.0 coverage (no wa
GREENLAND
ELLESMERE ISLAND
DEVON IS.
BYLOT IS.
BAFFIN ISLAND
80°
75°
70°
65°

Figure 3.1.1(g) Ice conditions in Baffin Bay and the Arctic archipelago, October 7-12, 1955

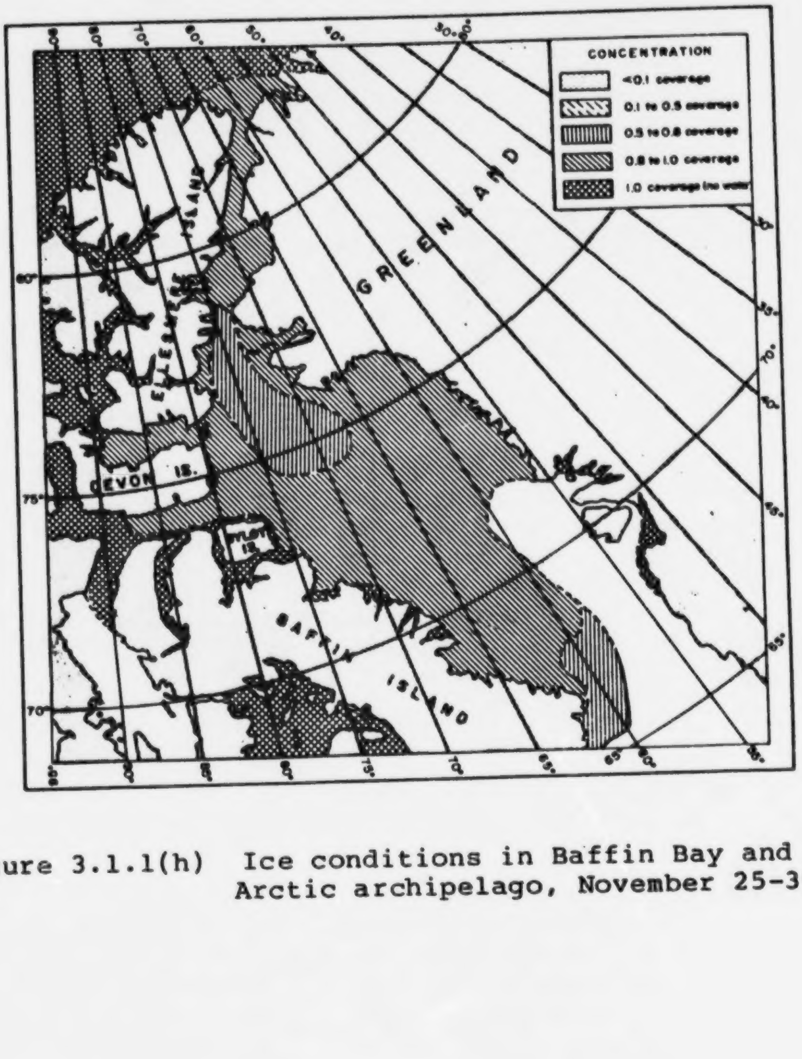
CONCENTRATION
<0.1 coverage
0.1 to 0.5 coverage
0.5 to 0.8 coverage
0.8 to 1.0 coverage
1.0 coverage (no water)
GREENLAND
ELLESMERE ISLAND
DEVON IS.
BYLOT IS.
BAFFIN ISLAND
80°
75°
70°
90°
80°
70°
60°
50°
40°
30°

Figure 3.1.1(h) Ice conditions in Baffin Bay and the Arctic archipelago, November 25-30, 1955

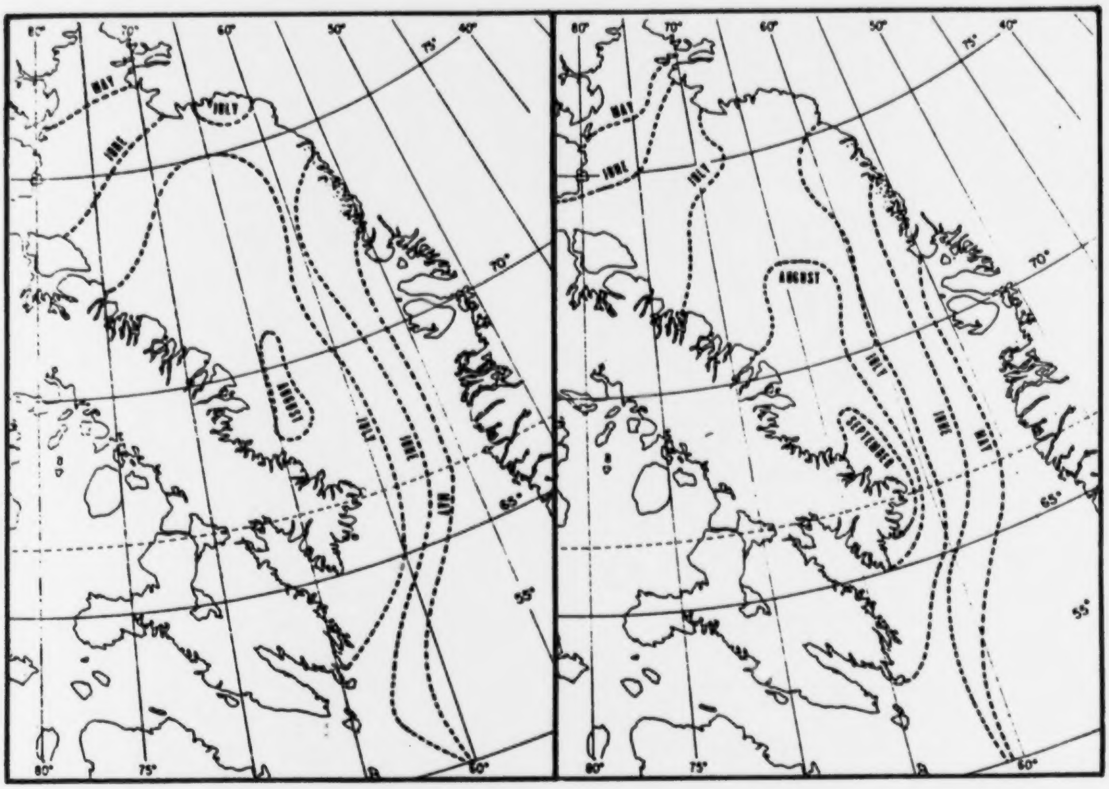
80°
70°
60°
50°
75°
40°
MAY
JUNE
JULY
AUGUST
70°
65°
55°
80°
75°
60°
MAY
JUNE
JULY
AUGUST
SEPTEMBER
JULY
JUNE
MAY
70°
65°
55°
80°
75°
60°

(a) (b)

Figure 3.1.2 Mean monthly limits of 4/10 to 4/10 ice cover: (a) 1952-1960; (b) 1961-1970. Note differing rates of clearance.

to enormously different situations for energy exchange between the atmospheric and water layers, wildlife feeding and migration patterns, and for the degree of threat posed by offshore operations.

While the statistical representations of the type presented in Appendix 1 offer simple and compact illustrations of ice-cover variability, their usefulness for more detailed analyses of the underlying processes is somewhat limited by the tendency of the averaging to:

a) suppress features of ice-cover change which occur on scales comparable to or smaller than the grid spacings; and,

b) blend together large numbers of historical ice configurations to produce artificial composites which are often never realized.

As a result, the basic pattern of ice growth, stabilization and decay must generally be extracted from original data sources such as the weekly AES or other ice charts and satellite imagery.

A review of such data (Marko, 1978) has drawn attention to the basic importance of a cross-channel ice edge or boundary which becomes established each winter at some point along the lengths of Barrow Strait and/or Lancaster Sound. This boundary separates the landfast or immobile ice of the Central Archipelago on its west from an eastern field composed of vast pieces of floe ice which continue to move irregularly eastward through the winter season. Specific examples of such edges are visible in the April 16, 1975 and February 8, 1976 NOAA images of Figures 3.1-3 and 3.1-4. In these instances, edge formation took place in the vicinity of Griffith and Prince Leopold Islands at respectively the western and eastern ends of Barrow Strait. A survey of the ice data extending back to 1961 indicates that stable winter ice edges have occurred at just five general locations in Parry Channel. These locations are indicated in Figure 3.1-5 and labelled according to years of occurrence. The distribution of positions is consistent with the "average" statistical configuration of Appendix IB which displayed a sudden jump in ice concentration west of roughly 90°W. This result evidently arises from:

1) The fact that in approximately one-half the surveyed years, stable ice edges were located near the 90°W Prince Leopold Island site; and,

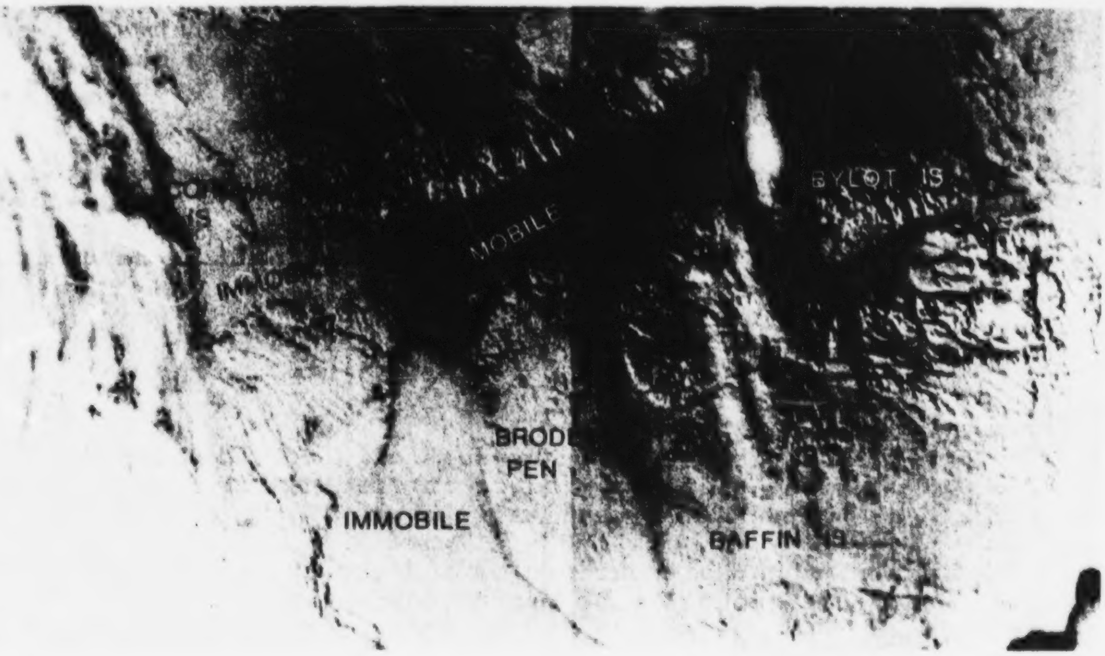
MOBILE
BYLOT IS
IMMOBILE
BRODE
PEN
IMMOBILE
BAFFIN IS

Figure 3.1-3 NOAA satellite imagery, Eastern Parry Channel, April 16, 1975

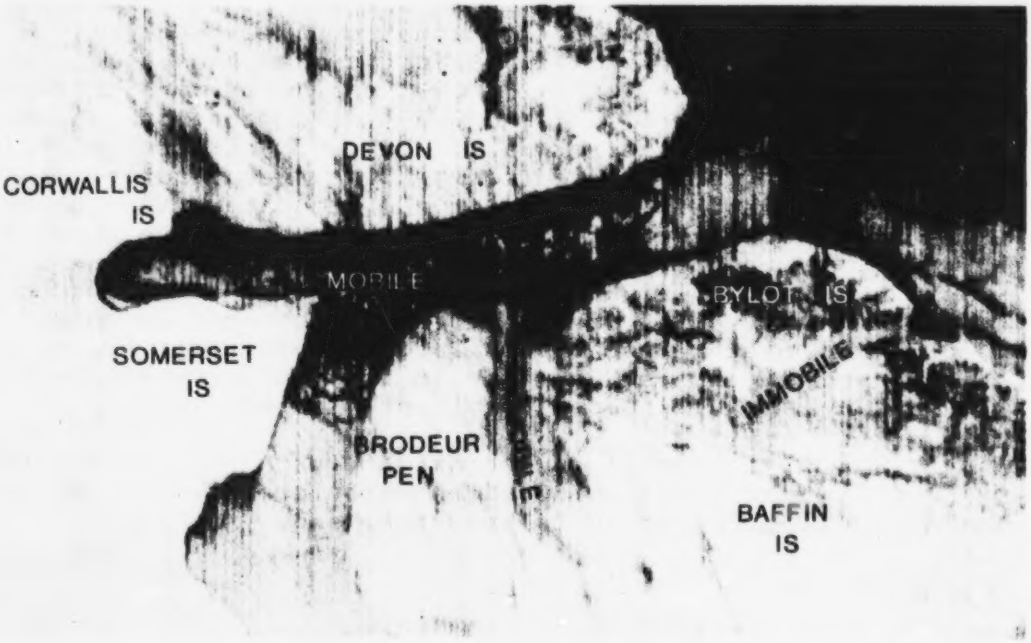
DEVON IS
CORWALLIS
IS
MOBILE
BYLOT IS
SOMERSET
IS
IMMOBILE
BRODEUR
PEN
BAFFIN
IS

Figure 3.1-4 NOAA satellite imagery, Eastern Parry Channel, February 8, 1976

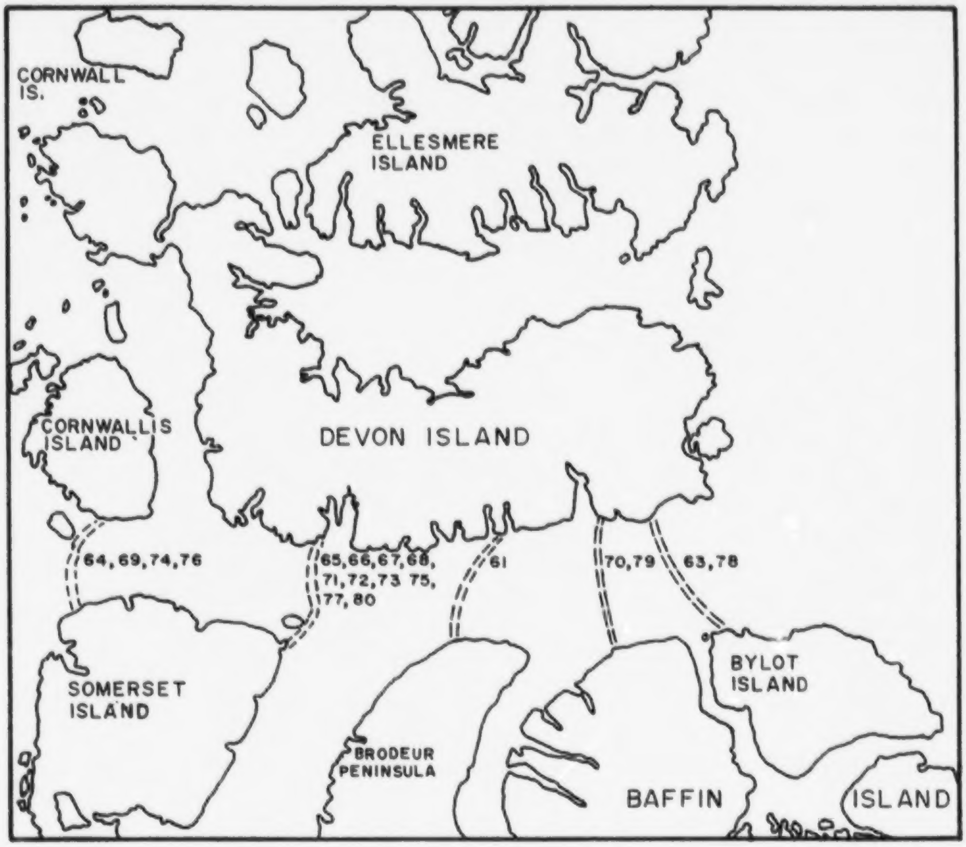
CORNWALL IS.
ELLESMERE ISLAND
CORNWALLIS ISLAND
DEVON ISLAND
64,69,74,76
65,66,67,68, 71,72,73 75, 77,80
61
70,79
63,78
SOMERSET ISLAND
BYLOT ISLAND
BRODEUR PENINSULA
BAFFIN
ISLAND

Figure 3.1.5 Approximate annual position of the stable winter landfast ice edge, 1961-1980

2) the edge positions in the remaining years were evenly divided between more easterly and more westerly sites, achieving a cancellation and leaving the discontinuity in average ice concentration near the most common 90°W site.

Nevertheless, it is to be noted that in approximately half the years considered, no long-lived ice-condition discontinuity occurred near 90°W.

Figures 3.1-6 and 3.1-7 illustrate the basic changes which occur in the Parry Channel ice cover for the two most frequently occurring positions of the annual ice edge, near Prince Leopold Island and Griffith Island. The sketched conditions were taken from the 1975 and 1976 NOAA satellite imagery (Milne and Smiley, 1978). For reference purposes, the corresponding seasonal ice concentrations have been mapped over the greater Baffin Bay region in Figures 3.1-8 and 3.1-9.

In the 1975 sequence (Figure 3.1-6), stabilization was evident at the Prince Leopold site during January. A mixture of vast and smaller floes and areas of thinner ice continued to move eastward away from the landfast ice edge at a typical rate of several km/day. Continued (until April) instability of the Prince Regent Inlet ice cover also resulted in a net winter export of ice from this latter body into Lancaster Sound. Otherwise, all side-channels and embayments were under immobile ice. Coast-paralleling shelves of landfast ice were also evident and separated from the main ice flow by linear zones of thin ice or open water whose widths seem to be increase or decrease under small cross-channel shifts of the mobile ice pack probably associated with changes in the north-south components of the surface winds. Particularly extensive landfast ice shelves occur along the coastlines of east Devon and northwestern Bylot Islands where they extend into waters many times deeper than the likely depths of the largest ice floe keels. Such keels are believed to play an important part in the stability of the landfast ice in the Beaufort Sea (Kovacs and Mellor, 1974). Data are presently inadequate to allow a comparable explanation of stability in the eastern Arctic.

The size and tone (indications of ice thickness) of the region just to the east of the Parry Channel ice edge is obviously determined by the relative balance of local ice growth and ice export by the prevailing easterly drift. It is anticipated that this situation would give a wedge-shaped cross-section to the Lancaster Sound ice cover (when viewed edgewise, perpendicular to the main Channel axis) with its thickest end adjacent to Baffin Bay.

The proportion of thinner, darker ice generally decreased through the winter until April when drastic reductions were noted in the coverage by thicker, larger floes. Such floes gradually drifted out into Baffin Bay during May, leaving the nearly ice-free Lancaster Sound surface indicated in the mid-June sketch of Figure 3.1-7. The small number of floes present at the latter time originated from the early break-up of Prince Regent Inlet, the deterioration of the Parry Channel ice edge and from the characteristic intrusive flow of ice out of Baffin Bay into northeastern Lancaster Sound. Some deterioration of the eastern Devon Island coastal ice shelves were evident at that time, although it should be noted that the ice sheet around Philpots Island is perhaps the most persistent landfast coastal feature of the region, remaining, in 1975, at least partially in place until the end of July.

The breakdown of the Parry Channel ice edge itself took place at the end of June, allowing the ice of Barrow Strait to move eastward, and establishing a new, short-lived ice edge in the vicinity of Griffith Island. The break-up of this new feature and the Wellington Channel ice cover followed in mid-July giving the indicated mid-August picture in which streams of rapidly deteriorating ice from the north and west were present in Barrow Strait and western Lancaster Sound. Much of this ice melted in situ, never reaching the eastern end of Lancaster Sound.

With the onset of refreezing in September, the regional surface was covered with a mixture of grey and grey-white ice with inclusions of year-old and older floes. The thin ice/open-water features evident in the November, 1975 sketch can be broken down into two categories:

1) a narrow lead or thin ice zone at the edge of the growing coastal landfast ice shelves along the northern border of Parry Channel. This lead is believed to be kept open by the prevailing northerly winds, and in 1975, extended as far west as western Viscount Melville Sound.

2) the predominantly cross-channel fractures or leads which were found to appear and disappear with time as the moving ice pack alternately became immobile and resumed its easterly drift.

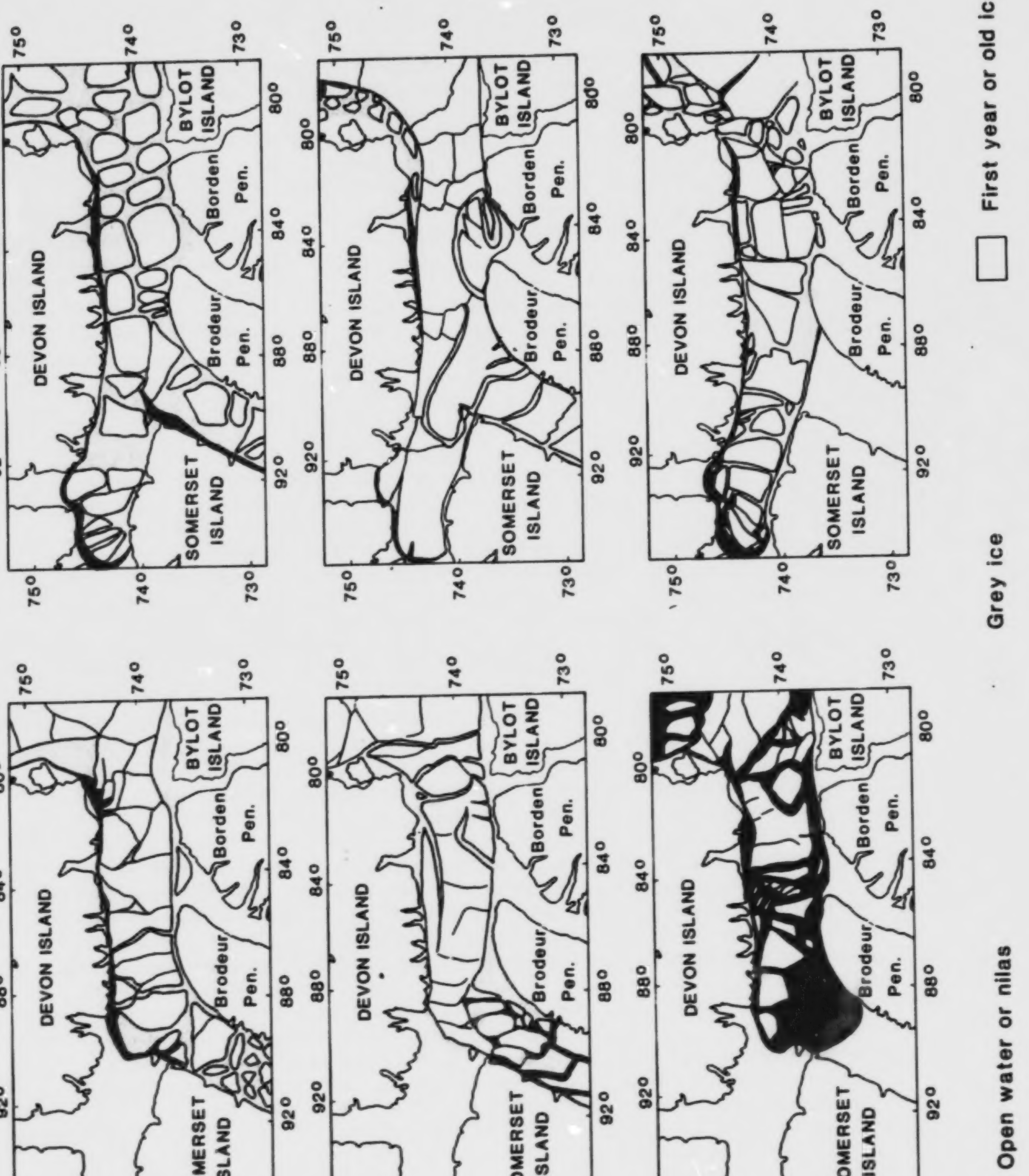
EARLY JANUARY
MID MARCH
LATE APRIL
DEVON ISLAND
SOMERSET ISLAND
BYLOT ISLAND
Borden Pen.
Brodeur Pen.
75°
74°
73°
92°
88°
84°
80°
Open water or nilas
Grey ice
First year or old ice

Figure 3.1.6 Ice freeze-up and breakup patterns, January-April, 1975 and 1976

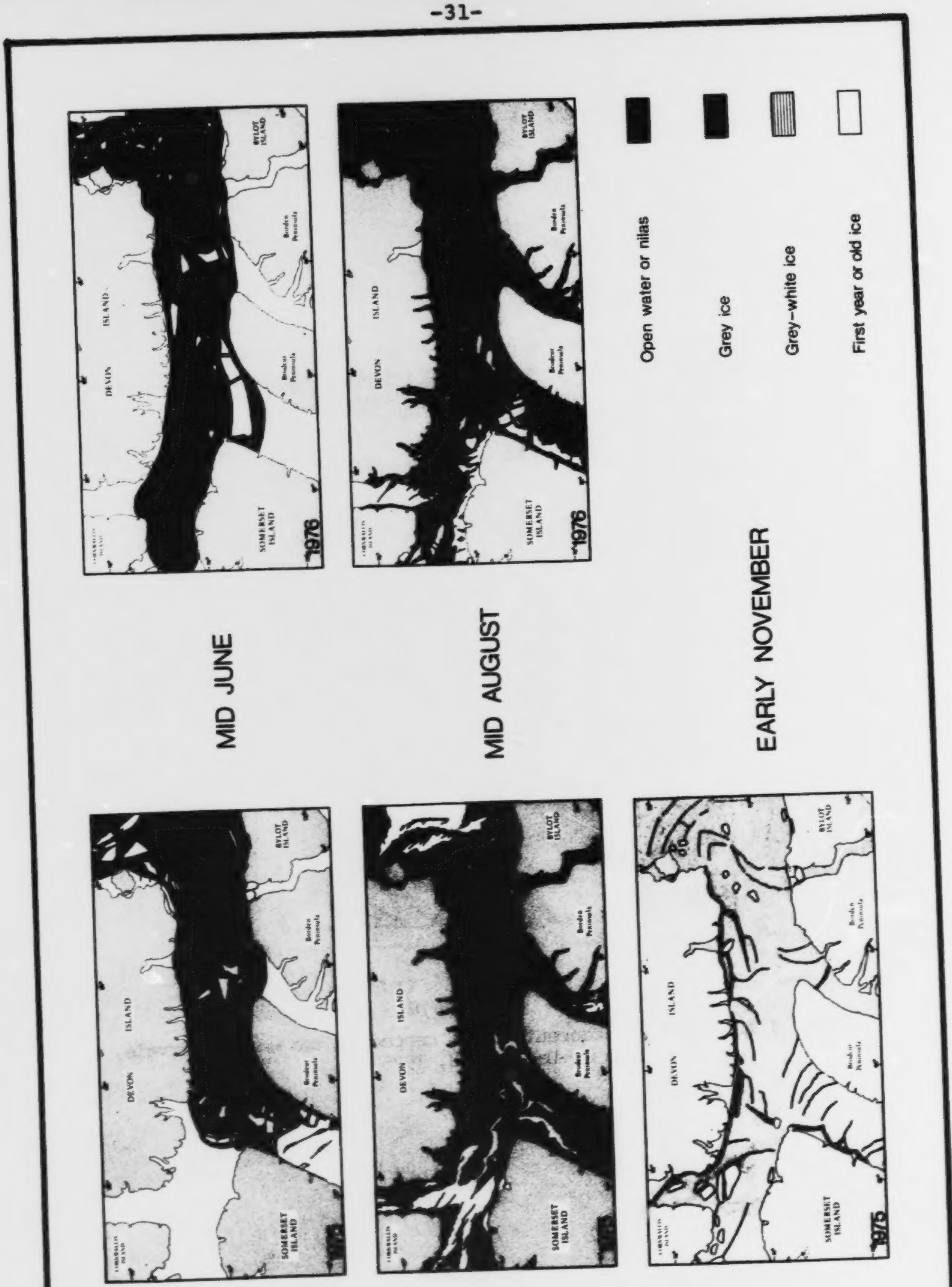
MID JUNE
MID AUGUST
EARLY NOVEMBER
DEVON ISLAND
SOMERSET ISLAND
BYLOT ISLAND
CORNWALLIS ISLAND
Borden Peninsula
Brodeur Peninsula
1976
1975
Open water or nilas
Grey ice
Grey-white ice
First year or old ice

Figure 3.1-7 Ice freeze-up and breakup patterns, June-November, 1975 and 1976

■	10/10 coverage (consolidated or landfast ice)
▓	7/10 - 9+/10 coverage
▒	4/10 - 6/10 coverage
░	1/10 - 3/10 coverage
OW	less than 1/10 coverage (open water)

Fig. 3.1.8 (a-m) Ice concentrations mapped at two week intervals, June 16-December 3, 1975

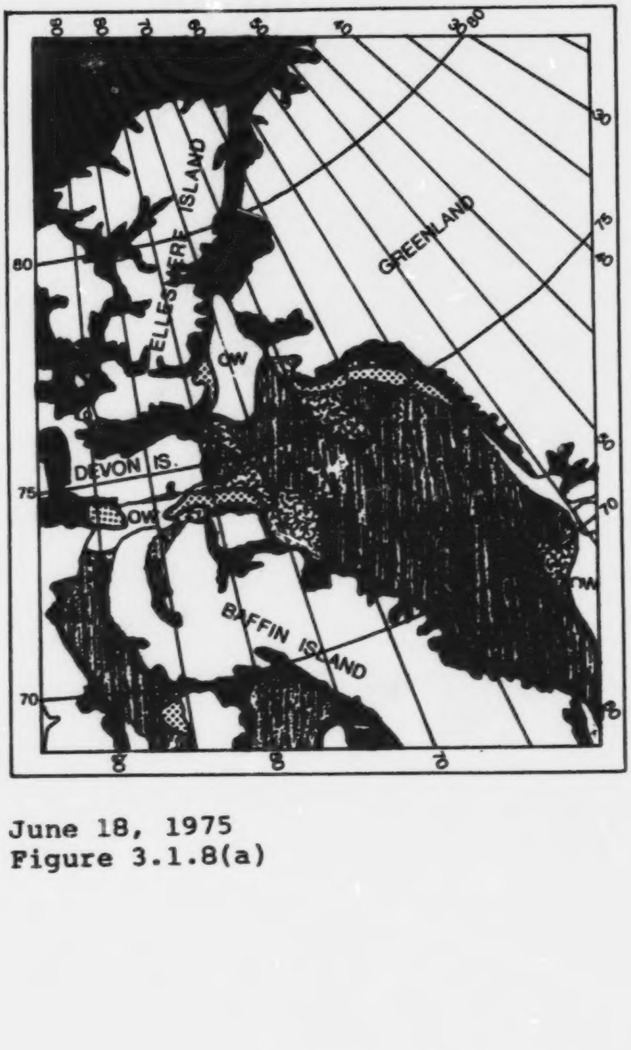
ELLESMERE ISLAND
GREENLAND
OW
DEVON IS.
OW
BAFFIN ISLAND
WL
80
75
70
30
75
80
70
60

June 18, 1975
Figure 3.1.8(a)

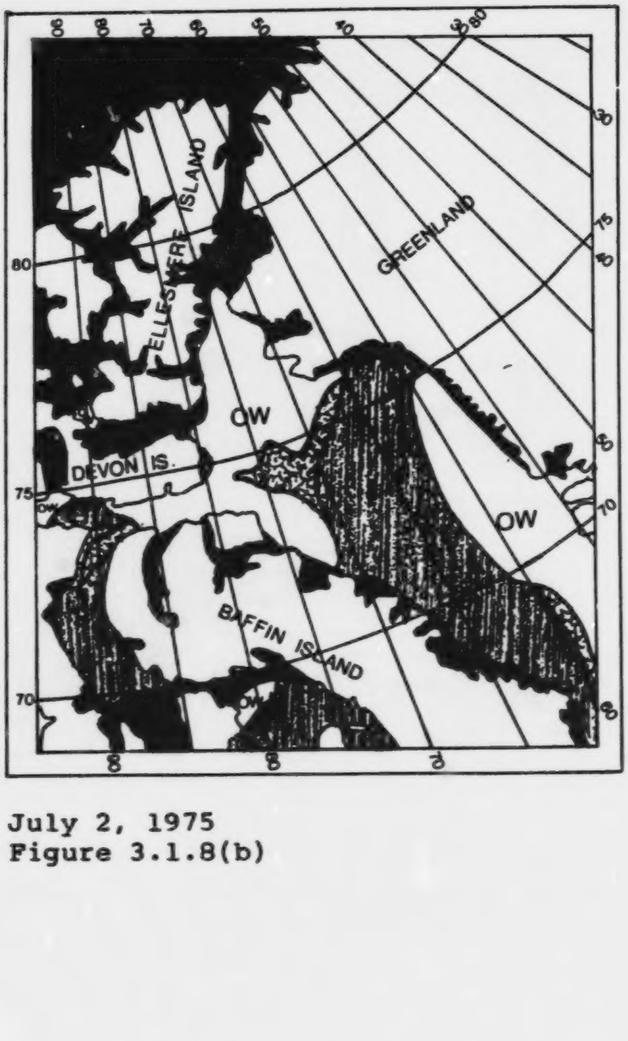
ELLESMERE ISLAND
GREENLAND
DEVON IS.
BAFFIN ISLAND
OW
OW
OW
OW
80
75
70
90
80
70
60
50
40
30
75
70
65
60

July 2, 1975
Figure 3.1.8(b)

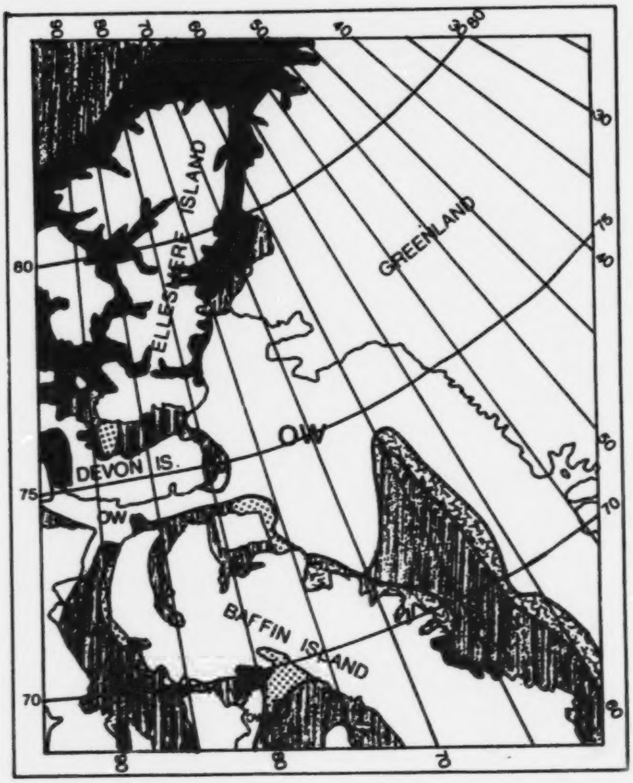
ELLESMERE ISLAND
GREENLAND
OW
DEVON IS.
OW
BAFFIN ISLAND
80
75
70
90
80
70
60
50
40
30
80
30
75
80
60
70
80
80
70

July 16, 1975
Figure 3.1.8(c)

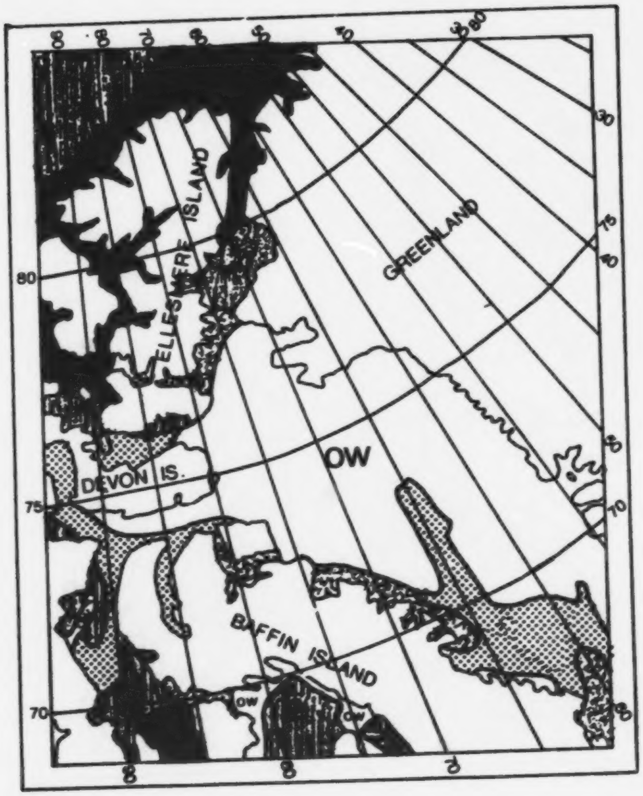
ELLESMERE ISLAND
GREENLAND
DEVON IS.
OW
BAFFIN ISLAND
OW
OW
80
75
70
90
80
70
60
50
40
30
75
70

July 30, 1975
Figure 3.1.8(d)

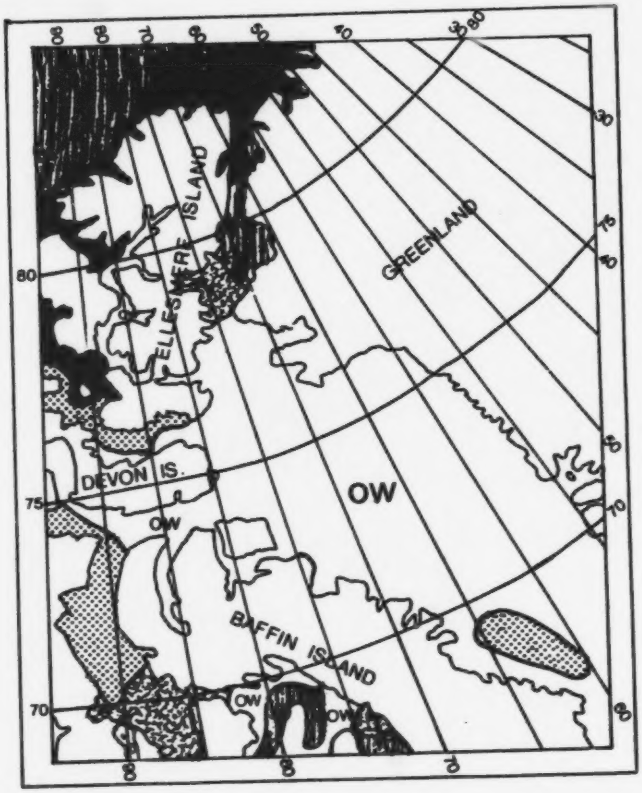
ELLESMERE ISLAND
GREENLAND
DEVON IS.
OW
OW
BAFFIN ISLAND
OW
OW
80
75
70

August 13, 1975
Figure 3.1.8(e)

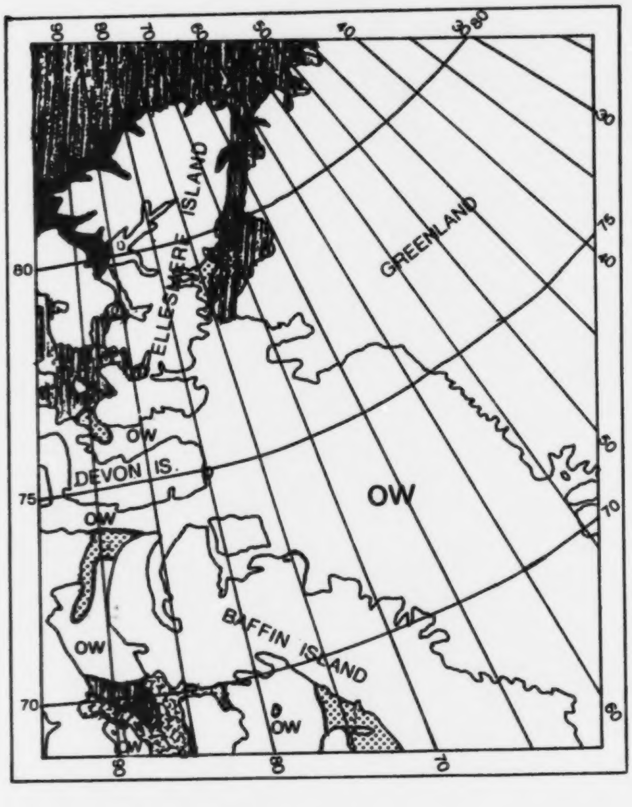
ELLESMERE ISLAND
GREENLAND
DEVON IS.
BAFFIN ISLAND
OW
OW
OW
OW
OW
OW
OW
80
75
70
90
80
70
60
50
40
30
80
30
75
80
50
70
60
90
80
70

August 27, 1975
Figure 3.1.8(f)

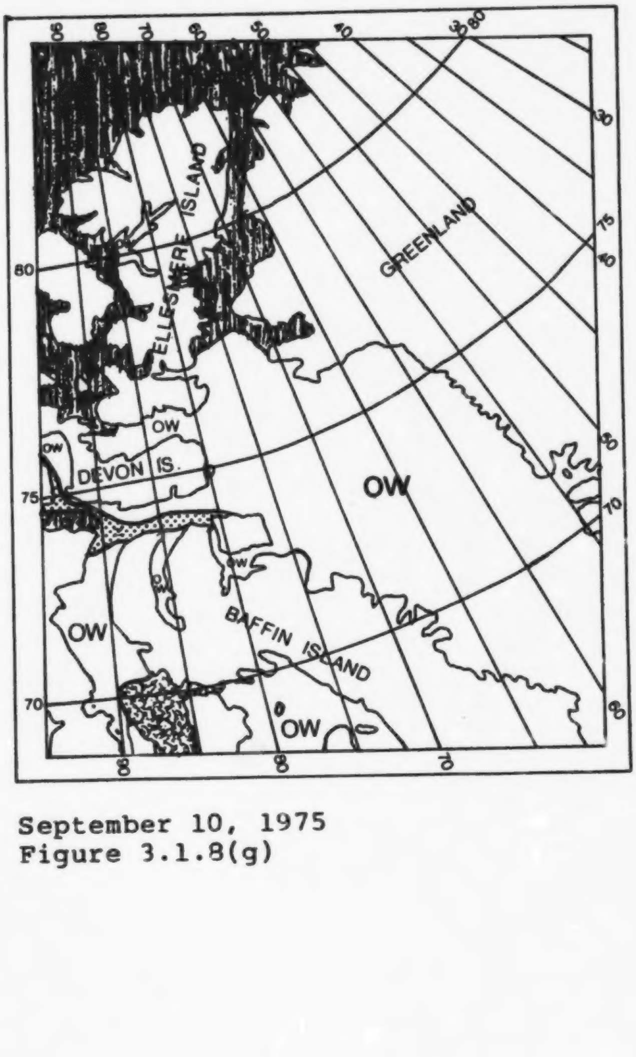
90
80
70
60
50
40
30
80
30
75
80
70
60
ELLESMERE ISLAND
GREENLAND
80
75
70
OW
OW
DEVON IS.
OW
OW
BAFFIN ISLAND
OW
OW
80
80
70

September 10, 1975
Figure 3.1.8(g)

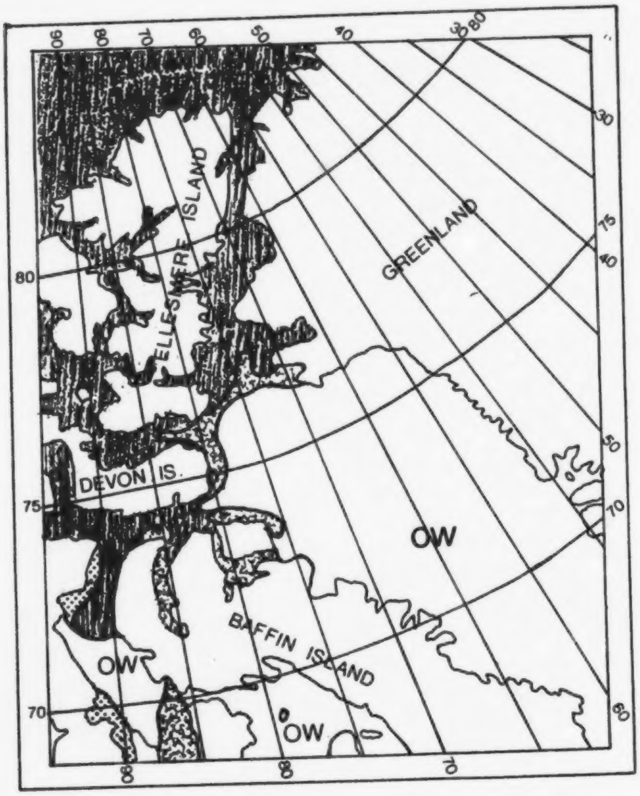
90
80
70
60
50
40
80
30
75
40
80
ELLESMERE ISLAND
GREENLAND
50
DEVON IS.
75
70
OW
BAFFIN ISLAND
OW
70
OW
60
90
80
70

September 24, 1975
Figure 3.1.8(h)

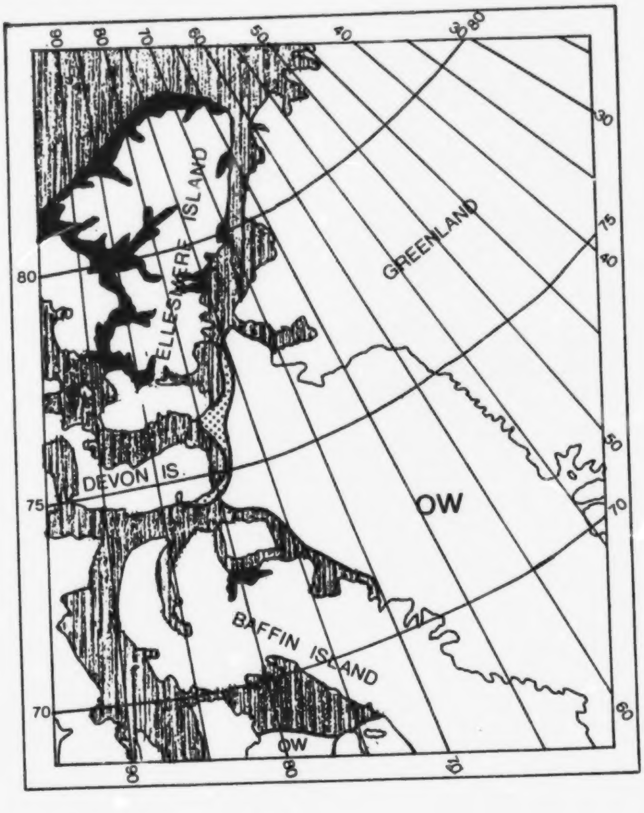
ELLESMERE ISLAND
GREENLAND
DEVON IS.
BAFFIN ISLAND
OW
OW
80
75
70
90
80
70
60
50
40
30
75
40
50
70
60
90
80
70

October 8, 1975
Figure 3.1.8(i)

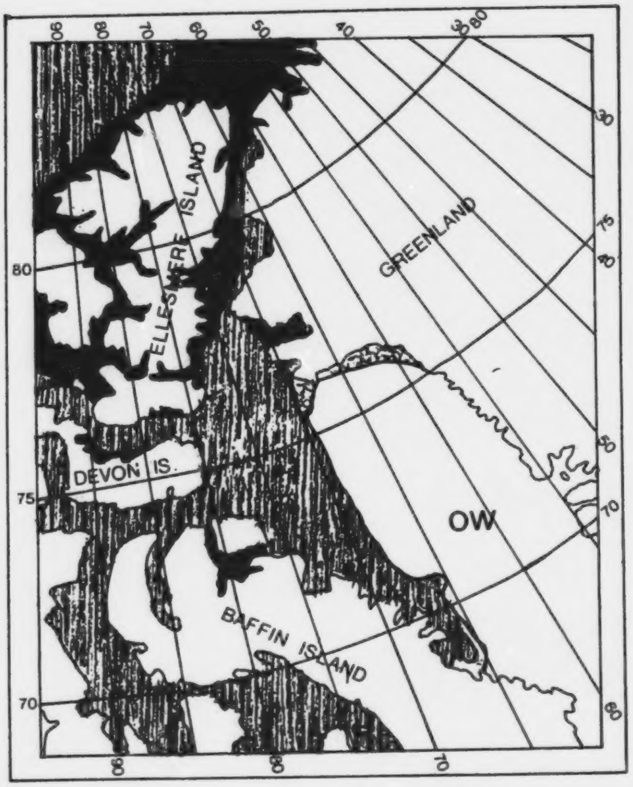
ELLESMERE ISLAND
GREENLAND
DEVON IS.
BAFFIN ISLAND
OW
90
80
70
60
50
40
30
75
70
65
60
80

October 22, 1975
Figure 3.1.8(j)

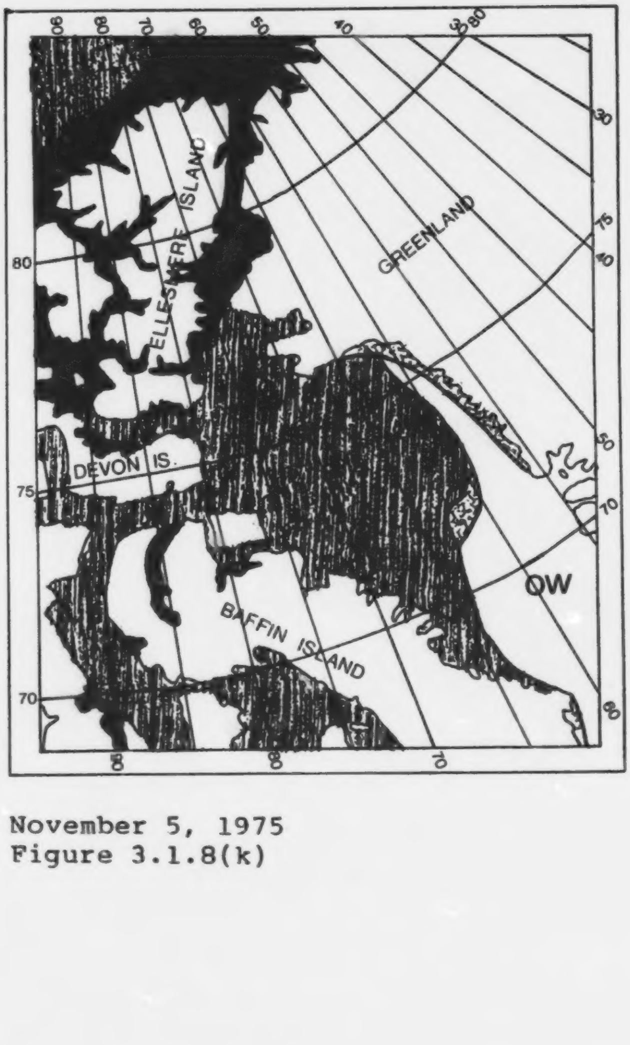
ELLESMERE ISLAND
GREENLAND
DEVON IS.
BAFFIN ISLAND
OW
90
80
70
60
50
40
30
80
75
70
60

November 5, 1975
Figure 3.1.8(k)

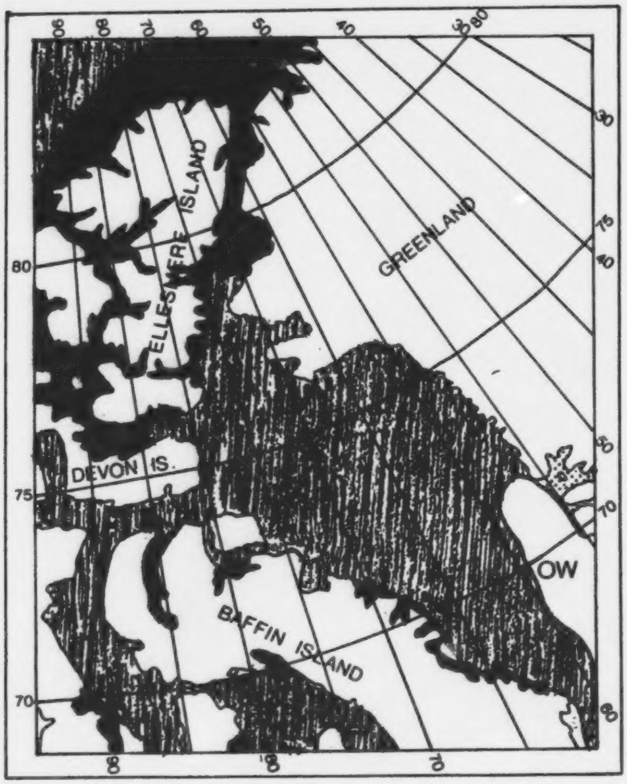
ELLESMERE ISLAND
GREENLAND
DEVON IS.
BAFFIN ISLAND
OW
80
75
70
90
80
70
60
50
40
30
80
75
70
60
90
80
70

November 19, 1975
Figure 3.1.8(1)

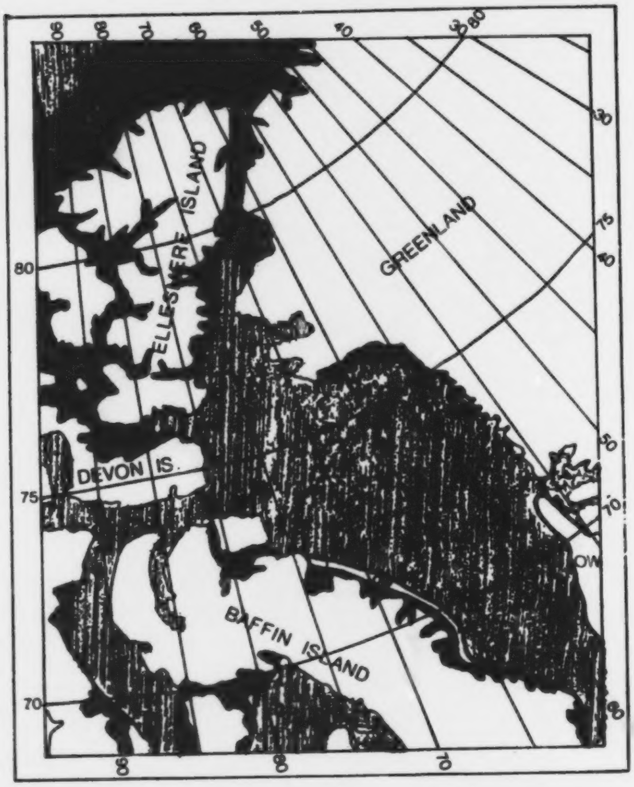
ELLESMERE ISLAND
GREENLAND
DEVON IS.
BAFFIN ISLAND
OW
80
75
70
90
80
70
60
50
40
30
80
75
70
60
50
70
90
80
70

December 3, 1975
Figure 3.1.8(m)

■ 10/10 coverage (consolidated or landfast ice)

▩ 7/10 - 9+/10 coverage

▒ 4/10 - 6/10 coverage

░ 1/10 - 3/10 coverage

OW less than 1/10 coverage (open water)

Fig. 3.1.9 (a-m) Ice concentrations mapped at two week intervals June 16-December 1, 1976

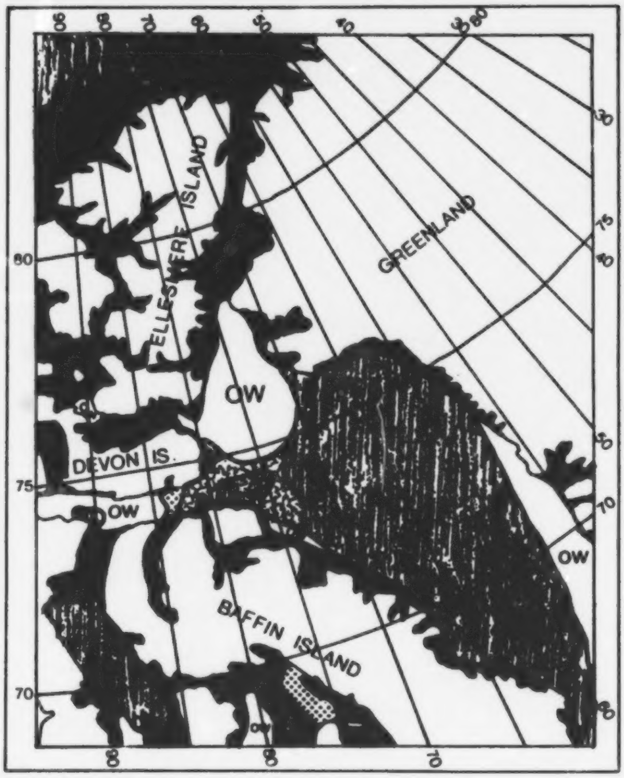
ELLESMERE ISLAND
GREENLAND
OW
DEVON IS.
OW
OW
BAFFIN ISLAND
OW
80
75
70
90
80
70
60
50
40
30
80
70
60
50
60
70
75
70
60
90
80
70

June 16, 1976
Figure 3.1.9(a)

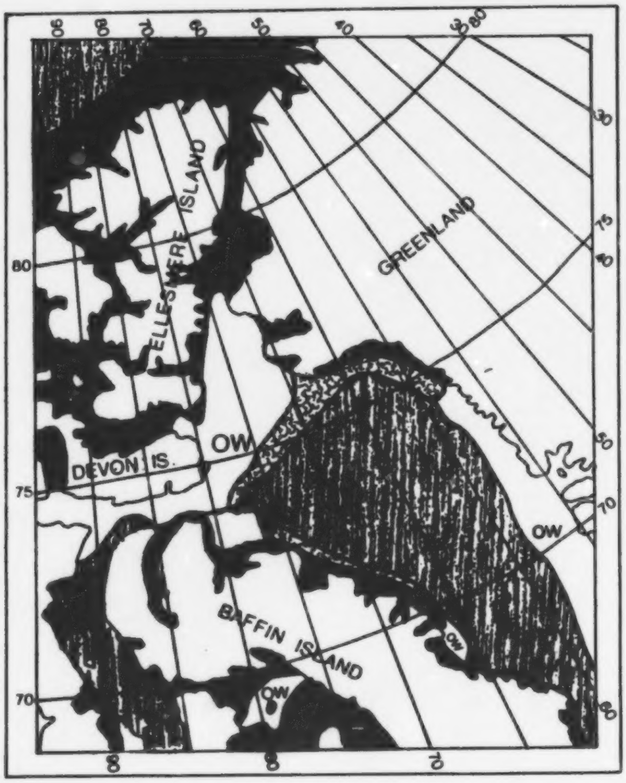
90
80
70
60
50
40
30
80
30
ELLESMERE ISLAND
GREENLAND
75
80
80
DEVON IS.
OW
75
50
70
OW
BAFFIN ISLAND
OW
OW
70
60
90
80
70

June 30, 1976
Figure 3.1.9(b)

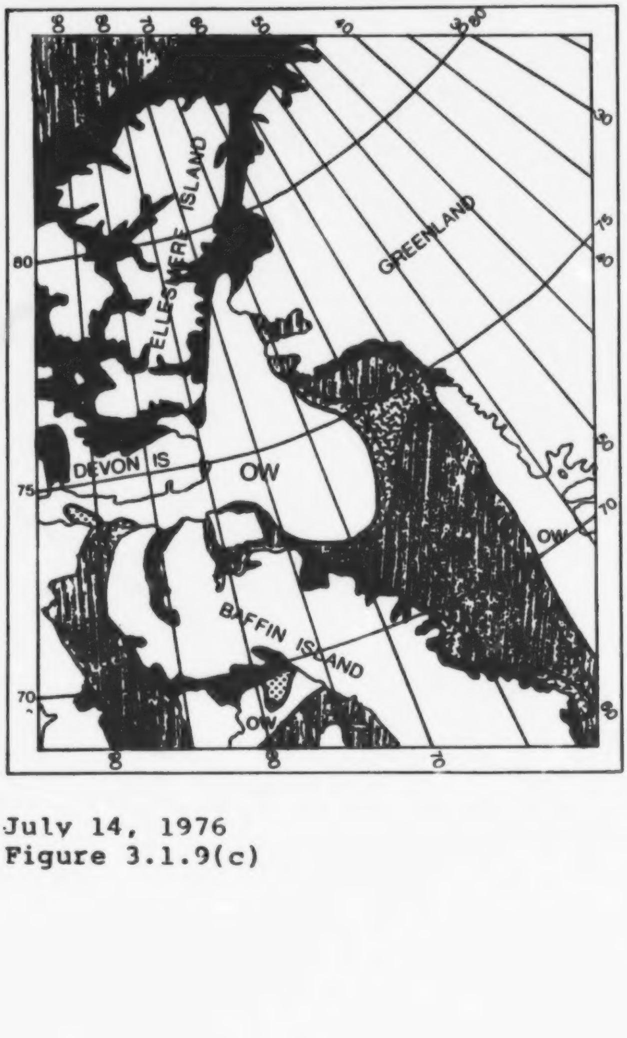
ELLESMERE ISLAND
GREENLAND
DEVON IS
OW
BAFFIN ISLAND
OW
OW
80
75
70
70

July 14, 1976
Figure 3.1.9(c)

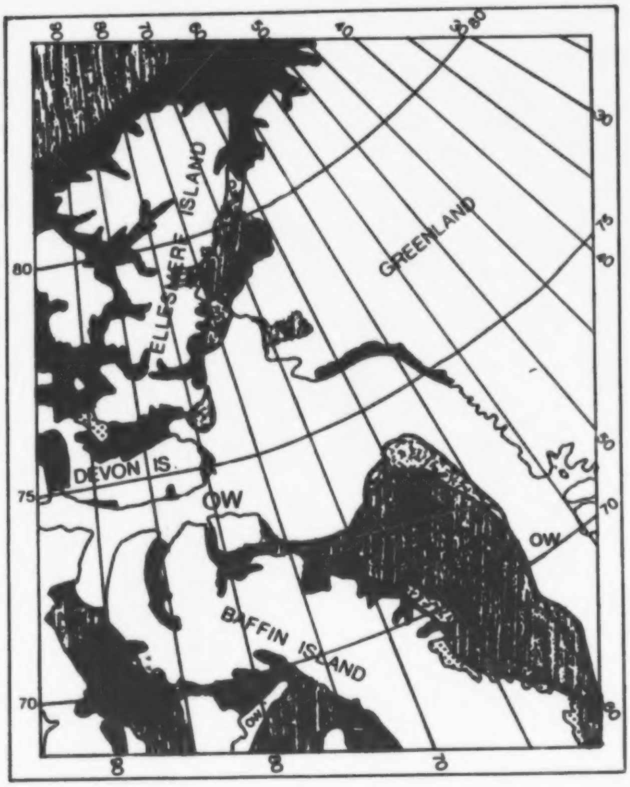
ELLESMERE ISLAND
GREENLAND
DEVON IS.
OW
BAFFIN ISLAND
OW
OW
80
75
70
30
40
50
60
70
80
90

July 28, 1976
Figure 3.1.9(d)

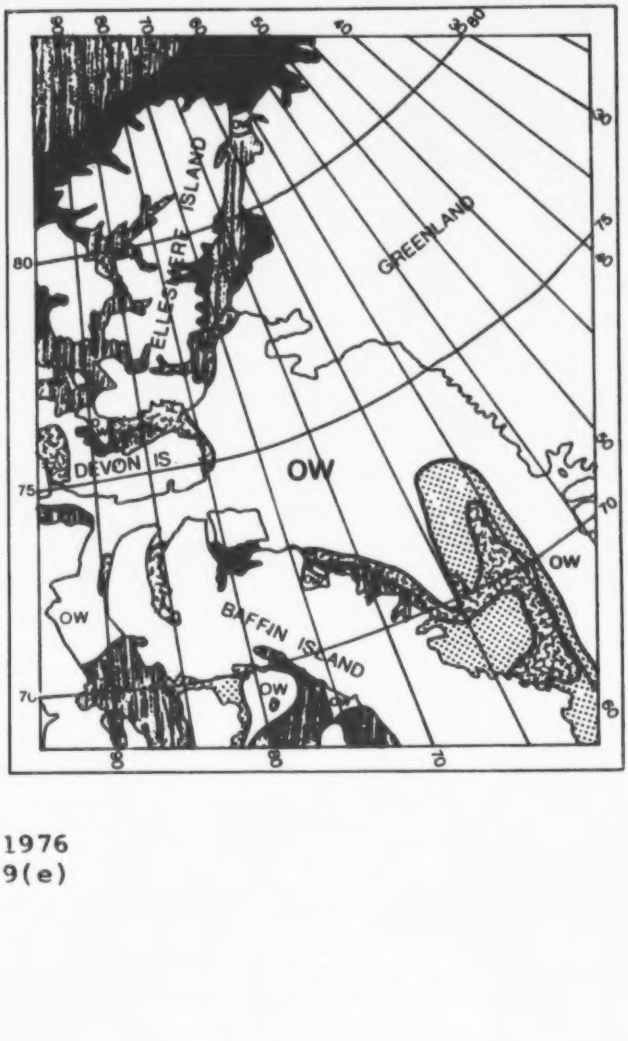
ELLESMERE ISLAND
GREENLAND
DEVON IS.
OW
OW
OW
OW
BAFFIN ISLAND
80
75
70
80
70
60
50
40
30
80
75
70
80
70

August 11, 1976
Figure 3.1.9(e)

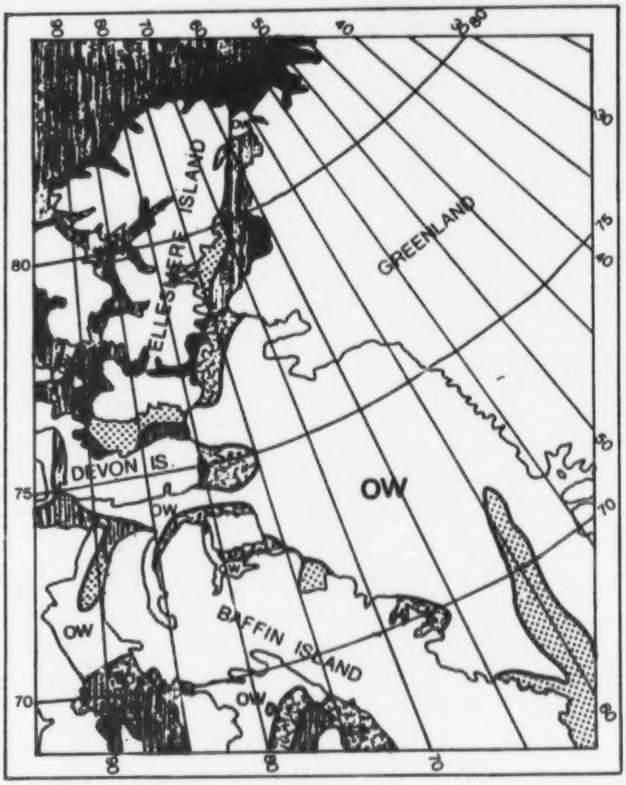
90
80
70
60
50
40
30
80
75
70
ELLESMERE ISLAND
GREENLAND
DEVON IS.
OW
OW
OW
OW
OW
BAFFIN ISLAND
80
70
60
70
80

August 25, 1976
Figure 3.1.9(f)

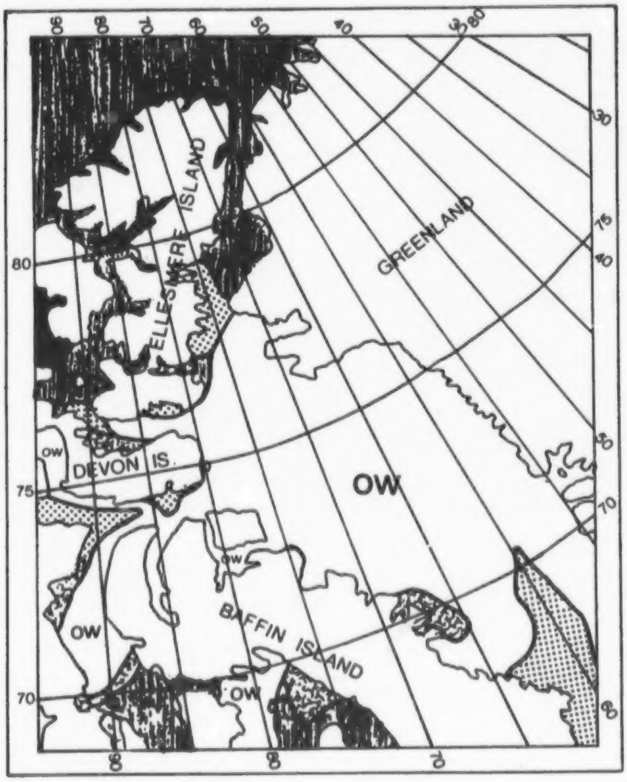
90
80
70
60
50
40
30
80
30
75
40
50
70
60
80
75
70
ELLESMERE ISLAND
GREENLAND
OW
DEVON IS.
OW
OW
BAFFIN ISLAND
OW
OW
90
80
70

September 8, 1976
Figure 3.1.9(g)

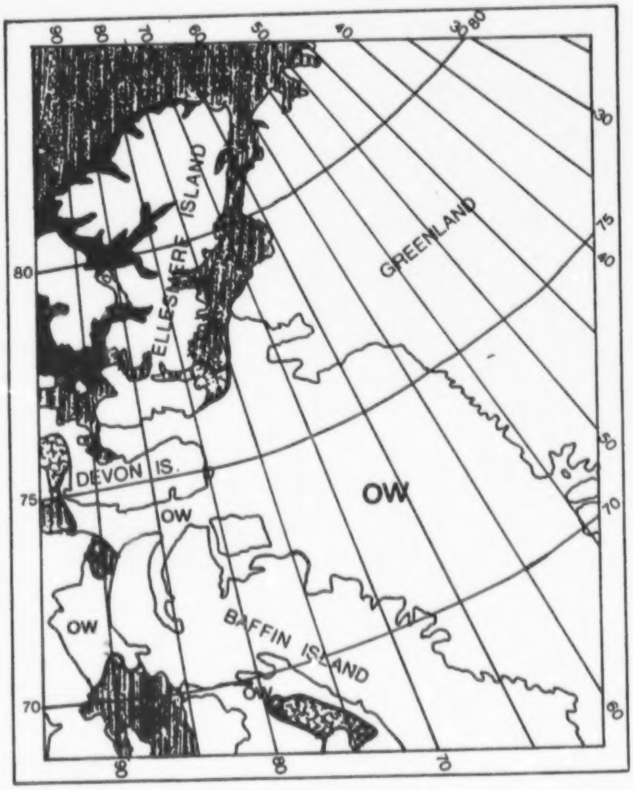
ELLESMERE ISLAND
GREENLAND
DEVON IS.
OW
OW
OW
OW
BAFFIN ISLAND
90
80
70
60
50
40
30
20
30
75
80
80
75
70
70
60
80
80
70

September 22, 1976
Figure 3.1.9(h)

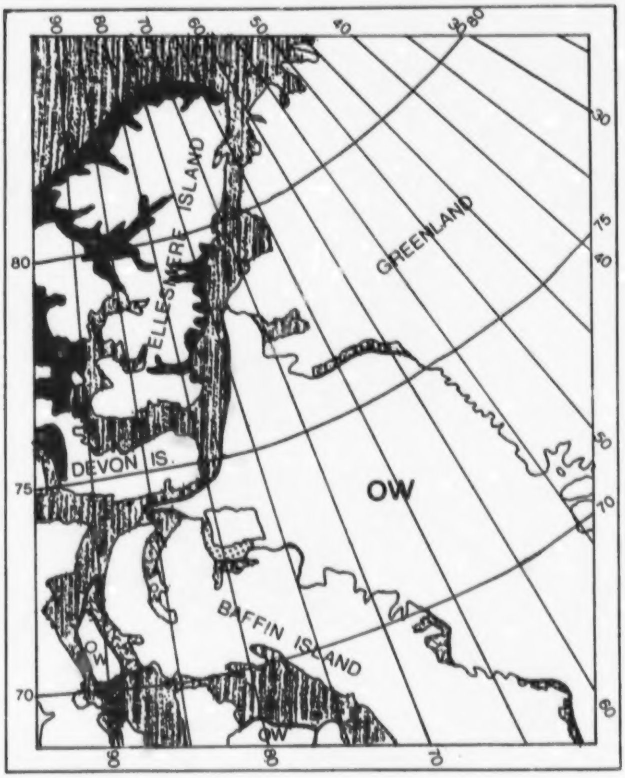
ELLESMERE ISLAND
GREENLAND
DEVON IS.
OW
BAFFIN ISLAND
OW
OW
90
80
70
60
50
40
80
30
75
70
60
80
75
70
80
80
70

October 6, 1976
Figure 3.1.9(i)

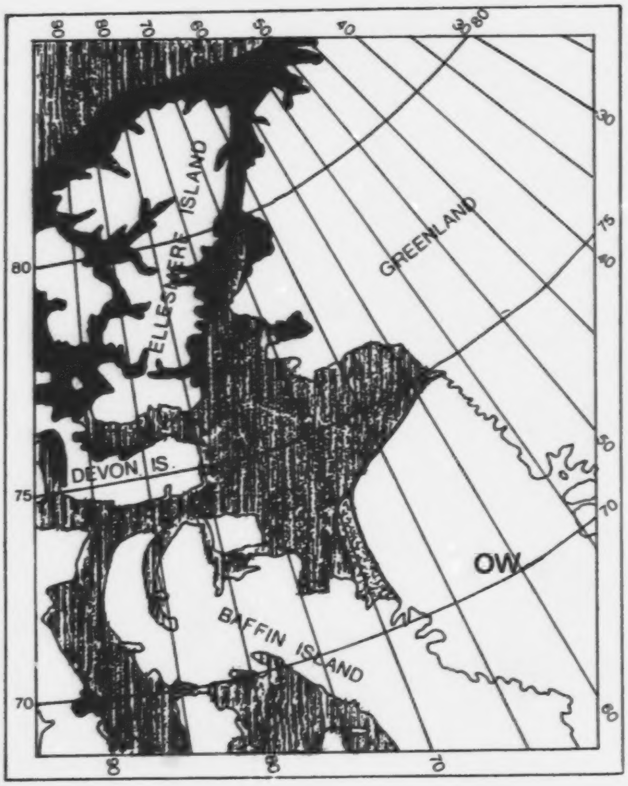
ELLESMERE ISLAND
GREENLAND
DEVON IS.
BAFFIN ISLAND
OW
80
75
70
90
80
70
60
50
40
30
80
30
75
40
50
70
60
80
80
70

October 20, 1976
Figure 3.1.9(j)

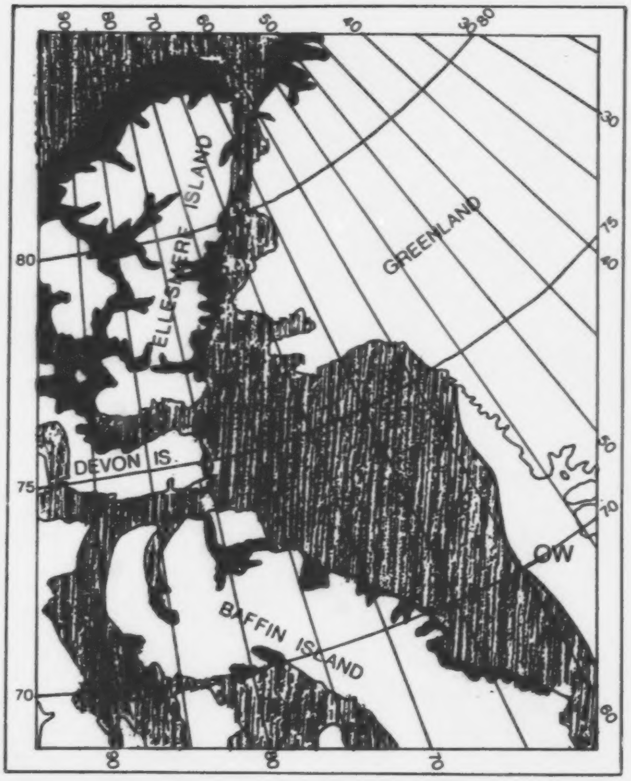
90
80
70
60
50
40
30
80
30
75
40
50
70
60
80
75
70
80
80
70
ELLESMERE ISLAND
GREENLAND
DEVON IS.
BAFFIN ISLAND
OW

November 3, 1975
Figure 3.1.9(k)

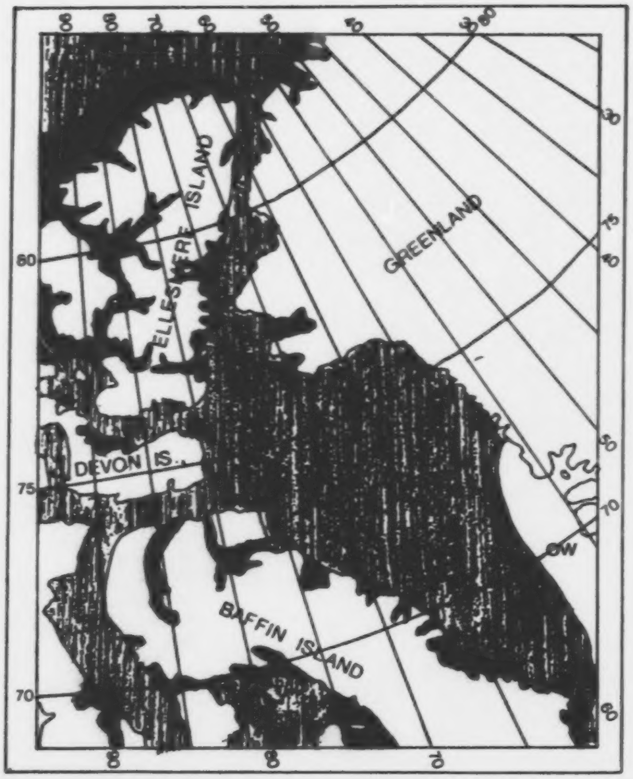
ELLESMERE ISLAND
GREENLAND
DEVON IS.
BAFFIN ISLAND
OW
80
75
70
80
75
70
60
50
40
30

November 17, 1976
Figure 3.1.9(1)

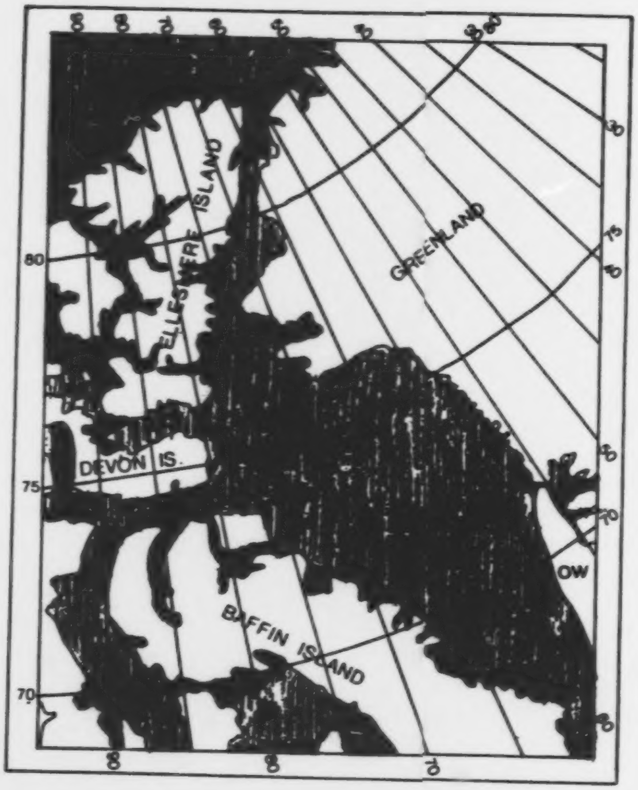
ELLESMERE ISLAND
GREENLAND
DEVON IS.
BAFFIN ISLAND
OW
80
75
70

December 1, 1976
Figure 3.1.9(m)

The northern perimeter lead eventually froze over in the landfast sectors of the Channel, typically losing visibility in December. The process of transient cross-channel lead formation, on the other hand, continued even with the gradual thickening of the ice cover. This may be seen in the NOAA images for December 23, 1975 and January 28, 1976 (Figure 3.1-10) and February 8, 1976 (Figure 3.1-9) NOAA images. The first of these images shows the existence of a stable, immobile ice cover lying to the west of a very wide arch which extends from Griffith Island far to the west with its main cross-channel portion to the south of Bathurst Island. A second edge also was evident, extending almost due south from Griffith Island. Extensive refreezing was evident at both edges of the January 28 image, with new cross-channel leads visible near the east end of Cornwallis Island and (more prominently) near Prince Leopold Island. However, by February 8, resumption of easterly motion had eliminated the latter two leads and re-established an ultimately stable boundary along the shorter Griffith Island line.

In spite of the more westerly position of the winter ice edge, the evolution of the 1976 ice surface proceeded with roughly the schedule of the previous year, with perhaps the largest difference arising from the later, second week in August, break-up of Wellington Channel. Otherwise, the typical May clearing led to largely open-water conditions in June with the countable number of vast or giant floes originating from the Prince Regent Inlet icefields and the Baffin Bay intrusive flow. The breakdown of the Parry Channel edge during the first week in July, led to the indicated later (August) flow of ice from Viscount Melville and MacDougall Sounds along the south side of Barrow Strait.

One other distinction of the 1976 season was the significantly later (relative to 1975) clearing of coastal ice from the eastern and northern shores of Bylot Island (Figures 3.1-9 and 3.1-10). Otherwise, in both 1975 and 1976, ice conditions of the Baffin Bay region followed the rough pattern of the "best year in five" configurations of Appendix 1A.

Data obtained over the past two decades of aerial and satellite observations indicate a general correlation of western positions of the Parry Channel ice edge with good ice conditions in Lancaster Sound and in the immediately adjoining sector of Baffin Bay. The implied relationship does not, of course, exclude the occurrence in such years of local anomalies such as unusually persistent shoreline ice concentrations or short periods of heavy conditions associated with "pulses" of ice moving southward from Jones and Smith Sounds.

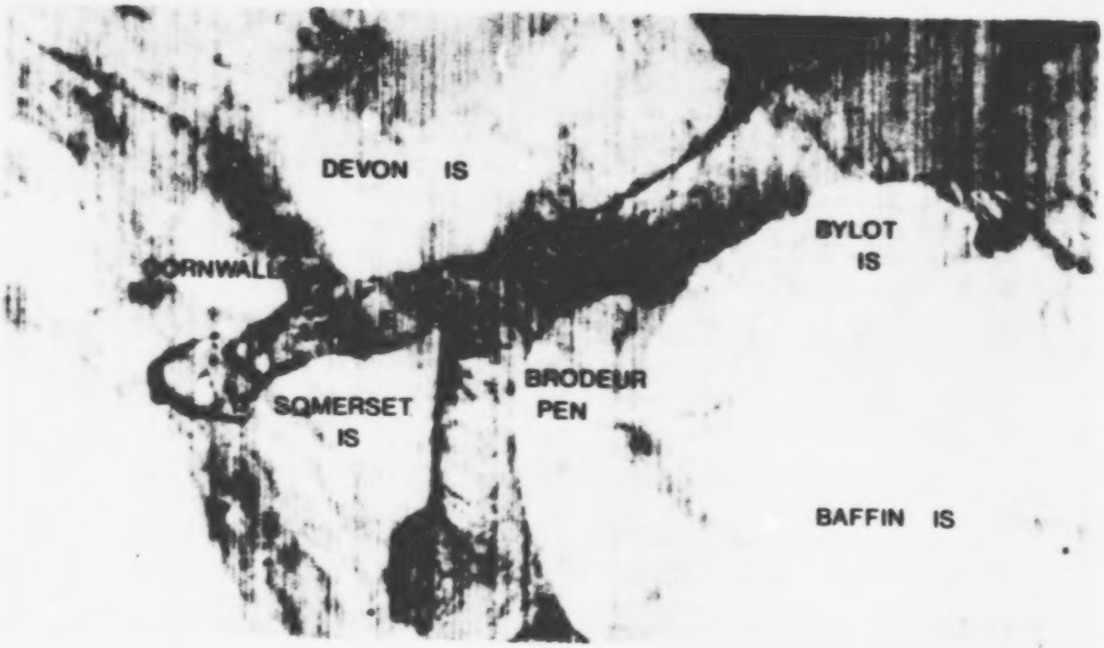
DEVON IS
CORNWALLIS
BYLOT IS
BRODEUR PEN
SOMERSET IS
BAFFIN IS

Figure 3.1-10(a): NOAA satellite imagery showing transient cross-channel lead formation, December 23, 1975.

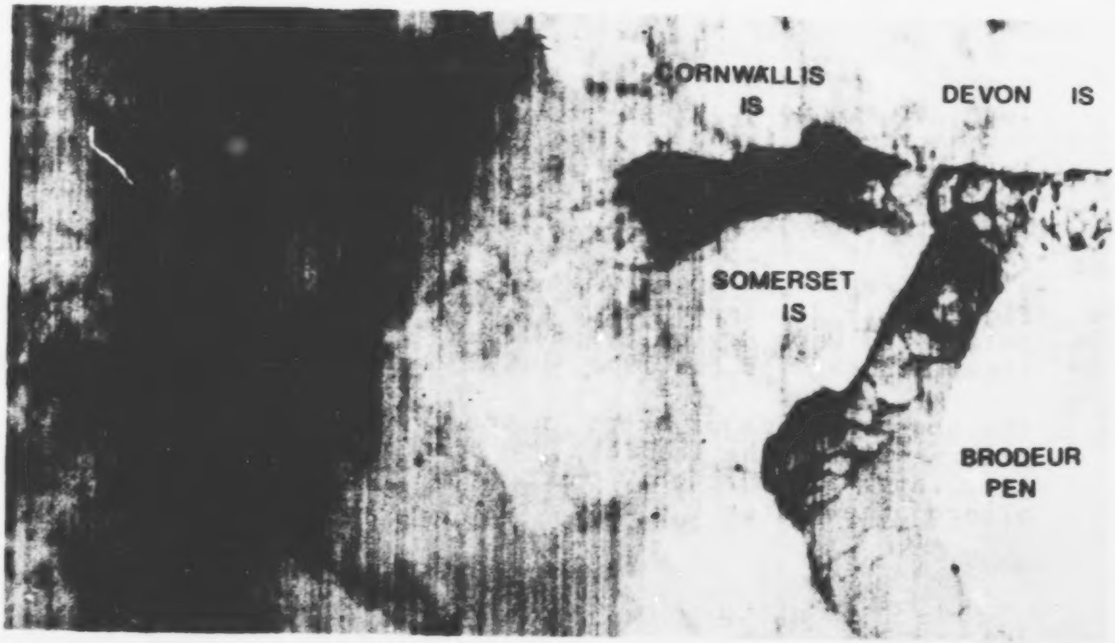
CORNWALLIS IS
DEVON IS
SOMERSET IS
BRODEUR PEN

Figure 3.1-10(b): NOAA satellite imagery showing transient cross-channel lead formation, January 28, 1976.

On the other hand, stabilization of the winter ice edge at positions to the east of 90°W has generally corresponded with poor ice conditions in the following summer period. The relationship in this case must be, in part, due to the resulting extended retention in the region of the unmelted portions of the ice packs of eastern Parry Channel, Prince Regent Inlet and (in some cases) Admiralty Inlet. Subsequent to the normal July breakdown of the landfast ice edge, ice from these bodies continues to drift into Baffin Bay through much of the remaining summer period.

The 1978 and 1979 seasons covered by the Petro-Canada-EAMES programs provided almost classic examples of poor ice years associated with landfast ice boundaries at the two most extreme eastern positions indicated in Figure 3.1-5.

The description of ice conditions in the latter two years are given below to facilitate the interpretation of other environmental data and to clarify, as much as possible, the characteristics of heavy regional ice years.

We begin by briefly summarizing the changes in the winter ice cover which led to the establishment of the respective 1978 and 1979 winter landfast ice edges. The key steps in this respect are indicated in Figure 3.1-11 and 3.1-12.

The January 20 image (Figure 3.1-11) taken in the first of these years illustrates the typical heavy ice conditions of Baffin Bay as well as the presence of characteristic rectilinear leads extending eastward toward the Greenland coast. At this time, a large portion of the eastern Archipelago ice cover was mobile with the Parry Channel landfast ice boundary lying along an extreme western line connecting Griffith, Lowther and Russel Islands. The following February 25 and March 10 images show respectively the stabilization of a new edge near Prince Leopold Island and its later supplantation by a still, more easterly edge in the vicinity of Sargent Point on the Brodeur Peninsula. Finally, a third, still more easterly edge (see March 26 image of Figure 3.1-12) was established between Cape Warrender, Devon Island and Cape Hay on Bylot Island. This edge became the final boundary of the 1977 - 1978 regional landfast ice cover.

The observable major steps in the described eastward progression of the landfast ice boundary took place over a time interval of roughly one month. The process drastically altered the winter ice conditions in Barrow Strait and

Lancaster Sound, leaving both areas under immobile ice covers. The period preceeding the final stabilization was characterized by weak, northerly winds (as determined from the AES surface pressure charts and the geostrophic assumption), but detailed analysis of the conditions accompanying events is complicated by the absence of actual wind and current data in Lancaster Sound.

The stabilization of the 1978 - 1979 winter ice cover took place in November, 1978, following several temporary stabilizations of the ice edges in Wellington Channel and Prince Regent Inlet and an earlier stabilization of Parry Channel along the Griffith-Lowther-Russell Island line, observed on November 3. In the November 28 NOAA image (Figure 3.1-12) however, a new boundary became visible, running from a point west of Cape Warrender on Devon Island to Cape Charles Yorke on the Borden Peninsula, somewhat to the west of the line of stabilization followed during the previous winter. In any case, little change was observed in the shape of this boundary (see the January 19, 1979 image - Figure 3.1-12) until February 1, when some detachment of ice was noted. Otherwise, the late November boundary remained intact until the break-up of the following summer. The stabilization process was apparently achieved without an eastward progression of temporary boundaries, as observed during the 1977 - 1978 winters. Instead, the events suggested a sudden immobilization of the still nominally thin ice cover of eastern Lancaster Sound. Circumstances were favorable for a rapid freeze-up in the area due to the heavy ice conditions of the previous summer, which limited the radiant heating of the surface water layer. In addition, bottom-moored current meters, placed 35m below the surface near Philpots and Bylot Islands, indicated (Fisseletal 1980) a significant reduction in current speeds corresponding to a general slowdown in area water movements during the November 1978 to March 1979 period. Unfortunately, there were no current measurements made in the immediate vicinity of the ice edge and, of course, no local surface wind measurements were available.

The progressions of the 1978 and 1979 ice seasons are summarized in Appendices 2 and 3 respectively in the form of both greater Baffin Bay and study area ice concentration mappings.

The earliest portions of the 1978 sequences indicate two major regions of clearing in northwestern Baffin Bay. These result from the usual May southward extension of the North Water and the accompanying clearing of ice to the east of the Parry

Figure 3.1-11(a)

NOAA satellite imagery, Eastern Parry
Channel, January 20, 1978

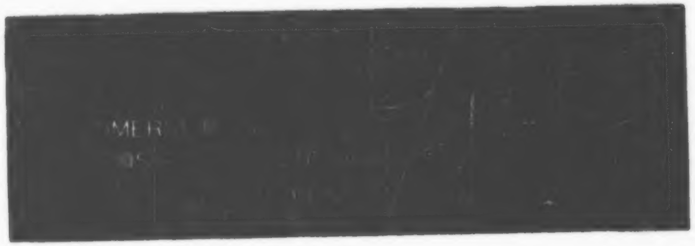

Figure 3.1-11(b)

NOAA satellite imagery, Eastern Parry
Channel, February 25, 1978

Figure 3.1-11(c)

NOAA satellite imagery, Eastern Parry
Channel, March 10, 1978

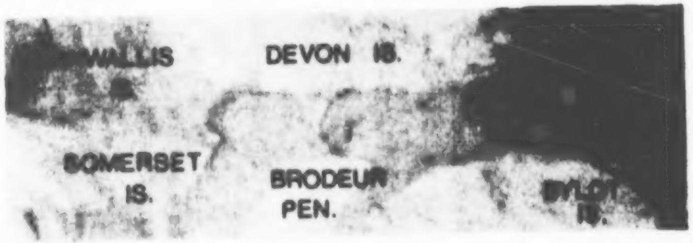
WALLIS
IS.
DEVON IS.
SOMERSET
IS.
BRODEUR
PEN.
BYLOT
IS.

Figure 3.1-11(d)

NOAA satellite imagery, Eastern Parry
Channel, March 26, 1978

Channel ice edge and off the east coast of Devon Island. The extent of the open-water regions produced in the latter areas were limited by the extreme eastern position of the ice edge and the rather slow progress of the Baffin Bay clearing which appeared to be roughly one month behind the "average" process of Appendix 1B. Heavy and moderate concentrations of ice were maintained near the Lancaster Sound entrance by Baffin Bay conditions prior to the mid-July break-up of the Parry Channel ice edge. The portion of this edge which extended to the east along the Bylot Island coastline was particularly long-lived, maintaining substantial concentrations of ice along the Island's north and east coasts, right up to the late September - early October start of new ice growth. The landfast ice shelf along the east coast of Devon Island was also exceptionally persistent, remaining almost completely in place until the early part of August.

The seasonal clearing of Baffin Bay was incomplete in both the central region and along the Baffin Island coastline. Similarly, considerable concentrations of ice remained in central and western Lancaster Sound until freeze-up, tending to concentrate along the southern side of Parry Channel. Ice also continued to be present in significant, time-varying quantities in the major sidearms of Wellington Channel and Prince Regent, Admiralty and Navy Board Inlets.

In 1979, in spite of the relatively small, westward shift of the winter landfast ice edge, generally lighter ice conditions were obtained. This circumstance could have been associated with the more normal progress of the clearing in Baffin Bay and/or favourable wind conditions that led to an earlier (late July) removal of the east Devon Island landfast ice shelf and prevented a persistence of shoreline ice concentrations off Bylot Island beyond mid-August. Continuing movements of ice out of more northern areas kept low-to-moderate concentrations of floes, usually of diameter less than 2 km, close to the east and southeast coasts of Devon Island. Heavy concentrations of floes up to 10 km diameter were also present from late August through much of September along the northern side of central and western Lancaster Sound, reversing the trend of the previous year in which ice tended toward the south shore of Parry Channel.

Heavy ice concentrations were evident throughout the Channel in mid-October, except for a narrow thin-ice or open-water zone near to and paralleling the south coast of Devon Island. The 1979 - 1980 landfast ice edge was stabilized near Prince Leopold Island.

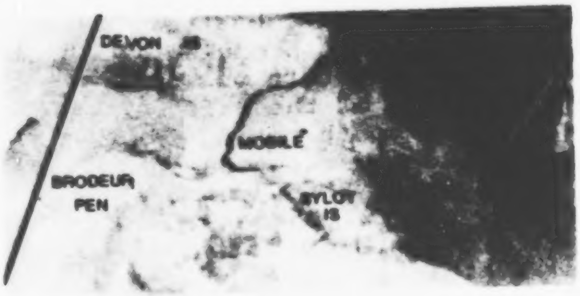
DEVON IS
MOBILE
BRODEUR
PEN
BYLOT
IS

Figure 3.1-12(a)

NOAA satellite imagery, Eastern Parry Channel, November 28, 1978

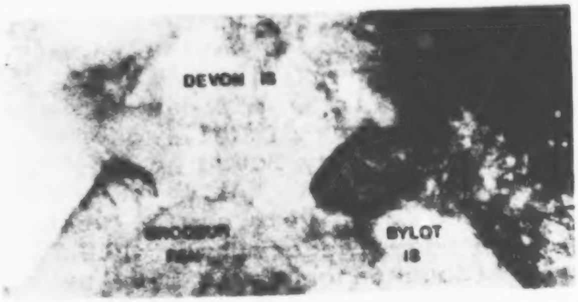
DEVON IS
BRODEUR
PEN
BYLOT
IS

Figure 3.1-12(b)

NOAA satellite imagery, Eastern Parry Channel, January 19, 1979

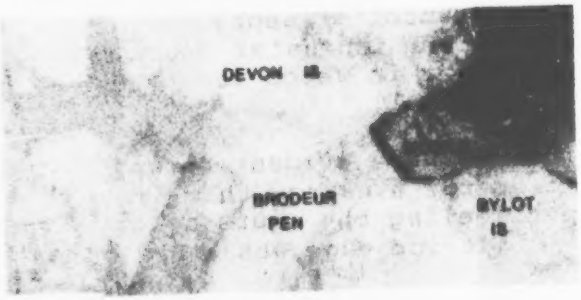
DEVON IS
BRODEUR
PEN
BYLOT
IS

Figure 3.1-12(c)

NOAA satellite imagery, Eastern Parry Channel, February 1, 1979

The above attempts at classification and description of ice seasons according to the corresponding positions of the Parry Channel landfast ice edge suggests an important systematic component of the year-to-year variability in surface conditions. However, little detailed evaluation has thus far been carried out of the degree to which the location and timing of landfast ice stabilizations correlate with larger spatial- and temporal-scale averages of the major environmental parameters of wind, temperature, etc. The alternative possibility, namely that the relevant phenomena occur on much shorter time and space scales would enhance the stochastic character of the winter events and greatly complicate the prediction problem. In any case, there is an obvious need for further study of the stabilization problem requiring careful monitoring of the current, wind and ice regimes at different area locations.

Finally, in the absence of any detailed understanding of the sources of variability, it is appropriate to give some documentation of the observed year-to-year changes in the timing of recongizable annual events. This has been done in Table 3.1.1 and its accompanying glossary.

Table 3.1.1

Approximate timings are given for repeatable annual ice events over the period 1973-1979. The date listed in each case corresponds to the week and month associated with the event in question. More detailed descriptions of the included events are given in the glossary.

	1970	1971	1972	1973	1974	1975	1976	1977	1978	1979	
1.	Formation of permanent Parry Channel ice edge	----	----	----	----	1 Nov 1973	3 Jan	2 Feb	1 Apr	2 Mar	1 Dec
2.	Lancaster Sound ice free (east of edges)	before 4 June	2 July	before 3 June	before 3 June	4 June	4 May	2 June	2 June	1 June	3 June
3.	Breakup of permanent ice edge	1 July	2 July	2 July	1 July	4 July	4 June	1 July	1 July	3 July	3 July
4.	Breakup of Wellington Channel	1 Aug	4 July	3 Aug	3 July	4 July	3 July	2 Aug	4 July	4 Aug	4 Aug
5.	Breakup of Prince Regent Inlet	2 July	4 July	2 Aug	1 Aug	4 July	1 July	3 July	2 July	1 Sept	4 Aug
6.	Breakup of Admiralty Inlet	1 Aug	4 July	2 Aug	1 Aug	4 July	3 July	1 Aug	4 July	2 Aug	4 Aug
7.	Breakup of Navy Board Inlet	2 Aug	4 July	2 Aug	4 July	4 July	3 July	1 Aug	4 July	2 Aug	3 Aug
8.	Breakup of Eclipse Sound	3 Aug	4 July	2 Sept	4 July	4 July	3 July	3 Aug	4 July	2 Aug	2 Aug

Table 3.1.1 (Cont'd)	1970	1971	1972	1973	1974	1975	1976	1977	1978	1979
9. Lady Ann Strait ice free (east of edge)	1 July	4 June	before 3 June	before 3 June	before 3 June	before 3 June	before 2 June	before 2 June	before 1 June	4 June
10. Breakup of N.E. Devon Is. fast ice	2 July	4 June	4 July	4 June	2 July	1 July	4 July	1 Aug	2 Aug	4 July
11. Breakup of Glacier Str.	4 July	4 July	2 Aug	1 Aug	3 July	2 July	4 July	1 Aug	2 Aug	1 Aug
12. Breakup of fast ice Jones Sound edge	2 Sept	4 Aug	never	2 Aug	2 Aug	4 July	3 Aug	1 Aug	1 Sept	4 Aug
13. Breakup of North Philpots Is.	1 Aug	1 Aug	1 Aug	4 June	3 July	3 July	1 Aug	1 Aug	3 Aug	1 Aug
14. Breakup of fast ice South Philpots Is.	1 Aug	3 July	1 Aug	4 June	3 July	3 July	4 July	4 July	3 Aug	4 July
15. Breakup of fast ice Capes Warrender-Sherard	4 July	4 June	before 3 June	4 June	1 July	4 June	1 July	1 July	3 July	2 July
16. Breakup of fast ice Croker Bay	2 Aug	4 July	1 Aug	4 June	4 July	1 July	1 Aug	4 July	1 Sept	3 July
17. Breakup of fast ice Maud Bight (Bylot)	4 July	2 July	3 July	4 July	1 July	1 July	3 July	4 July	2 Aug	4 July

Table 3.1.1 (Cont'd)	1970	1971	1972	1973	1974	1975	1976	1977	1978	1979
18. Breakup of fast ice E. Bylot Is.	2 July	1 Aug	1 July	1 July	1 July	2 July	4 July	1 Aug	2 Aug	4 July
19. Breakup of Pond Inlet	2 Aug	4 July	4 Aug	4 July	4 July	2 July	4 July	4 July	2 Aug	1 Aug
20. Breakup of fast ice Bucham Gulf	1 Aug	2 Aug	2 Aug	1 Aug	4 July	2 July	2 Aug	1 Aug	4 Aug	4 Aug
21. E. Parry Channel Conc. 5/10	3 Aug	3 July	1 Aug	4 July	3 June	2 July	2 June	4 July	2 Sept	never
22. E. Parry Channel conc. 1/10	2 Sept	4 July	1 Aug	1 Au	4 June	3 July	4 June	1 Aug	never	never
23. new ice in Lancaster Sound 8/10	1 Oct	1 Oct	4 Sept	1 Oct	2 Oct	3 Sept	1 Oct	2 Oct	3 Sept	4 Sept
24. Landfast ice in side channels	3 Oct	3 Oct	after 1 Nov	1 Nov	3 Oct	1 Nov	4 Oct	3 Nov	4 Oct	4 Oct

GLOSSARY of event location/description for Table 3.1.1

1. Formation of the permanent winter ice edge across Lancaster Sound or Barrow Strait

2. The area to the east of the permanent ice edge has an ice concentration of less than 1/10.

4.-8. Ice concentration of less than 9/10.

Table 3.1.1 (Cont'd)

9. The area to the east of the permanent ice edge has an ice concentration of less than 1/10.

10.-11. Ice concentration of less than 9/10.

11. See Figure 1.1

12. Ice concentration in Jones Sound less than 5/10.

13.-20. Ice concentration of less than 9/10.

13. Hyde Inlet (See Figure 1.1).

14. Bethune Inlet (See Figure 1.1).

15. South shore of Devon Island-Cape Warrender to Cape Sherard.

17. Between Cape Hay and Cape Liverpool-north shore of Bylot Island.

18. Bathurst Bay to Cape Graham More.

21.-22. Average concentration of ice, east of Cornwallis Island.

24. Admiralty Inlet, Navy Board Inlet, Wellington Channel.

3.2 Ice Characteristics

3.2.1 Thickness and Old Ice Fractions

From the discussion of the previous section (3.1) it is clear that the ice cover of Lancaster Sound and northwest Baffin Bay undergoes almost complete annual replacement even under the heaviest or "worst year in five" seasonal conditions. The local thickness of this cover is a function of the detailed energy balance in the upper water-and ice-layers, which depends upon many factors including the radiant energy input, ice drift speed, accumulated thickness of snow cover, air and water temperature, etc. Experimental data are given in Fig. 3.2-1 for two sheltered sites in the greater Lancaster Sound vicinity. They indicate both the range of year-to-year variability and typical rates of growth which depend to some extent upon measurement locale. A general limit of 2m is appropriate to the study area with an empirical growth curve (Fig. 3.2-2) (NORCOR, 1978) somewhat intermediate to the two experimental curves of Fig. 3.2-1 giving a late May, early June date for the start of the ablation period. Using the relationship

$$h = .55\Sigma\Theta \qquad \text{E.g. 3.2-1}$$

where h = ice thickness in cm and $\Sigma\Theta$ is the accumulated degree days above -1.8°C, Milne and Smiley (1978) found that ice drifting eastward at 15 km/day beginning on July 5 would lose 63 cm before reaching Navy Board Inlet some 17 days later. Under such conditions the original 180 cm typical ice thickness would be reduced to less than 117 cm in the vicinity of the entrance to Baffin Bay.

While "universal" curves of the type indicated in Figures 3.2.1 and 3.2.2 have their use, it is important to recognize the presence of systematic spatial- and time-dependencies in ice thickness and the fractional presence of old ice (ice having survived one or more summer melts). Experimental data on both aspects of the ice environment are hard to come by and much of our knowledge is speculative in nature and derived from the known characteristics of the ice movements.

It is particularly important to distinguish between the distribution of thickness and age obtained: a) in the absence of a cross-channel landfast ice edge and; (b) and (c) in the landfast and moving ice zones lying respectively to the west and east of such an edge.

In case a) the curves of Figure 3.2.2 are likely to be representative of the resulting almost uniformly thick regional ice cover and its old ice component which in Lancaster Sound originates primarily from the Sverdrup Basin (NORCOR, 1978). Some modification of the old ice relationship would be expected in Baffin Bay and in the extreme eastern end of Lancaster Sound where much of the older ice has its origin in Smith and Jones Sounds.

In the presence of a cross-channel landfast ice edge, relationships similar to those of Figure 3.2.2 retain approximate validity only in the immobilized portion of the ice cover (case b). Continuing movement of ice away from the eastern side of this edge should give a zone of moving ice which tends to thicken to the east at least up to the entrance to Baffin Bay. In this situation the shutting off of ice advection at the landfast ice edge also results in a gradual reduction of the old ice fraction in the mobile ice zone. An additional, smaller south to north increase in thickness may also be present in Lancaster Sound as a result of the greater winter drift speeds noted on the southern side of the waterway (Section 3.3). With a typical winter drift speed of 10 km/day ice forming, for example, at the Prince Leopold Island ice edge in March would increase its thickness by 51 cm (Milne and Smiley, 1978) before arriving, some 26 days later, to the north of Navy Board Inlet. Under the described circumstances a mean drift rate varying from 3 km/day to 15 km/day would give a 30 to 150 cm range for ice thickness in eastern Lancaster Sound.

Unfortunately, there are few measurements of offshore ice thickness in the study region available for comparison with these speculations. Some relevant data obtained on the May, 1970 voyage of the SS Manhatten are plotted in Figure 3.2.3 together with a sketch of the corresponding annual landfast ice boundary. Although the position of the latter feature can only be specified with limited accuracy on the basis of primitive satellite imagery, the data generally appear to have been obtained in the mobile ice zone to the east of the indicated boundary. In addition to the indicated range of measurements at each site, considerable site to site variability is evident with the thinnest ice appearing in the western and northwestern sections of the surveyed track, adjoining respectively the westernmost portion of the ice edge and southeastern Devon Island. Interpretation of these data in the light of the foregoing is difficult because of: the absence of information on earlier drift rates; the proximity of the ice edge to Baffin Bay and the general low measurement density. At present the principal import of the data is to confirm the existence of ice of mean thickness well below the typical 2 m regional limit in areas downstream of a landfast ice edge.

The only quantitative information on the fractional presence of old ice in the region study must be obtained from the recorded estimates made since 1959 in the aerial ice surveillance programs of the Atmospheric Environment Service. Although the accuracy of such estimates is somewhat open to question, these data have recently been processed and tabulated by Petro-Canada Ltd. for the period of 1959-1974 (Miller, private communication). They are presented in this report in terms of weekly cumulative probabilities for the occurrence of fractional old ice surface coverage at eleven selected sites (See Figure 3.2.4). As represented in Tables 3.2.1-3.2.11, these probabilities correspond to percentages of years in which the weekly old ice concentration equaled or fell below a given value (in tenths).

Considering first the data at sites #520 and #524 (Tables 3.2.1 and 3.2.2) along the expected principal path of old ice entry, it is seen that in roughly 20% of the years surveyed concentrations exceeded 3/10 in the period preceeding the month of August. In the months August through October percentages of occurrence for 10/10 old ice and concentrations in excess of 3/10 were respectively 23% and 62%. This late season rise in the amounts of old ice corresponds to the heavy outflow from Smith Sound and Kane Basin. A similar breakout is evident in the statistics for sites #540 and #541 (Tables 3.2.3 and 3.2.4) in, and immediately downstream of the Lady Ann Strait exit from Jones Sound. In the week of September 17 the data show a 45% occurrence for old ice concentrations exceeding 3/10.

At sites #557 and #558 off the east coast of Devon Island, the data (Tables 3.2.5 and 3.2.6) show generally lower probabilities for very high concentrations of old ice. In particular large influxes appeared to be most likely at the inshore site #557 where concentrations higher than 6/10 occurred in 20% of the years in late August or early September. Slightly lower concentrations were present with highest consistency during the month of October.

Comparisons of the records at sites 569 and 501 (Tables 3.2.7 and 3.2.8) suggest that the old ice appearing in the records of more northern stations tends to follow the intrusive flow which turns sharply across site #501. Although the overall statistics still show a probability of 30% or less for non-zero concentrations of old ice at the latter site, 10/10 coverage was recorded in 14% of the surveyed years.

At site #502 in the southerly portion of the intrusive flow the data (Table 3.2.9) resemble those obtained at the upstream site #501 generally corresponding to low or negligible concentrations occasionally interrupted in September ("10% probability) by heavy 10/10 fields of old ice.

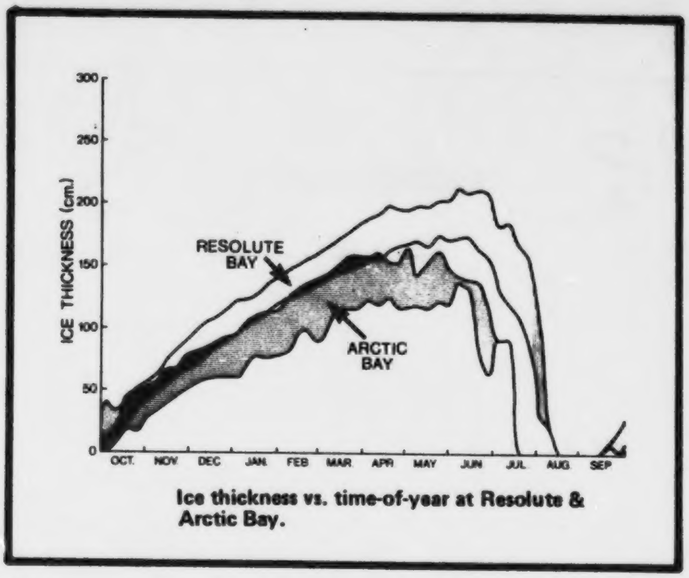

Figure 3.2.1 Ice thickness vs. time-of-year at Resolute and Arctic Bay. Shaded areas indicate year-to-year variability.

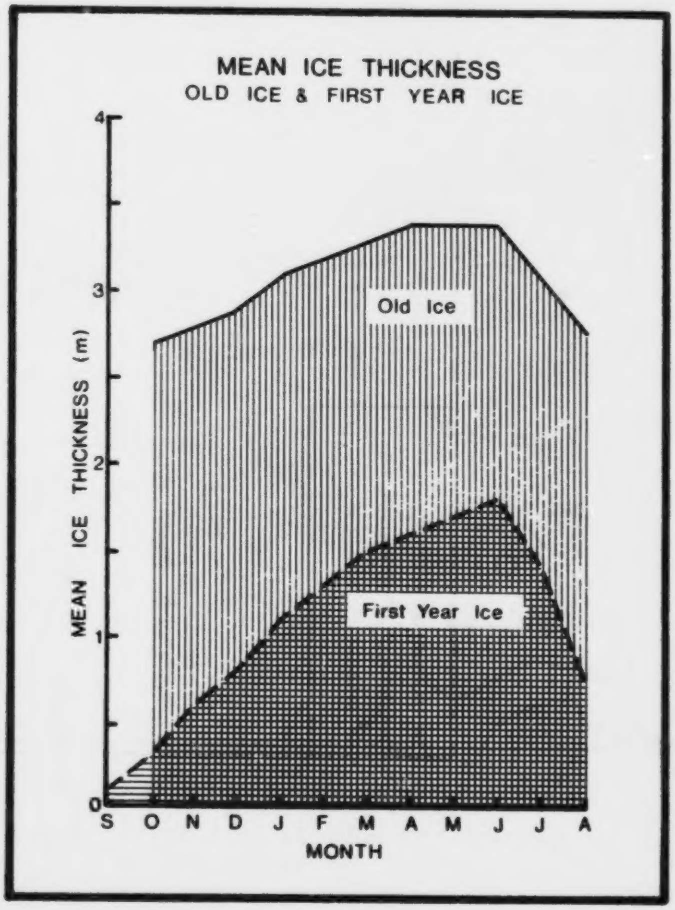

Figure 3.2.2 Theoretical growth curve of ice thickness in study area

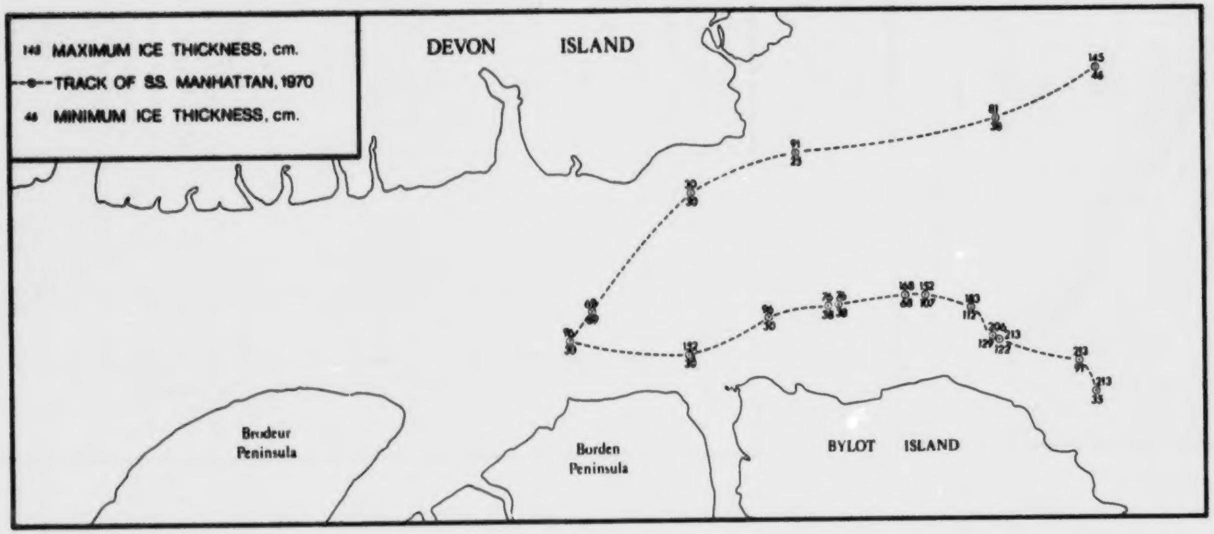
145 MAXIMUM ICE THICKNESS, cm.
TRACK OF S.S. MANHATTAN, 1970
46 MINIMUM ICE THICKNESS, cm.
DEVON ISLAND
Brodeur Peninsula
Borden Peninsula
BYLOT ISLAND
145
46
81
91
23
30
30
152
30
168
152
107
112
206
213
129
122
213
213
35

Figure 3.2.3 Ice thicknesses measured May 2-10, 1970 from the S.S. Manhattan

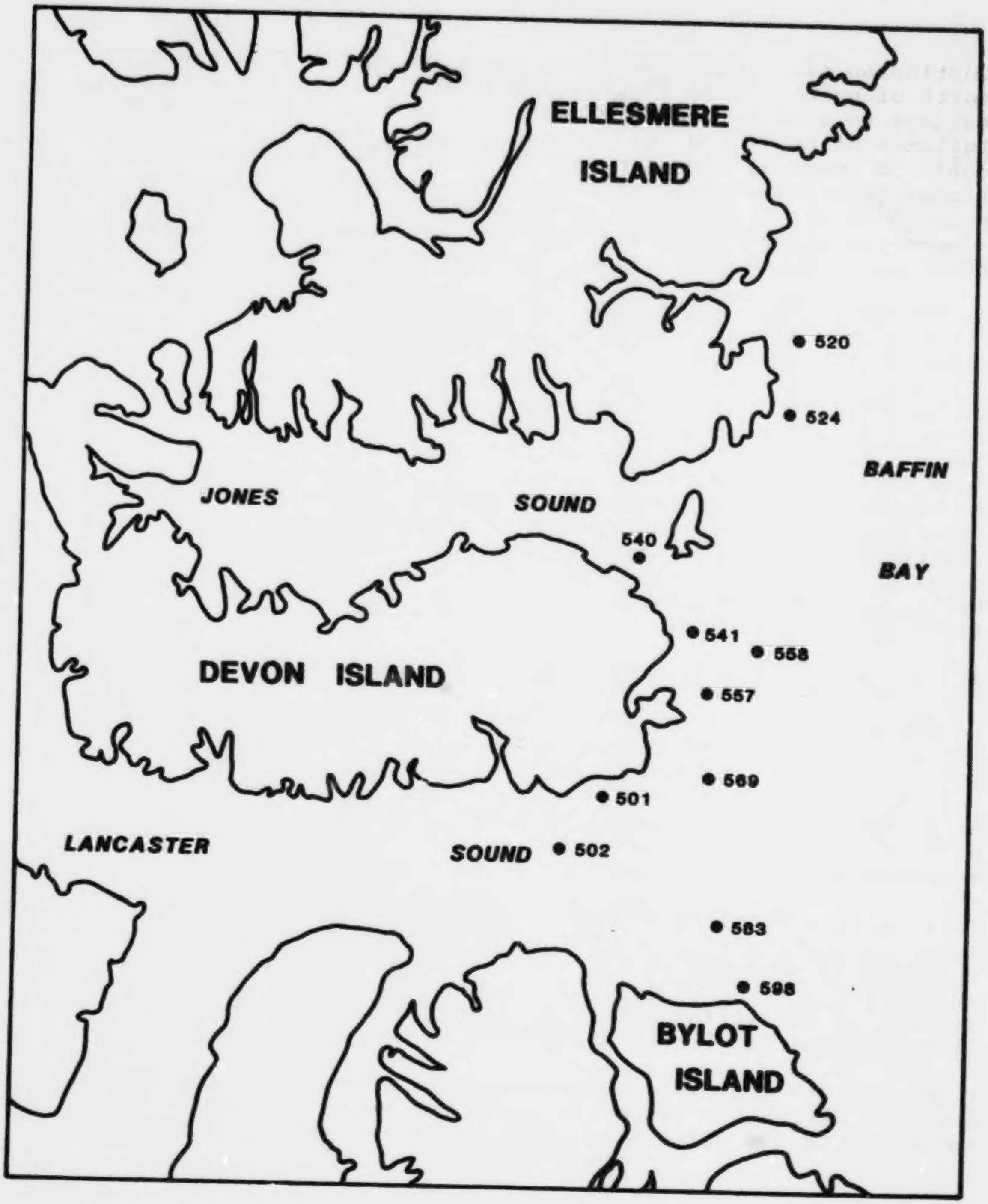
ELLESMERE
ISLAND
520
524
BAFFIN
JONES
SOUND
540
BAY
541
558
DEVON ISLAND
557
569
501
LANCASTER
SOUND
502
583
598
BYLOT
ISLAND

Figure 3.2.4 Location of AES ice survey sites referred to in text

Continuing along with the intrusive flow, sites #583 and #598 north of Bylot Island (Tables 3.2.10 and 3.2.11) are evidently subject to similar, somewhat narrower in time, late September influxes of heavy old ice concentrations. In the following month of October, the recorded concentrations are distinctly higher than those noted at sites #501 and #502 in the upstream portion of the intrusion. It is possible that the additional concentrations of old ice arise from the ice streams which, in the fall, move eastward along the southside of Parry Channel.

In summary, these statistical results, in effect, give a broad outline of the characteristic distributions of old ice in the study area. As indicated above, some questions remain as to the accuracy of the underlying numerical estimates particularly at the lower end of the old ice concentration range. More fundamentally, however, these data are limited in their application to environmental hazard assessment by the loss of spatial resolution inherent in the averaging process. As a result, hazards remain in areas of nominally zero old-ice fractions because of the spatial inhomogeneity of the ice distribution and the detectibility limits of aerial observation. To our knowledge no data are available on typical background levels of old ice present in nominally first year ice fields.

3.2.2 Typical Ice Pack Configurations and Floe Sizes

In the preceeding discussions, the regional distribution of ice has been considered largely in terms of mappings of the local fractional surface covered by floating ice. The resulting simplifications, necessary for tractability, effectively neglected details, such as ice pack shape and make-up in terms of floe sizes, which are almost certainly relevant to a description of the ice environment.

This deficiency is addressed in the present subsection in terms of examples of the most common physical ice pack features as observed in the Landsat satellite imagery and a very brief listing of data taken from AES aerial observer records of the surface coverage fraction associated with "large" floes (of linear dimensions in excess of 100 m).

Figures 3.2.5 and 3.2.6 contain typical examples of two common features designated respectively as ice belts and ice spirals. In the first instance, ice belts tend to be observed

BAFFIN BAY

ICE CONCENTRATION - OLD ICE
SITE = 520

CUMULATIVE PROBABILITY

1959 - 1974

0	1	2	3	4	5	6	7	8	9	10	DATE
50	50	63	88	88	88	88	100	100	100	100	May 21
43	71	86	100	100	100	100	100	100	100	100	May 28
50	75	100	100	100	100	100	100	100	100	100	Jun 04
38	63	75	88	88	88	88	100	100	100	100	Jun 11
56	67	78	78	78	100	100	100	100	100	100	Jun 18
100	100	100	100	100	100	100	100	100	100	100	Jun 25
100	100	100	100	100	100	100	100	100	100	100	Jul 02
82	82	82	100	100	100	100	100	100	100	100	Jul 09
91	91	91	91	91	91	91	100	100	100	100	Jul 16
69	69	69	77	77	85	85	92	100	100	100	Jul 23
62	69	69	69	69	77	77	85	92	92	100	Jul 30
47	47	47	60	73	80	87	93	93	93	100	Aug 06
43	50	50	57	64	71	71	79	93	100	100	Aug 13
36	36	36	57	57	71	71	71	79	86	100	Aug 20
50	50	50	64	64	64	71	71	79	93	100	Aug 27
38	38	38	38	46	54	69	69	69	77	100	Sep 03
50	50	50	50	67	67	83	83	92	92	100	Sep 10
23	23	23	69	69	77	85	85	92	100	100	Sep 17
23	23	23	38	46	46	69	69	85	85	100	Sep 24
7	7	7	21	43	57	71	71	86	100	100	Oct 01
21	21	21	43	57	57	79	86	100	100	100	Oct 08
9	9	9	36	55	64	82	91	91	100	100	Oct 15
17	17	17	42	50	67	92	92	100	100	100	Oct 22
18	18	27	36	55	82	91	100	100	100	100	Oct 29

Table 3.2.1 Weekly cumulative probabilities for the occurrence of fractional old ice surface coverage - Site 520. Probabilities correspond to percentages of years in which the weekly old ice concentration equaled or fell below a given value (in tenths)

ICE CONCENTRATION - OLD ICE

BAFFIN BAY

SITE = 524

CUMULATIVE PROBABILITY

1959 - 1974

0	1	2	3	4	5	6	7	8	9	10	DATE
86	100	100	100	100	100	100	100	100	100	100	May 21
63	75	75	88	88	100	100	100	100	100	100	May 28
86	100	100	100	100	100	100	100	100	100	100	Jun 04
90	100	100	100	100	100	100	100	100	100	100	Jun 11
73	73	73	82	82	100	100	100	100	100	100	Jun 18
80	80	90	90	90	100	100	100	100	100	100	Jun 25
86	100	100	100	100	100	100	100	100	100	100	Jul 02
100	100	100	100	100	100	100	100	100	100	100	Jul 09
92	92	92	92	92	92	92	100	100	100	100	Jul 16
87	87	87	93	93	100	100	100	100	100	100	Jul 23
93	93	93	93	93	93	93	93	100	100	100	Jul 30
75	75	83	83	83	92	100	100	100	100	100	Aug 06
58	67	75	83	83	83	83	83	92	92	100	Aug 13
46	46	46	54	54	77	77	77	85	85	100	Aug 20
53	53	60	67	67	67	80	80	80	87	100	Aug 27
36	36	36	36	64	71	79	79	79	79	100	Sep 03
58	58	58	58	75	75	83	83	92	92	100	Sep 10
15	15	15	46	54	62	69	77	77	85	100	Sep 17
36	36	36	43	50	57	79	79	86	86	100	Sep 24
8	8	8	31	54	77	85	85	85	100	100	Oct 01
27	27	33	53	60	60	73	87	100	100	100	Oct 08
8	8	17	33	50	75	83	92	92	100	100	Oct 15
14	14	21	43	57	71	93	93	100	100	100	Oct 22
17	33	42	42	58	100	100	100	100	100	100	Oct 29

Table 3.2.2 Weekly cumulative probabilities for the occurrence of fractional old ice surface coverage - Site 524

ICE CONCENTRATION - OLD ICE

BAFFIN BAY SITE = 540

CUMULATIVE PROBABILITY 1959 - 1974

0	1	2	3	4	5	6	7	8	9	10	DATE
80	90	90	90	90	100	100	100	100	100	100	May 21
89	89	89	100	100	100	100	100	100	100	100	May 28
100	100	100	100	100	100	100	100	100	100	100	Jun 04
100	100	100	100	100	100	100	100	100	100	100	Jun 11
90	90	90	90	90	90	90	90	90	90	100	Jun 18
100	100	100	100	100	100	100	100	100	100	100	Jun 25
90	100	100	100	100	100	100	100	100	100	100	Jul 02
91	100	100	100	100	100	100	100	100	100	100	Jul 09
93	100	100	100	100	100	100	100	100	100	100	Jul 16
100	100	100	100	100	100	100	100	100	100	100	Jul 23
93	93	93	93	100	100	100	100	100	100	100	Jul 30
87	87	87	93	100	100	100	100	100	100	100	Aug 06
93	93	100	100	100	100	100	100	100	100	100	Aug 13
87	87	87	87	87	100	100	100	100	100	100	Aug 20
73	73	73	73	73	80	87	87	87	87	100	Aug 27
80	80	80	80	80	80	80	87	87	87	100	Sep 03
93	93	93	93	93	93	93	93	100	100	100	Sep 10
36	45	45	55	73	73	73	73	73	91	100	Sep 17
69	69	69	69	77	85	85	85	85	85	100	Sep 24
31	31	38	62	77	77	92	92	92	100	100	Oct 01
27	40	40	60	60	67	73	93	93	100	100	Oct 08
38	46	69	77	85	92	100	100	100	100	100	Oct 15
21	36	57	79	79	93	100	100	100	100	100	Oct 22
45	45	64	82	100	100	100	100	100	100	100	Oct 29

Table 3.2.3 Weekly cumulative probabilities for the occurrence of fractional old ice surface coverage - Site 540

ICE CONCENTRATION - OLD ICE

BAFFIN BAY

SITE = 541

CUMULATIVE PROBABILITY

1959 - 1974

0	1	2	3	4	5	6	7	8	9	10	DATE
89	89	89	89	100	100	100	100	100	100	100	May 21
100	100	100	100	100	100	100	100	100	100	100	May 28
100	100	100	100	100	100	100	100	100	100	100	Jun 04
100	100	100	100	100	100	100	100	100	100	100	Jun 11
100	100	100	100	100	100	100	100	100	100	100	Jun 18
100	100	100	100	100	100	100	100	100	100	100	Jun 25
100	100	100	100	100	100	100	100	100	100	100	Jul 02
100	100	100	100	100	100	100	100	100	100	100	Jul 09
100	100	100	100	100	100	100	100	100	100	100	Jul 16
100	100	100	100	100	100	100	100	100	100	100	Jul 23
93	93	93	93	100	100	100	100	100	100	100	Jul 30
87	87	87	93	100	100	100	100	100	100	100	Aug 06
100	100	100	100	100	100	100	100	100	100	100	Aug 13
93	93	93	93	93	100	100	100	100	100	100	Aug 20
80	80	80	80	80	80	87	87	87	87	100	Aug 27
87	87	87	87	87	87	87	93	93	93	100	Sep 03
93	93	93	93	93	93	93	93	93	93	100	Sep 10
58	58	58	67	67	67	75	75	75	75	100	Sep 17
71	71	71	71	79	79	86	86	86	86	100	Sep 24
50	57	57	71	71	71	86	86	93	100	100	Oct 01
33	47	47	67	73	80	87	100	100	100	100	Oct 08
38	46	62	69	77	85	92	100	100	100	100	Oct 15
7	21	43	71	71	86	100	100	100	100	100	Oct 22
36	45	64	73	91	100	100	100	100	100	100	Oct 29

Table 3.2.4 Weekly cumulative probabilities for the occurrence of fractional old ice surface coverage - Site 541

ICE CONCENTRATION - OLD ICE

BAFFIN BAY SITE = 557

CUMULATIVE PROBABILITY 1959 - 1974

0	1	2	3	4	5	6	7	8	9	10	DATE
71	86	86	86	100	100	100	100	100	100	100	May 21
100	100	100	100	100	100	100	100	100	100	100	May 28
100	100	100	100	100	100	100	100	100	100	100	Jun 04
100	100	100	100	100	100	100	100	100	100	100	Jun 11
100	100	100	100	100	100	100	100	100	100	100	Jun 18
100	100	100	100	100	100	100	100	100	100	100	Jun 25
100	100	100	100	100	100	100	100	100	100	100	Jul 02
100	100	100	100	100	100	100	100	100	100	100	Jul 09
93	100	100	100	100	100	100	100	100	100	100	Jul 16
100	100	100	100	100	100	100	100	100	100	100	Jul 23
93	93	93	93	100	100	100	100	100	100	100	Jul 30
100	100	100	100	100	100	100	100	100	100	100	Aug 06
93	93	100	100	100	100	100	100	100	100	100	Aug 13
93	93	93	93	93	100	100	100	100	100	100	Aug 20
87	87	87	87	87	87	93	93	93	93	100	Aug 27
80	80	80	80	80	80	80	87	87	87	100	Sep 03
93	93	93	93	100	100	100	100	100	100	100	Sep 10
77	77	77	77	77	92	92	92	92	92	100	Sep 17
64	64	64	64	79	79	86	86	86	86	100	Sep 24
57	64	64	79	79	79	93	93	93	100	100	Oct 01
36	50	50	71	79	86	93	100	100	100	100	Oct 08
31	31	46	54	69	77	85	92	100	100	100	Oct 15
14	43	57	71	71	79	100	100	100	100	100	Oct 22
45	55	73	82	100	100	100	100	100	100	100	Oct 29

Table 3.2.5 Weekly cumulative probabilities for the occurrence of fractional old ice surface coverage - Site 557

ICE CONCENTRATION - OLD ICE

BAFFIN BAY

SITE = 558

CUMULATIVE PROBABILITY

1959 - 1974

0	1	2	3	4	5	6	7	8	9	10	DATE
88	88	88	88	100	100	100	100	100	100	100	May 21
100	100	100	100	100	100	100	100	100	100	100	May 28
100	100	100	100	100	100	100	100	100	100	100	Jun 04
100	100	100	100	100	100	100	100	100	100	100	Jun 11
100	100	100	100	100	100	100	100	100	100	100	Jun 18
92	92	92	92	92	100	100	100	100	100	100	Jun 25
92	92	92	100	100	100	100	100	100	100	100	Jul 02
100	100	100	100	100	100	100	100	100	100	100	Jul 09
93	100	100	100	100	100	100	100	100	100	100	Jul 16
100	100	100	100	100	100	100	100	100	100	100	Jul 23
100	100	100	100	100	100	100	100	100	100	100	Jul 30
100	100	100	100	100	100	100	100	100	100	100	Aug 06
100	100	100	100	100	100	100	100	100	100	100	Aug 13
100	100	100	100	100	100	100	100	100	100	100	Aug 20
100	100	100	100	100	100	100	100	100	100	100	Aug 27
100	100	100	100	100	100	100	100	100	100	100	Sep 03
100	100	100	100	100	100	100	100	100	100	100	Sep 10
100	100	100	100	100	100	100	100	100	100	100	Sep 17
80	80	80	80	80	80	87	87	87	87	100	Sep 24
93	93	93	100	100	100	100	100	100	100	100	Oct 01
50	64	64	79	86	93	100	100	100	100	100	Oct 08
40	40	40	70	80	90	100	100	100	100	100	Oct 15
29	43	64	79	79	79	100	100	100	100	100	Oct 22
36	55	64	73	91	100	100	100	100	100	100	Oct 29

Table 3.2.6 Weekly cumulative probabilities for the occurrence of fractional old ice surface coverage - Site 558

ICE CONCENTRATION - OLD ICE

BAFFIN BAY SITE = 569

CUMULATIVE PROBABILITY 1959 - 1974

0	1	2	3	4	5	6	7	8	9	10	DATE
88	100	100	100	100	100	100	100	100	100	100	May 21
100	100	100	100	100	100	100	100	100	100	100	May 28
100	100	100	100	100	100	100	100	100	100	100	Jun 04
91	100	100	100	100	100	100	100	100	100	100	Jun 11
82	91	91	100	100	100	100	100	100	100	100	Jun 18
92	92	92	92	92	100	100	100	100	100	100	Jun 25
92	92	92	100	100	100	100	100	100	100	100	Jul 02
83	92	92	100	100	100	100	100	100	100	100	Jul 09
100	100	100	100	100	100	100	100	100	100	100	Jul 16
100	100	100	100	100	100	100	100	100	100	100	Jul 23
100	100	100	100	100	100	100	100	100	100	100	Jul 30
100	100	100	100	100	100	100	100	100	100	100	Aug 06
100	100	100	100	100	100	100	100	100	100	100	Aug 13
100	100	100	100	100	100	100	100	100	100	100	Aug 20
100	100	100	100	100	100	100	100	100	100	100	Aug 27
100	100	100	100	100	100	100	100	100	100	100	Sep 03
100	100	100	100	100	100	100	100	100	100	100	Sep 10
100	100	100	100	100	100	100	100	100	100	100	Sep 17
93	93	93	93	93	93	93	93	93	93	100	Sep 24
93	93	93	100	100	100	100	100	100	100	100	Oct 01
71	79	79	86	86	93	100	100	100	100	100	Oct 08
55	55	64	82	100	100	100	100	100	100	100	Oct 15
36	50	79	86	86	86	100	100	100	100	100	Oct 22
33	75	83	92	92	100	100	100	100	100	100	Oct 29

Table 3.2.7 Weekly cumulative probabilities for the occurrence of fractional old ice surface coverage - Site 569

ICE CONCENTRATION - OLD ICE

BAFFIN BAY

SITE = 501

CUMULATIVE PROBABILITY

1959 - 1974

0	1	2	3	4	5	6	7	8	9	10	DATE
83	100	100	100	100	100	100	100	100	100	100	May 21
100	100	100	100	100	100	100	100	100	100	100	May 28
100	100	100	100	100	100	100	100	100	100	100	Jun 04
85	92	100	100	100	100	100	100	100	100	100	Jun 11
92	100	100	100	100	100	100	100	100	100	100	Jun 18
100	100	100	100	100	100	100	100	100	100	100	Jun 25
100	100	100	100	100	100	100	100	100	100	100	Jul 02
100	100	100	100	100	100	100	100	100	100	100	Jul 09
100	100	100	100	100	100	100	100	100	100	100	Jul 16
100	100	100	100	100	100	100	100	100	100	100	Jul 23
100	100	100	100	100	100	100	100	100	100	100	Jul 30
100	100	100	100	100	100	100	100	100	100	100	Aug 06
94	94	94	100	100	100	100	100	100	100	100	Aug 13
100	100	100	100	100	100	100	100	100	100	100	Aug 20
93	93	100	100	100	100	100	100	100	100	100	Aug 27
93	93	93	93	93	93	93	93	93	93	100	Sep 03
86	86	86	86	86	86	86	86	86	86	100	Sep 10
86	86	86	86	86	93	93	93	93	93	100	Sep 17
87	87	87	87	87	87	93	93	93	93	100	Sep 24
87	87	87	87	87	87	100	100	100	100	100	Oct 01
69	77	77	85	92	92	92	92	100	100	100	Oct 08
82	91	91	91	100	100	100	100	100	100	100	Oct 15
79	93	100	100	100	100	100	100	100	100	100	Oct 22
83	100	100	100	100	100	100	100	100	100	100	Oct 29

Table 3.2.8 Weekly cumulative probabilities for the occurrence of fractional old ice surface coverage - Site 501

ICE CONCENTRATION - OLD ICE

BAFFIN BAY SITE = 502

CUMULATIVE PROBABILITY 1959 - 1974

0	1	2	3	4	5	6	7	8	9	10	DATE
88	100	100	100	100	100	100	100	100	100	100	May 21
100	100	100	100	100	100	100	100	100	100	100	May 28
100	100	100	100	100	100	100	100	100	100	100	Jun 04
90	100	100	100	100	100	100	100	100	100	100	Jun 11
83	92	92	100	100	100	100	100	100	100	100	Jun 18
100	100	100	100	100	100	100	100	100	100	100	Jun 25
100	100	100	100	100	100	100	100	100	100	100	Jul 02
92	100	100	100	100	100	100	100	100	100	100	Jul 09
100	100	100	100	100	100	100	100	100	100	100	Jul 16
100	100	100	100	100	100	100	100	100	100	100	Jul 23
100	100	100	100	100	100	100	100	100	100	100	Jul 30
93	93	93	93	93	100	100	100	100	100	100	Aug 06
100	100	100	100	100	100	100	100	100	100	100	Aug 13
100	100	100	100	100	100	100	100	100	100	100	Aug 20
93	93	93	93	93	93	93	93	100	100	100	Aug 27
100	100	100	100	100	100	100	100	100	100	100	Sep 03
100	100	100	100	100	100	100	100	100	100	100	Sep 10
86	86	86	86	86	86	86	86	86	86	100	Sep 17
87	87	87	87	87	87	93	93	93	93	100	Sep 24
93	93	93	93	93	93	100	100	100	100	100	Oct 01
77	85	85	85	92	92	92	92	100	100	100	Oct 08
80	100	100	100	100	100	100	100	100	100	100	Oct 15
77	85	100	100	100	100	100	100	100	100	100	Oct 22
67	92	100	100	100	100	100	100	100	100	100	Oct 29

Table 3.2.9 Weekly cumulative probabilities for the occurrence of fractional old ice surface coverage - Site 502

ICE CONCENTRATION - OLD ICE

BAFFIN BAY

SITE = 583

CUMULATIVE PROBABILITY

1959 - 1974

0	1	2	3	4	5	6	7	8	9	10	DATE
88	100	100	100	100	100	100	100	100	100	100	May 21
100	100	100	100	100	100	100	100	100	100	100	May 28
100	100	100	100	100	100	100	100	100	100	100	Jun 04
91	100	100	100	100	100	100	100	100	100	100	Jun 11
80	90	90	100	100	100	100	100	100	100	100	Jun 18
92	92	92	92	92	100	100	100	100	100	100	Jun 25
92	92	92	100	100	100	100	100	100	100	100	Jul 02
92	92	92	100	100	100	100	100	100	100	100	Jul 09
100	100	100	100	100	100	100	100	100	100	100	Jul 16
100	100	100	100	100	100	100	100	100	100	100	Jul 23
100	100	100	100	100	100	100	100	100	100	100	Jul 30
100	100	100	100	100	100	100	100	100	100	100	Aug 06
100	100	100	100	100	100	100	100	100	100	100	Aug 13
100	100	100	100	100	100	100	100	100	100	100	Aug 20
100	100	100	100	100	100	100	100	100	100	100	Aug 27
100	100	100	100	100	100	100	100	100	100	100	Sep 03
100	100	100	100	100	100	100	100	100	100	100	Sep 10
100	100	100	100	100	100	100	100	100	100	100	Sep 17
88	88	88	88	88	88	88	88	88	88	100	Sep 24
80	80	80	87	87	87	87	87	100	100	100	Oct 01
75	75	75	83	92	100	100	100	100	100	100	Oct 08
55	73	73	73	91	100	100	100	100	100	100	Oct 15
43	50	79	86	86	93	100	100	100	100	100	Oct 22
42	75	83	92	92	92	100	100	100	100	100	Oct 29

Table 3.2.10 Weekly cumulative probabilities for the occurrence of fractional old ice surface coverage - Site 583

ICE CONCENTRATION - OLD ICE

BAFFIN BAY SITE = 598

CUMULATIVE PROBABILITY 1959 - 1974

0	1	2	3	4	5	6	7	8	9	10	DATE
86	100	100	100	100	100	100	100	100	100	100	May 21
100	100	100	100	100	100	100	100	100	100	100	May 28
100	100	100	100	100	100	100	100	100	100	100	Jun 04
80	100	100	100	100	100	100	100	100	100	100	Jun 11
80	90	90	100	100	100	100	100	100	100	100	Jun 18
82	82	82	91	91	100	100	100	100	100	100	Jun 25
92	92	92	100	100	100	100	100	100	100	100	Jul 02
85	85	85	92	92	100	100	100	100	100	100	Jul 09
92	92	100	100	100	100	100	100	100	100	100	Jul 16
100	100	100	100	100	100	100	100	100	100	100	Jul 23
100	100	100	100	100	100	100	100	100	100	100	Jul 30
93	93	93	93	93	100	100	100	100	100	100	Aug 06
100	100	100	100	100	100	100	100	100	100	100	Aug 13
100	100	100	100	100	100	100	100	100	100	100	Aug 20
100	100	100	100	100	100	100	100	100	100	100	Aug 27
100	100	100	100	100	100	100	100	100	100	100	Sep 03
100	100	100	100	100	100	100	100	100	100	100	Sep 10
100	100	100	100	100	100	100	100	100	100	100	Sep 17
88	94	94	94	94	94	94	94	94	94	100	Sep 24
80	87	87	93	93	93	93	93	100	100	100	Oct 01
79	79	79	79	86	93	93	93	93	93	100	Oct 08
55	64	64	64	82	91	100	100	100	100	100	Oct 15
43	50	79	86	86	93	100	100	100	100	100	Oct 22
50	83	92	92	92	92	100	100	100	100	100	Oct 29

Table 3.2.11 Weekly cumulative probabilities for the occurrence of fractional old ice surface coverage - Site 598

in the high speed cores of the regional near-surface current systems. Their shorter, cross-correct linear dimensions typically range from a fraction of a kilometer upward to 10 km. As indicated in the satellite imagery the long dimensions of the features can be one hundred or more kilometers. Such features are particularly common in September and October, when with the prevalence of higher old ice concentrations, these features can become major navigational and operational obstacles.

Much in the same manner that ice belts tend to be associated with regions of strong and unidirectional water flow, ice spirals are generally noted in areas of characteristically weak and variable surface currents. The spirals usually have a net drift and generally maintain their form for periods of at least three to four days (see the sequence of Figure 3.2.7) and, undoubtedly, correspond closely to the looping portions of the berg and drogued drifter trajectories noted in Section 3.4, and in Fissel et al (1980).

For convenience in its operational planning programs, Petro-Canada Ltd. has adopted a more specific classification scheme to allow simple representations of the encountered sea ice features. These categories are as follows:

1. Ice Fields: areas of pack ice consisting of floes, of any size, in concentrations of 3/10 or greater and whose areal coverage exceeds 100 km^2.
2. Ice Patches: Isolated collections of pack ice of area less than 100 km^2 and concentration equal to or in excess of 3/10.
3. Ice Belts: A region of pack ice exhibiting linear geometry with length being at least 5 times its transverse dimension. Minimum concentration and area requirements are 3/10 and 100 km^2 respectively.
4. Individual Floes: Any unique or identifiable floe or collection of ice in concentrations less than 3/10.
5. Ice Strip: A region of pack ice with the above characteristics of an ice-belt but of area less than 100 km^2.

The distinctions between categories are of course arbitrary and represent a rather gross attempt to represent an unlimited continuum of ice configurations for modelling and assessment purposes.

Unfortunately, there is little historical data available to allow estimates of frequency or composition (in terms of component floe size) for these features. Floe size data are particularly critical to operational evaluations since this parameter determines to a large extent the working modes of transport and drilling vessels.

The relevant information in this respect is available from the AES aerial data survey in terms of weekly listings of the fractional surface coverage due to "medium" floes, i.e. of linear dimensions in excess of 100 m. These data have been processed in terms of the accumulated probability format used above in describing the fractional presence of old ice. We have chosen here to represent a small portion of the data in terms of the percentage probabilities for exceeding respectively the 3/10 and 8/10 levels of surface coverage. Data are included for site #520 along the major northern path of ice approach (Figure 3.2.8), at site #502 in the southerly segment of the Lancaster Sound intrusion (Figure 3.2.9), and at site #598 in the easterly current region north of Bylot Island (Figure 3.2.10). As in the case of the overall ice coverage statistics, the northern site #520 clearly experiences the heaviest concentrations of larger floes. The probability is close to unity for complete coverage prior to mid-June and falls to only 50% for coverage in excess of the 3/10 level over the remainder of the summer and fall seasons. At the Lancaster Sound site #502, the probability for heavy (7-8/10) coverage by large floes remains low or negligible throughout the included May-October period (Figure 3.2.9). The 3/10 or moderate level of coverage appears to be significant (72%), only outside of the mid-July to October interval. Higher probabilities of both heavy and moderate floe coverage are evident (Figure 3.2.10) at site #598 possibly due to preferential movement along the south side of Parry Channel for floes arising from the initial breakup of the coastal and main channel landfast ice packs.

Further analysis of such statistics is unlikely to contribute significantly to the regional ice characterization. The classification relative to the 100 m floe dimension is too crude to be of much use in assessing impact. Greater interest

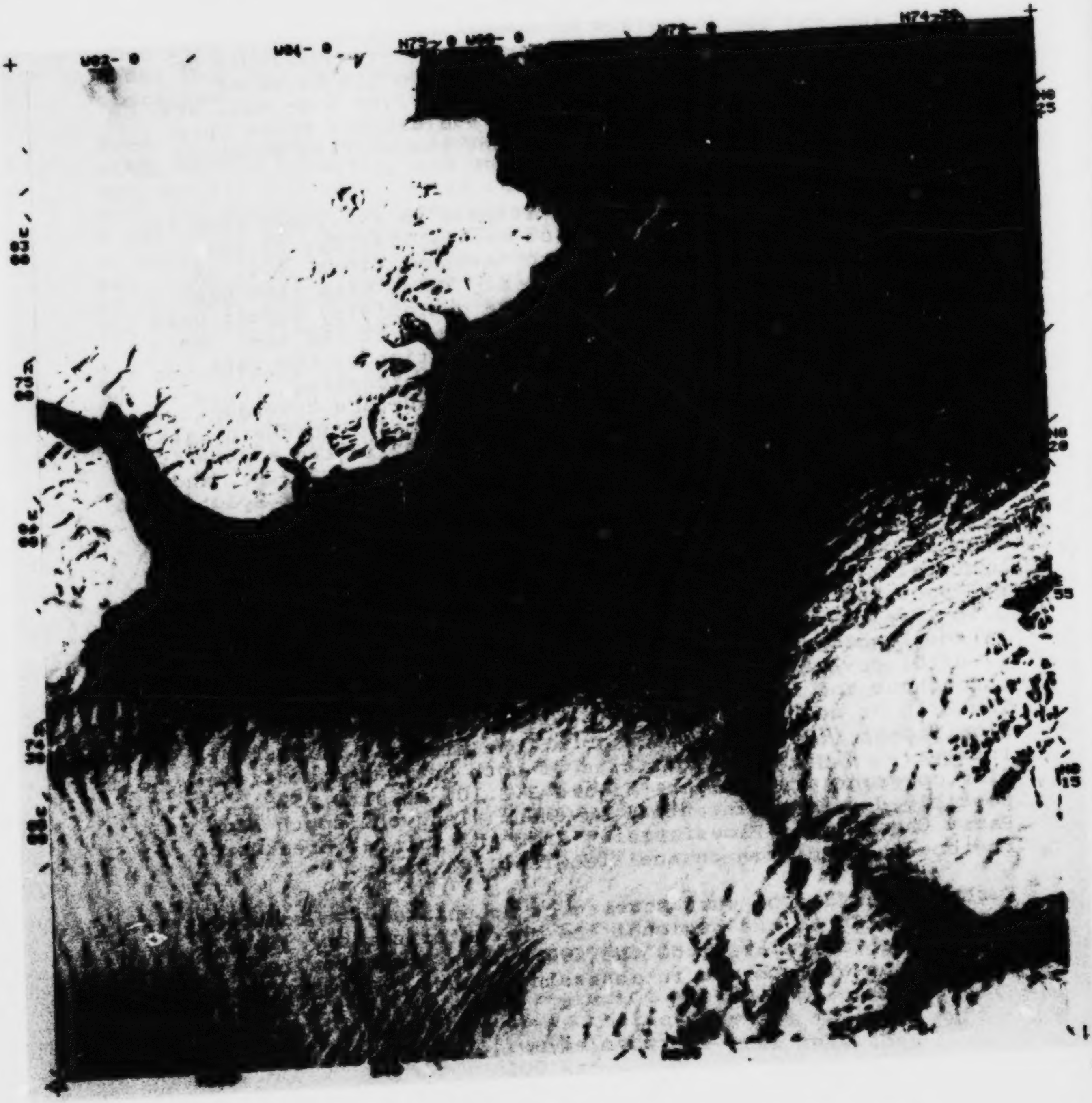

Figure 3:2.5 Landsat imagery, Sept. 17, 1977, showing an ice belt

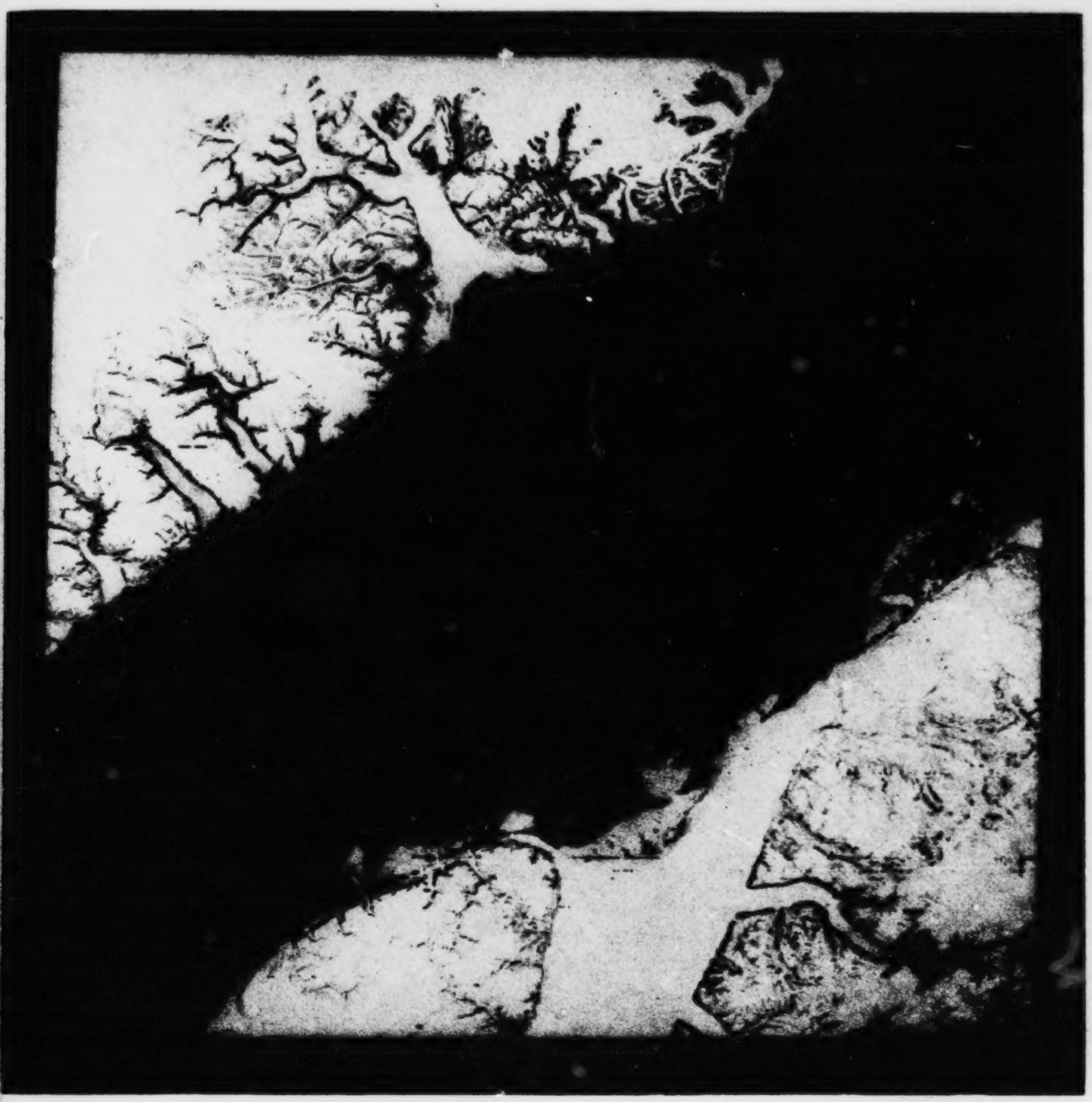

Figure 3.2.6 Landsat imagery, June 9, 1974, showing an ice spiral

Figure 3.2.7(a) Landsat imagery, June 20, 1974, eastern Lancaster Sound

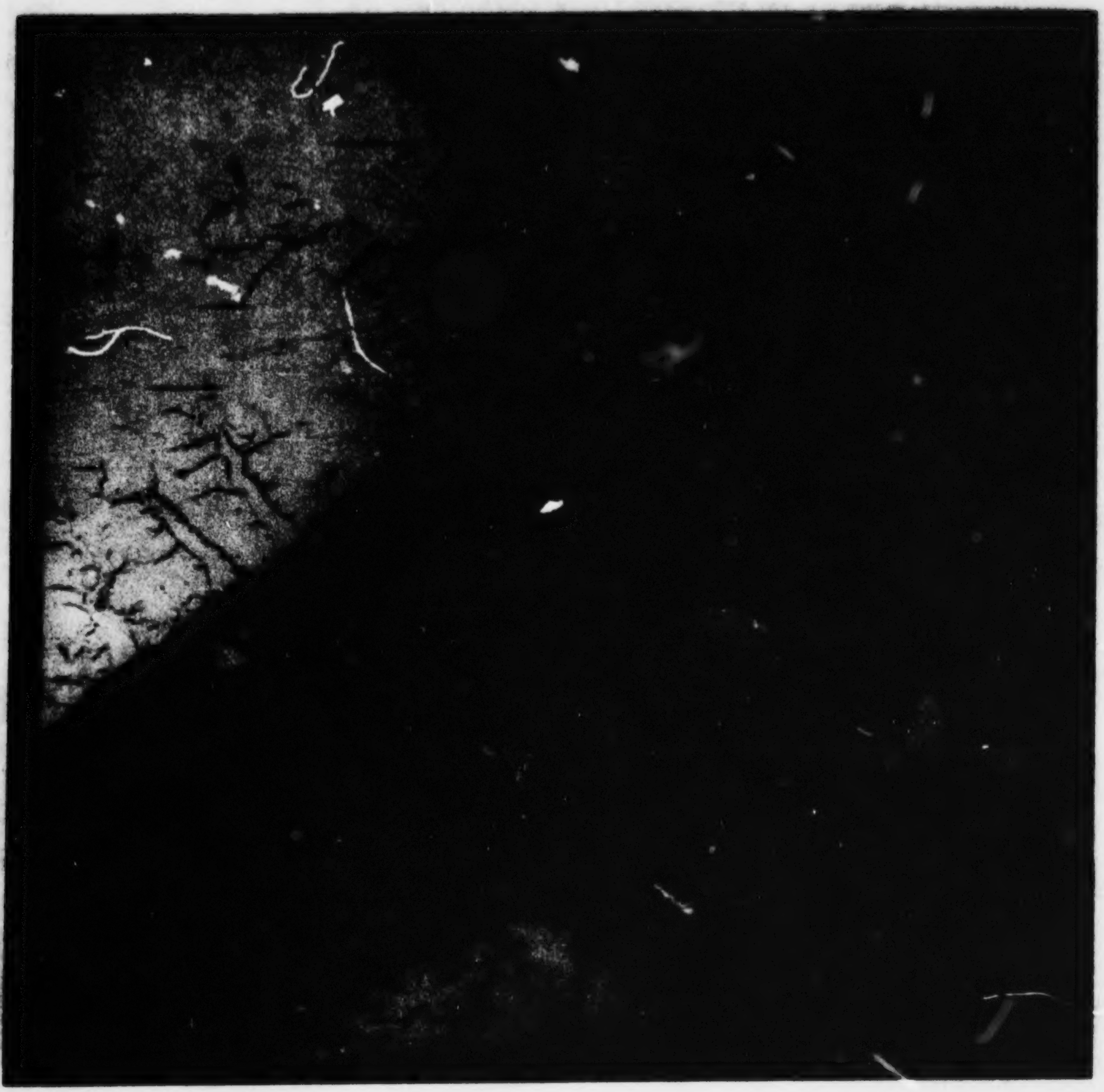

Figure 3.2.7(b) Landsat imagery, June 21, 1974, eastern Lancaster Sound

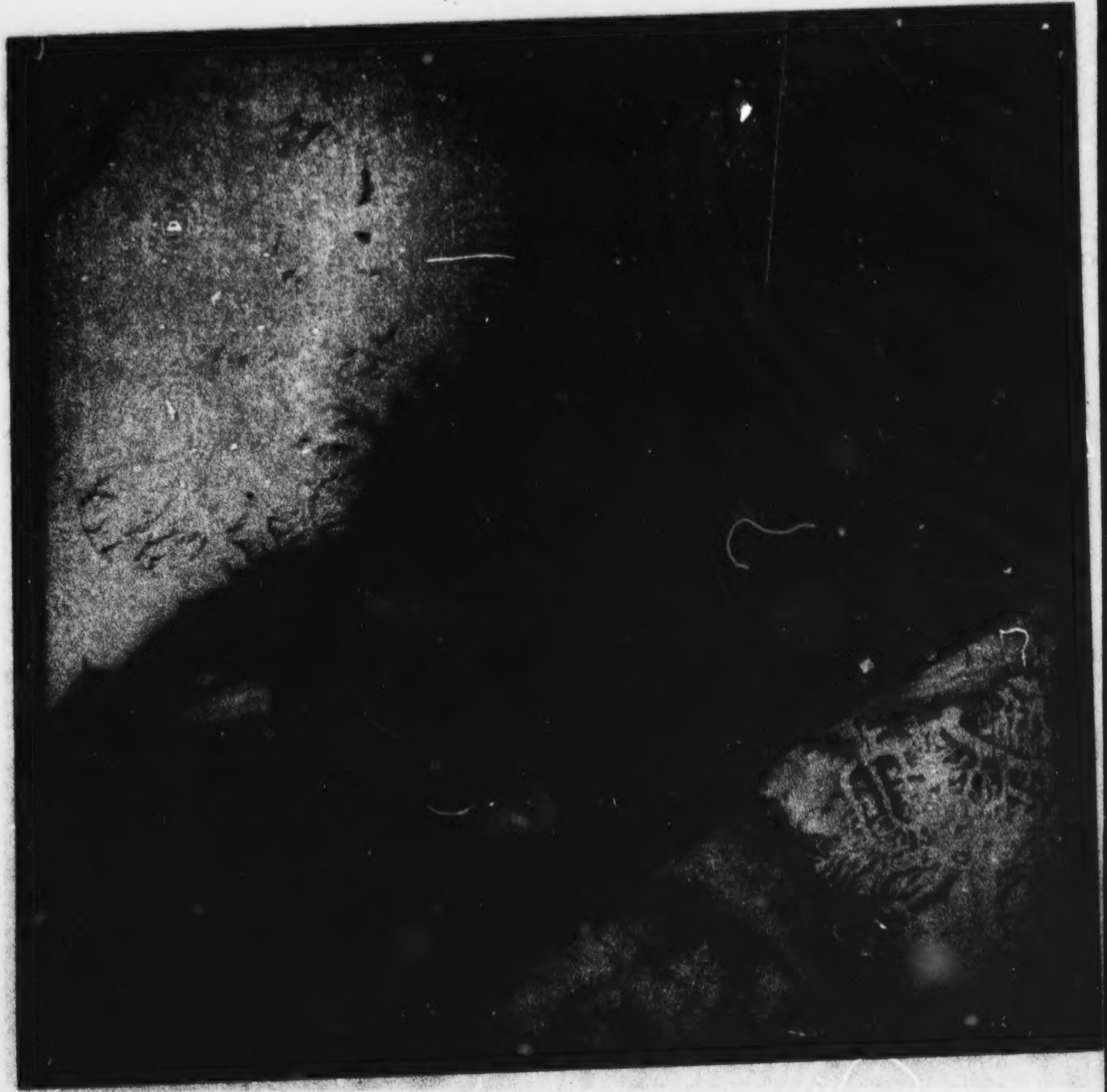

Figure 3.2.7(c) Landsat imagery, June 22, 1974, eastern Lancaster Sound

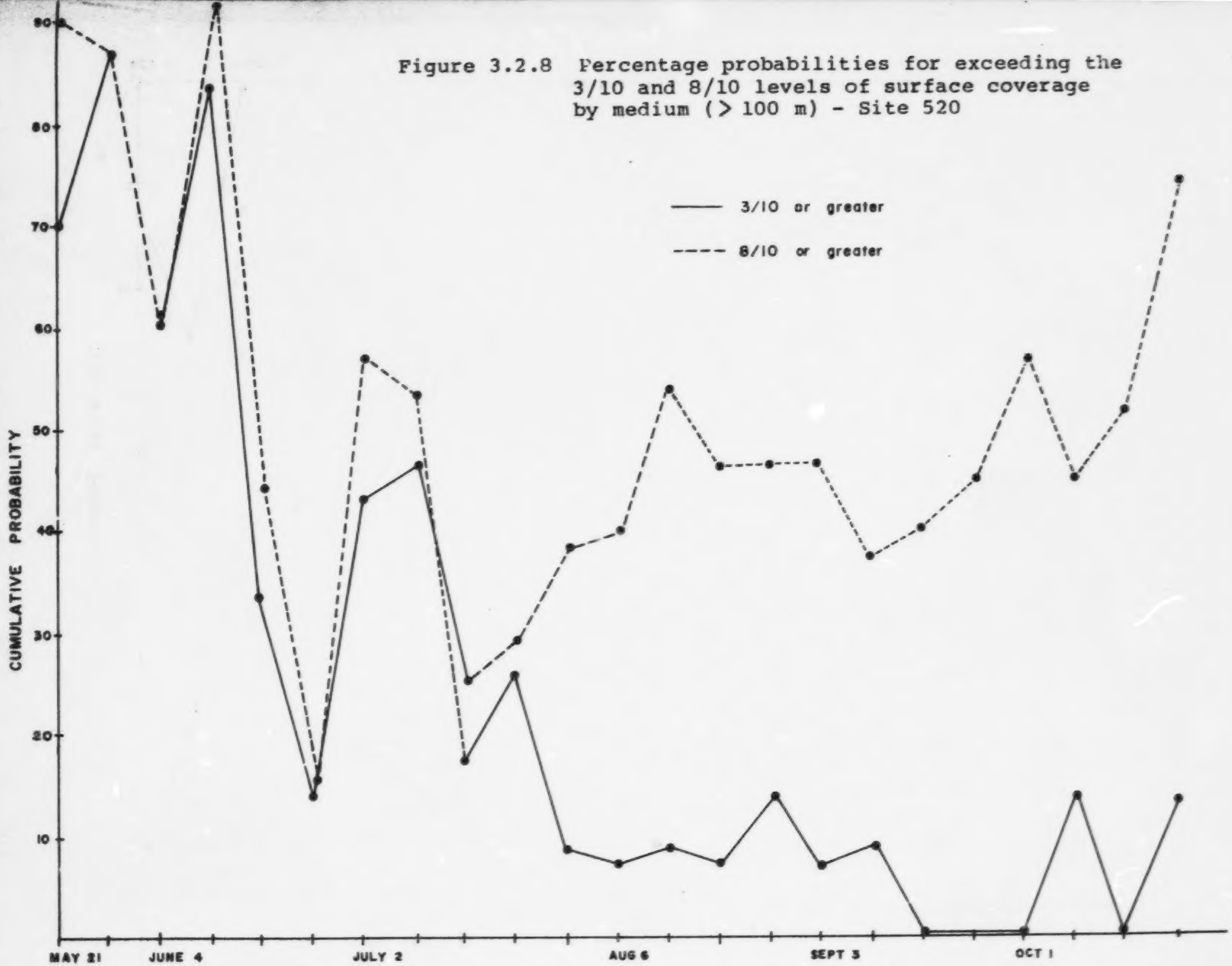

Figure 3.2.8 Percentage probabilities for exceeding the 3/10 and 8/10 levels of surface coverage by medium (> 100 m) - Site 520

Figure 3.2.9 Percentage probabilities for exceeding the 3/10 and 8/10 levels of surface coverage by medium floes - Site 502

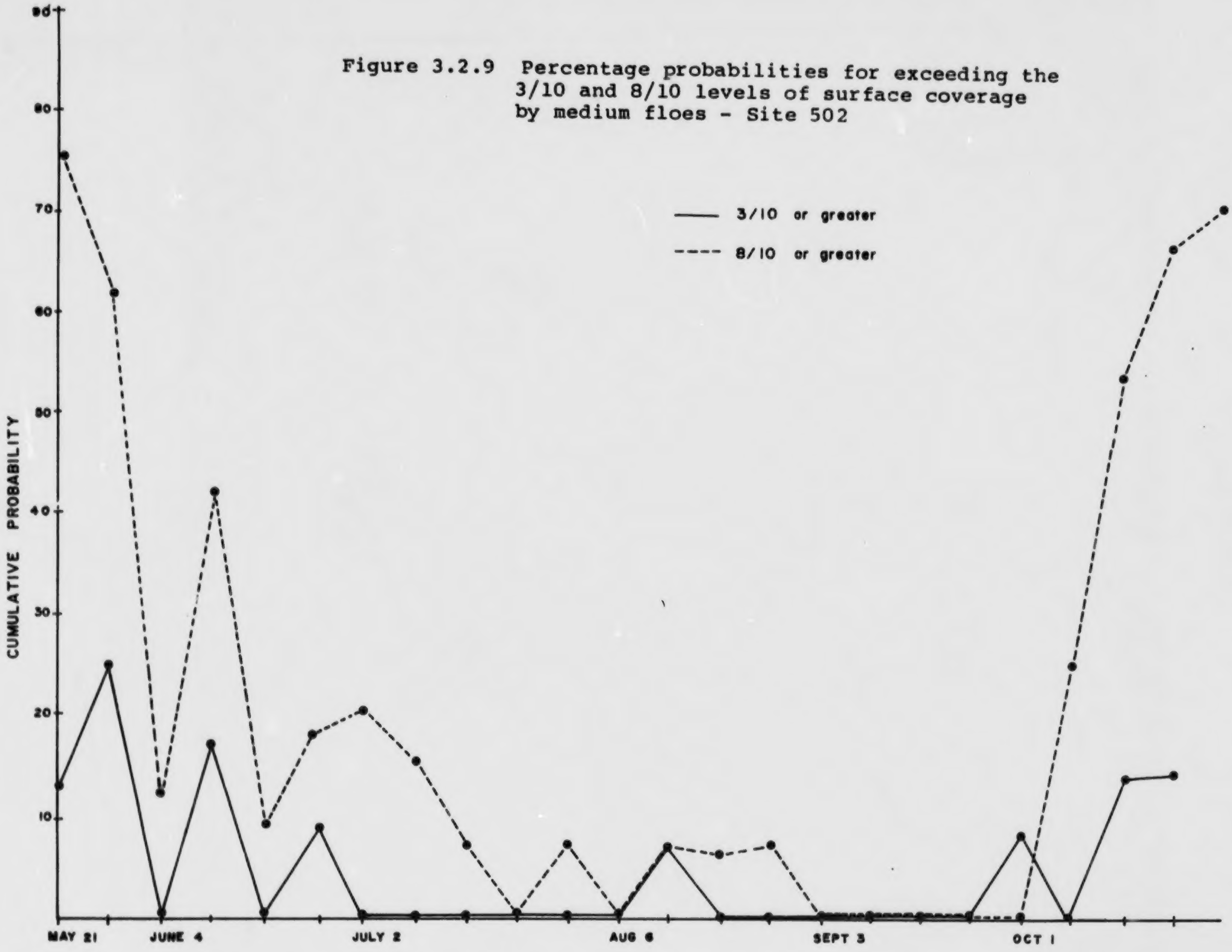

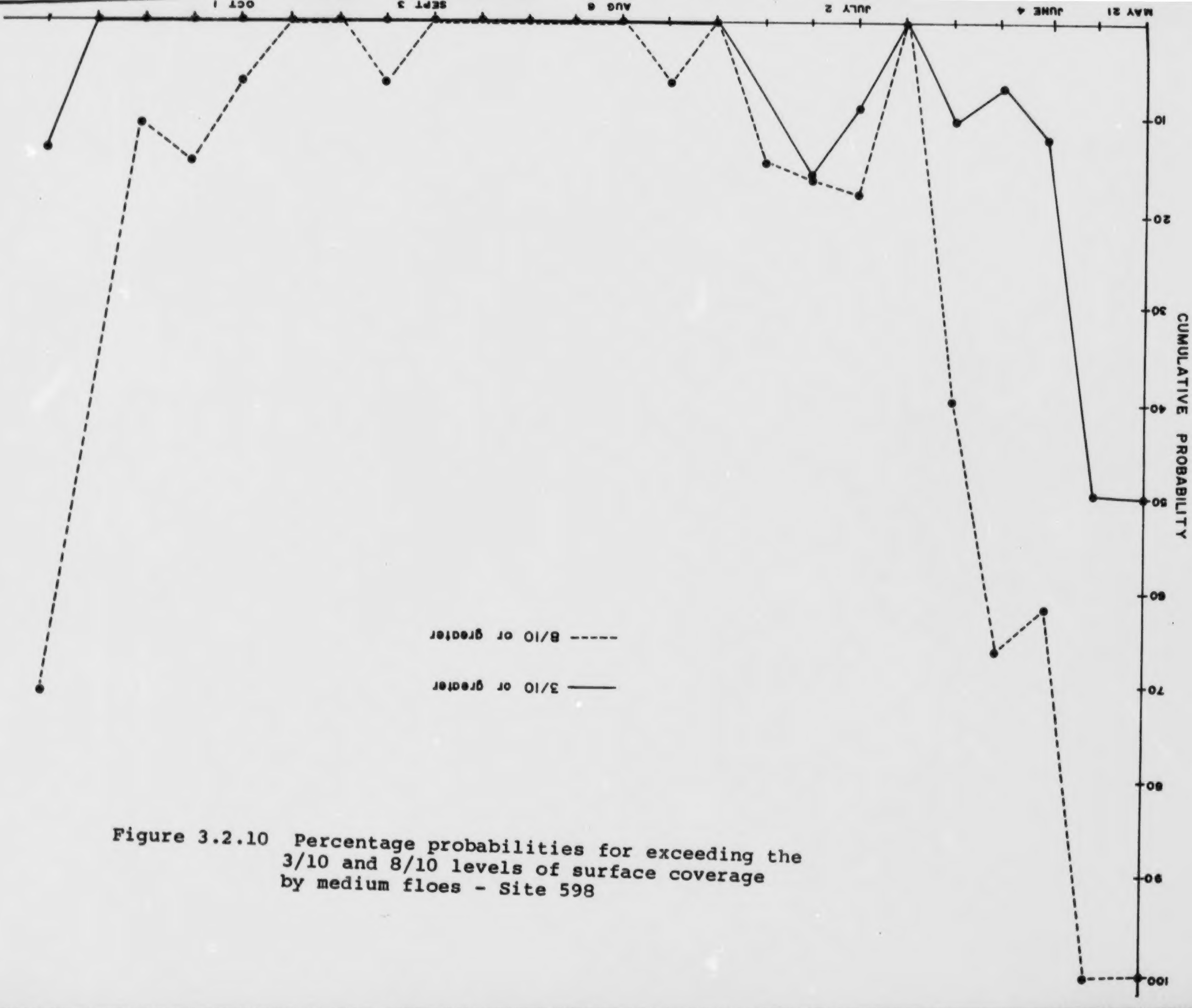

Figure 3.2.10 Percentage probabilities for exceeding the 3/10 and 8/10 levels of surface coverage by medium floes - Site 598

is justified in comparable statistics for large floes with dimensions on the order of kilometers or tens of kilometers which, in the absence of further improvements in avoidance techniques, may not be compatible with safe offshore exploration and transport activities.

3.3 Ice Movements

Until recently, data on ice movements were primarily obtained from the observations of mariners often made during lengthy drift voyages aboard ice-entrapped vessels. The trajectories of several famous such voyages are plotted in Figure 3.3-1. They indicate the easterly flow trend of Parry Channel and, as well, a tendency for this drift to take place in the southern half of the Channel. In Baffin Bay, a southerly trend was noted except in the east where a northerly coastal flow and otherwise more complex and erratic motions are suggested. Modern, long-term drift data from the NOAA satellites (Figure 3.3-2) more clearly confirm these trends and demonstrate additional features of the flow pattern such as the intrusive southerly movement off the east shore of Devon Island.

Most of these features reflect the predominant directions and magnitudes of the measured near-surface currents (Fissel et al., 1980). Unfortunately, however, in general, ice moves as a complicated sum of both the wind and water-driving forces, with the details greatly dependent upon the vertical structure of the air and water columns, time dependencies and other factors. Simplifications are usually only possible in areas where either the current or wind influence is totally dominant. Although current dominance is present in several sectors of the study region, in general the wind and current contributions to the ice motion are of comparable magnitude, greatly complicating calculations of the characteristic movements. Reliable ice-drift information is therefore only available from the experimental data which were obtained almost exclusively from the drifts of ice floes as observed in the satellite imagery of the 1973 - 1979 period.

Previously, Marko (1978) attempted to extract the time and spatial dependencies of the ice movements in Parry Channel using the daily floe displacement data obtained from the NOAA and Landsat satellite systems. The resulting daily averaged drift vectors are represented for both the summer (June to August) and "other" months in figure 3.3-3, according to the indicated zone scheme.

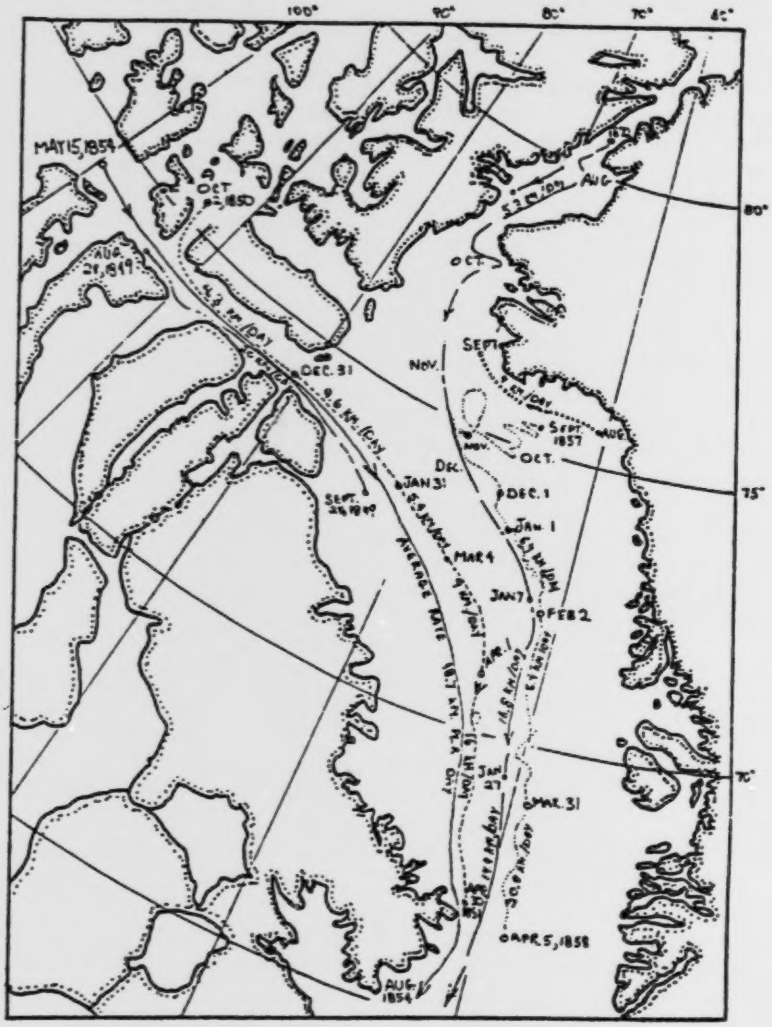
100°
90°
80°
70°
60°
80°
75°
70°
MAY 15, 1854
OCT 27, 1850
AUG. 27, 1849
4.3 KM/DAY
DEC. 31
9.6 KM/DAY
SEPT. 25, 1849
JAN 31
MAR 4
AVERAGE RATE 10.7 KM/DAY
AUG. 1854
5.3 KM/DAY
AUG.
OCT.
NOV.
SEPT.
KM/DAY
SEPT. 1857
AUG.
NOV.
OCT.
DEC.
DEC. 1
JAN. 1
JAN 7
FEB 2
16.5 KM/DAY
JAN 27
MAR. 31
30.8 KM/DAY
APR 5, 1858

Figure 3.3.1 Tracks of several ice beset vessels. Average net speeds are given for major segments of each track

The data in the non-summer months suggest a pronounced alignment of ice motion parallel to the axis of Parry Channel, with an average movement of 7 to 8 km/day. This figure applies only to periods of locally mobile ice conditions, and would, in some cases, be reduced in longer-term drifts due to the previously described (Section 3.1) temporarily landfast ice conditions. With the exception of the two westernmost zones where very slow movements were generally recorded, the average winter velocities exhibited little dependence upon position along the Channel axis. On the other hand, a very distinct cross-channel gradient was apparent, equivalent to velocity increases of 50% to 100% in the southern sectors (see Table 3.3-1).

The data suggest the continuing eastward movement of ice during the non-summer months in all areas of Parry Channel, including the extreme northeastern corner of Lancaster Sound. This result is consistent with long-term floe tracks obtained from the NOAA satellite imagery (Figure 3.3-2) of the November-to-February and March-to-May periods.

The average velocity data of the summer (June to August) period exhibited an even more distinct southern enhancement of the easterly movements. An examination of the actual recorded drifts indicates that the weak, easterly trends of the northern zones C and E result from a near-cancellation by comparable numbers of east-tending and west-tending floes. On the other hand, the strong southwesterly drift vector of the northeastern zone G clearly reflects the predominant strong flow trend of this region as reflected in all current (Fissel et al., 1980) and berg drift (Section 3.3-4) observations.

The significant southerly velocity components in the southern zones D, F and H, suggest the presence of large cross-channel motions during the summer season. The evidence for such motions is more clear-cut if data are excluded for the month of June when continuing landfast conditions in Prince Regent, Admiralty and Navy Board Inlets apparently limit the extent of cross-channel motion.

Unfortunately, the spatial scale of the zone scheme used in the cited analyses was appropriate to display only the grosser features of the eastern Parry Channel ice circulation. The resulting averaging tended to obscure the spatial structure within the zonal data; for example, by mixing the often north-south oriented velocities of the mid-channel regions

Figure 3.3-2 (a)

ICE FLOE TRACKS FROM NOAA SATELLITE IMAGERY
March - May, 1976 - 1978

1. May 22-27, 1978
2. May 17-18, 1978
3. May 22-25, 1976
4. April 1-10, 1978
5. May 24-28, 1976
6. May 15-27, 1977
7. April 15-21, 1977
8. April 1-10, 1978
9. May 26-30, 1977
10. April 19-22, 1977
11. May 19-27, 1977
12. March 10-16, 1977
13. May 22-28, 1976
14. May 19-25, 1977
15. May 6-9, 1978
16. May 22-27, 1978
17. May 7-20, 1977
18. May 15-16, 1976
19. April 23-May 7, 1976
20. May 22-27, 1978
21. April 19-20, 1977
22. May 7-20, 1977
23. May 22-28, 1978
24. May 22-25, 1976
25. May 12-20, 1978
26. May 26-30, 1977
27. May 22-28, 1976
28. April 1-10, 1978
29. May 27-28, 1976
30. March 1-10, 1977
31. April 1-10, 1978
32. April 15-21, 1977
33. May 13-14, 1978
34. May 6-8, 1978

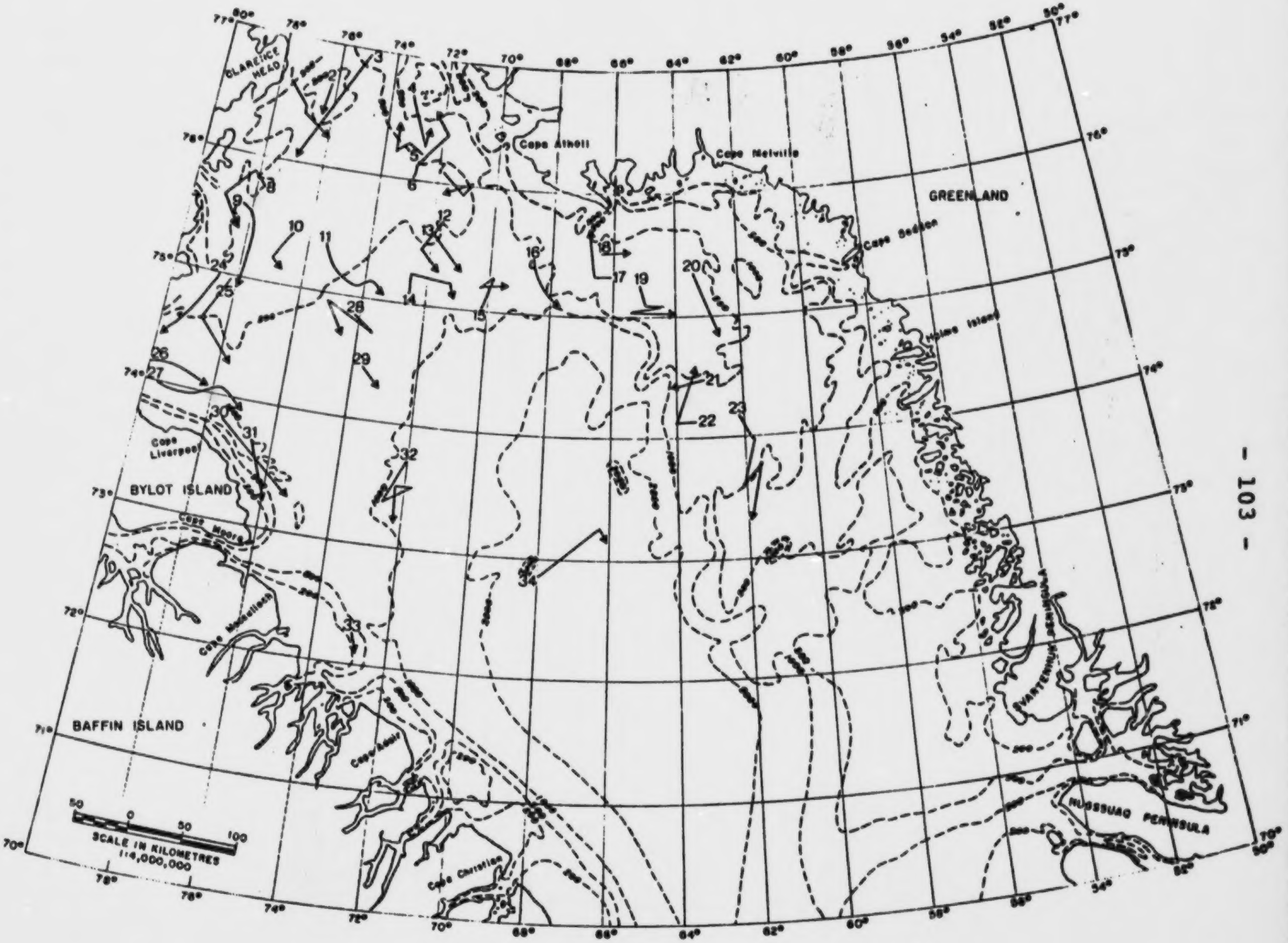
GREENLAND
Cape Melville
Cape Atholl
Cape Seddon
Holms Island
Clarence Head
Cape Liverpool
BYLOT ISLAND
Cape Hooper
Cape Macculloch
Cape Christian
BAFFIN ISLAND
NUGSSUAQ PENINSULA
SVARTENHUK PENINSULA
SCALE IN KILOMETRES
1:4,000,000
50 0 50 100

Figure 3.3.2(a)
Ice Floe Tracks from NOAA Satellite Imagery
March - May, 1976-1978

3.3-2 (b)

ICE FLOE DRIFT TRACKS FROM
NOAA SATELLITE IMAGERY
June - October 1976-1978

June 28-July 20, 1977
June 17-22, 1976
September 3-9, 1978
September 14-19, 1976
June 4-12, 1978
June 29-July 7, 1978
June 3-14, 1978
August 20-21, 1978
June 16-25, 1976
August 2-9, 1978
July 24-26, 1978
August 3-9, 1978
June 10-13, 1978
September 16-18, 1978
August 19-21, 1978
June 29-July 10, 1978
June 13-28, 1976
July 24-26, 1978
June 14-26, 1976
September 3-9, 1978
August 2-9, 1978
July 2-10, 1978
July 17-21, 1978
August 19-20, 1978
August 3-9, 1978
October 16-18, 1978
July 21-28, 1978
September 1-9, 1978

29. August 19-21, 1978
30. July 17-25, 1977
31. August 3-9, 1978
32. June 5-13, 1978
33. July 3-10, 1978
34. July 21-24, 1978
35. June 15-26, 1976
36. June 6-10, 1978
37. June 25-July 25,1977
38. June 5-12, 1978
39. July 4-12, 1978
40. July 17-25, 1977
41. June 5-12, 1978
42. July 4-12, 1978
43. September 3-9, 1978
44. June 25-July 25,1977
45. August 19-26, 1978
46. August 3-9, 1978
47. June 16-26, 1976
48. August 20-25, 1978
49. June 7-12, 1978
50. August 20-26, 1978
51. September 3-9, 1978
52. June 5-13, 1978
53. June 7-12, 1978
54. July 23-28, 1978
55. August 20-26, 1978
56. July 23-28, 1978

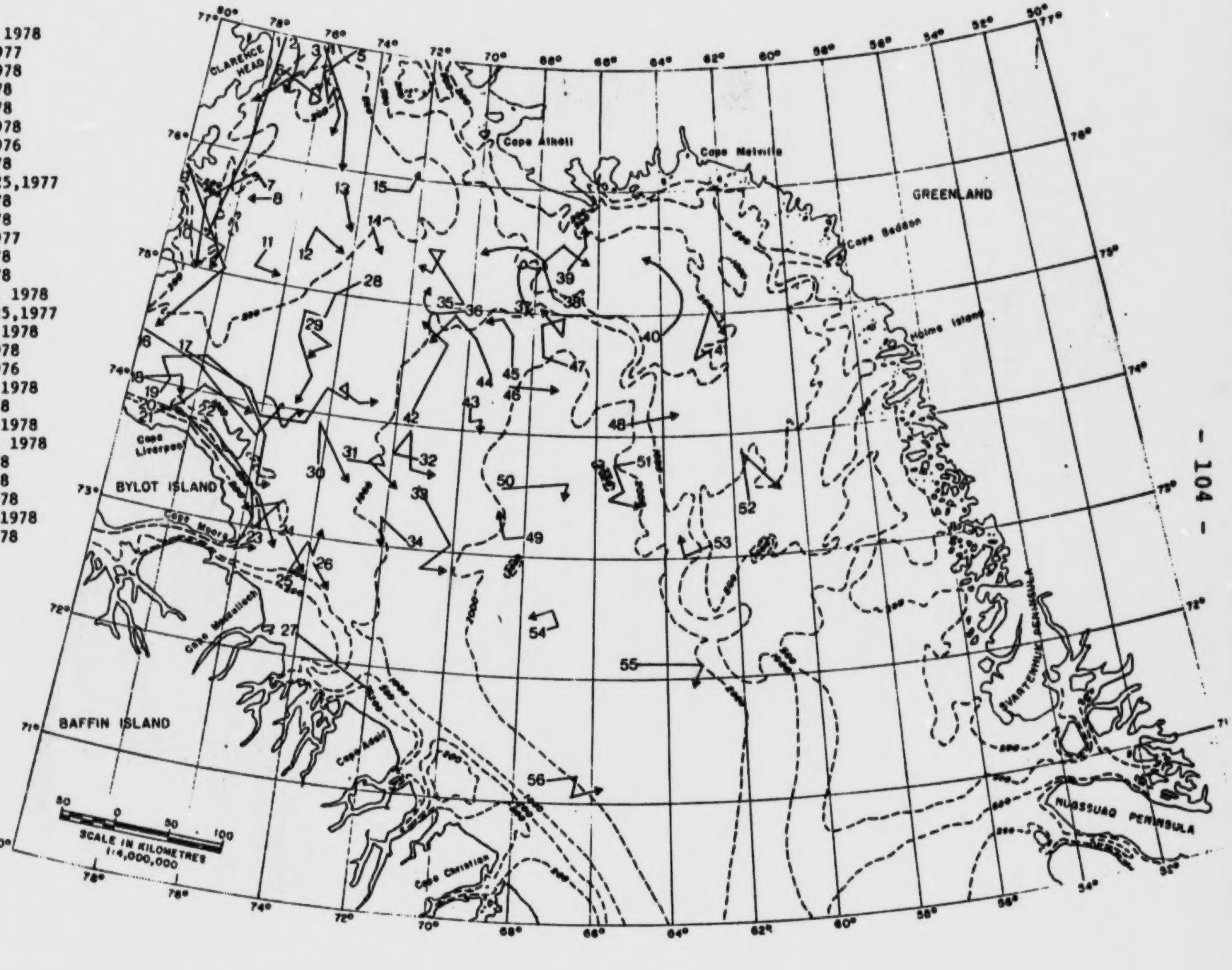
CLARENCE HEAD
Cape Atholl
Cape Melville
GREENLAND
Cape Seddon
Holms Island
SVARTENHUK PENINSULA
NUGSSUAQ PENINSULA
Cape Liverpool
BYLOT ISLAND
BAFFIN ISLAND
Cape Christian
SCALE IN KILOMETRES
1:4,000,000
50
0
50
100
80°
78°
76°
74°
72°
70°
68°
66°
64°
62°
60°
58°
56°
54°
52°
50°
77°
76°
75°
74°
73°
72°
71°
70°
2000
1000
500
200

Figure 3.3.2(b)
Ice Floe Drift Tracks from NOAA Satellite Imagery
June - October, 1976-1978

Figure 3.3-2(c)

ICE FLOE DRIFT TRACKS FROM NOAA SATELLITE IMAGERY
November-February, 1976-1979

1. Feb. 16-21, 1977
2. Jan. 13-16, 1979
3. Nov. 30-Dec. 2, 1977
4. Nov. 16-27, 1978
5. Dec. 8-14, 1978
6. Dec. 15-21, 1976
7. Feb. 3-24, 1978
8. Nov. 2-27, 1978
9. Dec. 16-20, 1977
10. Dec. 3-9, 1976
11. Feb. 11-12, 1978
12. Nov. 5-15, 1978
13. Dec. 9-20, 1977
14. Feb. 3-4, 1978
15. Dec. 8-18, 1978
16. Jan. 1-7, 1977
17. Nov. 2-15, 1978
18. Nov. 26-Dec. 3, 1977
19. Nov. 16-27, 1978
20. Jan. 4-8, 1977
21. Dec. 10-12, 1977
22. Dec. 17-20, 1977
23. Dec. 7-17, 1978
24. Jan. 1-3, 1978
25. Dec. 5-8, 1976
26. Nov. 2-12, 1978
27. Dec. 10-12, 1977
28. Nov. 16-27, 1978
29. Dec. 2-5, 1977
30. Feb.13-21, 1977
31. Jan. 1-3, 1978
32. Dec. 27-Jan. 5, 1979
33. Dec. 16-20, 1977
34. Dec. 3-11, 1977
35. Jan. 4-7, 1977
36. Jan. 1-3, 1978
37. Dec. 4-7, 1976
38. Jan.28-Feb.1, 1979
39. Jan. 1-3, 1978
40. Nov. 20-27, 1978
41. Dec. 10-23, 1977
42. Dec. 4-9, 1976
43. Dec. 7-10, 1976
44. Nov. 16-23, 1977
45. Dec. 31-Jan. 6, 1977
46. Feb. 11-26, 1978
47. Jan. 13-16, 1979
48. Jan. 11-13, 1978
49. Feb. 14-18, 1979
50. Dec. 31-Jan.5, 1977
51. Dec. 24-Jan.2, 1979
52. Dec. 7-16, 1978
53. Feb.11-15, 1978
54. Feb. 24-26, 1978
55. Dec. 4-8, 1976
56. Nov. 5-12, 1978
57. Jan.13-16, 1979
58. Dec. 9-12, 1978
59. Dec. 3-16, 1978
60. Feb. 13-18, 1977
61. Nov. 15-27, 1978

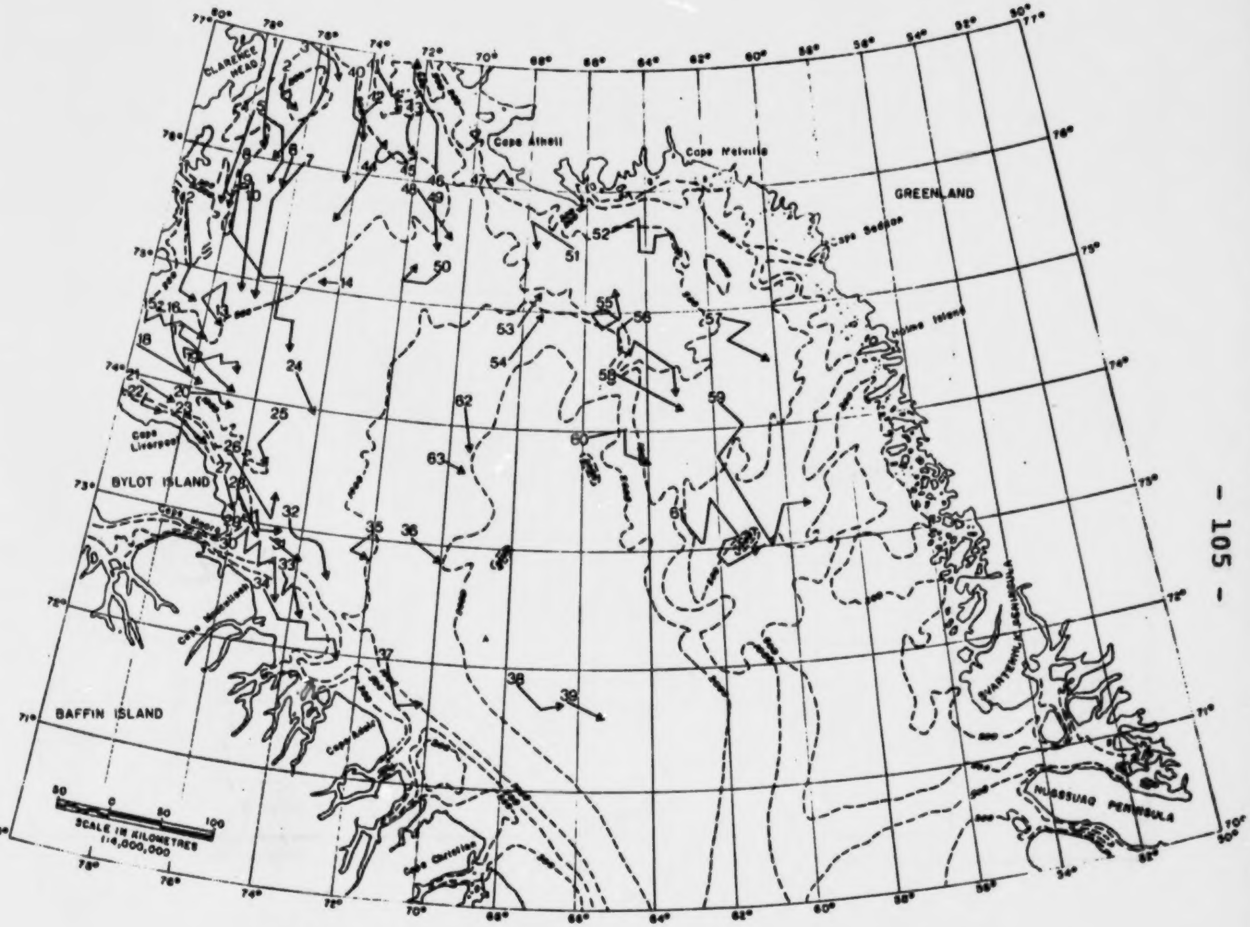
CLARENCE HEAD
Cape Atholl
Cape Melville
GREENLAND
Cape Seddon
Holms Island
Cape Liverpool
BYLOT ISLAND
BAFFIN ISLAND
Cape Christian
NUGSSUAQ PENINSULA
SCALE IN KILOMETRES
1:4,000,000
50 0 50 100
80° 78° 76° 74° 72° 70° 68° 66° 64° 62° 60° 58° 56° 54° 52° 50°
77° 76° 75° 74° 73° 72° 71° 70°

Figure 3.3.2(c)
Ice Floe Drift Tracks from NOAA Satellite Imagery
November - February, 1976-1979

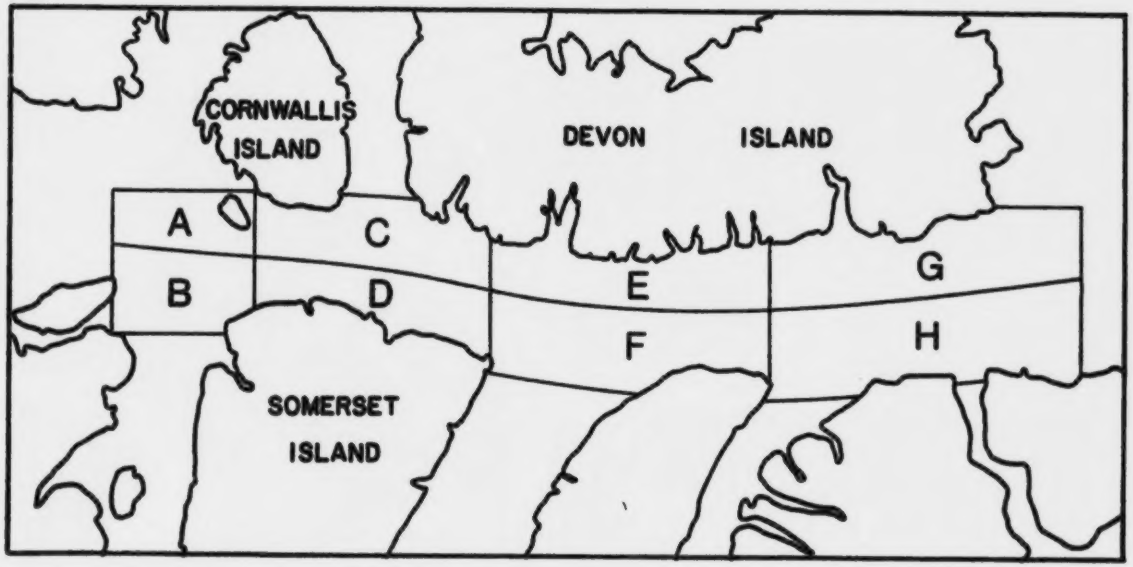
CORNWALLIS ISLAND
DEVON ISLAND
SOMERSET ISLAND
A
B
C
D
E
F
G
H

Figure 3.3.3(a) The division of Eastern Parry Channel into zones for the computation of average velocities

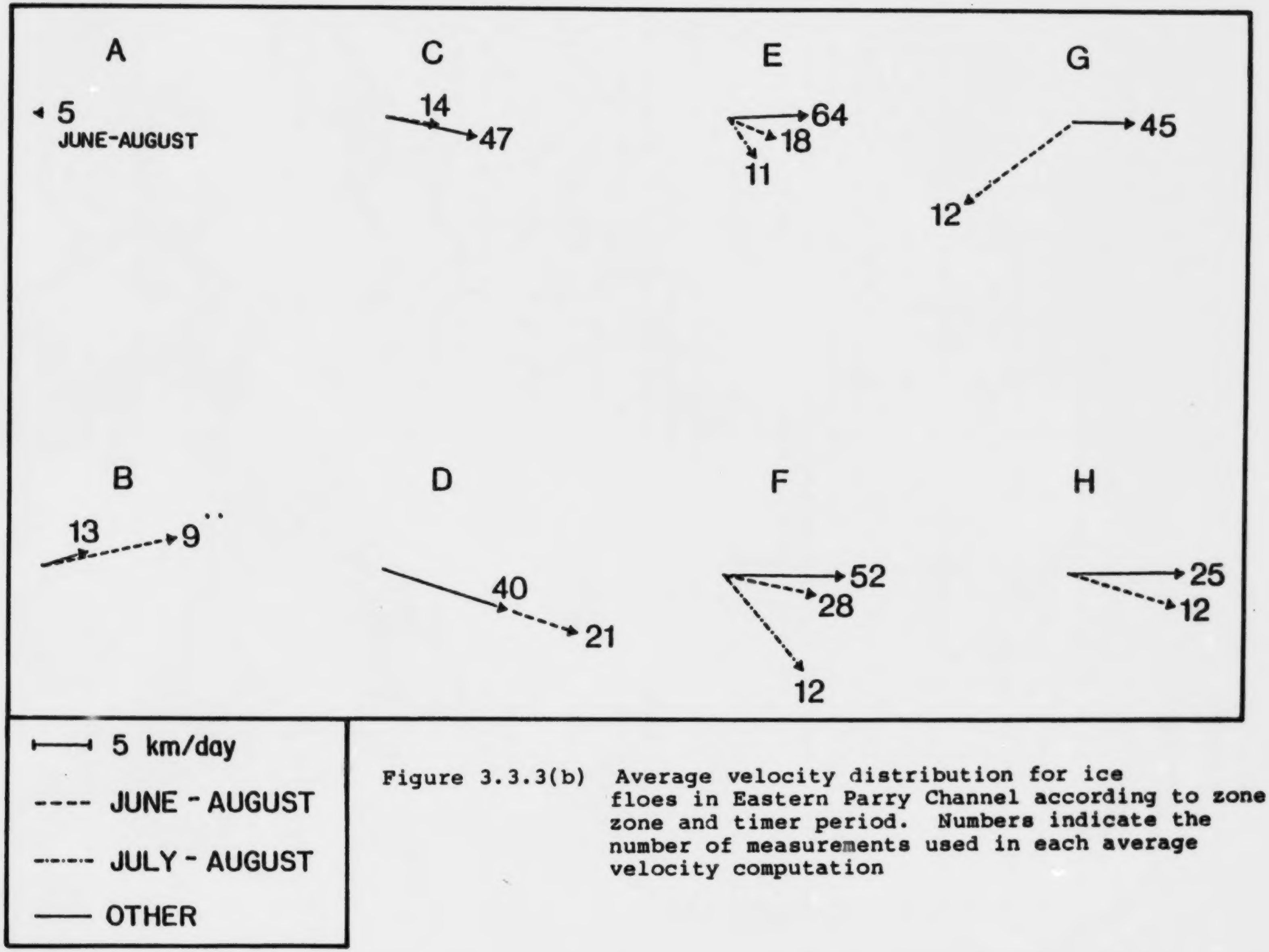
A
5
JUNE-AUGUST
C
14
47
E
64
18
11
G
45
12
B
13
9
D
40
21
F
52
28
12
H
25
12
5 km/day
JUNE - AUGUST
JULY - AUGUST
OTHER

Figure 3.3.3(b) Average velocity distribution for ice floes in Eastern Parry Channel according to zone zone and timer period. Numbers indicate the number of measurements used in each average velocity computation

Zone	n_s	v_{xs}	v_{ys}	n_{ns}	v_{xns}	v_{yns}
A	5	-0.7	0	--	--	--
B	9	12	3	13	4	1.2
C	14	4.3	-0.3	47	7.6	-1.4
D	17	-5.2	21	40	10.9	-3.2
E	18	4	-1.3	64	7.0	0.5
F	28	8.3	-1.6	52	10.3	-0.2
G	12	-9.4	-7.2	45	5.2	-0.3
H	14	8.9	-2.5	25	9.9	0.2

Table 3.3.1 A listing of the x (east) and y (north) components of the average summer(s) and non-summer (NS) velocities according to zone

with the generally orthogonal movements observed in more inshore areas. As a result, misleadingly small values were obtained for the easterly summer average velocities in the southern Channel zones. Comparison with the corresponding compilation of drift tracks (Figure 3.3-2) indicates the existence of a distinct region of rapid flow roughly aligned with the 74° parallel where typical ice movements are on the order of 40 to 50 km/day, considerably in excess of the calculated zonal averages.

A similar vector-averaging has been carried out as part of the present review using the complete set of March through November Landsat imagery and a finer averaging grid concentrated in the eastern Lancaster Sound - northwest Baffin Bay region. The resulting average vectors are plotted in Figures 3.3-4 and 3.3-5, together with the corresponding numbers of observations in each zone and shaded rectangles representing the uncertainties in the plotted results. In each case, rectangles were drawn with the lengths of their sides equal to twice the "root-mean-square" deviation of the zonal east-west and north-south velocity components.

The plotted summer vectors delineate more clearly the concentration of easterly flow in southern Parry Channel. Nevertheless, the average speeds in the pattern zones still fall below those commonly noted in the fast core of the ice movement. A similar reduction is evident in zone 26 where southwesterly flows of 50 km/day are normally observed. The latter result is probably associated with the small number of observations made in this zone due primarily to the characteristically short zone traversal time. As a result, the average value is probably aliased by a tendency for measurements to be obtained on the more slowly moving fraction of the floe population. This problem was even more strikingly present in the adjoining zone 12 off the east coast of Devon Island where no daily velocity measures were obtained. Drift buoy data (Fissel, Lemon and Birch, 1980) and the longer term NOAA satellite drift data of Figure 3.3.2 suggest velocities in this zone are typically southwestward and in the 30 to 50 km/day range.

The higher resolution data clearly follow the pattern of intrusive flow in eastern Lancaster Sound identified from satellite-tracked drifter trajectories and other measurements of near-surface currents (Fissel, Lemon and Birch, 1980) with reduced velocity magnitudes in the identified "central disordered zone". Westerly average velocities were confined to the extreme northeastern Parry Channel zones 4 and 5. No evidence was found in zones 7, 11 and 13 for a net westerly ice flow in any way comparable in magnitude to the easterly flow of southern Parry Channel. Nevertheless, the existence of such a movement cannot be dismissed in view of the still very coarse zonal scheme and the relatively small number drift observations. Additional measurements are needed to clarify the structures of the zones west of Cape Warrender and in the disordered mid-Channel region.

108

Fig. 3.3-4

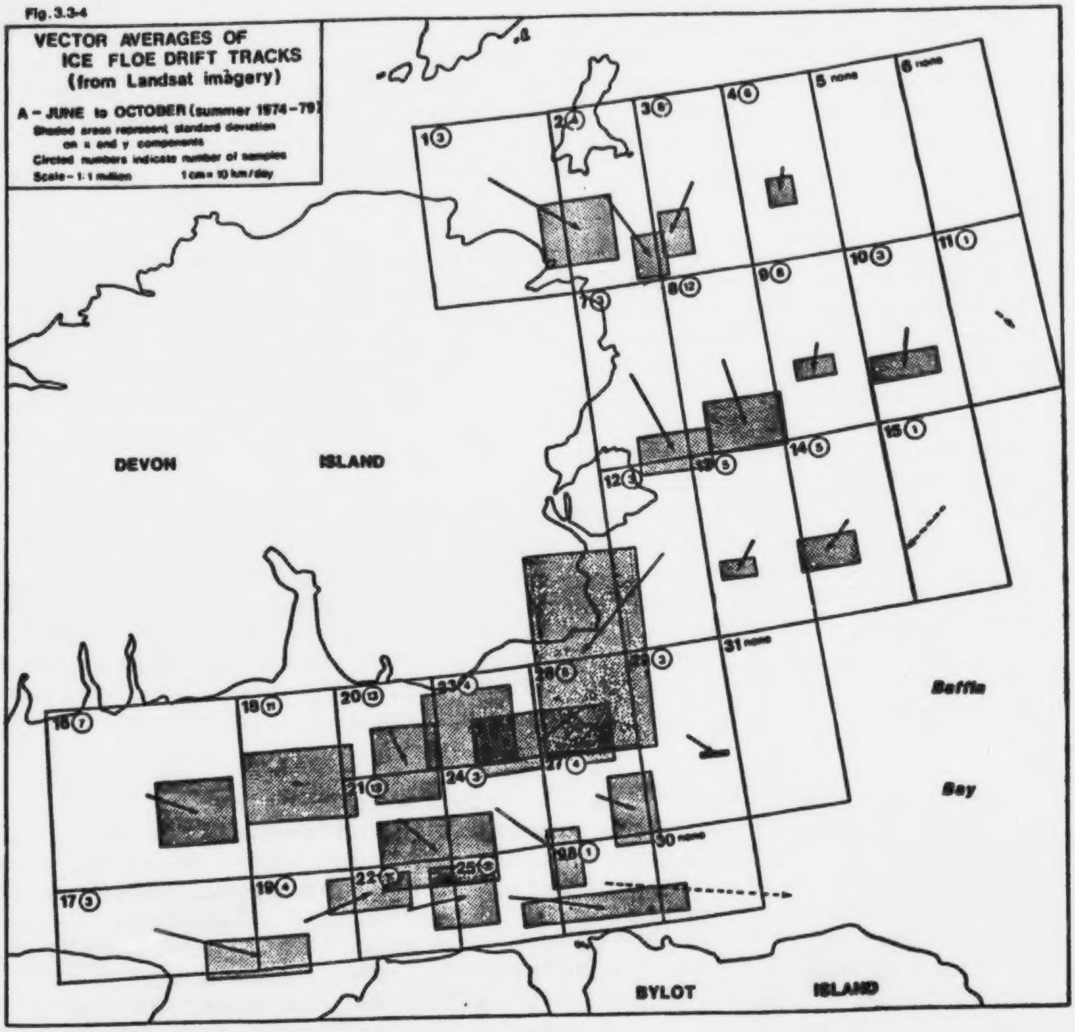
VECTOR AVERAGES OF
ICE FLOE DRIFT TRACKS
(from Landsat imàgery)
A - JUNE to OCTOBER (summer 1974-79)
Shaded areas represent standard deviation
on x and y components
Circled numbers indicate number of samples
Scale - 1:1 million
1 cm = 10 km/day
1③
2④
3⑥
4⑥
5 none
6 none
7③
8⑫
9⑥
10③
11①
12③
13⑤
14⑤
15①
16⑦
17③
18⑪
19④
20⑫
21⑬
22
23④
24③
25
26⑧
27④
28①
29③
30 none
31 none
DEVON
ISLAND
Baffin
Bay
BYLOT
ISLAND

Figure 3.3.4

Vector Averages of Ice Floe Drift Tracks
(from Landsat imagery)

A - June to October (summer 1974-79)

Shaded areas represent standard deviation
on x and y components
Circled numbers indicate number of samples
Scale - 1:1 million 1 cm = 10 km/day

107

Fig.3.3-5

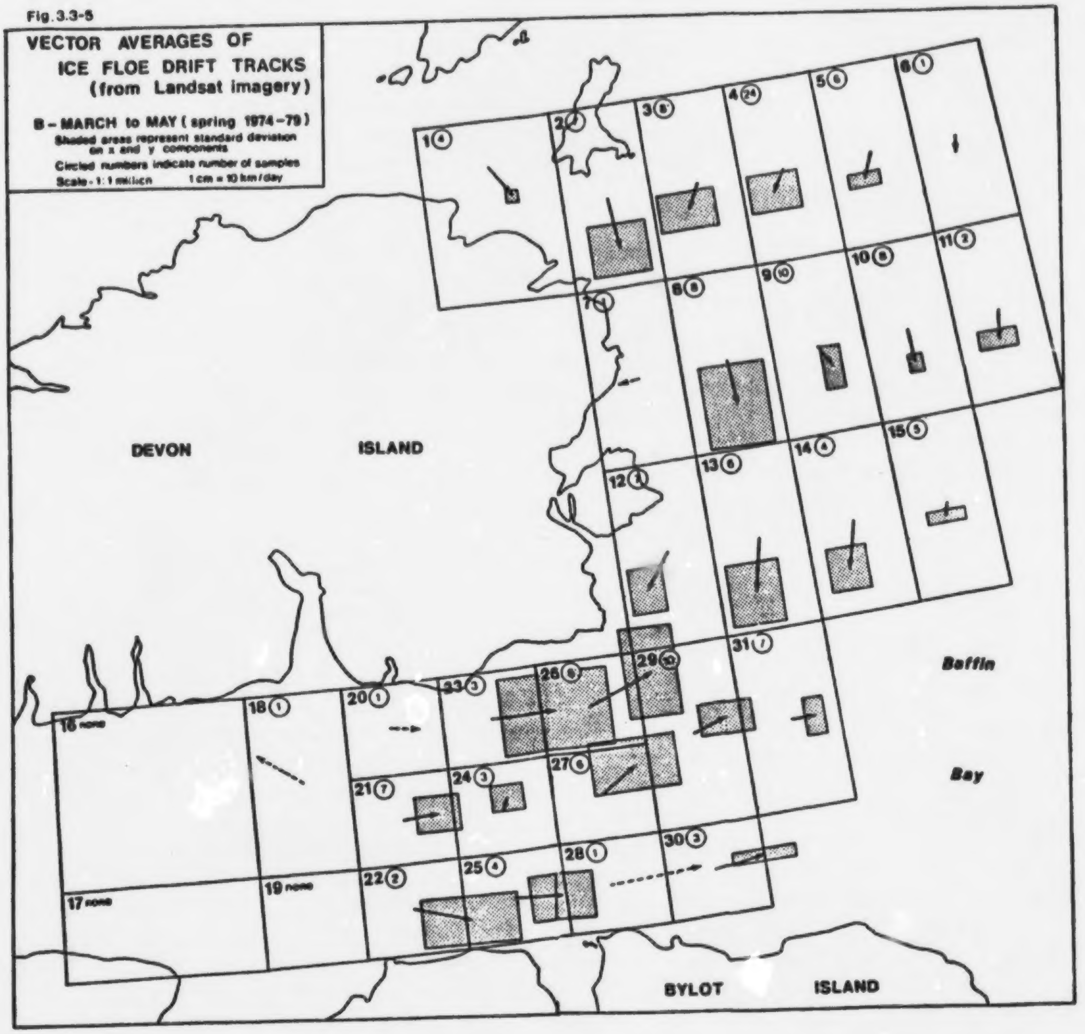
VECTOR AVERAGES OF
ICE FLOE DRIFT TRACKS
(from Landsat imagery)
B - MARCH to MAY (spring 1974-79)
Shaded areas represent standard deviation on x and y components
Circled numbers indicate number of samples
Scale - 1:1 million 1 cm = 10 km/day
DEVON
ISLAND
BYLOT
ISLAND
Baffin
Bay
1④
2
3⑧
4㉔
5⑥
6①
7
8⑧
9⑩
10⑧
11②
12②
13⑥
14④
15③
16 none
17 none
18①
19 none
20①
21⑦
22②
23③
24③
25④
26⑧
27⑥
28①
29⑩
30③
31⑦

Figure 3.3.5

Vector Averages of Ice Floe Drift Tracks
(from Landsat imagery)

A - March to May (spring 1974 - 79)

Shaded areas represent standard deviation
on x and y components
Circled numbers indicate number of samples
Scale - 1:1 million 1 cm = 10 km/day

The data in northern Baffin Bay indicate a rapid 30 to 40 km/day movement out of Jones Sound and a confinement of the strong southerly flow to a zone roughly 55 km wide adjoining the east coast of Devon Island. Average speeds in this region typically exhibit a threefold west to east falloff.

The spring (March to May) velocity grid of Figure 3.3.5 differs from the summer results in the reduced velocity magnitudes of the fastest flow regions of southern Parry Channel and to the east of Devon Island. A more general reduction in velocities would be evident if the late April and May contributions were excluded from the averaging process leaving the data more typical of the winter period. Unfortunately, the limited amount of late February-March Landsat data are not yet sufficient to support such an averaging scheme.

Nevertheless, the early spring-late winter data clearly demonstrate a very significant seasonal reversal of flow in zones 23 and 26 giving a uniformly easterly sense to the ice drift in all areas of Lancaster Sound east of the landfast ice edge and in the immediately adjoining segment of Baffin Bay. Oceanographic and wind measurements would be necessary to ascertain whether this reversal reflects a reduction in the intrusive current flow or is in fact a result of the increased importance of wind and/or internal ice forces in the winter-early spring period.

3.4 Icebergs

3.4.1 Background

The International Ice Patrol has estimated (I.I.P., 1977) that 85% of the icebergs which reach the Grand Banks of Newfoundland originate from the tidewater glaciers of west Greenland (Figure 3.4.1). These glaciers annually calve some 10,000 to 20,000 bergs into the adjoining waters of Baffin Bay. The prevailing current and ice drift patterns (See Fissel, Lemon, Birch, 1980 and Section 3.3) tend to move these bergs northward along the west Greenland coast with numerous groundings and refloatings until at latitudes north of roughly 76°N, they move west and encounter the influence of the Baffin or Canadian Current which flows southward along the western side of Baffin Bay. The latter flow follows the eastern coastlines of Ellesmere and Devon Islands, and carries the bergs through the northwest Baffin Bay - Lancaster Sound study region on route to more southern waters.

Of the other sources of Newfoundland bergs, namely east Greenland (10%) and the glaciers and ice-shelves of Ellesmere, Devon and Bylot Islands, only the latter make any substantial contributions to the berg populations of northwest Baffin Bay.

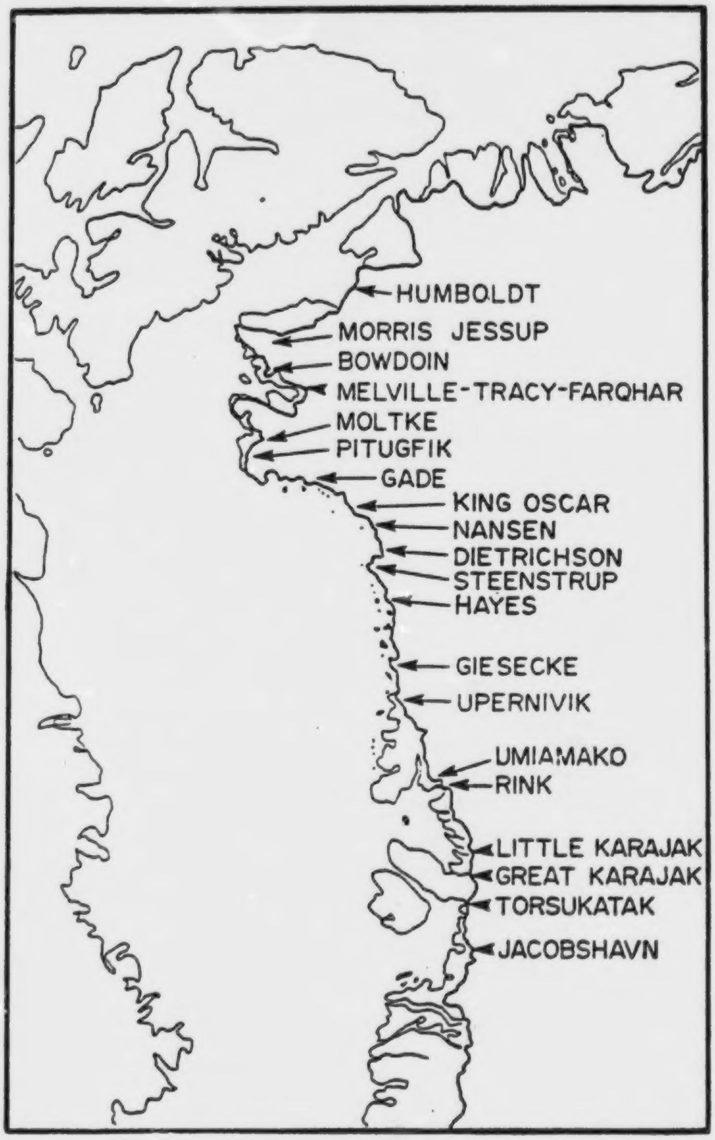
HUMBOLDT
MORRIS JESSUP
BOWDOIN
MELVILLE-TRACY-FARQHAR
MOLTKE
PITUGFIK
GADE
KING OSCAR
NANSEN
DIETRICHSON
STEENSTRUP
HAYES
GIESECKE
UPERNIVIK
UMIAMAKO
RINK
LITTLE KARAJAK
GREAT KARAJAK
TORSUKATAK
JACOBSHAVN

Figure 3.4.1 Major iceberg - producing glaciers of West Greenland

As indicated in Section 2, much of the general information available on the berg circulation was obtained from the numerous shipboard and aerial surveys carried out by the International Ice Patrol, the U.S. Coast Guard and Canadian Government agencies. These efforts included the tracking of individual bergs and a small number of very extensive berg counts which gave a measure of the berg distributions at particular moments in time over the greater Baffin Bay - Davis Strait region.

The results of the earliest of these counting surveys, carried out photographically by the U.S. Coast Guard in 1949, are presented in Figure 3.4.2. The principal features of the recorded distribution are the extremely high berg numbers in Melville Bay and along the west Greenland coastline. Generally lower but still substantial densities were also observed off the east coasts of Devon and Ellesmere Islands. A trend toward lower berg concentrations was evident in areas north of roughly 70°N and surrounding the main northwest - southeast axis of the survey region. Somewhat higher berg concentrations were recorded along the Baffin Island coast.

Results from a later, 1969, survey using both photographic and radar methods are presented in Figure 3.4.3 with a higher (2x) spatial resolution. They indicate again the tendency for the highest concentrations of bergs to accumulate in Melville Bay and along the west Greenland coast. However, berg numbers were greatly reduced in these areas relative to the 1949 results, with much of the factor of five difference between the 1949 and 1969 overall totals arising from the lower 1969 densities in these regions. Other differences in the 1969 distribution are the negligible berg concentrations off the east coast of Devon Island and the general shift of the axial region of low berg density toward the western shore of Baffin Bay - Davis Strait.

While these results contribute to the overall picture of the larger-scale circulation, it is difficult to distinguish true year to year variability from changes in observational techniques and conditions.

A previous review (A.P.O.A., 1973) has approached the berg distribution problem through a brute force averaging and contouring of all berg density data recorded by the International Ice Patrol and the Canadian Department of Transport, Meteorological Branch. For completeness the results of this process have been presented in Figure 3.4.4 a-c for the periods: September - October 1963 - 1969; 1968 - 1970; and, August-October, 1971. The listed numerical values correspond to the commonly used units of bergs/1,000 square

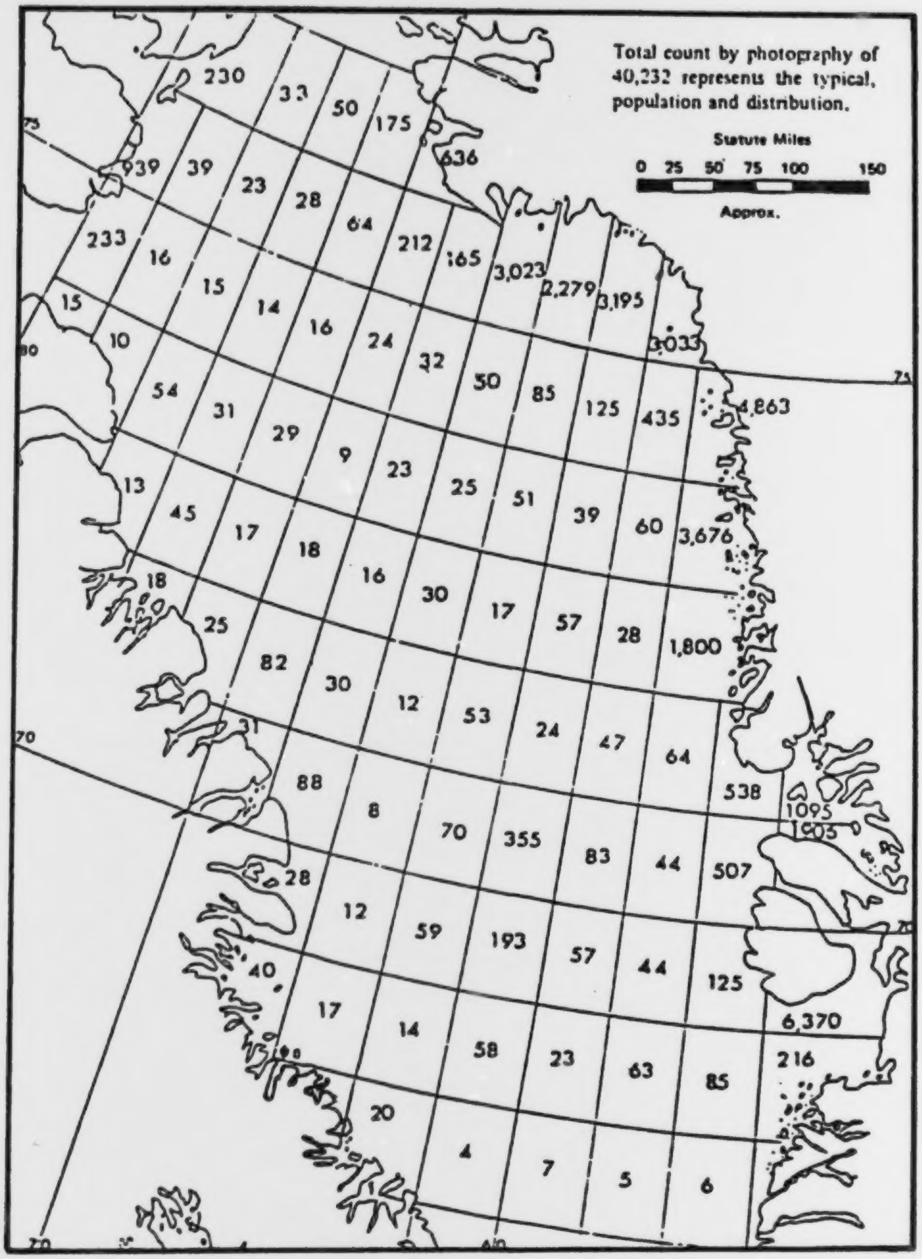
Total count by photography of 40,232 represents the typical, population and distribution.
Statute Miles
0 25 50 75 100 150
Approx.
230
33
50
175
636
939
39
23
28
64
212
165
3,023
2,279
3,195
3,033
233
16
15
14
16
24
32
50
85
125
435
4,863
15
10
54
31
29
9
23
25
51
39
60
3,676
13
45
17
18
16
30
17
57
28
1,800
18
25
82
30
12
53
24
47
64
31
88
8
70
355
83
44
507
538
1095
1905
28
12
59
193
57
44
125
40
17
14
58
23
63
85
6,370
216
20
4
7
5
6
75
80
75
70
70
70
60

Figure 3.4.2 August, 1949 IIP iceberg counts in Baffin Bay and adjacent waterways

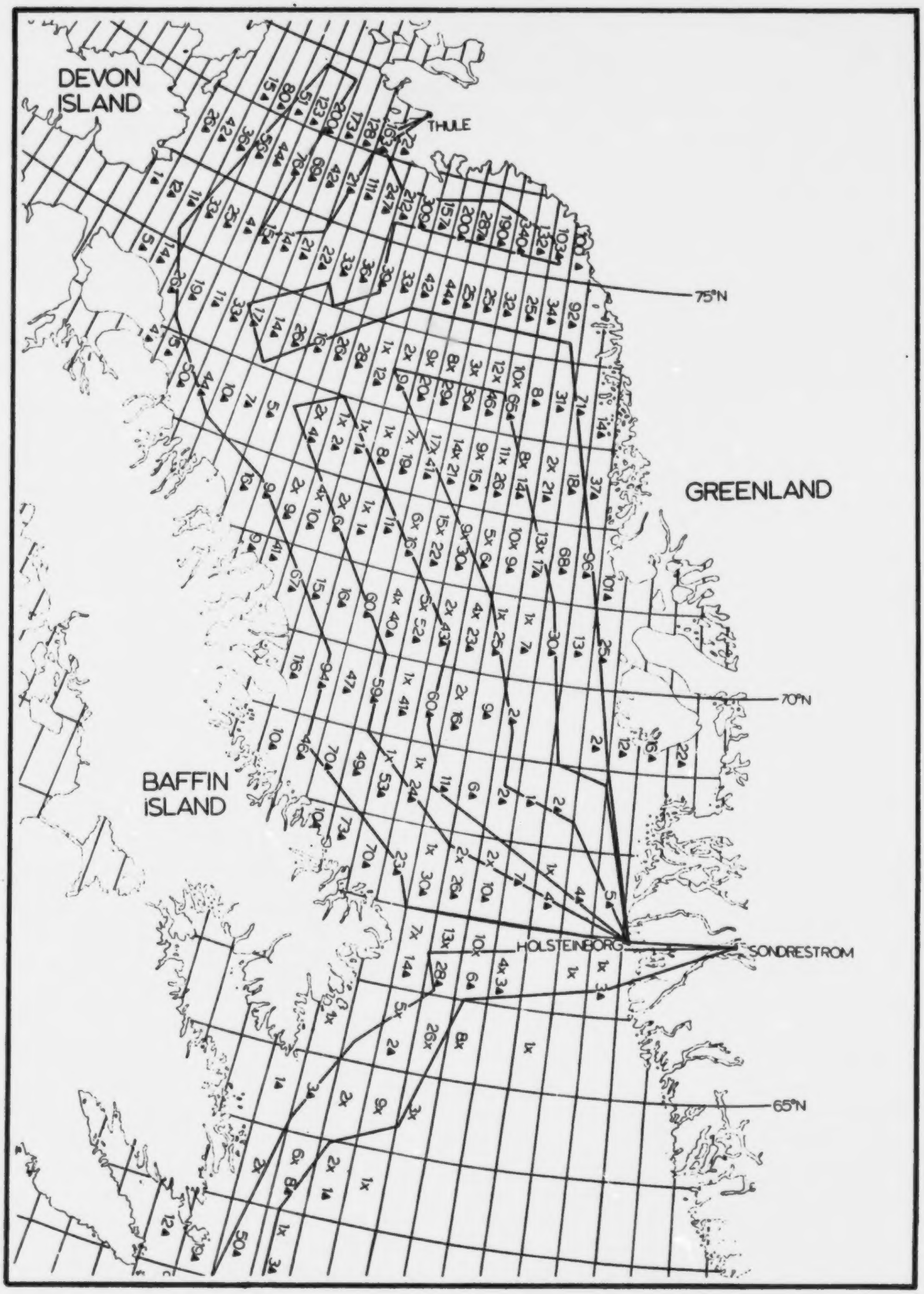
DEVON ISLAND
THULE
75°N
GREENLAND
70°N
BAFFIN ISLAND
HOLSTEINBORG
SONDRESTROM
65°N

Figure 3.4.3 1969 iceberg counts in Baffin Bay (IIP, 1970). Separate listings are given in each zone for confirmed iceber sightings (▲) and berg-like radar targets (X).

nautical miles. The results of 1949 and 1969 can be put in similar terms by dividing the numerical values in Figures 3.4.2 and 3.4.3 by 2.04 and 1.02 respectively. While the contours of Figure 3.4.4 follow very roughly the known surface current circulation of Baffin Bay, the differences between the patterns of the individual averaging periods are qualitative. Additionally, the basic inhomogeneity of the berg distributions tend to be obscured by the contouring and common procedure of counting berg numbers on the basis of 1,000 sq.n.m. averaging zones. Data presented below confirm the impression that bergs tend to concentrate in narrow zones which coincide with the rapid flow cores of the regional surface and near-surface current systems. The widths of these cores are often on the order of a few nautical miles. In such cases rectangular box average densities are clearly inadequate to represent important aspects of the berg distribution.

The general requirement for highly detailed information on the northwest Baffin Bay - Lancaster Sound region forces a reliance, in the current review, upon the most recent studies of the area; primarily those carried out in the 1978-1979 Petro-Canada-EAMES programs.

The four iceberg-related components of the latter study are described below in some detail.

1. Satellite-Tracking

   Intermediate resolution (in time and space) tracking of selected bergs was carried out in both 1978 and 1979 utilizing 20 radio-pulse emitting platforms placed on the berg surfaces with the aid of a ship-based helicopter. Platform positions were tracked through the Nimbus-NASA and Tiros-System ARGOS satellite and data-processing facilities. Position fixes were obtained at rates ranging from 2/day to 12/day with accuracies of "2.5 km (1978) and .5 km (1979). Platforms released in 1978 have now been tracked for 2 years on a continuous basis. The more precise System ARGOS monitoring of platforms released in 1979 was terminated in November of that year for economic reasons. A subsequent check ascertained that 9 of the latter platforms were still operating in late summer, 1980. Position monitoring has now been resumed for ungrounded bergs. The initial positions of the 22 tracked bergs are plotted in Figure 3.4.5. The discrepancy between this number and the complement of 20 platforms arose from the transfer of two platforms from grounded to freely moving bergs.

2. Iceberg Profiling

   A 1978 iceberg dimension study utilized photographic and sonar techniques to obtain measurements of the under and above-water dimensions of 35 selected bergs.

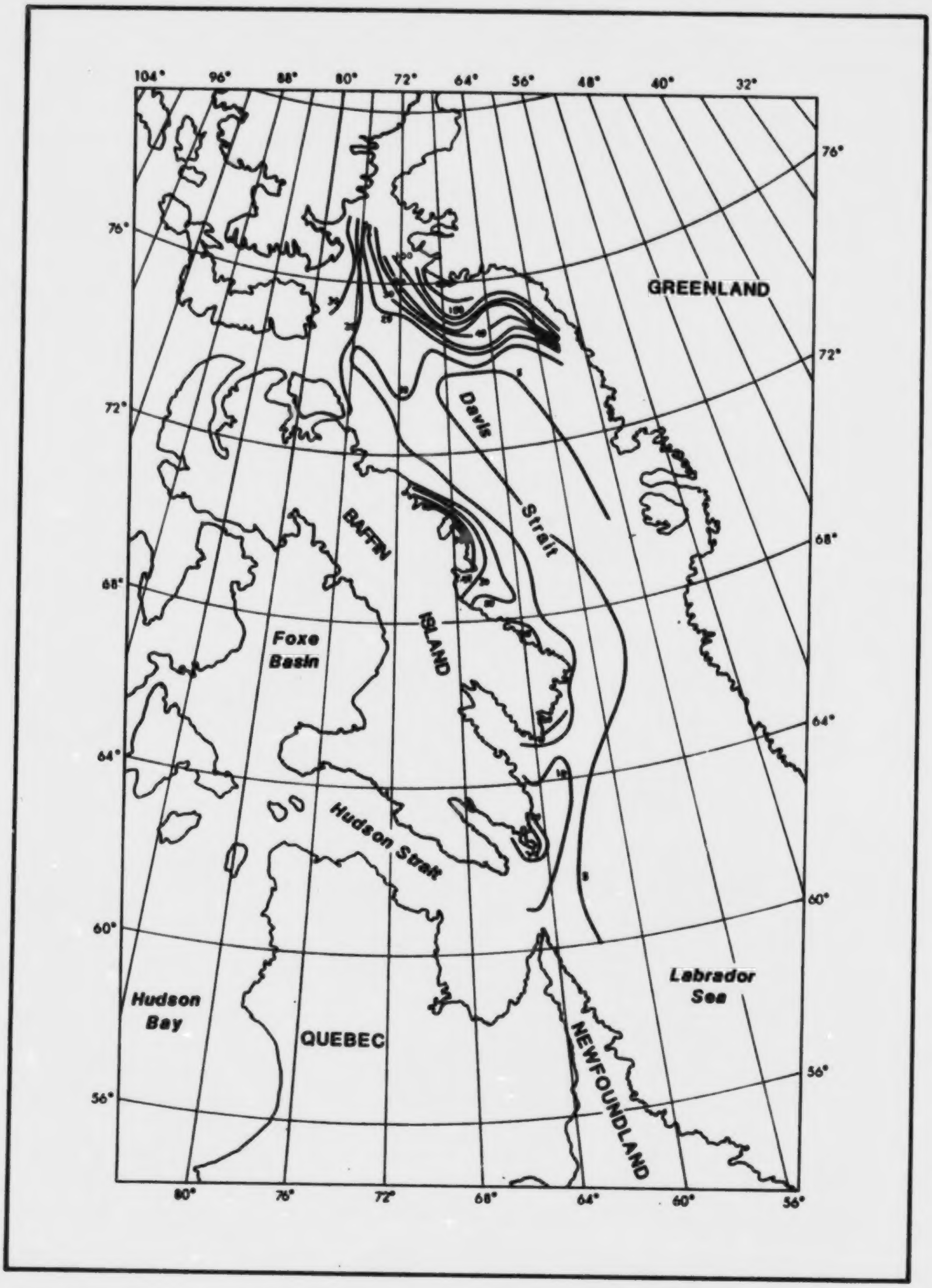
104°
96°
88°
80°
72°
64°
56°
48°
40°
32°
76°
72°
68°
64°
60°
56°
80°
76°
72°
68°
64°
60°
56°
GREENLAND
Davis
Strait
BAFFIN
ISLAND
Foxe
Basin
Hudson Strait
Hudson
Bay
QUEBEC
NEWFOUNDLAND
Labrador
Sea
100

Figure 3.4.4(a) Iceberg densities, September and October, 1963-1969 (Densities in bergs per 1000 sq. nautical miles)

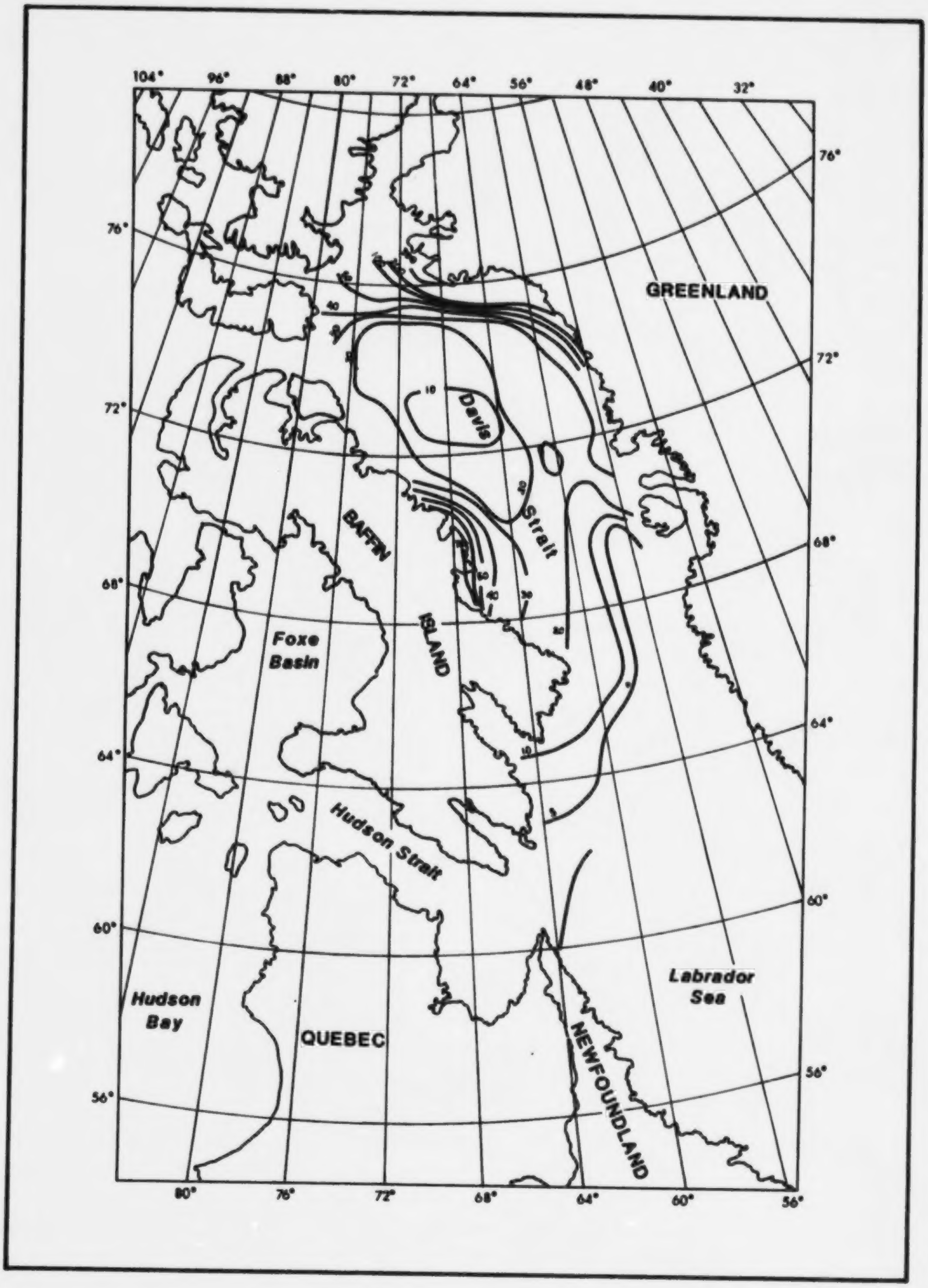
104°
96°
88°
80°
72°
64°
56°
48°
40°
32°
76°
72°
68°
64°
60°
56°
76°
72°
68°
64°
60°
56°
80°
76°
72°
68°
64°
60°
56°
GREENLAND
40
20
10
10
Davis
Strait
20
50
40
30
20
10
5
BAFFIN
ISLAND
Foxe
Basin
Hudson Strait
Hudson
Bay
QUEBEC
Labrador
Sea
NEWFOUNDLAND

Figure 3.4.4(b) Iceberg densities, 1968-1970 (Densities in bergs per 1000 sq. nautical miles)

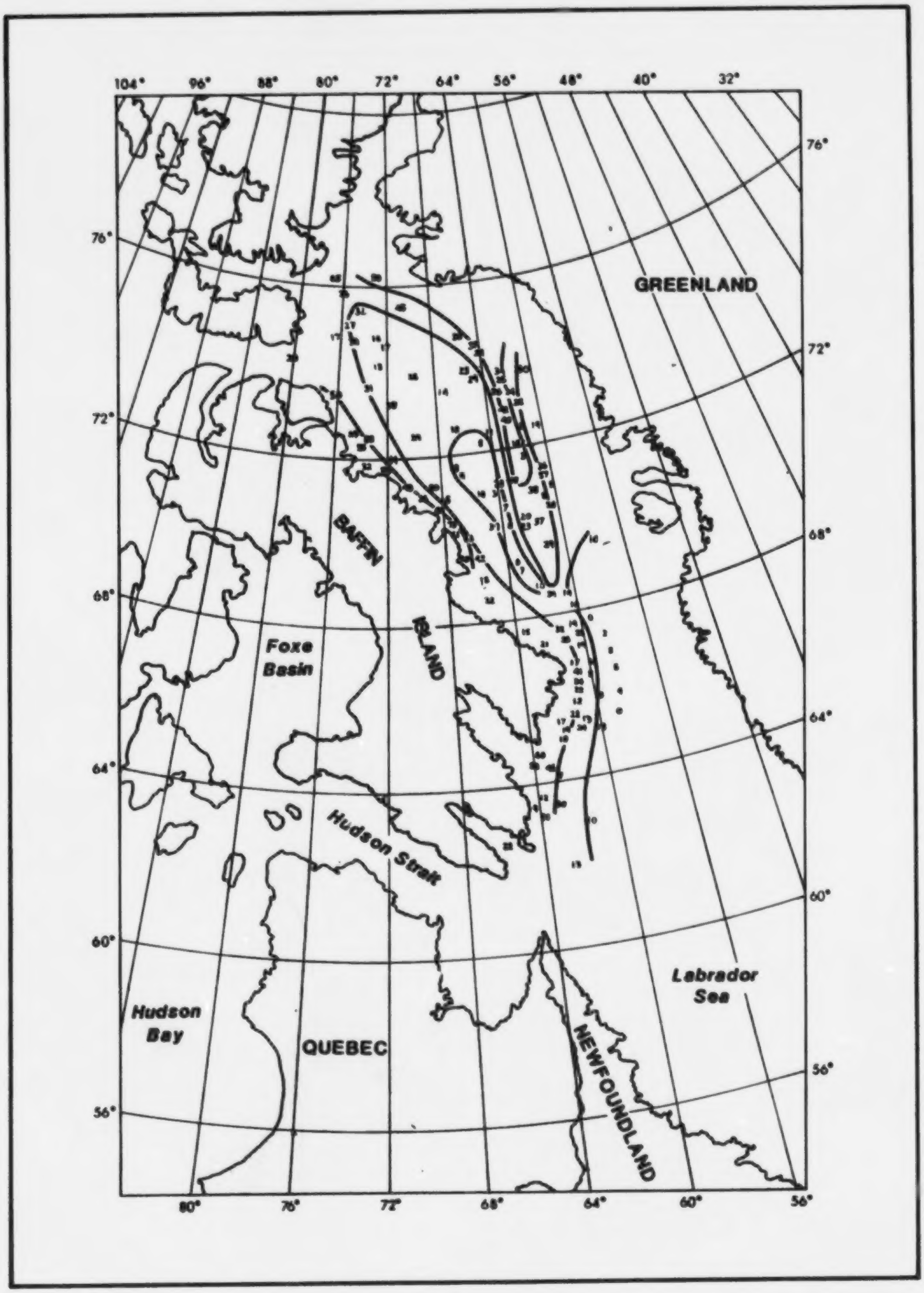
104°
96°
88°
80°
72°
64°
56°
48°
40°
32°
76°
72°
68°
64°
60°
56°
80°
76°
72°
68°
64°
60°
56°
GREENLAND
BAFFIN
ISLAND
Foxe
Basin
Hudson Strait
Hudson
Bay
QUEBEC
NEWFOUNDLAND
Labrador
Sea

Figure 3.4.4(c) Iceberg densities, August-October, 1971 (densities in bergs per 1000 sq. nautical miles)

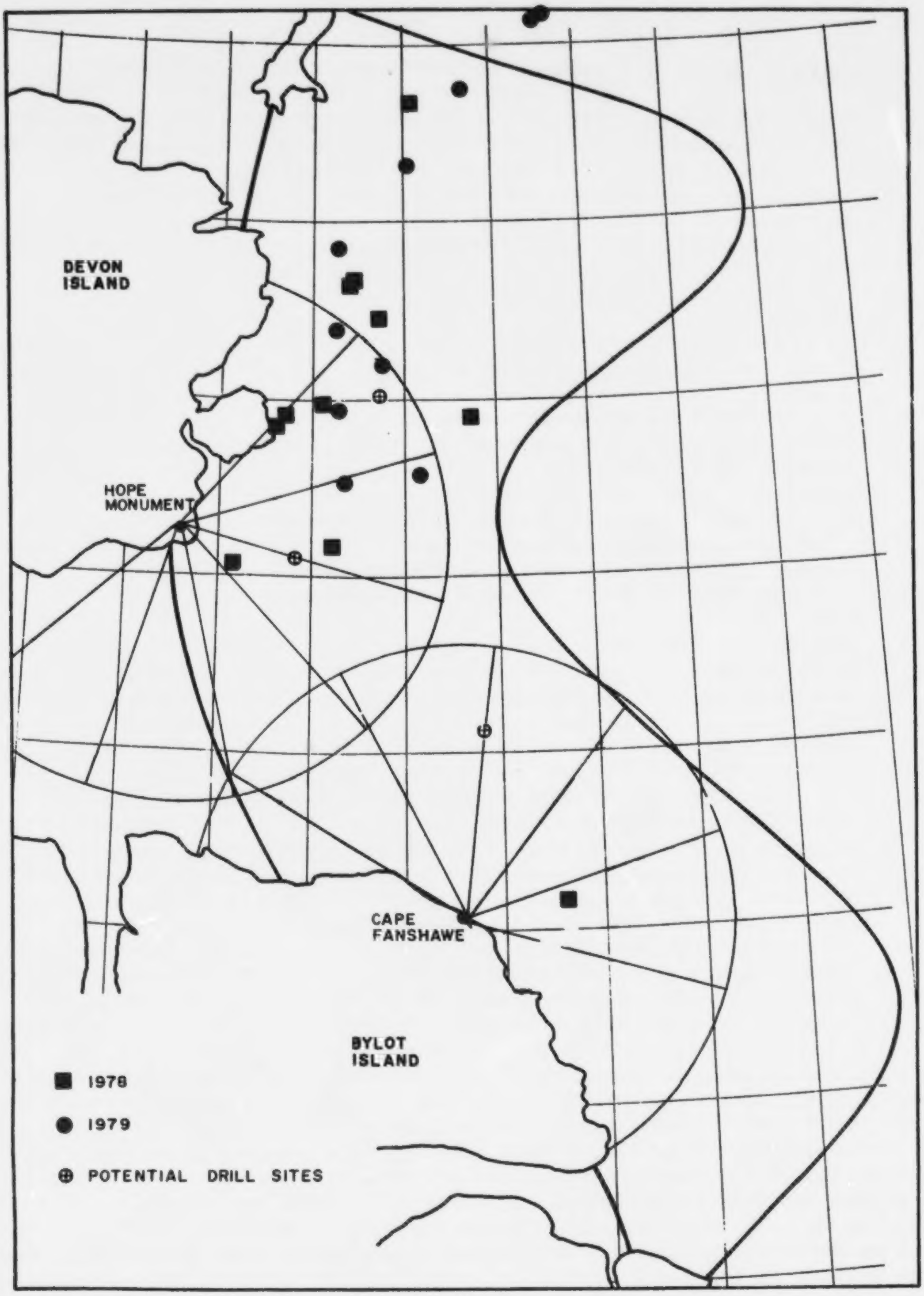
DEVON ISLAND
HOPE MONUMENT
CAPE FANSHAWE
BYLOT ISLAND
■ 1978
● 1979
⊕ POTENTIAL DRILL SITES

Figure 3.4.5 Initial positions of satellite-tracked bergs, during the 1978 and 1979 seasons, shown relative to the boundaries of the aerial survey (bold lines) and the 1978 Hope Monument and Cape Fanshawe radar tracking stations

3. Aerial Iceberg Surveys

Fixed-wing aircraft observation flights were maintained on an almost daily basis over the July to October periods of both 1978 and 1979. Photographic and radar techniques were used in conjunction with satellite navigation to establish berg numbers, positions, shape classifications and above-water physical dimensions. The approximate area of coverage is indicated in Figure 3.4.5 along with the positions of prospective drill sites.

4. Land-Based Radar Scanning

Radar stations were maintained at two land sites from early July to late September, 1978. Station locations were:

a) at 450 m elevation on Hope Monument near the southeastern corner of Devon Island and;
b) at 596 m elevation near Cape Fanshawe on the northeastern coast of Bylot Island.

The respective zones of coverage are delineated for each station in Figure 3.4.5. Sensitivity of detection decreased with distance resulting in an increasing preference for larger, favourably shaped (for reflection) bergs. This complication and the general strong shape-dependence of berg radar visibility limited the use of this technique to establish the intermediate scale (" 25 n.m.) distribution of berg numbers. To facilitate interpretation, other data including theodolite-determined berg positions, berg and sea ice photographs and meteorological observations were routinely recorded at both stations. Additional automatic air pressure, temperature and wind recording facilities were maintained at sea level sites near Cape Sherard on Devon Island and Cape Liverpool, Bylot Island.

The outlined studies represent but two calendar years of observations almost completely concentrated in summer periods which, at least in the vicinity of the eastern entrance to Lancaster Sound, were characterized by "worst year in five" ice conditions. The northern Baffin Bay ice conditions, on the other hand were markedly different in the two years (Section 3.1). Clearly the extent to which the observed details represent typical or extreme behaviour can only be established by continued study including perhaps some monitoring of northern berg source and entrapment regions. At the present time however, the data still undoubtedly represents the most extensive and detailed information base yet accumulated on environmentally relevant berg properties and thus must serve as the principal source for the descriptions of the iceberg environment given below. Of course, reference to earlier works, chiefly the 1972 A.P.O.A. study, will also be made for completeness and to extend the period of time covered by the results.

3.4.2 Intrinsic Iceberg Parameters

3.4.2.1 Numbers

According to the World Meteorlogical Network an iceberg is defined as "a massive piece of ice, more than 5 meters above sea level, which has broken away from a glacier and which may be afloat or aground". In practice, distinctions between bergs and the smaller categories of land-ice masses (i.e. "bergy bits" and "growlers") are often determined by the method of observation. Thus, while no fixed criteria were established in the Petro-Canada-EAMES land-based radar studies, an examination of accompanying photographic data suggests that the dimensions critical to strong radar signal return, namely berg length (maximum above-water horizontal dimension) and sail height, were generally in excess of 50 m and 5 m respectively. On the other hand the Petro-Canada-EAMES aerial surveys of 1978 and 1979 utilized a simple minimum length criterion in accord with both the plan-view method of observation and the need to minimize re-identification difficulties due to the more frequent "roll-overs" of shorter bergs. A 50 m value was used in the 1978 survey. Subsequent improvements in documentation procedures and an increased interest in small bergs allowed a reduction of this minimum length to 30 m in the 1979 aerial program.

This change, the differing lengths of the observation periods (103 days in 1978 versus 72 days in 1979) and an altered spatial distribution of flying time complicated comparison of the two annual berg populations. Nevertheless a review of the individual zone data indicated that 1979 berg numbers were approximately 20% fewer than those recorded in 1978. Typical daily distributions of various sized bergs are illustrated in Figure 3.4.6 for August 7 and 24, 1979. The apparent concentration of bergs seen in the northern portion of the survey area is a common but not general characteristic of the region. The underlying pattern of flow (See Section 3.4.3) is such that most bergs follow similar paths through the region ensuring that above average berg concentrations in northern areas ultimately lead, after an appropriate delay, to similar downstream increases.

Some measure of the time dependence of berg density may be obtained from the 6 hour berg totals plotted in Figure 3.4.7 a-f on the basis of the observation record of the Hope

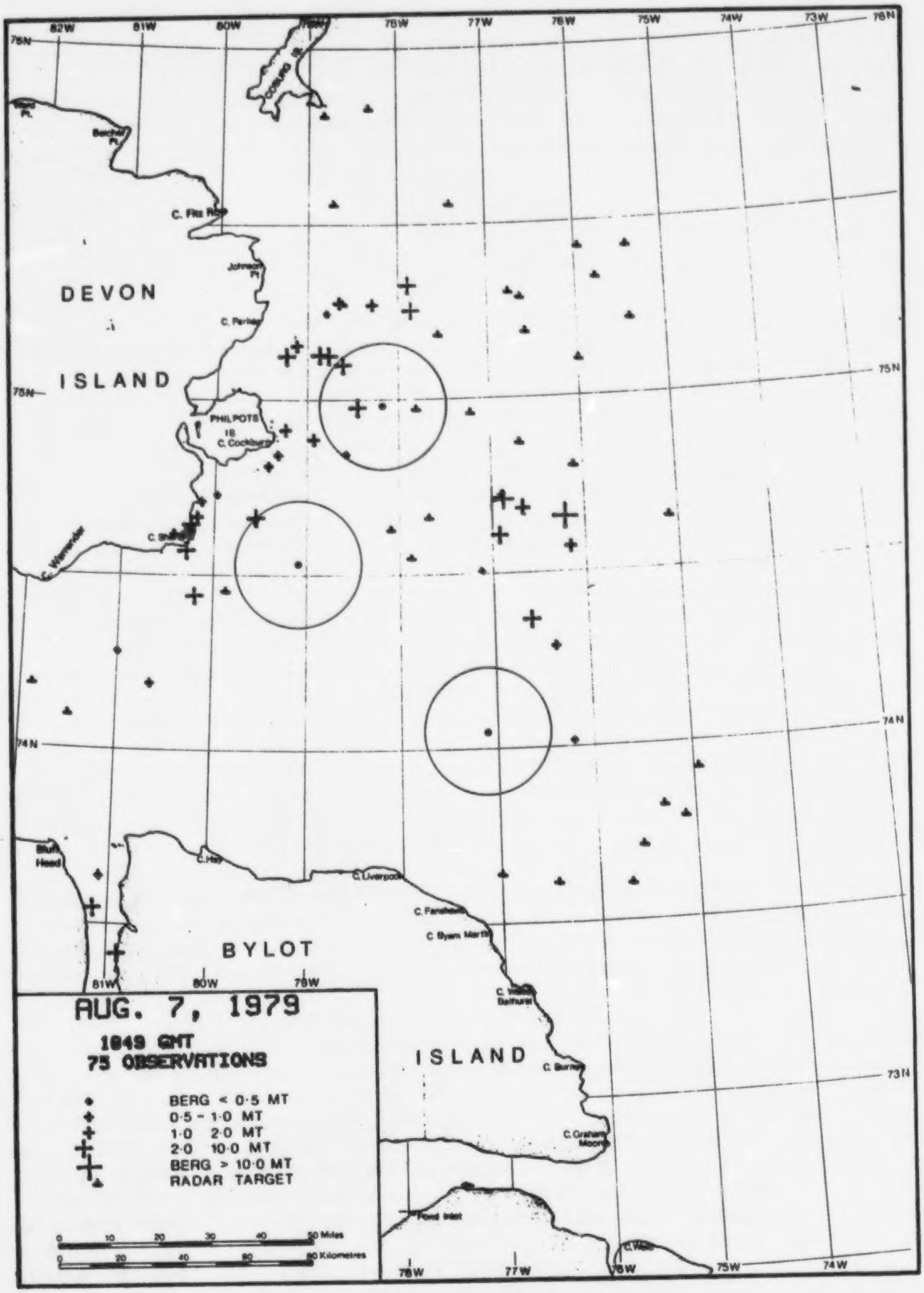
82W
81W
80W
79W
78W
77W
76W
75W
74W
73W
76N
75N
74N
73N
COBURG IS.
Beecher Pt.
C. Fitz Roy
Johnson Pt.
C. Parker
DEVON
ISLAND
PHILPOTS IS
C. Cockburn
C. Sherard
C. Warrender
Bluff Head
C. Hay
C. Liverpool
C. Fanshawe
C. Byam Martin
C. Walter Bathurst
BYLOT
ISLAND
C. Burney
C. Graham Moore
Pond Inlet
AUG. 7, 1979
1849 GMT
75 OBSERVATIONS
BERG < 0·5 MT
0·5 - 1·0 MT
1·0 2·0 MT
2·0 10·0 MT
BERG > 10·0 MT
RADAR TARGET
0 10 20 30 40 50 Miles
0 20 40 60 80 Kilometres

Figure 3.4.6(a) Distribution of icebergs, August 7, 1979

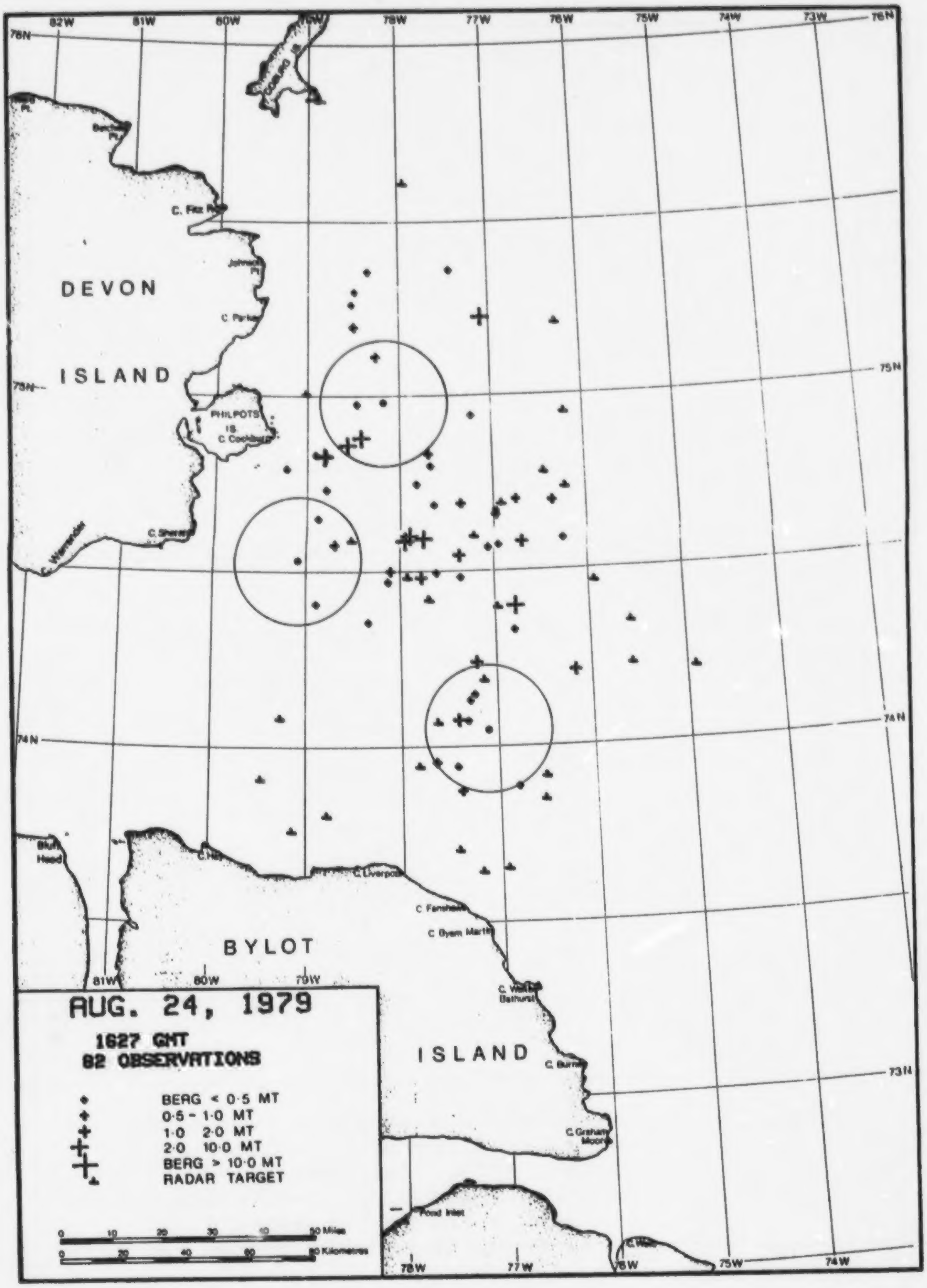
82W
81W
80W
79W
78W
77W
76W
75W
74W
73W
76N
75N
74N
73N
DEVON
ISLAND
PHILPOTS IS.
C. Fitz Roy
C. Parker
C. Sherard
C. Warrender
BYLOT
ISLAND
Bluff Head
C. Liverpool
C. Fanshawe
C. Byam Martin
C. Walter Bathurst
C. Burney
C. Graham Moore
Pond Inlet
AUG. 24, 1979
1627 GMT
82 OBSERVATIONS
BERG < 0·5 MT
0·5 - 1·0 MT
1·0 2·0 MT
2·0 10·0 MT
BERG > 10·0 MT
RADAR TARGET
0
10
20
30
40
50 Miles
0
20
40
60
80 Kilometres

Figure 3.4.6(b) Distribution of icebergs, August 24, 1979

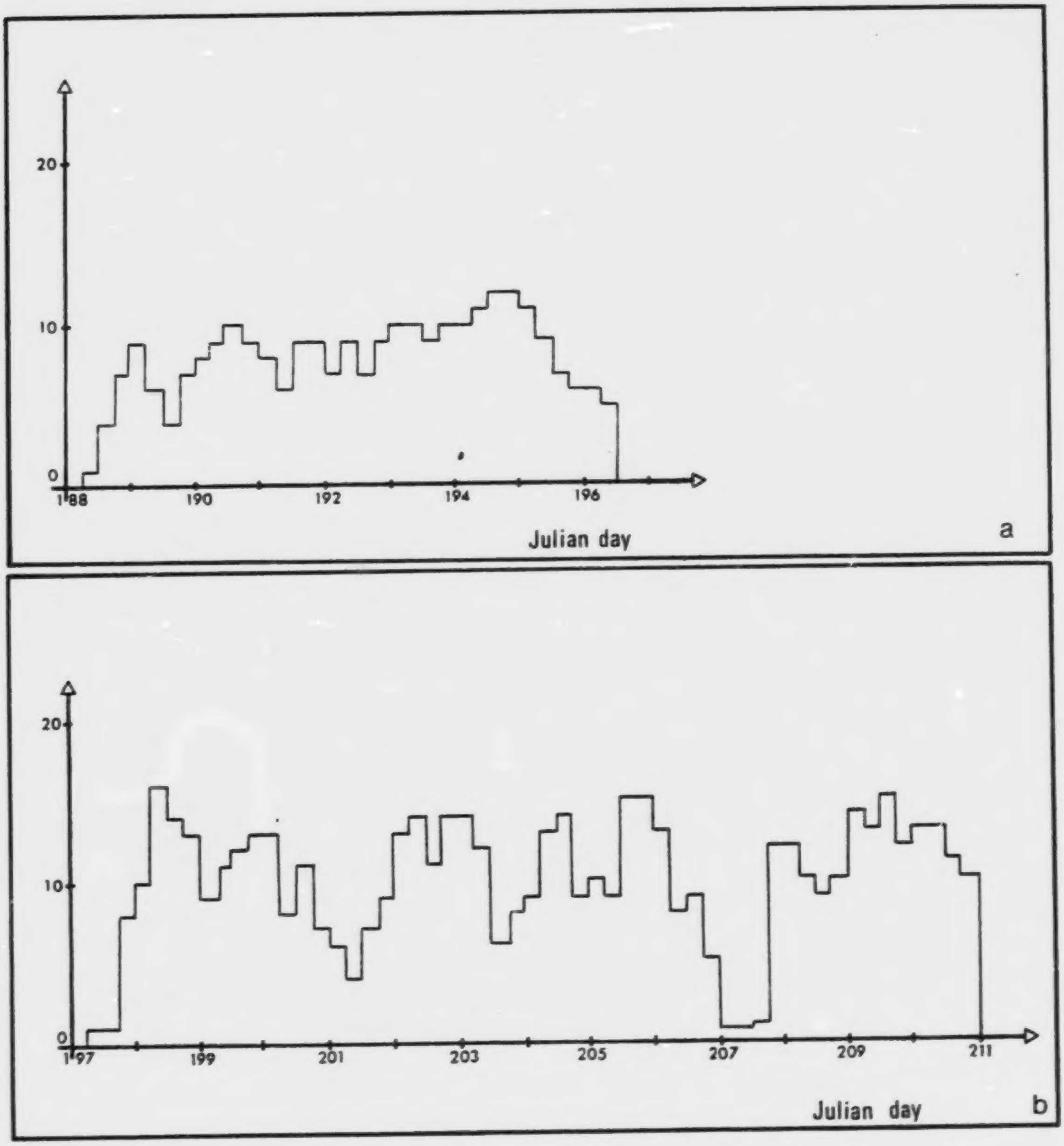

Figure 3.4.7 Number of bergs observed over 6-hour periods from the Hope Monument radar station, 1978: (a) Week 1; (b) Weeks 2 and 3; (c) Weeks 4 and 5; (d) Weeks 6 and 7; (e) Weeks 8 and 9; (f) Weeks 10 and 11

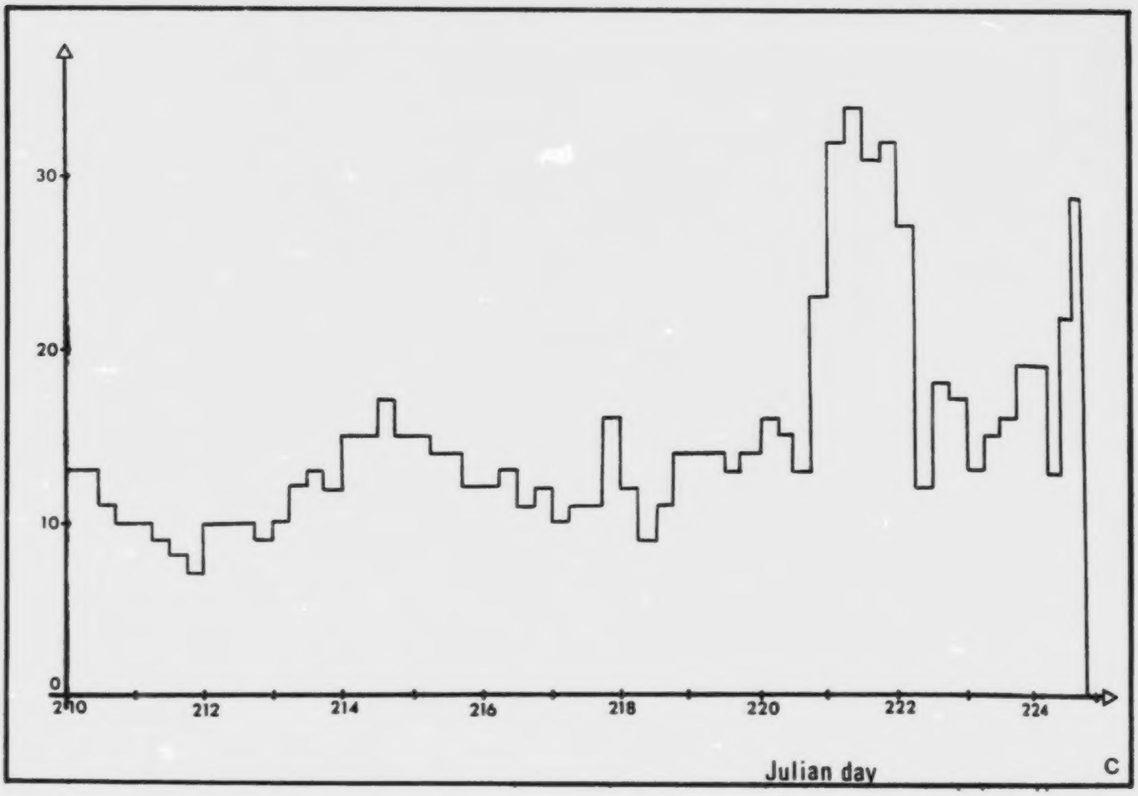

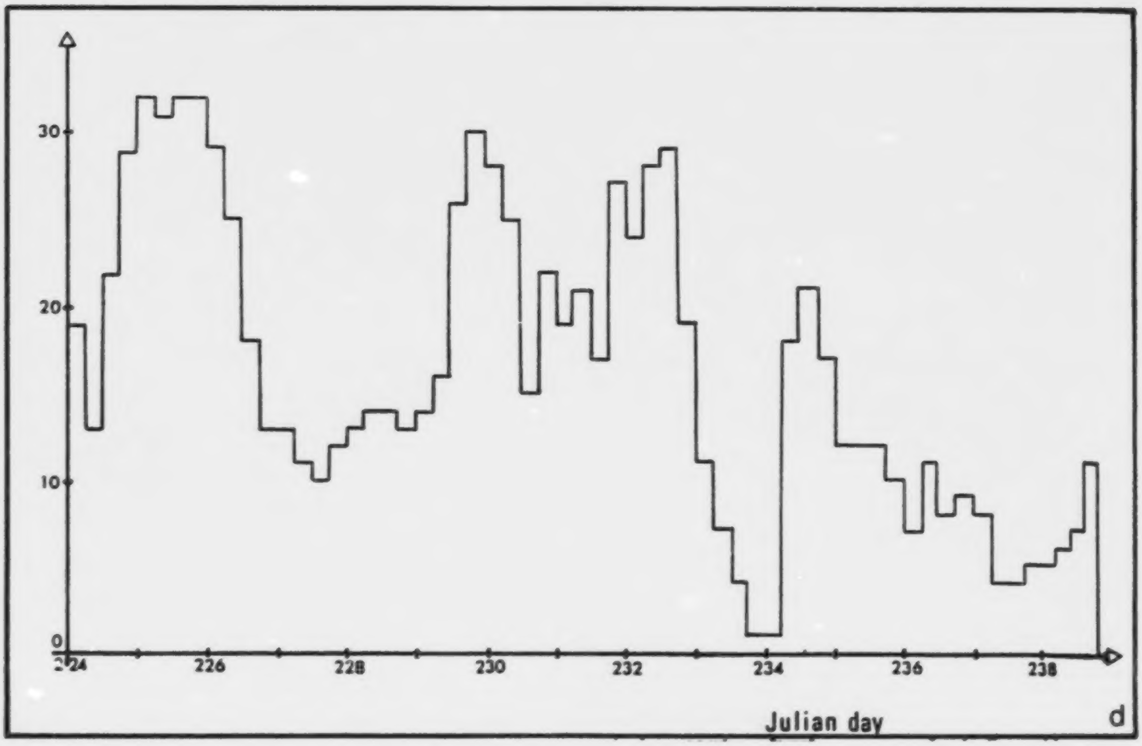

Figure 3.4.7 (Continued)

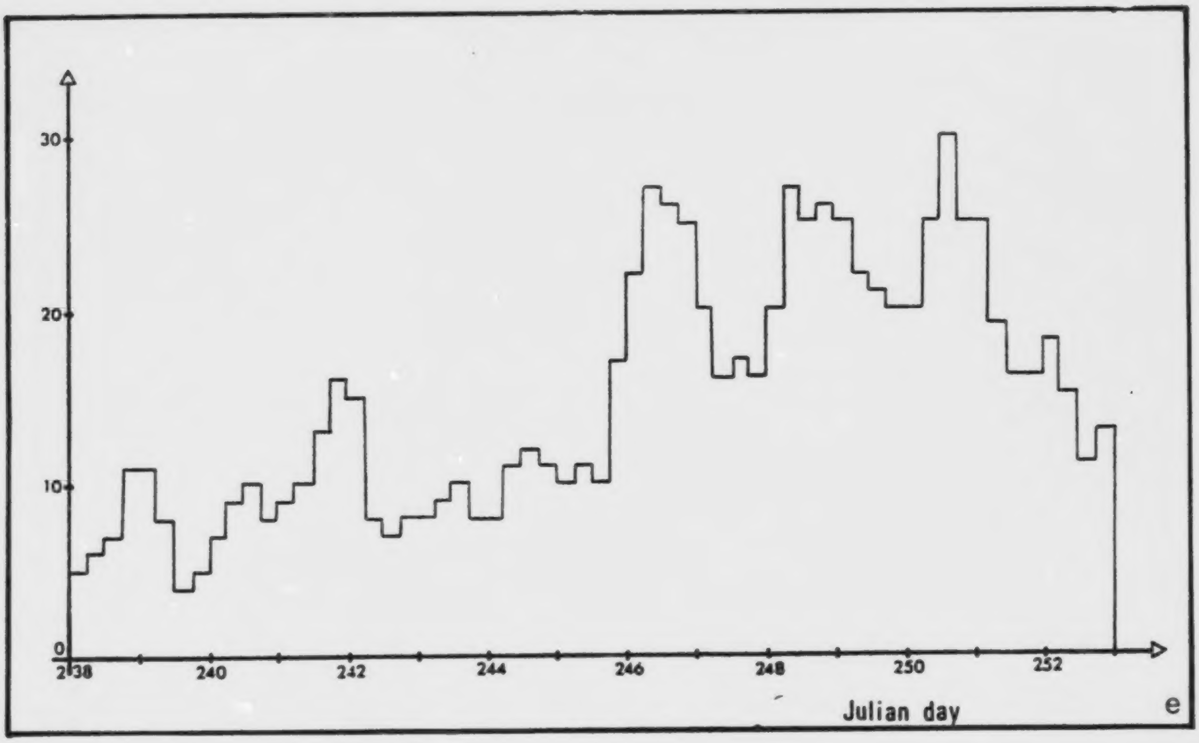

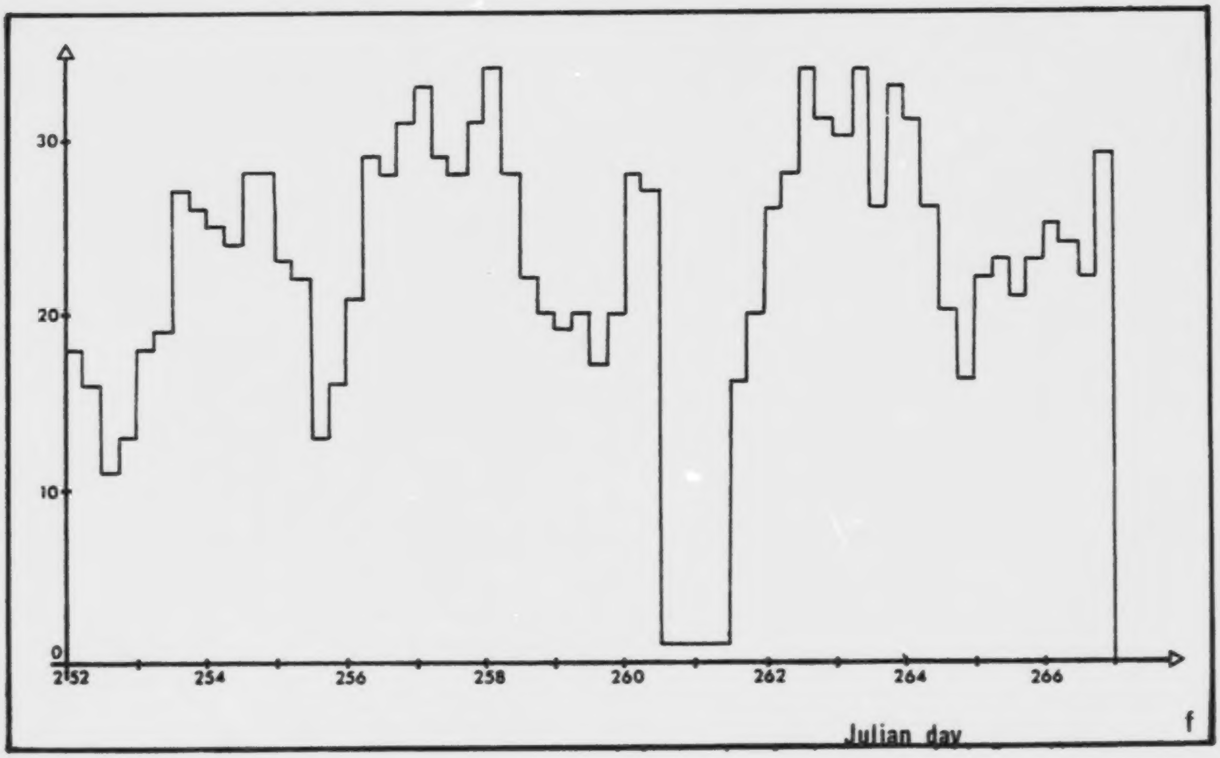

Figure 3.4.7 (Continued)

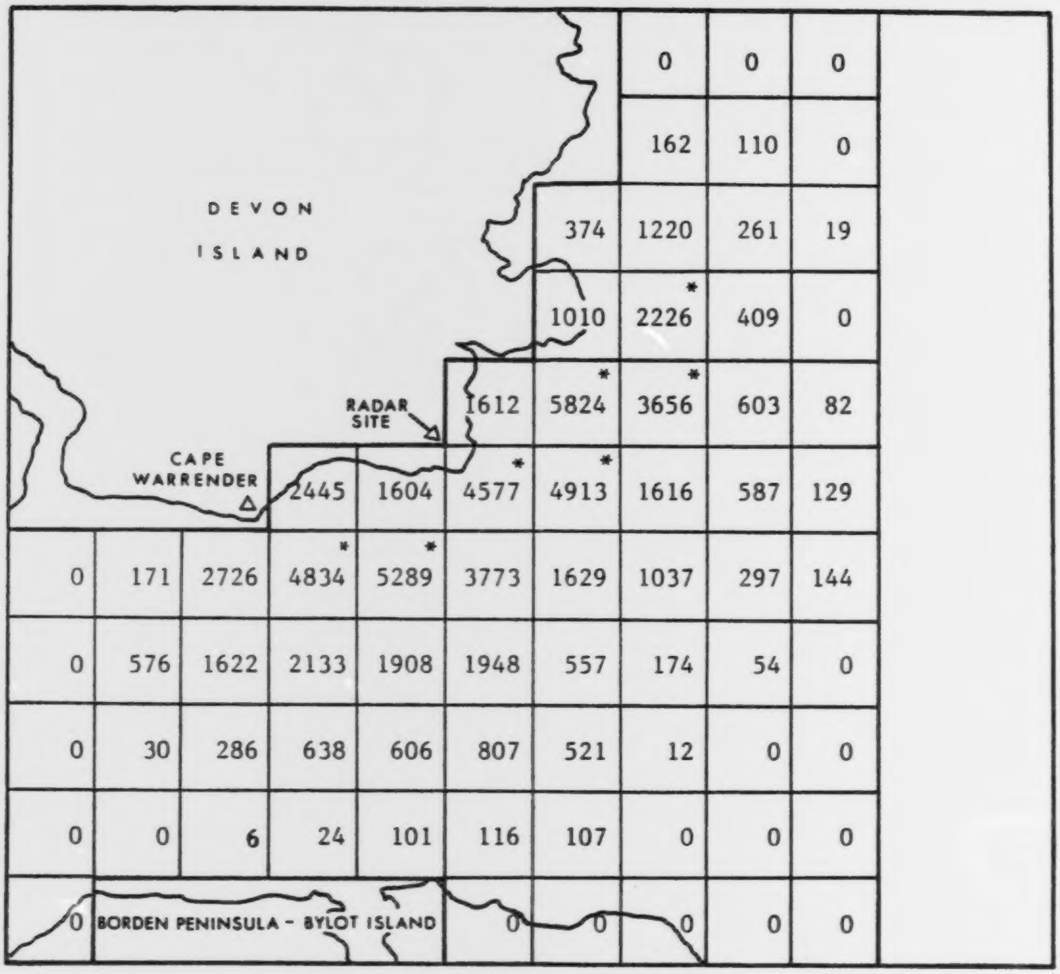
DEVON ISLAND
RADAR SITE
CAPE WARRENDER
BORDEN PENINSULA - BYLOT ISLAND

							0	0	0
							162	110	0
						374	1220	261	19
						1010	* 2226	409	0
					1612	* 5824	* 3656	603	82
			2445	1604	* 4577	* 4913	1616	587	129
0	171	2726	* 4834	* 5289	3773	1629	1037	297	144
0	576	1622	2133	1908	1948	557	174	54	0
0	30	286	638	606	807	521	12	0	0
0	0	6	24	101	116	107	0	0	0
0					0	0	0	0	0

Figure 3.4.8 Overall distribution of berg observations from Hope Monument radar station; 1978. Areas marked with asterisks are typically associated with large ice and water velocities

Monument radar station obtained over an 11 week period in 1978 (deLange Boom, MacNeill and Buckley, 1979). Aside from periods of station shutdown, the total number of bergs under observation in any 6-hour period usually ranged from 10 to 30 bergs with the trend being toward the low end of this range prior to day 220 when greater variability and generally greater numbers of bergs began to appear. Detectable "pulses" of high berg numbers appeared on days 221, 225 and 230 - 232 as well as a 10-day (days 235 - 245) interval of diminished densities. Overall the observed berg numbers followed a pattern of apparently random fluctuation superimposed upon a slow steadily rising function of time.

The use of these radar data as a probe of the spatial distribution of bergs was of course complicated by the strong range dependence of the detection sensitivity. Nevertheless making the simple assumption of azimuthal symmetry it was possible to use the overall distribution of berg observations (Figure 3.4.8) to deduce an underlying spatial non-uniformity in the form of a core of high berg density paralleling the eastern and southeastern coastlines of Devon Island. Such areas are denoted by asterisks in Figure 3.4.8 and are typically associated with large ice and water velocities (see Section 3.3 and Fissel, Lemon and Birch, 1980, as well as the berg motion discussion of Section 3.4.3). Elsewhere berg observation density fell off according to distance and spatial structure was unresolved. The observed pattern is consistent with the distribution of observations recorded by the M.V. Orion (Figure 3.4.9) and with the coarser trends inferred from A.E.S. data (Figure 3.4.10) which indicated a strong confinement of berg populations to the eastern end of Lancaster Sound.

3.4.2.2 Shapes

Classification of icebergs according to general categories of shape and form has been primarily motivated by the belief that such data offer easy methods of estimating iceberg age and underwater dimensions. In the first instance the relationship is based upon an observed linkage between berg shape and extent of deterioration since calving and entry into the marine environment. On the other hand, the use of berg shape data to obtain difficult to observe underwater information is based upon approximate and somewhat questionable empirical relationships which have been assumed to exist between the raios of maximum underwater depth (draft) and maximum above water height (sail) for bergs of a given shape category. These relationships, if valid, would minimize the need for underwater data, for example, in the estimation of berg drift and bottom-scouring probabilities.

Unfortunately, there has been little consistency in the terminology and criteria used in the recording of shape data.

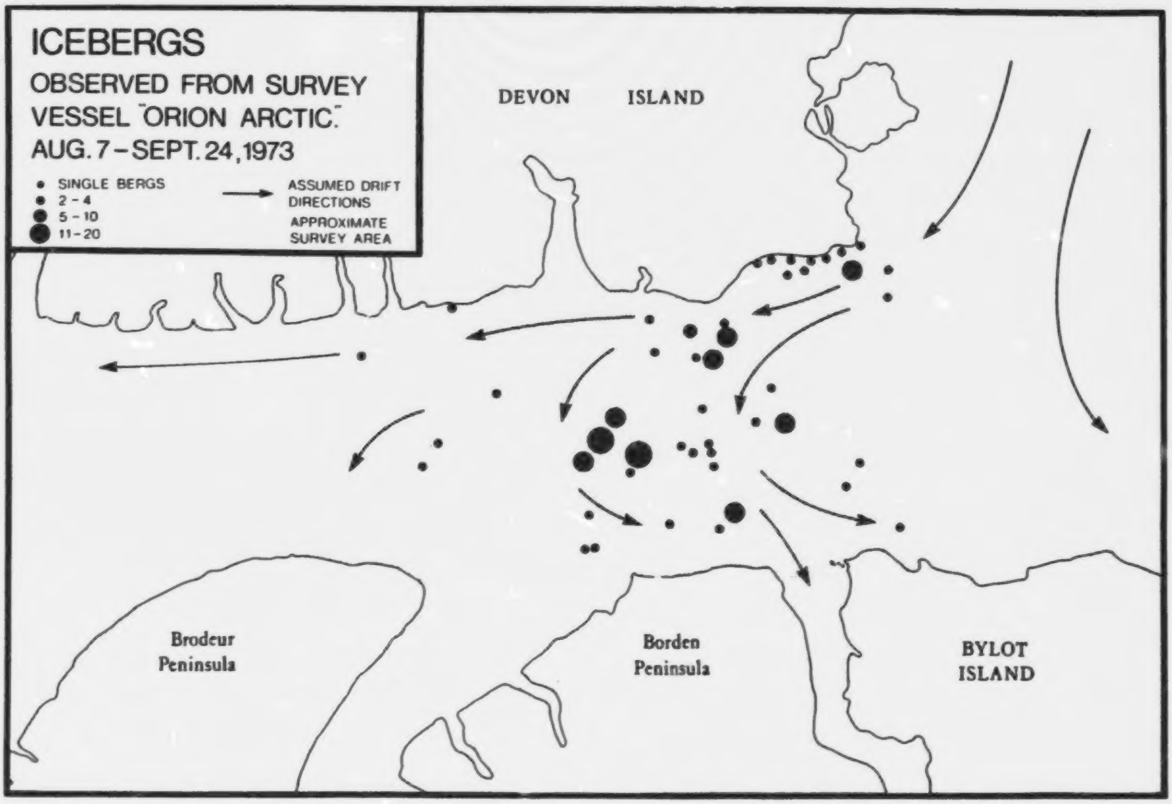
ICEBERGS
OBSERVED FROM SURVEY VESSEL "ORION ARCTIC."
AUG. 7 - SEPT. 24, 1973
● SINGLE BERGS
● 2 - 4
● 5 - 10
● 11 - 20
ASSUMED DRIFT DIRECTIONS
APPROXIMATE SURVEY AREA
DEVON ISLAND
Brodeur Peninsula
Borden Peninsula
BYLOT ISLAND

Figure 3.4.9 Icebergs observed from Survey Vessel "Orion Arctic" August 7 - September 24, 1973

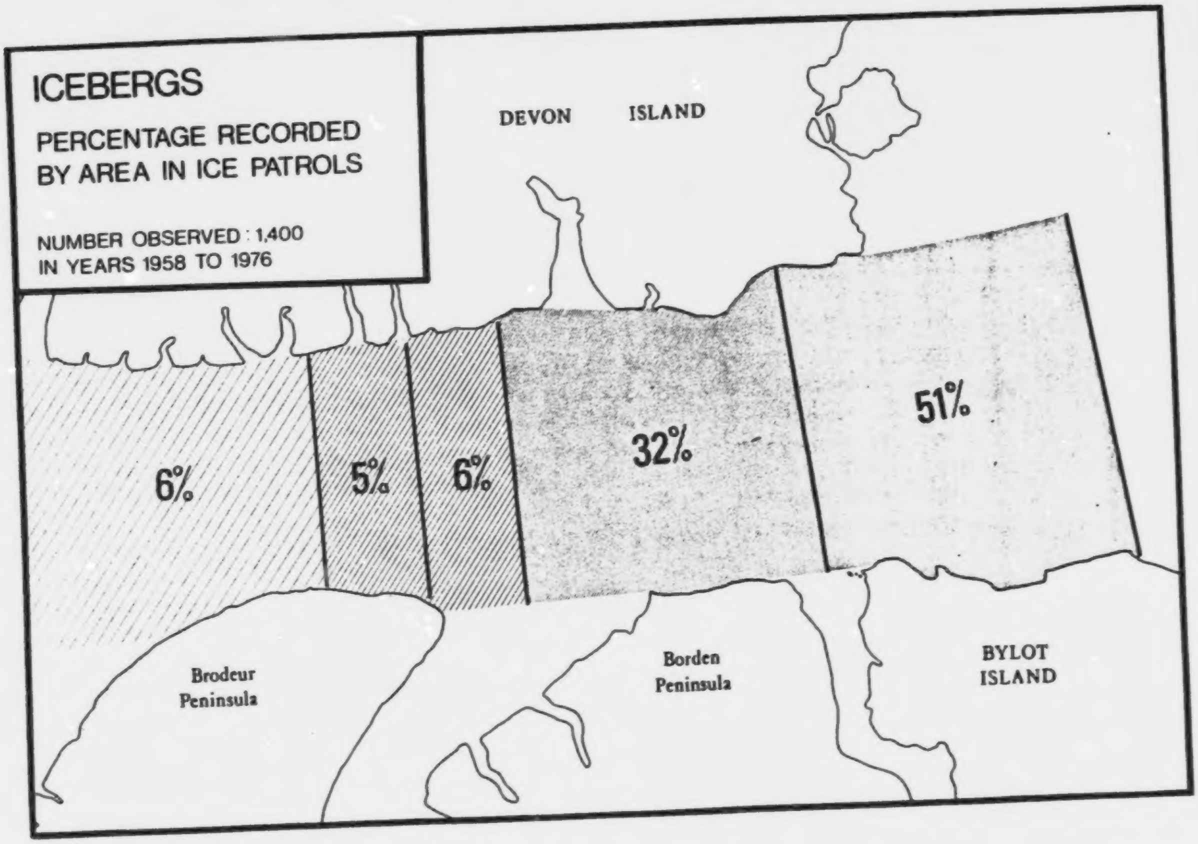
ICEBERGS
PERCENTAGE RECORDED BY AREA IN ICE PATROLS
NUMBER OBSERVED : 1,400
IN YEARS 1958 TO 1976
DEVON ISLAND
6%
5%
6%
32%
51%
Brodeur Peninsula
Borden Peninsula
BYLOT ISLAND

Figure 3.4.10 Icebergs percentage recorded by area in ice patrols

Categories have been variously labelled as "picturesque Greenland", "tabular", "tilted tabular", "broken tabular", "blocky", "perfectly spherical", "domed", "horned and winged" and "drydock" (Smith, 1928; NORDCO, 1979; A.P.O.A., 1973, Robe, 1975; Miller, 1980). The classification scheme of the present review is based upon the terminology used in the 1978 and 1979 Petro-Canada-EAMES field studies and is illustrated in Figure 3.4.11. The categories generally correspond to increasing age or extent of sea immersion proportional to the degree of geometric irregularity, with the tabular and drydock types usually representing the initial and final stages respectively of the iceberg life cycle. In practice, however, there is much room for ambiguity in the age-shape relationships depending, among other things, upon berg origin and the particular trajectory and ice conditions encountered by the berg enroute to the observation site.

The Petro-Canada-EAMES shape data were obtained from the 1978 photographic records of the Bylot Island radar station (NORDCO, 1979) and from berg and ice reconnaissance flights undertaken in 1979 (Miller, 1980). Results are listed in Table 3.4.1 for both sources together with similar data* obtained in 1972 for the Baffin Bay portion of the *M.V. Hans Egede* cruise (A.P.O.A., 1973). This table also includes values of the draft/sail parameter ϕ appropriate to each category as obtained by averaging the berg dimension data gathered both from the work of Robe (1975) and from the detailed 1978 Petro-Canada-EAMES documentation of 35 bergs (ICE, 1979).

Table 3.4.1

Distribution of Berg Shapes

	Tabular $\phi=4.4$	Tilted Tabular $\phi=3.9$	Blocky $\phi=3.9$	Pinnacled $\phi=2.7$	Domed $\phi=6.0$	Drydocked $\phi=2.4$
NORDCO (1979)	28%	13%	22%	26%	7%	2%
Miller (1980)	17%	--	42%	28%	15%	--
A.P.O.A. (1973)	30%	--	23%	16%	30%	2%

---

* Inclusion of this data in Table 3.4.1 was made assuming the following correspondence of P.C.-EAMES/A.P.O.A. shape categories: Tabular/Weathered Tabular; Blocky/Picturesque Greenland; Pinnacled/Pinnacled; Domed/Perfectly Spherical and Drydocked/Horned and Winged.

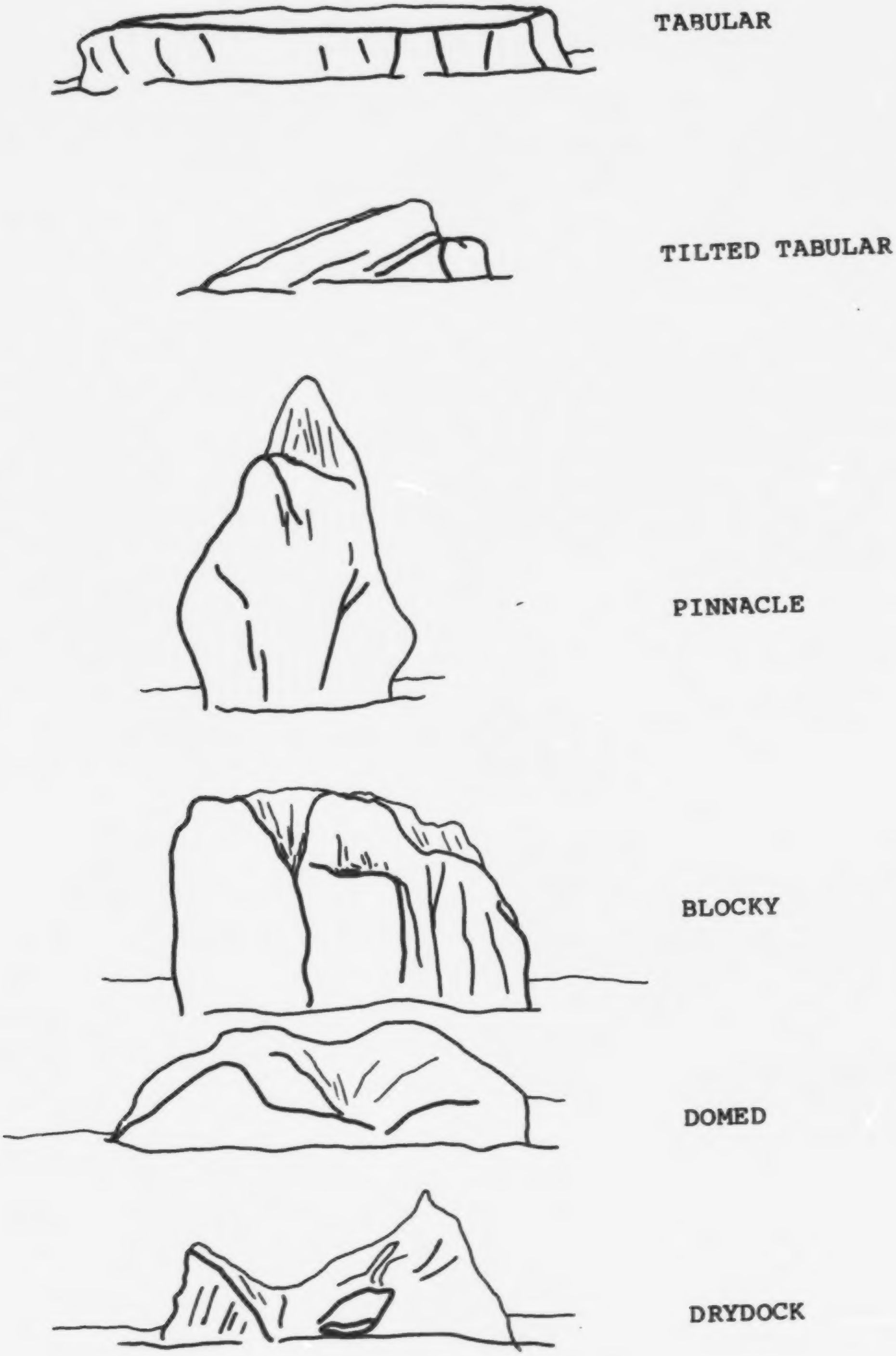
TABULAR
TILTED TABULAR
PINNACLE
BLOCKY
DOMED
DRYDOCK

Figure 3.4.11 Classification terminology of iceberg shapes.

Unfortunately, the analysis of Robe (1975) has cast considerable doubt upon the statistical basis for a category-dependent draft/sail ratio. It was concluded that no significant difference could be established between the different category ratios. Our re-analysis of Robe's results together with additional more recent data (ICE, 1979) confirmed this conclusion to the 95% level of certainty. On a lesser level (68% certainty) some distinction is possible between the domed and pinnacled - drydocked categories which are nominally associated with extremely large and small ratios respectively. in general however, the recommendation of Robe (1975) suggesting the use of a shape-independent value of $\phi = 3.95$ as a depth estimating guideline seems appropriate.

The shape distribution data themselves exhibit no clear-cut trend except that the majority of bergs tend to fit in the tabular, tilted tabular and blocky categories generally associated with relatively young berg populations. Many of the differences between the various survey results could be attributed to differences of judgement and possible overlapping and confusion of criteria. Clearly some consistency must be established in the classification process if iceberg shape data are to be deemed worthy of even qualitative analysis.

3.4.2.3 Dimensions

Distributions of above-water berg dimensions are represented in Figures 3.4.12 - 3.4.15 on the basis of the 1978 and 1979 aerial berg surveys.* Comparable data are also included in the first three of these Figures as obtained from the 1972 M.V. Hans Egede survey (A.P.O.A., 1973). In the case of the 1978 and 1979 results, maximum, mean, median and 10% and 90% exceedance values are also listed. Particular note should be taken of the maximum recorded dimensions of: 760 m (length); 96 m (peak height) and 63 million tonnes mass. The largest draft recorded in the accompanying survey (ICE, 1979) of 35 different bergs was 220 m.

---

* The 1978 and 1979 height and mass distributions were obtained from:

a) direct measurements and calculations based upon detailed stereographic surveys of 293 bergs;

b) height and mass values calculated from length and area data for the remainder of the berg populations using regressions derived from the detailed 293 berg data sets.

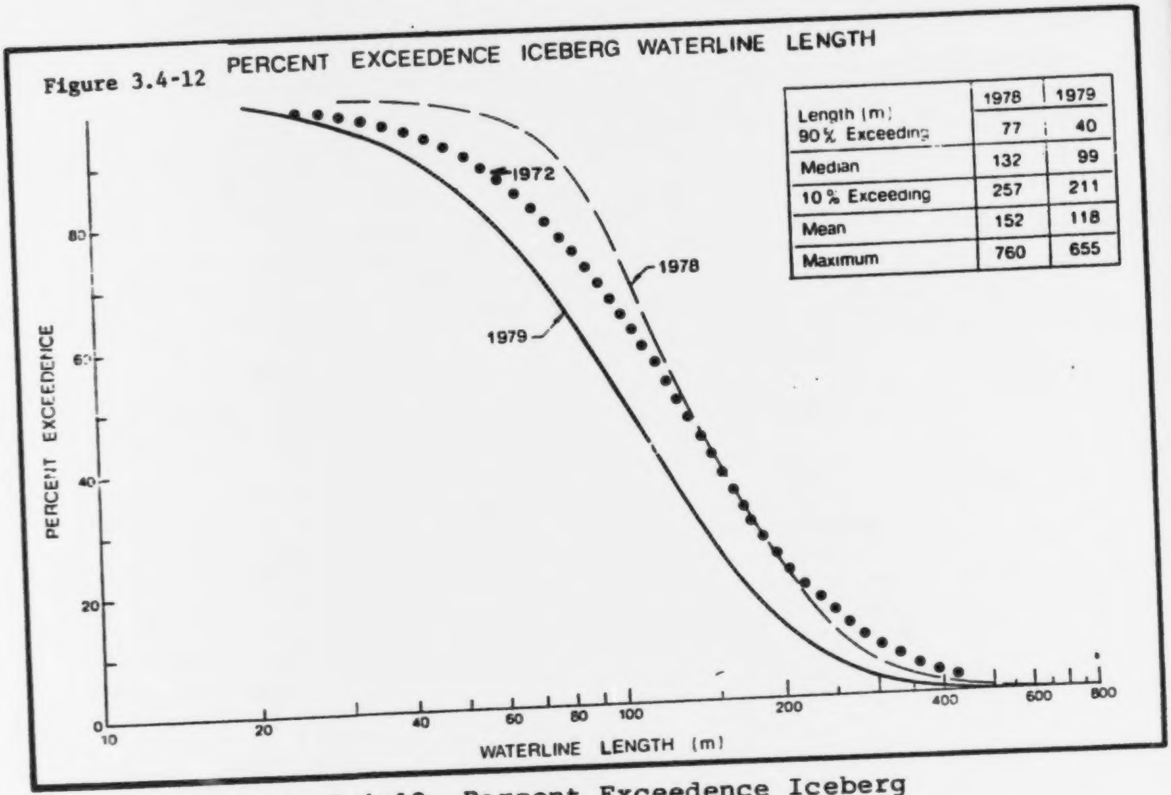
Figure 3.4-12 PERCENT EXCEEDENCE ICEBERG WATERLINE LENGTH

Length (m)	1978	1979
90 % Exceeding	77	40
Median	132	99
10 % Exceeding	257	211
Mean	152	118
Maximum	760	655

Figure 3.4.12 Percent Exceedence Iceberg Waterline Length

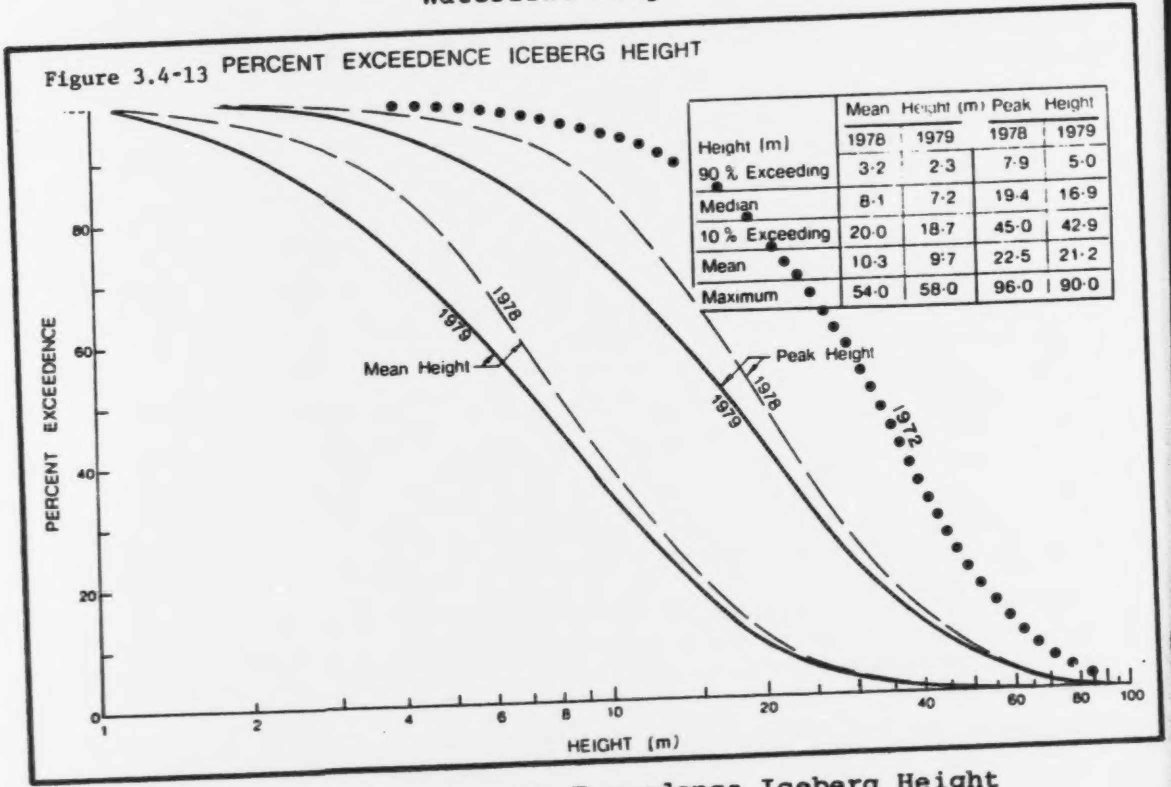
Figure 3.4-13 PERCENT EXCEEDENCE ICEBERG HEIGHT

Height (m)	Mean Height (m)		Peak Height	
	1978	1979	1978	1979
90 % Exceeding	3·2	2·3	7·9	5·0
Median	8·1	7·2	19·4	16·9
10 % Exceeding	20·0	18·7	45·0	42·9
Mean	10·3	9·7	22·5	21·2
Maximum	54·0	58·0	96·0	90·0

Figure 3.4.13 Percent Exceedence Iceberg Height

Figure 3.4-14 PERCENT EXCEEDENCE ICEBERG WATERLINE AREA

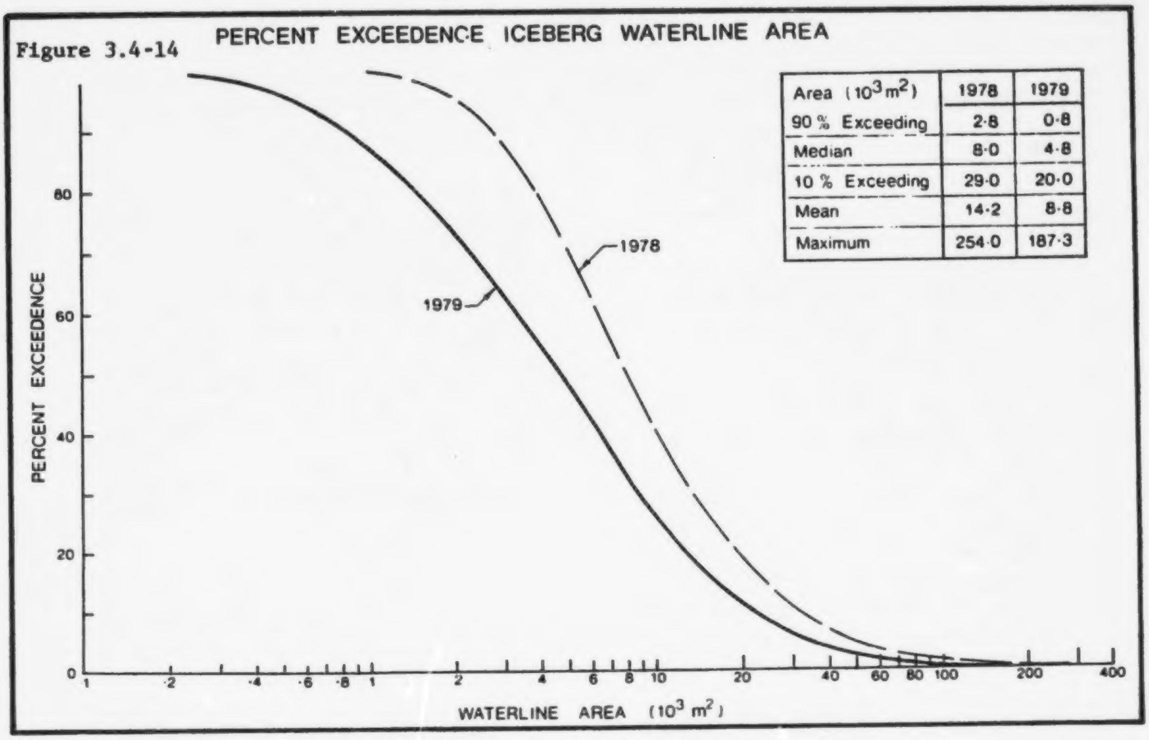

Area ($10^3 m^2$)	1978	1979
90 % Exceeding	2·8	0·8
Median	8·0	4·8
10 % Exceeding	29·0	20·0
Mean	14·2	8·8
Maximum	254·0	187·3

Figure 3.4.14 Percent Exceedence Iceberg Waterline Area

Figure 3.4-15 PERCENT EXCEEDENCE ICEBERG MASS

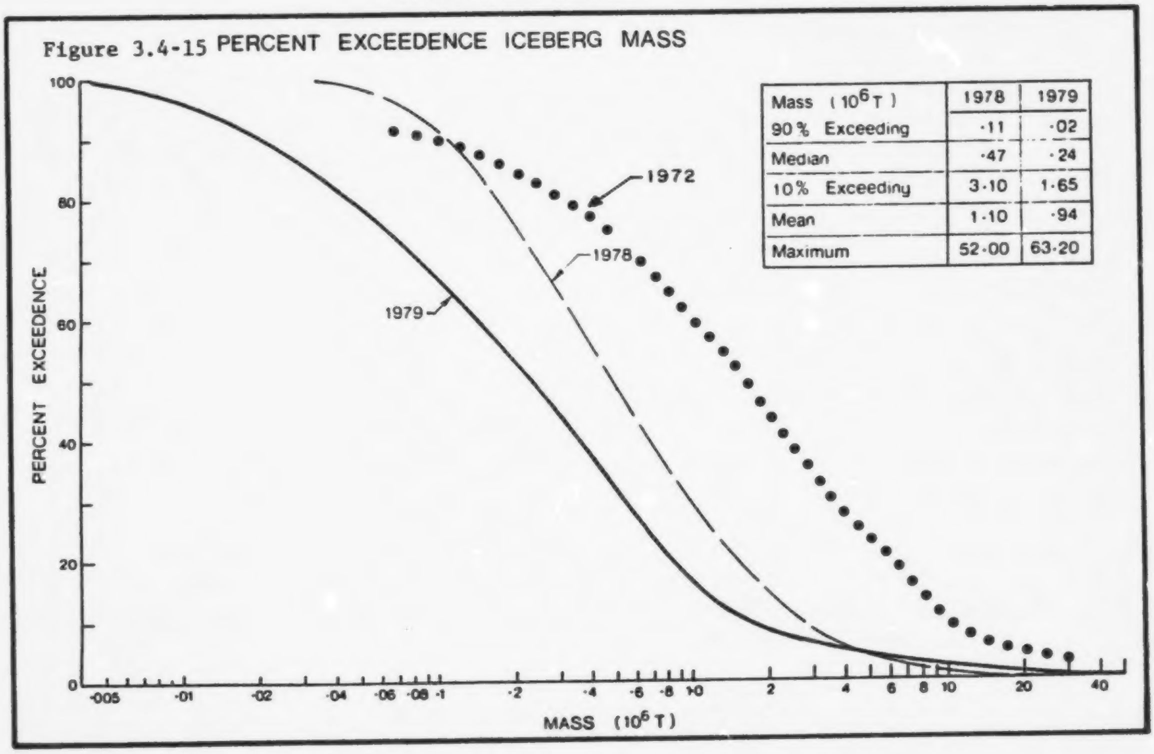

Mass (10^6 T)	1978	1979
90 % Exceeding	·11	·02
Median	·47	·24
10 % Exceeding	3·10	1·65
Mean	1·10	·94
Maximum	52·00	63·20

Figure 3.4.15 Percent Exceedence Iceberg Mass

When account is taken of the increased attention given to small bergs in 1979, the length distributions of Figure 3.4.12 reflect the general impression of little significant difference between the 1978 and 1979 dimensional data sets.

In Figure 3.4.12 the additional 1979 small berg data produced an almost uniform 40 m offset relative to the 1978 results. The 1972 distribution was closely bracketted by the 1978 and 1979 results except at the lower and upper ends of the length scale where increased densities were observed in the early survey. Deviations from the 1978 and 1979 distributions were much more pronounced in the height and mass data of 1972, which in terms of averages exceeded the later results by 50% and 300% respectively. Some attempt has been made (NORCOR, 1979) to attribute these differences to:

a) the inclusion of Davis Strait data in the 1972 survey and;

b) its accompanying restriction to the late season period (September - October) when presumably smaller bergs would have preferentially disappeared from the sampled population.

While these arguments may have some validity, it is equally likely that the apparent differences in the 1972 distributions can be attributed to the methods (unspecified) used to choose the documented berg population (measurements were made on but 350 of the 2,000 bergs seen in the Hans Egede survey).

In the absence of additional and directly comparable data, it must be assumed that the distributions of Figure 3.4.12 - 3.4.15 are representative of the berg population in eastern Lancaster Sound and northwest Baffin Bay.

3.4.3 Iceberg Motion

The detailed prediction of the movements of an individual iceberg remains a formidable if not impossible task. Leaving aside remaining uncertainties in mechanisms, such a capability requires precise and continuing data on berg geometry and on the turbulent atmospheric and oceanic boundary layers. As in the case of floe ice, the impracticality of obtaining such data has created the need for extensive berg motion data in order to:

a) establish the general characteristics of the iceberg motion in the area of interest and;

b) to serve as a base for continuing work on predictive models.

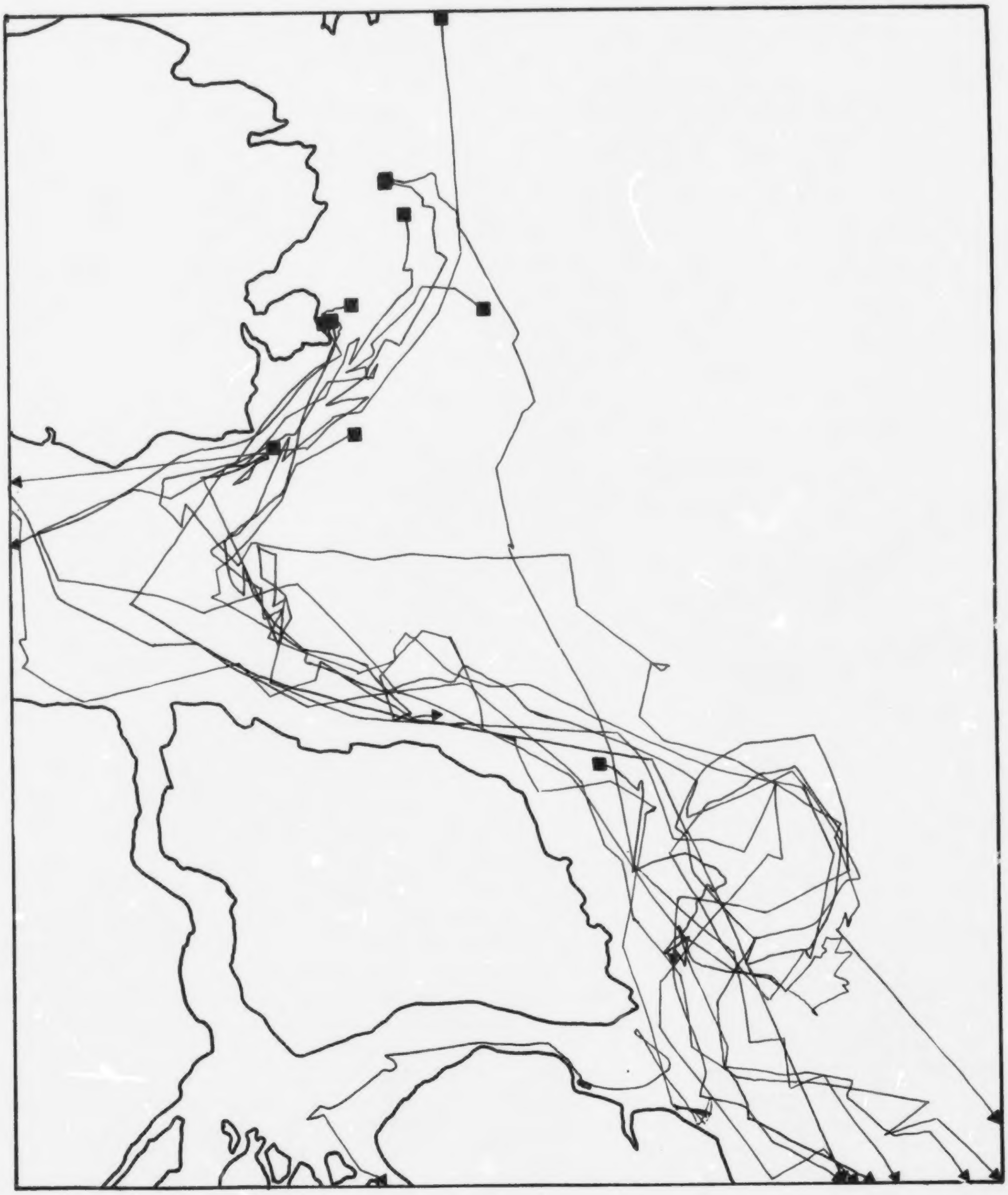

Figure 3.4.16 Trajectories of berg drifts from Satellite - tracked data, 1978

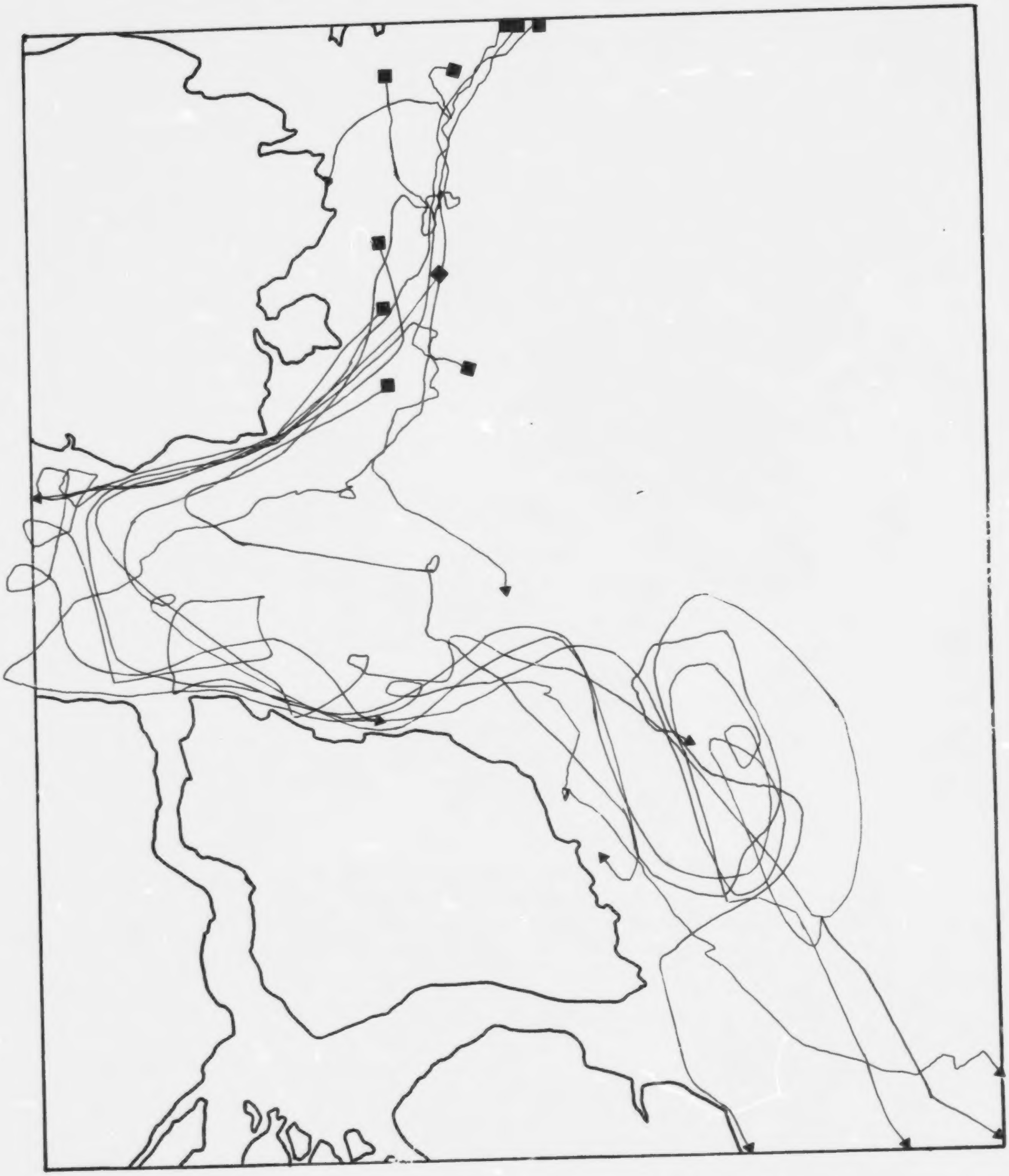

Figure 3.4.17 Trajectories of berg drifts from satellite - tracked data, 1979 (Fissel, 1980)

In the Petro-Canada-EAMES studies, iceberg motion was monitored on several spatial and temporal scales according to the resolutions and measurement frequencies characteristic of the utilized aerial observation radar, land-based radar , and satellite-tracking radar techniques.

The general features of the regional berg drift are perhaps most readily illustrated through the satellite-tracking data [Fissel (1980), Arctic Sciences Ltd. (1980 a, b)] which offer a moderately accurate (mean errors of .5 to 2.5 km) position information at frequencies of 2 to 12 times/day over periods in excess of a full calendar year. The regional trajectories of all bergs tracked in this manner have been plotted in Figures 3.4.16 and 3.4.17 on the basis of respectively, the 1978 and 1979 data. No attempt has been made in these Figures to distinguish dates or other features related to rates of berg movement. Instead, the accumulated mass of trajectory data itself is suggestive of major features of the annual berg circulations. The existence of an intrusive flow into Lancaster Sound is clearly the dominant feature of the circulation. Approximately 90% of the bergs, originally located in a 30 n.m. wide strip off the east coast of Devon Island, eventually find their way into the eastern end of the Sound. The common path of entry skirts the southeastern corner of Devon Island, near Cape Sherard, passing through the zones where large berg numbers were observed in both the 1978 Hope Monument radar study and in the 1974 cruise of the M.V. Orion (Section 3.4.2.1). The narrowing of the trajectory envelopes in this region corresponded to minimum across-stream widths of 10 n.m. and 3 n.m. for 1978 and 1979 respectively. The greater constriction of the berg paths in 1979 also corresponded to increased penetration of Lancaster Sound with respectively 70%, as opposed to 44%, of the bergs reaching as far west as the 81.8°W. line of Cape Warrender. The majority of 1978 bergs crossed to the south side of Parry Channel near 80°W. in strong contrast to the 82°W region favoured in the 1979 crossings. Substantial penetration of Lancaster Sound west of the roughly 83°W boundary of Figures 3.4.16 and 3.4.17 was achieved by only 2 bergs in overlapping intervals (September 18 - October 10, September 21 - October 2) of 1978. These bergs followed complicated, looping trajectories in the western region, each reaching roughly 85°W before moving eastward again and out of Lancaster Sound.

A survey of detailed trajectory data (see below) suggests that, after entry near Cape Sherard, a typical berg has a 7 to 10 day residence time in Lancaster Sound west of 79°W. East of 79°W the exit flow of bergs out of the Sound is slowed considerably by the prevalence of counter-clockwise looping to the northwest and north of Cape Fanshawe. To the east of 78°W the trajectories swing to the northeast before turning southward again beyond the 76°W line. Subsequent drift in the area east of Bylot island is dominated by large diameter counter-clockwise looping with typical periods for the larger structures being on the order of 10 days.

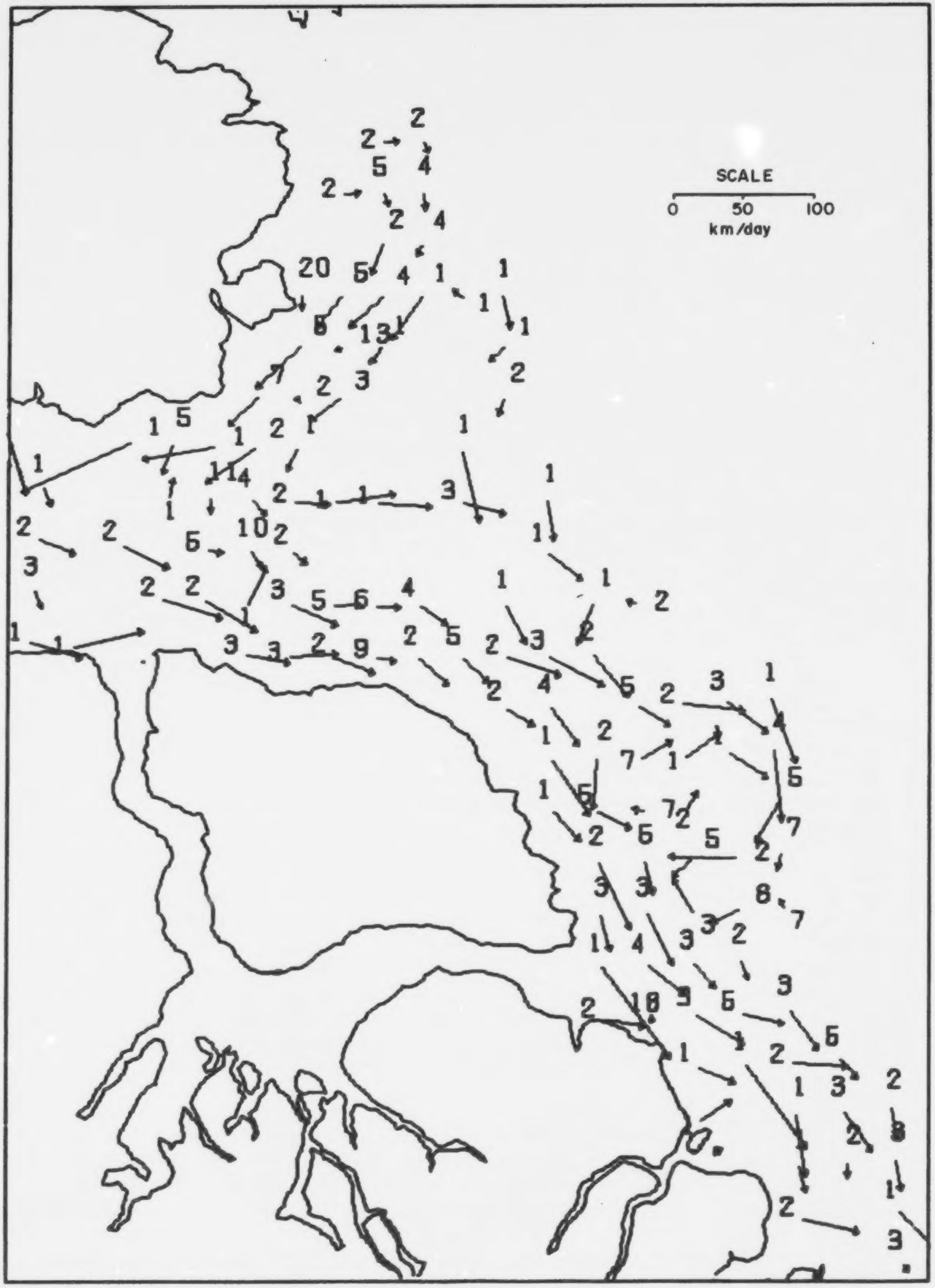
SCALE
0
50
100
km/day

Figure 3.4.18(a) Average velocity vectors, from 1978 Satellite-tracked berg data (1 inch = 100 km/day)

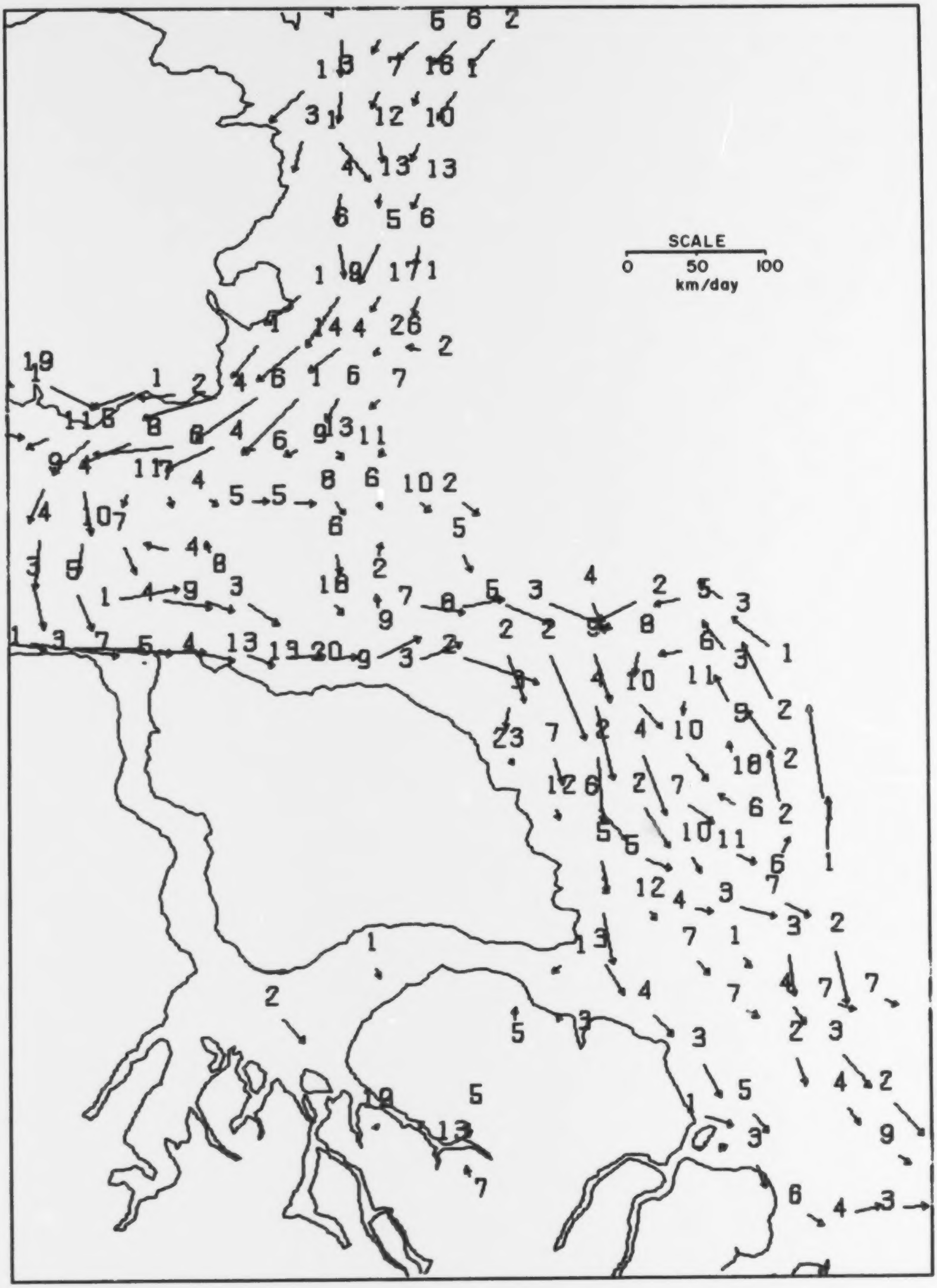
SCALE
0
50
100
km/day

Figure 3.4.18(b) Average velocity vectors, from 1979 Satellite-tracked berg data (1 inch = 100 km/day)

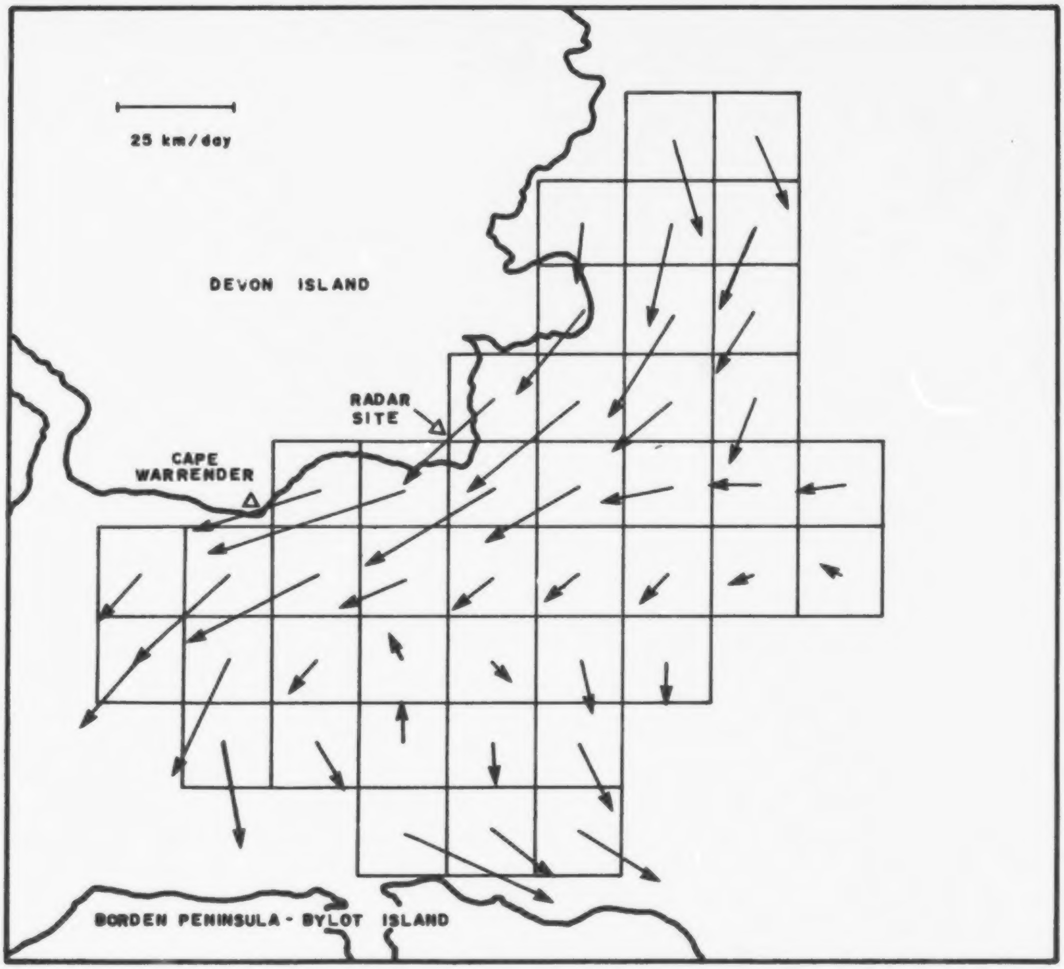
25 km/day
DEVON ISLAND
RADAR SITE
CAPE WARRENDER
BORDEN PENINSULA - BYLOT ISLAND

Figure 3.4.19 Average zonal velocity vectors, from 1978 Hope Monument radar-tracked berg data

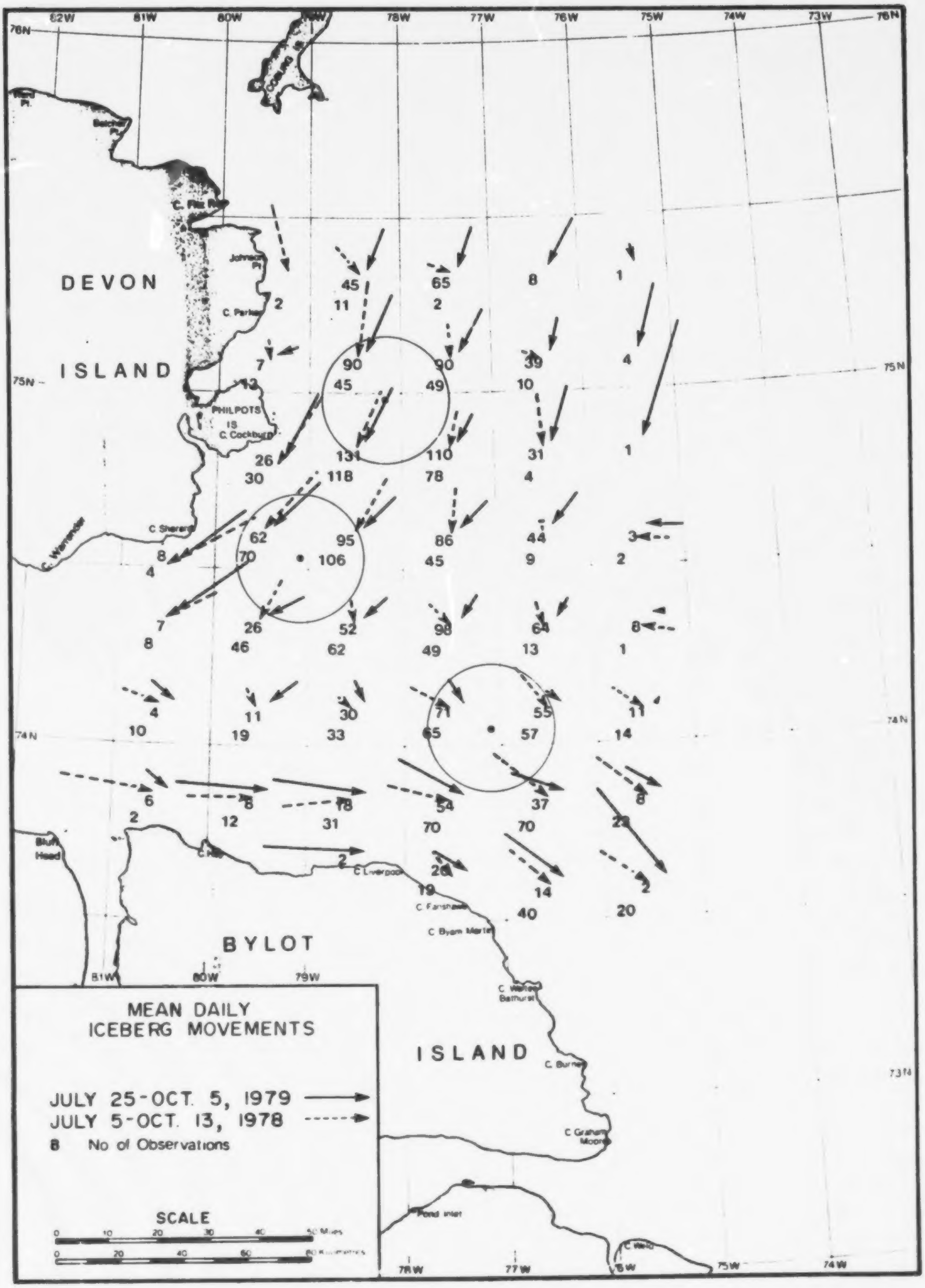
DEVON
ISLAND
PHILPOTS IS
C. Cockburn
C. Sherard
C. Warrender
Johnson Pt.
C. Parker
Belcher Pt.
C. Fitz Roy
Coburg Is.
BYLOT
ISLAND
Bluff Head
C. Hay
C. Liverpool
C. Fanshawe
C. Byam Martin
C. Walter Bathurst
C. Burney
C. Graham Moore
Pond Inlet
C. Weld
MEAN DAILY ICEBERG MOVEMENTS
JULY 25-OCT. 5, 1979
JULY 5-OCT. 13, 1978
8 No. of Observations
SCALE
0 10 20 30 40 50 Miles
0 20 40 60 80 Kilometres
82W
81W
80W
79W
78W
77W
76W
75W
74W
73W
76N
75N
74N
73N

Figure 3.4.20 Average velocity vectors, from 1978 1979 serial observations (1978 dashed)

Some measure of the rates of berg movement along the trajectories of Figures 3.4.16 and 3.4.17 may be obtained from the average velocity vectors represented in Figure 3.4.18a, b. In this case each vector represents the average of all velocities computed in each of the indicated 18.5 km by 18.5 km zones on the basis of adjoining satellite "fixes" of berg position.

Similar zonal or box averages have also been computed (See Figure 3.4.19) from the weekly average velocities obtained in the 1978 Hope Monument radar study (deLange Boom, McNeill and Buckley, 1979) and from the 1978 and 1979 aerial observation programs (NORCOR, 1980). (Figure 3.4.20). In spite of the different time intervals used in the respective velocity calculations (2 to 12 hours for satellite tracking; 20 minutes for radar- and one or more days for aerial observation-data) the alternative representations are in reasonable agreement in most regions of overlap.

The average velocity data and the accumulation of trajectories indicate few substantive differences between the 1978 and 1979 berg circulations. The results are consistent with a relatively unchanging pattern of berg motion which greatly resembles in detail the circulation of floe ice (Wilson and Marko, 1980) and the flow of the upper portion of the water column as deduced from satellite-tracked drifters, current meter and water mass measurements (Fissel, Lemon and Birch, 1980). These results as well as other features of the circulation such as the presence of repetitive looping or eddying motions are inexplicable in terms of direct atmospheric forcing mechanisms. The alternative, namely the dominant influence of the upper level water currents is to be expected on the basis of the high ratio of under- to above-water berg surface areas and from the large magnitudes of the currents in the region's zones of rapid flow. Significant wind influence and a consequent higher variability would be expected to be confined to areas outside of the main core of rapid water movement.

Interpretation of berg drift data may be simplified in terms of the simple classifaction scheme introduced by Fissel et al (1980) relative to the regional pattern of near-surface water flow. In this scheme, near-surface currents are considered in each of the 8 adjoining zones indicated in Figure 3.4.21. Zone boundaries are denoted by shading and a distinction is also made, through additional darkening of a 10 km wide zone, following the perimeters of all land masses. The latter delineates a distinct near-shore zone where significant differences such as smaller-scale spatial variability, enhanced tidal effect and motions associated with local wind regimes are commonly noted relative to adjoining off-shore areas. In the individual off-shore zones vectors of varying length and darkness are used to denote respectively the magnitude and degree of variability in the near-surface

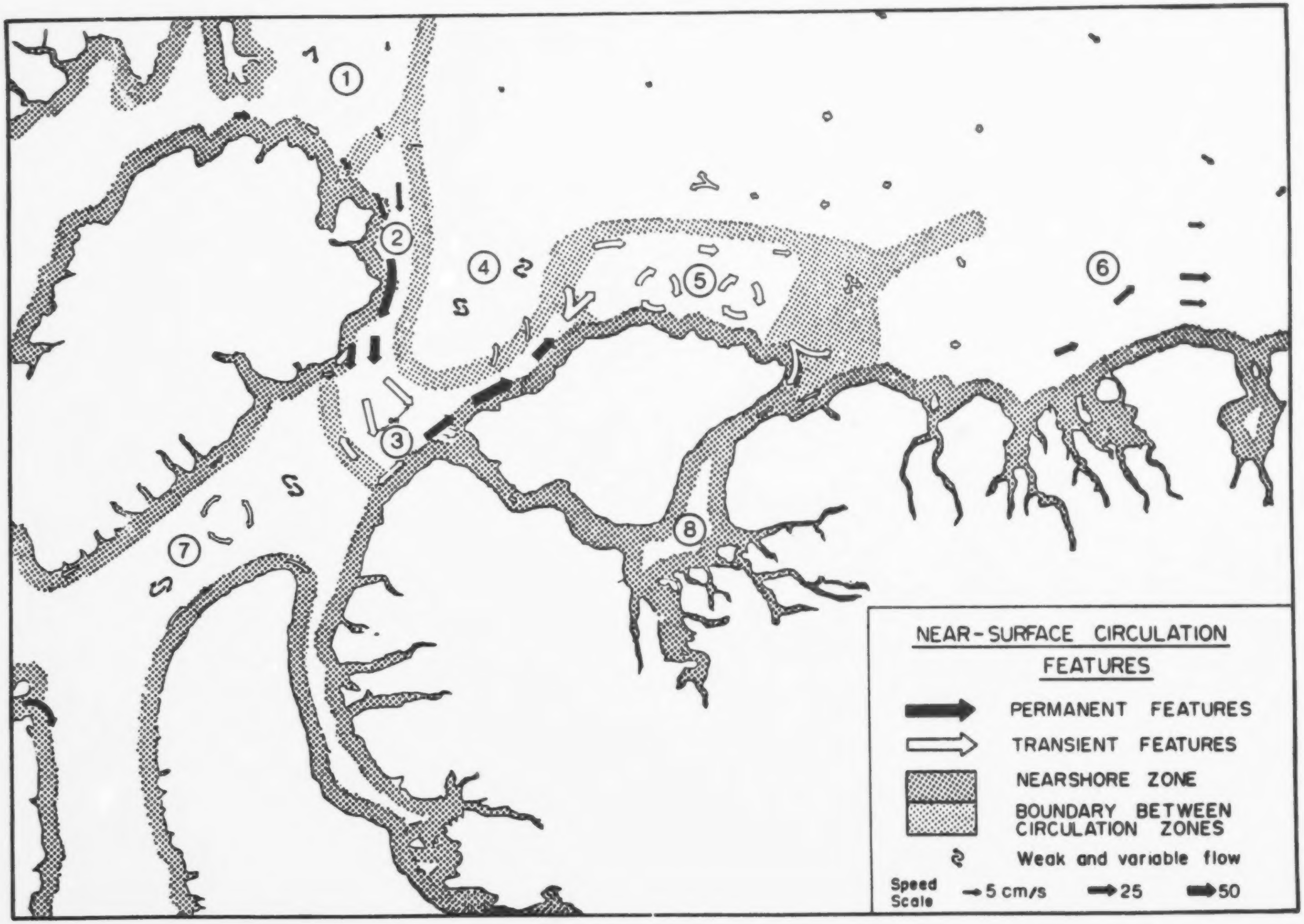
①
②
③
④
⑤
⑥
⑦
⑧
NEAR-SURFACE CIRCULATION FEATURES
PERMANENT FEATURES
TRANSIENT FEATURES
NEARSHORE ZONE
BOUNDARY BETWEEN CIRCULATION ZONES
Weak and variable flow
Speed Scale
5 cm/s
25
50

Figure 3.4.21 Regional pattern of near surface water flow at one scheme

flows. In the following paragraphs berg drift data are reviewed and summarized in each of these zones and related to the indicated characteristics of the water movements.

Region 1 - Northern Boundary Zone

In this region water mass and some drifter data indicate steady southeasterly flow at moderate speed out of Jones Sound through Lady Ann Strait with higher variability south-southwesterly flow further to the east in Baffin Bay.

Aside from the small amount of radar and aerial observer data available in the southern portion of this region (Figures 3.4.9 and 3.4.20), detailed information on berg movements was primarily obtained from the satellite-tracked berg data. Four trajectories of particular interest are represented in Figures 3.4.22-3.4.25. The first of these represents perhaps the most typical pattern of berg flow through the region with an average 10 km/day south-southwesterly velocity being maintained in the north and increasing somewhat to the south of 75°30'. A similar overall net drift is evident in Figure 3.4.23, with, however, an intervening period of complex looping in the September 11-16 interval when the previously considered berg (Figure 3.4.22) also deviated from its overall south-tending drift. The final two trajectories (Figures 3.4.24 and 3.4.25) represent common deviations from the average flow reflecting respectively a rapid in-shore berg movement and a southeasterly and easterly flow which moved berg 1446 far enough off-shore to by-pass the intrusive flow near the mouth of Lancaster Sound.

Region 2 - East of Devon Island

The near surface current data generally confirm the existence of a persistent south-southwesterly flow nominally 25 km in width centered a similar distance off the east coast of Devon Island. This flow is normally bounded by an inshore current of cold Arctic water moving out of Lady Ann Strait and eastern boundary region characterized by time dependent meanders and eddy-like structures (Figure 3.4.26). The pattern of berg drift in the main core of the current flow is displayed in the radar-determined velocity averages (Figures 3.4.19). Data in the complex meander region to the east of the main flow are available primarily from the satellite-tracking results (Figure 3.4.18) and aerial observations (Figure 3.4.20). Satellite and radar data (Figures 3.4.22-3.4.25, 3.4.27 and 3.4.28) show the characteristically small deviations from a broad overall south-southwesterly berg flow. Particular note should be made of the track of berg #1446 which evidently moved south-southeastward over the September 7-10 (averaging 20 km/day) without entering the intrusive flow of the Lancaster Sound entrance.

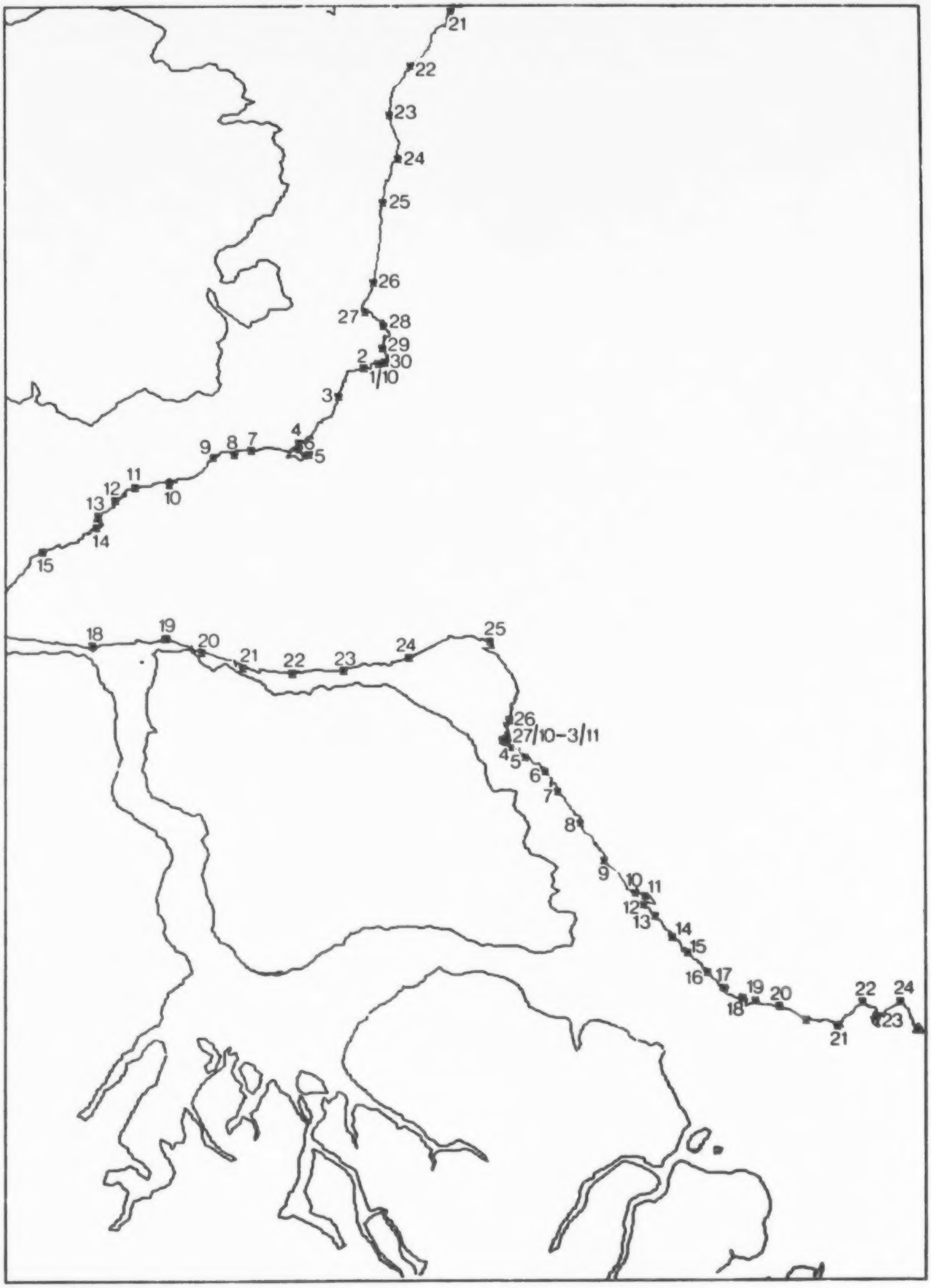
21
22
23
24
25
26
27
28
29
30
2
1/10
3
4
6
5
9
8
7
11
12
13
10
14
15
18
19
20
21
22
23
24
25
26
27/10-3/11
4
5
6
7
8
9
10
11
12
13
14
15
16
17
19
20
18
22
24
23
21

Figure 3.4.22 Satellite-tracked berg trajectory:
ID 1986, 8/9/79 to 24/11/79

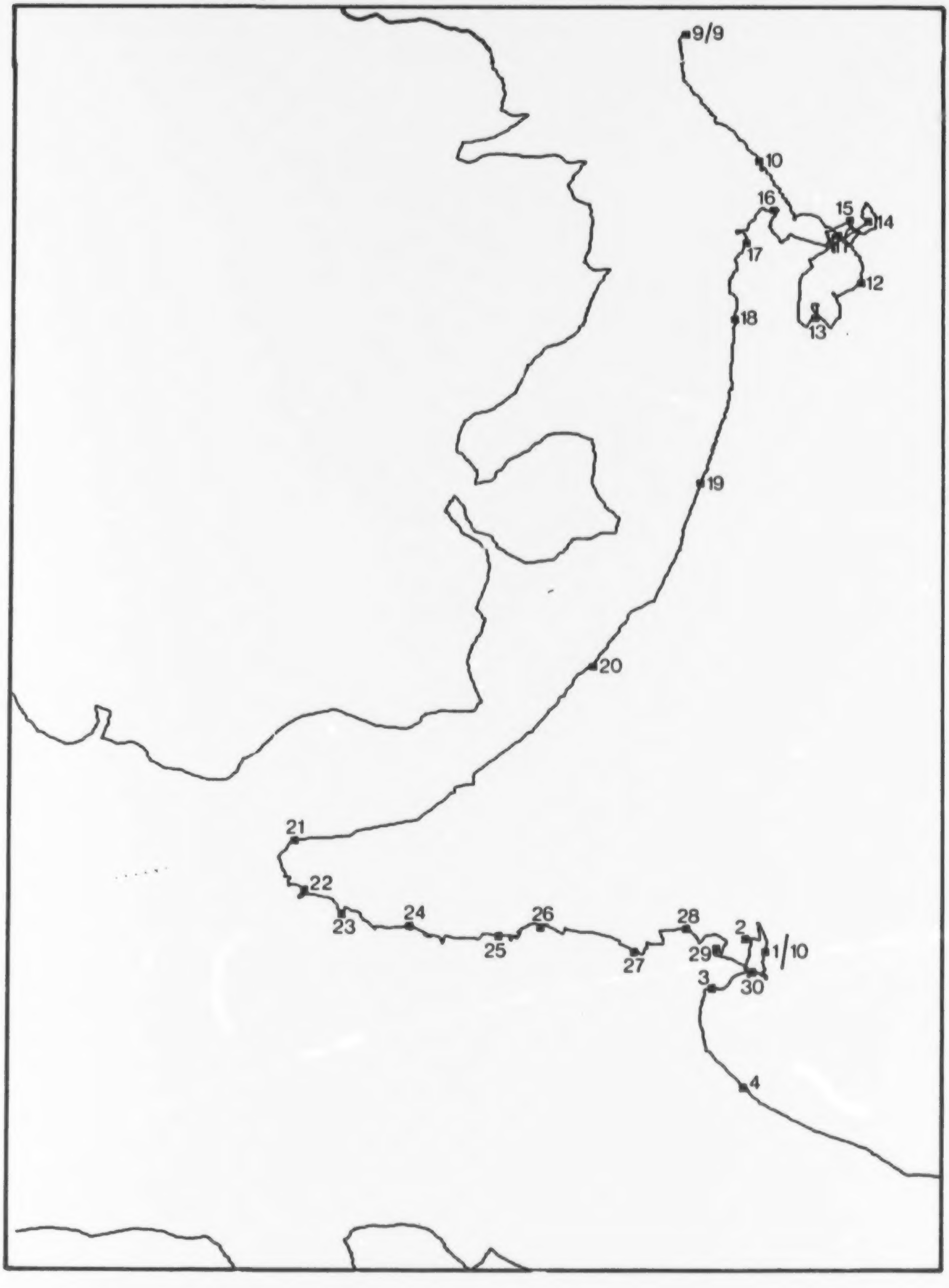
9/9
10
16
15
14
17
12
18
13
19
20
21
22
23
24
25
26
27
28
2
1/10
29
3
30
4

Figure 3.4.23 Satellite-tracked berg trajectory:
ID 1995, 9/9/79 to 4/10/79

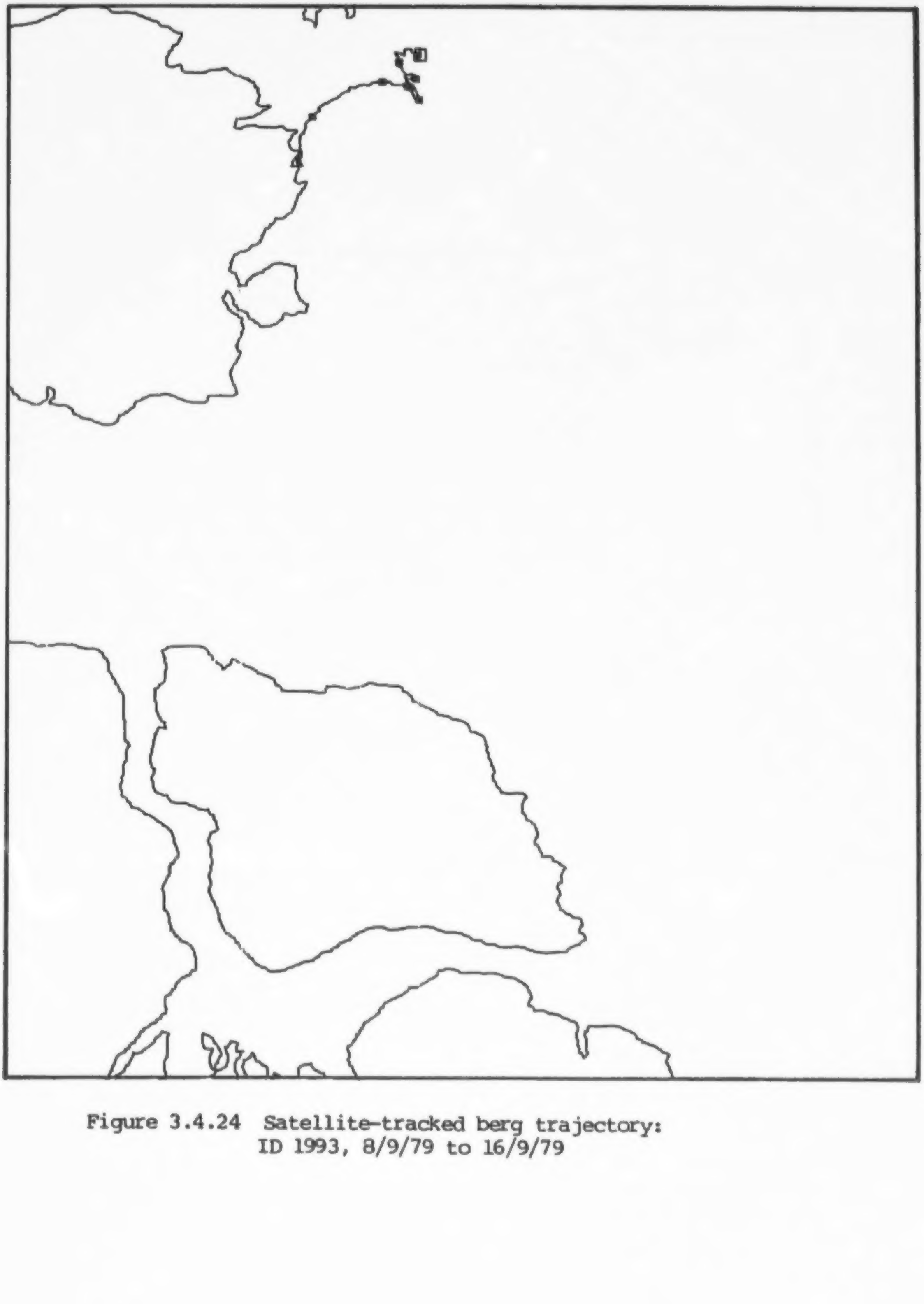

Figure 3.4.24 Satellite-tracked berg trajectory:
ID 1993, 8/9/79 to 16/9/79

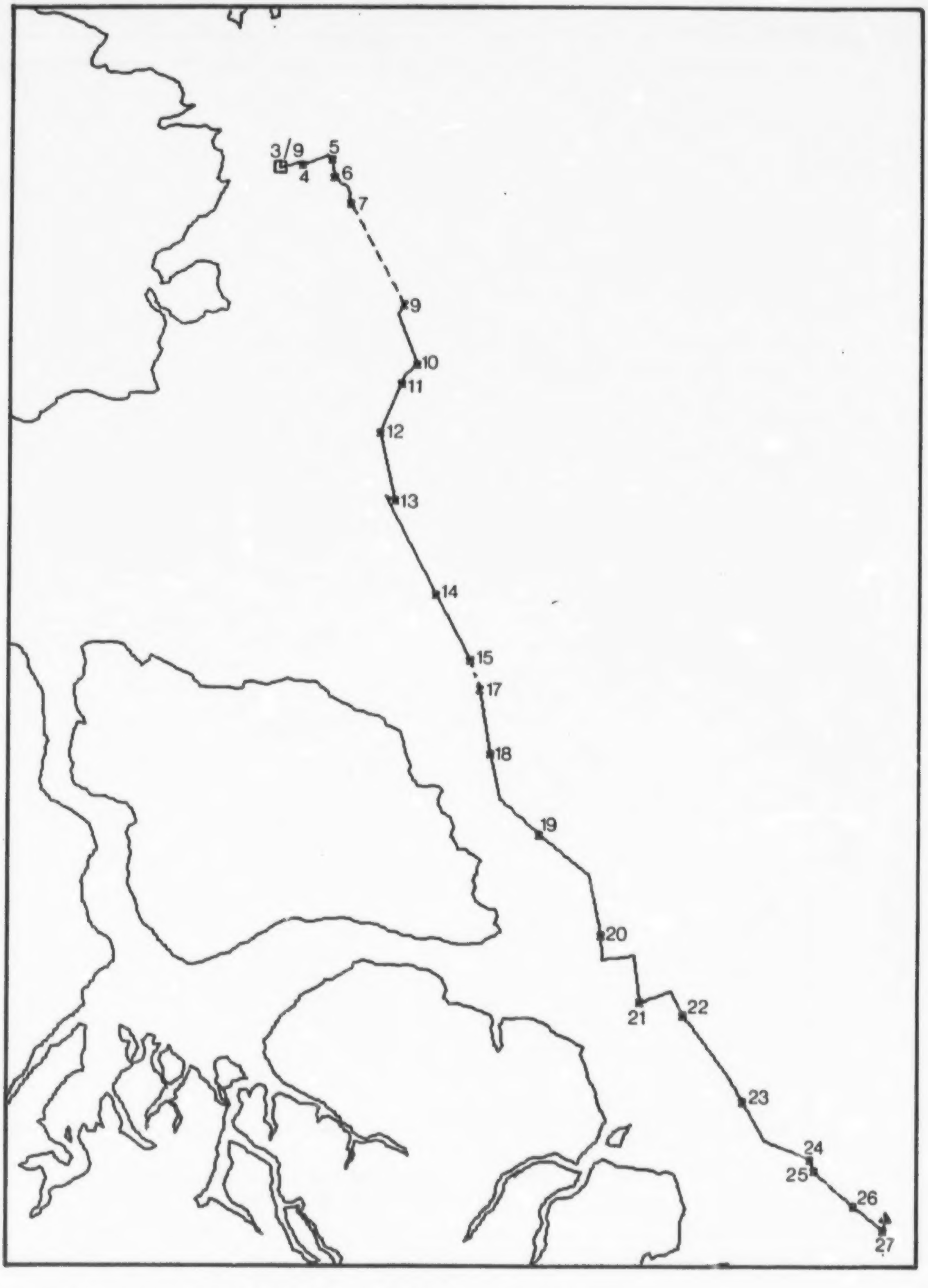
3/9
4
5
6
7
9
10
11
12
13
14
15
17
18
19
20
21
22
23
24
25
26
27

Figure 3.4.25 Satellite-tracked berg trajectory:
ID 1446, 3/9/78 to 27/9/78

Region 3 - The Intrusive Current of Eastern Lancaster Sound

The principal features of the Lancaster Sound intrusion are well established from moored current meter, water mass and drogued drifter measurements. The envelopes of the majority of drifers released in the 1979 experiments (Figure 3.4.29) indicate: a) the narrow zone of west-southwesterly flow near southeast Devon Island; b) the easterly return regime north of Bylot island and, c) the intervening zone where a south-tending current crosses Lancaster Sound.

Two patterns of flow are indicated in the latter crossing region alternatively leading to a direct link-up with the exit flow north of Bylot Island or a southwestward drift toward the Borden Peninsula followed by movement either into the Navy Board Inlet-Eclipse Sound system or a looping northward drift and later eastward and southward movements into Baffin Bay or Navy Board Inlet.

The convergent character of the intrusive current is apparent from the radar tracks of Figure 3.4.30. As indicated above by the satellite-tracked berg data, the position and width of the narrow core of berg flow are time-dependent (see Figure 3.4.27a). Typical velocities in this area are on the order of 50 km/day (Figures 3.4.18 and 3.4.20) (The smaller values of Figure 3.4.19 presumably reflect the magnitude reduction expected from measurements of net displacement over longer periods of one or more days). As indicated by the average velocity pattern, bergs in the intrusive flow generally penetrate Lancaster Sound to at least the longitude of Cape Warrender, following trajectories similar to those displayed in Figure 3.4.28. The deviation from this behaviour previously noted in the preponderance of 1978 trajectories (Figure 3.4.16) is likely to be the result of the fortuitous entry of bergs into the southeast Devon Island convergent current coincident with winds of appropriate speed, direction and duration to produce a deflection out of the normal flow and into the adjoining central disordered zone (Figure 3.4.21). This possibility is most likely for bergs travelling on the outside- or southern-portion of the southeast Devon Island current core. Examples of such deflection are presented in Figure 3.4.27a (berg #5024) and Figure 3.4.32.

Other deviations from the principal pattern of drift occur in the crossing region where current data and the averaged berg drift velocities of Figure 3.4.19 suggest the possibility of continuation of the southwestward flow into the neighborhood of the Borden Peninsula. Subsequent northerly movements could introduce bergs into central Lancaster Sound (Region 7). Unfortunately, possibly as a result of range limitations, no conclusive evidence of such berg movements was obtained from radar data. The only satellite-tracked berg to approach the Borden Peninsula on the assumed southwesterly track (see Figure 3.4.17) actually entered the crossing region through

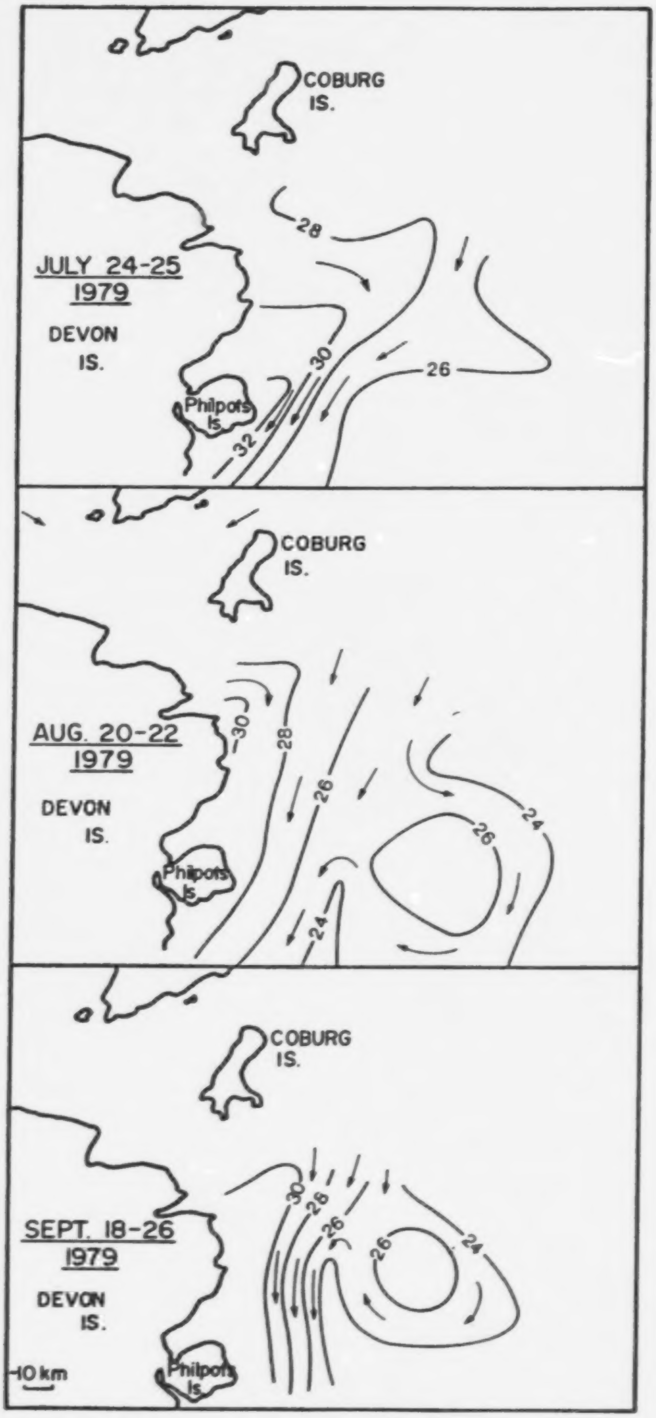
COBURG IS.
JULY 24-25 1979
DEVON IS.
Philpots Is.
28
30
32
26
COBURG IS.
AUG. 20-22 1979
DEVON IS.
Philpots Is.
30
28
26
24
26
24
COBURG IS.
SEPT. 18-26 1979
DEVON IS.
Philpots Is.
10 km
30
28
26
26
24

Figure 3.4.26 Near-surface current data, summer 1979 (Dynamic height in cm., 300 db reference level) (Fissell, Lemon, Birch, 1980)

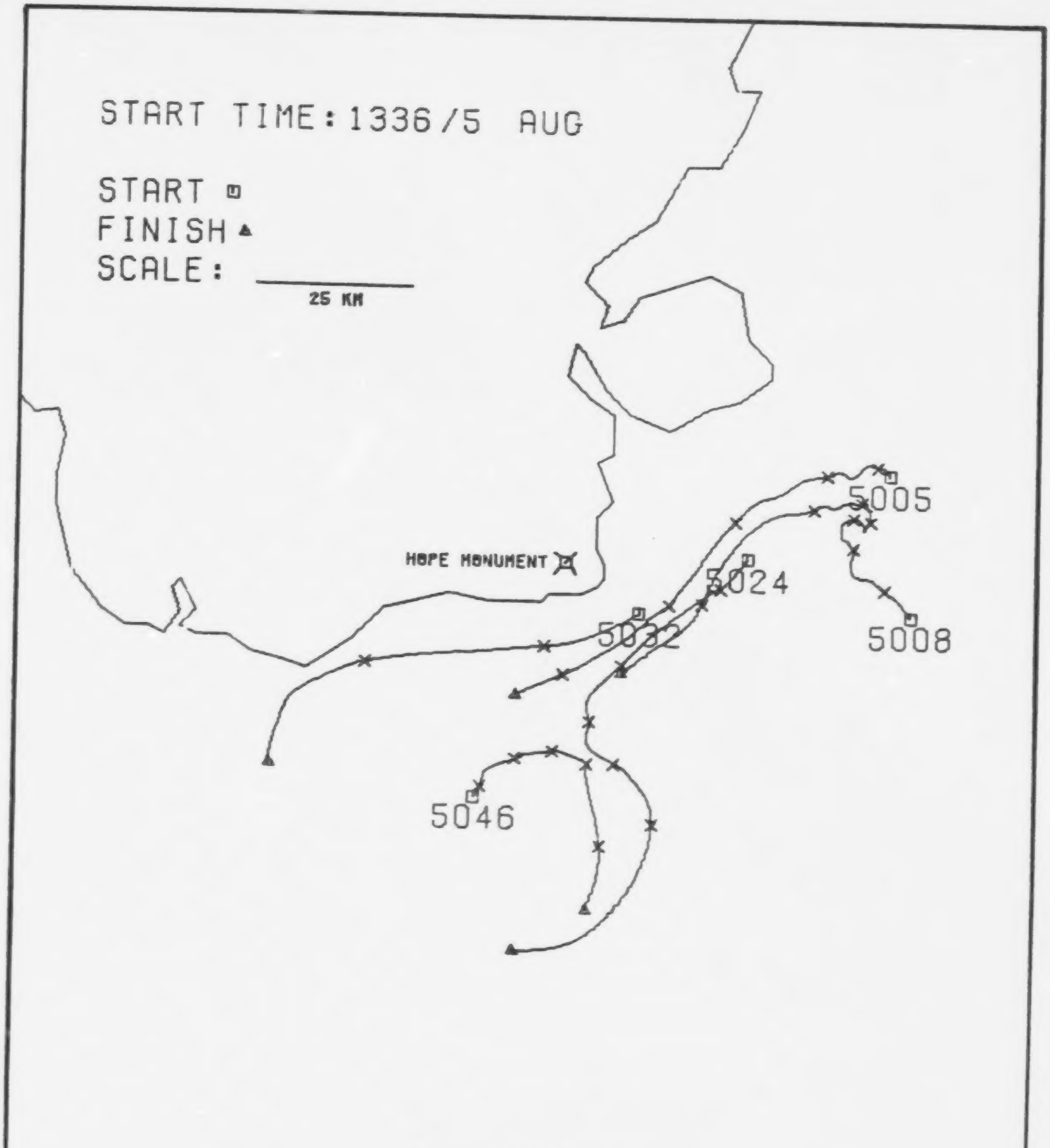
START TIME:1336/5 AUG
START ◻
FINISH ▲
SCALE:
25 KM
HOPE MONUMENT
5005
5024
5032
5008
5046

Figure 3.4.27(a) Radar-tracked berg trajectories - August 5-11, 1978 (de Lange Boom, MacNeill, Buckley, 1979)

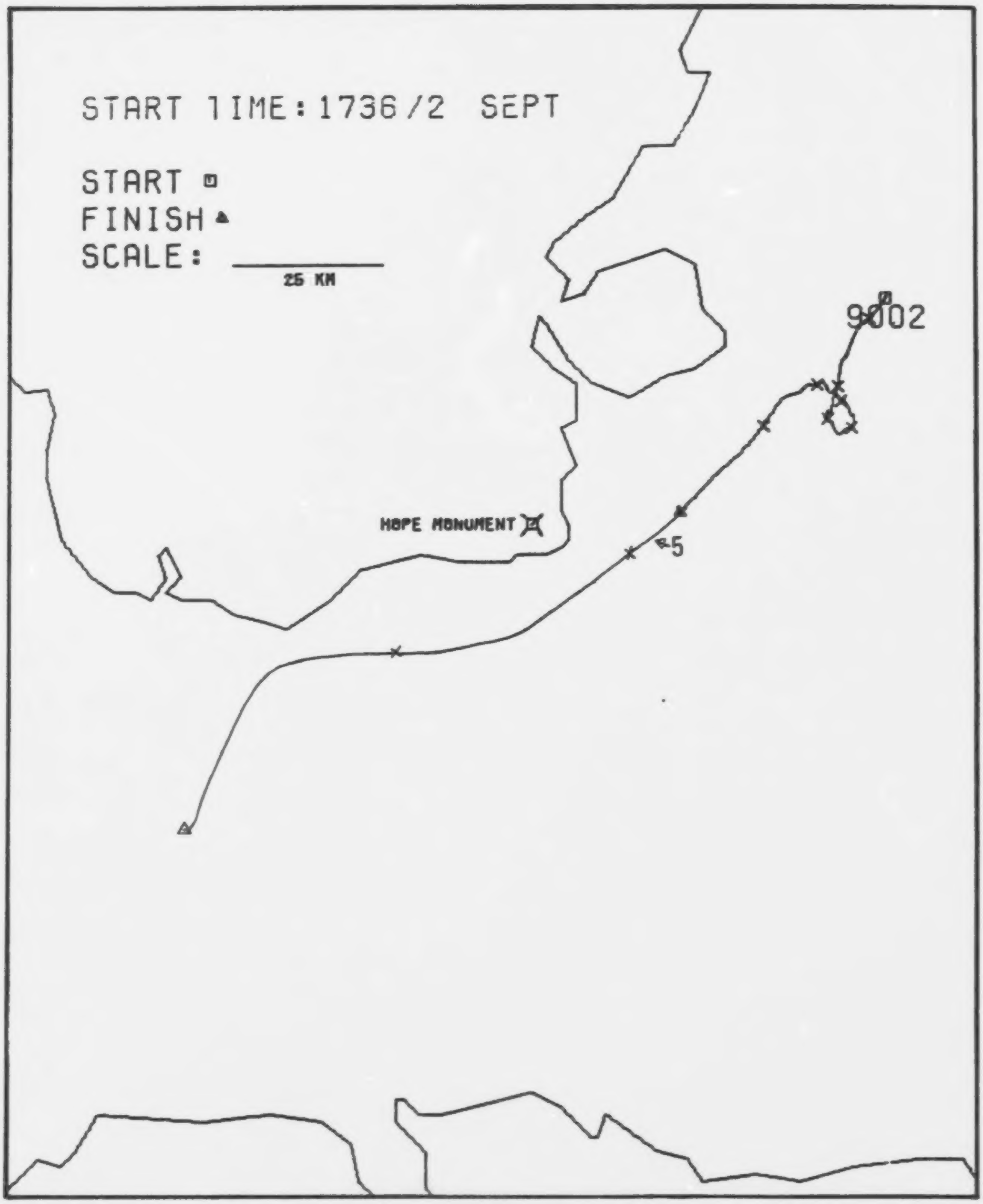
START TIME:1736/2 SEPT
START
FINISH
SCALE:
25 KM
9002
HOPE MONUMENT
5

Figure 3.4.27(b) Radar-tracked berg trajectories - September 2-8, 1978 (de Lange Boom, MacNeill, Buckley, 1979)

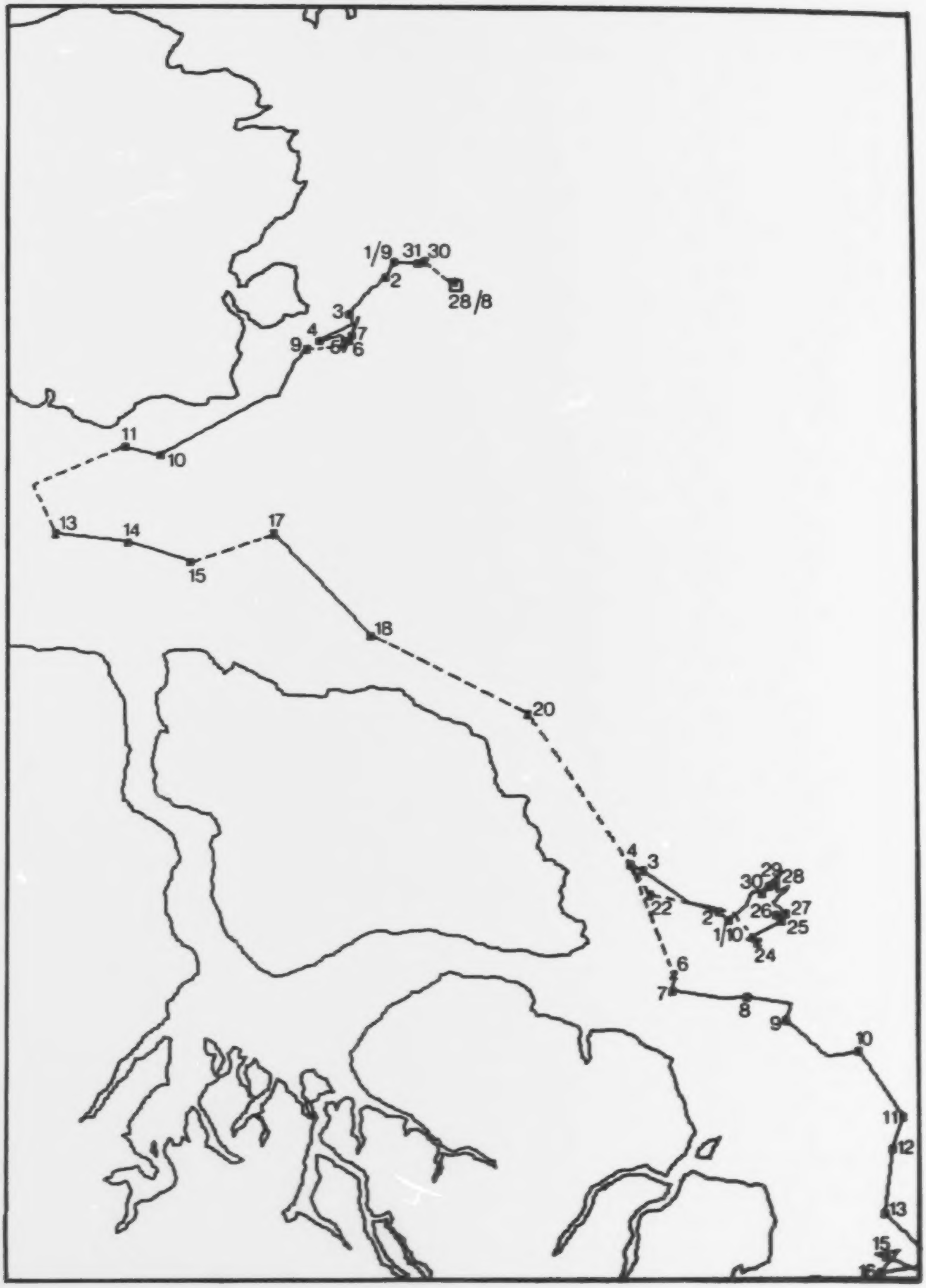
1/9
31
30
2
28/8
3
4
7
9
5
6
11
10
13
14
17
15
18
20
4
3
1
22
30
29
28
26
27
2
25
1/10
24
6
7
8
9
10
11
12
13
15
16

Figure 3.4.28 Satellite-tracked berg trajectory:
ID 1163, 38/8/78 to 22/12/78
(Fissel, 1980)

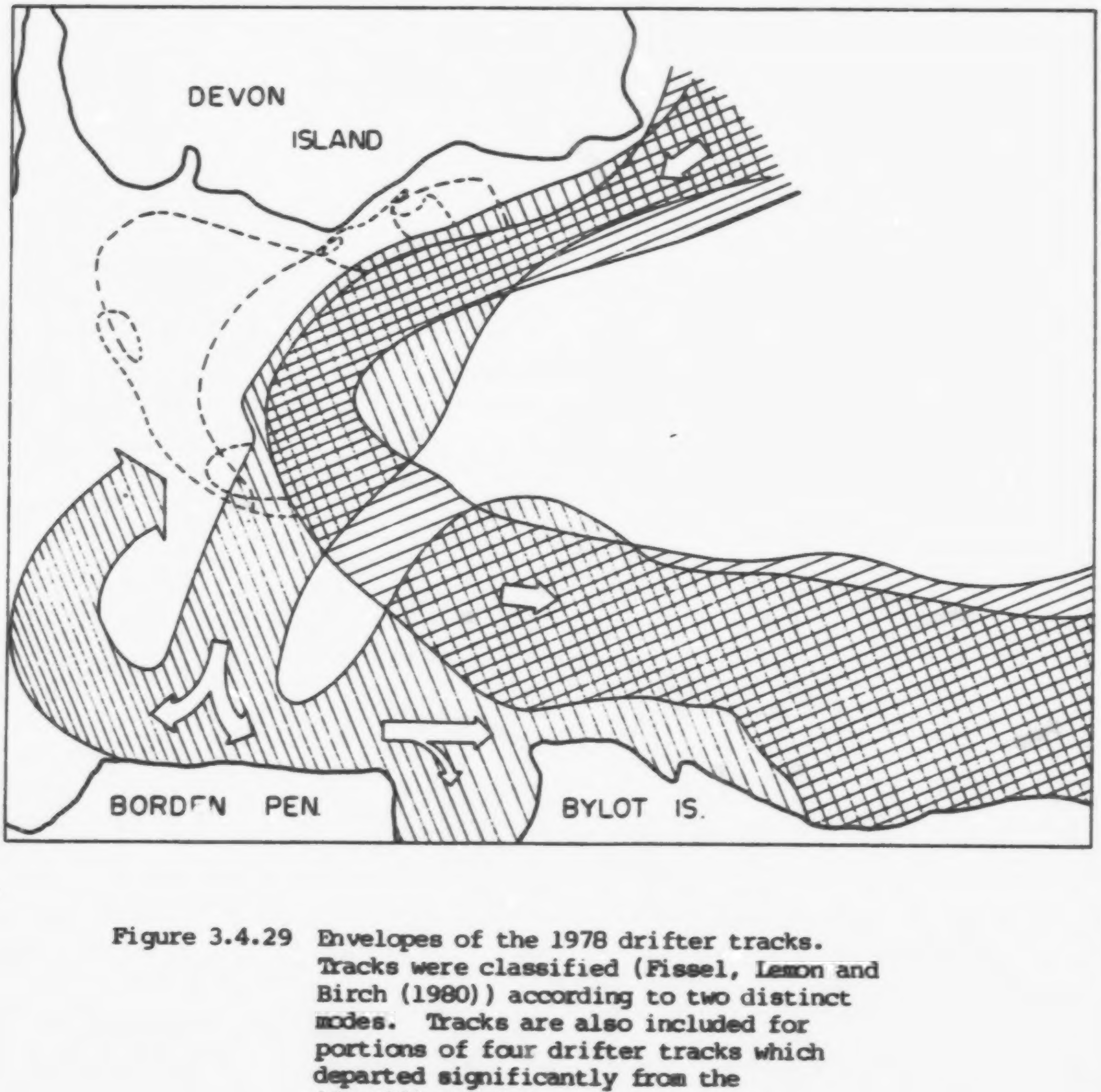
DEVON
ISLAND
BORDEN PEN.
BYLOT IS.

Figure 3.4.29 Envelopes of the 1978 drifter tracks. Tracks were classified (Fissel, Lemon and Birch (1980)) according to two distinct modes. Tracks are also included for portions of four drifter tracks which departed significantly from the identified modes.

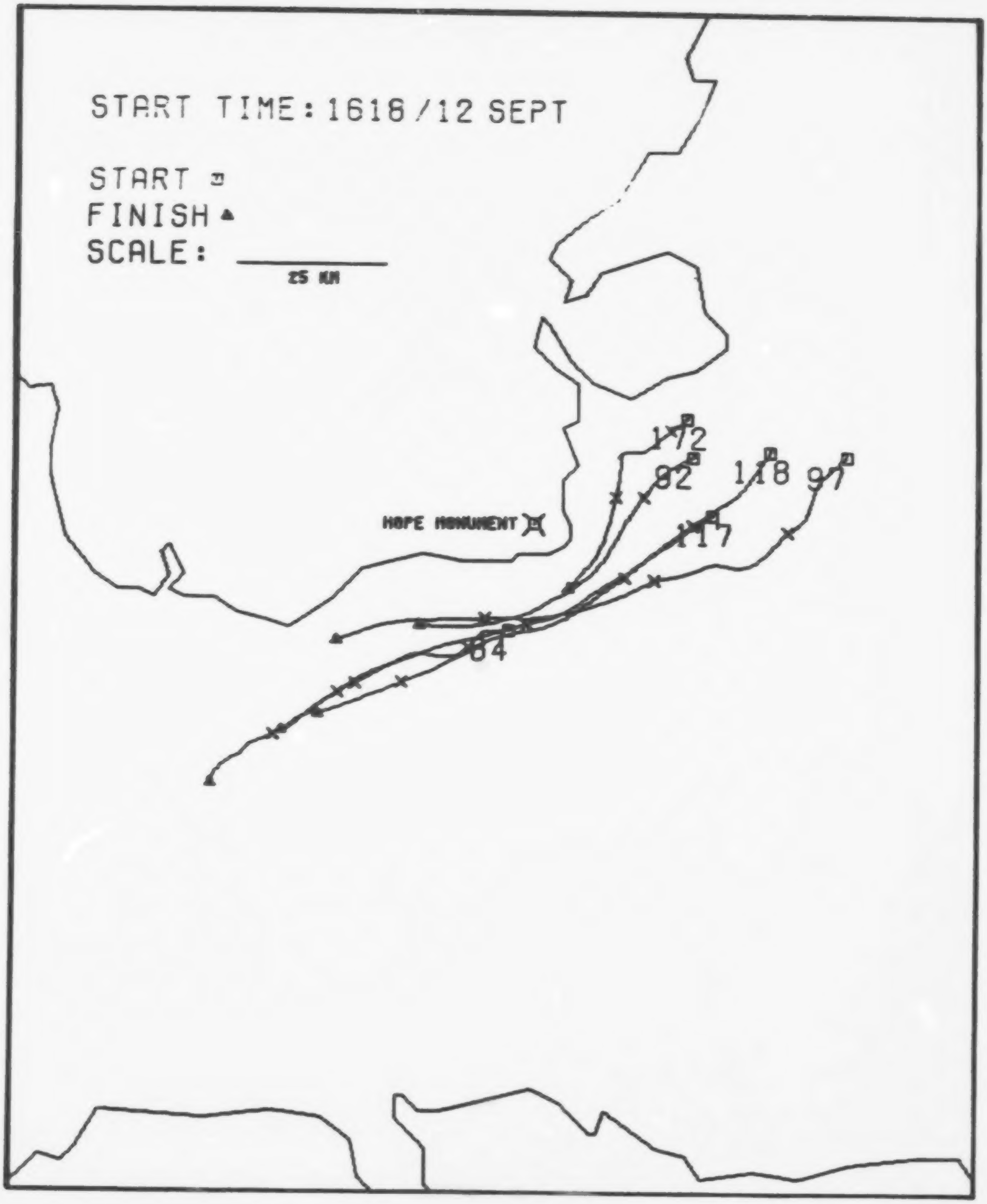
START TIME: 1618/12 SEPT
START □
FINISH ▲
SCALE:
25 KM
HOPE MONUMENT
172
82
118
97
117
84

Figure 3.4.30 Radar-tracked berg trajectories: September 12-18, 1978 (de Lange Boom, MacNeill, Buckley, 1979)

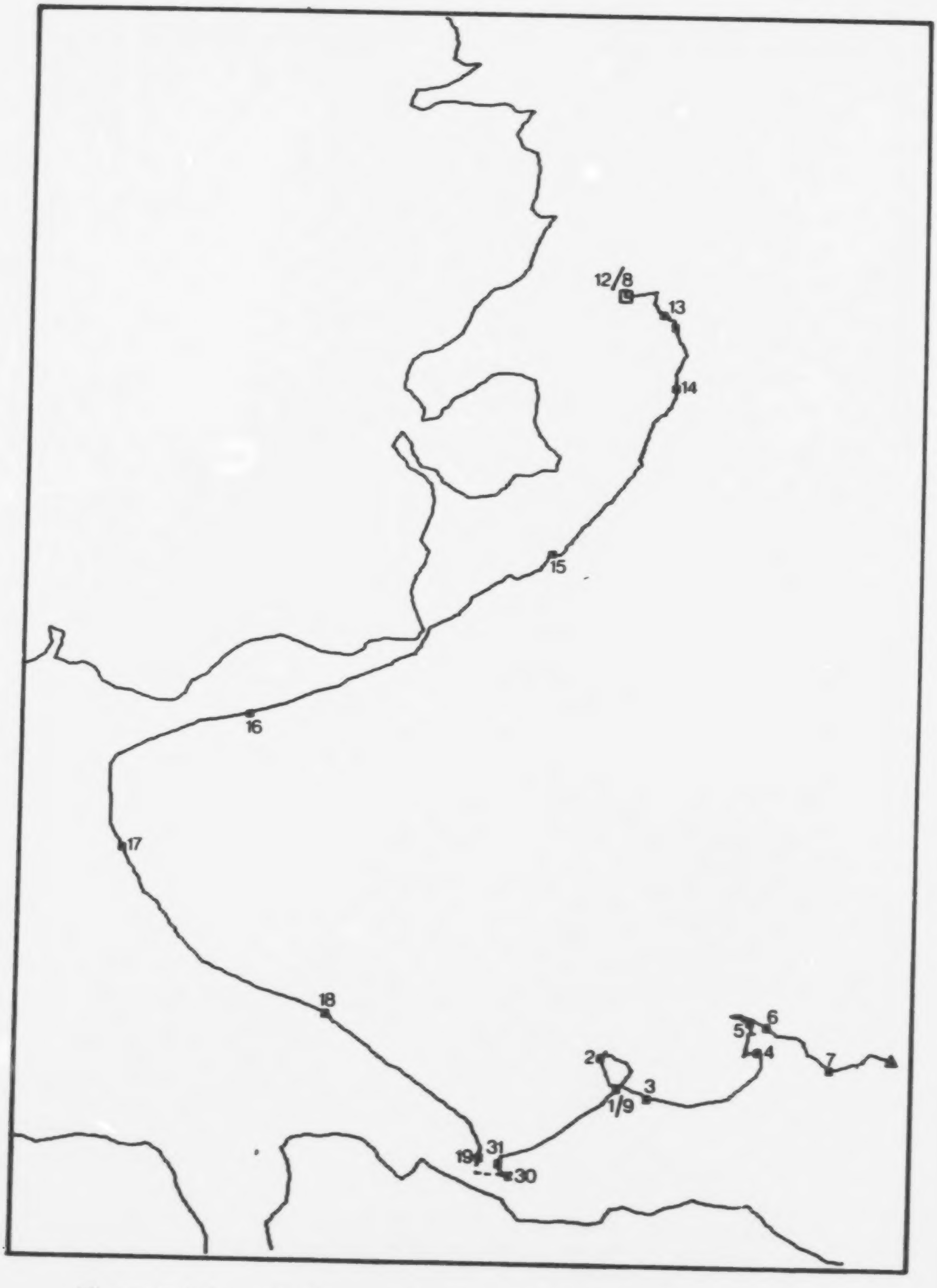
12/8
13
14
15
16
17
18
19
31
30
1/9
2
3
4
5
6
7

Figure 3.4.31 Satellite-tracked berg trajectories: ID 1990, 12/8/79 to 7/9/79 (Fissell, 1980)

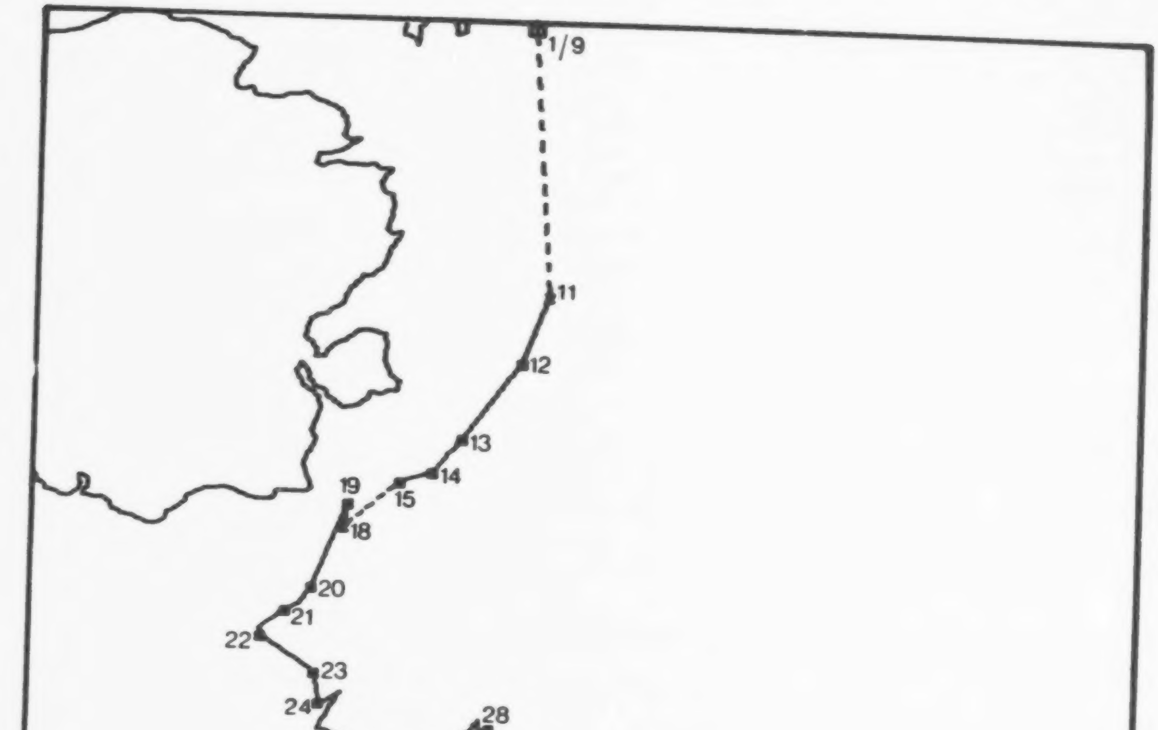
1/9
11
12
13
14
15
19
18
20
21
22
23
24
28
27
26
25
29
30
8
1/10
7
6
5
2
9
4
10
3
11
12
13

Figure 3.4.32 Satellite-tracked berg trajectories: ID 1223, 1/9/78 to 13/10/78 (Fissell, 1980)

the central disordered zone and quickly exited Lancaster Sound via the coastal flow. The only documented instances (2) of entry into central Lancaster Sound occurred in 1978 with the points of entry being in the northern half of the Sound west-southwest of Cape Warrender. Similarly no observations were obtained of berg entry into Navy Board Inlet.

The return portion of the intrusive berg flow is amply documented by the averaged velocity data sets (Figure 3.4.18-20), detailed trajectories (Figures 3.4.22, 3.4.31 and 3.4.32) and the identified weekly patterns of movement (Figure 3.4.33). (NORDCO, 1979). Typical daily rates of movement range from 25 to 35 km/day with characteristic looping zones occurring to the north of Cape Liverpool and to the east of Cape Fanshawe. These latter features and the directionality of flow are strongly time dependent, determining to the same extent the directness of subsequent return to southerly movement in the adjoining Eddy Zone east of Bylot Island (Zone 5).

Region 4 - The Central Disordered Zone

In this area of weak and variable flow there appears to be little net movement in the upper 300 m of the water column. Current speeds and drifter velocities are generally low with much evidence of transient looping or eddy-like structures of both the clockwise and counterclockwise types. It is important to note that none of the drogued drifters which have entered this zone have been observed to exit the regiion to the north or west thus implying an overall easterly and southerly drift trend.

The most complete sets of berg drift data in this region were obtained from the Hope Monument radar station (de Lange Boom et al, 1979). The corresponding velocity averages (Figure 3.4.19) suggest a distinct southerly trend in the eastern sector with a net gyral flow prevailing in the west. However, although a previous analysis (de Lange Boom et al, 1979) deduced a disordered region circulation in the form of two adjoining, oppositely rotating gyres (see Figure 3.4.34), there is little actual evidence in the trajectory data supporting the permanent existence of such structures. (See Figure 3.4.16 and 3.4.17).

Instead the disordered zone motion would appear to be governed by time dependent low to moderate speed structures in the upper water column and surface winds. The latter may be the primary agent in extracting bergs from the adjacent intrusive current. Estimates of the extent of wind influence are difficult to achieve with the general dearth of wind data in the offshore regime. Nevertheless there is some evidence in the satellite-tracked trajectory data suggestive of the possibility that bergs frequently maintain a sustained drift fully or partially through the disordered region in a

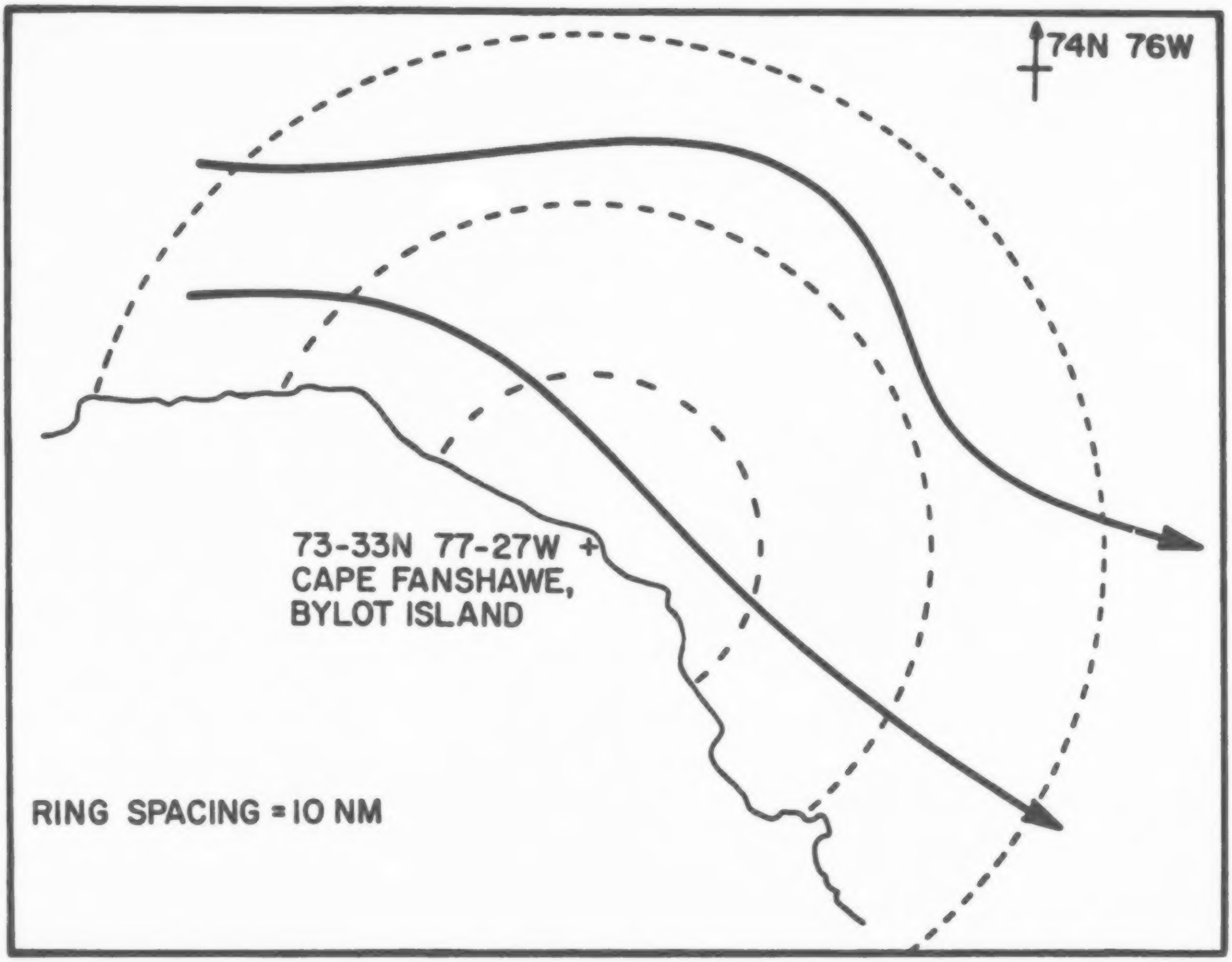
74N 76W
73-33N 77-27W
CAPE FANSHAWE,
BYLOT ISLAND
RING SPACING = 10 NM

Figure 3.4.33(a) General iceberg drift pattern, July 13-27 (NORDCO, 1979)

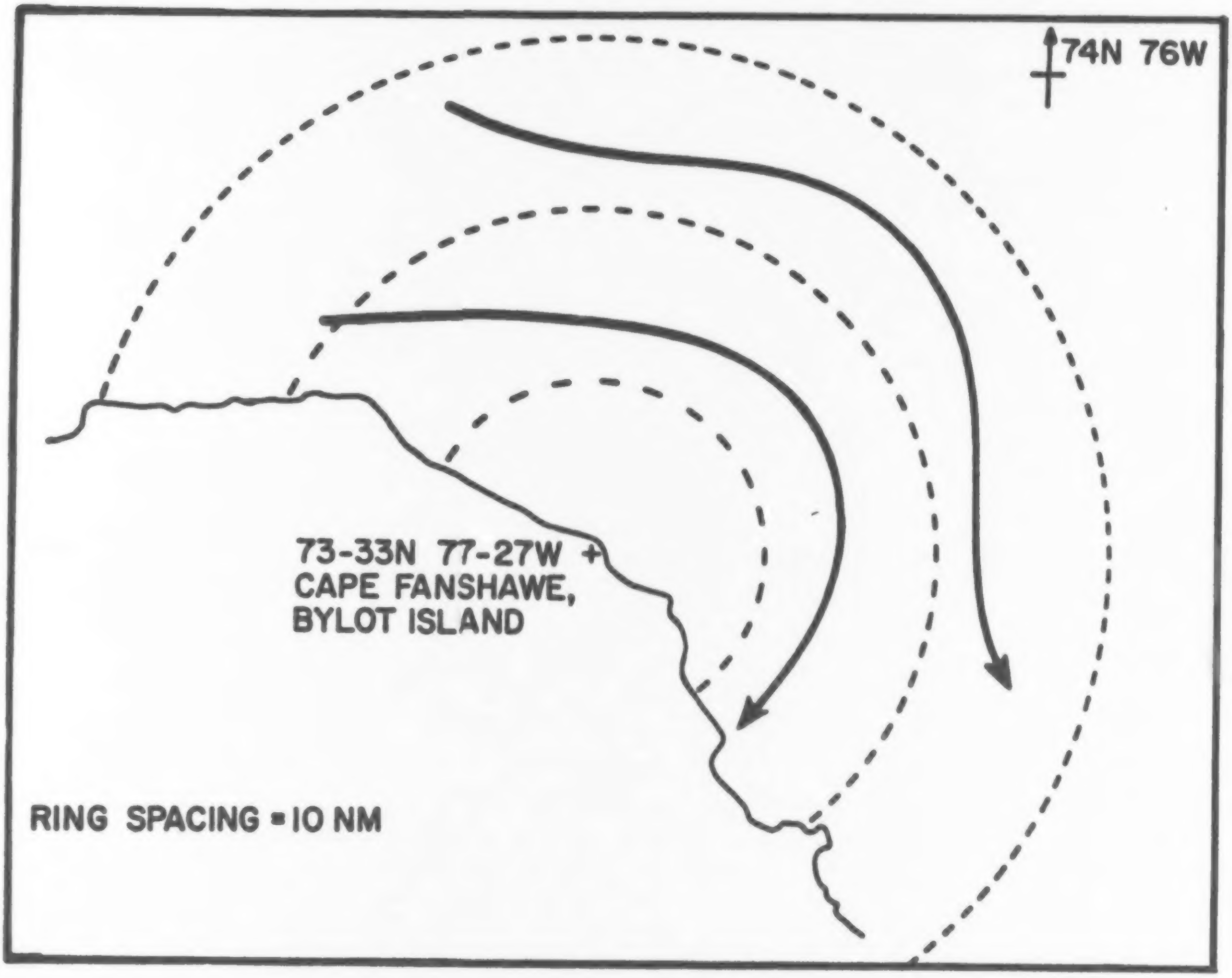
74N 76W
73-33N 77-27W
CAPE FANSHAWE,
BYLOT ISLAND
RING SPACING = 10 NM

Figure 3.4.33(b) General iceberg drift pattern, July 28 - August 3 (NORDCO, 1979)

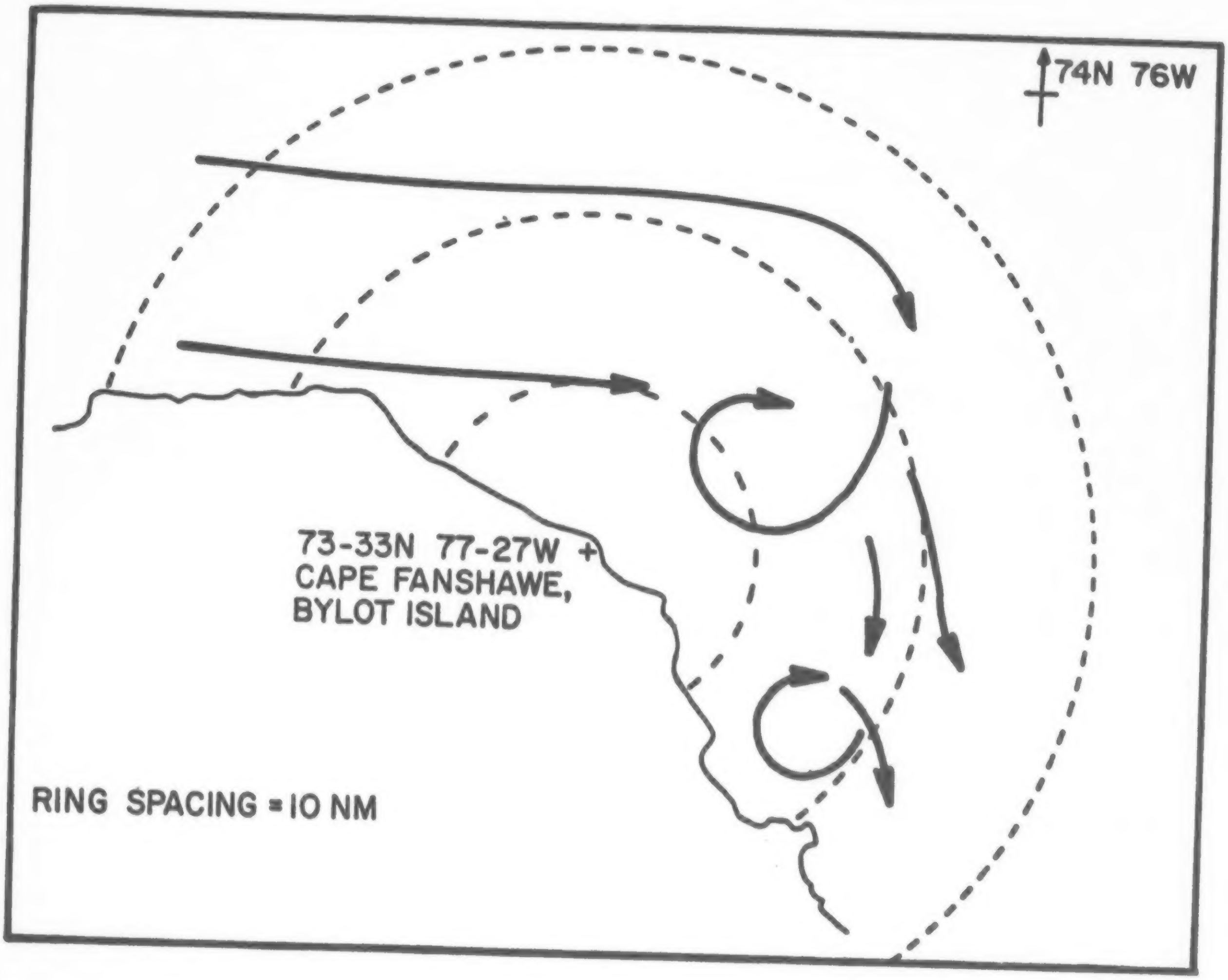
74N 76W
73-33N 77-27W
CAPE FANSHAWE,
BYLOT ISLAND
RING SPACING = 10 NM

Figure 3.4.33(c) General iceberg drift pattern, August 4-10 (NORDCO, 1979)

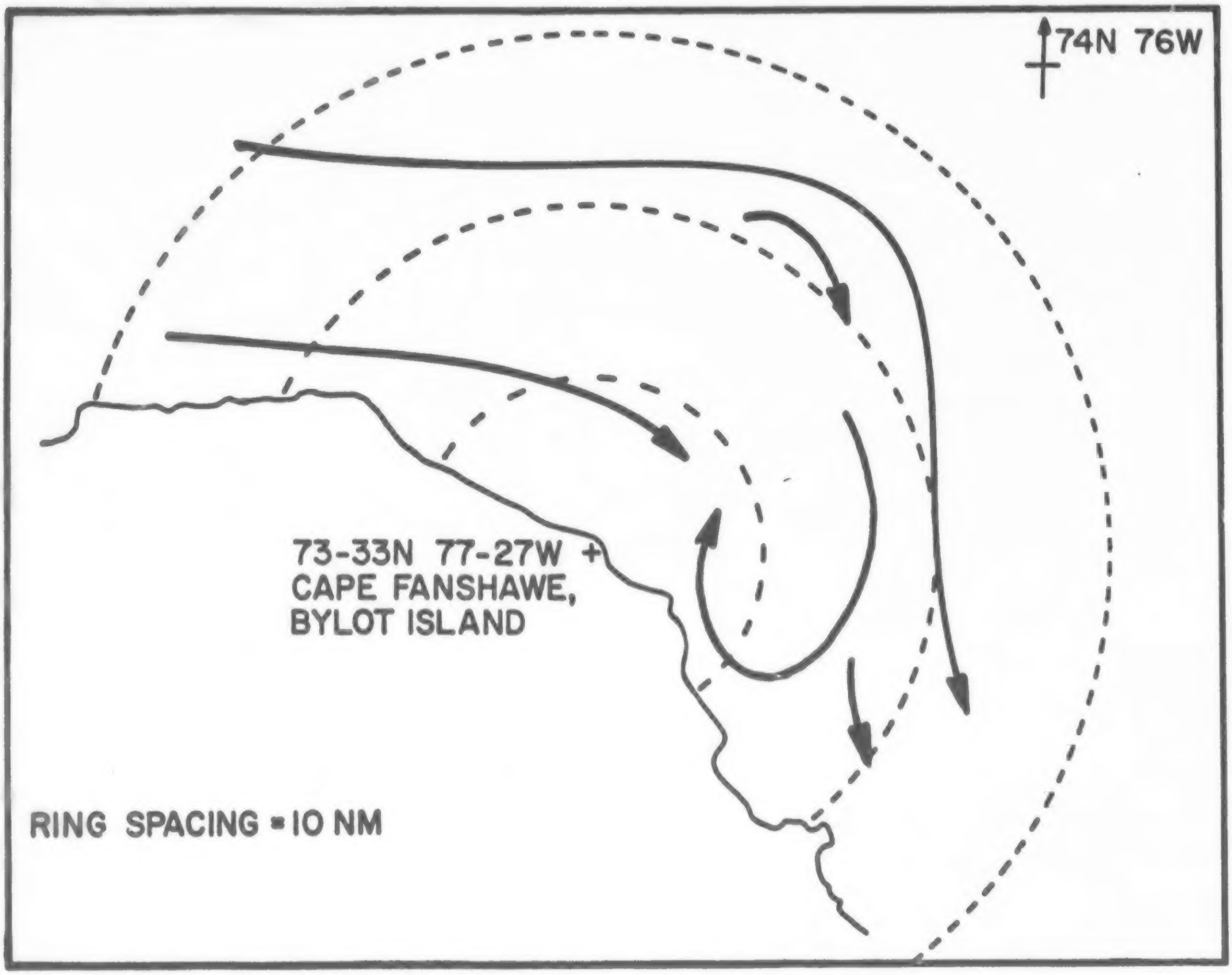
74N 76W
73-33N 77-27W
CAPE FANSHAWE,
BYLOT ISLAND
RING SPACING = 10 NM

Figure 3.4.33(d) General iceberg drift pattern, August 11-17 (NORDCO, 1979)

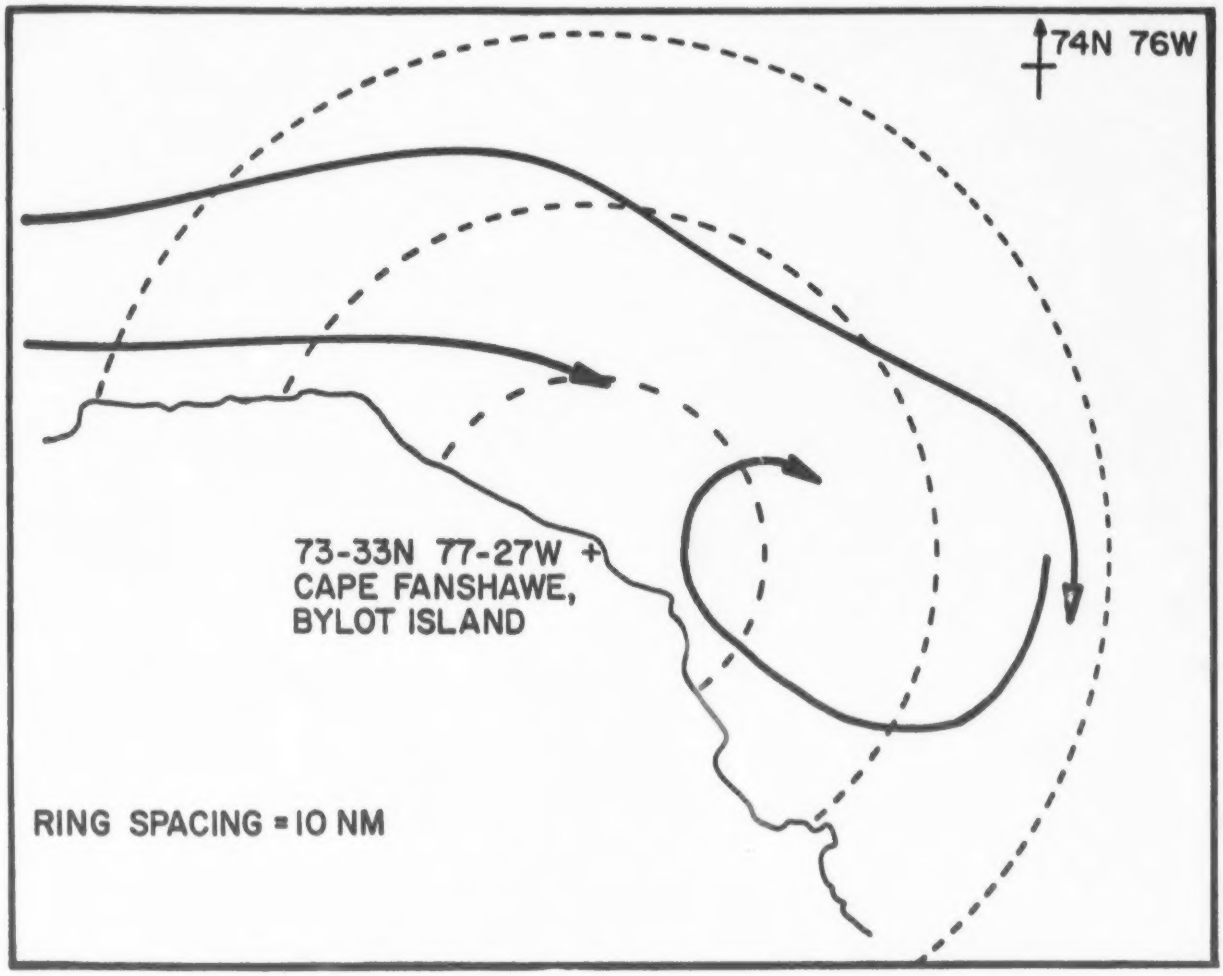
74N 76W
73-33N 77-27W
CAPE FANSHAWE,
BYLOT ISLAND
RING SPACING = 10 NM

Figure 3.4.33(e) General iceberg drift pattern, August 18-24 (NORDCO, 1979)

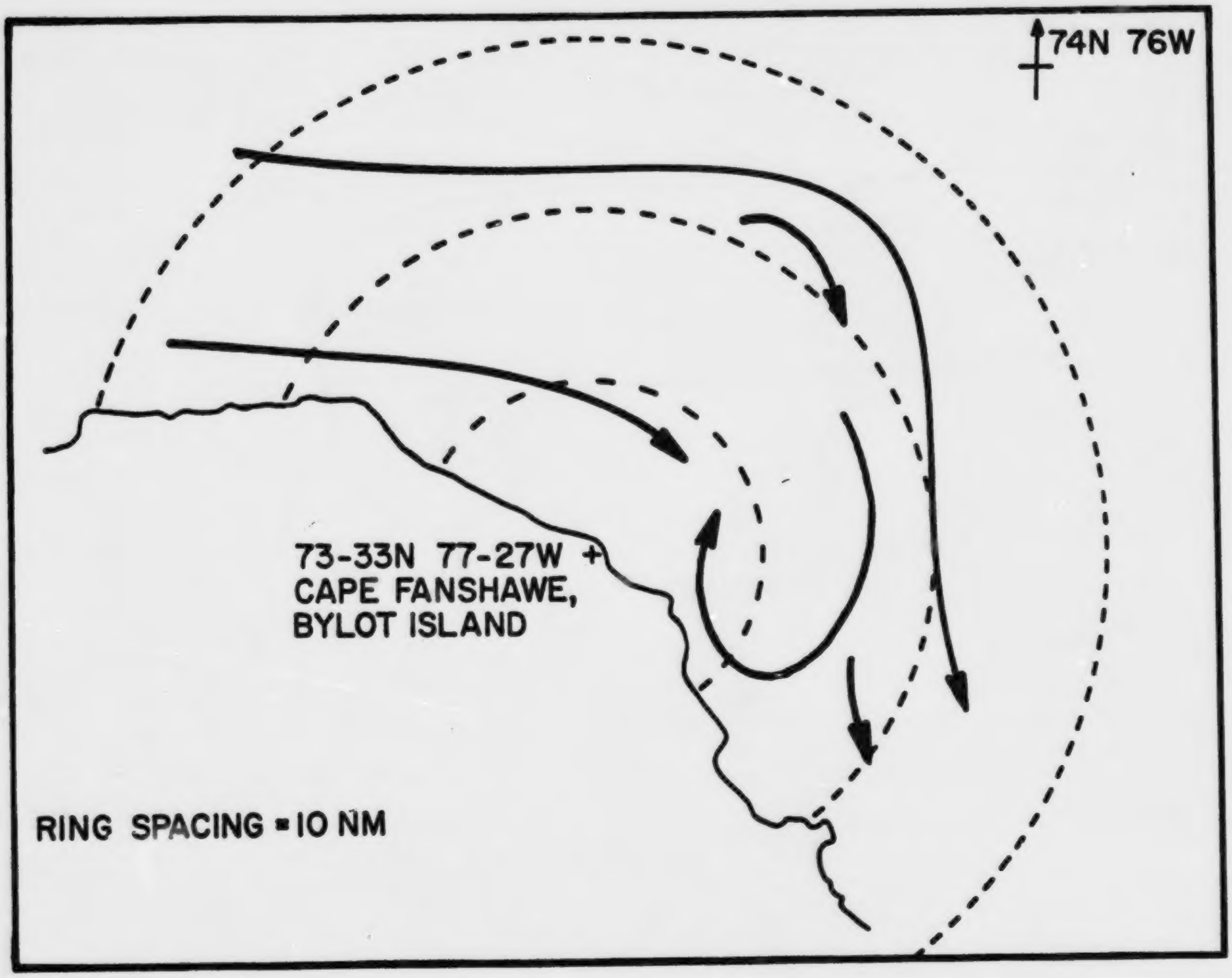
74N 76W
73-33N 77-27W
CAPE FANSHAWE,
BYLOT ISLAND
RING SPACING = 10 NM

Figure 3.4.33(d) General iceberg drift pattern, August 11-17 (NORDCO, 1979)

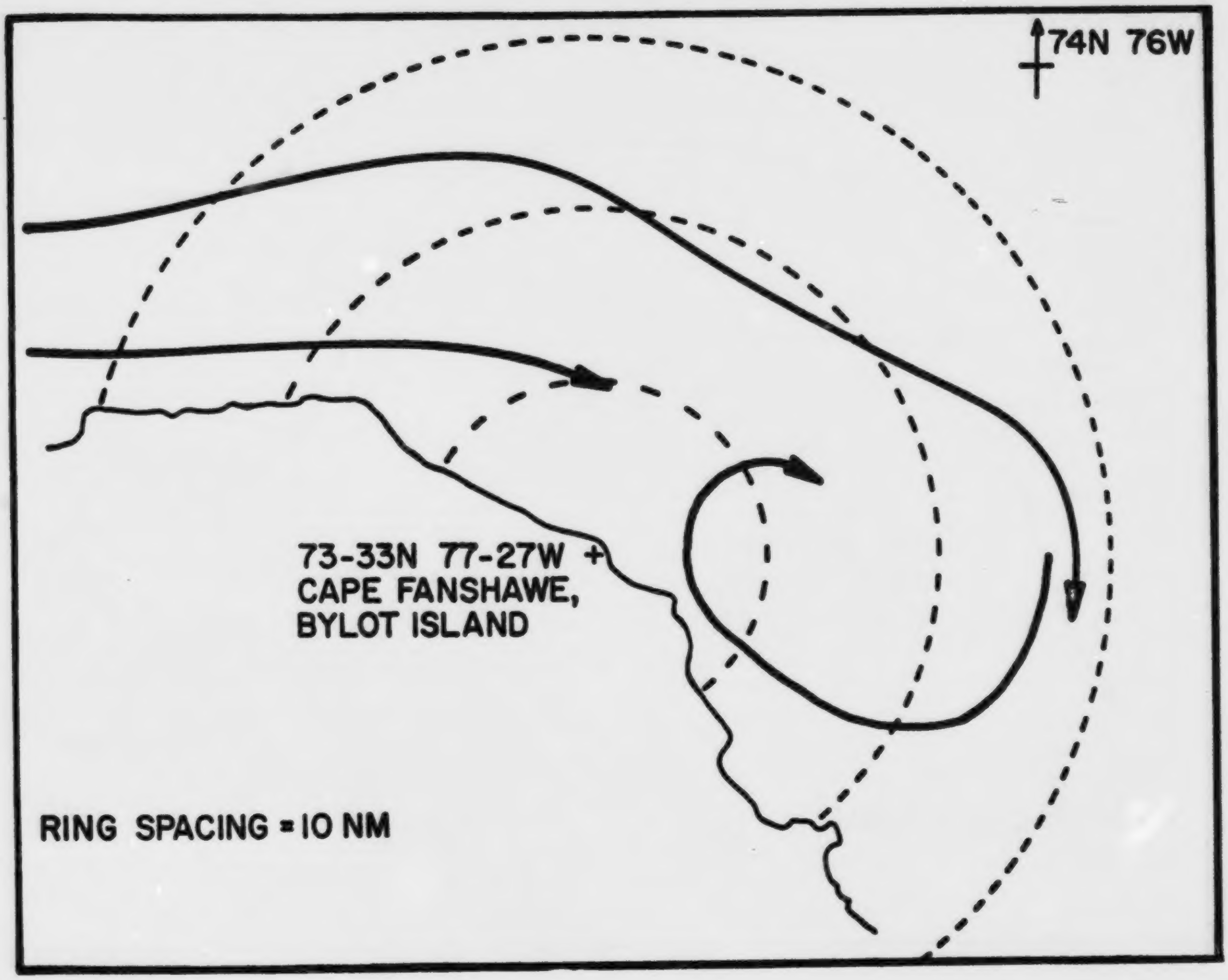
74N 76W
73-33N 77-27W
CAPE FANSHAWE,
BYLOT ISLAND
RING SPACING = 10 NM

Figure 3.4.33(e) General iceberg drift pattern, August 18-24 (NORDCO, 1979)

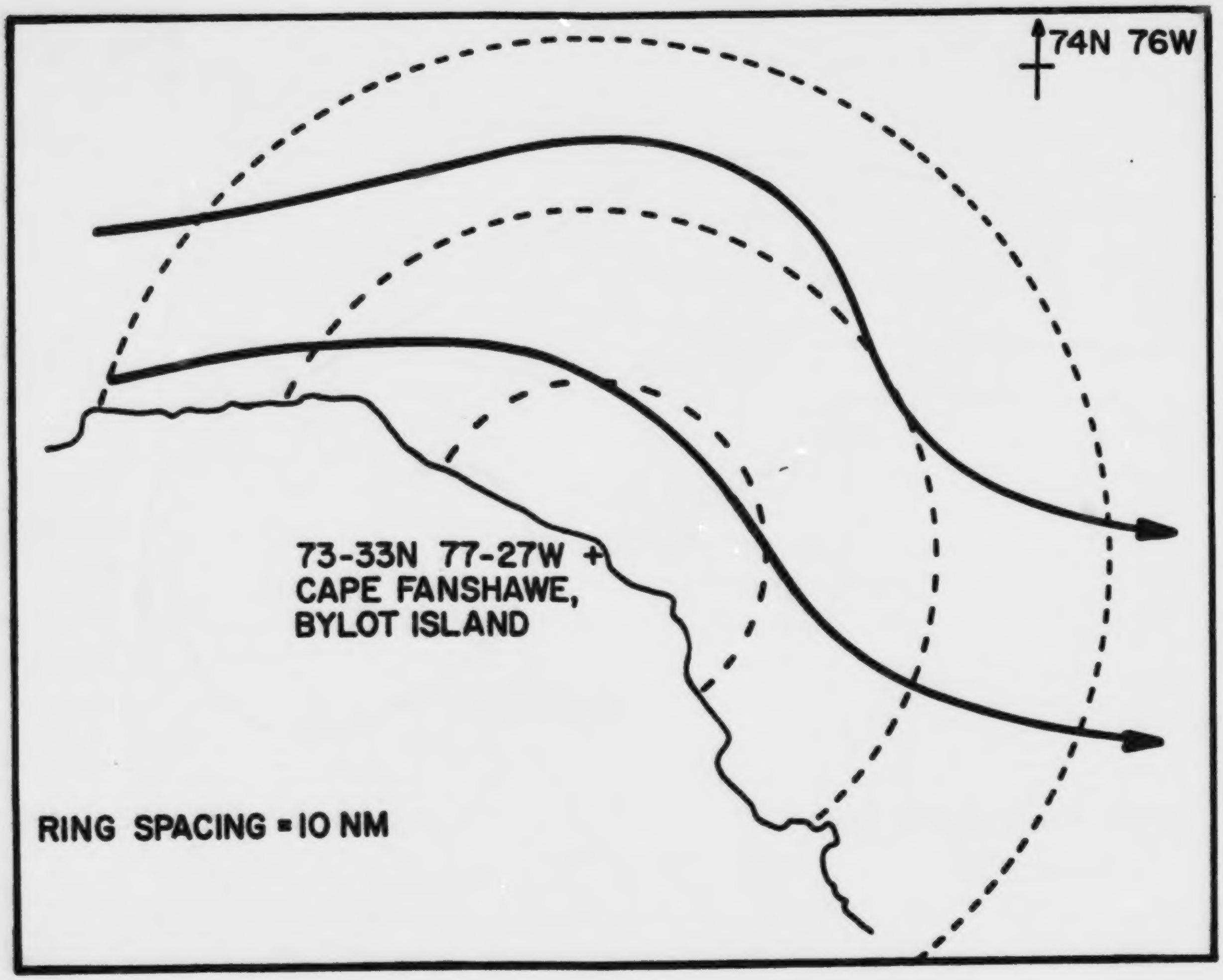
74N 76W
73-33N 77-27W
CAPE FANSHAWE,
BYLOT ISLAND
RING SPACING = 10 NM

Figure 3.4.33(f) General iceberg drift pattern, August 25-31 (NORDCO, 1979)

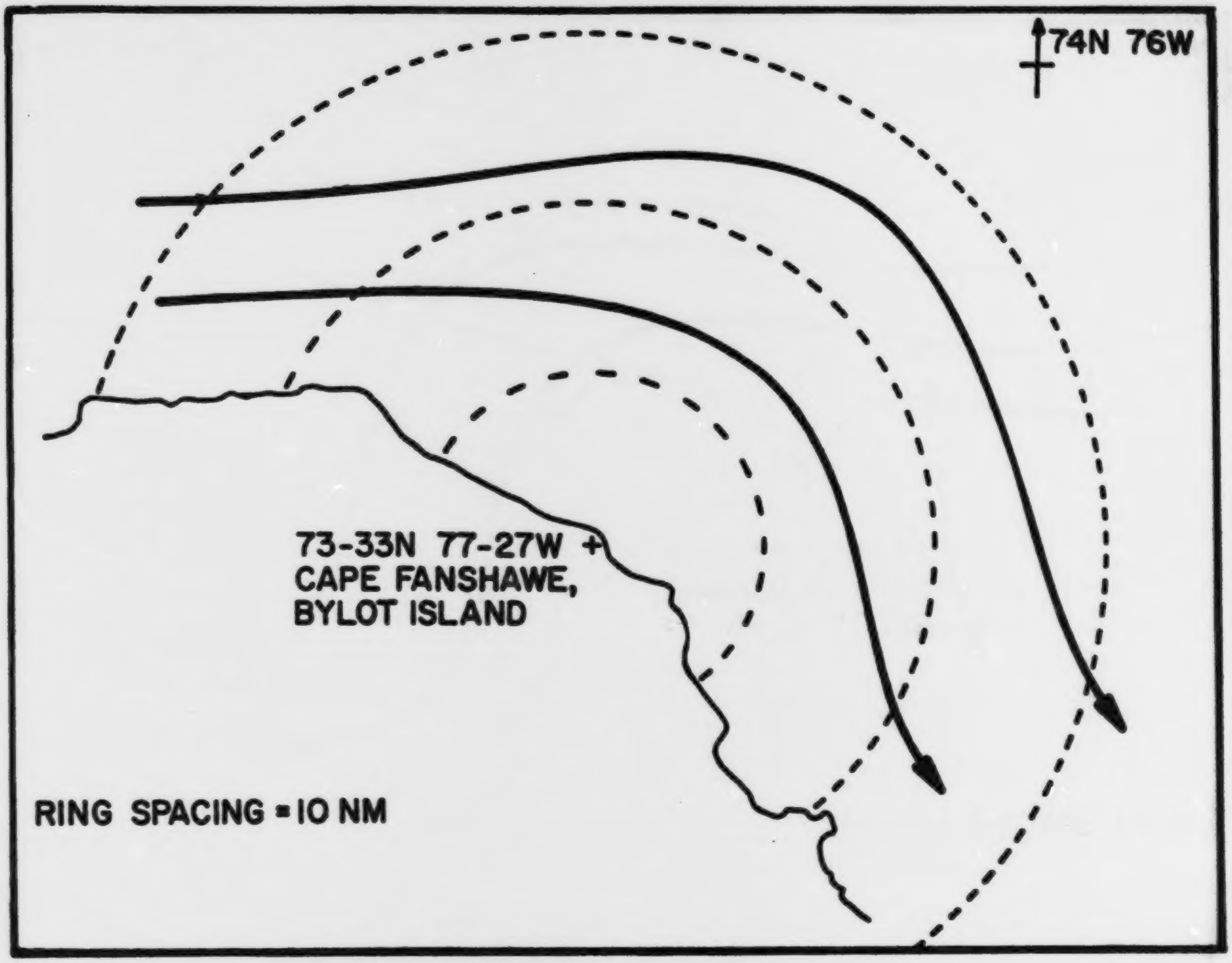
74N 76W
73-33N 77-27W
CAPE FANSHAWE,
BYLOT ISLAND
RING SPACING = 10 NM

Figure 3.4.33(g) General iceberg drift pattern, September 1-7 (NORDCO, 1979)

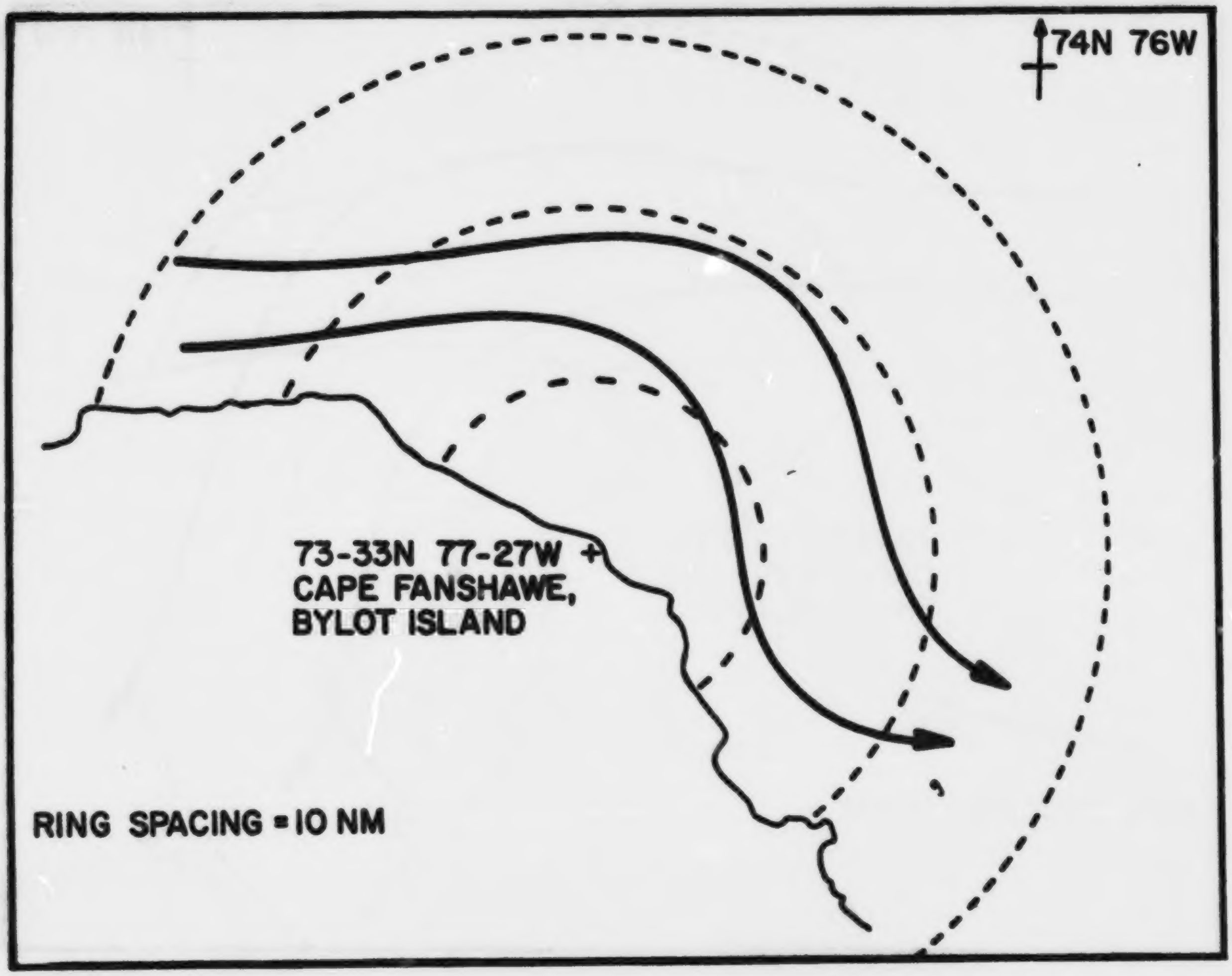
74N 76W
73-33N 77-27W
CAPE FANSHAWE,
BYLOT ISLAND
RING SPACING = 10 NM

Figure 3.4.33(h) General iceberg drift pattern, September 8-14 (NORDCO, 1979)

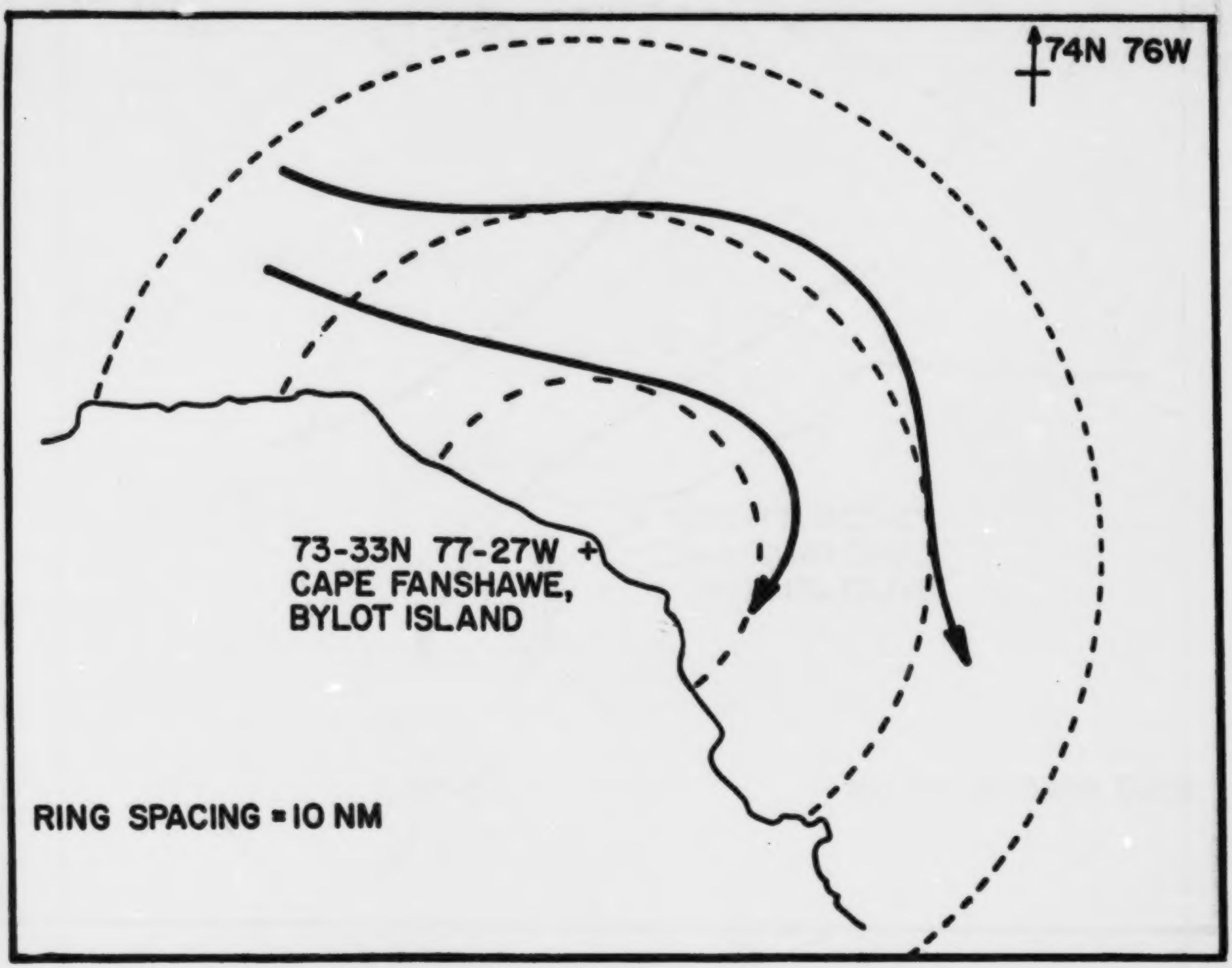
74N 76W
73-33N 77-27W
CAPE FANSHAWE,
BYLOT ISLAND
RING SPACING = 10 NM

Figure 3.4.33(i) General iceberg drift pattern, September 15-21 (NORDCO, 1979)

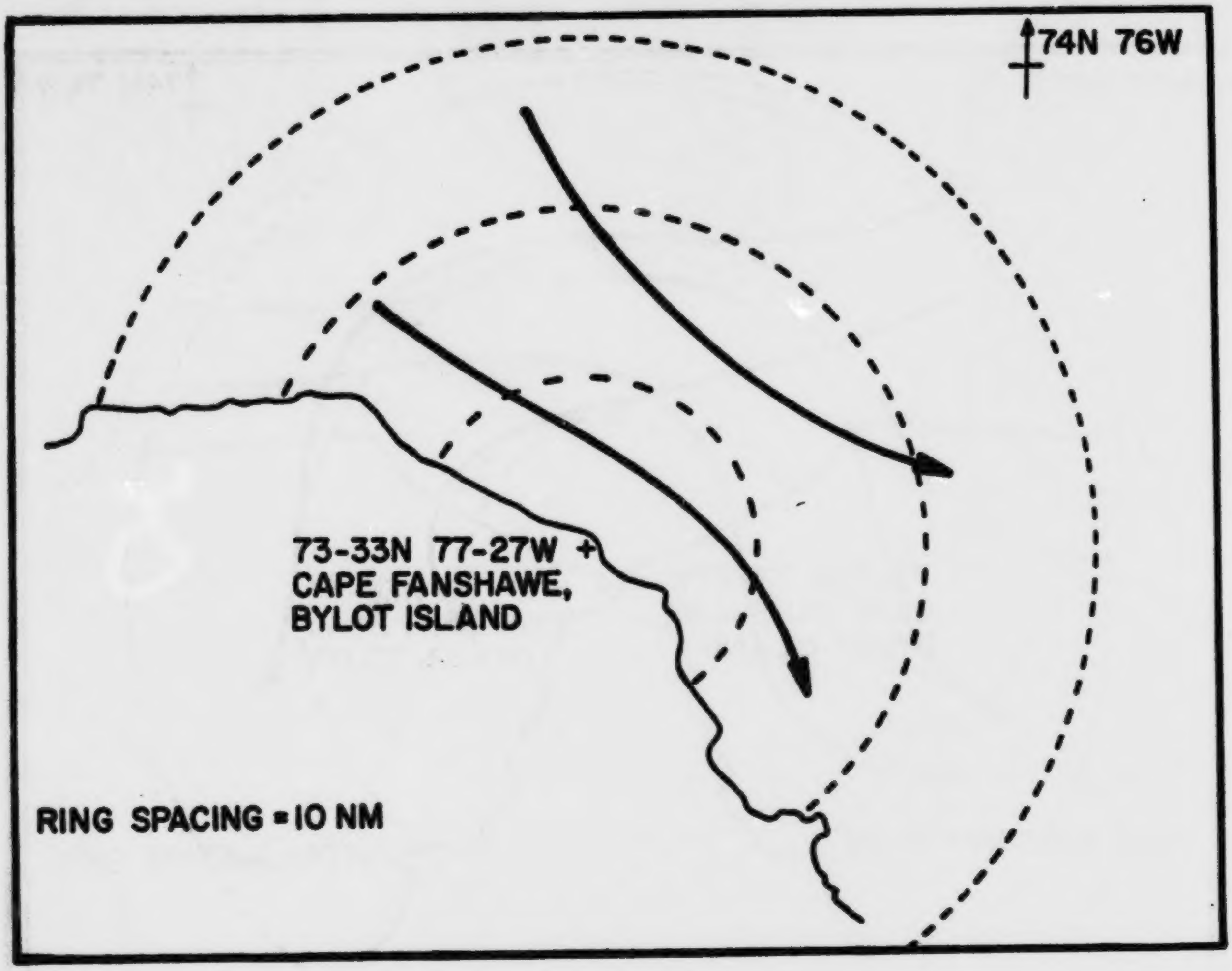
74N 76W
73-33N 77-27W
CAPE FANSHAWE,
BYLOT ISLAND
RING SPACING = 10 NM

Figure 3.4.33(j) General iceberg drift pattern, September 22-28 (NORDCO, 1979)

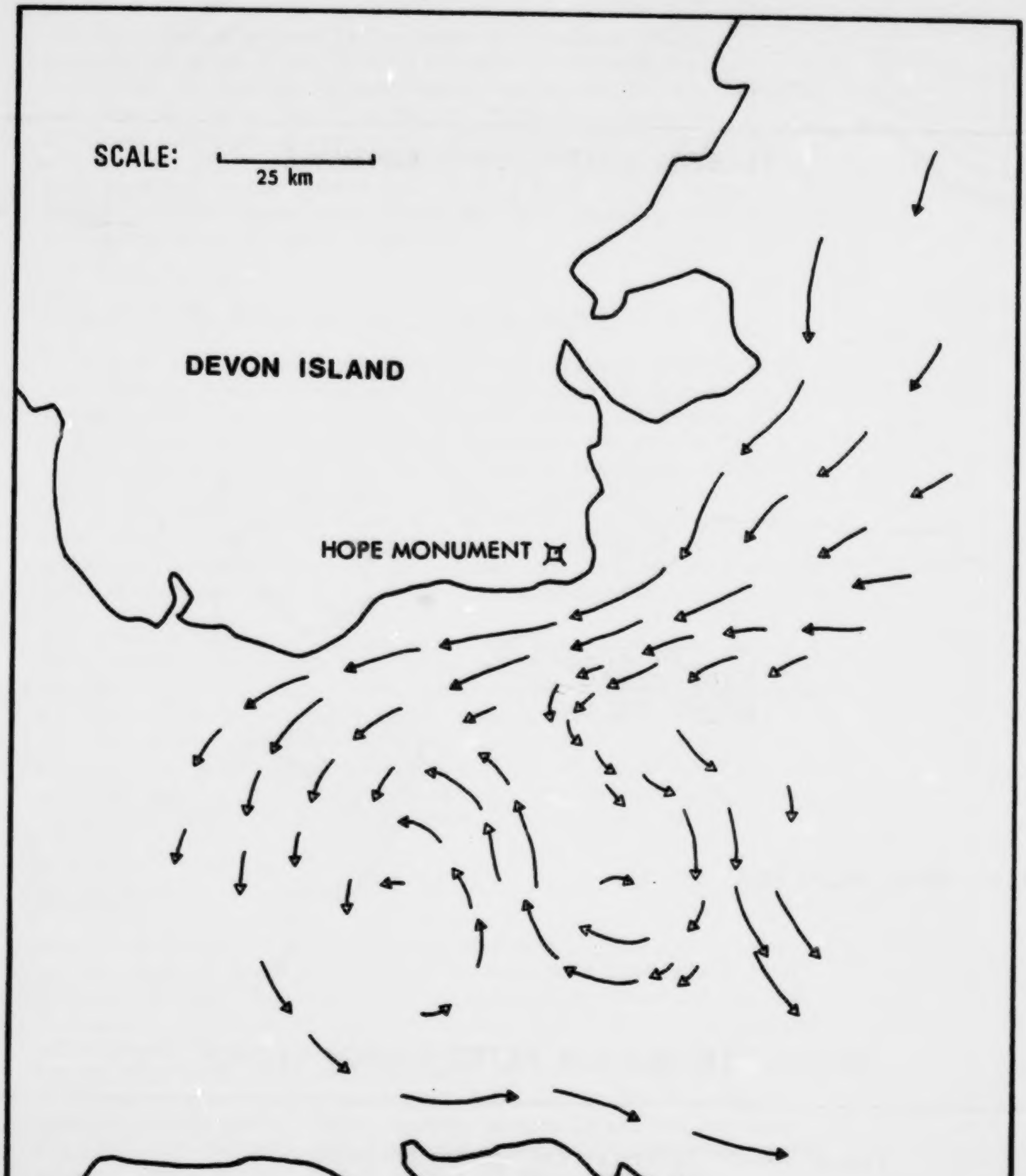
SCALE:
25 km
DEVON ISLAND
HOPE MONUMENT
BYLOT ISLAND

Figure 3.4.34 A general pattern of iceberg circulation deduced from radar-tracked iceberg data (de Lange Boom, MacNeill, Buckley, 1979)

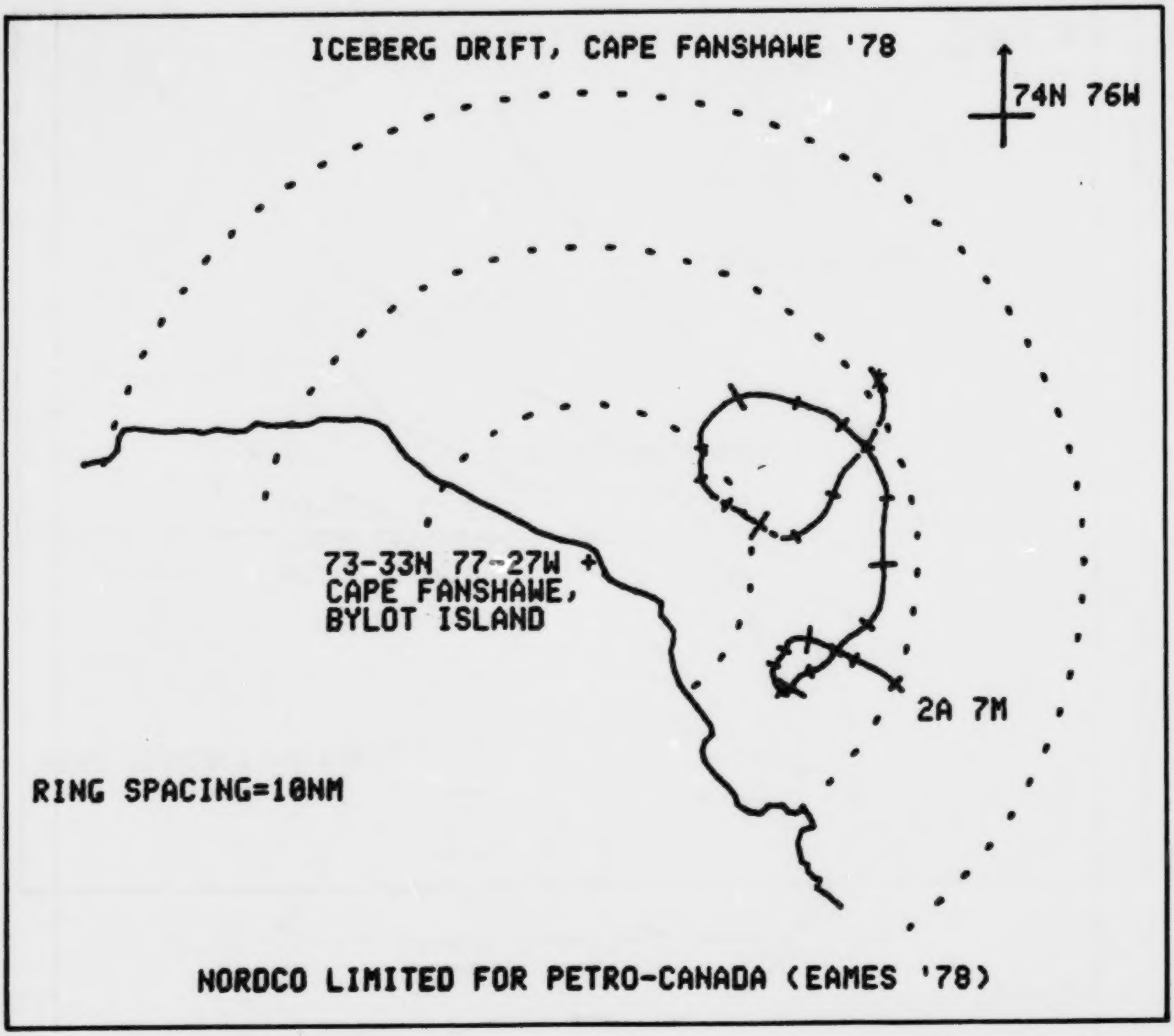
ICEBERG DRIFT, CAPE FANSHAWE '78
74N 76W
73-33N 77-27W
CAPE FANSHAWE,
BYLOT ISLAND
2A 7M
RING SPACING=10NM
NORDCO LIMITED FOR PETRO-CANADA (EAMES '78)

Figure 3.4.35 Radar-tracked iceberg trajectory:
ID 02A07, 1978

direction roughly paralleling that of original entry. Examples of such drift from the northern and eastern boundaries of the region are found in Figures 3.4.23, 3.4.27a and 3.4.32. This behaviour may be associated with the existence of minimum levels of persistence and strength for wind fields capable of extracting bergs out of the intrusive flow regime. These levels both may be high enough that, in general, an extracted berg continues to follow the wind until it leaves the disordered zone.

Region 5 - The Eddy Zone East of Bylot Island

The important features of the water circulation in this region include the continued separation of the current from the Bylot Island coastline noted in the adjacent sector of region 3 and the presence of quasi-stationary eddies in the region extending outward some 70 km to the east of the Bylot Island coastline. The two principal locations for the latter structures are roughly 20 km northeast of Cape Fanshawe and some 24 km northeast of Cape Birney. Exclusive of periods of eddying, the net displacements of drogued drifters in the area generally range from 25 to 50 km/day southeasterly.

The results from the Cape Fanshawe radar station and the satellite-tracking indicate essentially identical features in the berg drift results. (See for example the weekly patterns of figure 3.4.33 and the trajectories of 3.4.32 and 3.4.35.) The indicated periods of rotation (8-10 days) are typical as are the eddy positions. The possibility of rapid and direct southeasterly berg passages inshore of the primary eddy zone is well illustrated by the trajectory of figure 3.4.25.

Region 6 -

The oceanographic data (Fissel, Lemon and Birch, 1980) taken to the east of Bylot and Baffin Islands show that the Baffin Current (or the Canadian Current) takes form south of the east entrance to Pond Inlet, appearing as a reasonably well defined entity near 72°30'. Average current velocities of 15-20 km/day southeast were recorded near 71°30' with maximum speeds over the continental slope at the edge of the shelf roughly some 30 km offshore. Drift speeds in the latter region were typically 30 km/day. The flow was observed to continue to the edge of Davis Strait with a factor of two reduction in magnitude in 1979 relative to the previous year.

The only berg data available in the Baffin Current region were obtained from the 1978 and 1979 satellite-tracking programs, which yielded 12 trajectories which either partially or completely traversed the region.

The general interpretation of the resulting data is more difficult than in the previously discussed more northern areas due to the comparatively high regional probability of berg grounding. As a result the net rates of movement along

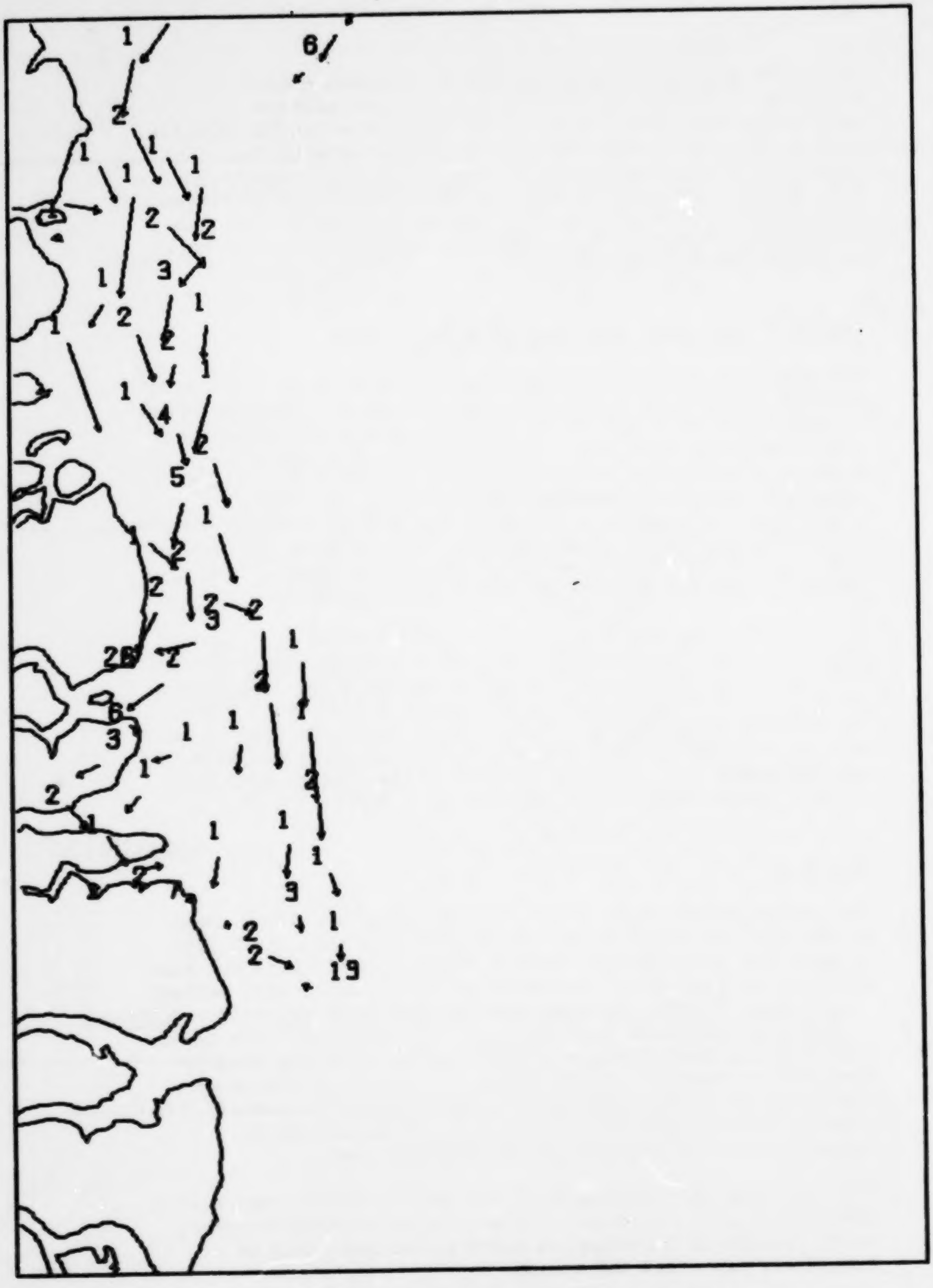
1
6
2
1
1
1
1
2
2
1
3
1
1
2
2
1
1
4
2
5
1
2
2
2
2
3
1
2B
2
2
6
1
1
1
3
1
2
2
1
1
1
1
2
9
1
2
2
19

Figure 3.4.36 Average velocity vectors, from 1978 satellite-tracked berg data (1 inch = 100 km/day)

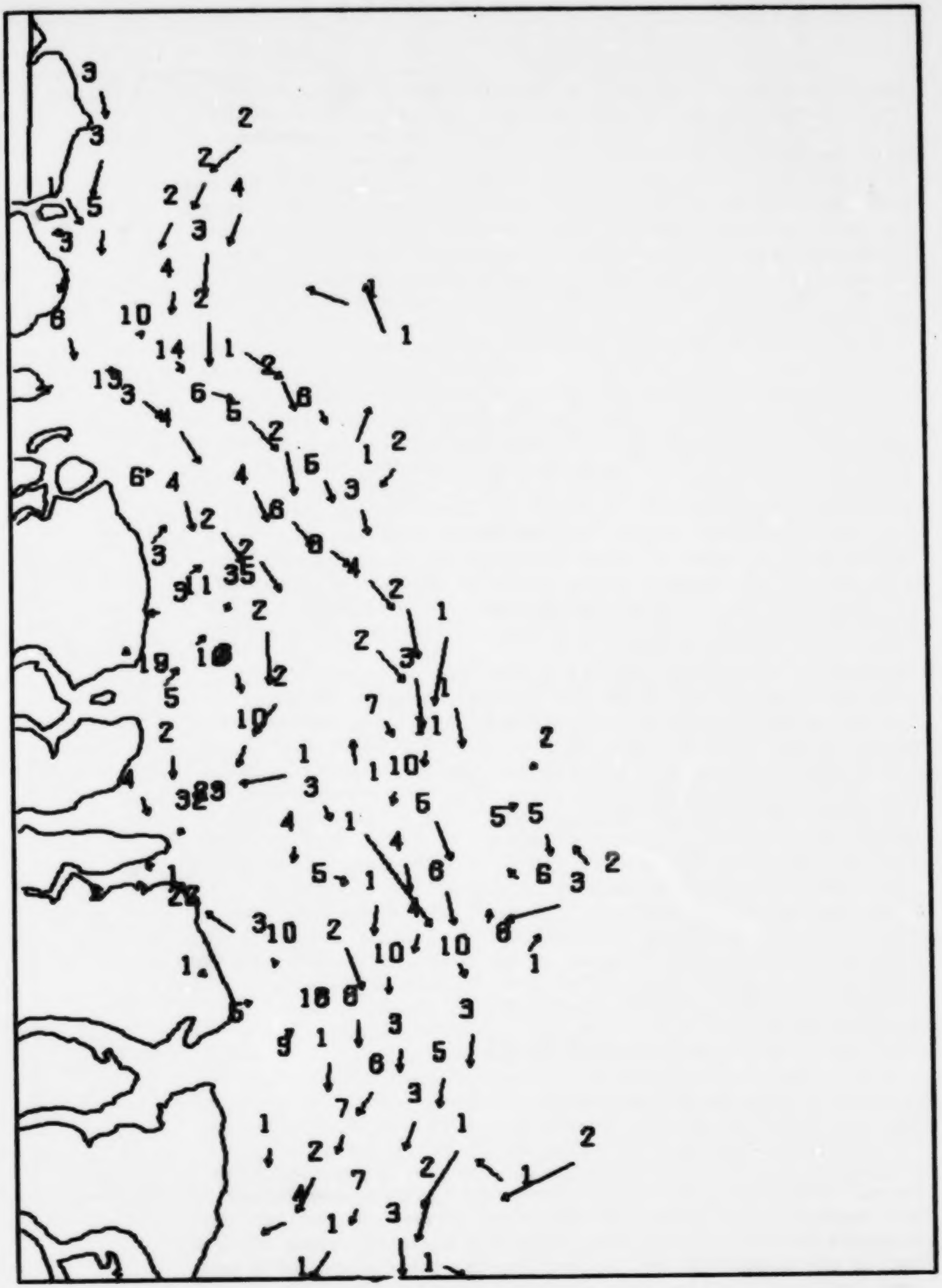

Figure 3.4.37 Average velocity vectors, from 1979 satellite-tracked berg data (1 inch = 100 km/day)

similar paths can vary widely depending upon timing, berg draft, local ice conditions and other factors. Some measure of the characteristic local berg velocities may be obtained from the average velocities of Figure 3.4.36 and 3.4.37. As in Figure 3.4.18 (which includes average velocity data for the northern portion of this region) the averaging was carried out on the velocities computed from pairs of adjoining position fixes exclusive of periods of obvious berg grounding. The data indicate the overall coast-paralleling nature of the drift. The accuracy with which spatial variations in drift velocity may be detected is somewhat limited by the small number of individual berg velocity measurements. Nevertheless the 1978 data in the northern portion of the region generally indicate that maximum drift rates of 30 to 35 km/day occurred in the zone centered some 30 km out from the coastline. As seen from the simplified trajectories of the bergs sketched in Figures 3.4.38a, b, the bergs initially tracked in 1978 reached as far south as 70°30' before the freeze-up essentially immobilized all bergs in November and December. The 1979 velocities appear to be somewhat smaller than those of the previous year although the limited amount of data do not justify the drawing of any detailed conclusion comparable to the factor of two differences noted in the 1978 and 1979 average near-surface currents (Fissel, Lemon and Birch, 1980).

Instead, a comparison of the trajectories of Figure 3.4.38 with those obtained in the 1979 tracking program (Figure 3.4.39) reveals considerable similarities in the respective annual drift trends. Thus, in each year a drifter (#1413 (1978) and #1990 (1979)) entered the region in mid-September, followed a close-inshore path until it either closely skirted the shoreline (1978) or ran aground in the vicinity of Cape Christian in early October. A good part of the reduced 1979 velocity averages in northern areas no doubt resulted from the highly erratic path followed by berg #1162 in the period preceding the usual September dates of berg entry into the region (Figure 3.4.40a). Significantly, greater net southerly movements were recorded in the latter year particularly in the track of berg #1162 which moved from roughly 72°30'N to 67°30'N over the September 23-October 24 interval (see detailed tracks of Figure 3.4.40a, b). Comparisons of the 1979 end points with the trajectories in Figures 3.4.38 and 3.4.39 illustrate the spatial overlap of populations which originally entered the region in adjoining years. Tracking of the berg populations into areas below 67°N was limited by the higher transmitter failure rates in the Davis Strait area, presumably due to rolling of the progressively deteriorating bergs. Continuing data from the Nimbus tracking system and the resumption of ARGOS coverage later suggested that leading elements of both tracked berg populations passed south of 62°N during the summer of 1980 suggesting the possibility of a one year berg transit time from eastern Lancaster Sound to Labrador.

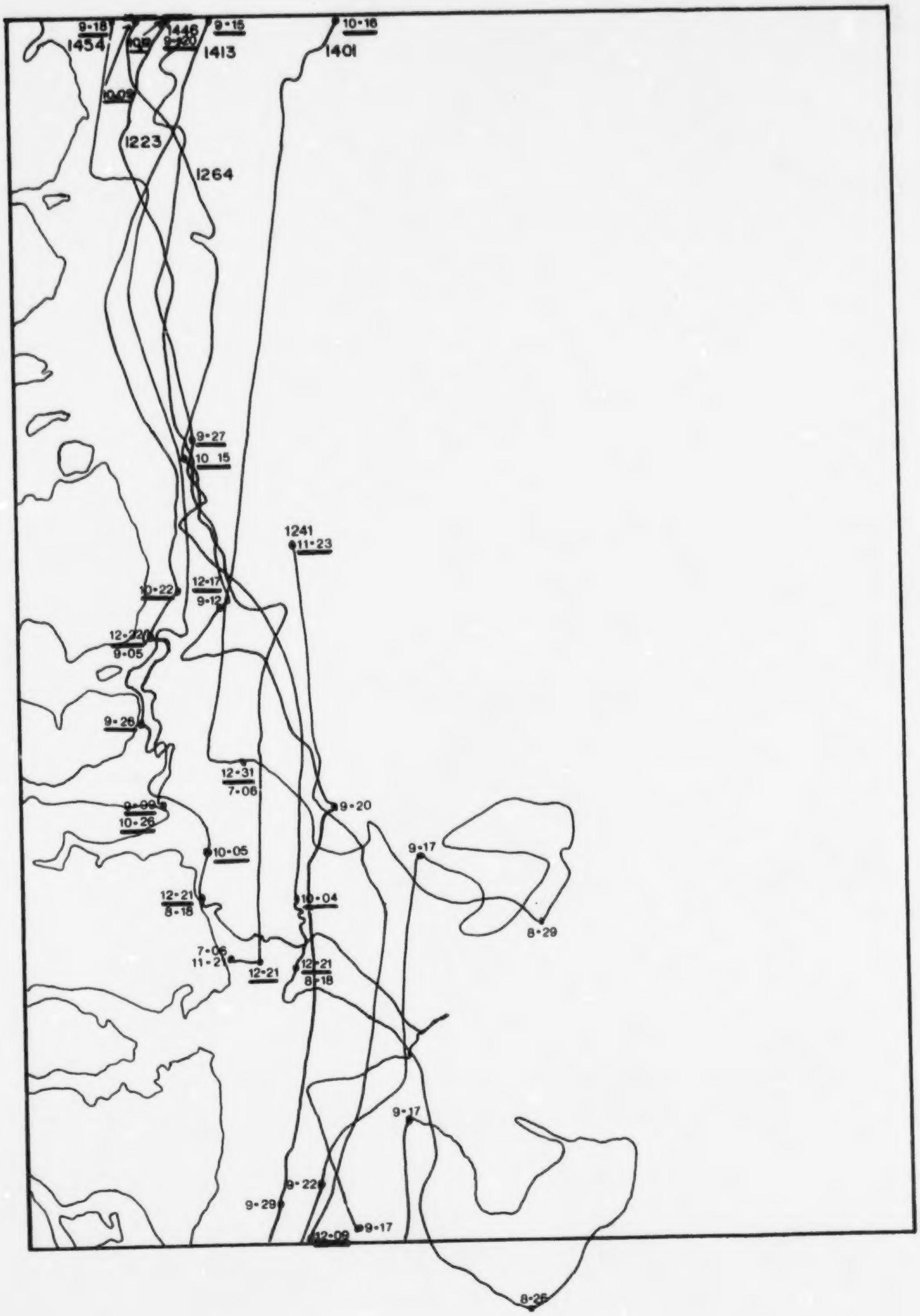
9-18
1454
10?
1446
9-20
9-15
1413
10-16
1401
10-09
1223
1264
9-27
10 15
1241
11-23
10-22
12-17
9-12
12-22
9-05
9-26
12-31
7-06
9-20
9-09
10-26
10-05
9-17
8-29
12-21
8-18
10-04
7-06
11-21
12-21
12-21
8-18
9-17
9-22
9-29
12-09
9-17
8-26

Figure 3.4.38(a) Simplified trajectories of satellite-tracked berg: - 1978 drops (1978 dates are underlined, 1979 dates are not underlined)

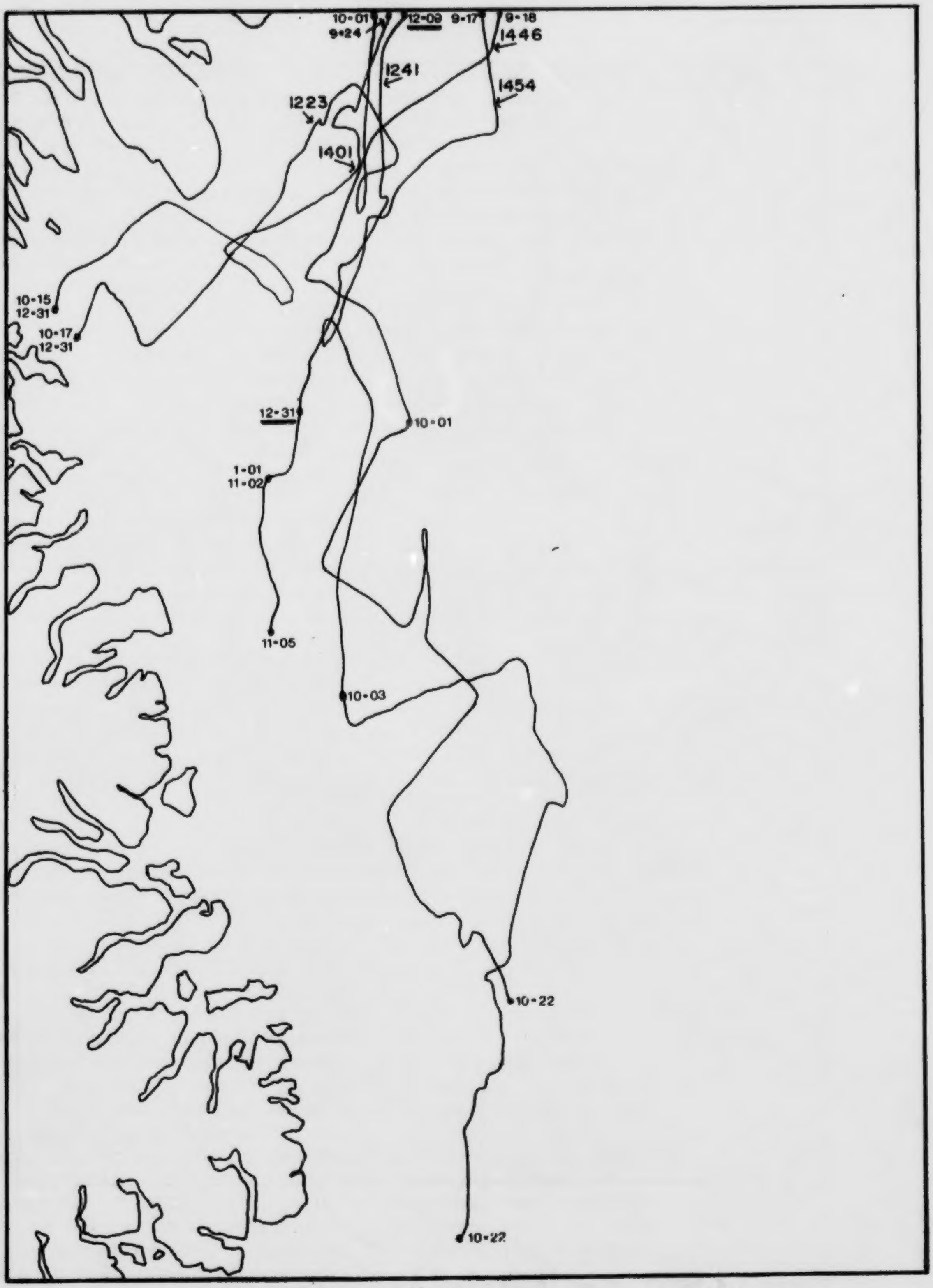
10-01
9-24
12-09
9-17
9-18
1446
1241
1454
1223
1401
10-15
12-31
10-17
12-31
12-31
10-01
1-01
11-02
11-05
10-03
10-22
10-22

Figure 3.4.38(b) Simplified trajectories of satellite-tracked berg: - 1978 drops (cont'd) (1978 dates are underlined, 1979 dates are not underlined)

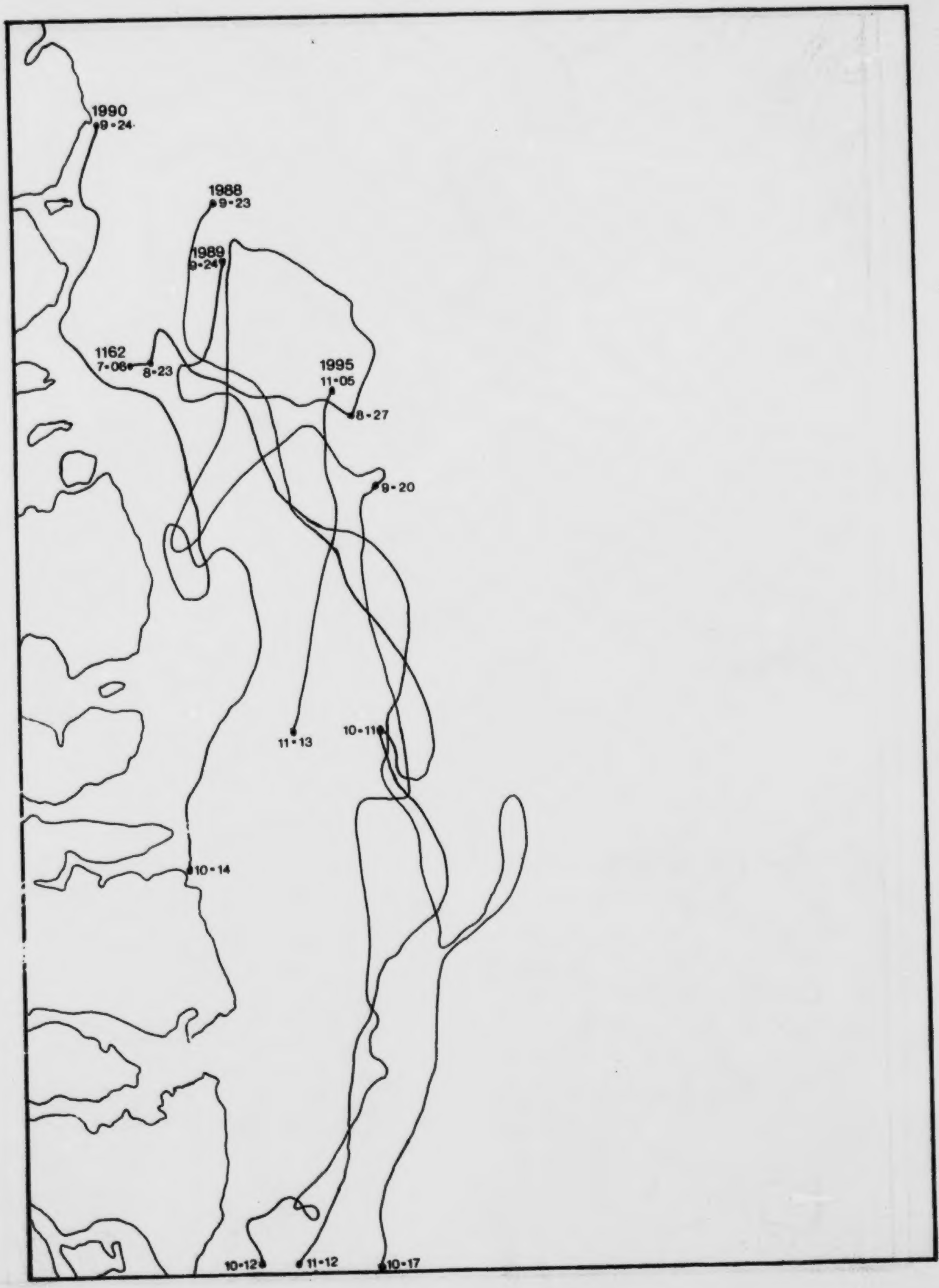
1990
9-24
1988
9-23
1989
9-24
1162
7-06
8-23
1995
11-05
8-27
9-20
11-13
10-11
10-14
10-12
11-12
10-17

Figure 3.4.39(a) Simplified trajectories of satellite-tracked bergs - 1979 placements

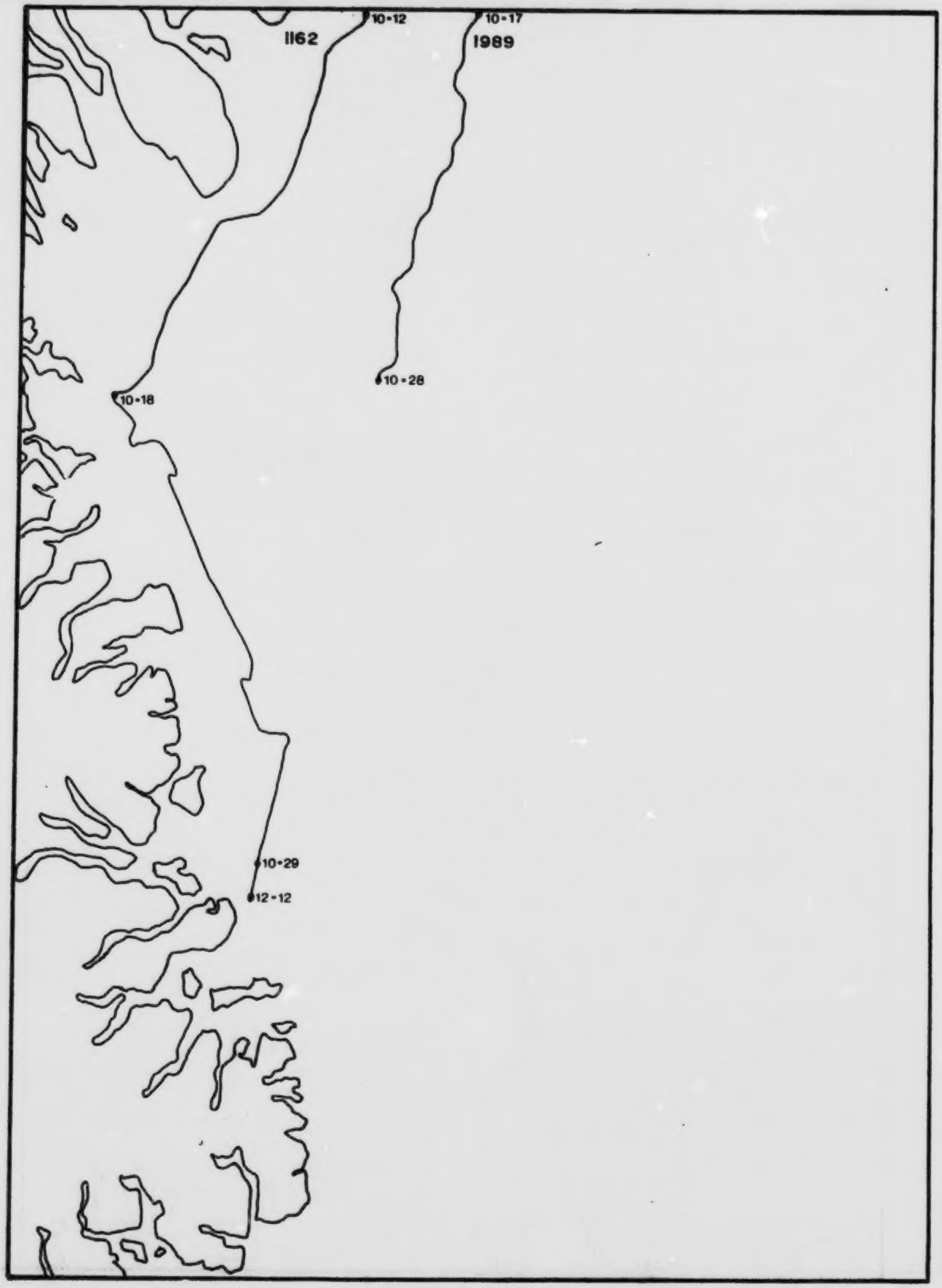
10-12
1162
10-17
1989
10-28
10-18
10-29
12-12

Figure 3.4.39(b) Simplified trajectories of satellite-tracked bergs - 1979 placements (cont'd)

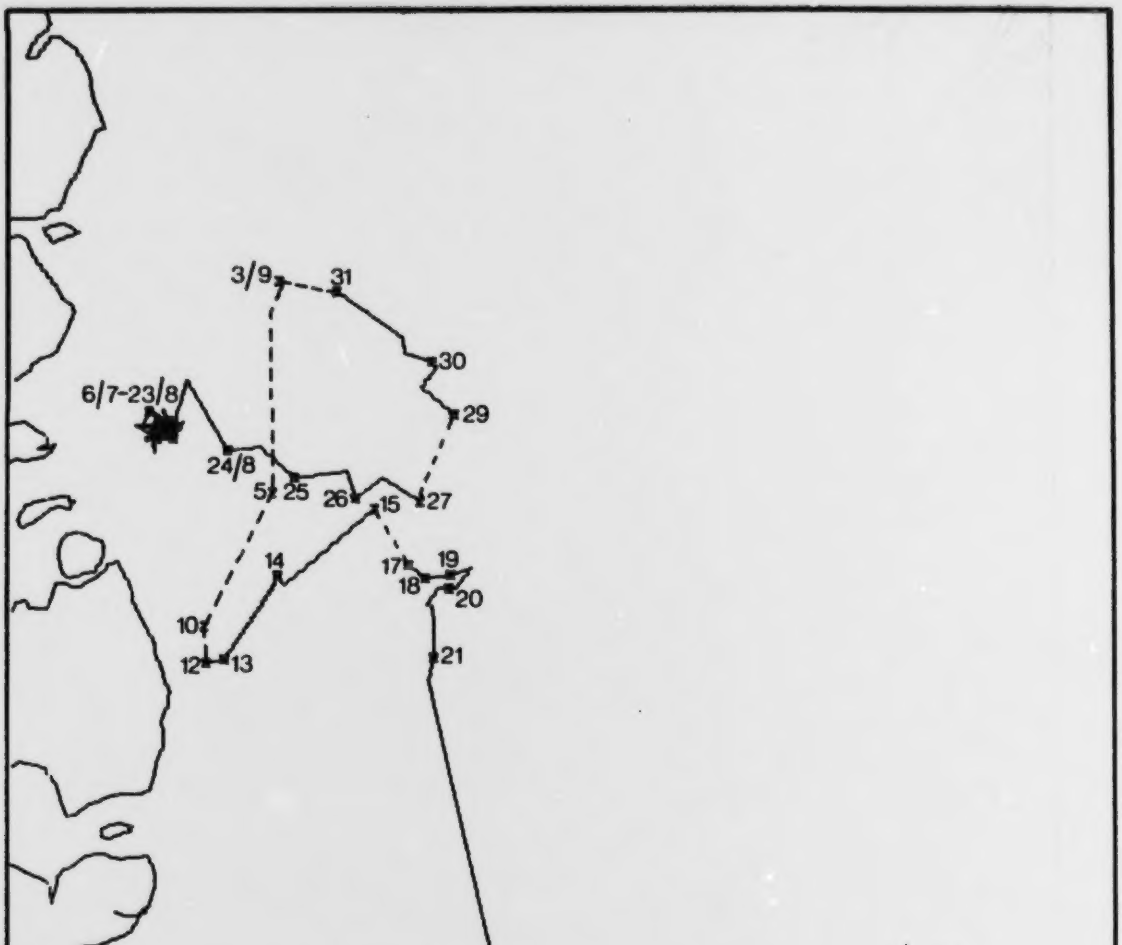
3/9
31
30
29
6/7-23/8
24/8
5
25
26
15
27
14
17
19
18
20
10
12
13
21
22
24
26
27
28
29
8
3
1/10
11

Figure 3.4.40(a) Satellite-tracked berg trajectory, ID 1162, 6/7/79 to 11/10/79 (Fissel, 1980)

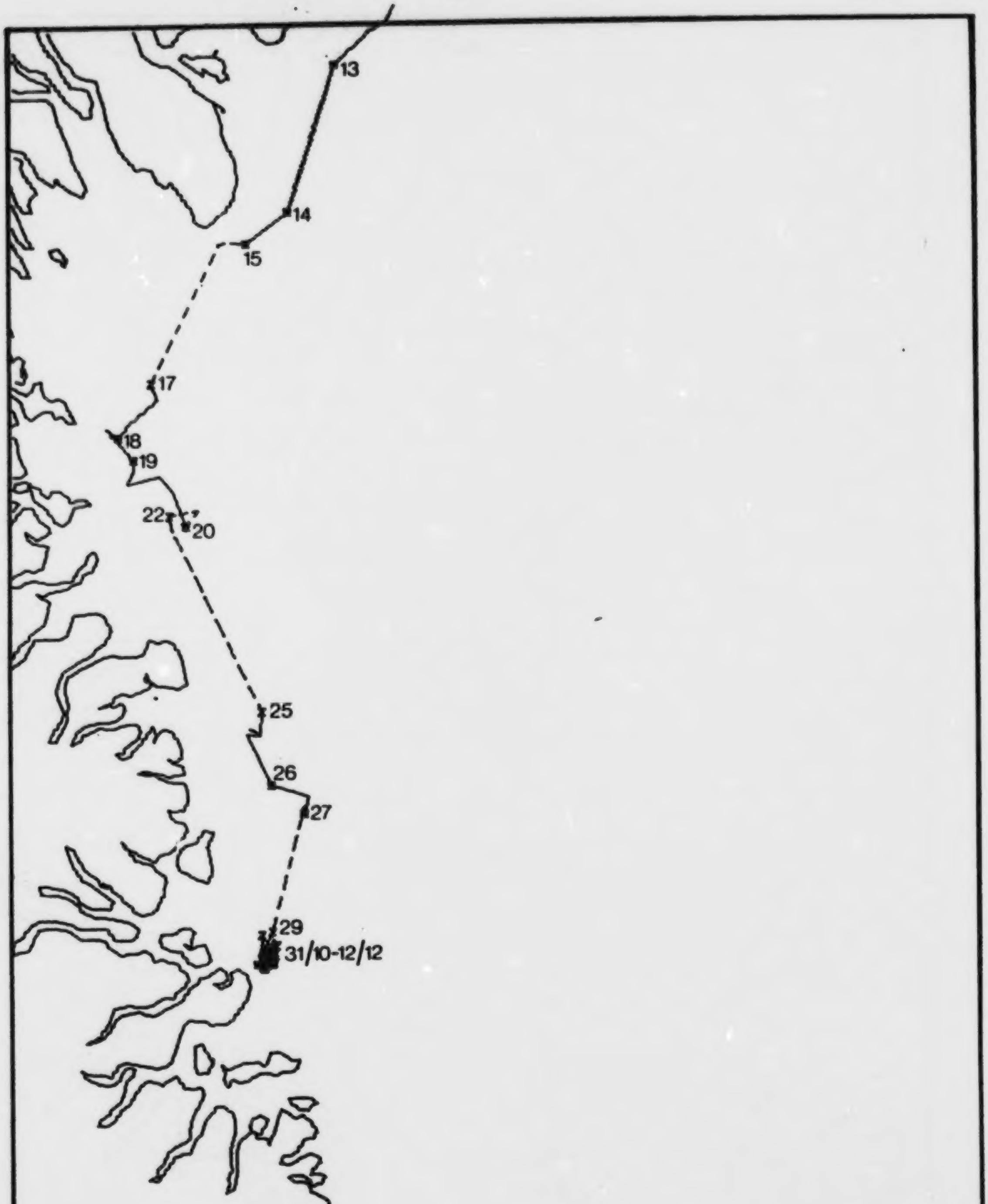
13
14
15
17
18
19
22
20
25
26
27
29
31/10-12/12

Figure 3.4.40(b) Satellite-tracked berg trajectory, ID 1162, 11/10/79 to 12/12/79 (Fissel, 1980)

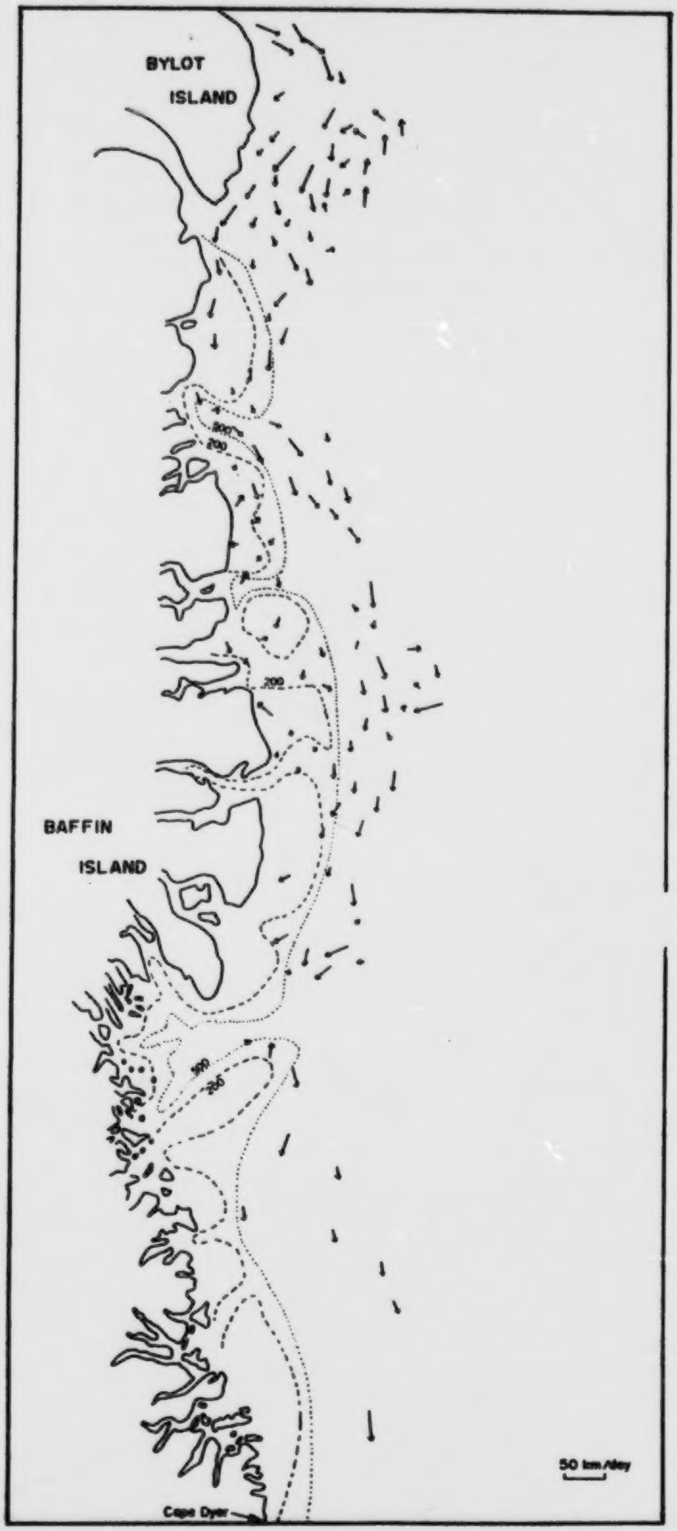
BYLOT
ISLAND
BAFFIN
ISLAND
200
500
50 km/day
Cape Dyer

Figure 3.4.41 The 1978-1979 box averaged daily iceberg drift vectors. The 200 m and 500 m bottom contours are included for comparative purposes

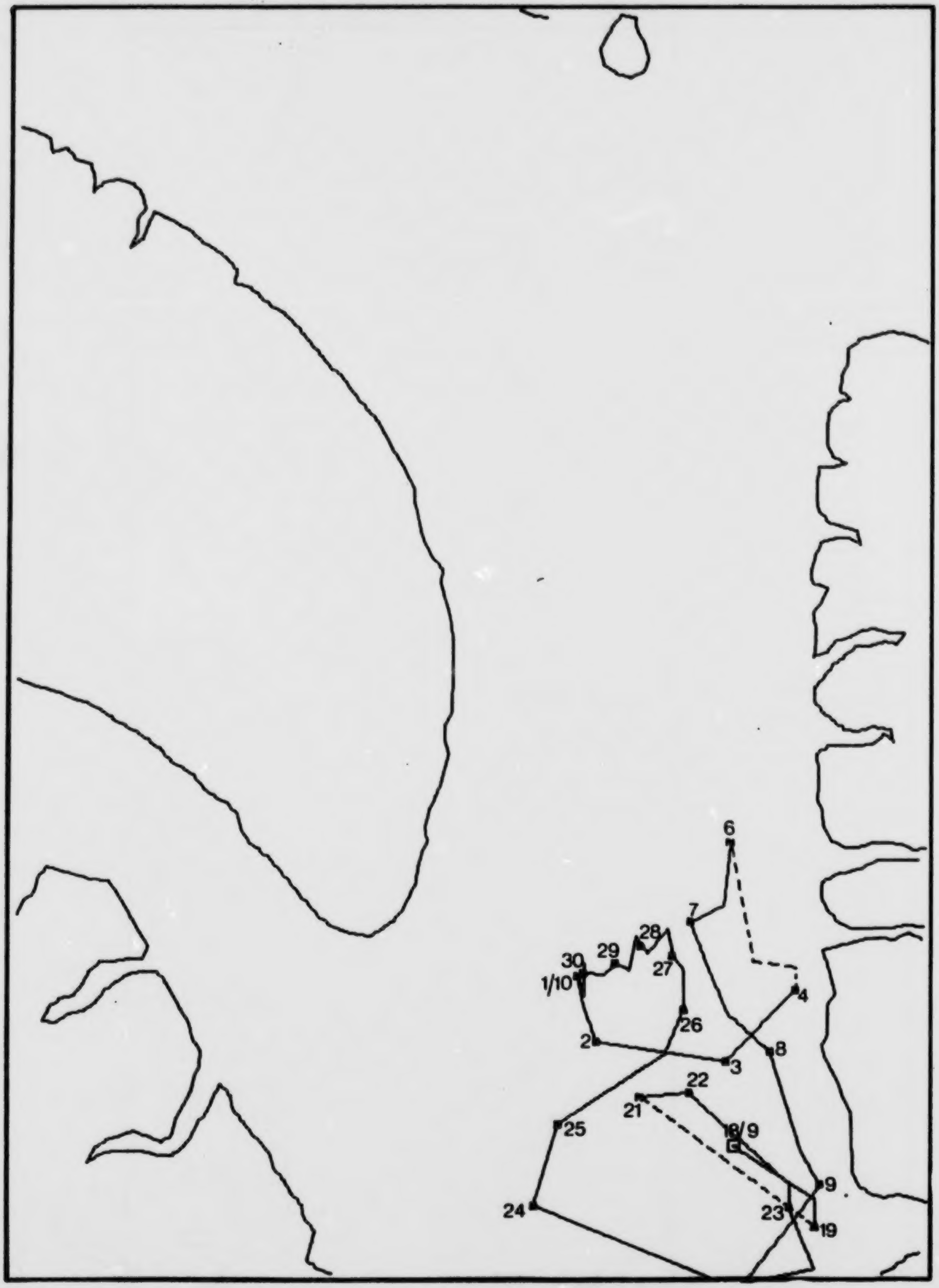
6
7
28
29
30
27
1/10
26
4
2
8
3
22
21
18/9
25
9
24
23
19

Figure 3.4.42 Satellite-tracked berg trajectory, ID 1241, 18/9/78 to 9/10/78 (Fissell, 1980)

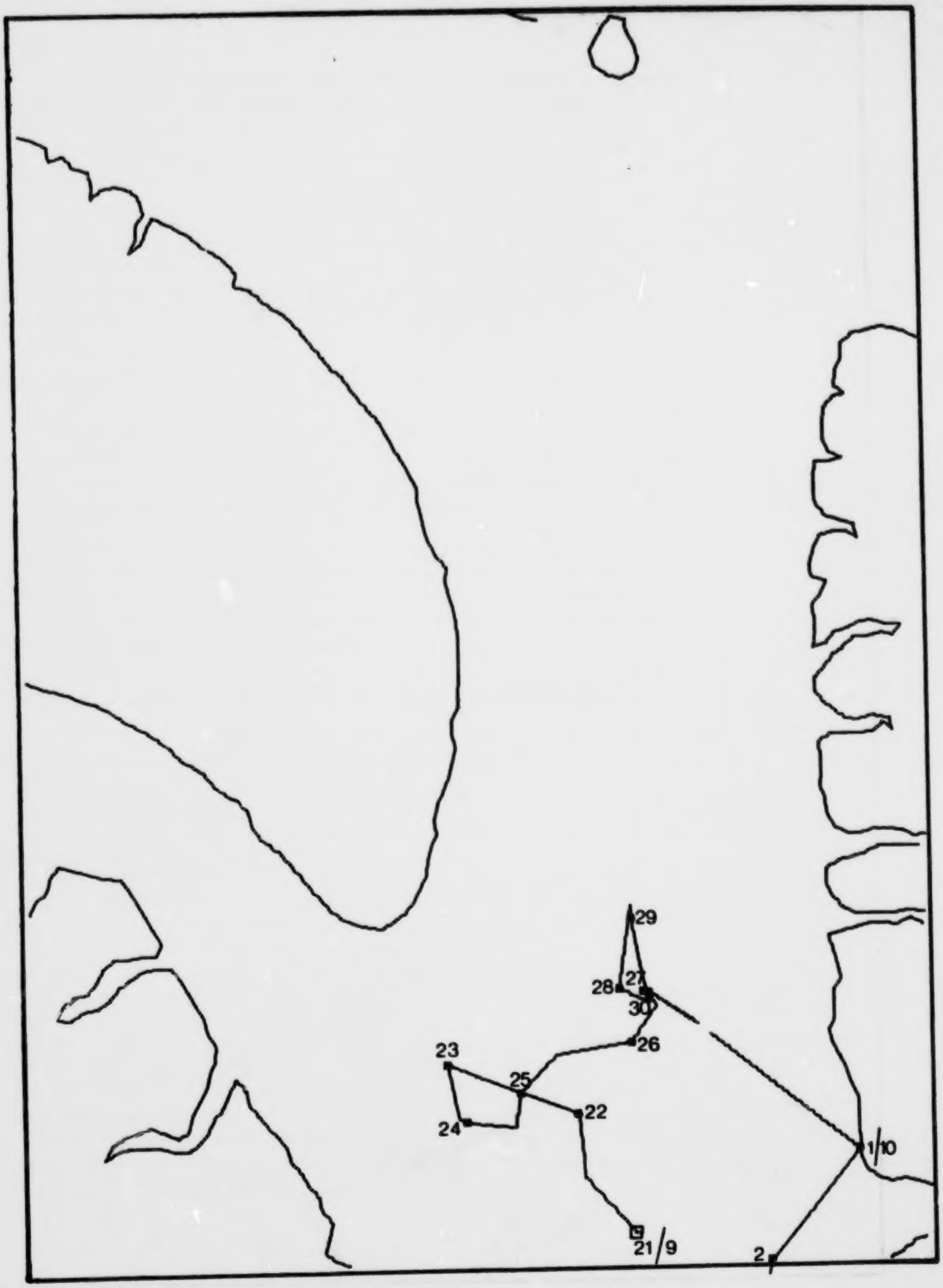
29
28
27
30
26
23
25
22
24
1/10
21/9
2

Figure 3.4.43 Satellite-tracked berg trajectory, ID 1264, 21/9/78 to 2/10/78 (Fissell, 1980)

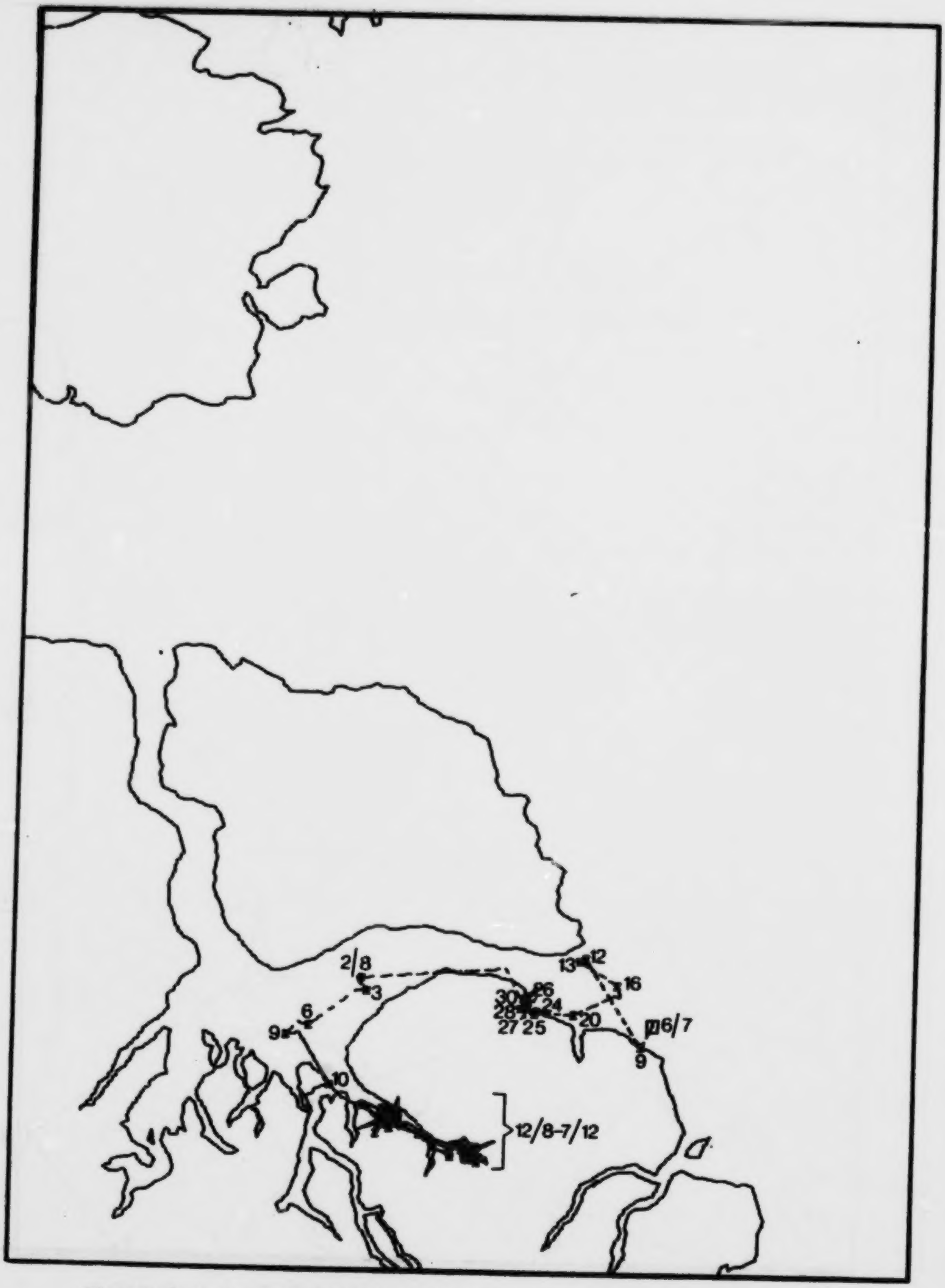
2/8
3
6
9
10
13
12
16
30
26
24
28
27
25
20
6/7
9
12/8-7/12

Figure 3.4.44 Satellite-tracked berg trajectory, ID 1462, 6/7/79 to 7/12/79 (Fissell, 1980)

These satellite-tracked data have been recently reviewed (Marko, Birch and Wilson, 1981) specifically with regard to implications for long term berg drift rates. It was found that a critical element of the problem was the tendency for berg motions to follow the topographic contours of the sea-bottom. This characteristic, noted in near-surface current studies (Fissel, Lemon and Birch, 1980), led to high densities of shoreward berg movements over each of several narrow underwater canyons which traverse the Baffin Island continental shelf (see the 200 m and 500 m contours in the combined 1978-1979 average berg velocity plot of Figure 3.4-41). Bergs diverted in this manner have a high probability of grounding on the adjoining shallow portions of the shelf under wind and other coastal influences.

Thus, although freely moving bergs tended to move southeasterly at, very roughly, a 15 km/day sustained rate, the frequency and duration of berg immobilization (by grounding or ice entrapment) were found to be the controlling factors in net movement. Moreover, once a berg was immobilized, the critical step in the resumption appeared to be the break-up and clearing of the landfast ice shelves during August and September. Of the 15 bergs studied, the average duration of the southeasterly drift from Bylot Island to Cape Dyer was 2 to 3 years.

Region 7 - Western and Central Lancaster Sound Region

In this area summer current data indicate the prevalence of weak and variable flows. Typically large eddy-type structures are present which do not appear to have any particular preferred sense of rotation or location. The most persistent flow in the region was an easterly regime in the south side of the Sound.

Berg data in this region consist primarily of the tracks of berg #'s 1241 and 1264 which moved into the area in mid and late September 1978 in the northern half of the Channel shortly after entering the Cape Sherard segment of the intrusive flow (see Figure 3.4.16). The subsequent berg paths, indicated in Figures 3.4.42 and 3.4.43, exhibit both clockwise and counterclockwise looping segments and an initial slow westerly and later easterly drift. Movement across the Sound is evident in Figure 3.4.43, but, as in the case of the current and drifter observations (Fissel, Lemon and Birch, 1980), no pattern of movement is obvious. In both cases bergs moved again to the northern side of the Channel before rejoining the intrusive flow in early October.

Region 8 - The Navy Board Inlet-Eclipse Sound-Pond Inlet Region

The berg data in this region consists of the July 7, 1971 to December 12, 1979 portion of the trajectory of berg #1462 (Figure 3.4.44) which moved, in this period, from the eastern entrance of Pond Inlet into the eastern extremity of Oliver Sound. The indicated path followed the southern border of the Inlet, as distinguished from the movements of three drifter buoys (Fissel, Lemon and Birch, 1980) which were observed to enter and leave the waterway in the east on its northern and southern sides respectively in a flow similar to that of the Lancaster Sound intrusion.

Other data of relevance were the resulting statistics on berg penetration of the northern and eastern ends respectively of Navy Board and Pond Inlets. In the first instance, none of the eighteen bergs tracked through the intrusive current region were observed to enter region 8. The data in the east at the Pond Inlet entrance correspond to an entrappment of one out of a complement of 10 (ten) tracked bergs.

4. Summary and Recommendations

After a review of the general body of ice research, the major elements of the Lancaster Sound-northwest Baffin Bay ice environment were examined with respect to identifying data patterns of behaviour and typical levels of variablity relevant to assessments of impact from proposed regional developments. Separate, but, of course interrelated treatments were given to ice of land origin (icebergs, bergy bits, etc.) and ice which forms on the sea surface (sea ice). Icebergs have been a principal focus of much previous work in the north Baffin Bay region and were the major target for study in the Petro-Canada-EAMES ice programs. Sea ice data on the other hand have largely been obtained through remote sensing techniques or more specifically from fixed-wing aircraft observer records and from satellite imagery.

The records of sea ice and berg motion are remarkably similar and bear a common relationship to the identified regional near-surface current patterns (Fissel, Lemon and Birch, 1980), suggesting an overall dominance of ocean current influence. This similarity applied to features of high repeatability, such as the fast current cores of the Lancaster Sound Intrusive flow and, as well, to intermittent eddy-like features in which bergs, sea ice and drogued drifters followed common looping trajectories.

The characteristic seasonal sea ice distributions were subject to the dual influence of the Baffin Bay pack ice and the great sheet of immobilized or landfast ice which covers most of the waterways of the Arctic Archipelago over the November to July period. Analysis of historical and recent patterns of ice coverage identified the fundamental influence of the position of the eastern boundary of this ice sheet in eastern Parry Channel as a determinant of summer ice conditions in Lancaster Sound and in the adjoining sector of Baffin Bay. For as yet unidentified reasons, there is a wide year to year variation in the position of this ice edge giving extreme conditions in which, over the May to mid-July period, the entire Barrow Strait-Lancaster Sound waterway may be alternatively under ten-tenths or zero-tenths ice coverage. Superimposed upon this highly variable annual trend is the comparatively steady flow of water and ice down the western side of Baffin Bay including its intrusive segment which penetrates Lancaster Sound to roughly the 82° line of longitude. Variability in this flow often controls the rates of clearing along the east coasts of Devon, Bylot and Baffin Islands and this flow can inject considerable concentrations of ice into eastern Lancaster Sound regardless of the position of the landfast ice edge.

In spite of the obvious complexity of this situation, analysis of patterns of ice accumulation appears to be possible in terms of ice edge position, the known current structures and surface wind conditions. Characteristic "best year in five", "average" and "worst year in five" patterns identified on a purely statistical basis from AES ice observer data were related to specific examples of annual conditions and the corresponding positions of the Channel landfast ice edge.

The results of two years of berg observations generally indicated small year to year variability with, for example, a perhaps 20% reduction occurring in 1979 relative to the previous year. Changes in the annual average berg drift velocities were of similar magnitude. A crude estimate on the basis of satellite-tracked berg trajectories indicated that less than 10% of the bergs moving past the east Devon Island coastline penetrate Lancaster Sound. Berg trajectories were strongly confined to the fast cores of the current system with occasional deviations into areas of persistent eddying motion with the prominent zone off the east coast of Bylot Island.

Particular features of the berg data worthy of note include the small, "20%, difference in the respective annual number of bergs noted in the two year study and the fact that the majority of bergs tend to be confined to the high speed and stability sectors of the near-surface current cores.

Future research efforts should be directed toward compiling the bases of simultaneous wind, ice and water column data that would allow:

a) Detailed clarification of the processes responsible for the formation and stabilization of the coastal and cross-channel landfast ice edges in Lancaster Sound-Barrow Strait. A predictive model of cross-channel edge location and approximate stabilization date would be a major contribution to regional and operational planning. More immediately however, enough understanding of mechanisms must be gained to allow assessment of the likely impact of development on this important feature.

b) Identification of the sources of variability in the clearing rates of the Baffin Bay pack ice. Such an effort would no doubt amount to both original new work and interfacing with the accumulated results of earlier studies such as the North Water Project. The dynamics of the Baffin Bay ice cover are only poorly understood and have sufficient significance for independent study.

c) Higher spatial resolution characterization of the multiyear ice fraction, particularly in the low concentration or nearly pure first year ice regimes.

d) A more detailed description of the spatial and temporal distribution of floes using size categories more directly relevant to present operational capabilities.

Data collected in these efforts (surface winds, ice thickness and strengths of currents, etc.) would not only be of use in establishing the details of the regional ice processes, but, also would be directly applicable to exploration, production and transport planning.

Bibliography

Aber, P.G. and E. Vowinckel (1972), Evaluation of North Water Spring Ice Cover from Satellite Photographs, Arctic 25 pp. 263-271.

Allen, J.H. (1972), Iceberg Study, Saglek, Labrador, Memorial University Press, St. John's, Nfld.

APOA (1973), Environmental Conditions in Baffin Bay and Davis Strait, Marex Ltd., 100 p.

Arctic Sciences Ltd., 1980a, Interim Report: Movement of satellite-tracked drifters and icebergs, June 6-12, 1980. Prepared for Petro-Canada Ltd. by Arctic Sciences Ltd., Sidney, B.C.

Arctic Sciences Ltd., 1980b. Interim Report No. 2: Movement of satellite-tracked drifters and icebergs, August 12-October 21, 1980. Prepared for Petro-Canada Ltd. by Arctic Sciences Ltd., Sidney, B.C.

Arsenault, L.D., D. Waung, M. Holtz, M.R. Vant and R.O. Ramseir(1976), Remote Sensing Applications-- Sea Ice Dynamics, Interim Progress Report ICP 4-2 Prepared for Arctic Island Pipeline Program, Environment Canada, Edmonton.

Barry, R.G., J.D. Jacobs and others (1978), Energy Budget Studies in Relation to Fast-Ice Break-up Processes in Davis Strait, Occasional Paper No. 26, Institute of Arctic and Alpine Research, Boulder, Colo., 284 pp.

Bilello, M.A. (1960), Formation, Growth and Decay of Sea Ice in the Canadian Arctic Archipelago, Research Report 65, U.S. Army Snow, Ice and Permafrost Res. Est., Wilmette, Ill.

Bilello, M.A. (1964), Ice Thickness Observations -- North American Arctic and Sub/arctic, 1960-1962, Cold Regions Research and Engineering Laboratory Report 43.

Black, W.A., 1965, Sea ice survey, Queen Elizabeth Islands region, summer, 1962. Geographical Branch, Dept. of Energy, Mines and Resources, Ottawa, Ont.

Bradford, J.D. (1972), A Preliminary Report of the Observation of Sea Ice Pressure and its Effect on Merchant Vessels Under Icebreaker Escort, in Sea Ice, an International conference at Reykjavik, Iceland, pp. 154-158.

Bradford, J.D. (1978), Icebreaking Capability of CCES Labrador in Western Barrow Strait, October 23-28, 1973, Dept. of Fisheries and Environment Report, 12 pp.

Bradley, R.S. (1973), Seasonal Climatic Fluctuations on Baffin Island during the Period of Instrumental Records, Arctic, 26, pp. 240-243.

Broida, S. and W.S. Richardson (1972), Surface Current Measurements by Expended Probes, U.S. Coast Guard Technical Report Project 726520, 7 pp.

Brown, A.L. (1954), An Analytical Method of Ice Potential Calculation, U.S. Hydrographic Office Technical Report. TR-5.

Callaway, E.B. (1954), An Analysis of Environmental Factors Affecting Ice Growth, U.S. Hydrographic Office Report TR-7.

Corton, E.L. (1954),The Ice Budget of the Arctic Pack and its Application to Ice Forecasting, U.S. Hydrographic Office Report. TR-6.

Crane, R.G. (1978), Seasonal Variations of Sea Ice Extent in the Davis Strait-Labrador Sea Area and Relationships with Synoptic Scale Atmospheric Calculation, Arctic 31 pp. 434-447.

Dawson, W.B. (1907), The Currents in Belle Ile Strait, Dept. of Marine and Fisheries, pp. 1-43.

deLange Boom, B.R. and L.W. Davidson (1977), Radar Tracking of Ice in the Byam Martin Island Area, Seakem Ltd. under contract to Environment Canada.

deLange Boom, M.R. MacNeill and J.R. Buckley (1979), Iceberg Tracking in Northwestern Baffin Bay and Eastern Lancastern Sound from the Hope Monument Radar Camp, prepared for Petro-Canada Ltd. by SeaKem Oceanography 214. pp.

Deutsches Hydrographisches Institut (1950), Alas des Eisverhaltnisse des Nordatlantischen Ozeans und Ubersichtskarten des Eisverhaltnisse des Nord-und Sudpolargebietes, Hamburg.

Dunbar, M. (1969), The Geographical Position of the North Water, Arctic 22, pp. 438-441.

Dunbar, M. (1972), Increasing Severity of Ice Conditions in Baffin Bay and Davis Strait and its Effect on the Extreme Limits of Ice, in Sea Ice, an International Conference, Reykjavik, Iceland, pp. 87-93.

Dunbar, M. (1979), Fall Ice Drift in Nares Strait as observed by Sideways Looking Airborne Radar, Arctic 32 pp. 283-307.

Ekman, V.W. (1905), On the influence of the Earth's rotation on ocean currents. Arkf. Mat. Astr. och Fysik. K. Sv. Vet-Akad, Stockholm, Band 2, pp. 52.

Feazel, C.T. and R.C. Kollmeyer (1972), Major Ice Producing Glaciers of West Greenland, in Sea-Ice, an international conference at Reykjavik, Iceland, pp. 140-145.

ENCO (1974), The Northwest Passage, An Environmental Study Related to Offshore Operations with Emphasis in Lancaster Sound. (Carried out for Norlands Petroleum Ltd.).

Fissel, D.B., D. Lemon and J.R. Birch (1980), The Physical Oceanography of Western Baffin Bay and Lancaster Sound Report prepared for Petro-Canada Ltd. by Arctic Sciences Ltd., 345 p.

Fissel, D.B., 1980, Satellite-tracked iceberg movements in Baffin Bay and Lancaster Sound, summer 1978 and 1979. Data Report No. 7 prepared for Petro-Canada Ltd. by Arctic Sciences, ltd., Sidney, B.C.

Hamburg, A. (1884), Hydrografisk-Kemiska Iakttogelser under den Svensa Expeditionen til Gronland 1883, Bihtill K. Sv. Vet-Akad. Ilandl., 9 pp 1-65.

ICE (1979), Arctic Iceberg Dimension Project, prepared for Petro-Canada Ltd. by ICE Engineering Ltd. 57 pp.

IIP, 1950, International ice observations and ice patrol services in the North Atlantic Ocean - Season of 1949. U.S. Coast Guard Bull, No. 36.

IIP, 1963, Report of the International Ice Patrol Service. U.S. Coast Guard Bull, No. 49.

IIP (1964), Report of the International Ice Patrol Service in the North Atlantic Ocean, pp.

IPP (1967), Report of the International Ice Patrol Service in the North Atlantic Ocean, pp.

IIP (1967), Report of the International Ice Patrol Service in the North Atlantic Ocean, pp.

IIP, 1970, Report of the International Ice Patrol Service. U.S. Coast Guard Bull, No. 56.

IIP, 1971, Report of the International Ice Patrol Service in the North Atlantic Ocean. U.S. Coast Guard Bull, No. 57.

IIP, 1977, "International Ice Patrol". Published by the U.S. Coast Guard, 19 pp.

Ito, H. and F. Muller (1975), Horizontal Movement of Fast Ice in North Water.

Jacobs, J.D., R.G. Barry and R.L. Weaver (1975), Fast Ice Characteristics with Special Reference to the Eastern Canadian Arctic, Polar Record, pp. 521-536.

Jacobs, J.D. and J.R. Newell (1979), Recent Year-to-Year Variations in Seasonal Temperatures and Sea Ice Conditions in the Eastern Canadian Arctic, Arctic 32, pp. 345-354.

Kolchak, A.V. (1928), The Arctic Pack and the Polynya, Problems of Polar Research, The American Geographical Society Special Publication No. 7, New York, pp. 125-141.

Kovacs, A. and M. Mellor, 1974, Sea ice morphology and ice as a geologic agent in the Southern Beaufort Sea, In: Proc. of the Symp. on Beaufort Sea Coastal and Shelf Research, Arctic Institute of North America, pp. 113-161.

Krummel, O. (1907), Handbuch der Ozeanographic, Vol. I, Leipzig, 526 pp.

Kukla, G.J. (1978), Recent changes in snow and ice climatic change, J. Gribbin, Ed., Cambridge Univ. Press, pp. 114-129.

Lake, R.A. and E.L. Lewis (1970), Salt Rejection by Sea Ice During Growth, J. Geophys, Res. 75, pp. 583-597.

Lake, R.A. and E.L. Lewis (1972), The Microclimate Beneath Growing Sea Ice, in Sea Ice, an international conference Reykjavik, Iceland, pp. 241-245.

Lewis, E.L. and E.R. Walker (1970), The Water Structure Under a Growing Sea Ice Sheet, J. Geophys. Res. 75, pp. 6836-6845.

Lindsay, D.J. (1976), Sea Ice Atlas of Arctic Canada, 1961-1968, Energy, Mines and Resources, Canada, Ottawa, 213 pp.

Lindsay, D.J. (1977), Sea Ice Atlas of Arctic Canada, 1969-1974, Energy, Mines and Resources, Canada, 219 pp.

Løken, O.H., C.S.L. Ommanney and G. Holdsworth (1972), Iceberg Studies in the Glaciology Division, Environment Canada, in Sea Ice, an international conference, Reykjavik, Iceland, pp. 146-151.

MacNeill, M.R., B.R. de Lange Boom and D. Ramsden, 1978. Radar tracking of ioce in the Griffith Island area of barrow Strait, NWT. Contractor Report Series, Institute of Ocean Sciences, Patricia Bay, Sidney, B.C.

Malmgren, F. 1927, The properties of sea ice. The scientific results of the "Maud" expedition, 1918-1925.

Markham, W.E., 1975, Ice climatology in the Beaufort Sea. Beaufort Sea Project Technical Report No. 26.

Markham, W.E., unpublished, Ice climatology of Lancaster Sound, Manuscript.

Marko, J.R., 1975, Satellite observations of the Beaufort Sea ice cover. Beaufort Sea Project Technical Report No. 34, BSP, DOE.

Marko, J.R., 1977, A satellite-based study of sea ice dynamics in the central Canadian Arctic Archipelago. Contractor Report Series 77-4, Institute of Ocean Sciences, Patricia Bay, Sidney, B.C. 106 pp.

Marko, J.R. 1978, A satellite imagery study of Eastern Parry Channel. Contractor Report Series 78-5, Institute of Ocean Sciences, Patricia Bay, Sidney, B.C.

Marko, J.R. and M.A. Wilson (1980), Ice Velocities in Lancaster Sound-Northwest Baffin Bay as Determined from Landsat and NOAA Satellite Imagery, prepared for Petro-Canada Ltd. by Arctic Sciences Ltd., 67 pp.

Marko, J.R., J.R. Birch and M.A. Wilson, 1981. A study of long-term satellite-tracked iceberg drifts in Baffin Bay and Davis Strait. To be published.

Maykut, G.A. and N. Untersteines (1971), Some Results from a Time-Dependent Thermodynamic Model of Sea Ice, 76, pp. 1550-1575.

Mecking, L.(1907), Die Treibesier sheinungen bei Neufundland in inhrer Abhanyigkeit von W. Herunggsverhultnissen Annalen d'Hydrographic und Maritimem Meteorologic, 35 pp. 348-355 and pp. 296-409.

Melling, H., to be published. Ice drift and deformation in the Southeastern Beaufort Sea.

Milne, A.R. (1963), Acoustics under Arctic Sea Ice, McClure Strait, August-September, 1961, Canada Pacific Naval Laboratory Report 63-1.

Milne, A.R., 1970, Transition from moving to fast ice in Western Viscount Melville Sound. Arctic, 23: 45-46.

Milne, A.R. and B.D. Smiley (1978), Offshore Drilling in Lancaster Sound: Possible Environmental Hazards, Institute of Ocean Sciences, Patricia Bay, a5 pp.

Miller, J. (1980), Unpublished memorandum.

Mowat, F. (1960), Ordeal by Ice, McClelland and Stewart Ltd., Toronto, 422 pp.

Muller, F., H. Blatter, R. Braithwaite, H. Ito, G. Kappenberger, A. Uhmura, K. Schroff and A. Zust (1975), Glaciological and Climatological Investigation of the North Water Polynyd in Northern Baffin Bay, A Progress Report on North Water Activities, internal report. 149 pp.

Nielsen, J.W. (1909a), Forelobig Meddelelse om Undersogelser over Vestgronlands Hydrografi, Foretagne under "Tjalfe" - Expedition 1908 Beretn. og Kundgorelser vedrorende kilcnierne: Gronl. pp. 24-27.

Nielsen, J.W. (1909b), Forelobig Meddelelseom de fra Briggen "Tjalfe" foretagne hydrografishe Undersogelseunne i Sommerem. Beretn. og Kundgorelser vedrorende kiloniere i Gronl., (5) pp. 106-110.

Nielsen, J.W. (1928), Waters round Greenland. Greenland 1, pp. 185-230, C.A. Reitzel, Copenhagen.

NORCOR (1978), A Study of Ice Conditions Along Marine Shipping Routes in the Arctic Archipelago, prepared for Ministry of Transport by NORCOR Ltd., 50 pp.

NORCOR (1979), Aerial Iceberg Surveys Baffin Bay 1978, prepared for Petro-Canada Ltd. by NORCOR Ltd., 60 pp. plus appendices

NORCOR (1980), Aerial Iceberg Surveys Baffin Bay 1979, prepared for Petro-Canada Ltd. by NORCOR Ltd., 79 pp. plus appendices

NORDCO (1979), A Study of Ice Drift in Lancaster Sound, July-October, 1978 prepared for Petro-Canada Ltd. by NORDCO Ltd., 92 pp. plus appendices

PETTERSON, O. (1883), On the properties of water and ice. Vega Expeditionens vetenskapliga iakttagelser, II pp. 247-323, Stockholm, F. and G. Beijers Forlag

PRITCHARD, R.S. R. Reimer and M.D. Coon (1979), Ice Flow through Straits, Proceedings of an international conference on Port and Ocean Engineering under Arctic Conditions, Aug. 13-18, 1979 pp. 61-74.

Rodman, H. (1890), Reports on Ice and Ice Movements in the North Atlantic Ocean, U.S. Navy Hydrographic Office, No. 93, 26 pp.

Seifert, W.J. (unpublished) Sea Ice Maps of the Queen Elizabeth Island Region, Polar Continental Shelf Project, DEMR, Ottawa.

Smith, E.H. (1928), The Marion Expedition to Davis Strait and Baffin Bay, Scientific Results, Part 3, U.S. Treasury Department, Coast Guard Bulletin No. 19, 221 pp.

Sodhi, D.S. (1977), Ice Arching and the Drift of Pack Ice through Restricted Channels. Cold Regions Research and Engineering Laboratory Report 77-18, 11 pp.

Steenstrup, K.J.V. (1893), Bidgragtil Kjendskab til Braeerne ug Brae Isen i Nord Gronland, meddelelseom Gronland, Vol. 4, pp. 71-112.

Sverdrup, H.U. (1928), The Wind-Drift of the Ice on the North Siberian Shelf. The Norwegian North Polar Expedition with the Mad. 1918-1925. Scientific Results. Vol. IV. No. 1. pp. 1-46. Bergen.

Sverdrup, H.U. (1929), The Waters on the North Siberian Shelf. Ibid. Vol. IV, No. 2, pp. 1-75. Bergen.

Swithinbank, C. (1960), Ice Atlas of Arctic Canada, Defence Research Board, Ottawa.

U.S. Naval Hydrographic Office (1956, 1958, 1960-64) Report of the Ice Observing and Forecast Program, Special Publications, Washington, D.C.

Verral, R.I., J.H. Granton, and A.R. Milne (1974), An Ice Drift Measurement in Western Parry Channel, Arctic, 27, pp. 47-52.

Vowinckel, E. and S. Orvig (1966), Energy Balance of the Arctic, 5, The Head Budget of the Arctic Ocean, Arch. Meteorol. Geophys. Bioklimatol., A, 14 pp. 303-325.

Walker, E.R. (1975), Oil Ice and Climate in the Beaufort Sea, Beaufort Sea Project Technical Report No. 35, Dept. of Fisheries and Environment, Institute of Ocean Sciences, Sidney, B.C.

Walmsley, J.L. (1966), Ice Cover and Surface Heat Fluxes in Baffin Bay, McGill University Marine Sciences Centre Manuscript Rept. No. 2.

Walsh, J.E. and C.M. Johnson (1979), An Analysis of Sea Ice Fluctuations, 1953-77, J. Phys. Oceanog. 9, pp. 580-591.

Wandel, C.F. (1891), On de Hydrogryphisko Forhold Davis-Straedet Medel om Gronl., 7, 57-1B.

Welsh, J.P., Dr. and S.M. Phillips (1973),Iceberg Drift from Surface Currents, U.S. Coast Guard Bulletin No. 59, Appendix B, 5 pp.

Weyprecht, K. (1897), Metamorphosen des Polareises. Verag von Moritz Perles, Vienna. pp. 1-284.

Wittman, W.I., 1972, Comment on the paper of Lø, Ommanney and Holdsworth (1972), In: Sea Ice, an international conference, Reykjavik, Iceland, pp. 151.

APPENDIX 1A

Ice concentration maps derived from AES digitized ice parameter data. Results are given for semi-monthly intervals over the May to October period, based upon 20 percentile values of the ice concentrations.

Legend

$\frac{10}{10}$ concentration

$\frac{7}{10}$ - $\frac{9}{10}$ concentration

$\frac{4}{10}$ - $\frac{6}{10}$ concentration

$\frac{1}{10}$ - $\frac{3}{10}$ concentration

less than $\frac{1}{10}$ concentration

"NI" means the area was not included in the study.

APPENDIX IA

May 21 (20)

Ice concentration maps derived from AES digitised ice parameter data. Results are given for semi-monthly intervals over the May to October period, based upon 20 percentile values of the ice concentrations.

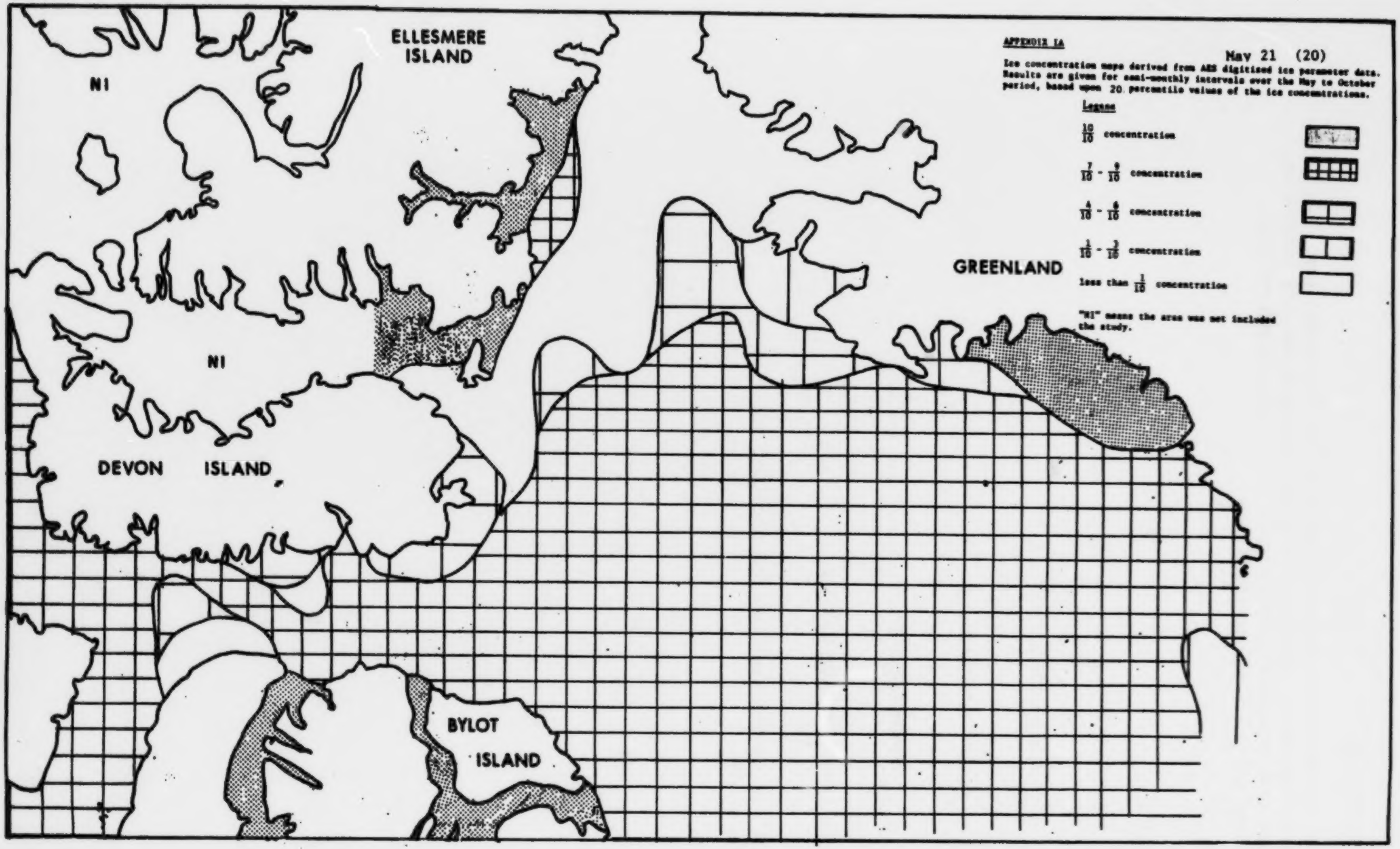

ELLESMERE ISLAND
NI
NI
DEVON ISLAND
GREENLAND
BYLOT ISLAND

Legend

$\frac{10}{10}$ concentration ▩

$\frac{7}{10}$ - $\frac{9}{10}$ concentration ▦

$\frac{4}{10}$ - $\frac{6}{10}$ concentration ⊞

$\frac{1}{10}$ - $\frac{3}{10}$ concentration ◫

less than $\frac{1}{10}$ concentration ☐

"NI" means the area was not included the study.

APPENDIX IA

June 4 (20)

Ice concentration maps derived from AES digitized ice parameter data. Results are given for semi-monthly intervals over the May to October period, based upon 20 percentile values of the ice concentrations.

Legend

$\frac{10}{10}$ concentration ▩

$\frac{7}{10}$ - $\frac{9}{10}$ concentration ▦

$\frac{4}{10}$ - $\frac{6}{10}$ concentration ⊞

$\frac{1}{10}$ - $\frac{3}{10}$ concentration ◫

less than $\frac{1}{10}$ concentration ▭

"NI" means the area was not included the study.

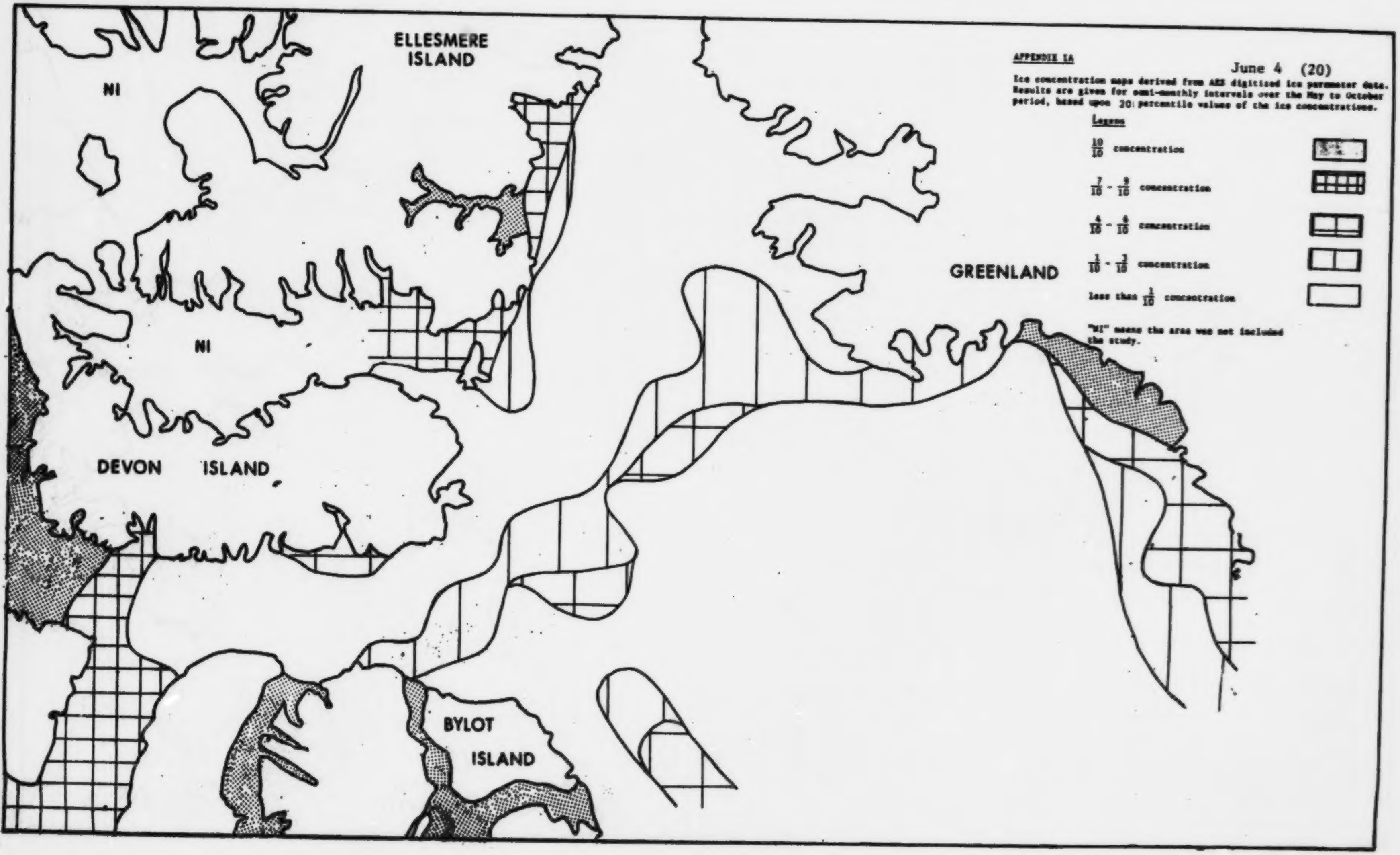
ELLESMERE ISLAND
NI
NI
DEVON ISLAND
GREENLAND
BYLOT ISLAND

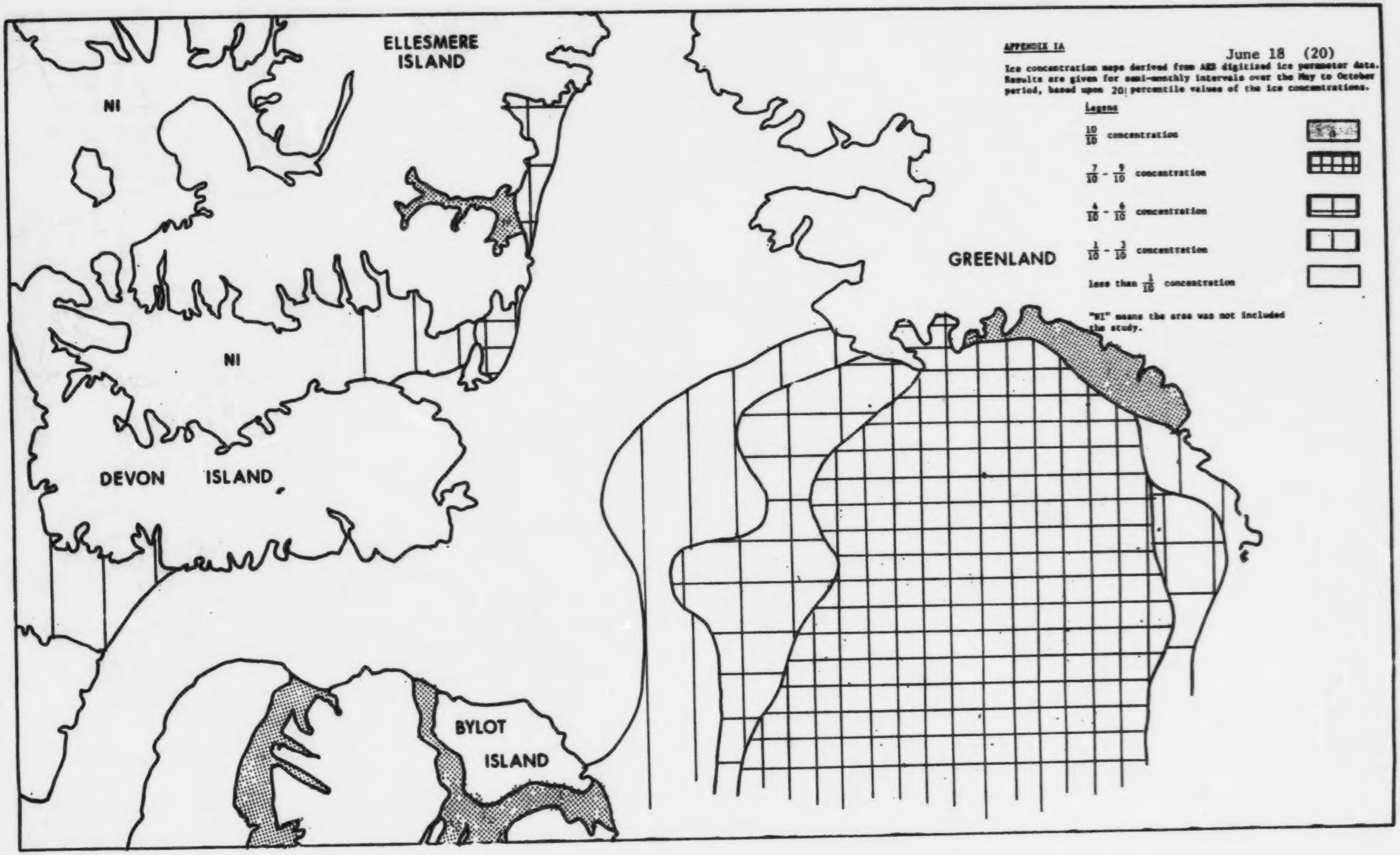

APPENDIX IA

June 18 (20)

Ice concentration maps derived from AES digitized ice perimeter data. Results are given for semi-monthly intervals over the May to October period, based upon 20 percentile values of the ice concentrations.

Legend

$\frac{10}{10}$ concentration	▩
$\frac{7}{10} - \frac{9}{10}$ concentration	▦
$\frac{4}{10} - \frac{6}{10}$ concentration	⊞
$\frac{1}{10} - \frac{3}{10}$ concentration	◫
less than $\frac{1}{10}$ concentration	☐

"NI" means the area was not included the study.

ELLESMERE ISLAND
NI
NI
DEVON ISLAND
GREENLAND
BYLOT ISLAND

APPENDIX 1A

July 2 (20)

Ice concentration maps derived from AES digitized ice parameter data. Results are given for semi-monthly intervals over the May to October period, based upon 20 percentile values of the ice concentrations.

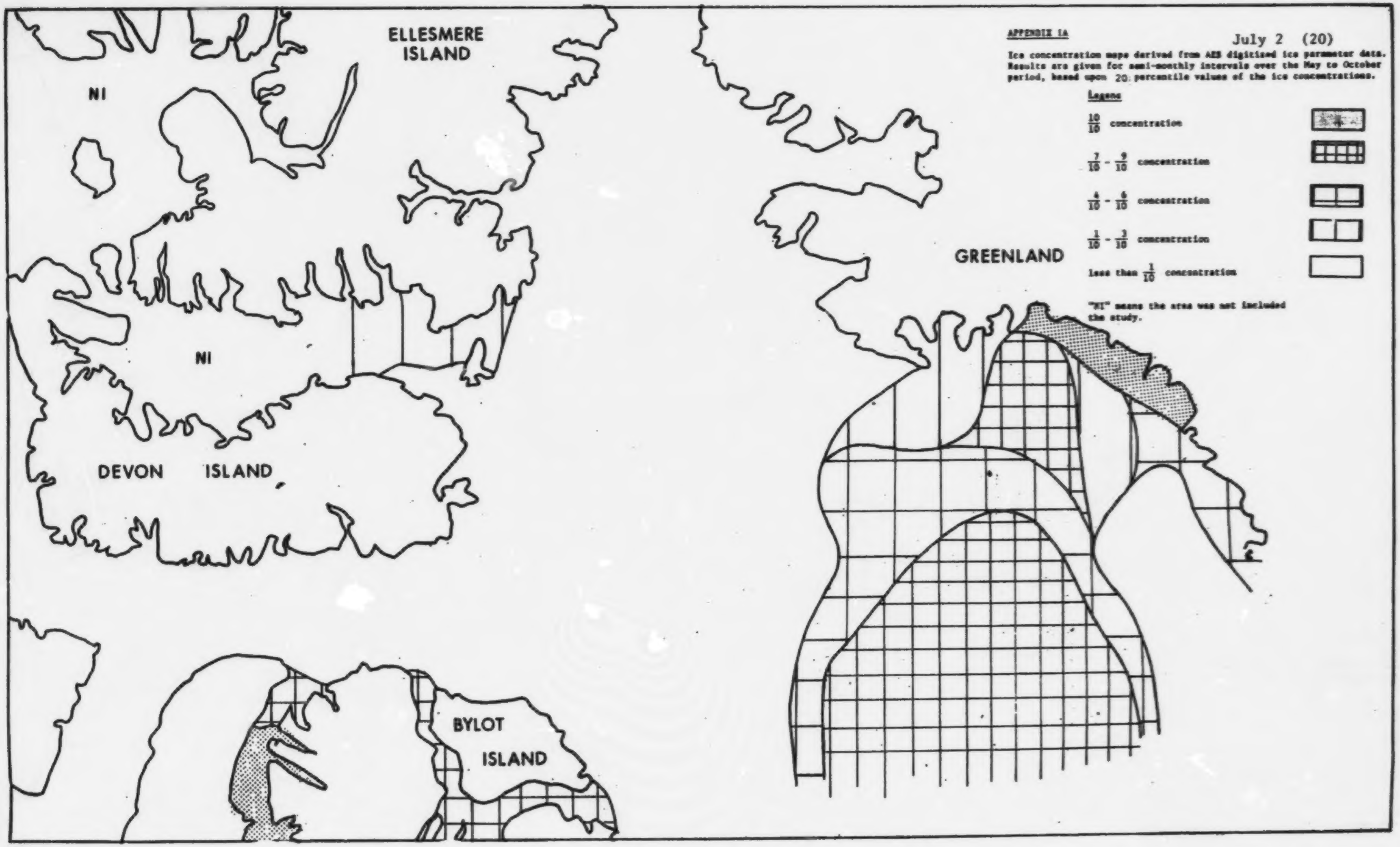
ELLESMERE ISLAND
NI
NI
DEVON ISLAND
GREENLAND
BYLOT ISLAND

Legend

$\frac{10}{10}$ concentration ▨

$\frac{7}{10}$ - $\frac{9}{10}$ concentration ▦

$\frac{4}{10}$ - $\frac{6}{10}$ concentration ⊞

$\frac{1}{10}$ - $\frac{3}{10}$ concentration ◫

less than $\frac{1}{10}$ concentration ▭

"NI" means the area was not included the study.

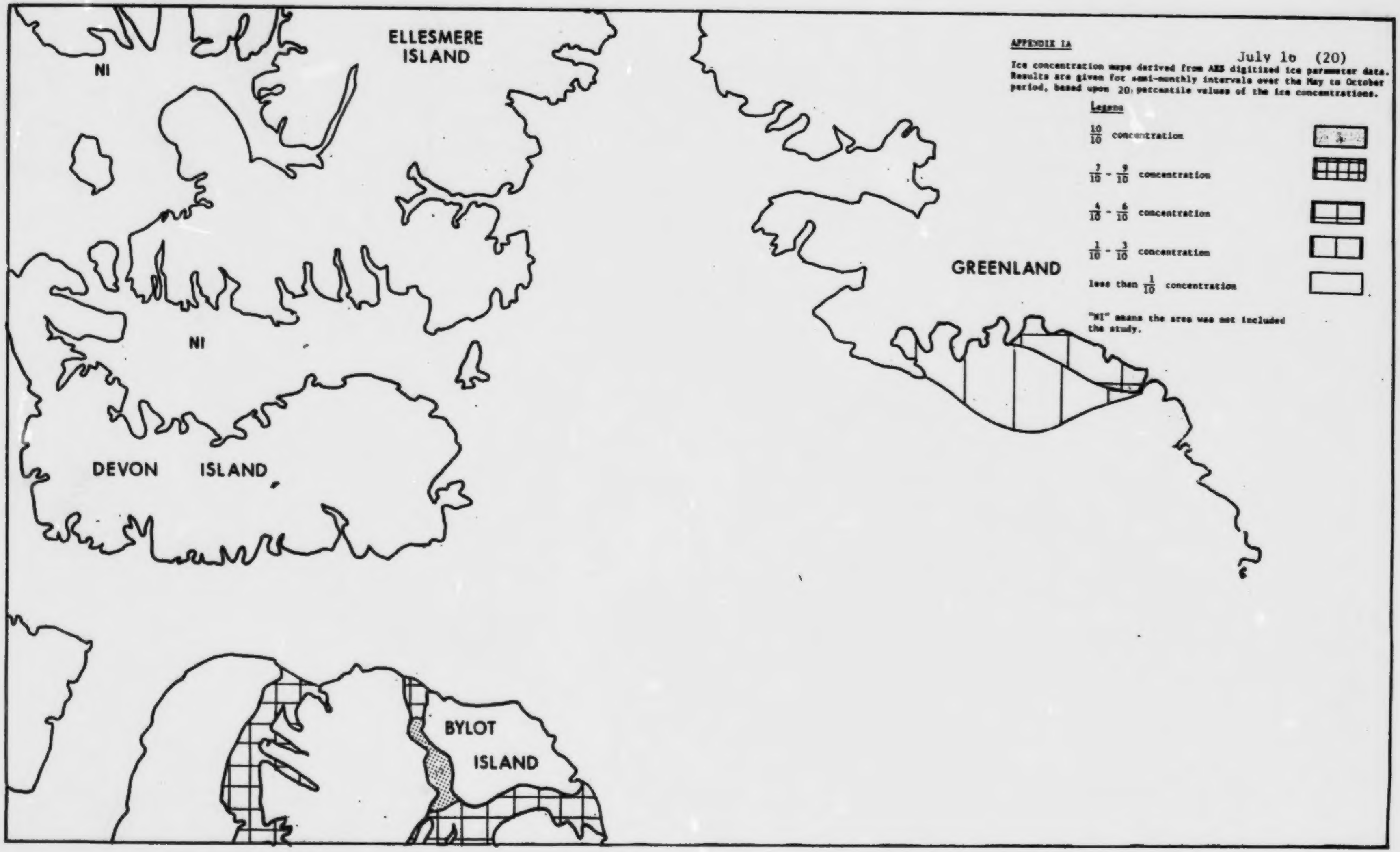
ELLESMERE ISLAND
NI
NI
DEVON ISLAND
GREENLAND
BYLOT ISLAND

APPENDIX IA

July 16 (20)

Ice concentration maps derived from AES digitized ice parameter data. Results are given for semi-monthly intervals over the May to October period, based upon 20 percentile values of the ice concentrations.

Legend

$\frac{10}{10}$ concentration ▩

$\frac{7}{10}$ - $\frac{9}{10}$ concentration ▦

$\frac{4}{10}$ - $\frac{6}{10}$ concentration ⊞

$\frac{1}{10}$ - $\frac{3}{10}$ concentration ◫

less than $\frac{1}{10}$ concentration ▭

"NI" means the area was not included the study.

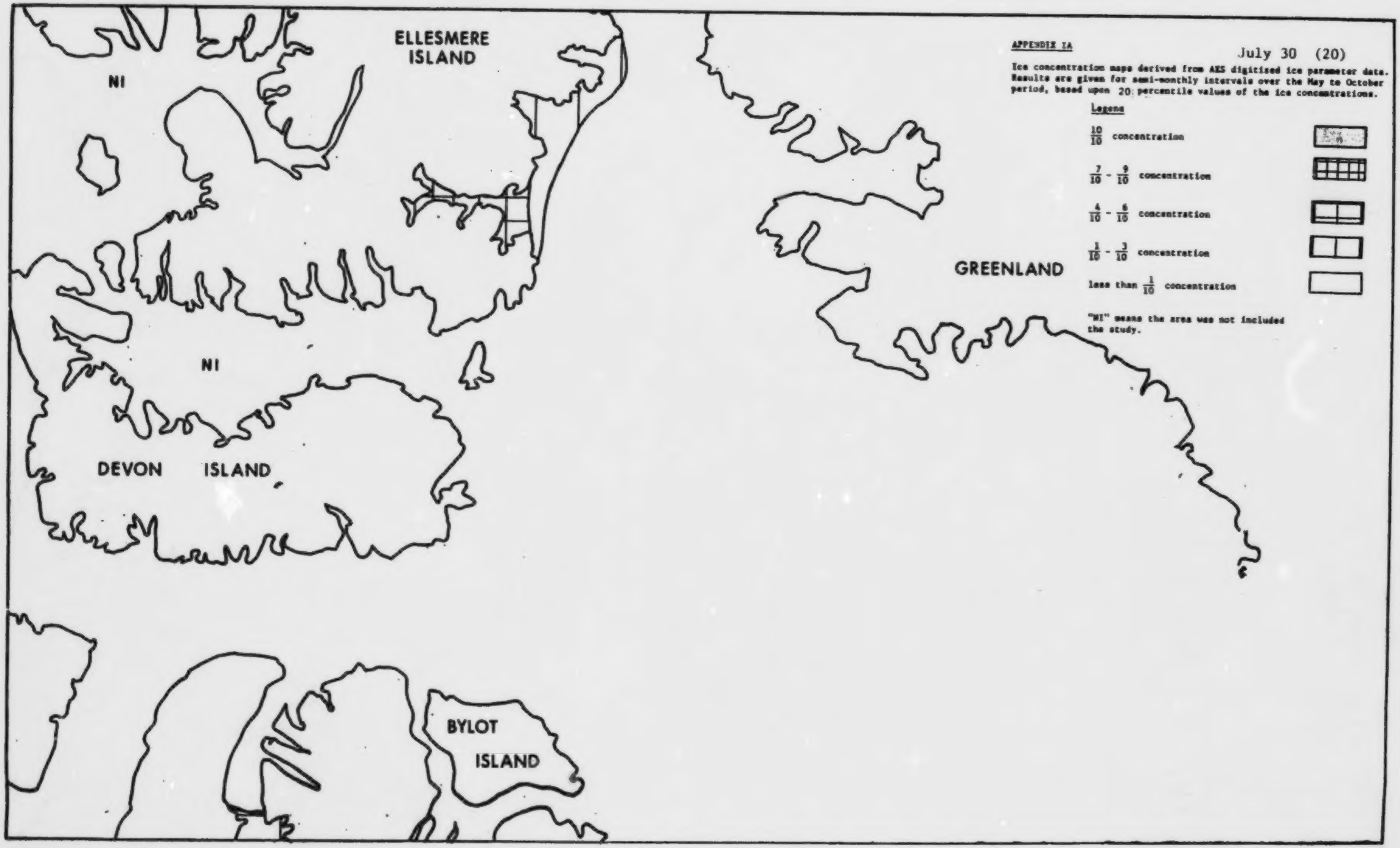
ELLESMERE
ISLAND
NI
NI
DEVON ISLAND
GREENLAND
BYLOT
ISLAND

APPENDIX IA

July 30 (20)

Ice concentration maps derived from AES digitised ice parameter data. Results are given for semi-monthly intervals over the May to October period, based upon 20 percentile values of the ice concentrations.

Legend

$\frac{10}{10}$ concentration	▨
$\frac{7}{10}$ - $\frac{9}{10}$ concentration	▦
$\frac{4}{10}$ - $\frac{6}{10}$ concentration	⊞
$\frac{1}{10}$ - $\frac{3}{10}$ concentration	◫
less than $\frac{1}{10}$ concentration	▭

"NI" means the area was not included the study.

ELLESMERE ISLAND
NI
NI
DEVON ISLAND
BYLOT ISLAND
GREENLAND

APPENDIX IA

August 13 (20)

Ice concentration maps derived from AES digitized ice parameter data. Results are given for semi-monthly intervals over the May to October period, based upon 20 percentile values of the ice concentrations.

Legend

$\frac{10}{10}$ concentration ▓

$\frac{7}{10}$ - $\frac{9}{10}$ concentration ▦

$\frac{4}{10}$ - $\frac{6}{10}$ concentration ⊞

$\frac{1}{10}$ - $\frac{3}{10}$ concentration ◫

less than $\frac{1}{10}$ concentration ▭

"NI" means the area was not included the study.

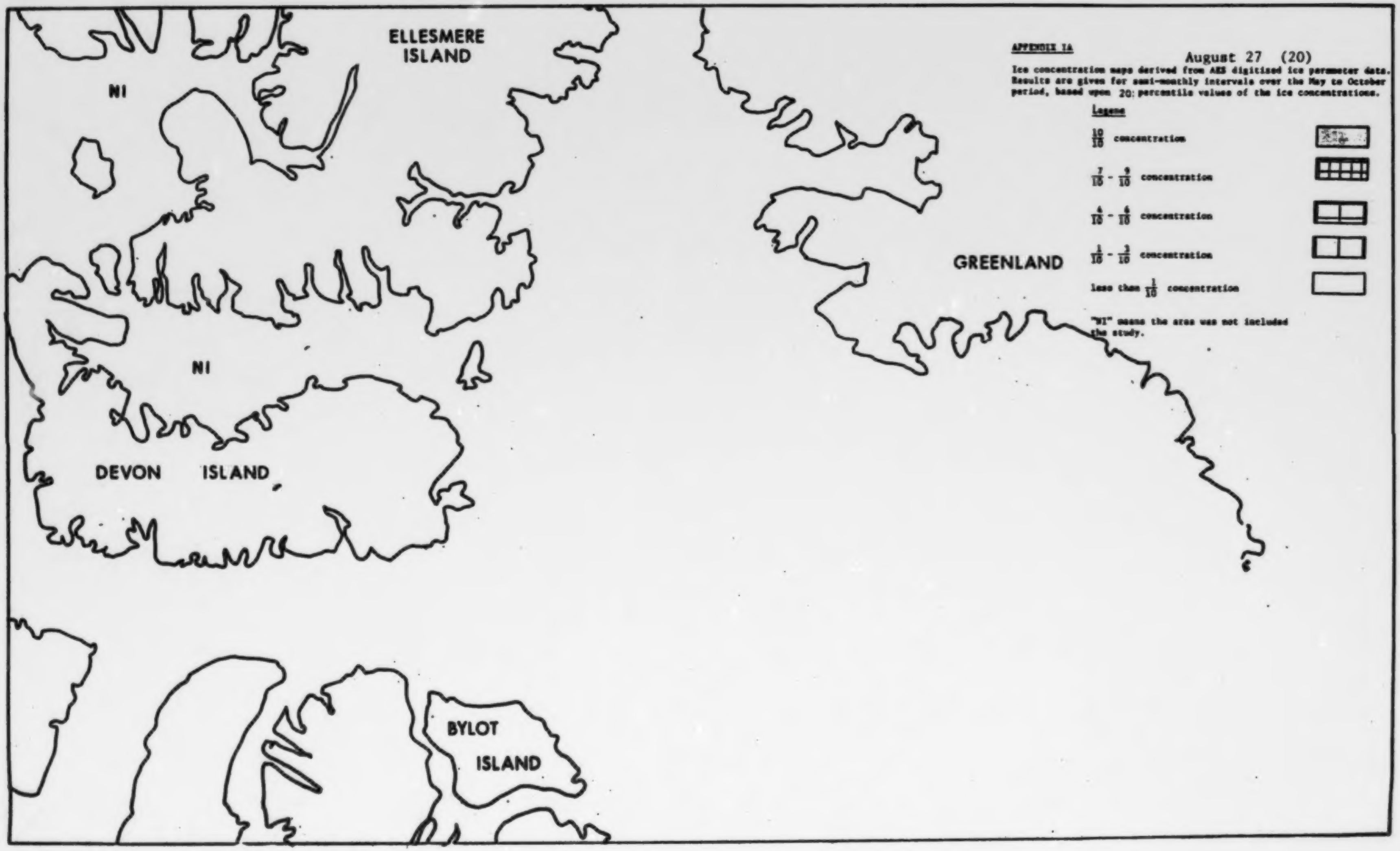
ELLESMERE ISLAND
NI
NI
DEVON ISLAND
GREENLAND
BYLOT ISLAND

APPENDIX 1A

August 27 (20)

Ice concentration maps derived from AES digitised ice parameter data. Results are given for semi-monthly intervals over the May to October period, based upon 20: percentile values of the ice concentrations.

Legend

$\frac{10}{10}$ concentration	▨
$\frac{7}{10}$ - $\frac{9}{10}$ concentration	▦
$\frac{4}{10}$ - $\frac{6}{10}$ concentration	⊞
$\frac{1}{10}$ - $\frac{3}{10}$ concentration	◫
less than $\frac{1}{10}$ concentration	▭

"NI" means the area was not included the study.

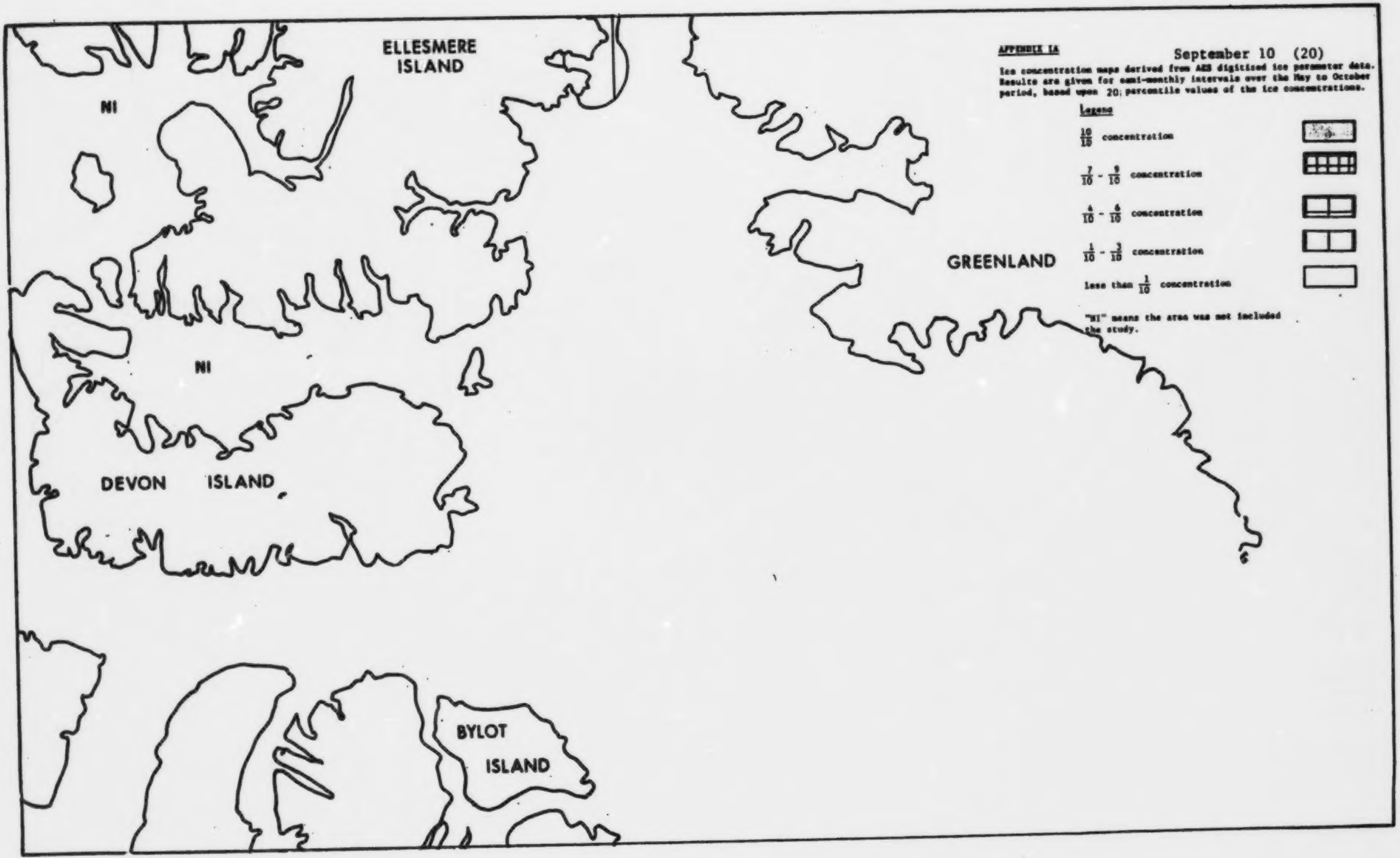
ELLESMERE ISLAND
NI
NI
DEVON ISLAND
GREENLAND
BYLOT ISLAND

APPENDIX IA

September 10 (20)

Ice concentration maps derived from AES digitised ice parameter data. Results are given for semi-monthly intervals over the May to October period, based upon 20 percentile values of the ice concentrations.

Legend

$\frac{10}{10}$ concentration ▩

$\frac{7}{10}$ - $\frac{9}{10}$ concentration ▦

$\frac{4}{10}$ - $\frac{6}{10}$ concentration ⊟

$\frac{1}{10}$ - $\frac{3}{10}$ concentration ◫

less than $\frac{1}{10}$ concentration ▭

"NI" means the area was not included the study.

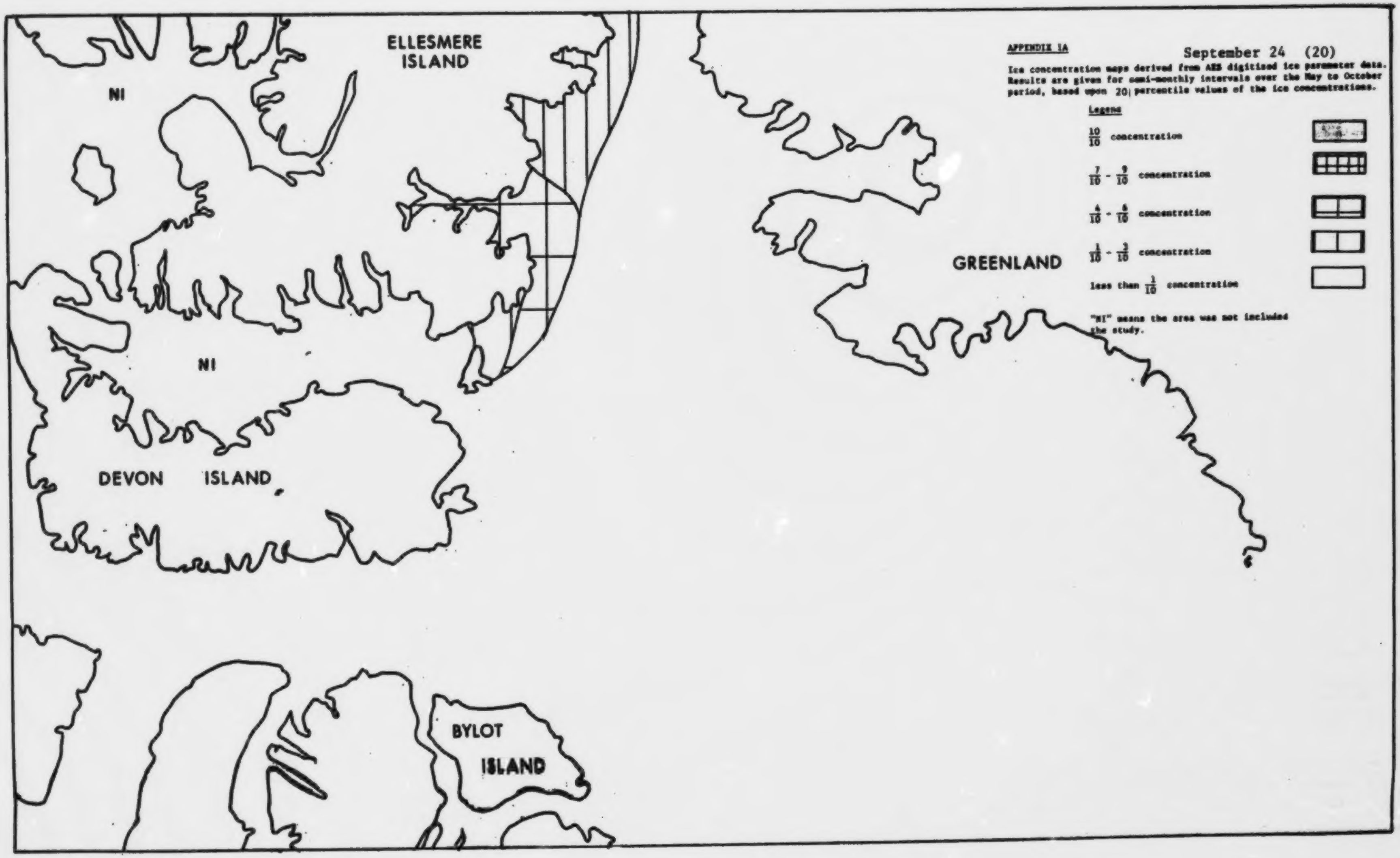

ELLESMERE ISLAND
NI
NI
DEVON ISLAND
GREENLAND
BYLOT ISLAND

APPENDIX 1A

September 24 (20)

Ice concentration maps derived from AES digitized ice parameter data. Results are given for semi-monthly intervals over the May to October period, based upon 20 percentile values of the ice concentrations.

Legend
$\frac{10}{10}$ concentration
$\frac{7}{10}$ - $\frac{9}{10}$ concentration
$\frac{4}{10}$ - $\frac{6}{10}$ concentration
$\frac{1}{10}$ - $\frac{3}{10}$ concentration
less than $\frac{1}{10}$ concentration

"NI" means the area was not included the study.

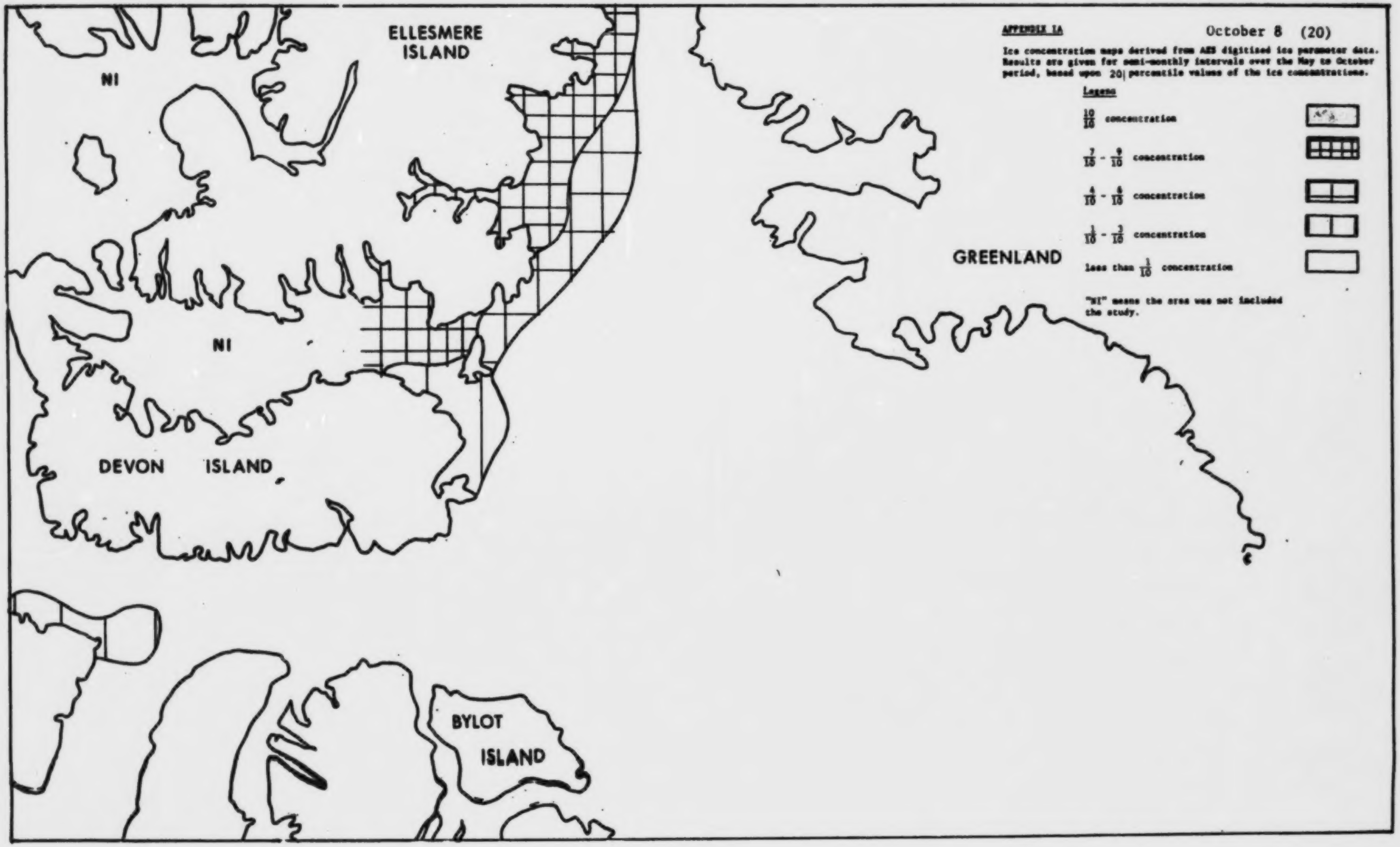

APPENDIX IA

October 8 (20)

Ice concentration maps derived from AES digitized ice parameter data. Results are given for semi-monthly intervals over the May to October period, based upon 20 percentile values of the ice concentrations.

Legend
$\frac{10}{10}$ concentration
$\frac{7}{10}$ - $\frac{9}{10}$ concentration
$\frac{4}{10}$ - $\frac{6}{10}$ concentration
$\frac{1}{10}$ - $\frac{3}{10}$ concentration
less than $\frac{1}{10}$ concentration
"NI" means the area was not included the study.
ELLESMERE ISLAND
NI
NI
DEVON ISLAND
GREENLAND
BYLOT ISLAND

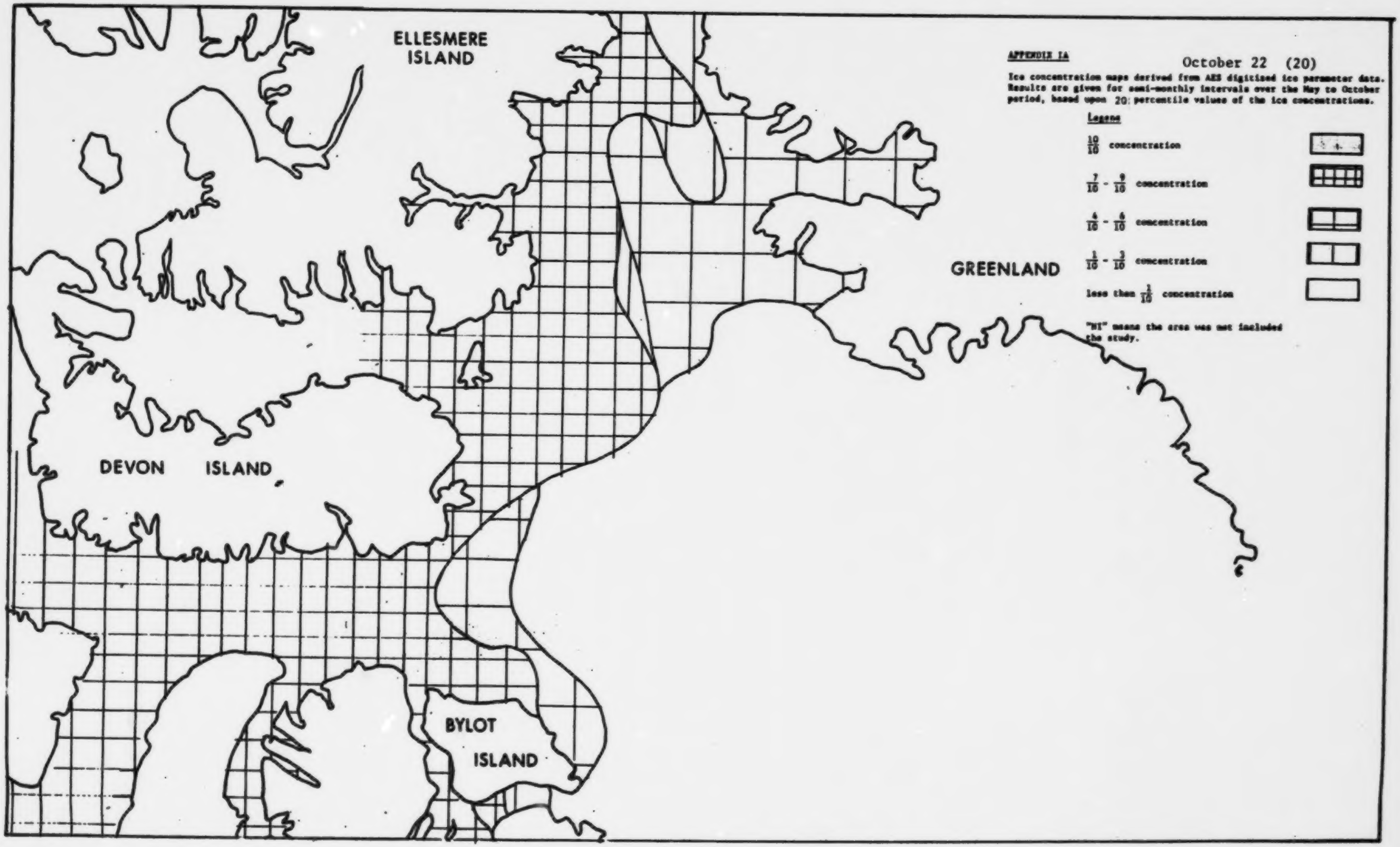

APPENDIX IA

October 22 (20)

Ice concentration maps derived from AES digitized ice parameter data. Results are given for semi-monthly intervals over the May to October period, based upon 20 percentile values of the ice concentrations.

Legend
$\frac{10}{10}$ concentration
$\frac{7}{10}$ - $\frac{9}{10}$ concentration
$\frac{4}{10}$ - $\frac{6}{10}$ concentration
$\frac{1}{10}$ - $\frac{3}{10}$ concentration
less than $\frac{1}{10}$ concentration
"NI" means the area was not included the study.
ELLESMERE ISLAND
GREENLAND
DEVON ISLAND
BYLOT ISLAND

APPENDIX 1B

Ice concentration maps derived from AES digitized ice parameter data. Results are given for semi-monthly intervals over the May to October period, based upon 50 percentile values of the ice concentrations.

Legend

$\frac{10}{10}$ concentration

$\frac{7}{10}$ - $\frac{9}{10}$ concentration

$\frac{4}{10}$ - $\frac{6}{10}$ concentration

$\frac{1}{10}$ - $\frac{3}{10}$ concentration

less than $\frac{1}{10}$ concentration

"NI" means the area was not included in the study.

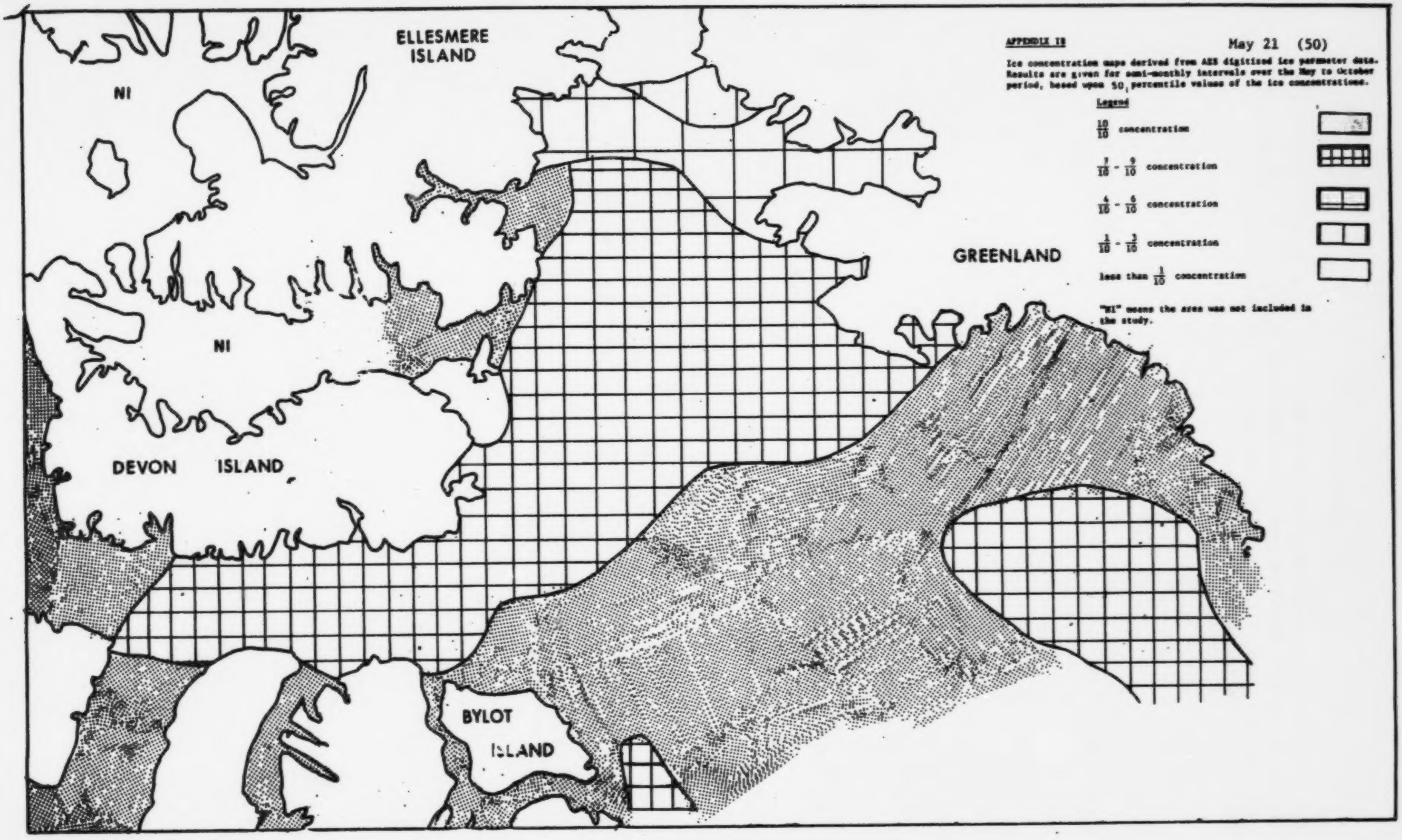

ELLESMERE ISLAND
NI
NI
DEVON ISLAND
GREENLAND
BYLOT ISLAND
Legend
$\frac{10}{10}$ concentration
$\frac{7}{10}$ - $\frac{9}{10}$ concentration
$\frac{4}{10}$ - $\frac{6}{10}$ concentration
$\frac{1}{10}$ - $\frac{3}{10}$ concentration
less than $\frac{1}{10}$ concentration
"NI" means the area was not included in the study.

APPENDIX IB

May 21 (50)

Ice concentration maps derived from AES digitised ice parameter data. Results are given for semi-monthly intervals over the May to October period, based upon 50 percentile values of the ice concentrations.

June 4 (50)

APPENDIX IB

Ice concentration maps derived from AES digitized ice parameter data. Results are given for semi-monthly intervals over the May to October period, based upon 50 percentile values of the ice concentrations.

Legend

$\frac{10}{10}$ concentration ▨

$\frac{7}{10}$ - $\frac{9}{10}$ concentration ▦

$\frac{4}{10}$ - $\frac{6}{10}$ concentration ⊞

$\frac{1}{10}$ - $\frac{3}{10}$ concentration ◫

less than $\frac{1}{10}$ concentration ☐

"NI" means the area was not included in the study.

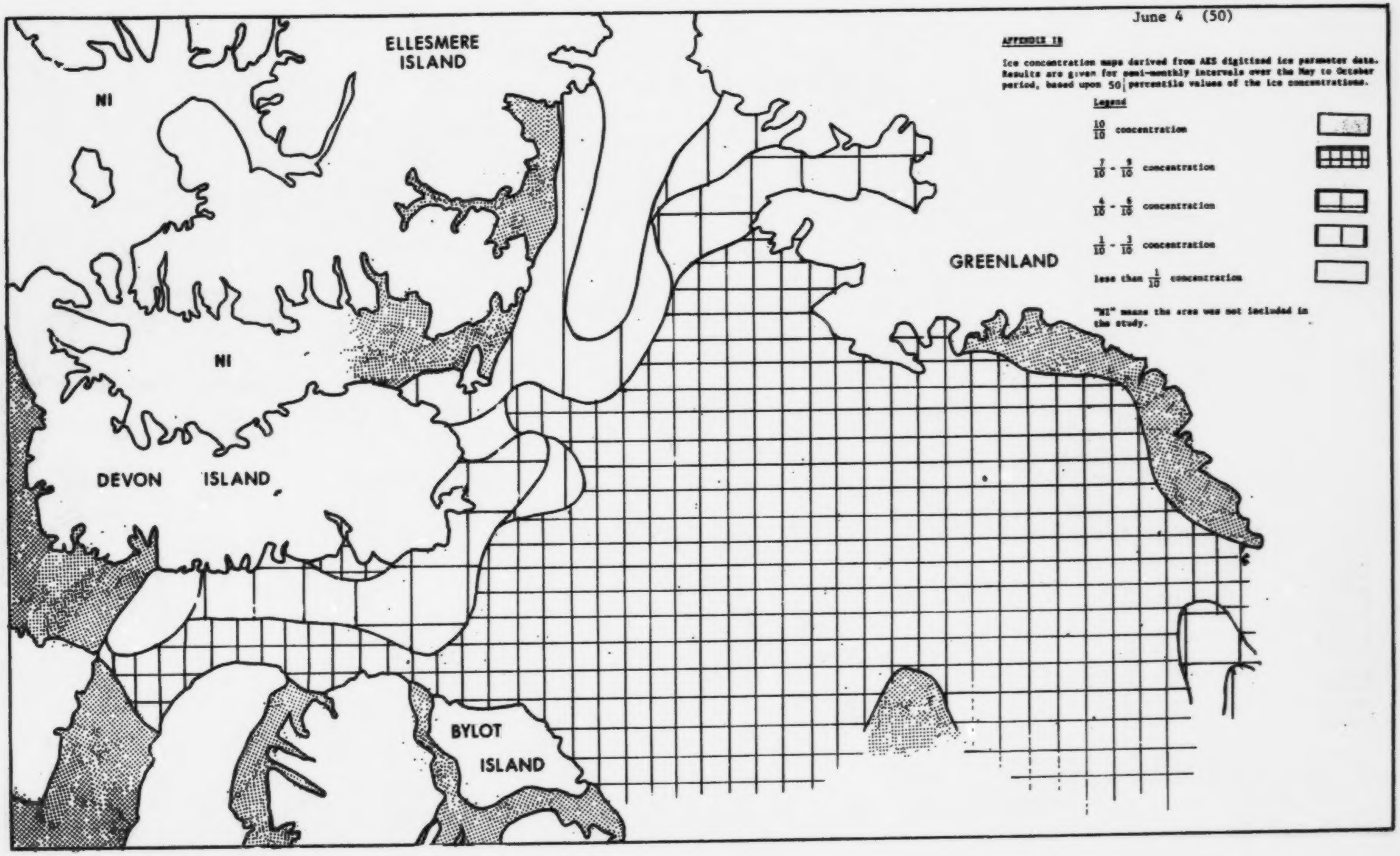
ELLESMERE ISLAND
NI
NI
DEVON ISLAND
GREENLAND
BYLOT ISLAND

APPENDIX IB

June 18 (50)

Ice concentration maps derived from AES digitized ice perimeter data. Results are given for semi-monthly intervals over the May to October period, based upon 50 percentile values of the ice concentrations.

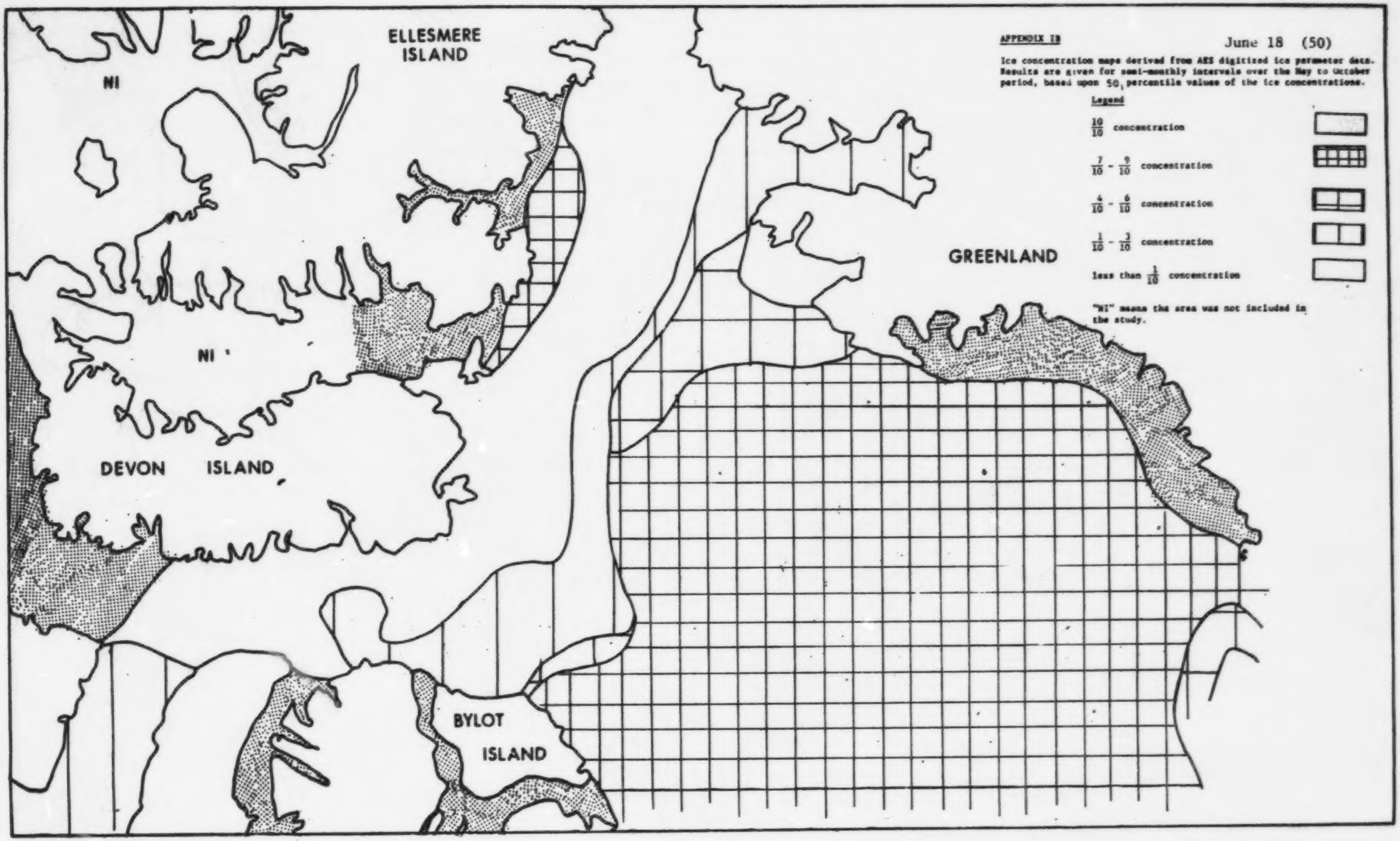
Legend
$\frac{10}{10}$ concentration
$\frac{7}{10}$ - $\frac{9}{10}$ concentration
$\frac{4}{10}$ - $\frac{6}{10}$ concentration
$\frac{1}{10}$ - $\frac{3}{10}$ concentration
less than $\frac{1}{10}$ concentration
"NI" means the area was not included in the study.
ELLESMERE ISLAND
NI
NI
DEVON ISLAND
GREENLAND
BYLOT ISLAND

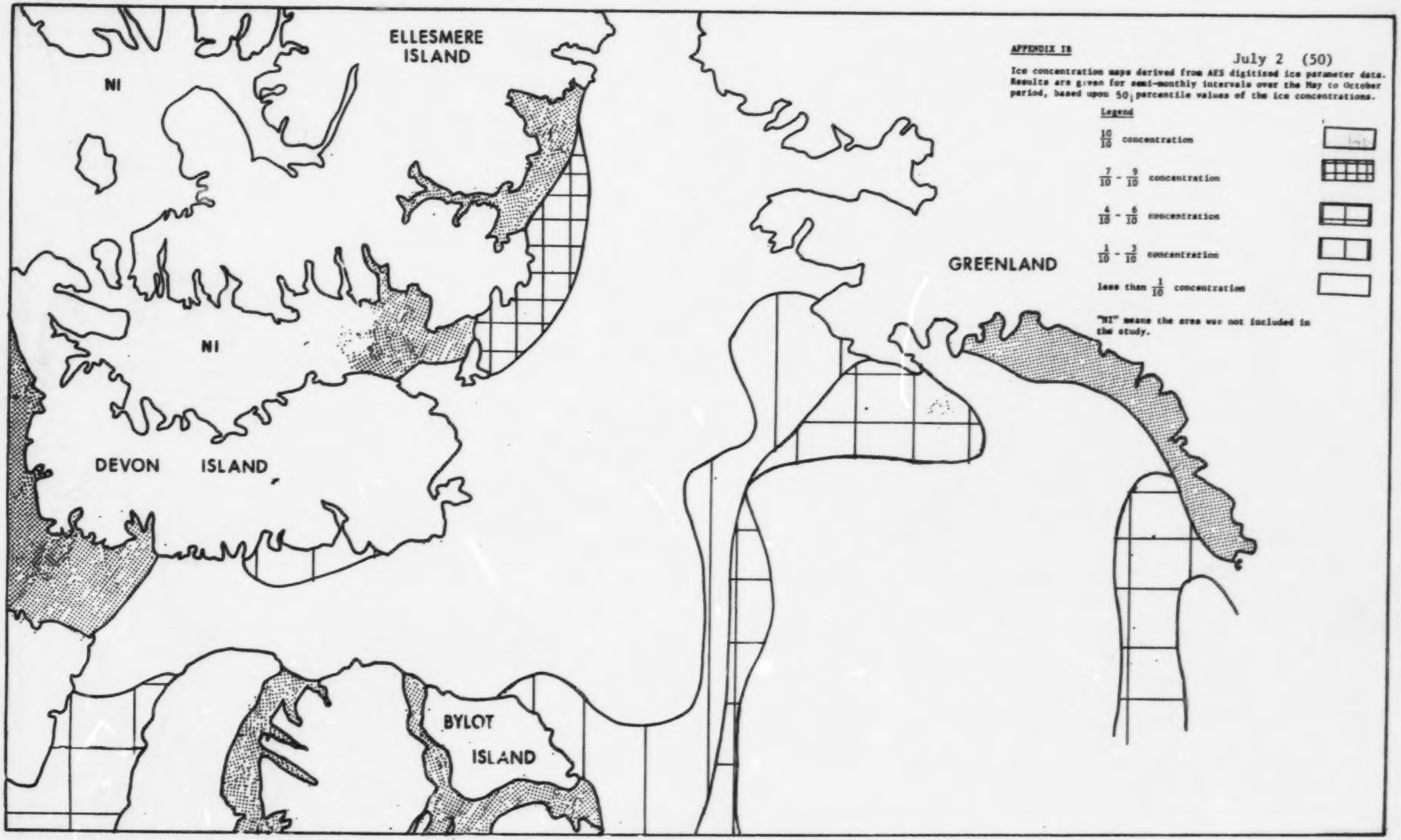

ELLESMERE ISLAND
NI
NI
DEVON ISLAND
GREENLAND
BYLOT ISLAND

APPENDIX IB

July 2 (50)

Ice concentration maps derived from AES digitized ice parameter data. Results are given for semi-monthly intervals over the May to October period, based upon 50 percentile values of the ice concentrations.

Legend

$\frac{10}{10}$ concentration ▨
$\frac{7}{10}$ - $\frac{9}{10}$ concentration ▦
$\frac{4}{10}$ - $\frac{6}{10}$ concentration ⊞
$\frac{1}{10}$ - $\frac{3}{10}$ concentration ◫
less than $\frac{1}{10}$ concentration ▭

"NI" means the area was not included in the study.

APPENDIX 18 July 16 (50)

Ice concentration maps derived from AES digitized ice parameter data. Results are given for semi-monthly intervals over the May to October period, based upon 50 percentile values of the ice concentrations.

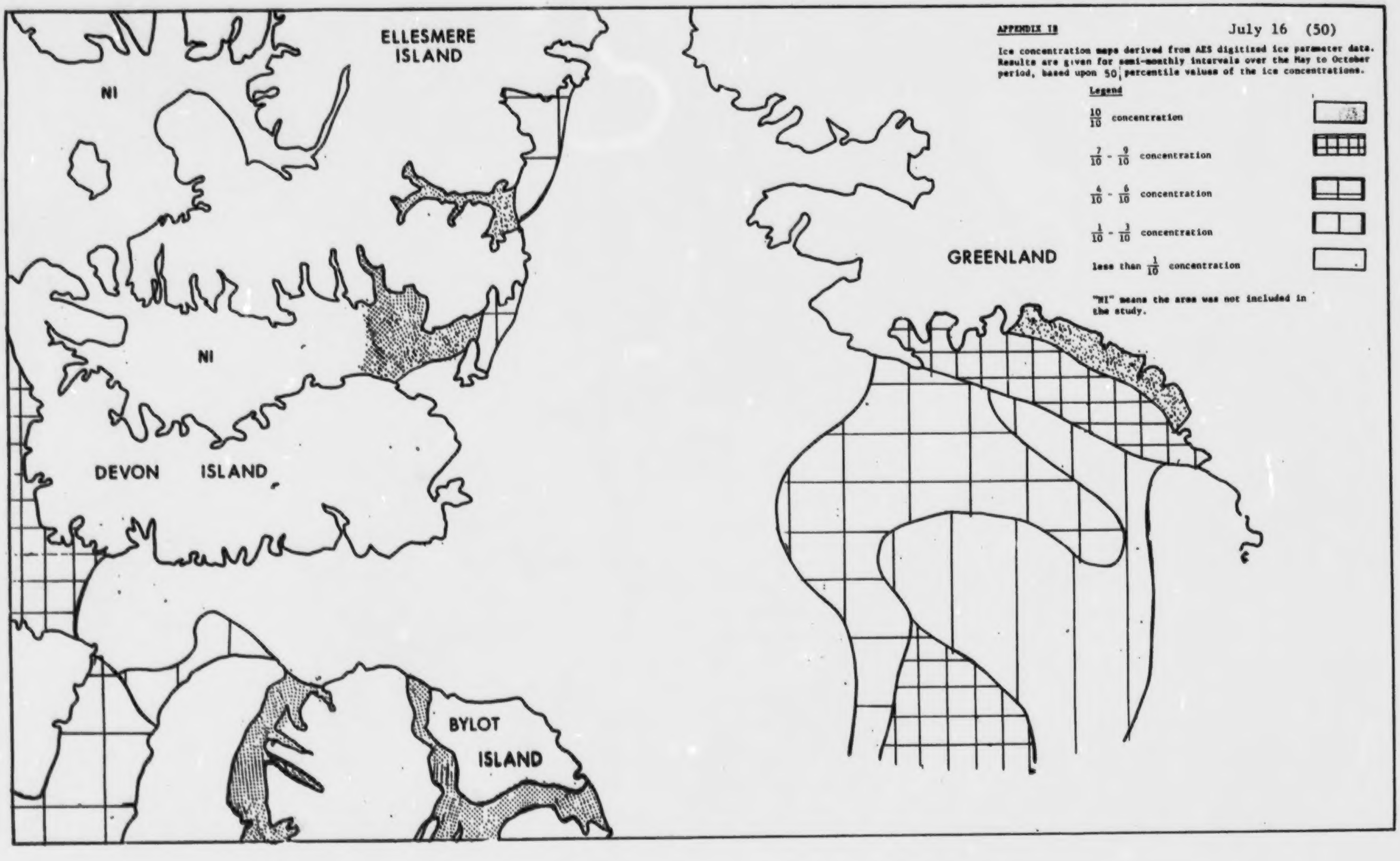

ELLESMERE ISLAND
NI
NI
DEVON ISLAND
BYLOT ISLAND
GREENLAND

Legend

$\frac{10}{10}$ concentration	▒
$\frac{7}{10}$ - $\frac{9}{10}$ concentration	▦
$\frac{4}{10}$ - $\frac{6}{10}$ concentration	⊞
$\frac{1}{10}$ - $\frac{3}{10}$ concentration	◫
less than $\frac{1}{10}$ concentration	☐

"NI" means the area was not included in the study.

APPENDIX IB

July 30 (50)

Ice concentration maps derived from AES digitized ice parameter data. Results are given for semi-monthly intervals over the May to October period, based upon 50 percentile values of the ice concentrations.

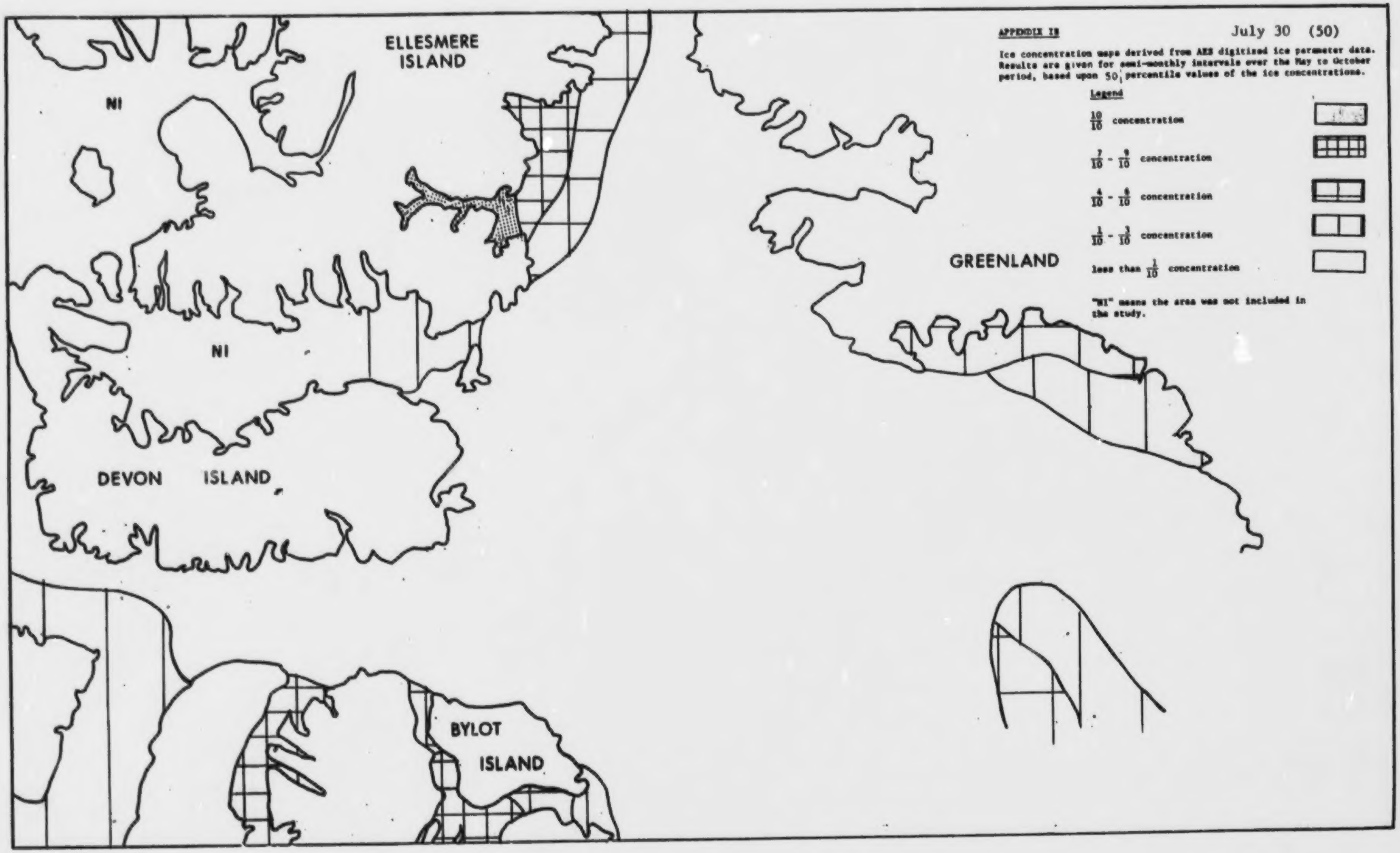
ELLESMERE ISLAND
NI
NI
DEVON ISLAND
GREENLAND
BYLOT ISLAND

Legend

$\frac{10}{10}$ concentration

$\frac{7}{10}$ - $\frac{9}{10}$ concentration

$\frac{4}{10}$ - $\frac{6}{10}$ concentration

$\frac{1}{10}$ - $\frac{3}{10}$ concentration

less than $\frac{1}{10}$ concentration

"NI" means the area was not included in the study.

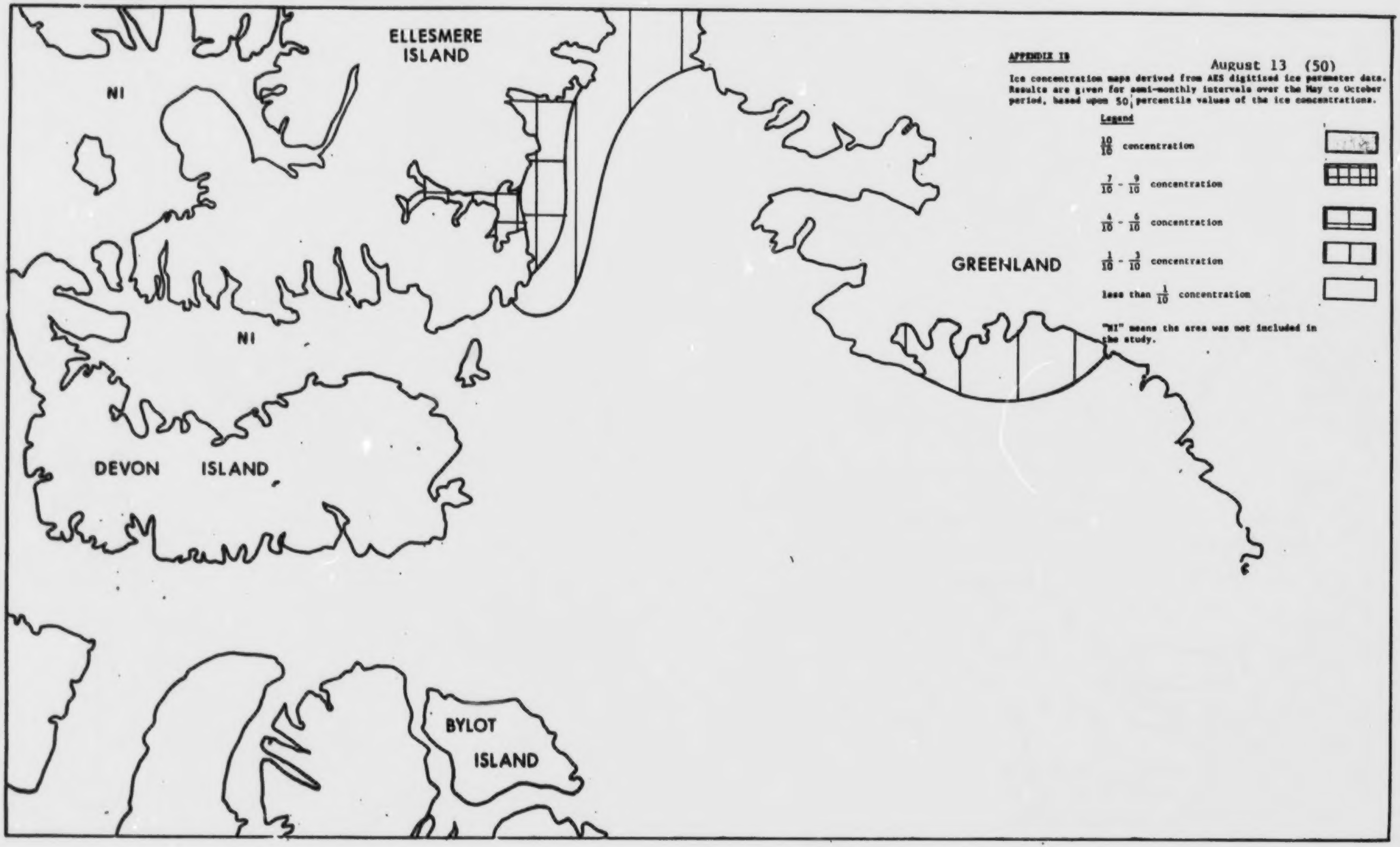
ELLESMERE ISLAND
NI
NI
DEVON ISLAND
GREENLAND
BYLOT ISLAND

APPENDIX 1B

August 13 (50)

Ice concentration maps derived from AES digitised ice parameter data. Results are given for semi-monthly intervals over the May to October period, based upon 50 percentile values of the ice concentrations.

Legend

$\frac{10}{10}$ concentration	▨
$\frac{7}{10}$ - $\frac{9}{10}$ concentration	▦
$\frac{4}{10}$ - $\frac{6}{10}$ concentration	⊞
$\frac{1}{10}$ - $\frac{3}{10}$ concentration	◫
less than $\frac{1}{10}$ concentration	☐

"NI" means the area was not included in the study.

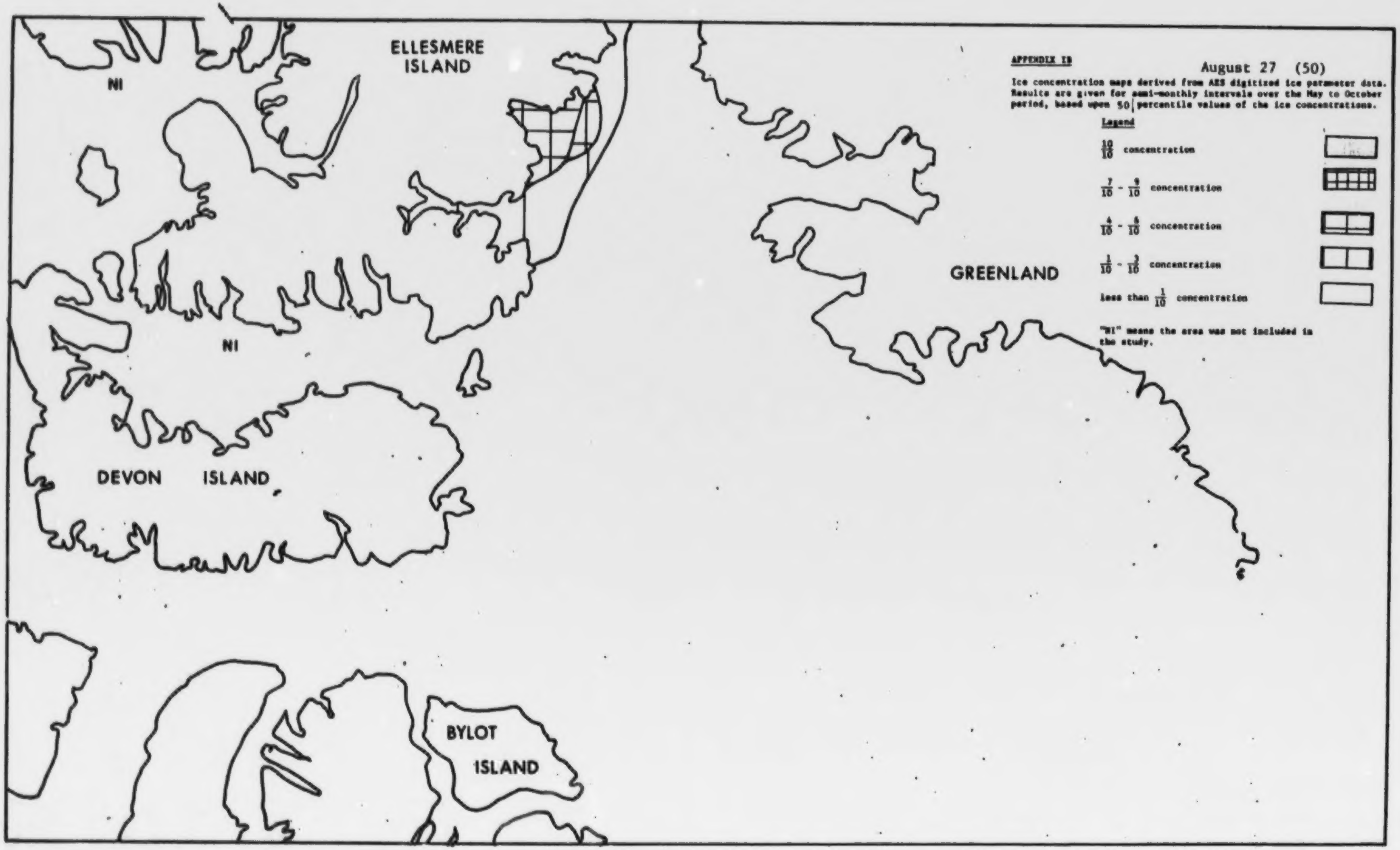

ELLESMERE ISLAND
NI
NI
DEVON ISLAND
GREENLAND
BYLOT ISLAND

APPENDIX IB

August 27 (50)

Ice concentration maps derived from AES digitized ice parameter data. Results are given for semi-monthly intervals over the May to October period, based upon 50 percentile values of the ice concentrations.

Legend

$\frac{10}{10}$ concentration	▨
$\frac{7}{10}$ - $\frac{9}{10}$ concentration	▦
$\frac{4}{10}$ - $\frac{6}{10}$ concentration	⊞
$\frac{1}{10}$ - $\frac{3}{10}$ concentration	◫
less than $\frac{1}{10}$ concentration	☐

"NI" means the area was not included in the study.

APPENDIX IB

September 10 (50)

Ice concentration maps derived from AES digitized ice parameter data. Results are given for semi-monthly intervals over the May to October period, based upon 50 percentile values of the ice concentrations.

Legend

$\frac{10}{10}$ concentration	▨
$\frac{7}{10}$ - $\frac{9}{10}$ concentration	▦
$\frac{4}{10}$ - $\frac{6}{10}$ concentration	⊞
$\frac{1}{10}$ - $\frac{3}{10}$ concentration	◫
less than $\frac{1}{10}$ concentration	▭

"NI" means the area was not included in the study.

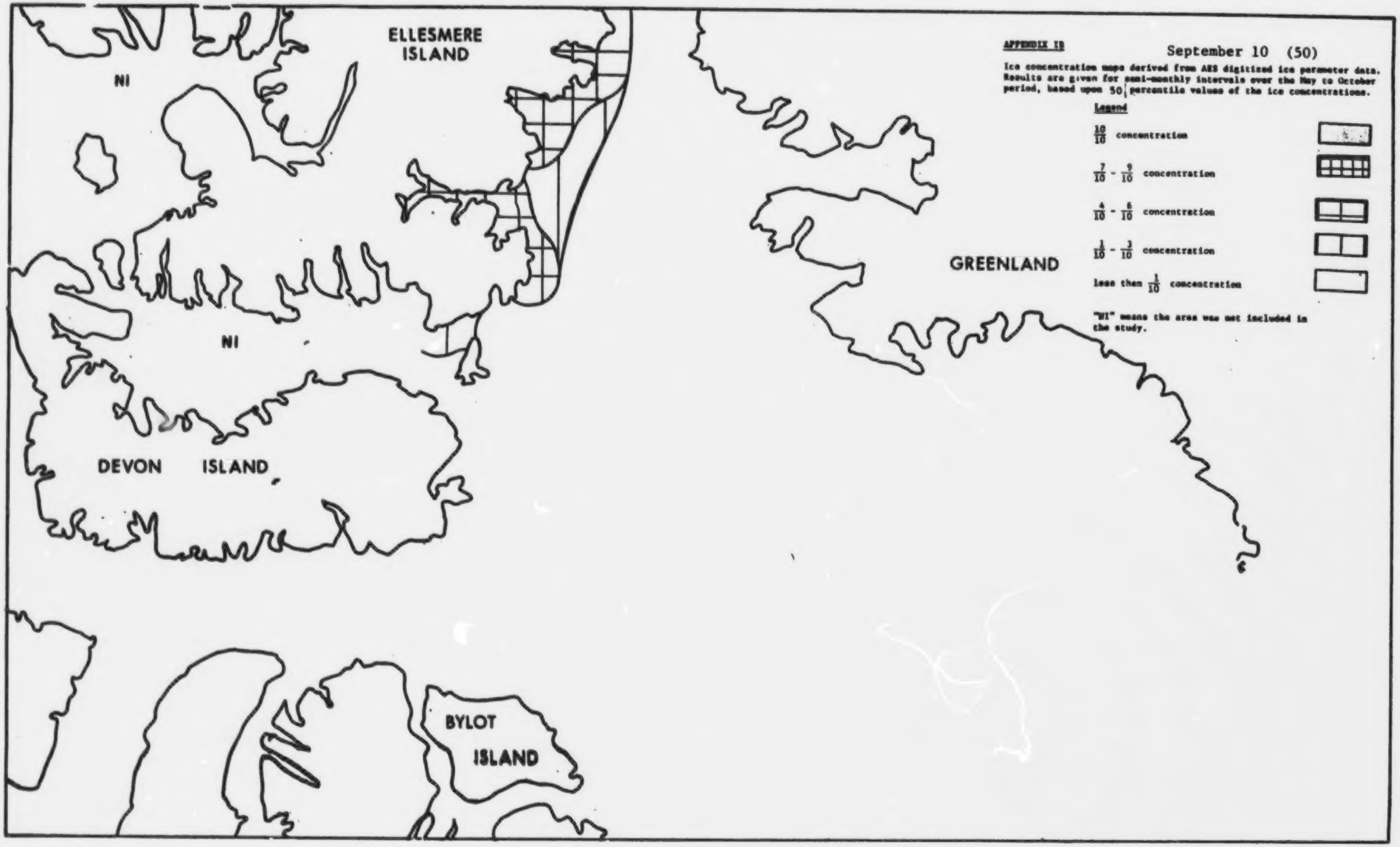
ELLESMERE ISLAND
NI
NI
DEVON ISLAND
GREENLAND
BYLOT ISLAND

APPENDIX IB

September 24 (50)

Ice concentration maps derived from AES digitized ice parameter data. Results are given for semi-monthly intervals over the May to October period, based upon 50 percentile values of the ice concentrations.

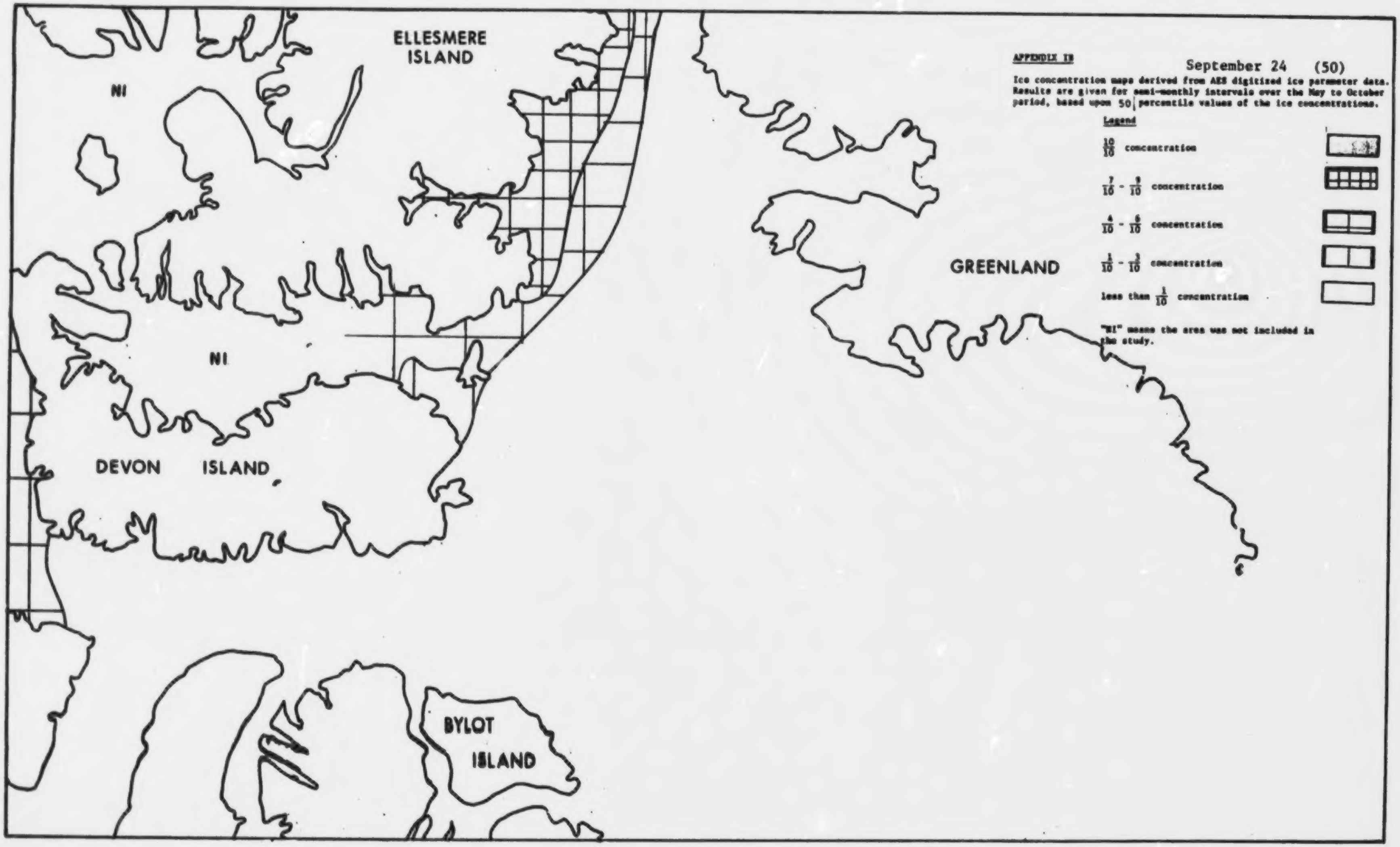
Legend
$\frac{10}{10}$ concentration
$\frac{7}{10}$ - $\frac{9}{10}$ concentration
$\frac{4}{10}$ - $\frac{6}{10}$ concentration
$\frac{1}{10}$ - $\frac{3}{10}$ concentration
less than $\frac{1}{10}$ concentration
"NI" means the area was not included in the study.
ELLESMERE ISLAND
NI
NI
DEVON ISLAND
GREENLAND
BYLOT ISLAND

APPENDIX IB

October 8 (50)

Ice concentration maps derived from AES digitized ice parameter data. Results are given for semi-monthly intervals over the May to October period, based upon 50 percentile values of the ice concentrations.

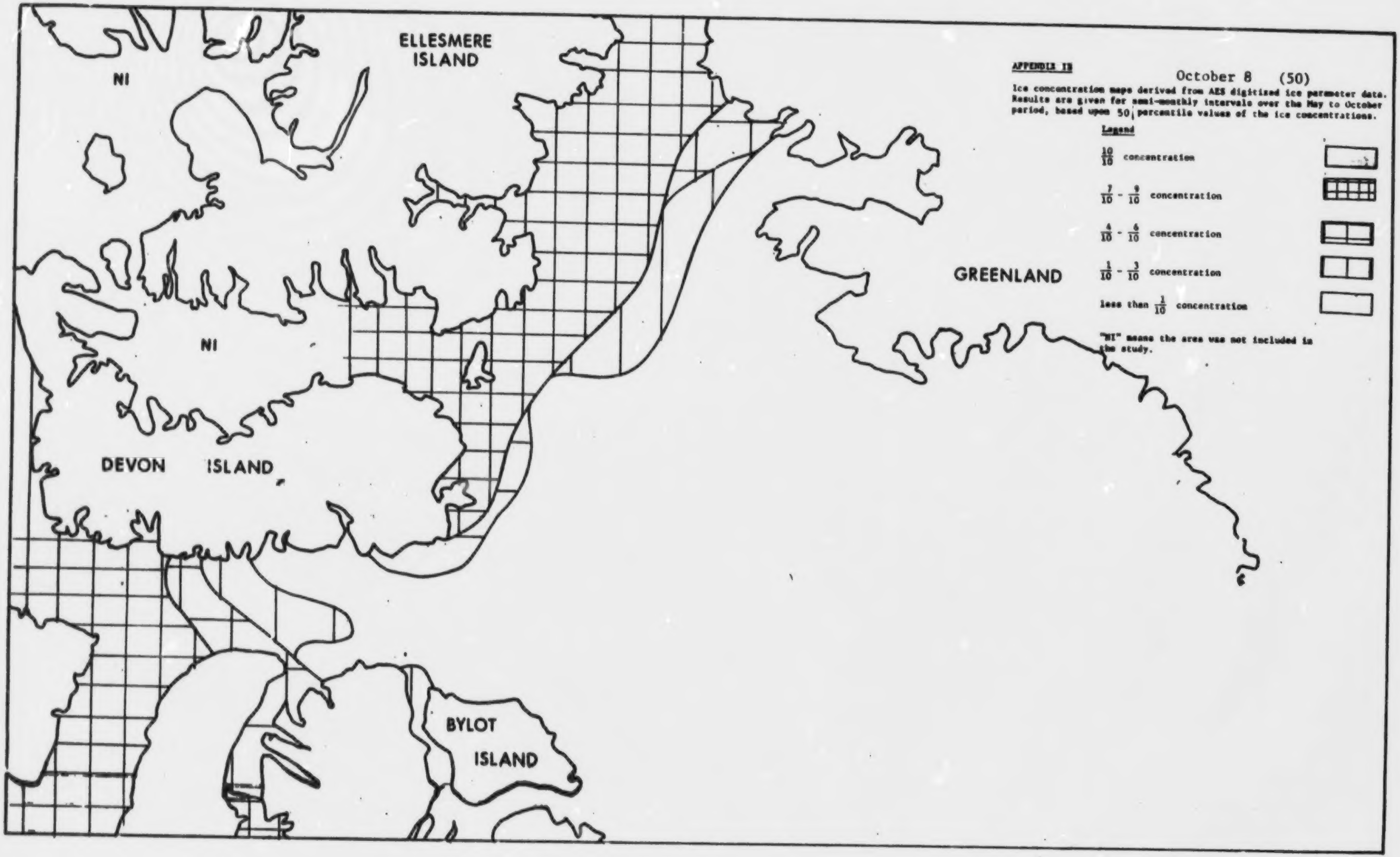
ELLESMERE ISLAND
NI
NI
DEVON ISLAND
GREENLAND
BYLOT ISLAND
Legend
$\frac{10}{10}$ concentration
$\frac{7}{10}$ - $\frac{9}{10}$ concentration
$\frac{4}{10}$ - $\frac{6}{10}$ concentration
$\frac{1}{10}$ - $\frac{3}{10}$ concentration
less than $\frac{1}{10}$ concentration

"NI" means the area was not included in the study.

APPENDIX 1B

October 22 (50)

Ice concentration maps derived from AES digitized ice parameter data. Results are given for semi-monthly intervals over the May to October period, based upon 50 percentile values of the ice concentrations.

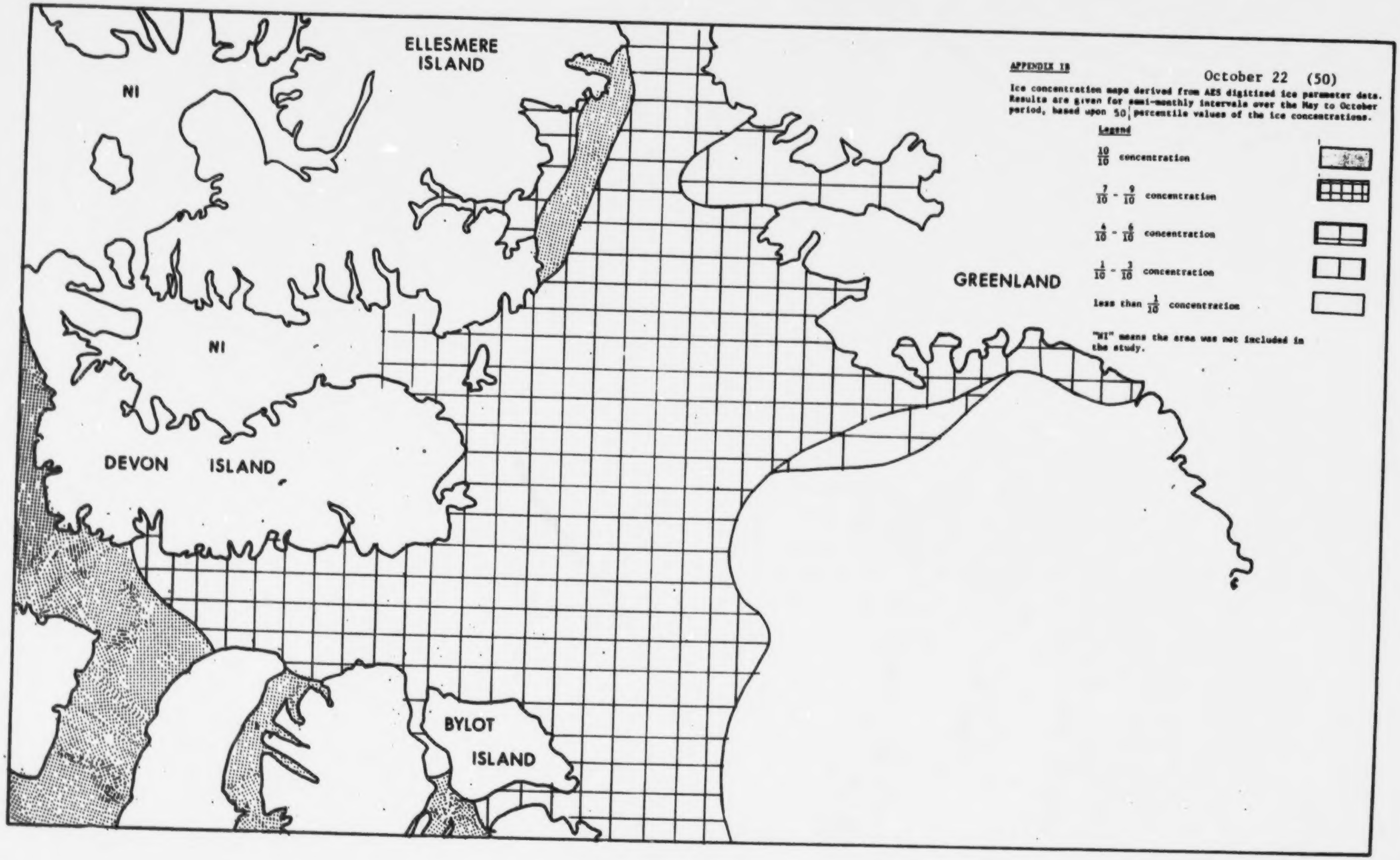
Legend
$\frac{10}{10}$ concentration
$\frac{7}{10}$ - $\frac{9}{10}$ concentration
$\frac{4}{10}$ - $\frac{6}{10}$ concentration
$\frac{1}{10}$ - $\frac{3}{10}$ concentration
less than $\frac{1}{10}$ concentration
"NI" means the area was not included in the study.
ELLESMERE ISLAND
NI
NI
GREENLAND
DEVON ISLAND
BYLOT ISLAND

APPENDIX 1C

Ice concentration maps derived from AES digitized ice parameter data. Results are given for semi-monthly intervals over the May to October period, based upon 80 percentile values of the ice concentrations.

Legend

$\frac{10}{10}$ concentration

$\frac{7}{10}$ - $\frac{9}{10}$ concentration

$\frac{4}{10}$ - $\frac{6}{10}$ concentration

$\frac{1}{10}$ - $\frac{3}{10}$ concentration

less than $\frac{1}{10}$ concentration

"NI" means the area was not included in the study.

APPENDIX IC

May 21 (80)

Ice concentration maps derived from AES digitized ice parameter data. Results are given for semi-monthly intervals over the May to October period, based upon 80 percentile values of the ice concentrations.

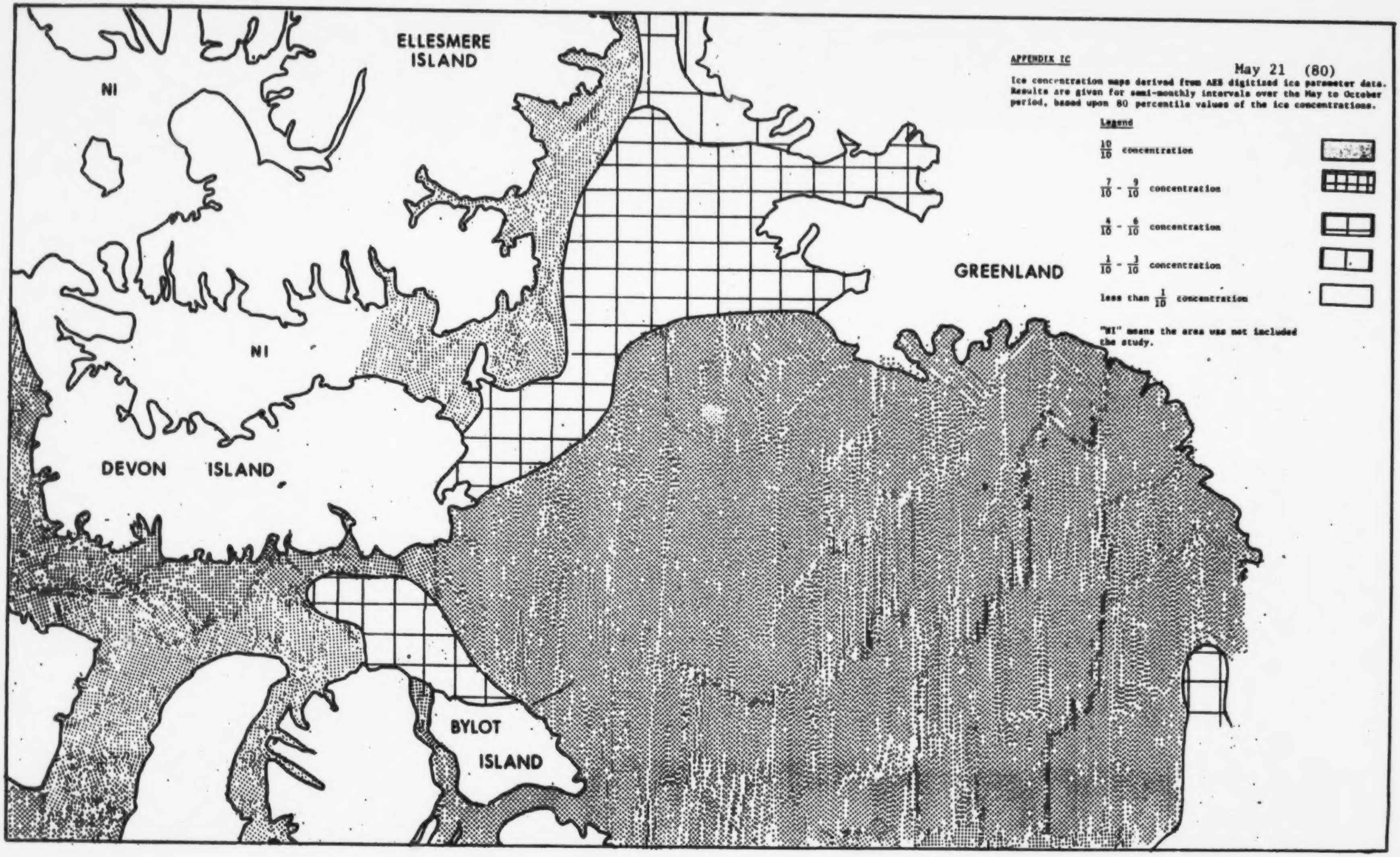
Legend
$\frac{10}{10}$ concentration
$\frac{7}{10}$ - $\frac{9}{10}$ concentration
$\frac{4}{10}$ - $\frac{6}{10}$ concentration
$\frac{1}{10}$ - $\frac{3}{10}$ concentration
less than $\frac{1}{10}$ concentration
"NI" means the area was not included the study.
ELLESMERE ISLAND
NI
NI
DEVON ISLAND
GREENLAND
BYLOT ISLAND

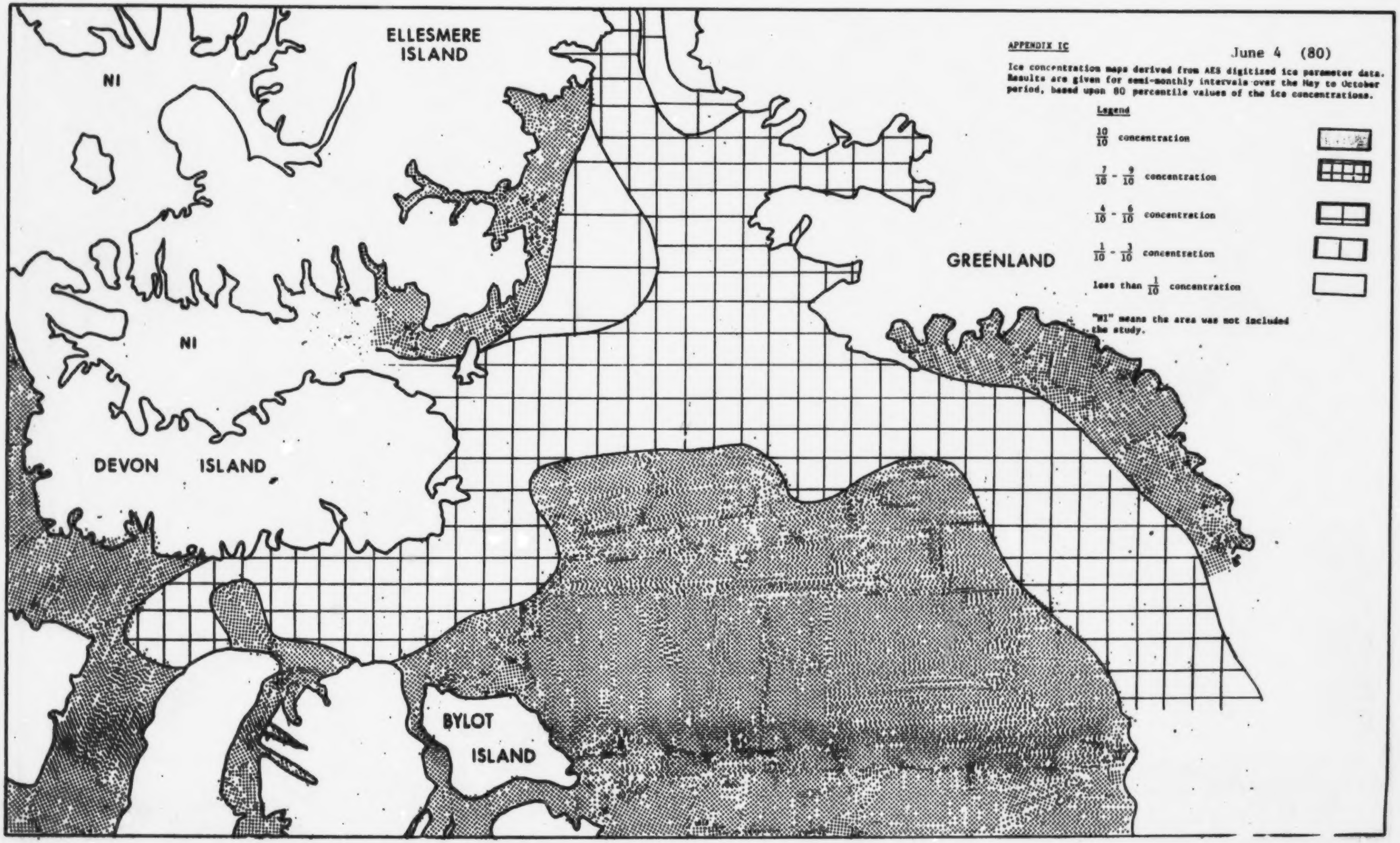

APPENDIX IC

June 4 (80)

Ice concentration maps derived from AES digitized ice parameter data. Results are given for semi-monthly intervals over the May to October period, based upon 80 percentile values of the ice concentrations.

Legend
$\frac{10}{10}$ concentration
$\frac{7}{10}$ - $\frac{9}{10}$ concentration
$\frac{4}{10}$ - $\frac{6}{10}$ concentration
$\frac{1}{10}$ - $\frac{3}{10}$ concentration
less than $\frac{1}{10}$ concentration
"NI" means the area was not included the study.
ELLESMERE ISLAND
NI
NI
DEVON ISLAND
GREENLAND
BYLOT ISLAND

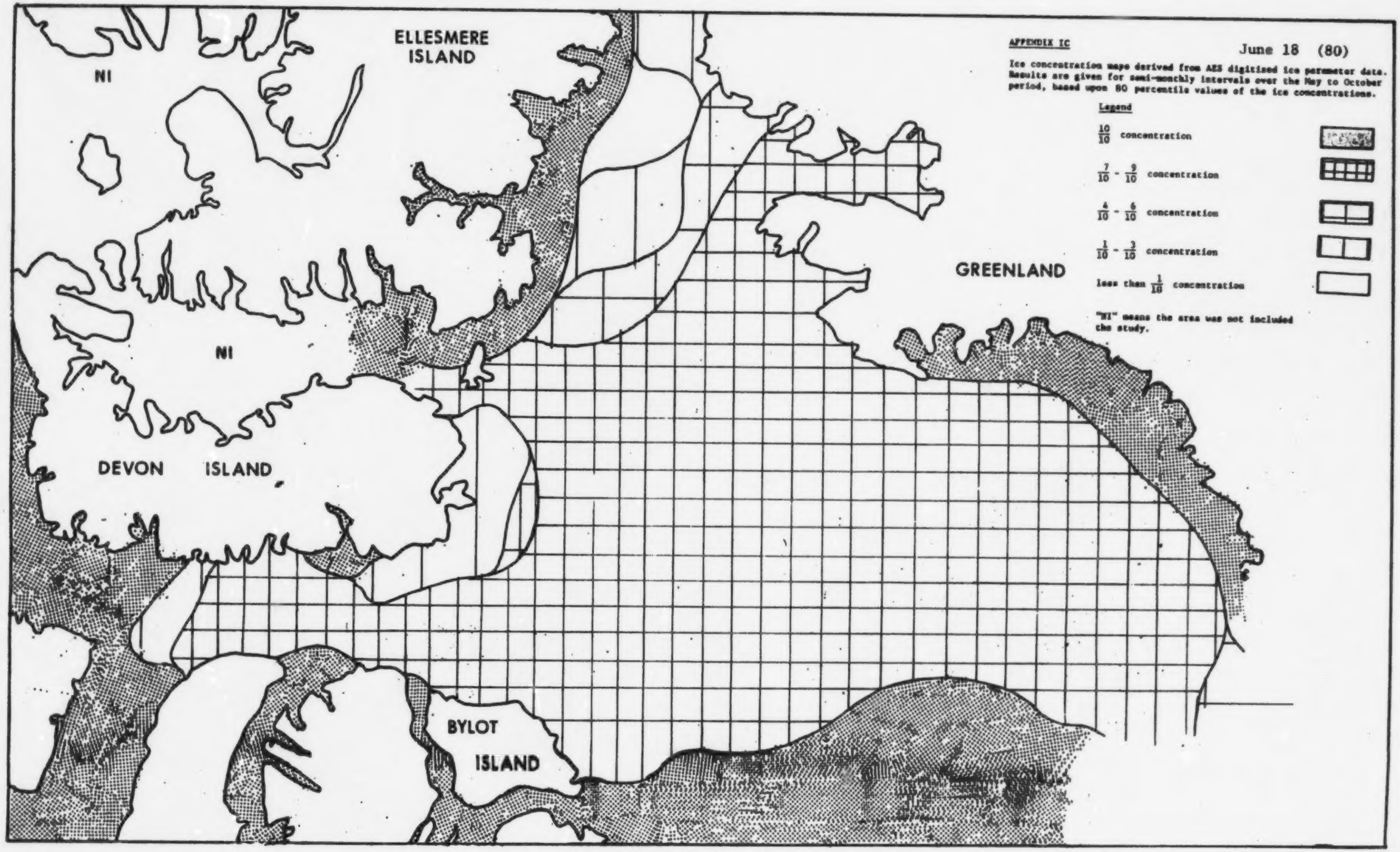
ELLESMERE ISLAND
NI
NI
DEVON ISLAND
GREENLAND
BYLOT ISLAND

APPENDIX IC

June 18 (80)

Ice concentration maps derived from AES digitized ice parameter data. Results are given for semi-monthly intervals over the May to October period, based upon 80 percentile values of the ice concentrations.

Legend

$\frac{10}{10}$ concentration ▩

$\frac{7}{10}$ - $\frac{9}{10}$ concentration ▦

$\frac{4}{10}$ - $\frac{6}{10}$ concentration ⊞

$\frac{1}{10}$ - $\frac{3}{10}$ concentration ◫

less than $\frac{1}{10}$ concentration ▭

"NI" means the area was not included the study.

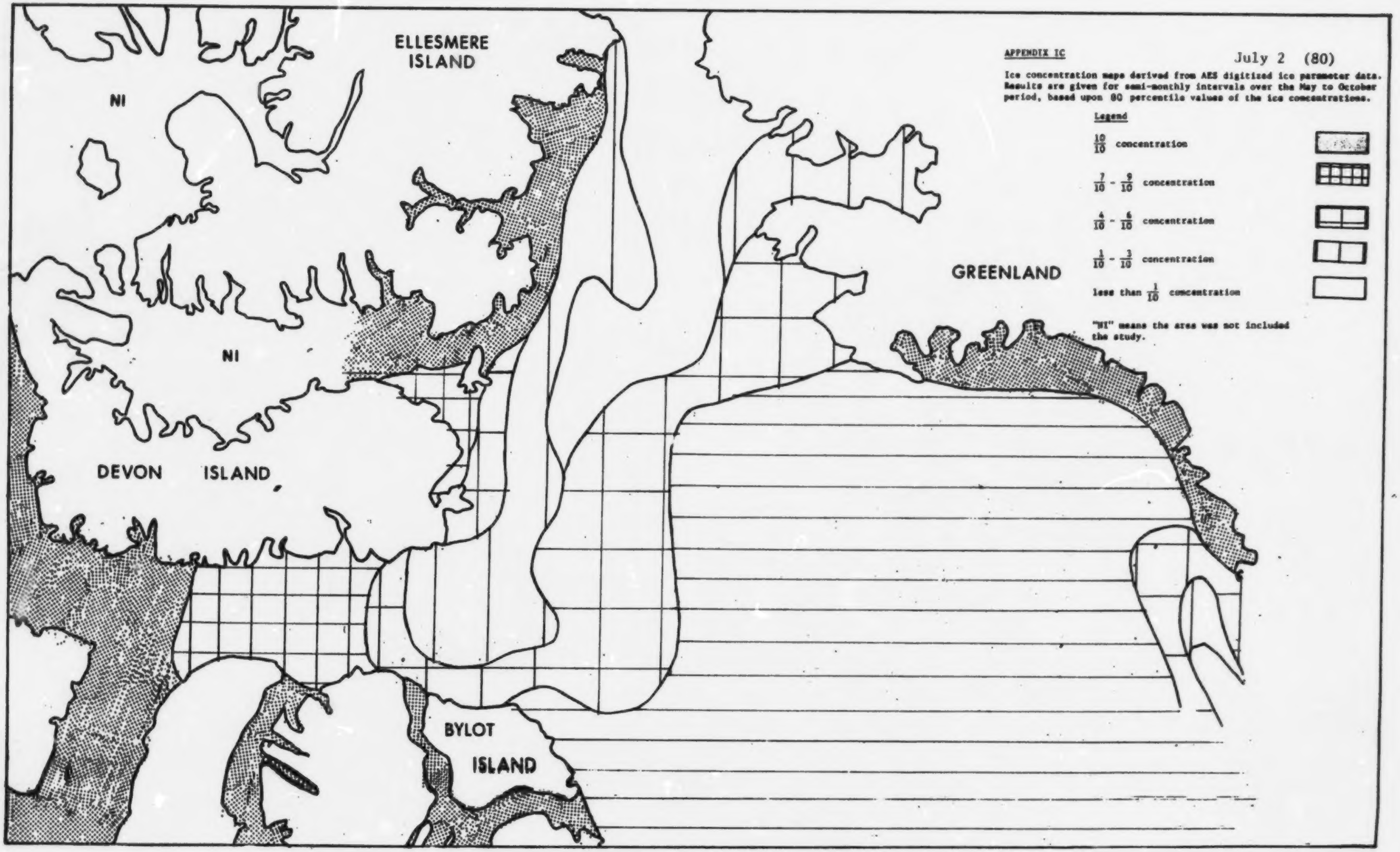

ELLESMERE ISLAND
NI
NI
DEVON ISLAND
GREENLAND
BYLOT ISLAND

APPENDIX IC

July 2 (80)

Ice concentration maps derived from AES digitized ice parameter data. Results are given for semi-monthly intervals over the May to October period, based upon 80 percentile values of the ice concentrations.

Legend
$\frac{10}{10}$ concentration
$\frac{7}{10}$ - $\frac{9}{10}$ concentration
$\frac{4}{10}$ - $\frac{6}{10}$ concentration
$\frac{1}{10}$ - $\frac{3}{10}$ concentration
less than $\frac{1}{10}$ concentration

"NI" means the area was not included the study.

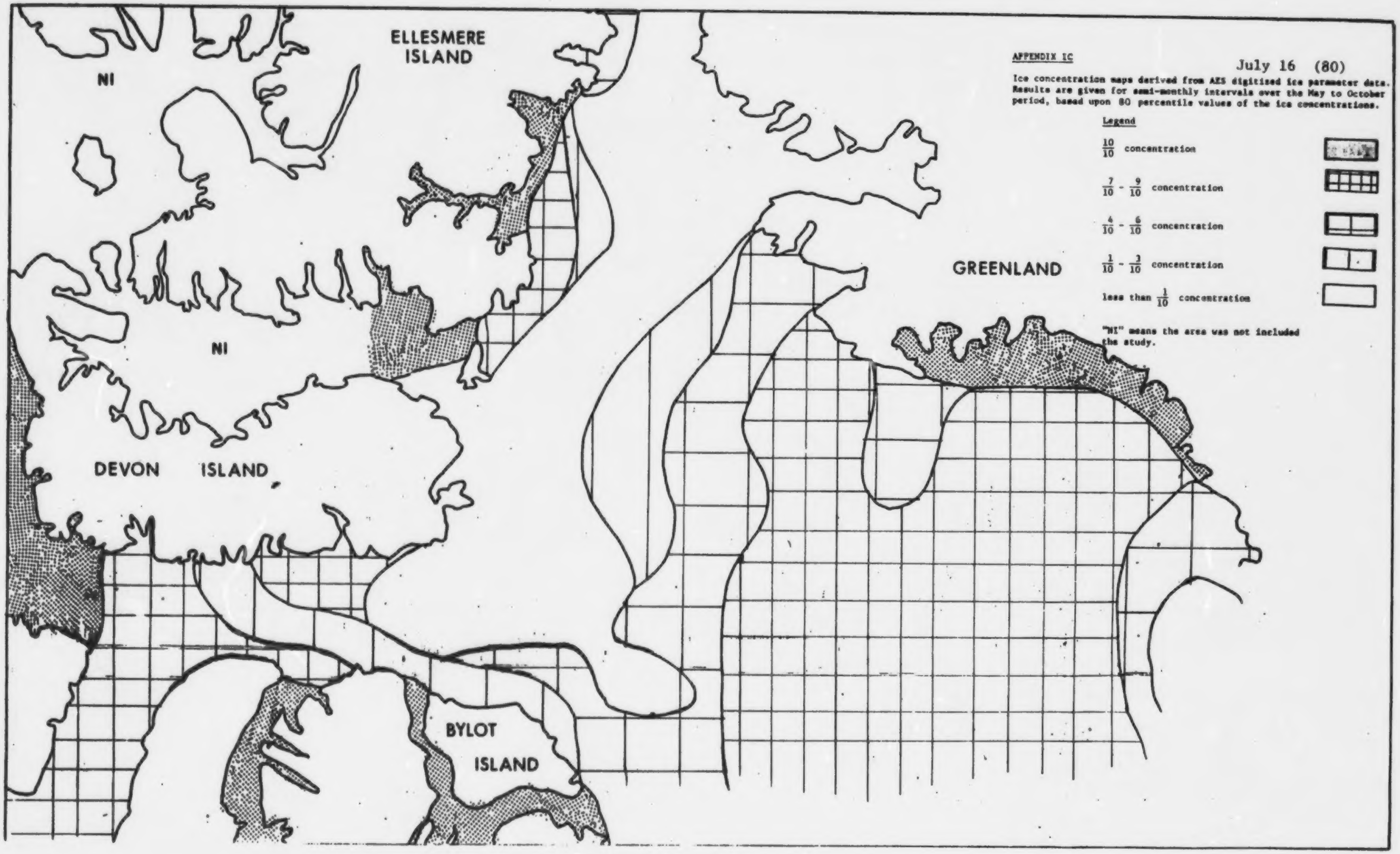

ELLESMERE ISLAND
NI
NI
DEVON ISLAND
GREENLAND
BYLOT ISLAND

APPENDIX IC

July 16 (80)

Ice concentration maps derived from AES digitized ice parameter data. Results are given for semi-monthly intervals over the May to October period, based upon 80 percentile values of the ice concentrations.

Legend

$\frac{10}{10}$ concentration	▩
$\frac{7}{10}$ - $\frac{9}{10}$ concentration	▦
$\frac{4}{10}$ - $\frac{6}{10}$ concentration	⊞
$\frac{1}{10}$ - $\frac{3}{10}$ concentration	◫
less than $\frac{1}{10}$ concentration	□

"NI" means the area was not included the study.

APPENDIX IC

July 16 (80)

Ice concentration maps derived from AES digitized ice parameter data. Results are given for semi-monthly intervals over the May to October period, based upon 80 percentile values of the ice concentrations.

Legend

$\frac{10}{10}$ concentration	▒
$\frac{7}{10}$ - $\frac{9}{10}$ concentration	▦
$\frac{4}{10}$ - $\frac{6}{10}$ concentration	⊞
$\frac{1}{10}$ - $\frac{3}{10}$ concentration	◫
less than $\frac{1}{10}$ concentration	☐

"NI" means the area was not included the study.

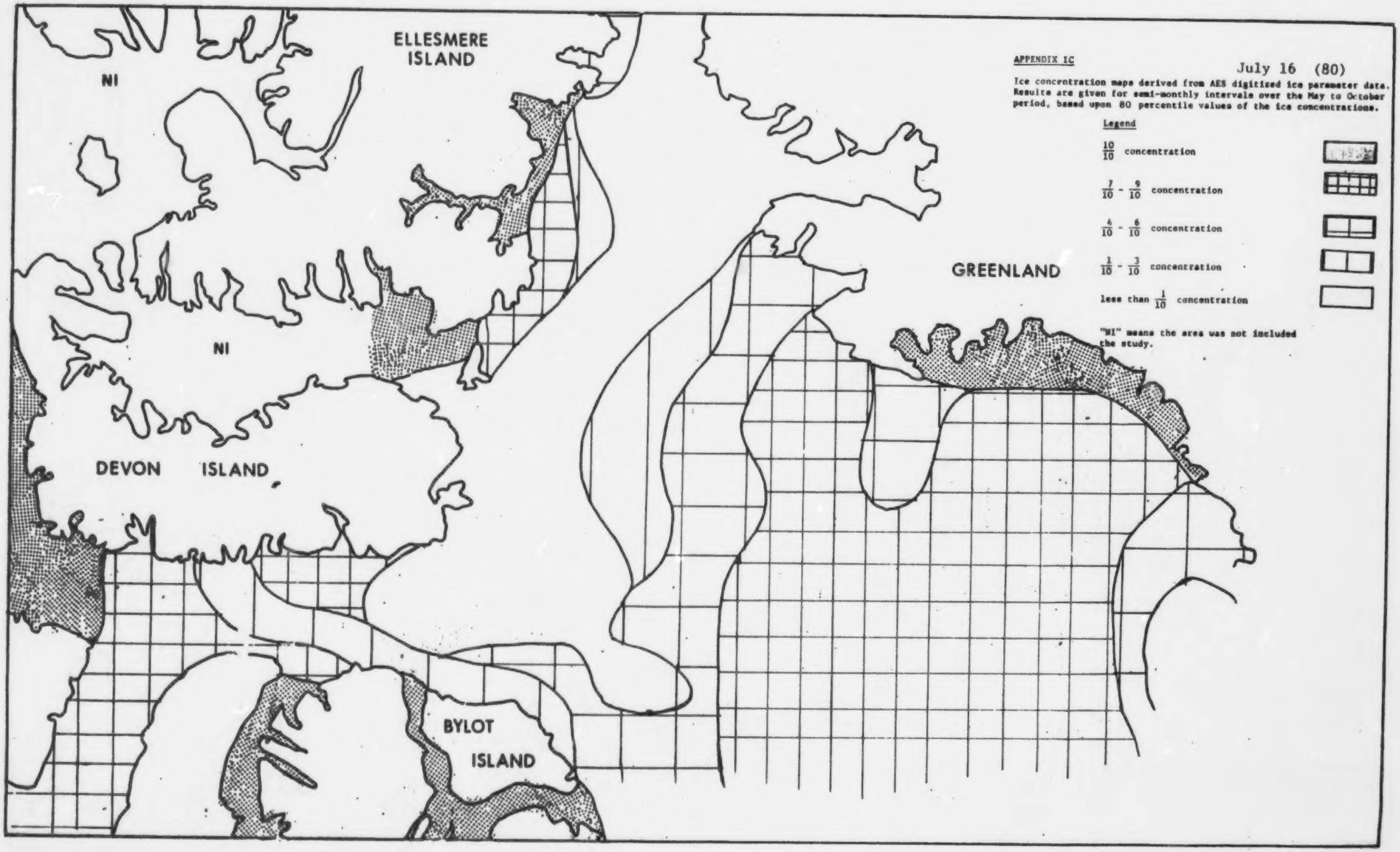
ELLESMERE ISLAND
NI
NI
DEVON ISLAND
GREENLAND
BYLOT ISLAND

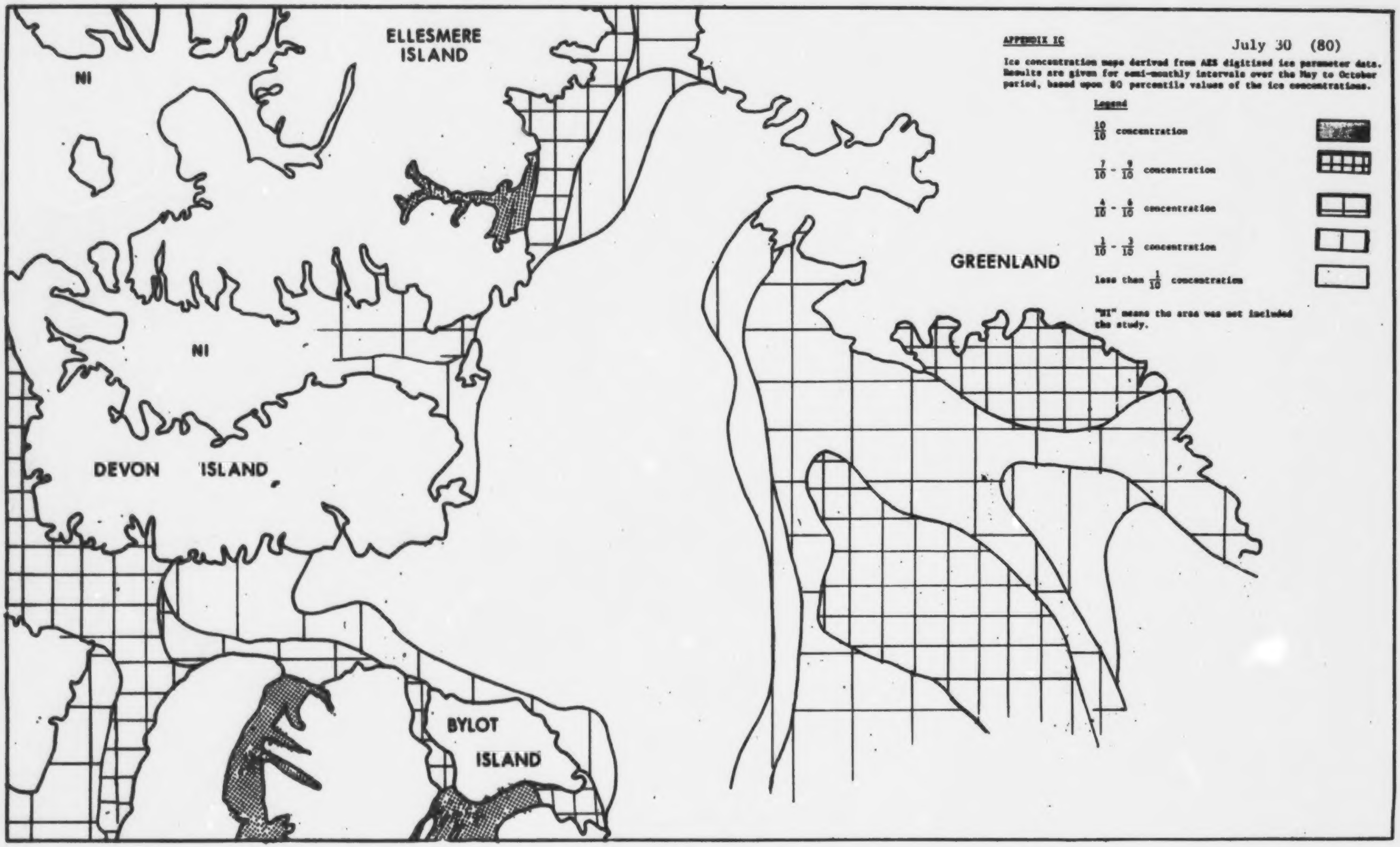

APPENDIX IC

July 30 (80)

Ice concentration maps derived from AES digitized ice parameter data. Results are given for semi-monthly intervals over the May to October period, based upon 80 percentile values of the ice concentrations.

Legend
$\frac{10}{10}$ concentration
$\frac{7}{10}$ - $\frac{9}{10}$ concentration
$\frac{4}{10}$ - $\frac{6}{10}$ concentration
$\frac{1}{10}$ - $\frac{3}{10}$ concentration
less than $\frac{1}{10}$ concentration
"NI" means the area was not included the study.
ELLESMERE ISLAND
NI
NI
DEVON ISLAND
GREENLAND
BYLOT ISLAND

APPENDIX IC

August 13 (80)

Ice concentration maps derived from AES digitized ice parameter data. Results are given for semi-monthly intervals over the May to October period, based upon 80 percentile values of the ice concentrations.

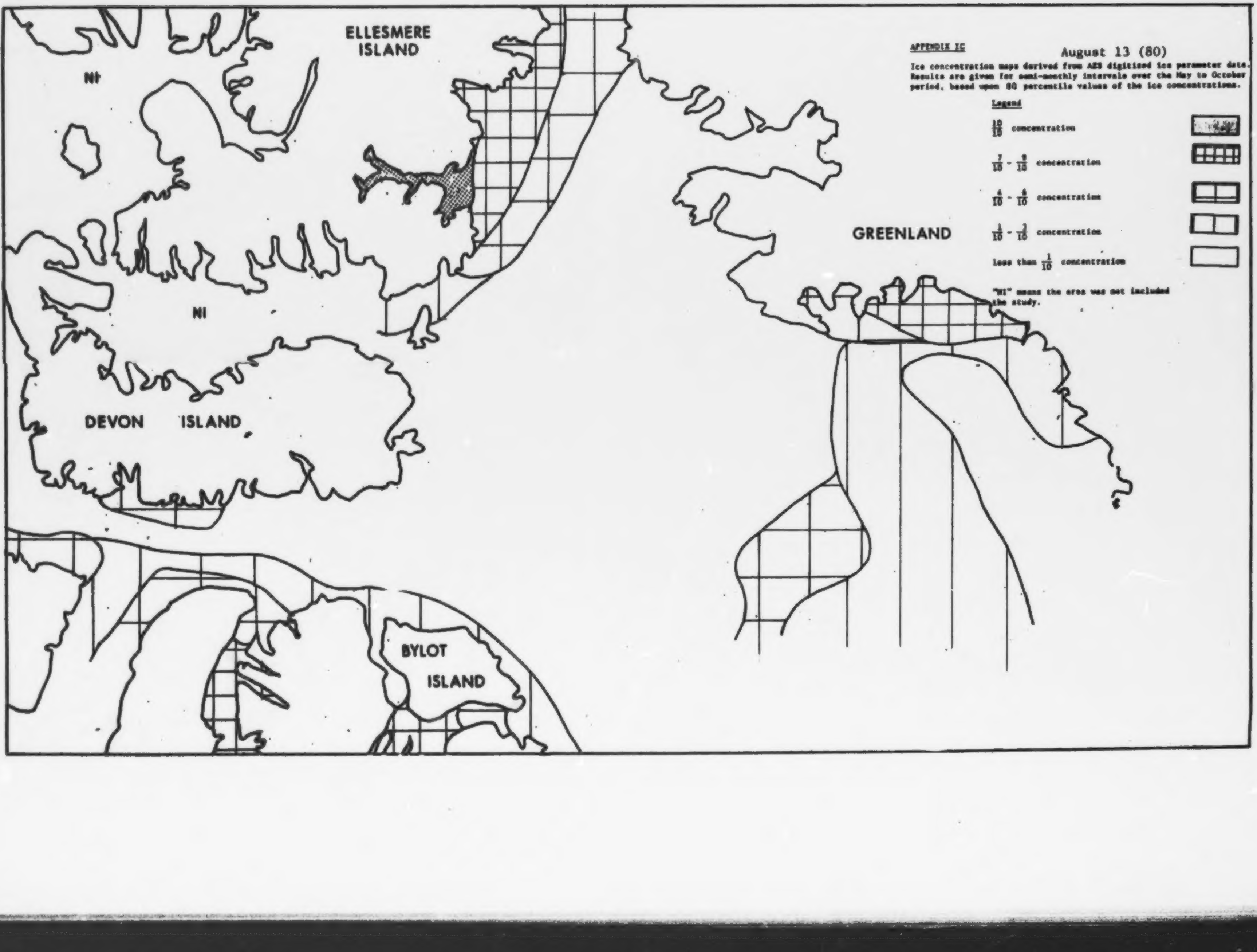
ELLESMERE ISLAND
NI
NI
DEVON ISLAND
GREENLAND
BYLOT ISLAND
Legend
$\frac{10}{10}$ concentration
$\frac{7}{10}$ - $\frac{9}{10}$ concentration
$\frac{4}{10}$ - $\frac{6}{10}$ concentration
$\frac{1}{10}$ - $\frac{3}{10}$ concentration
less than $\frac{1}{10}$ concentration
"NI" means the area was not included the study.

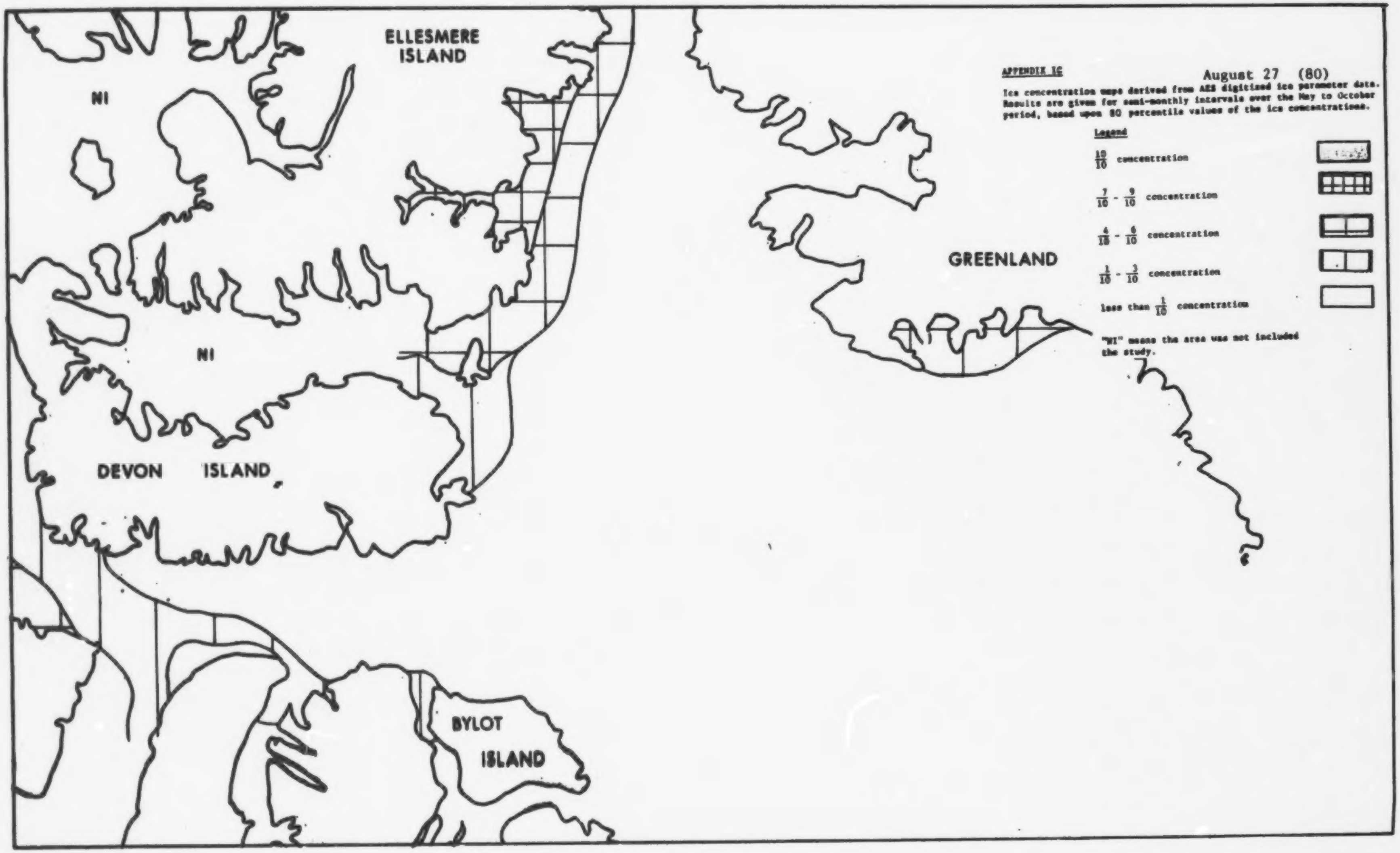

ELLESMERE ISLAND
NI
NI
DEVON ISLAND
GREENLAND
BYLOT ISLAND

APPENDIX IC

August 27 (80)

Ice concentration maps derived from AES digitized ice parameter data. Results are given for semi-monthly intervals over the May to October period, based upon 80 percentile values of the ice concentrations.

Legend

$\frac{10}{10}$ concentration	▒
$\frac{7}{10}$ - $\frac{9}{10}$ concentration	▦
$\frac{4}{10}$ - $\frac{6}{10}$ concentration	⊞
$\frac{1}{10}$ - $\frac{3}{10}$ concentration	◫
less than $\frac{1}{10}$ concentration	☐

"NI" means the area was not included the study.

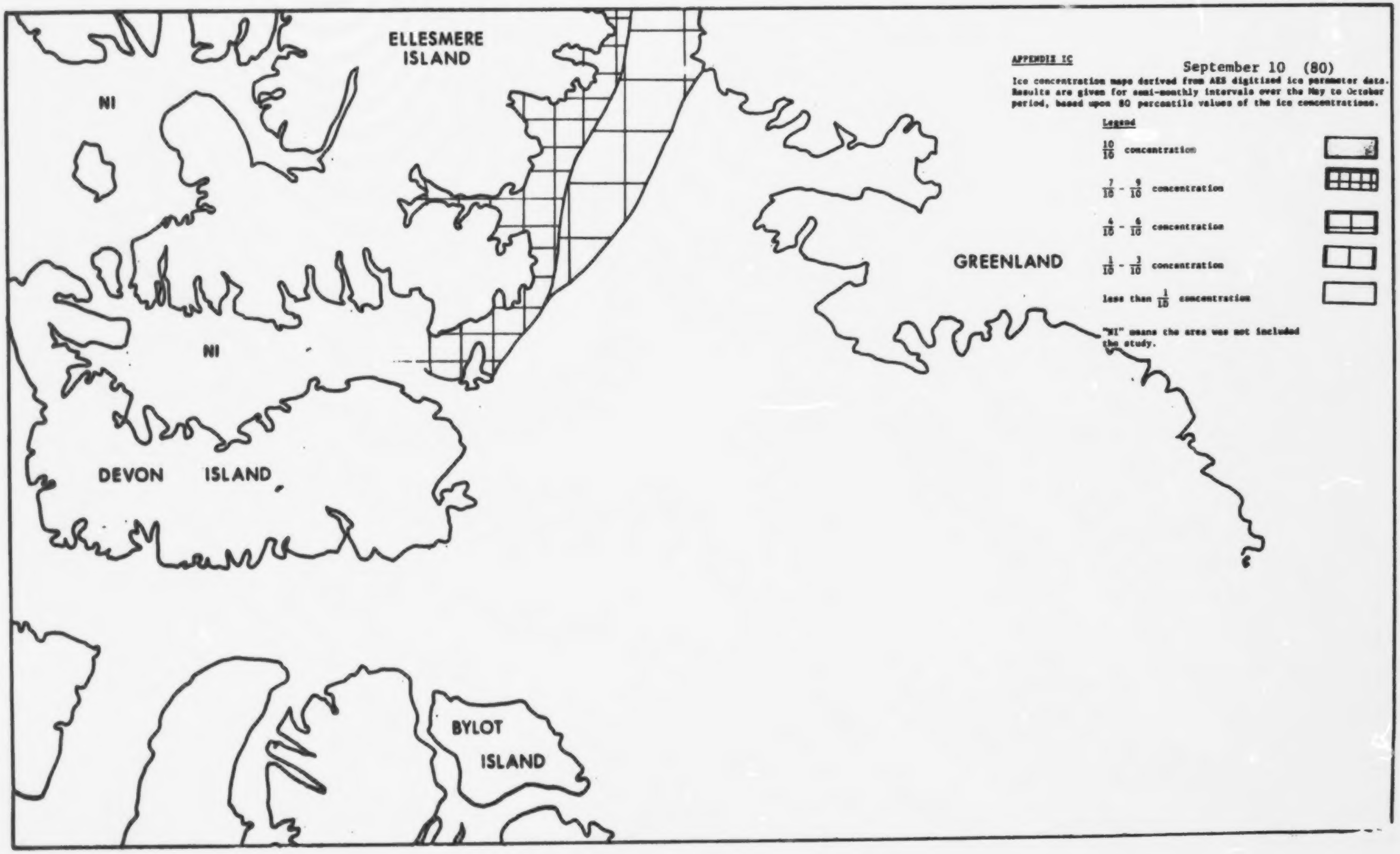

ELLESMERE ISLAND
NI
NI
DEVON ISLAND
GREENLAND
BYLOT ISLAND
Legend
$\frac{10}{10}$ concentration
$\frac{7}{10}$ - $\frac{9}{10}$ concentration
$\frac{4}{10}$ - $\frac{6}{10}$ concentration
$\frac{1}{10}$ - $\frac{3}{10}$ concentration
less than $\frac{1}{10}$ concentration

APPENDIX IC

September 10 (80)

Ice concentration maps derived from AES digitized ice parameter data. Results are given for semi-monthly intervals over the May to October period, based upon 80 percentile values of the ice concentrations.

"NI" means the area was not included the study.

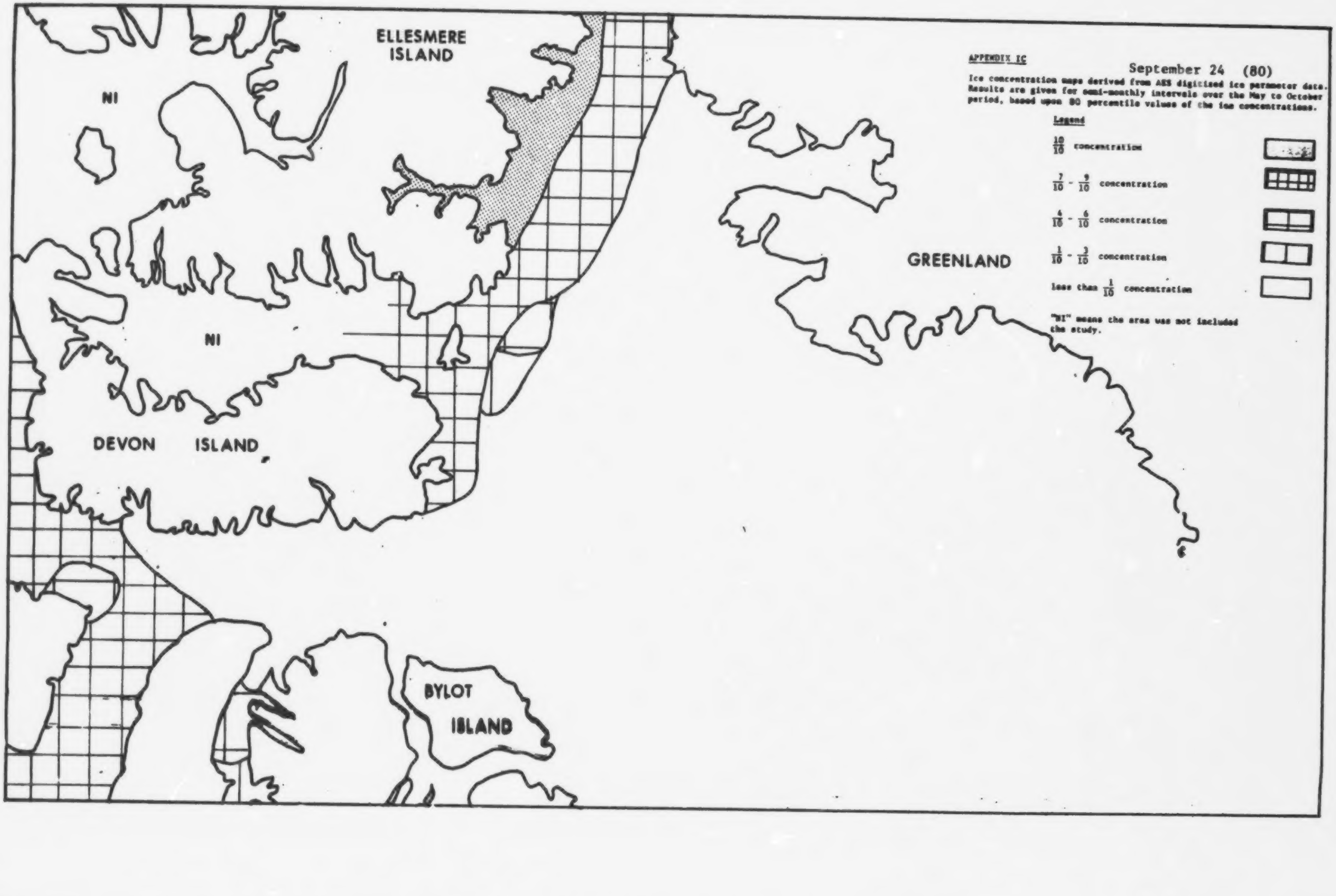
ELLESMERE ISLAND
NI
NI
DEVON ISLAND
GREENLAND
BYLOT ISLAND

APPENDIX IC

September 24 (80)

Ice concentration maps derived from AES digitized ice parameter data. Results are given for semi-monthly intervals over the May to October period, based upon 80 percentile values of the ice concentrations.

Legend

$\frac{10}{10}$ concentration ▩

$\frac{7}{10}$ - $\frac{9}{10}$ concentration ▦

$\frac{4}{10}$ - $\frac{6}{10}$ concentration ▤

$\frac{1}{10}$ - $\frac{3}{10}$ concentration ◫

less than $\frac{1}{10}$ concentration ▭

"NI" means the area was not included the study.

APPENDIX IC

October 8 (80)

Ice concentration maps derived from AES digitized ice parameter data. Results are given for semi-monthly intervals over the May to October period, based upon 80 percentile values of the ice concentrations.

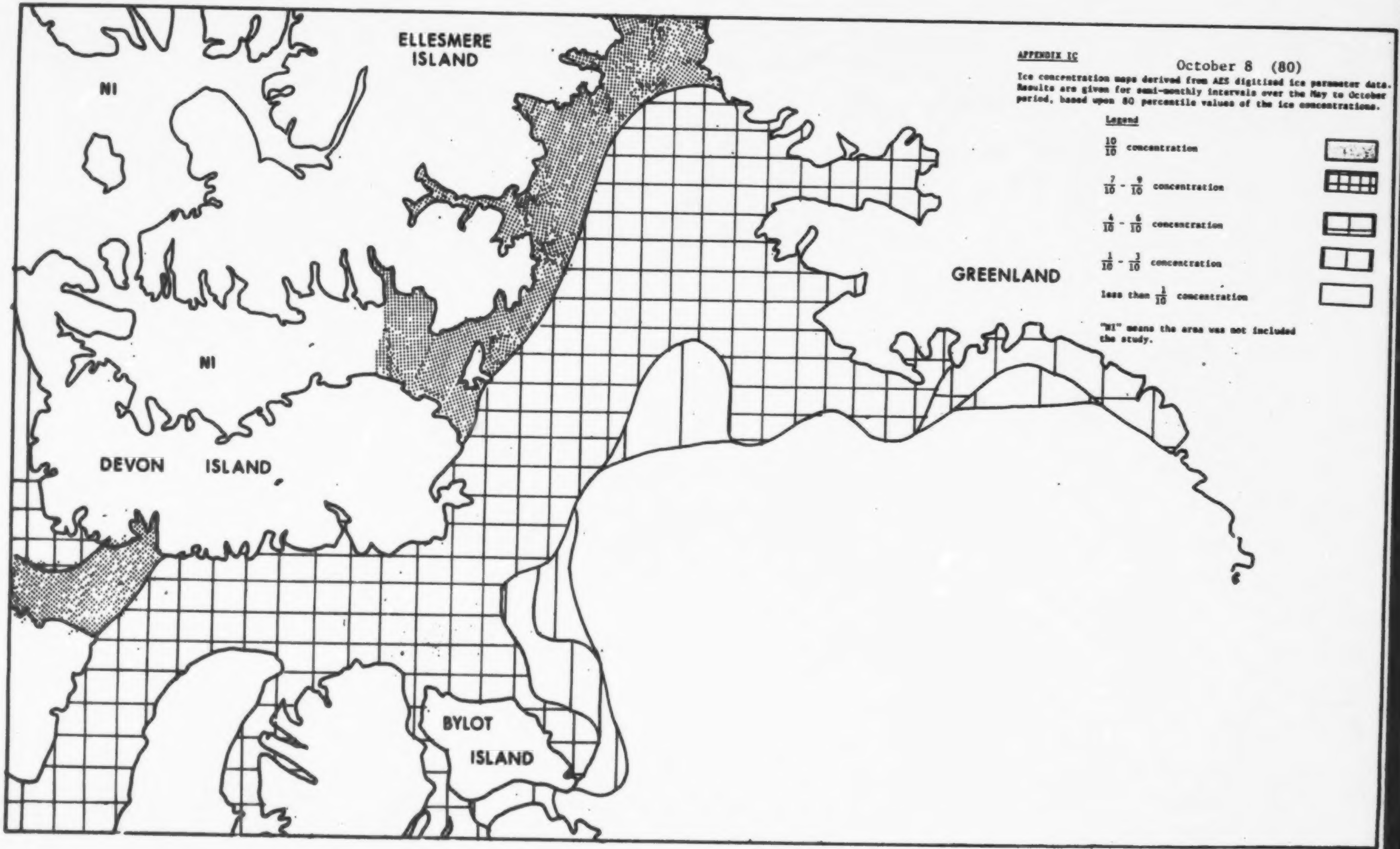
ELLESMERE ISLAND
NI
NI
DEVON ISLAND
GREENLAND
BYLOT ISLAND

Legend

$\frac{10}{10}$ concentration	▨
$\frac{7}{10}$ - $\frac{9}{10}$ concentration	▦
$\frac{4}{10}$ - $\frac{6}{10}$ concentration	⊞
$\frac{1}{10}$ - $\frac{3}{10}$ concentration	◫
less than $\frac{1}{10}$ concentration	☐

"NI" means the area was not included the study.

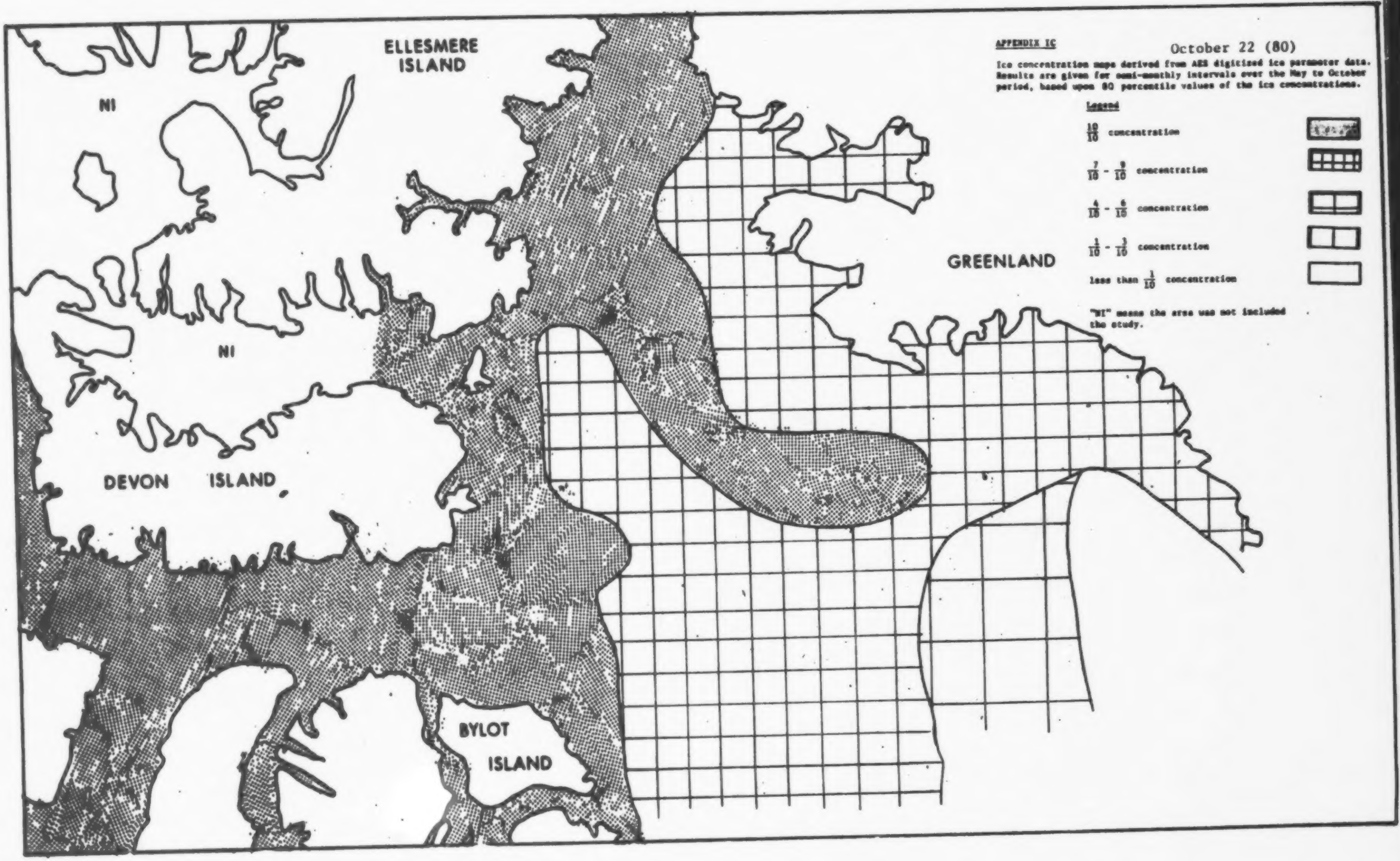

ELLESMERE ISLAND
NI
NI
DEVON ISLAND
GREENLAND
BYLOT ISLAND

APPENDIX IC

October 22 (80)

Ice concentration maps derived from AES digitized ice parameter data. Results are given for semi-monthly intervals over the May to October period, based upon 80 percentile values of the ice concentrations.

Legend

$\frac{10}{10}$ concentration ▩

$\frac{7}{10}$ - $\frac{9}{10}$ concentration ▦

$\frac{4}{10}$ - $\frac{6}{10}$ concentration ▤

$\frac{1}{10}$ - $\frac{3}{10}$ concentration ◫

less than $\frac{1}{10}$ concentration ▭

"NI" means the area was not included the study.

APPENDIX 2A

Ice concentrations mapped at two week Intervals, June 6 - 5, 1978.
December 5, 1978

KEY TO ICE CONCENTRATION MAPS

■	10/10 coverage (consolidated or landfast ice)
▩	7/10 - 9+/10 coverage
▒	4/10 - 6/10 coverage
░	1/10 - 3/10 coverage
OW	less than 1/10 coverage (open water)

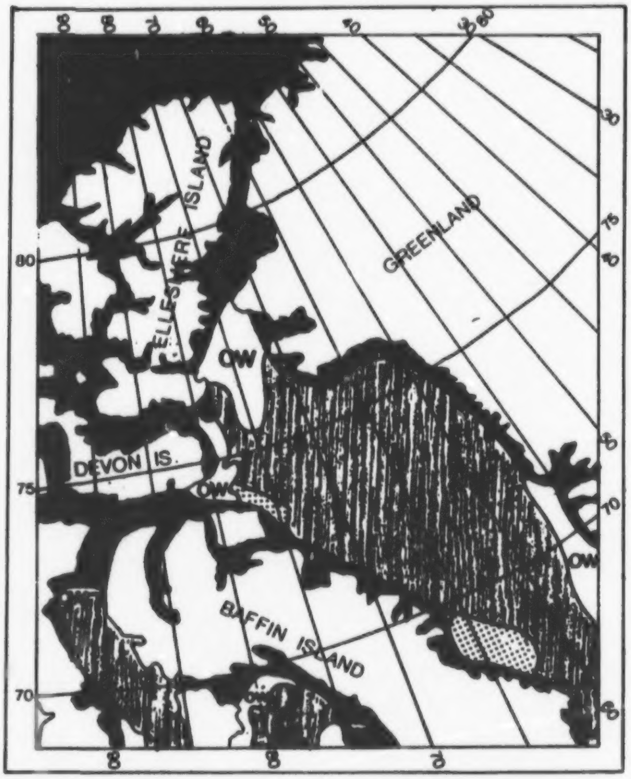

ELLESMERE ISLAND
GREENLAND
OW
DEVON IS.
OW
OW
BAFFIN ISLAND
80
75
70

June 6, 1978

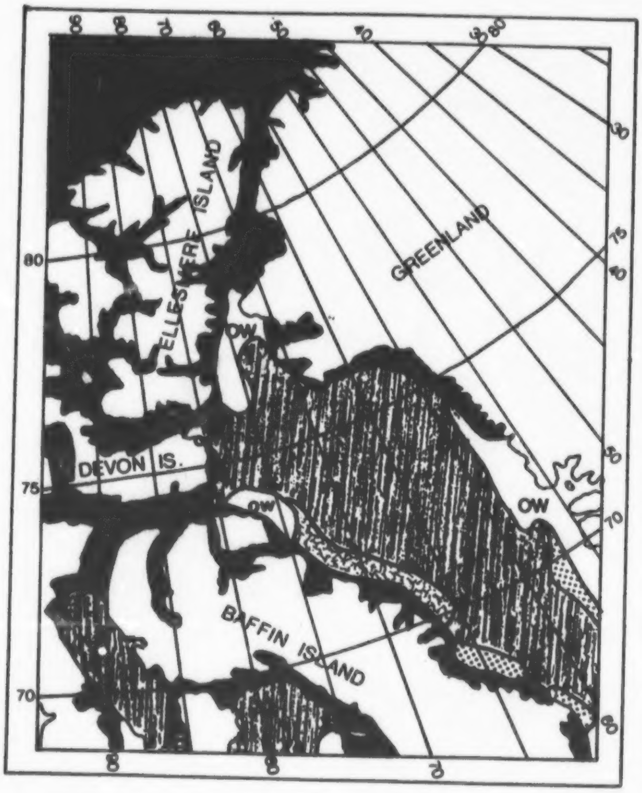
ELLESMERE ISLAND
GREENLAND
DEVON IS.
BAFFIN ISLAND
OW
OW
OW
OW
80
75
70

June 20, 1978

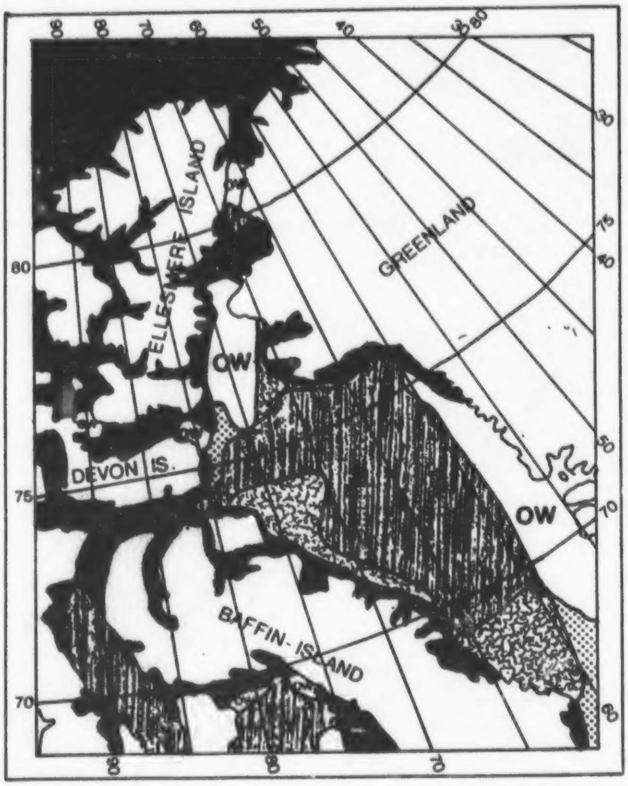
90
80
70
60
50
40
30
80
30
75
40
70
60
50
70
60
80
80
75
70
80
60
70
ELLESMERE ISLAND
GREENLAND
DEVON IS.
BAFFIN ISLAND
OW
OW
OW

July 4, 1978

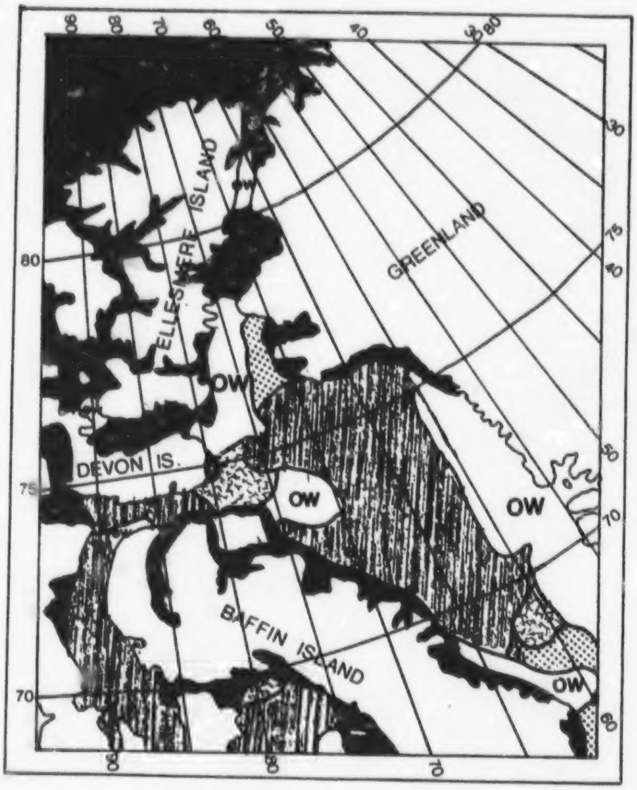

ELLESMERE ISLAND
GREENLAND
DEVON IS.
BAFFIN ISLAND
OW
OW
OW
OW
OW
90
80
70
60
50
40
30
80
80
75
75
70
70
80
75
70
60
90
80
70

July 18, 1978

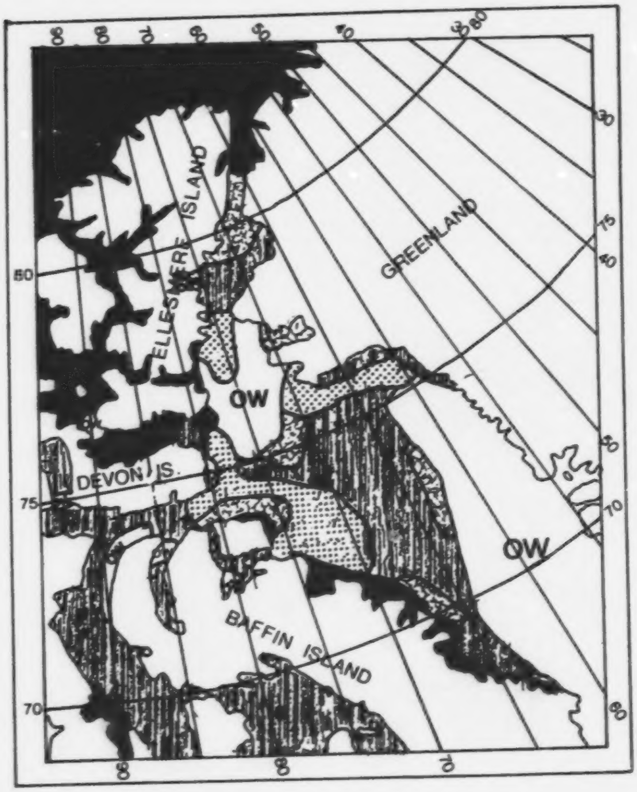
90
80
70
60
50
40
30
80
30
ELLESMERE ISLAND
GREENLAND
75
40
80
OW
DEVON IS.
75
50
70
OW
BAFFIN ISLAND
70
60
90
80
70

August 1, 1978

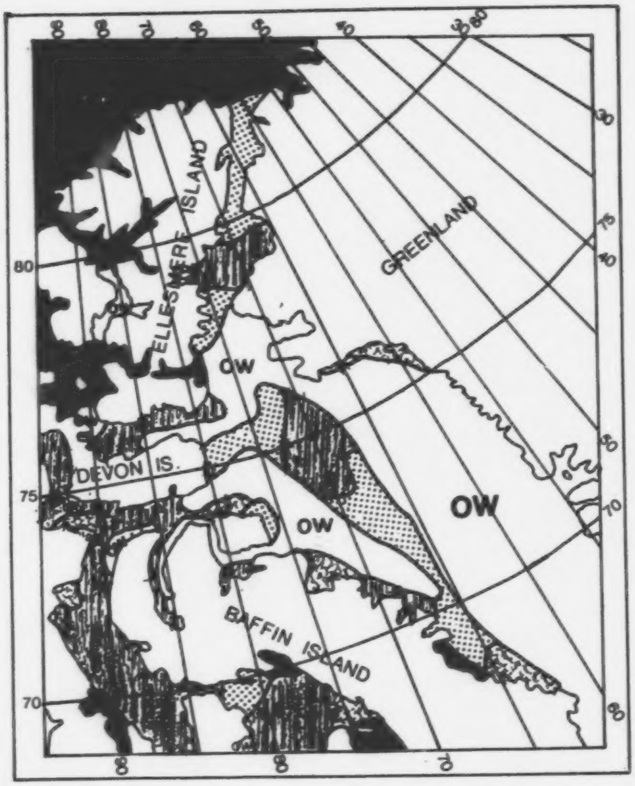
ELLESMERE ISLAND
GREENLAND
OW
DEVON IS.
OW
OW
BAFFIN ISLAND
80
75
70

August 15, 1978

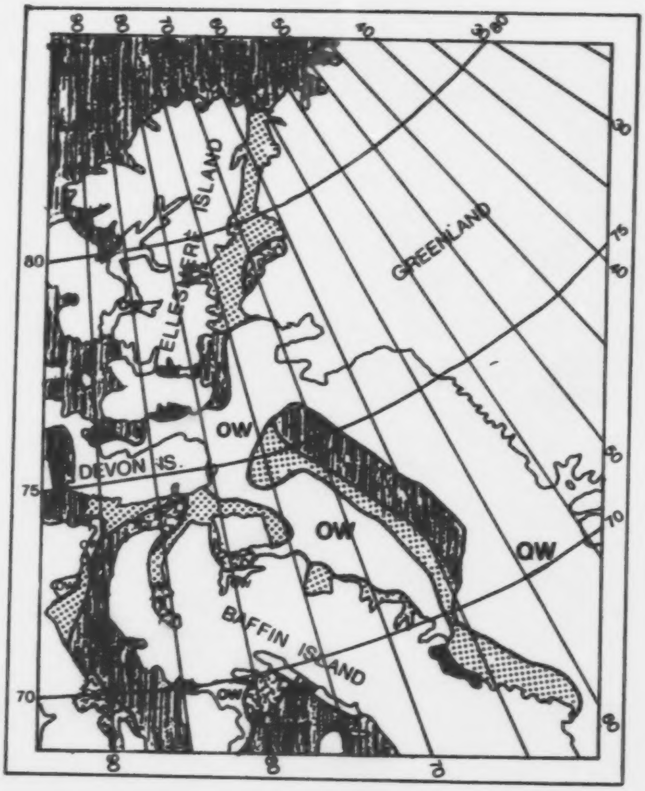
ELLESMERE ISLAND
GREENLAND
DEVON IS.
OW
OW
OW
OW
BAFFIN ISLAND
80
75
70
75
70

August 29, 1978

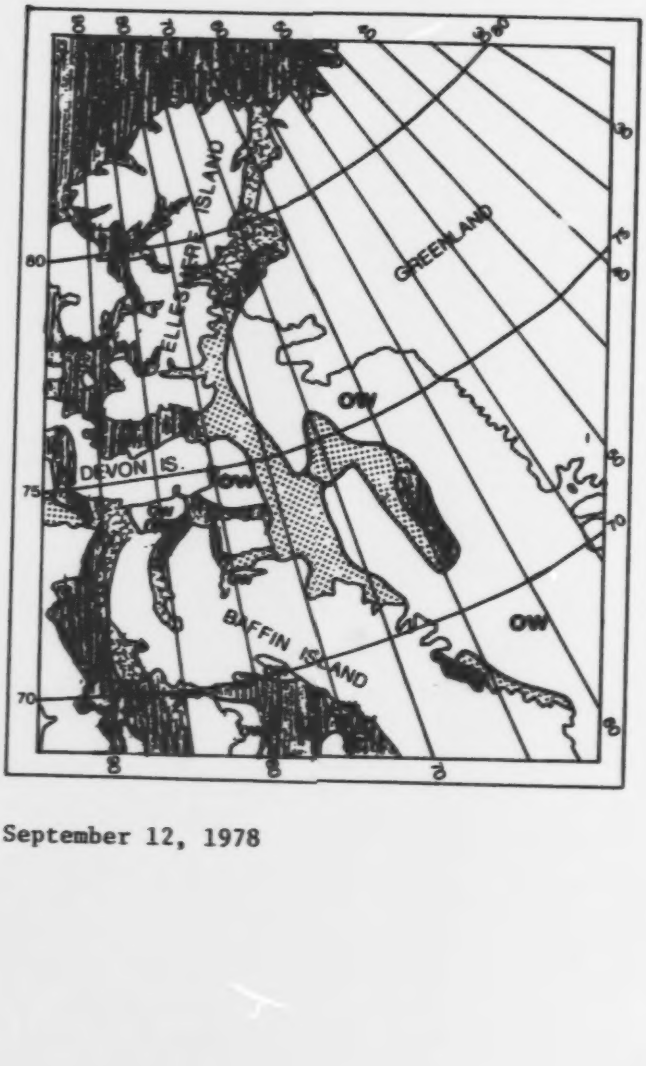
ELLESMERE ISLAND
GREENLAND
OW
DEVON IS.
OW
OW
BAFFIN ISLAND
80
75
70

September 12, 1978

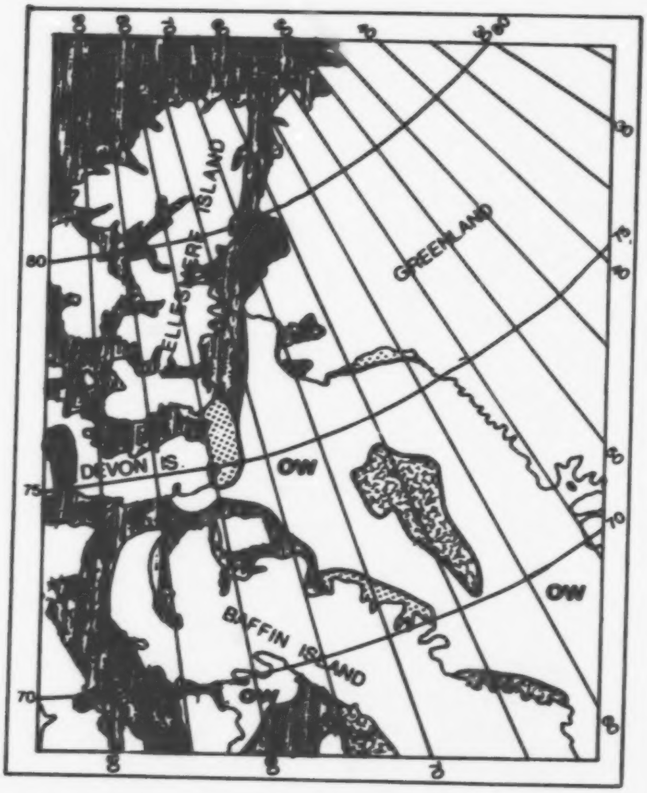
ELLESMERE ISLAND
GREENLAND
DEVON IS.
OW
OW
BAFFIN ISLAND
OW
80
75
70
60
70

September 26, 1978

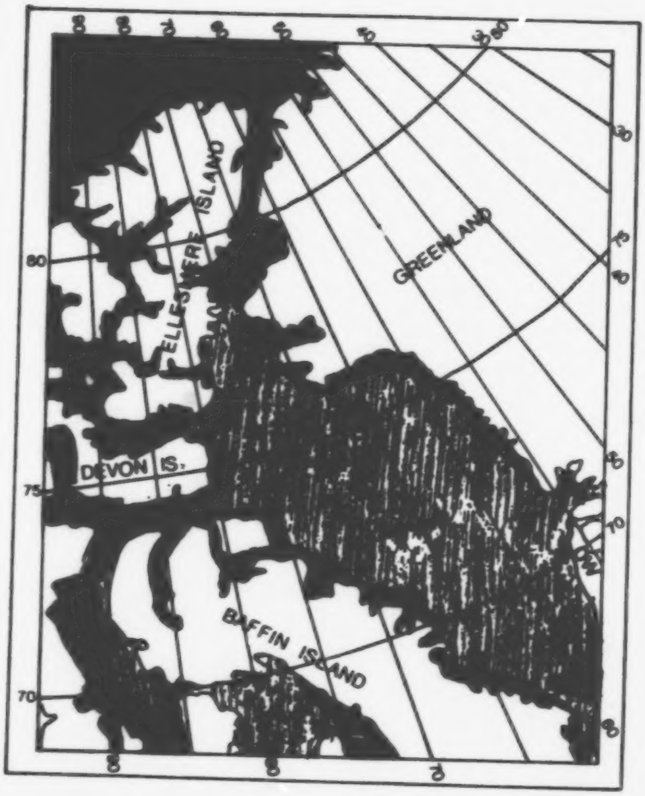
ELLESMERE ISLAND
GREENLAND
DEVON IS.
BAFFIN ISLAND
80
75
70

December 5, 1978

APPENDIX 2B

Ice conditions in Lancaster Sound and Northwest Baffin Bay, June 6, 1978 - December 5, 1978.

SYMBOLOGY

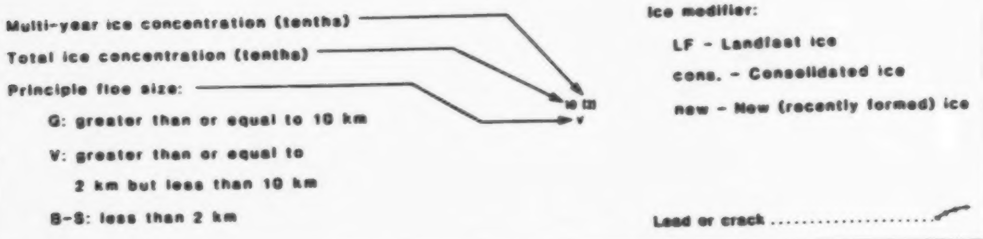
Multi-year ice concentration (tenths)
Total ice concentration (tenths)
Principle floe size:
G: greater than or equal to 10 km
V: greater than or equal to 2 km but less than 10 km
B-S: less than 2 km
10 (3)
V
Ice modifier:
LF - Landfast ice
cons. - Consolidated ice
new - New (recently formed) ice
Lead or crack

LEGEND

- ■ Fast ice (LF), Consolidated ice (cons.)
- □ Recently formed thin ice (new)
- □ Fracture zone
- ■ Very close pack
- □ Close pack
- ■ Open pack
- □ Very open pack
- ◪ Open water (O.W.), Bergy water (B.W.)

JUNE 6, 1978

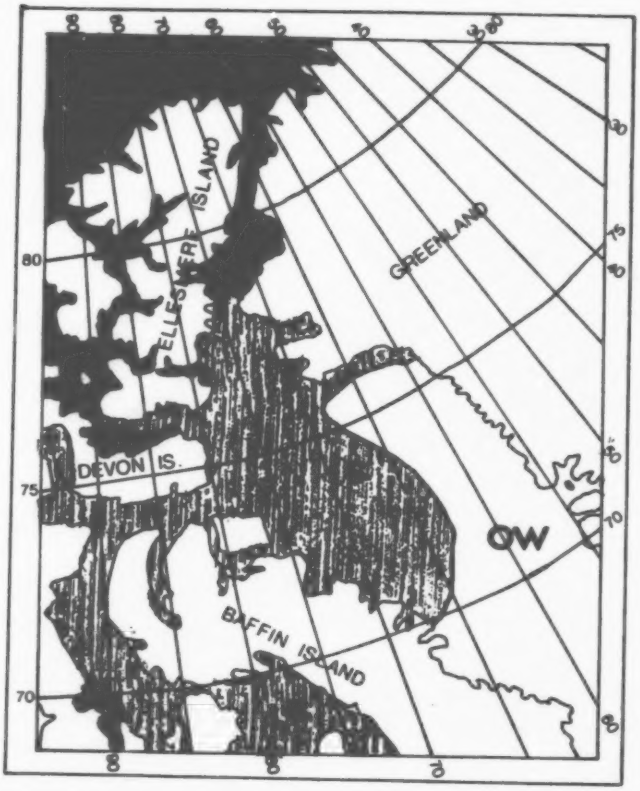
ELLESMERE ISLAND
GREENLAND
DEVON IS.
BAFFIN ISLAND
OW
80
75
70
70

October 10, 1978

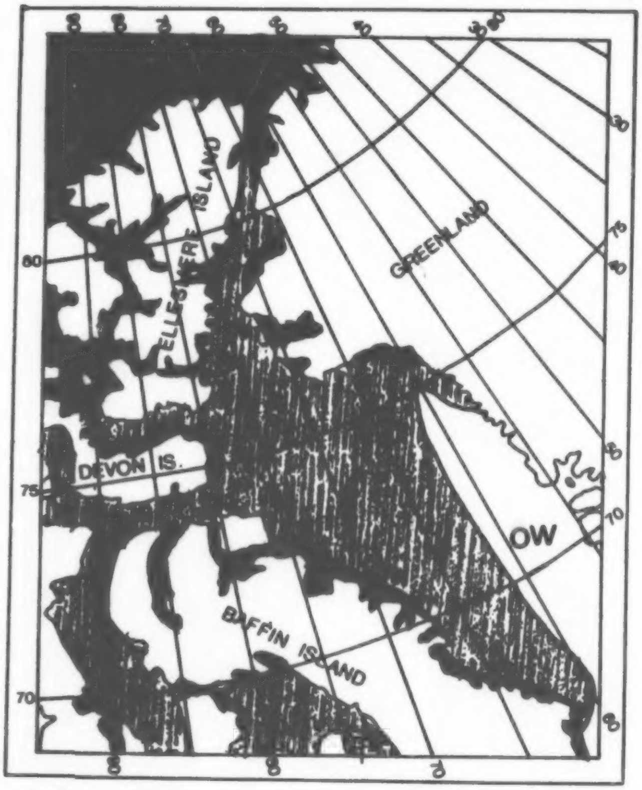
ELLESMERE ISLAND
GREENLAND
80
DEVON IS.
75
OW
70
BAFFIN ISLAND
70

October 24, 1978

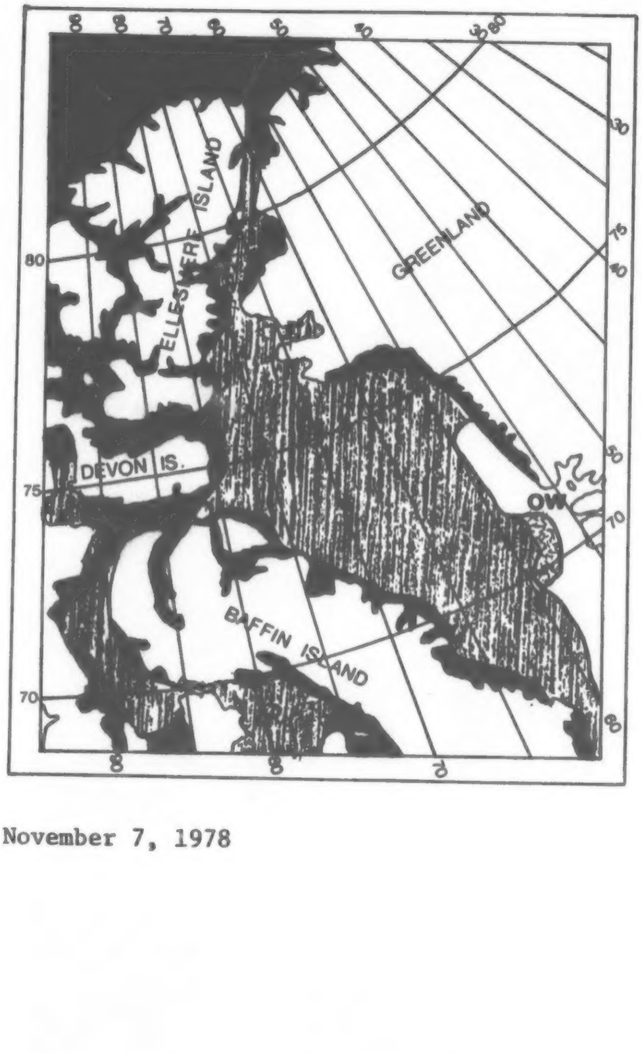
ELLESMERE ISLAND
GREENLAND
DEVON IS.
BAFFIN ISLAND
OW
80
75
70

November 7, 1978

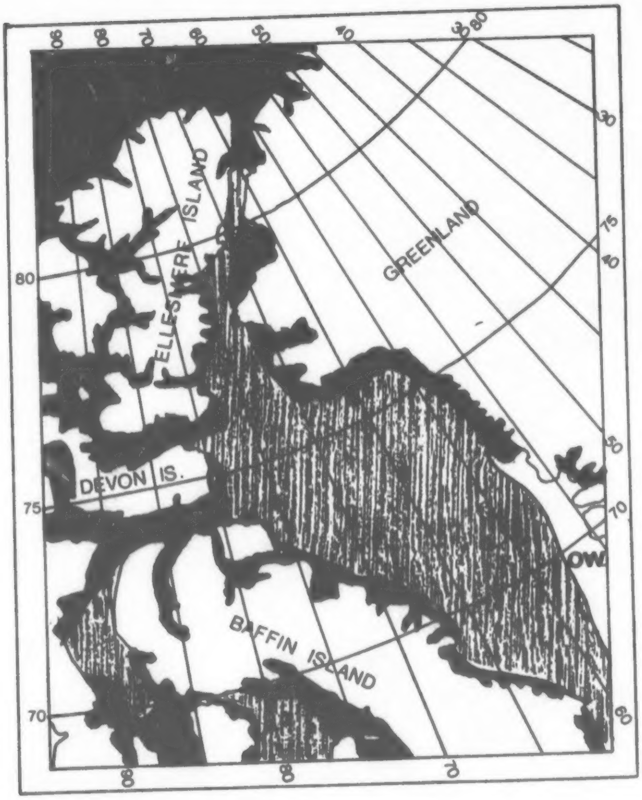
90
80
70
60
50
40
30
80
30
75
40
80
ELLESMERE ISLAND
GREENLAND
DEVON IS.
75
50
70
OW
BAFFIN ISLAND
70
60
80
80
70

November 21, 1978

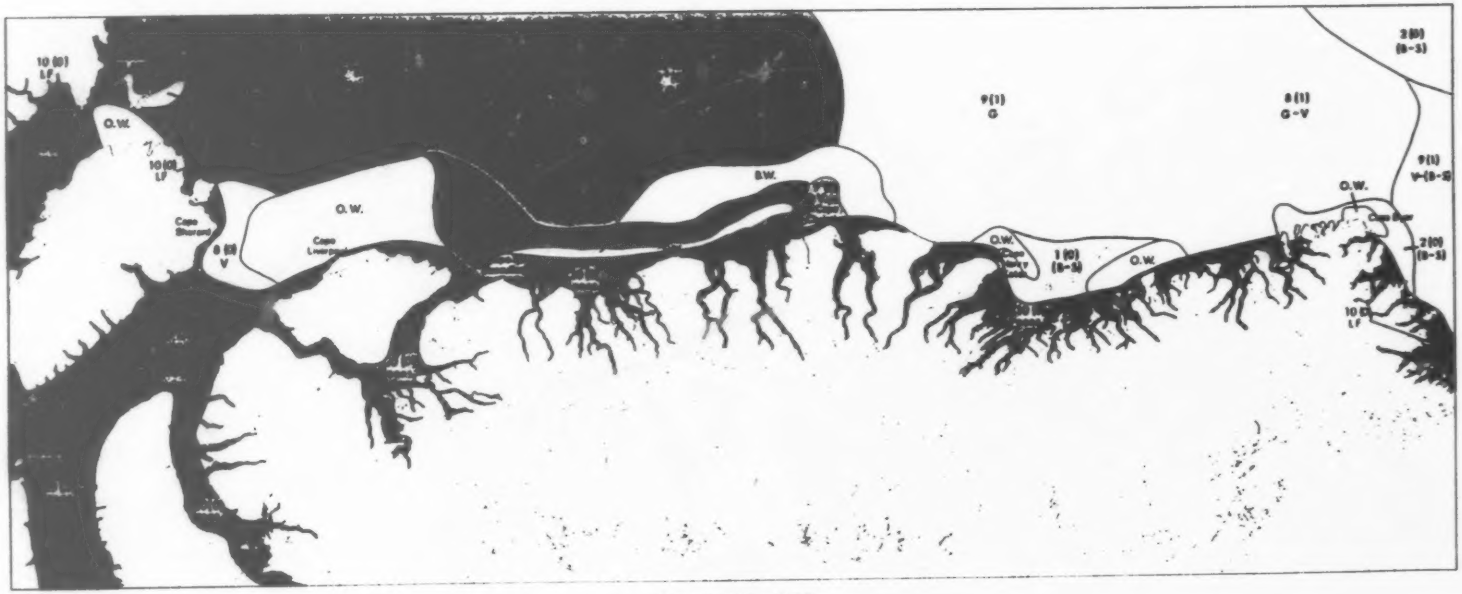
10 (0)
LF
O.W.
10 (0)
LF
Cape
Sherard
8 (0)
V
O.W.
Cape
Liverpool
B.W.
9 (1)
G
O.W.
1 (0)
(B-S)
O.W.
8 (1)
G-V
2 (0)
(B-S)
9 (1)
V-(B-S)
O.W.
Cape Byam
2 (0)
(B-S)
10 (0)
LF

JUNE 20, 1978

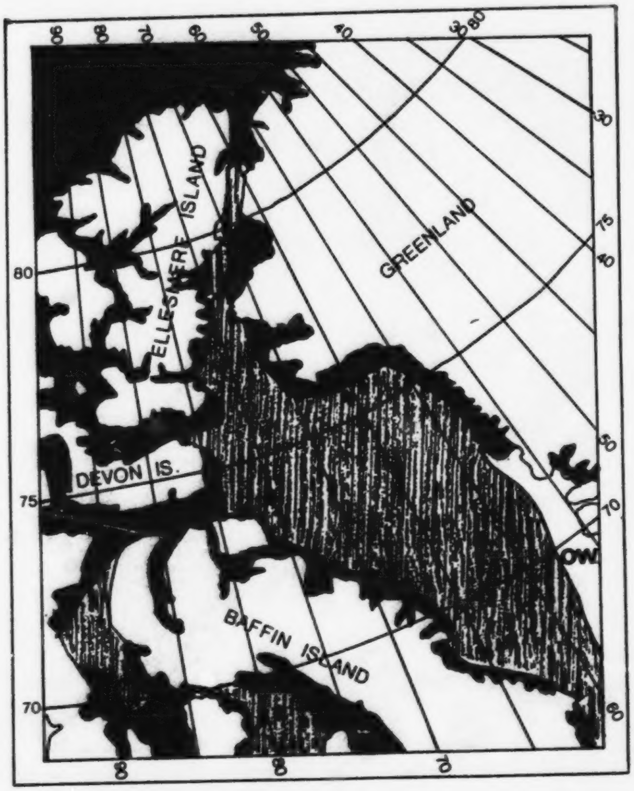
90
80
70
60
50
40
30
80
30
75
40
ELLESMERE ISLAND
GREENLAND
80
DEVON IS.
75
50
70
OW
BAFFIN ISLAND
70
60
90
80
70

November 21, 1978

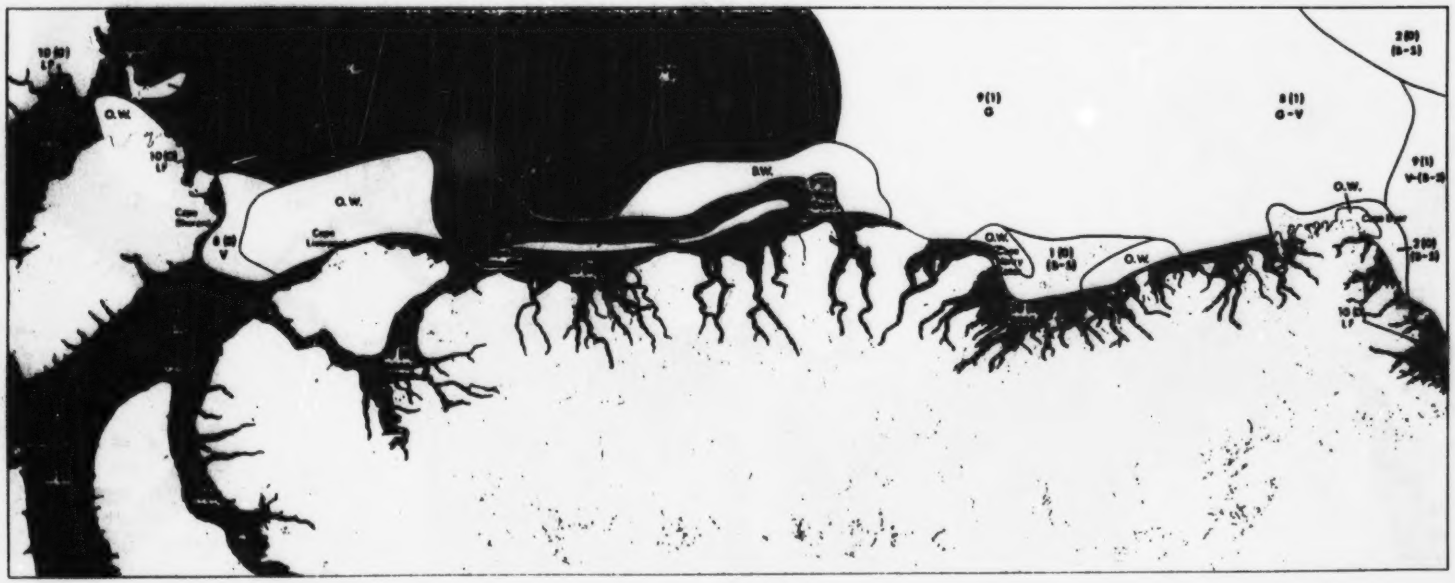

10 (0)
LF
O.W.
10 (0)
LF
8 (0)
V
O.W.
S.W.
9 (1)
G
O.W.
1 (0)
O.W.
8 (1)
G-V
2 (0)
9 (1)
O.W.
2 (0)
10 (0)
LF

JUNE 20, 1978

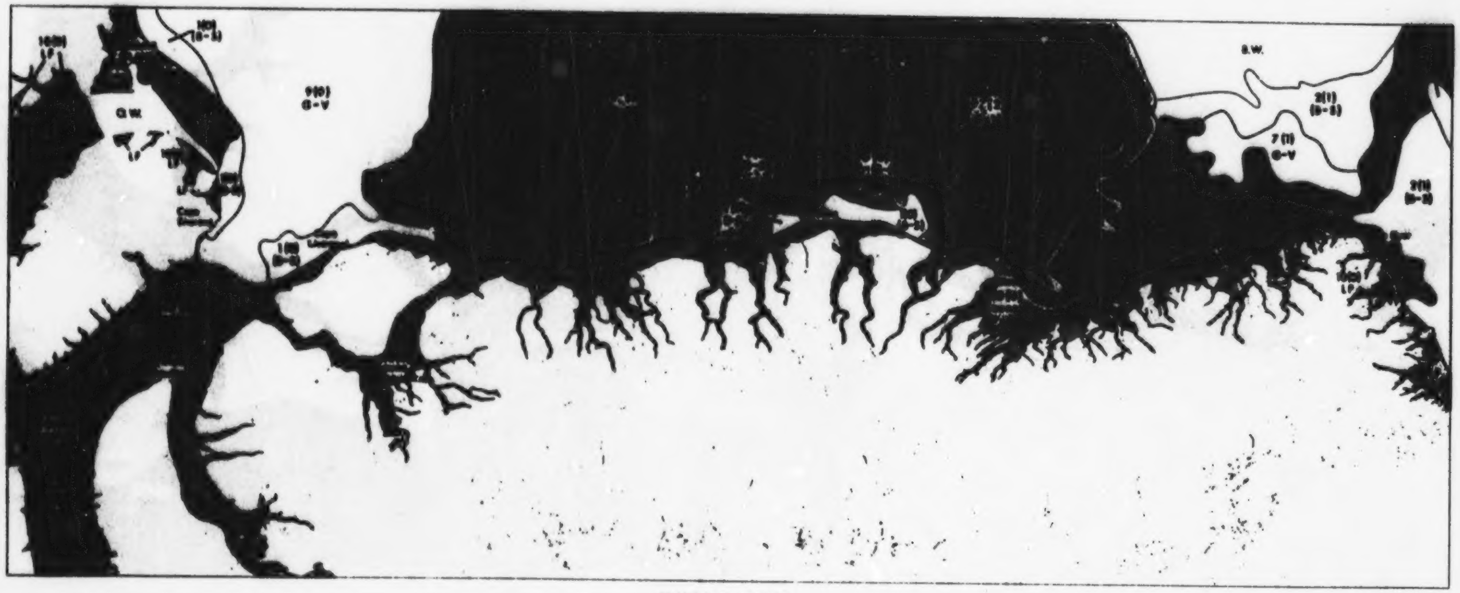

JULY 4, 1978

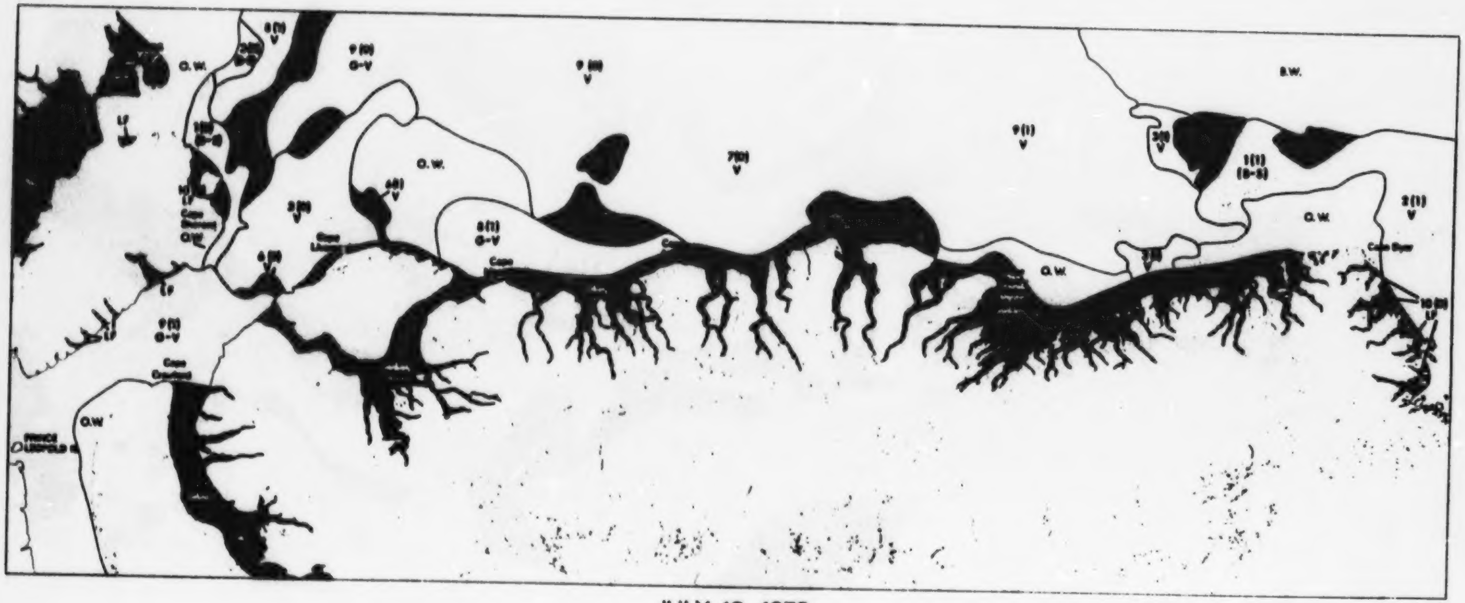
O.W.
O.W.
O.W.
O.W.
O.W.
B.W.
9(1)
V
7(0)
V
Cape Crawford
PRINCE LEOPOLD IS.

JULY 18, 1978

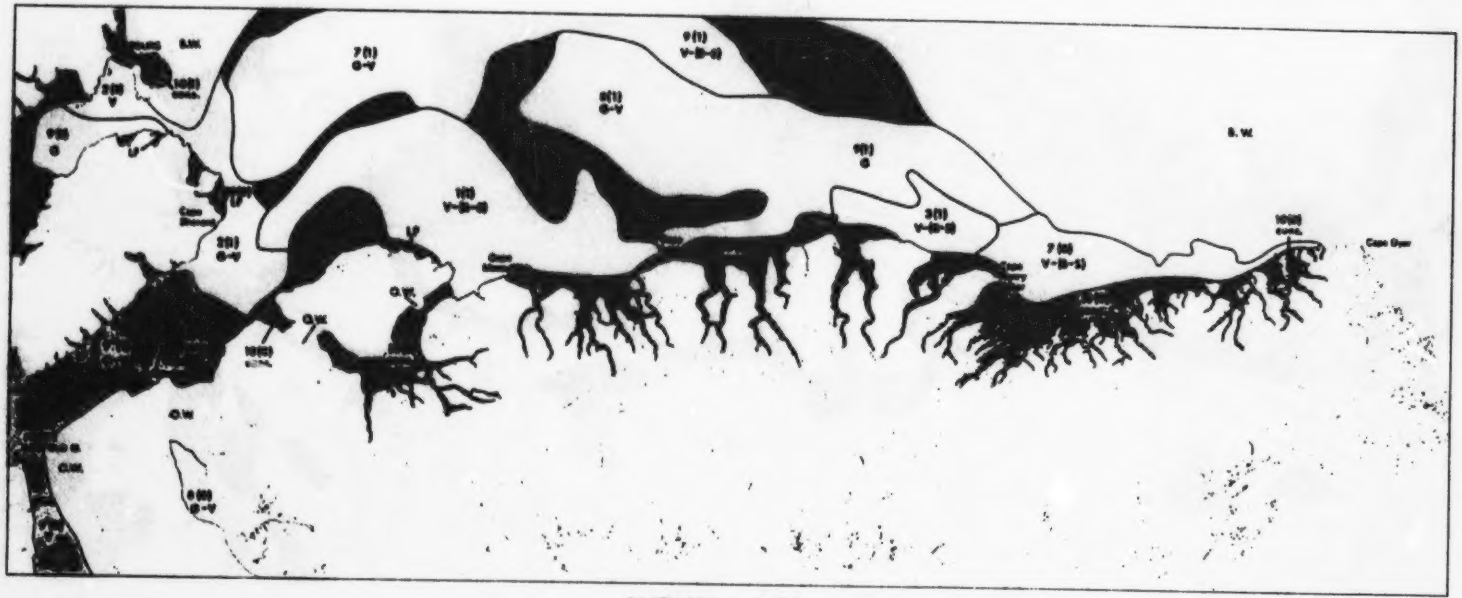
S.W.
7 (1)
G-V
9 (1)
V-(B-G)
5(1)
G-V
1(1)
V-(B-G)
9(1)
G
3(1)
V-(B-G)
7 (2)
V-(B-S)
10(2)
cont.
S.W.
Cape Dyer
3(1)
G-V
O.W.
O.W.
O.W.
10(2)
cont.
8 (2)
G-V

AUGUST 1, 1978

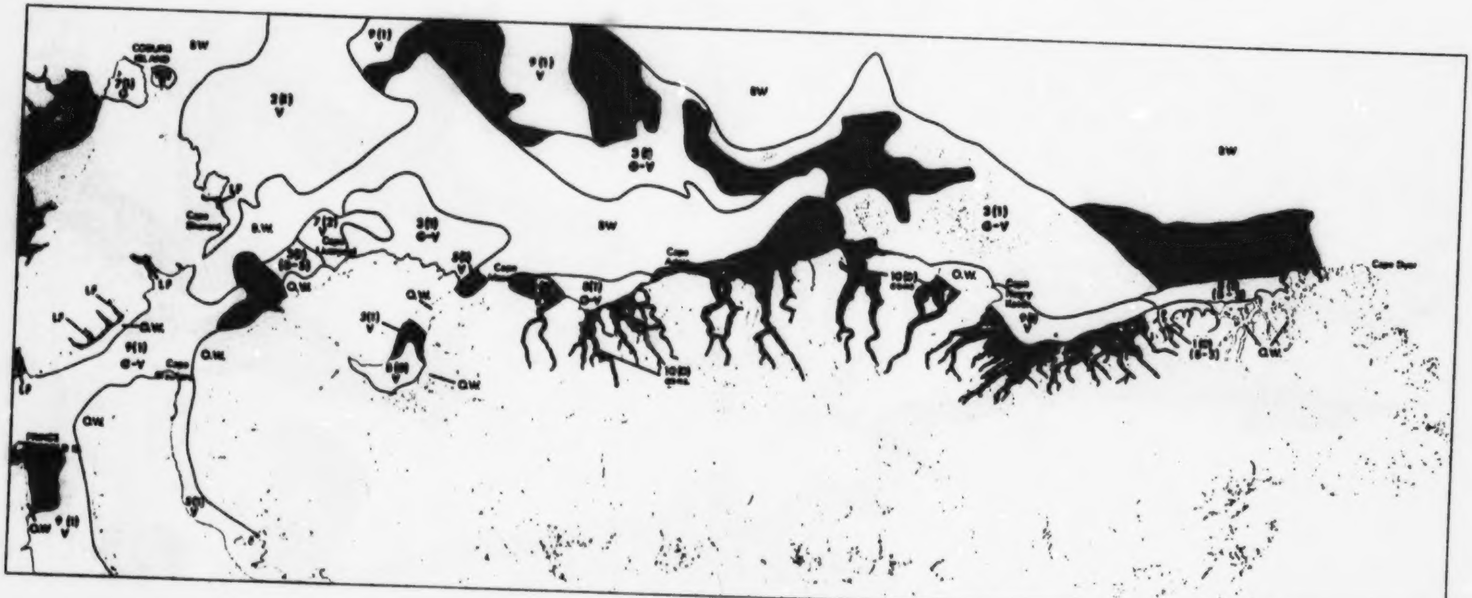
COBURG ISLAND
SW
9 (1)
V
3 (1)
G-V
O.W.
LF
Cape Dyer

AUGUST 15, 1978

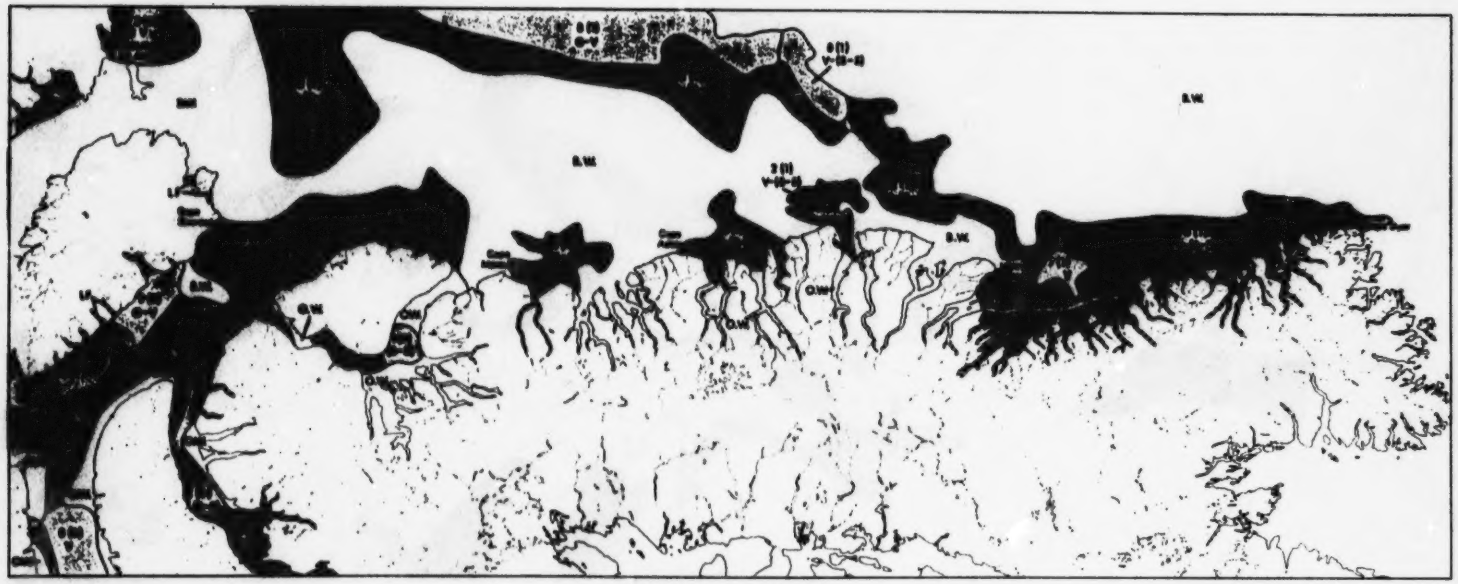
S.W.
S.W.
S.W.
O.W.
O.W.

AUGUST 29, 1978

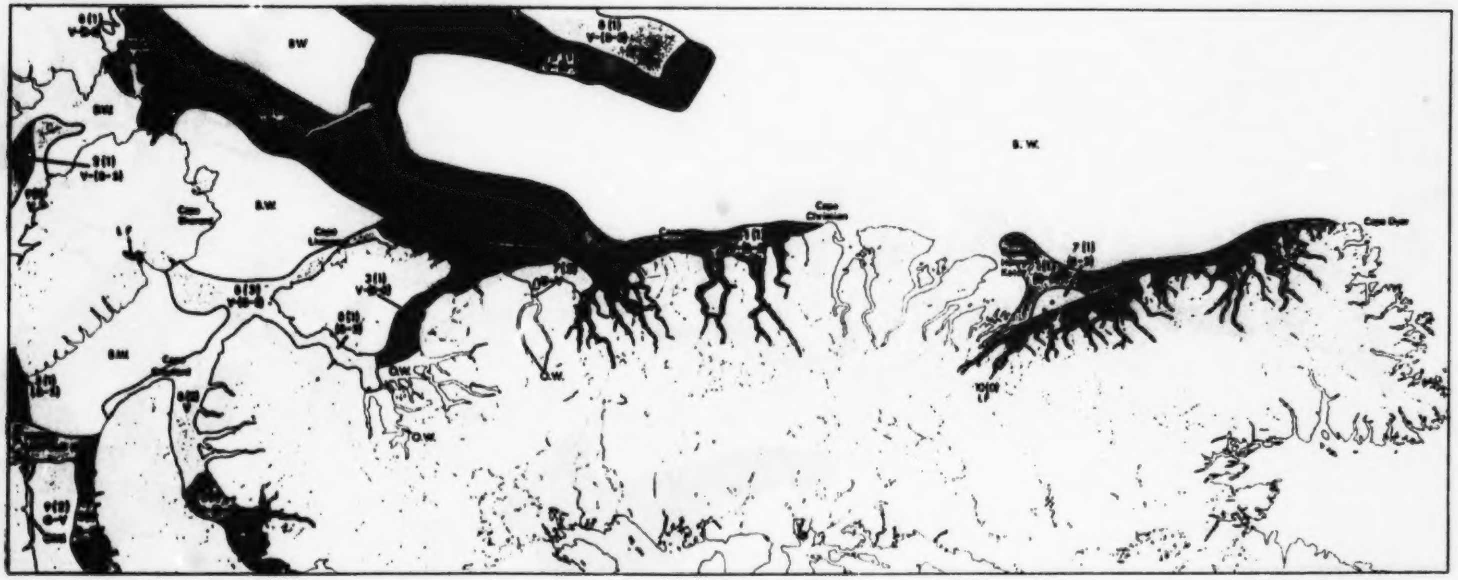
S.W.
Cape Christian
Cape Dyer
7 (1)
O.W.
O.W.
S.W.

SEPTEMBER 12, 1978

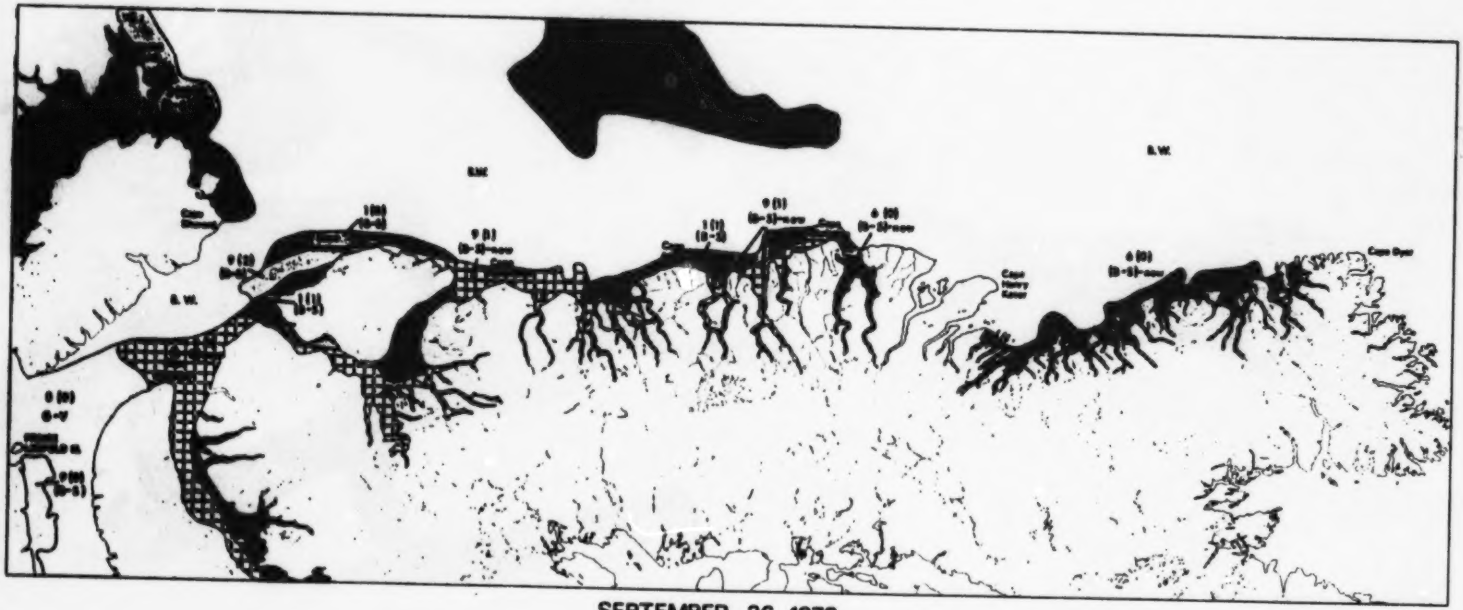
S.W.
Cape Henry Kater
Cape Dyer

SEPTEMBER 26, 1978

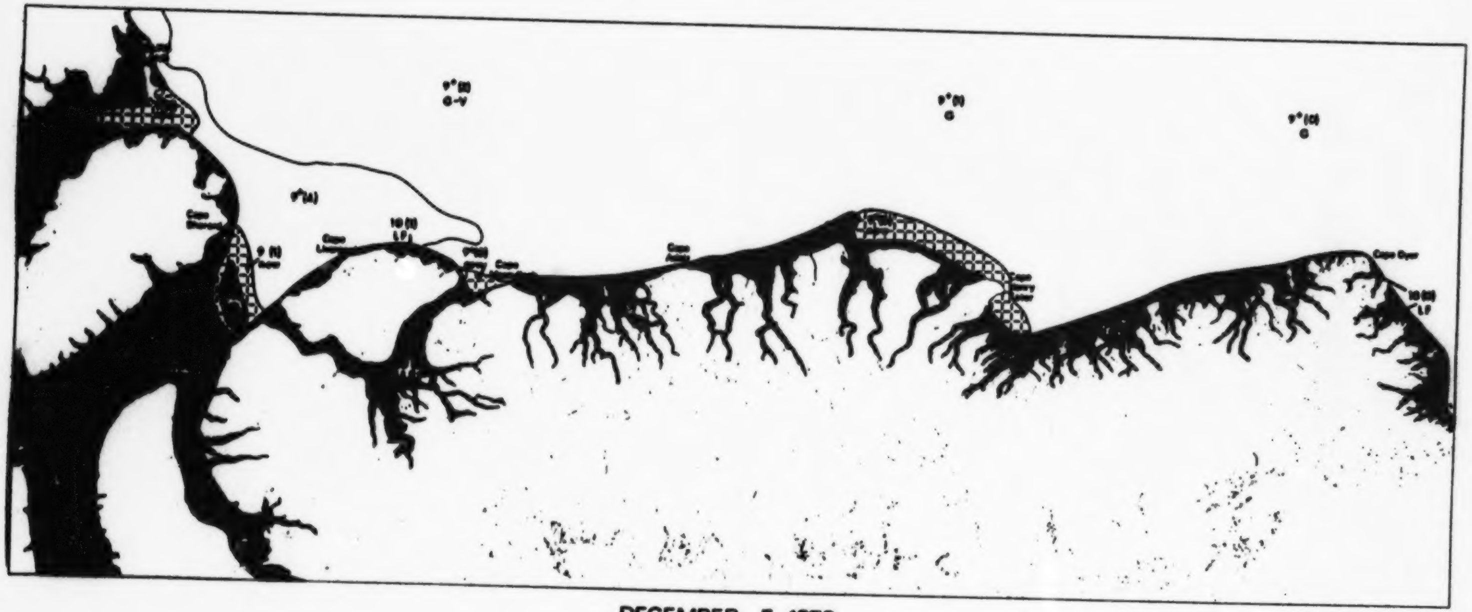

G-V
G
G
Cape Dyer
LF

DECEMBER 5, 1978

APPENDIX 3A

Ice concentrations mapped at two week Intervals, June 12 - vember 13, 1979.
November 13, 1979

KEY TO ICE CONCENTRATION MAPS

■	10/10 coverage (consolidated or landfast ice)
▩	7/10 - 9+/10 coverage
▦	4/10 - 6/10 coverage
░	1/10 - 3/10 coverage
OW	less than 1/10 coverage (open water)

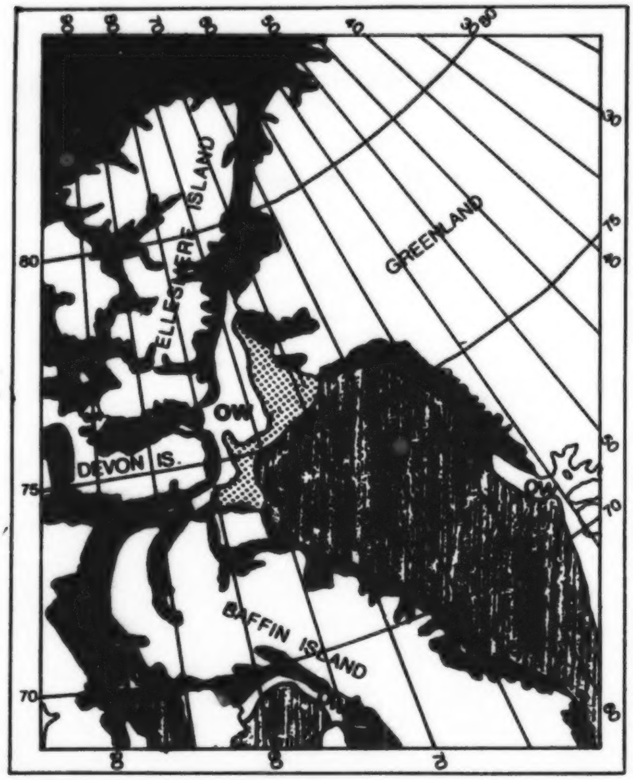
ELLESMERE ISLAND
GREENLAND
OW
DEVON IS.
OW
BAFFIN ISLAND
80
75
70

June 12, 1979

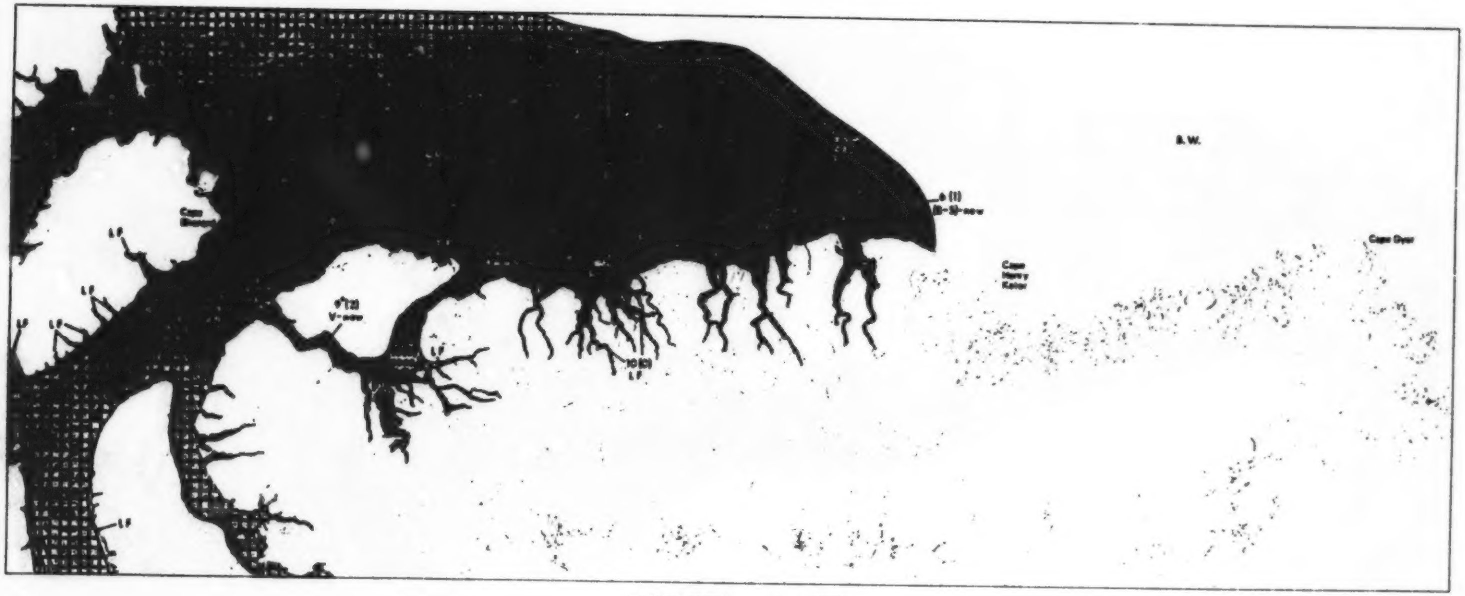
B. W.
6 (1)
(3-5)-new
Cape Dyer
Cape Henry Kater
10(2)
LF
9(2)
V-new
LF
LF
LF
LF
LF
LF

OCTOBER 10, 1978

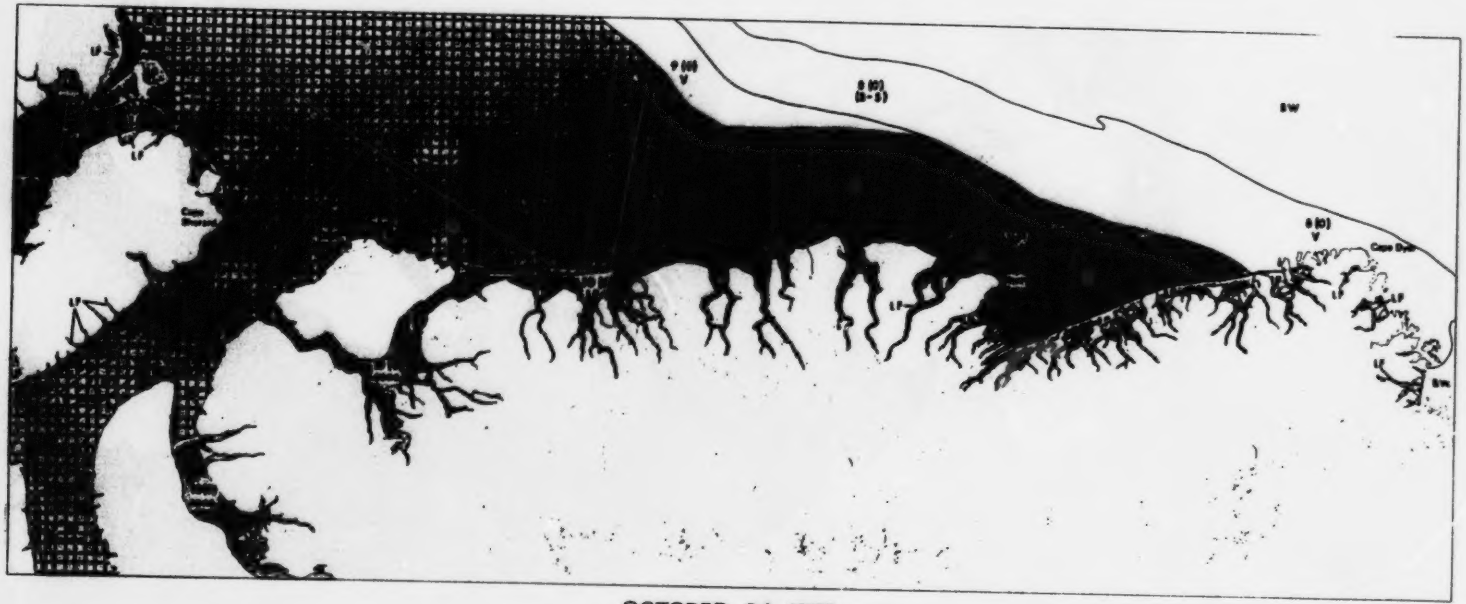
SW
Cape Dyer
LF
LF
SW

OCTOBER 24, 1978

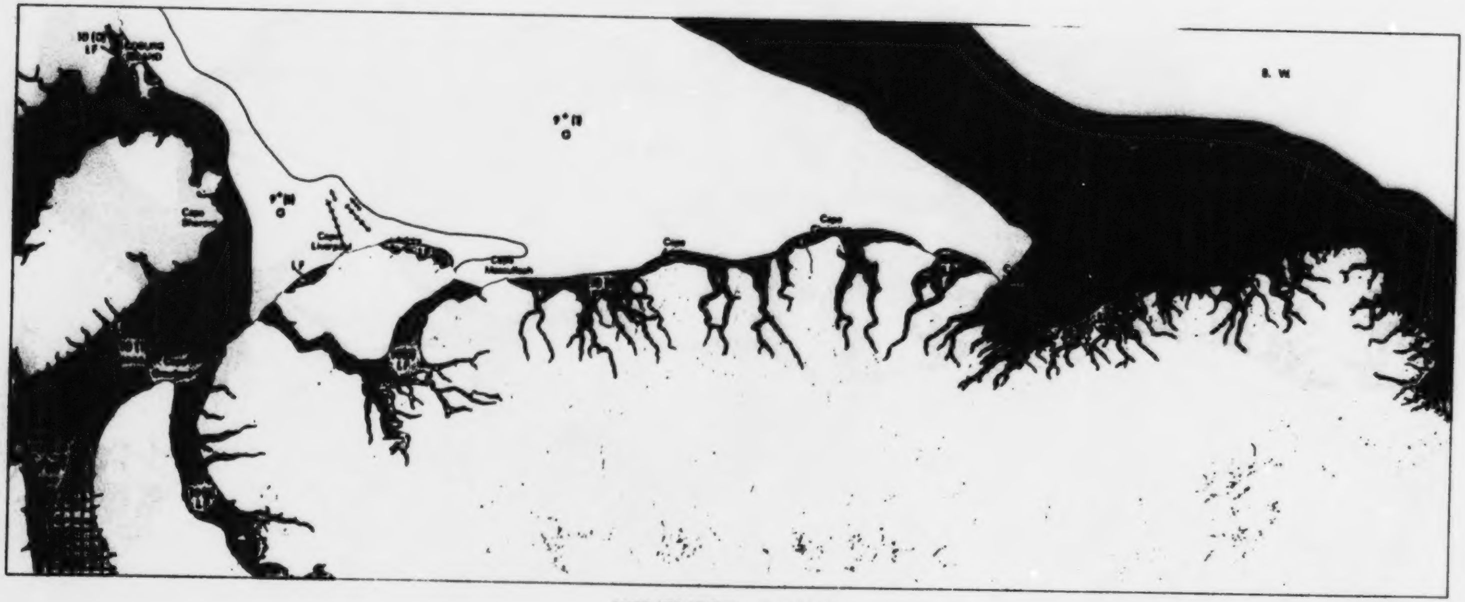
Cape Liverpool
S. W

NOVEMBER 7, 1978

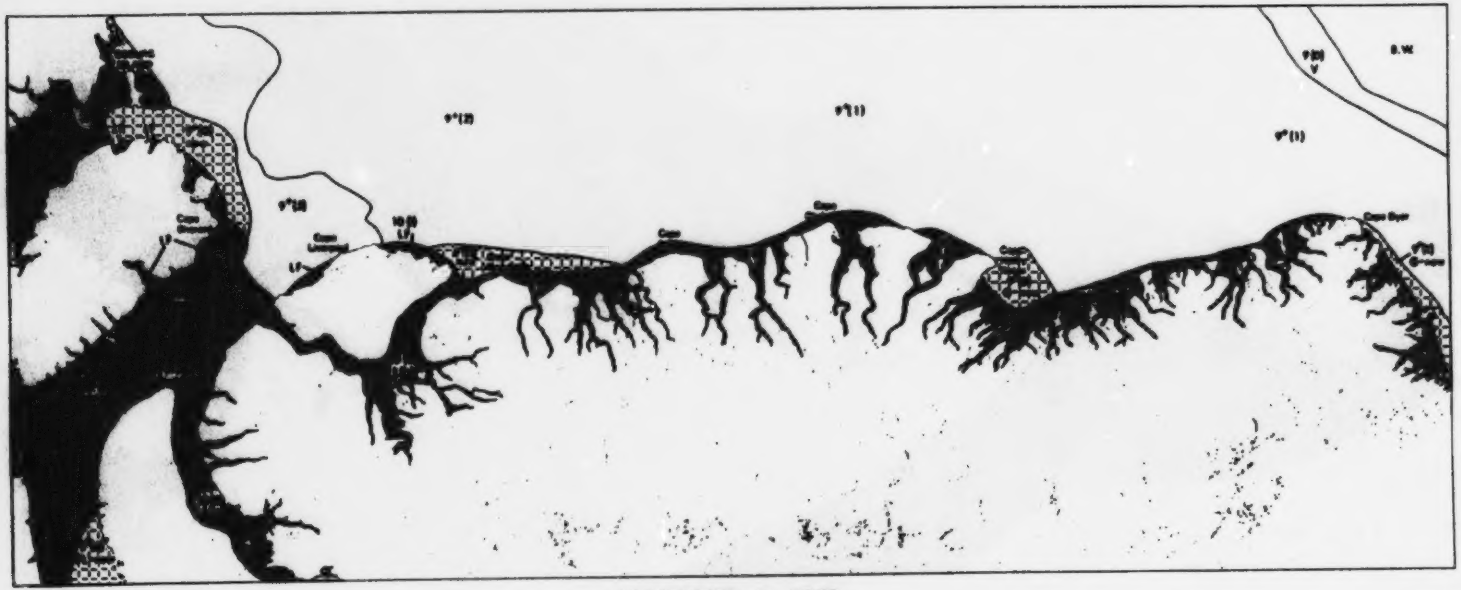
S.W
9°(1)
9°(1)
9°(2)
9°(2)
10 (1)

NOVEMBER 21, 1978

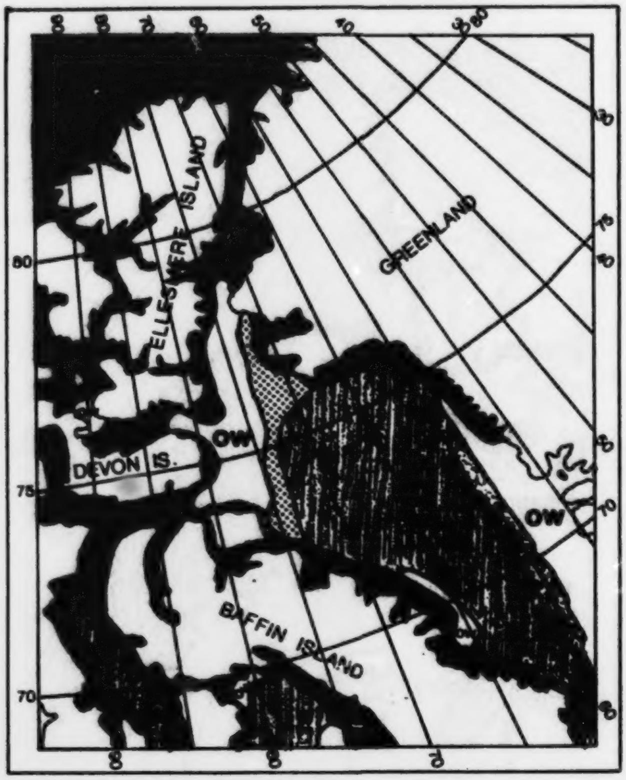
ELLESMERE ISLAND
GREENLAND
DEVON IS.
OW
OW
BAFFIN ISLAND
80
75
70
50
40

June 26, 1979

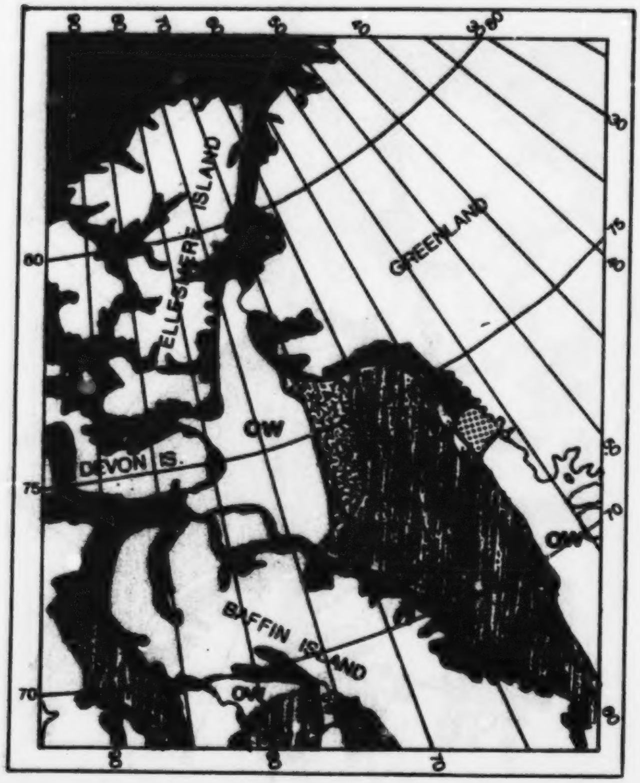
ELLESMERE ISLAND
GREENLAND
OW
DEVON IS.
OW
BAFFIN ISLAND
OW
80
75
70
70
75
80
70

July 10, 1979

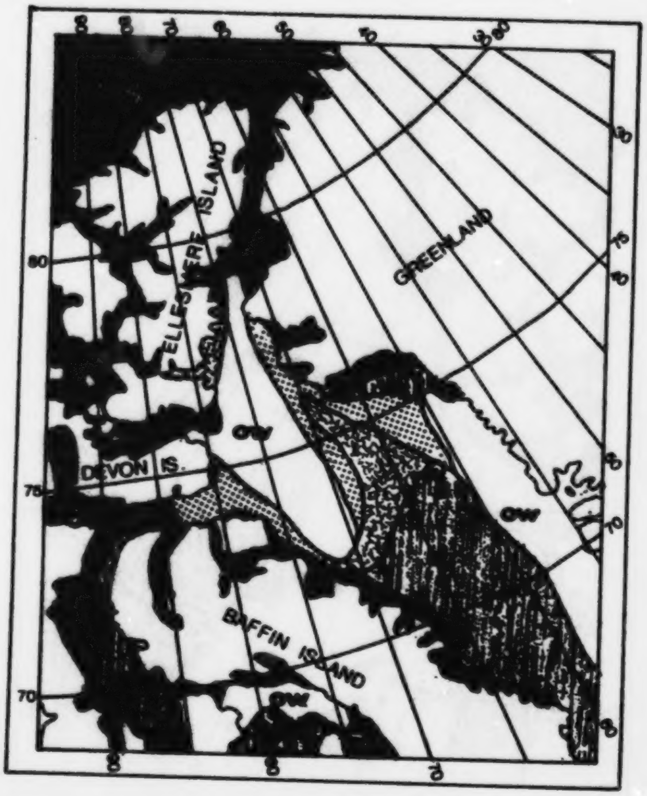
ELLESMERE ISLAND
GREENLAND
DEVON IS.
BAFFIN ISLAND
OW
OW
OW
80
75
70

July 24, 1979

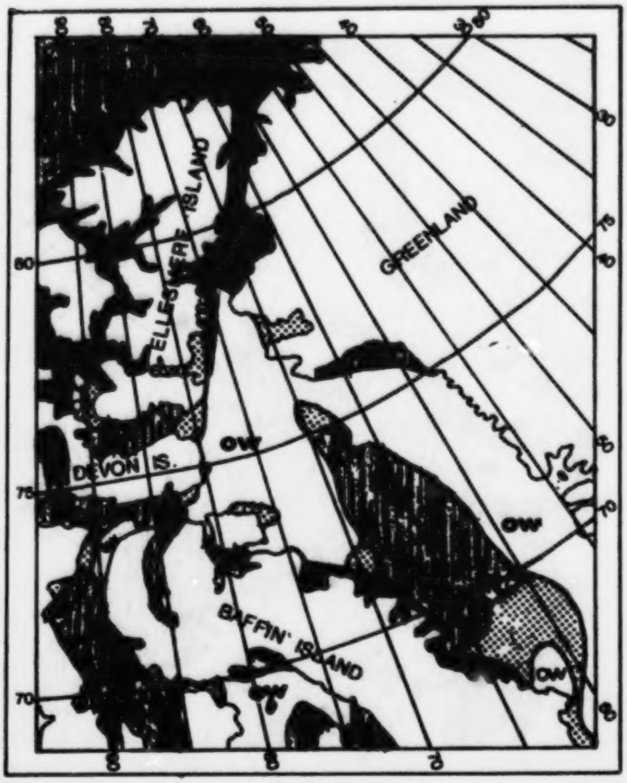
ELLESMERE ISLAND
GREENLAND
DEVON IS.
BAFFIN ISLAND
OW
OW
OW
OW
80
75
70
80
75
70

August 7, 1979

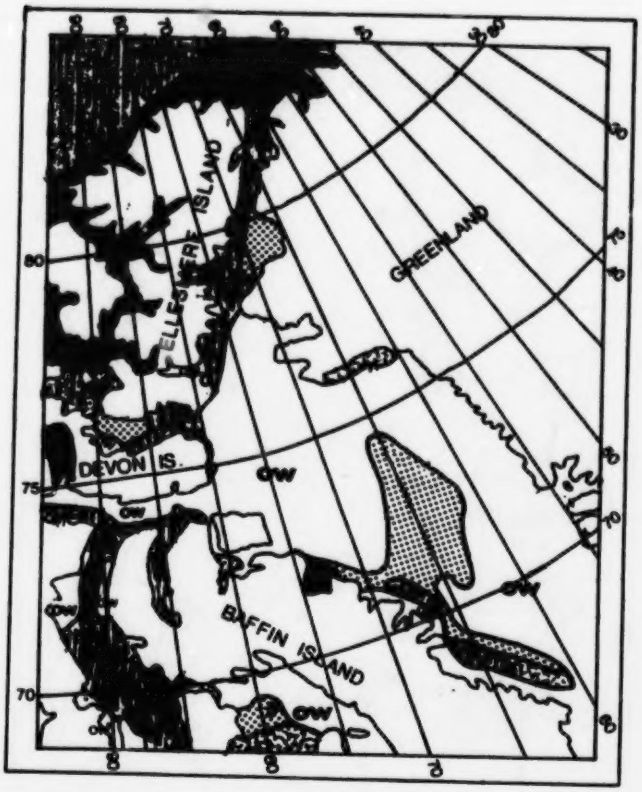
ELLESMERE ISLAND
GREENLAND
DEVON IS.
BAFFIN ISLAND
OW
OW
OW
OW
OW
80
75
70
80
75
70
65

August 21, 1979

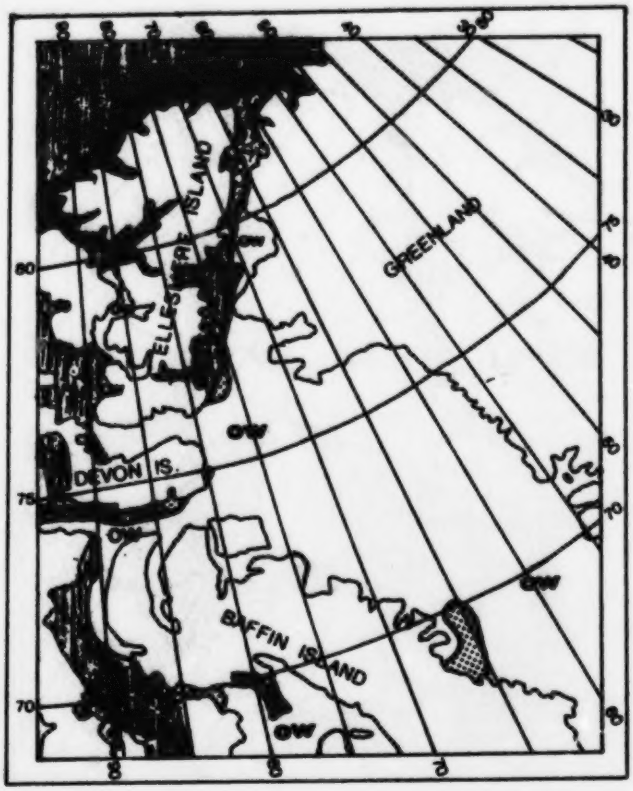
ELLESMERE ISLAND
GREENLAND
DEVON IS.
BAFFIN ISLAND
OW
OW
OW
OW
OW
80
75
70

September 4, 1979

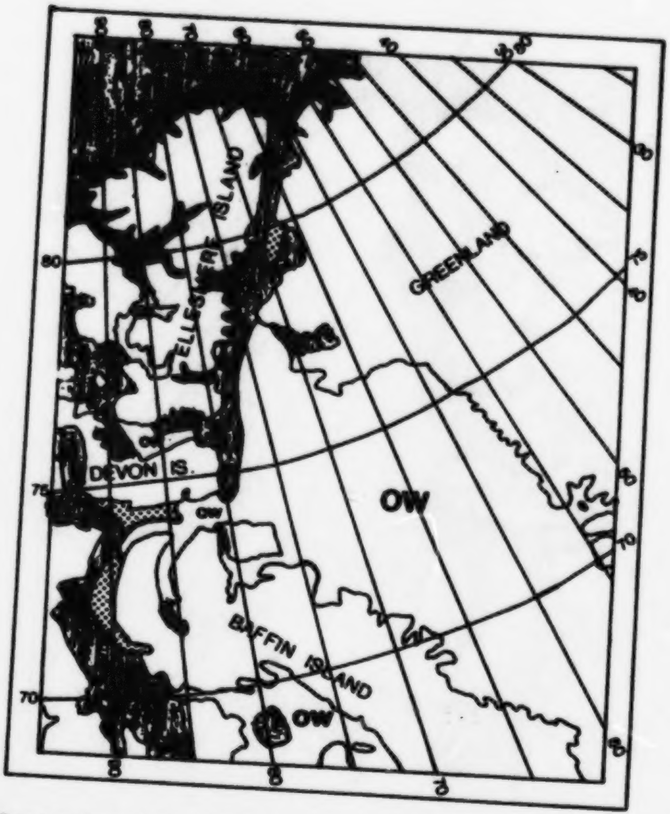
ELLESMERE ISLAND
GREENLAND
DEVON IS.
BAFFIN ISLAND
OW
OW
OW
OW
80
75
70

September 18, 1979

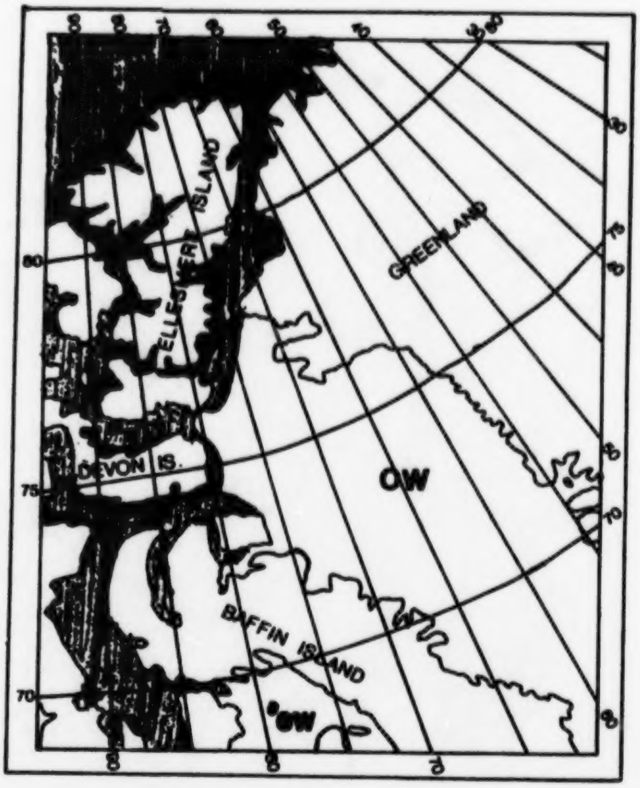
ELLESMERE ISLAND
GREENLAND
DEVON IS.
OW
BAFFIN ISLAND
OW
80
75
70

October 2, 1979

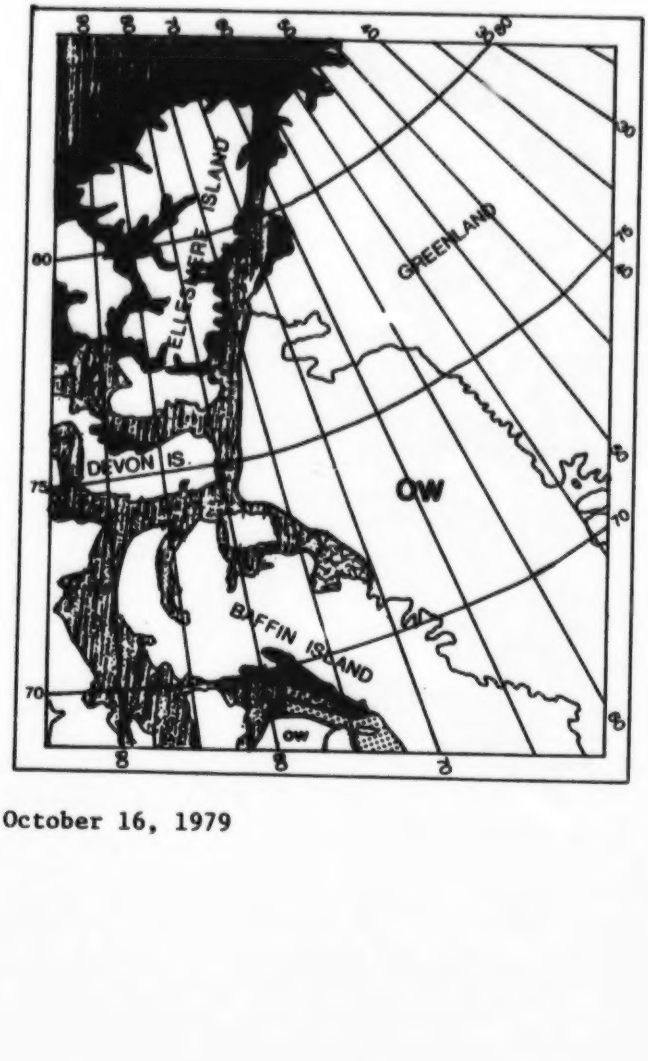
ELLESMERE ISLAND
GREENLAND
80
75
70
40
30
DEVON IS.
OW
BAFFIN ISLAND
OW

October 16, 1979

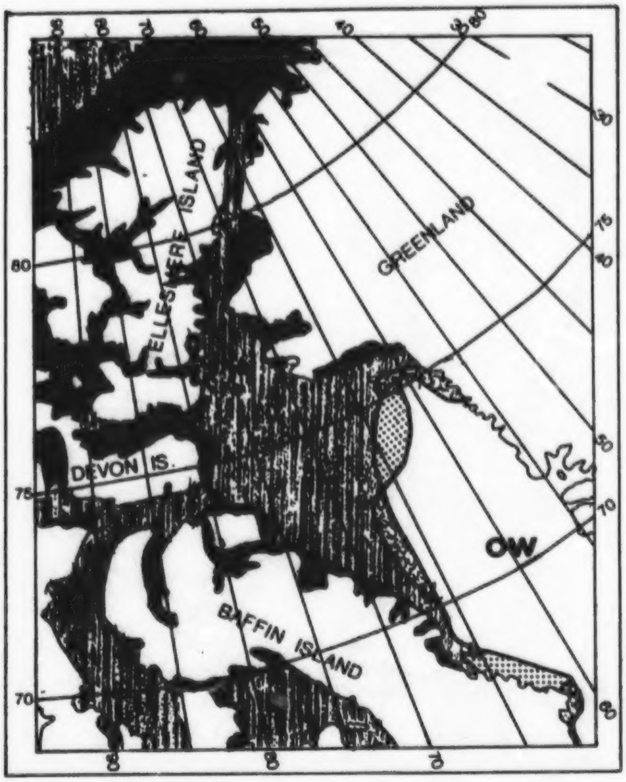
ELLESMERE ISLAND
GREENLAND
DEVON IS.
BAFFIN ISLAND
OW
80
75
70

October 30, 1979

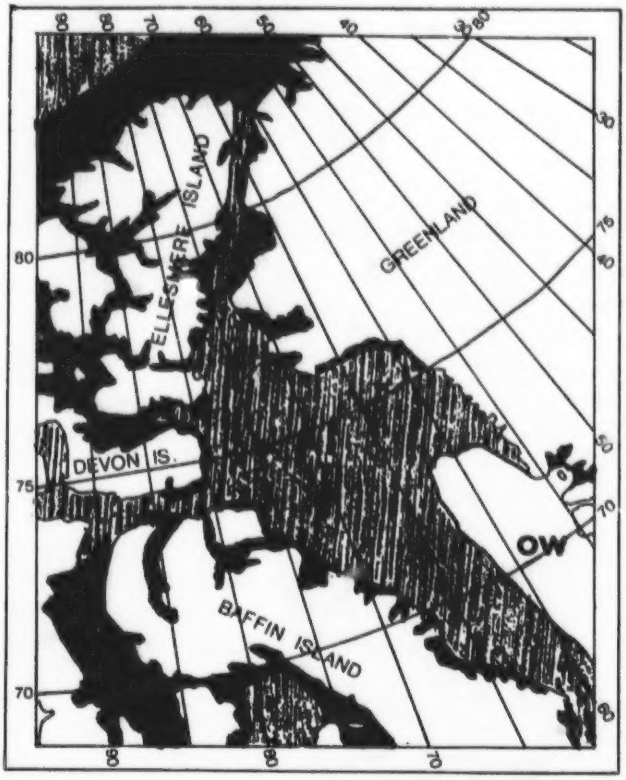
ELLESMERE ISLAND
GREENLAND
DEVON IS.
BAFFIN ISLAND
OW
80
75
70
60
50
40
30

November 13, 1979

APPENDIX 3B

Ice conditions in Lancaster Sound and Northwest Baffin Bay, June 12, 1979 - November 13, 1979.

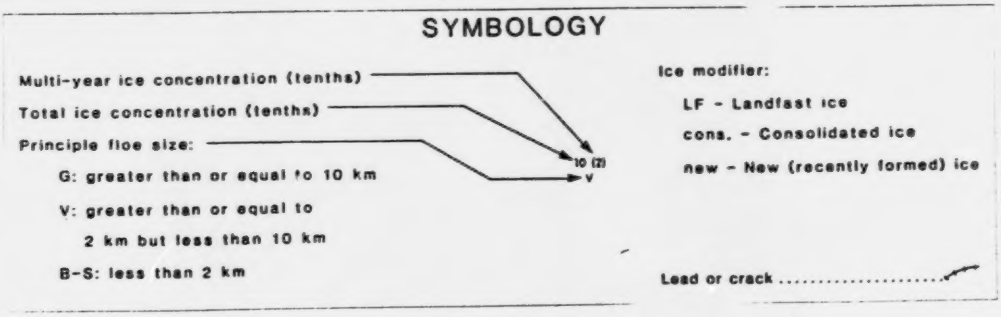

SYMBOLOGY

Multi-year ice concentration (tenths)

Total ice concentration (tenths)

Principle floe size:

G: greater than or equal to 10 km

V: greater than or equal to 2 km but less than 10 km

B-S: less than 2 km

Ice modifier:

LF - Landfast ice

cons. - Consolidated ice

new - New (recently formed) ice

Lead or crack ....

LEGEND

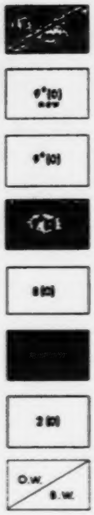

Fast ice (LF), Consolidated ice (cons.)

Recently formed thin ice (new)

Fracture zone

Very close pack

Close pack

Open pack

Very open pack

Open water (O.W.), Bergy water (B.W.)

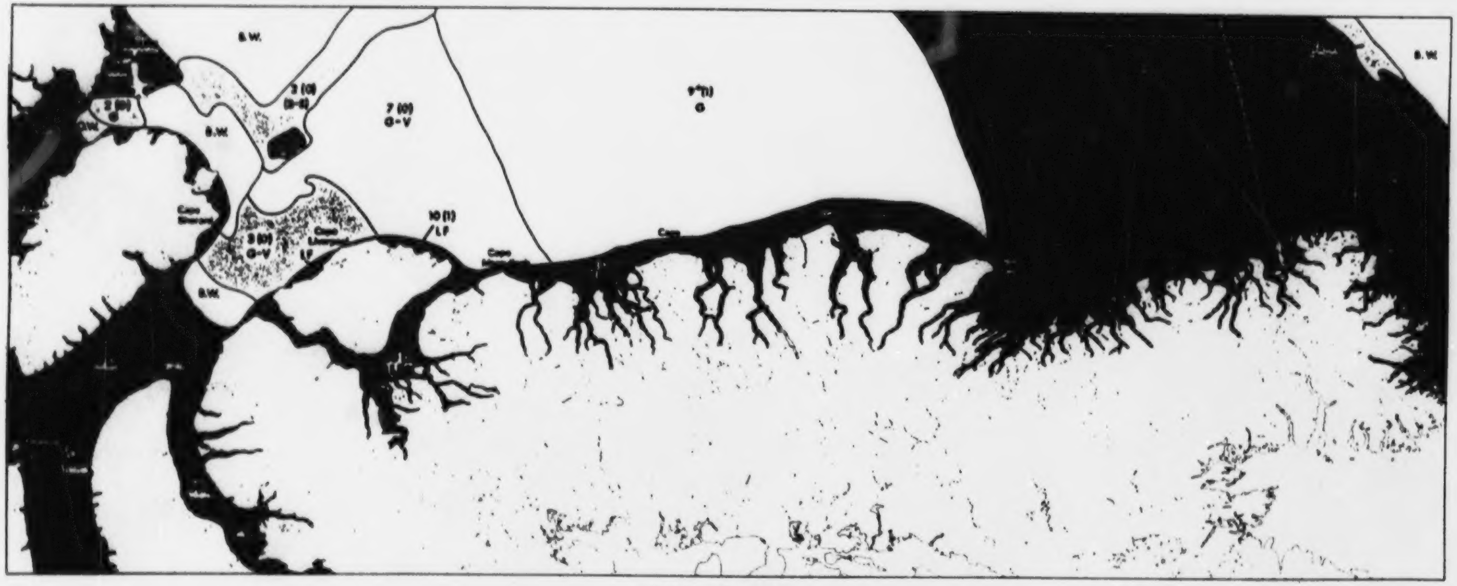
S.W.
2 (0)
G
S.W.
3 (0)
7 (0)
G-V
9 (1)
G
3 (0)
G-V
LF
10 (1)
LF
S.W.
S.W.

JUNE 12, 1979

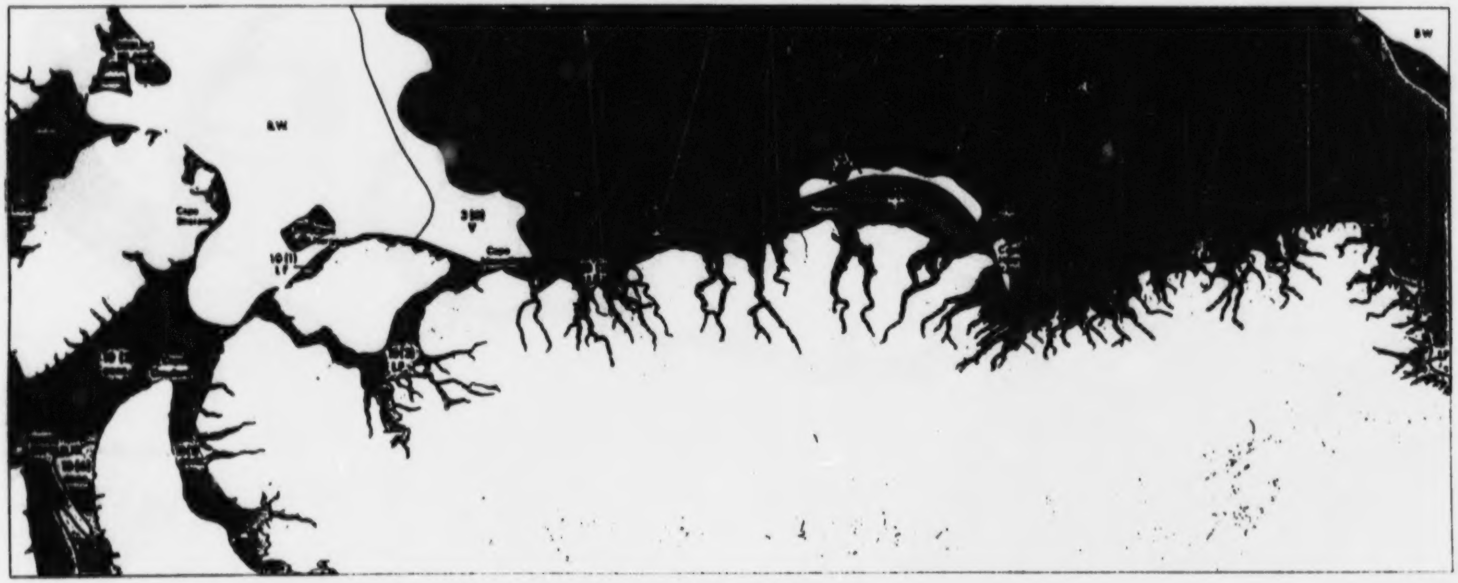

JUNE 26, 1979

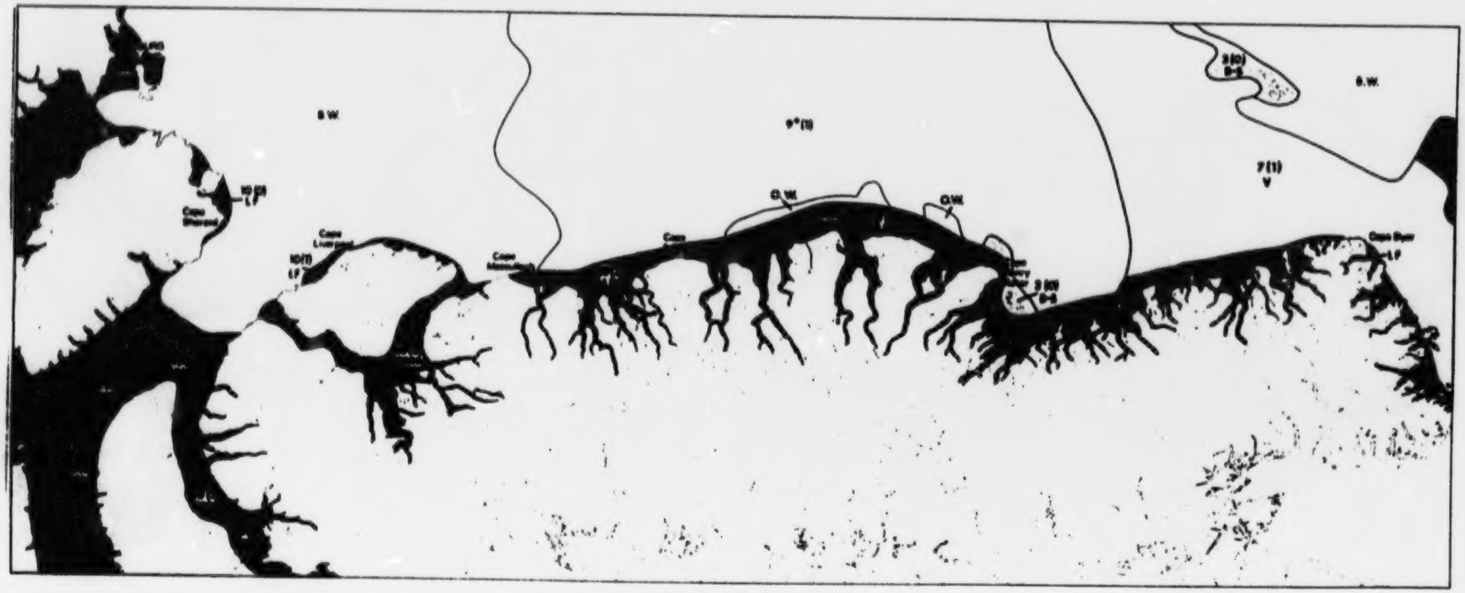
B.W.
Cape Sherard
Cape Liverpool
9⁺(1)
O.W.
O.W.
7(1)
V
B.W.

JULY 10, 1979

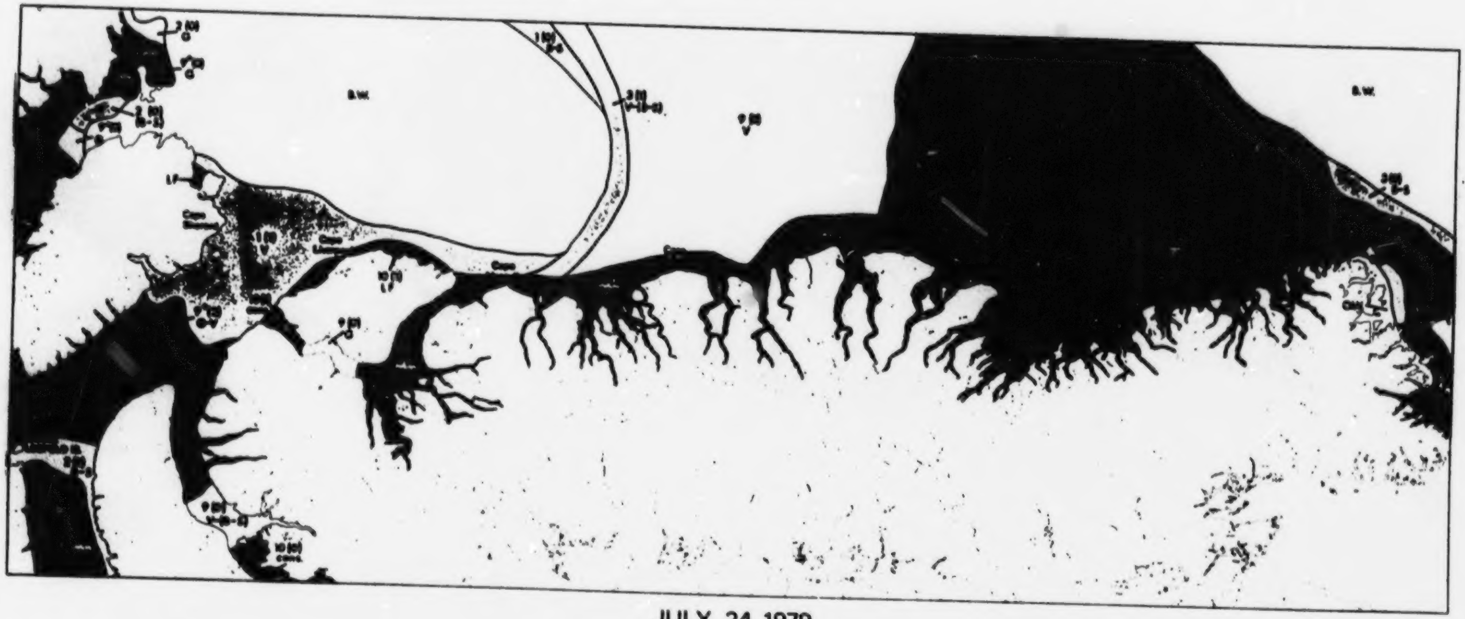

JULY 24, 1979

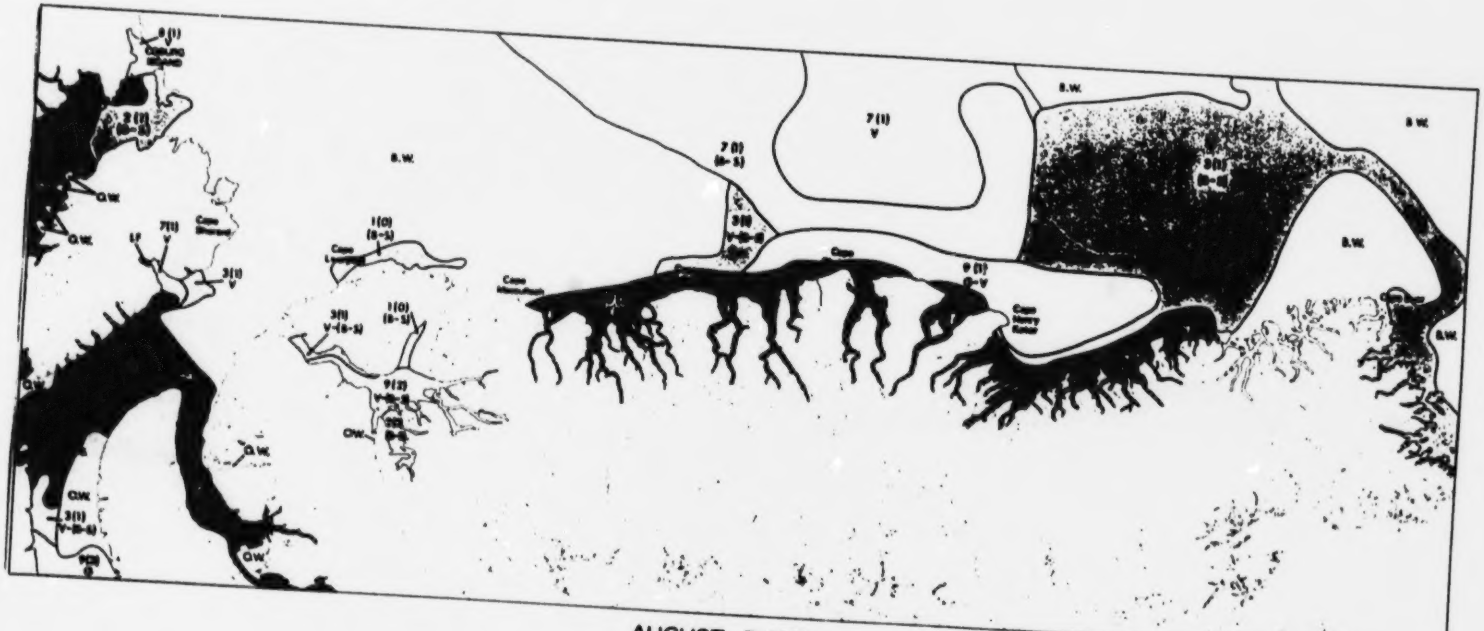
B.W.
O.W.
7(I)
V
3(I)
V
1(O)
(B-S)
3(I)
V-(B-S)
1(O)
(B-S)
9(2)
3(I)
7 (I)
(B-S)
7 (I)
V
9 (I)
O-V
Cape
Henry

AUGUST 7, 1979

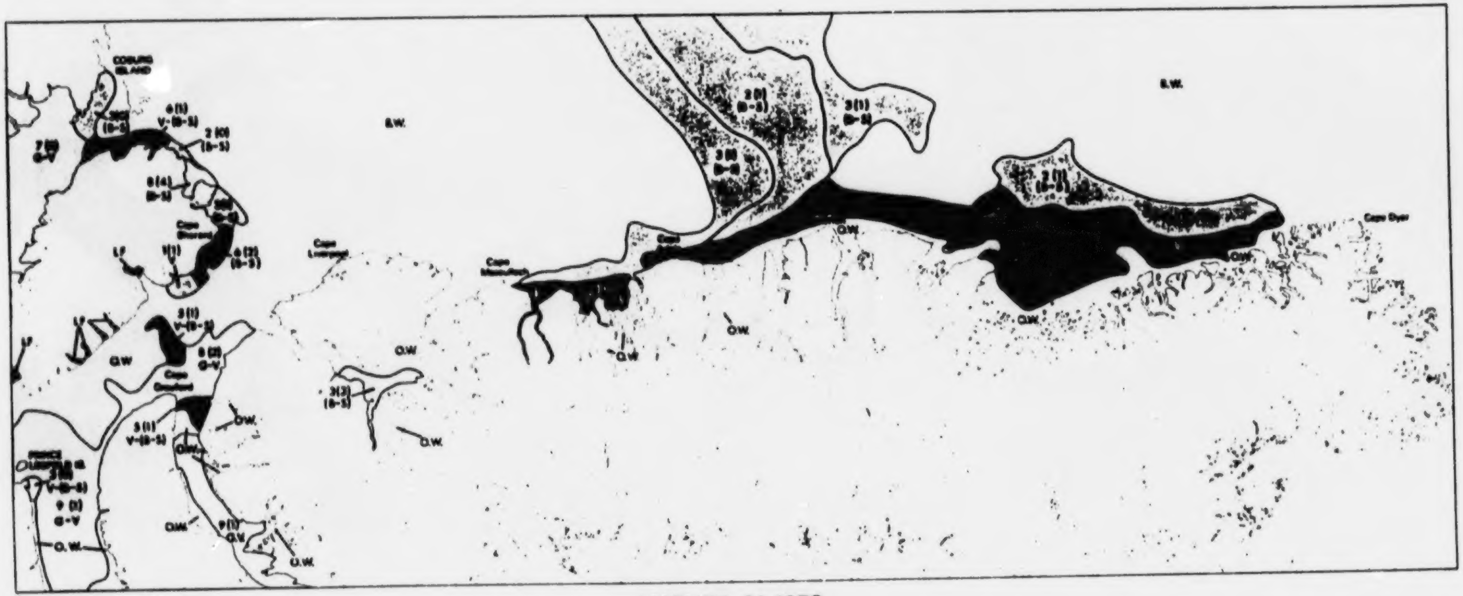
COBURG ISLAND
S.W.
S.W.
O.W.
O.W.
O.W.
O.W.
O.W.
O.W.
Cape Liverpool
Cape Dyer
2(1)
3(1)

AUGUST 21, 1979

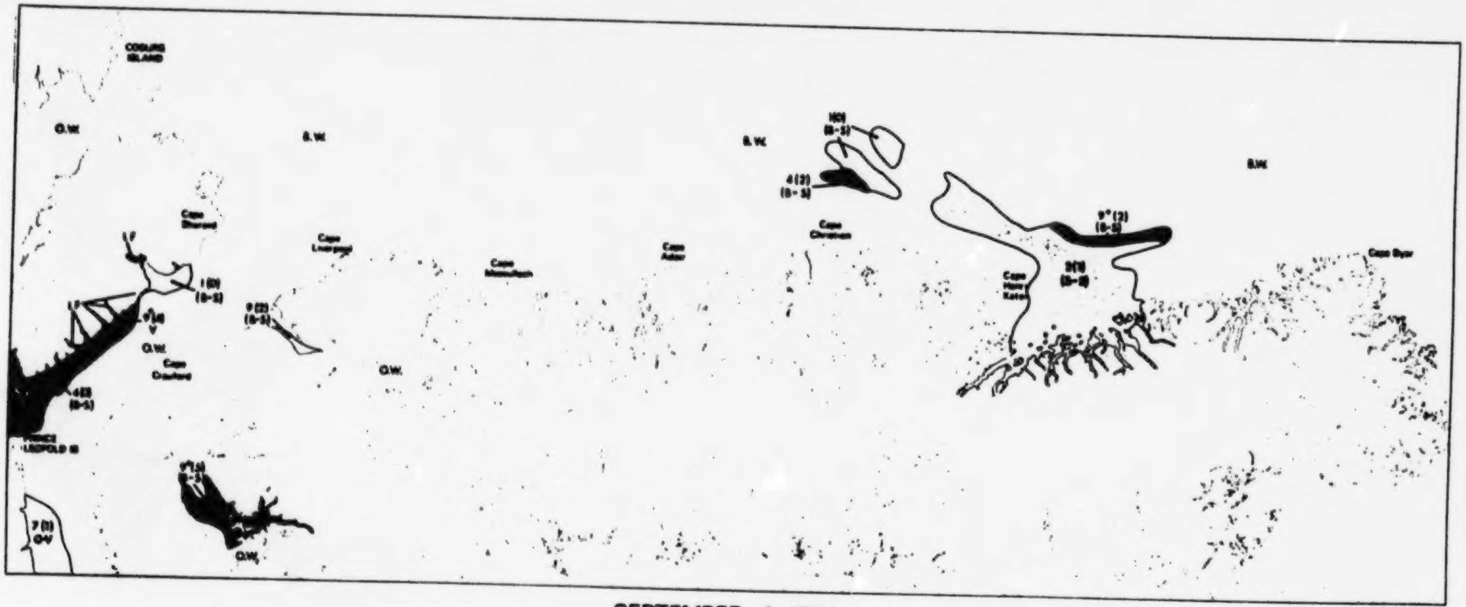
COBURG ISLAND
O.W.
B.W.
Cape Sherard
Cape Liverpool
1 (3)
(0-5)
9 (2)
(0-5)
9⁺(4)
O.W.
Cape Crawford
4 (2)
(0-5)
PRINCE LEOPOLD IS
9⁺(4)
(0-5)
O.W.
7 (1)
O-V
O.W.
Cape Macculloch
Cape Adair
B.W.
1 (2)
(0-5)
4 (2)
(0-5)
Cape Christian
9⁺(2)
(0-5)
Cape Henry Kater
3 (1)
(0-8)
O.W.
B.W.
Cape Dyer

SEPTEMBER 4, 1979

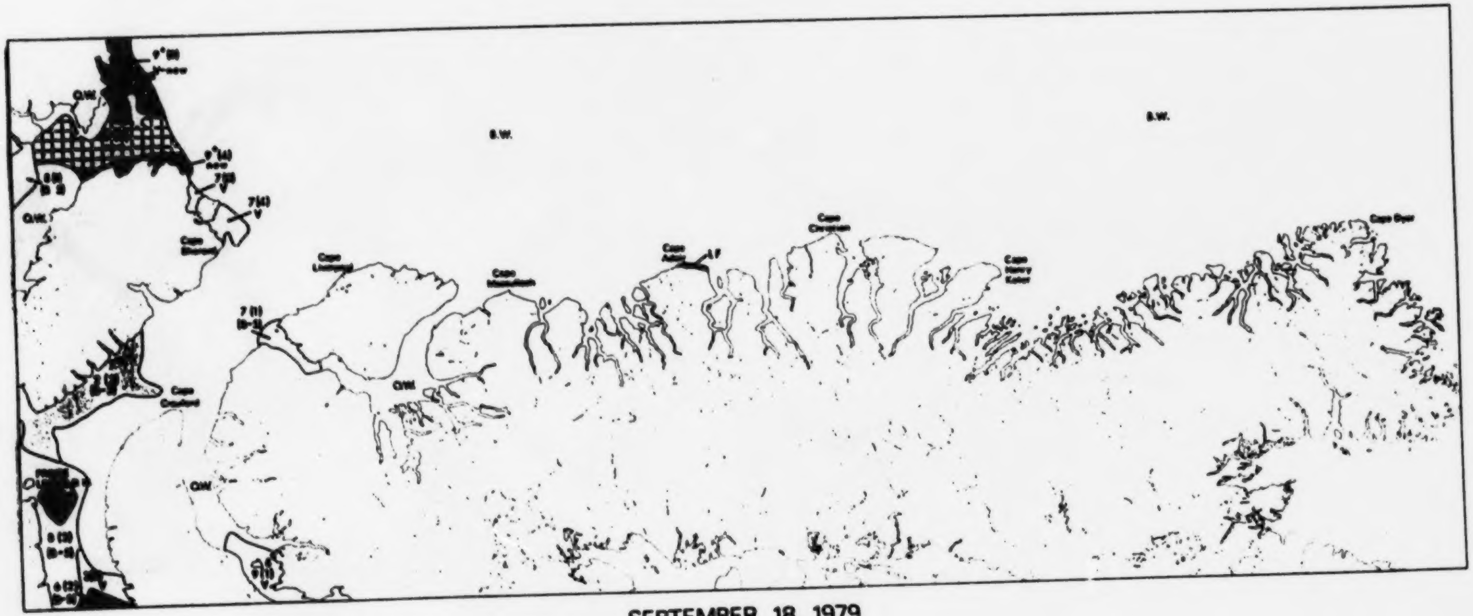

B.W.
B.W.
O.W.
O.W.
O.W.
O.W.
7(2)
V
7(4)
V
7 (1)
Cape Sherard
Cape Liverpool
Cape Macculloch
Cape Crauford
Cape Adair
Cape Christian
Cape Henry Kater
Cape Dyer

SEPTEMBER 18, 1979

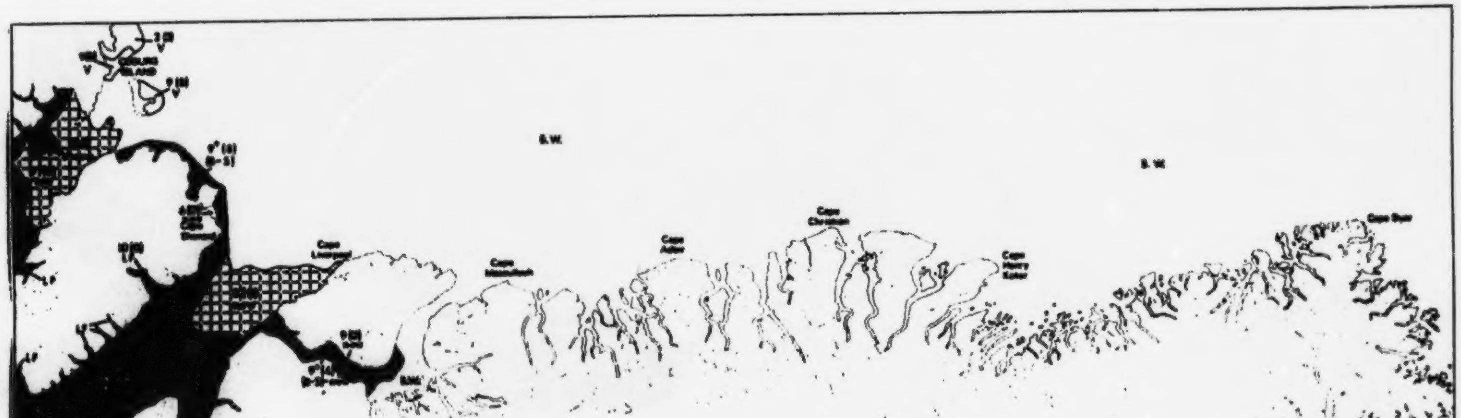

S.W.
Cape Liverpool
Cape Adair
Cape Christian
S.W.
Cape Henry Kater
Cape Dyer

OCTOBER 2, 1979

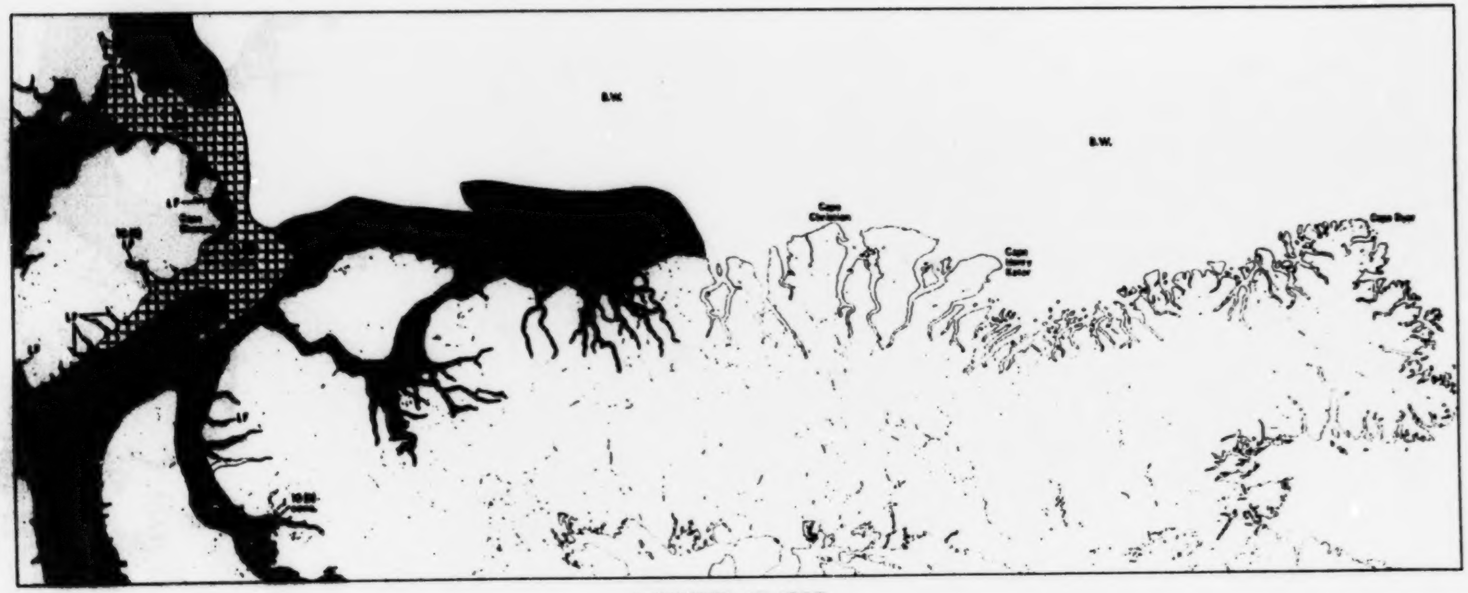
B.W.
B.W.
Cape Christian
Cape Henry Kater
Cape Dyer

OCTOBER 16, 1979

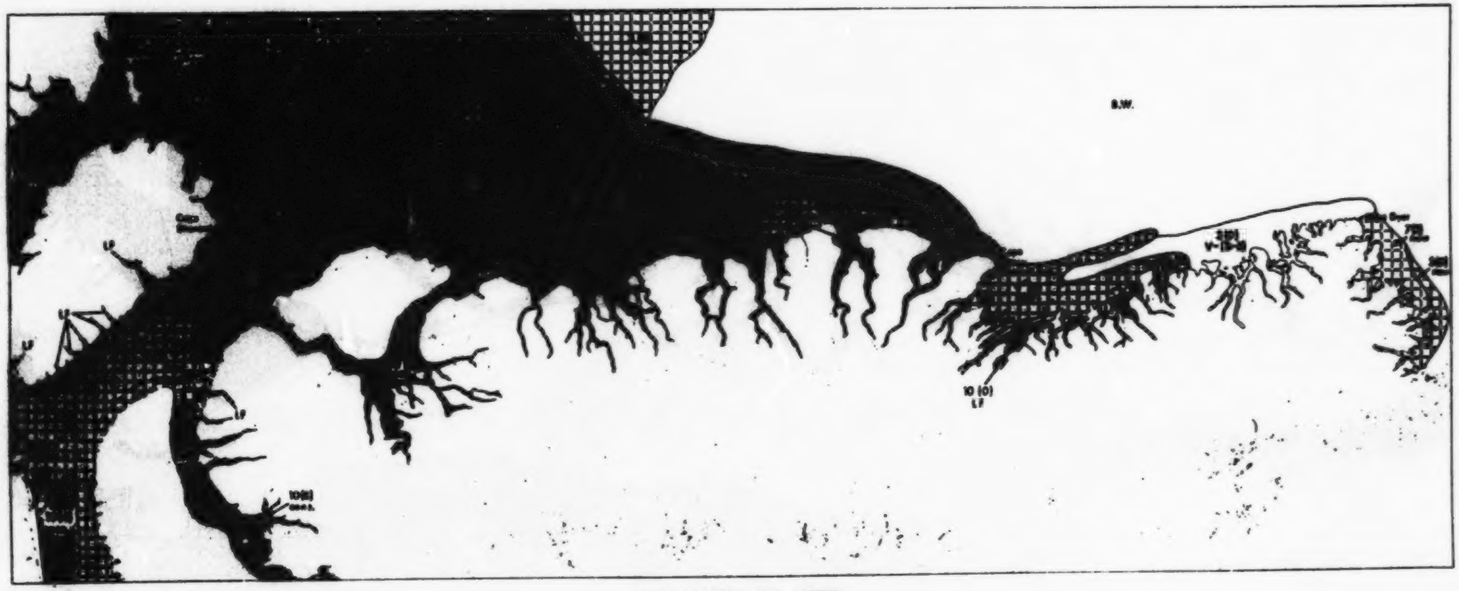

OCTOBER 30, 1979

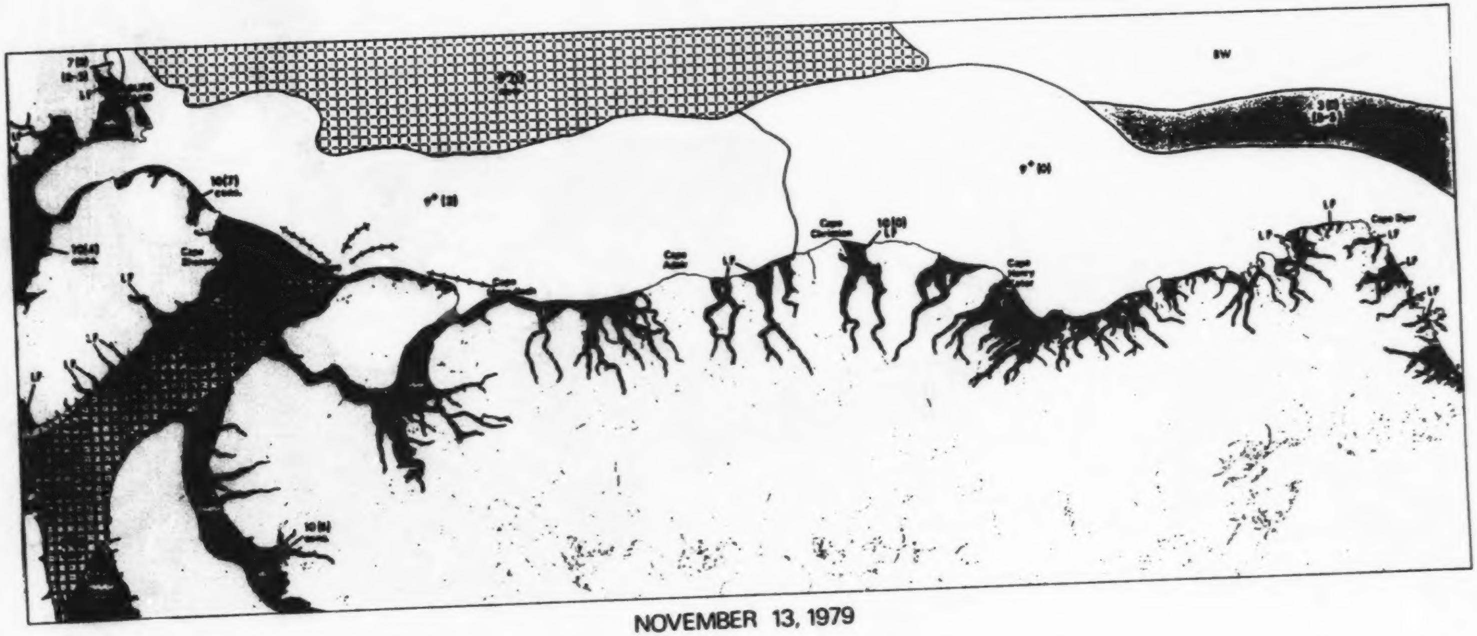
LF
10 (7)
cont.
Cape Adair
LF
Cape Christian
10 (0)
LF
Cape Henry Kater
SW
LF
Cape Dyer
LF
LF
LF

NOVEMBER 13, 1979